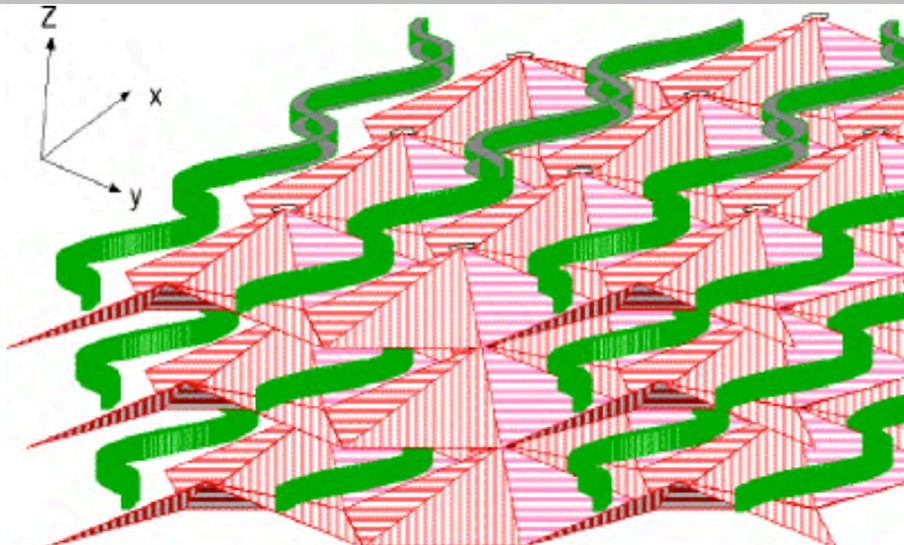


Superconductivity

The Structure Scale of the Universe

Twenty Third Edition – December 08, 2015

Richard D. Saam
 525 Louisiana Ave
 Corpus Christi, Texas 78404 USA
 e-mail: rdsam@att.net
<http://xxx.lanl.gov/abs/physics/9905007>



PREVIOUS PUBLICATIONS

First Edition, October 15, 1996
<http://xxx.lanl.gov/abs/physics/9705007>
 Second Edition, May 1, 1999
<http://xxx.lanl.gov/abs/physics/9905007>, version 19
 Third Edition, February 23, 2002
<http://xxx.lanl.gov/abs/physics/9905007>, version 20
 Fourth Edition, February 23, 2005
<http://xxx.lanl.gov/abs/physics/9905007>, version 21
 Fifth Edition, April 15, 2005
<http://xxx.lanl.gov/abs/physics/9905007>, version 22
 Sixth Edition, June 01, 2005
<http://xxx.lanl.gov/abs/physics/9905007>, version 23
 Seventh Edition, August 01, 2005
<http://xxx.lanl.gov/abs/physics/9905007>, version 24
 Eighth Edition, March 15, 2006
<http://xxx.lanl.gov/abs/physics/9905007>, version 25
 Ninth Edition, November 02, 2006
<http://xxx.lanl.gov/abs/physics/9905007>, version 26
 Tenth Edition, January 15, 2007
<http://xxx.lanl.gov/abs/physics/9905007>, version 27
 Eleventh Edition, June 15, 2007
<http://xxx.lanl.gov/abs/physics/9905007>, version 28

Twelfth Edition, December 6, 2007
<http://xxx.lanl.gov/abs/physics/9905007>, version 29
 Thirteenth Edition, January 15, 2008
<http://xxx.lanl.gov/abs/physics/9905007>, version 30
 Fourteenth Edition, March 25, 2008
<http://xxx.lanl.gov/abs/physics/9905007>, version 31
 Fifteenth Edition, February 02, 2009
<http://xxx.lanl.gov/abs/physics/9905007>, version 32
 Sixteenth Edition, May 12, 2009
<http://xxx.lanl.gov/abs/physics/9905007>, version 33
 Seventeenth Edition, March 15, 2010
<http://xxx.lanl.gov/abs/physics/9905007>, version 34
 Eighteenth Edition, November 24, 2010
<http://xxx.lanl.gov/abs/physics/9905007>, version 35
 Nineteenth Edition, May 10, 2011
<http://xxx.lanl.gov/abs/physics/9905007>, version 36
 Twentieth Edition, December 08, 2011
<http://xxx.lanl.gov/abs/physics/9905007>, version 37
 Twenty First Edition, August 15, 2012
<http://xxx.lanl.gov/abs/physics/9905007>, version 38
 Twenty Second Edition, December 08, 2013
<http://xxx.lanl.gov/abs/physics/9905007>, version 39

ABSTRACT

Superconductivity is presented as a resonant space filling cellular 3D tessellating triangular structure (trisine) consistent with universe conservation of energy and momentum ‘elastic nature’, universal parameters (G , H , h , c and k_b), Maxwells’ permittivity and permeability concepts, Lemaitre Big Bang universe expansion, a Higgs mechanism, de Broglie matter wave hypothesis, Einstein’s energy momentum stress tensor and Charge-Conjugation, Parity-Change and Time-Reversal (CPT) theorem (discrete Noether’s theorem) without recourse to net matter-antimatter annihilation concepts. These trisine lattice elastic structures scale as visible energies $m_i c^2 / (\text{permeability} \times \text{permittivity})$ and black body energies as $m_i c^2 / (\text{permittivity})$ each related to their reflective energy values $m_i c^2 / (\text{permeability_reflective} \times \text{permittivity_reflective})$ and $m_i c^2 / (\text{permittivity_reflective})$ by their near equality at the nuclear dimension defined by the speed of light(c). Both visible and reflective trisine lattices are scalable over 15 orders of magnitude from nuclear to universe dimensions with a constant cellular mass (m_i) (110.12275343 x electron mass or 56.2726 MeV/c²) and constant Hubble to Newton gravity ratio ‘ H_U/G_U ’. The standard model weak and strong forces and up, down, strange, charm, bottom and top particles are defined as nuclear trisine entities maintained at the nuclear density 2.34E14 g/cm³, radius 8.75E-14 cm and temperature 8.96E13 K. The trisine lattice scales to the present universe density of 6.38E-30 g/cm³, Hubble radius of curvature of 2.25E28 cm and temperature 8.11E-16 K. The trisine present universe mass and density could be considered a candidate for the ‘dark energy’ for interpreting present universe data observations. In the proposed trisine dark energy, each particle of mass m_i is contained in a present universe trisine cell volume of 15,733 cm³ resonating at 29,600 seconds. In this context, the universe present cosmic microwave background radiation (CMBR) black body temperature($m_i c^2 / (\text{permittivity}) = 2.729/k_b$ K) is linked to an ubiquitous extremely cold ($m_i c^2 / (\text{permeability} \times \text{permittivity}) = 8.11E-16/k_b$ K) universe ‘dark energy’ temperature thermally supporting an equally cold ‘dark matter’ in the form of colligative nucleosynthetic hydrogen/helium Bose Einstein Condensate(BEC) electromagnetically undetected but gravitationally affecting galactic rotation curves and lensing phenomena. Trisine momentum $m_i c$ space predicts an deceleration value with observed universe expansion and consistent with observed Pioneer 10 & 11 deep space translational and rotational deceleration, flat galactic rotation curves, local universe deceleration relative to supernovae Type 1a standard candles (not the reverse supernovae Type 1a universe expansion acceleration as conventionally reported) and all consistent with the notion that:

An object moving through momentum space will accelerate.

The ubiquitous trisine mass 56 MeV/c² is expressed in Voyager accelerated Anomalous Cosmic Rays, EGRET and FERMI spacecraft data. There is an indication that higher FERMI detected energies falling in intensity by -1/3 power and cosmic ray flux by -23/8 power are an indication of early Big Bang nucleosynthetic processes creating what is known as dark matter dictated by the relationship between reflective dark energy $k_b T_c = m_i c^2 / (\text{permeability_reflective} \times \text{permittivity_reflective})$ and back round radiation (presently CMBR) $k_b T_b = m_i c^2 / (\text{permittivity_reflective})$. Trisine resonant time oscillations have been observed in Gravity Probe B gyro, Active Galactic Nuclei (AGN), telluric atmospheric sodium material superconductors and top quark oscillations. Entanglement and ‘Action at a Distance’ is explained in terms of trisine visible and reflective properties. Nuclear asymptotic freedom as a reflective concept is congruent with the Universe early nucleosynthetic expansion. Also, a reasonable value for the cosmological constant is derived having dimensions of the visible universe. A changing gravitational constant ‘ G_U ’ is consistent with observed galaxy cluster dynamics as a function of ‘ z ’ and also with the recently observed Higg’s particle. Also, a 93 K superconductor should lose weight close to reported results by Podkletnov and Nieminen. Also this trisine model predicts 1, 2 and 3 dimensional superconductors, which has been verified by observed magnesium diboride (MgB₂) superconductor critical data. Also, the dimensional characteristics of material superconductor stripes are explained. Also dimensional guidelines are provided for design of room temperature superconductors and beyond and which are related to practical goals such as fabricating a superconductor with the energy content equivalent to the combustion energy of gasoline. These dimensional guidelines have been experimentally verified by Homes’ Law and generally fit the parameters of a superconductor operating in the “dirty” limit. Confirmation of the trisine approach is represented by correlation to Koide Lepton relation at nuclear dimensions. Also, there is good correlation between, the cosmological constant and a characteristic lattice angle of 22.8 degrees. Also, spacecraft with asymmetrical flyby gravity assist from the earth or other planets would experience modified energy characteristics due to interaction with universe resonant tidal effects or De Broglie matter waves imparted to the earth or planets and subsequently to the spacecraft. Also, the concept of critical volume is introduced for controlled study of characteristics associated with CPT symmetry Critical Optical Volume Energy (COVE) within the context of the Lawson Criterion. A \$1.5 billion - 10 year experimental plan is proposed to study and implement this concept under laboratory conditions here on earth.

Table of Contents

1. Introduction
2. Trisine Model Development
 - 2.1 Defining Model Relationships
 - 2.2 Trisine Geometry
 - 2.3 Trisine Characteristic Wave Vectors
 - 2.4 Trisine Characteristic De Broglie Velocities
 - 2.5 Dielectric Permittivity And Magnetic Permeability
 - 2.6 Fluxoid And Critical Fields
 - 2.7 Superconductor Resonant Internal Pressure, Casimir Force And Deep Space Thrust Force (Pioneer 10 & 11)
 - 2.8 Superconducting Resonant Current, Voltage And Conductance (And Homes' Law)
 - 2.9 Superconductor Resonant Apparent Weight Reduction In A Gravitational Field
 - 2.10 BCS Verifying Constants and Maxwell's Equations
 - 2.11 Cosmological Parameters
 - 2.12 Superconducting Resonant Variance At T/T_c
 - 2.13 Superconductor Resonant Energy Content
 - 2.14 Superconductor Resonant Gravitational Energy
 - 2.15 Black Body Relationships
 - 2.16 The Concept of Critical Optical Volume Energy (COVE) and Schwinger Pair Production
3. Discussion
4. Conclusion
5. Variable And Constant Definitions (Including Planck dimensions)
- Appendices
 - A. Trisine Number, Trisine Mass And B/A Ratio Derivation
 - B. Debye Model Normal And Trisine Reciprocal Lattice Wave Vectors
 - C. One Dimension And Trisine Density Of States
 - D. Ginzburg-Landau Equation And Trisine Structure Relationship
 - E. Heisenberg Uncertainty Within The Context of De Broglie Condition
 - F. Equivalence Principle In The Context Of Work Energy Theorem
 - G. Koide Constant for Leptons - tau, muon and electron
 - H. Active Galactic Nuclei Tidal Dimension in Oscillating Dark Energy Matter Medium
 - I. Dimensional Analysis of h, G, c, H
 - J. CMBR and Universe Luminosity Equivalence
 - K. Hydrogen Bose Einstein Condensate as Dark Matter
 - L. Model Development For Classical Fluid Shear and Fluid Drop Modification
 - M. Classical Phase Separation
 - N. Authority for Expenditure (Project Cost Estimate)
 6. References

Introduction

1.

The trisine structure is a geometrical lattice model for the superconductivity phenomena based on Gaussian surfaces (within the context of Maxwell Displacement (D) concept) encompassing superconducting Cooper CPT Charge conjugated pairs (discrete Noether's theorem entities). This Gaussian surface has the same configuration as a particular matrix geometry as defined in reference [1], and essentially consists of mirror image non-parallel surface pairs. Originally, the main purpose of the engineered lattice [1] was to control the flow of particles suspended in a fluid stream and generally has been fabricated on a macroscopic scale to remove particles in industrial fluid streams on the order of m^3/sec . This general background is presented in Appendices L and M. In the particular configuration discussed in this report, a more generalized conceptual lattice is described wherein there is a perfect elastic resonant character to fluid and particle flow. In other words there is 100 percent conservation of energy and momentum (elastic or resonant condition), which defines the phenomenon of superconductivity.

The superconducting model presented herein is a logical translation of this geometry [1] in terms of classical and quantum theory to provide a basis for explaining aspects of the superconducting phenomenon and integration of this phenomenon with nuclear, electromagnetic and gravitational forces at all time scales over the age of the universe (from the Big Bang to present) (in terms of z) within the context of references[1-151].

This approach is an attempt to articulate a geometrical model for superconductivity in order to anticipate dimensional regimes in which one could look for higher performance materials or photonic media an approach that leads to universal understanding. This approach addresses specific particles such as polarons, exitons, magnons, plasmons and the standard model quarks and gluons as an expression of superconductivity in a given material or photonic medium, but which mask the essence of superconductivity as an expression of virtual particles by Dirac Schwinger pair production/annihilation. Indeed, the dimensionally correct (*mass, length, time*) trisine structure or lattice as presented in this report may be expressed in terms of something very elementary and that is the Charge Conjugate Parity Change Time Reversal (CPT) Theorem as a basis for creating resonant virtual particle structures adjacent to the Heisenberg Uncertainty and consistent with dimensional (*mass, length, time*) correctness or numerical consistency

with fundamental constants (\hbar, G, c, H & k_b) (encompassing the Planck units) as well as conformance with Maxwell equations[41], Lemaitre cosmology[122] and Einstein's general relativity.

The vacuum energy density as derived by Milonni[45], may not have the extremely high value of $1E14$ erg/cm³ due to an undefined boundary condition assumption that is more physically represented by universe parameters (\hbar, G, c, H & k_b) describing nature independent of particular '*mass, length and time*' dimensions.

As a corollary:

If a fundamental constant (\hbar, G, c, H & k_b) functional relationship describing nature is in terms of *mass, length and time*, then a functional relationship with arbitrary dimensionality ($dim1, dim2, dim3$) equally describing nature is established with ($dim1, dim2, dim3$) functionally linked back to (*mass, length, time*).

Model numerical and dimensional coherency is maintained at less than the trisine uncertainty factor ($1-g_s$) = .01 on a Excel spreadsheet and Mathcad dimensional analysis software with name plate calculation precision at 15 significant digits.

Traditionally, superconductivity or resonance is keyed to a critical temperature (T_c), which is representative of the energy at which the superconductive resonant property takes place in a material or photonic medium. The material or photonic medium that is characterized as a superconductor has this property at all temperatures below the critical temperature.

Temperature(T) is related to energies (E_{ϵ, k_m}) associated with permittivity (ϵ) and permeability (k_m) through the Boltzmann constant (k_b) adjacent to the Heisenberg Uncertainty $E_{\epsilon, k_m} TIME = \hbar/2$ at a characteristic mass(m).

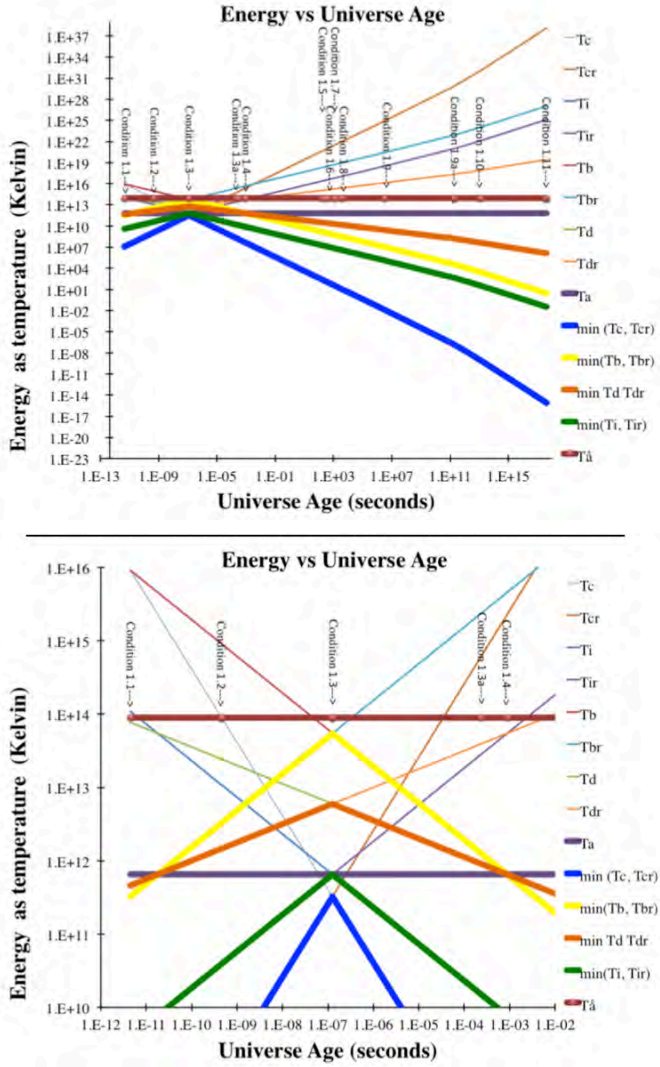
$$\frac{\hbar}{TIME} = k_b T = E_{\epsilon, k_m} = mv^2 = \epsilon k_m mc^2$$

Various quantum mechanical separable temperature ($T's$) such as T_c, T_b, T_a, T_p, T_r and T_i are to be defined as various expressions of permittivity (ϵ) and permeability (k_m) with the acknowledgement of group and phase velocities.

In terms of the trisine model, any critical temperature (T_c) can be inserted, but for the purposes of this report, eleven universe expansion conditions of critical temperatures (T_c) and associated black body temperatures (T_b) (and other $T's$) are selected as scaled with universe permittivity (ϵ) and permeability (k_m) and associated magnetic and electrical fields as well as various thermodynamic properties. This

approach can be placed in the context of the universe adiabatic expansion where these particular temperatures (T_c) and associated black body (T_b) existed at a particular universe age from the time of nucleosynthesis to present galactic formation from dark matter within the superconducting ‘dark energy’ milieu. In this scenario, this cold dark matter would primarily be hydrogen and helium but would not detract from the observed hydrogen and helium abundances as observed in early universe stellar formation.

Figure 1.1 Universe Expansion Concept as a superconducting (elastic resonant) permittivity (ϵ) permeability (k_m) medium as measured by indicator temperatures (T) constrained by the speed of light (c) and numerically presented in conditions 1.1 to 1.11 with expanded view at conditions 1.1 to 1.4.



This approach logically indicates that most of the mass of the universe (dark energy) is at the critical temperature (T_c) which is presently extremely cold at 8.11E-16 K and in

thermal equilibrium with the ‘dark baryonic matter’ having the chemical nature (mainly hydrogen and helium) of nucleosynthesis period in the early universe. Baryonic ‘dark’ matter presently at 8.11E-16 K (quantum mechanically distinct from the cosmic microwave background radiation T_b presently at 2.73 K) could be in a dense ($\sim 1 \text{ g/cm}^3$) particulate colligative Bose Einstein Condensate (BEC) phase since it has been demonstrated in the laboratory that hydrogen BECs are created at much warmer temperatures on the order of 1E-7 K (BEC_{ST} - see Appendix K). Conceptually, the universe expansion can be likened to a CO₂ fire extinguisher adiabatic discharge with the resultant CO₂ particle cold fog analogous to the universe dark matter. A small portion of this dark matter ‘fog’ gravitationally collapses into the luminous matter (stars, galaxies etc.) that is observed in the celestial sphere while the substantial residual remains as ~meter sized masses within galactic interstellar space and surrounding halos only observed by its gravitational effects.

More precisely, universe time evolution is dictated by adiabatic process at universe Hubble expansion H_U (initially at an extremely high 8.48E25 sec⁻¹) with the fundamental conservation of energy adiabatic expansion

$$T_{c2}/T_{c1} = (\rho_{U2}/\rho_{U1})^{2/3}$$

between Hubble expansion H_{U1} and Hubble expansion H_{U2} where:

$$H_U = (1/\sqrt{3})(\text{section/cavity})(k_b T_c / m_c c) = 1/Age_U.$$

The universe expansion is within the context of solutions to the Einstein field equations with H_U and G_U directly related by the speed of light (c) and the Dirac constant (\hbar):

$$G_{\mu\nu} = \frac{8\pi G_U}{c^4} T_{\mu\nu}$$

$$U = \frac{H_U}{G_U} = \frac{4\pi\rho_U}{H_U} = \frac{4m_t^3 c}{\pi\hbar^2} = 3.46E-11 \quad (\text{g cm}^{-3} \text{ sec})$$

where the Newton gravitational parameter (G_U) varies $\sim 1/Age_U$ inversely with universe age coordinate time (Age_U) while incremental proper time ($\Delta\tau$) is approximately zero. The universe expands with Hubble radius of curvature R_U and the volume of lattice component cavity’s at the universe age Age_U . Then lattice dimension $B \sim Age_U^{1/3}$. The different rates of B and R_U change with Age_U may explain the presently observed universe acceleration. We as observers

are imbedded in the universe lattice 3D tessellated *cavity* structure and bounded by the gross universe volume V_U . All transitions are smooth from the Big Bang (no initial Guth inflationary period is required).

$$\frac{1}{Age_U} = H_U = \frac{1}{\sqrt{3}} \frac{k_b T_c}{cavity} \frac{section}{m_t c} = \sqrt{\frac{8\pi}{2} G_U \rho_U}$$

$$\frac{1}{Age_{Ur}} = H_{Ur} = \frac{1}{\sqrt{3}} \frac{k_b T_c}{cavity_r} \frac{section_r}{m_t c} = \sqrt{\frac{8\pi}{2} G_{Ur} \rho_{Ur}}$$

$$\rho_U = \frac{m_t}{cavity} = \frac{2}{8\pi} \frac{H_U^2}{G_U} = \frac{M_U}{V_U} = \frac{3M_U}{4\pi R_U^3}$$

$$\rho_{Ur} = \frac{m_t}{cavity_r} = \frac{2}{8\pi} \frac{H_{Ur}^2}{G_{Ur}} = \frac{M_{Ur}}{V_{Ur}} = \frac{3M_{Ur}}{4\pi R_{Ur}^3}$$

$$R_U = \sqrt{3}cAge_U = \frac{\sqrt{3}c}{H_U} \quad \frac{G_U m_t M_U}{R_U} = m_t c^2$$

$$R_{Ur} = \sqrt{3}cAge_{Ur} = \frac{\sqrt{3}c}{H_{Ur}} \quad \frac{G_{Ur} m_t M_{Ur}}{R_{Ur}} = m_t c^2$$

$$\frac{G_U M_U H_U}{c^3} = \frac{G_{Ur} M_{Ur} H_{Ur}}{c^3} = \frac{(G_U G_{Ur} M_U M_{Ur} H_U H_{Ur})^{1/2}}{c^3} = 3^{1/2}$$

$$(M_U M_{Ur})^{1/2} = \frac{g_s m_t}{3\alpha}$$

$$\frac{1}{2} g_e g_s \frac{m_t}{m_e} \frac{e_\pm \hbar}{2m_e v_\pm} = cavity H_c$$

$$1/\alpha = \hbar c/e^2$$

$$\frac{m_t}{m_e} = 4\pi^{3/4} \sqrt{\frac{2\hbar c}{g_e e^2}} = 4\pi^{3/4} \sqrt{\frac{2}{g_e \alpha}}$$

$$2g_e g_s \pi^{3/4} \sqrt{\frac{2}{g_e \alpha}} \frac{e_\pm \hbar}{2m_e v_\pm} = cavity H_c$$

$$cavity = \frac{4\pi Age_U m_t}{U} = \frac{4\pi m_t}{U H_U} = 2\sqrt{3}AB^2$$

$$section = 2\sqrt{3}B^2 \quad \frac{section}{cavity} = \frac{1}{A} \quad \frac{B}{A} = 2.379760996$$

$$sherd = \frac{M_{Upresent}}{M_U} \quad sherd_{present} = 1$$

('present' values are in trisine condition 1.11 green)
universe constant mass = $M_U sherd = 3.02E+56$ g

universe constant energy = $M_U c^2 sherd = 2.72E+77$ erg

Universe Newtonian Gravitational constant G =

$$G_U sherd^{-1/2} = G_{Ur} sherd_r^{-1/2} = 6.6725985E-8 \text{ cm}^3 \text{ sec}^{-2} \text{ g}^{-1}$$

$$\text{Universe Total Volume } V_{UT} = M_U sherd \frac{cavity}{m_t}$$

Most cosmological observation assumes a constant Newtonian gravitational parameter (G) with the Universe age making a conversion necessary.

Trisine condition header information have the following universe temperature, size and time definitions:

$$Age_{UG} = Age_U \sqrt{\frac{G_U}{G}} = Age_U \sqrt{\frac{R_U c^2}{GM_U}}$$

$$Age_{UGr} = Age_{Ur} \sqrt{\frac{G_{Ur}}{G}} = Age_U \sqrt{\frac{R_{Ur} c^2}{GM_{Ur}}}$$

$$Age_{UGv} = Age_U \sqrt{\frac{R_U c^2}{G(M_U + M_v)}}$$

$$Age_{UGvr} = Age_{Ur} \sqrt{\frac{R_{Ur} c^2}{G(M_{Ur} + M_{vr})}}$$

$Age_{UGv} = Age_{UG} = Age_U = 13.7E+09$ years at the present time

$$T_a = \frac{m_t c^2}{k_b}$$

$$T_{\dot{a}} = g_d m_t c^2 / (a k_b)$$

$$T_d = \frac{m_t c^2}{\sqrt{\varepsilon} k_b} \quad T_{dr} = \frac{m_t c^2}{\sqrt{\varepsilon_r} k_b}$$

$$T_b = \frac{m_t c^2}{\varepsilon k_b} \quad T_{br} = \frac{m_t c^2}{\varepsilon_r k_b}$$

$$T_i = \frac{m_t c^2}{(k_{mx} \varepsilon_x)^{1/2} k_b} \quad T_{ir} = \frac{m_t c^2}{(k_{mxr} \varepsilon_{xr})^{1/2} k_b}$$

$$T_c = \frac{m_t c^2}{2k_{mx} \varepsilon_x k_b} \quad T_{cr} = \frac{m_t c^2}{2k_{mxr} \varepsilon_{xr} k_b}$$

$$T_j = \frac{1}{4} \frac{m_t c^2}{(k_m \varepsilon)^2} \frac{1}{k_b} \quad T_{jr} = \frac{1}{4} \frac{m_t c^2}{(k_{mr} \varepsilon_r)^2} \frac{1}{k_b}$$

$$k_m = \frac{1}{\varepsilon} \frac{1}{\frac{1}{\varepsilon_x k_{mx}} + \frac{1}{\varepsilon_y k_{my}} + \frac{1}{\varepsilon_z k_{mz}}} \quad \varepsilon = \frac{3}{\frac{1}{\varepsilon_x} + \frac{1}{\varepsilon_y} + \frac{1}{\varepsilon_z}}$$

$$k_{mr} = \frac{1}{\varepsilon_r} \frac{1}{\frac{1}{\varepsilon_{xr} k_{mxr}} + \frac{1}{\varepsilon_{yr} k_{myr}} + \frac{1}{\varepsilon_{zr} k_{mzr}}} \quad \varepsilon_r = \frac{3}{\frac{1}{\varepsilon_{xr}} + \frac{1}{\varepsilon_{yr}} + \frac{1}{\varepsilon_{zr}}}$$

$$z_B = \frac{B_{\text{present}}}{B} - 1 \quad z_R = \frac{R_{\text{Upresent}}}{R_U} - 1$$

1.1	z_R	3.79E+46	z_R	3.79E+46	unitless
	z_B	3.36E+15	z_B	3.36E+15	unitless
	T_a	6.53E+11	T_a	6.53E+11	$^{\circ}K$
	T_b	9.14E+15	T_{br}	3.27E+11	$^{\circ}K$
	T_c	9.14E+15	T_{cr}	1.17E+07	$^{\circ}K$
	T_d	7.73E+13	T_{dr}	4.62E+11	$^{\circ}K$
	T_i	1.09E+14	T_{ir}	3.90E+09	$^{\circ}K$
	T_j	7.98E+22	T_{jr}	1.30E+05	$^{\circ}K$
	ε_x	5.96E-03	ε_{xr}	1.67E+02	unitless
	ε_y	5.96E-03	ε_{yr}	1.67E+02	unitless
	ε_z	7.32E-05	ε_{zr}	2.05E+00	unitless
	ε	7.14E-05	ε_r	2.00E+00	unitless
	k_{mx}	5.99E-03	k_{mr}	1.67E+02	unitless
	k_{my}	4.49E-03	k_{myr}	1.25E+02	unitless
	k_{mz}	2.16E-02	k_{mzr}	6.04E+02	unitless
	k_m	2.00E-02	k_{mr}	5.61E+02	unitless

	ρ_U	2.41E+17	ρ_{Ur}	1.10E+04	g/cm ³
	B	6.58E-15	B_r	1.84E-10	cm
	$cavity$	4.16E-43	$cavity_r$	9.12E-30	cm ³
	R_U	5.93E-19	R_{Ur}	1.30E-05	cm
	V_U	8.74E-55	V_{Ur}	9.24E-15	cm ³
	V_{Utotal}	1.25E+39	$V_{Utotalr}$	9.24E-15	cm ³
	M_U	2.11E-37	M_{Ur}	1.02E-10	g
	M_v	5.14E-26	M_{vr}	5.14E-26	g
	M_{Utotal}	3.03E+56	$M_{Utotalr}$	3.03E+56	G
	$time_{\pm}$	2.63E-27	$time_{r\pm}$	2.06E-18	sec
	$1/time_{\pm}$	3.81E+26	$1/time_{r\pm}$	4.86E+17	/sec
	H_U	8.75E+28	H_{Ur}	3.99E+15	/sec
	G_U/G	3.79E+46	G_{Ur}/G	1.73E+33	unitless
	$sherd$	1.43E+93	$sherd_r$	2.98E+66	unitless
	Age_U	1.14E-29	Age_{Ur}	2.51E-16	sec
	Age_{UG}	2.22E-06	Age_{UGr}	1.04E+01	sec
	Age_{UGv}	4.50E-12	Age_{UGvr}	3.53E-03	sec
	$BCST$	2.58E+01	$BCST$	2.58E+01	sec

This energy conjunction at $T_c = T_b$ marks the beginning of the universe where time and space are not defined in a group phase reflection condition where $v_d \sim v_e \gg c$. The universe mass (M_U) is nominally at 2.08E-37 gram the radiation mass (M_v) $\sim m_t/2$. This point corresponds to the ankle condition in the observed cosmic ray spectrum as presented in Figure 4.33.1

1.2	z_R	3.67E+43	z_R	3.67E+43	unitless
	z_B	3.32E+14	z_B	3.32E+14	unitless
	T_a	6.53E+11	T_a	6.53E+11	$^{\circ}K$
	T_b	9.05E+14	T_{br}	3.30E+12	$^{\circ}K$
	T_c	8.96E+13	T_{cr}	1.19E+09	$^{\circ}K$
	T_d	4.80E+13	T_{dr}	8.89E+09	$^{\circ}K$
	T_i	1.08E+13	T_{ir}	3.94E+10	$^{\circ}K$
	T_j	7.67E+18	T_{jr}	1.35E+09	$^{\circ}K$
	ε_x	6.02E-02	ε_{xr}	1.65E+01	unitless
	ε_y	6.02E-02	ε_{yr}	1.65E+01	unitless

ε_z	7.39E-04	ε_{zr}	2.03E-01	unitless
ε	7.21E-04	ε_r	1.98E-01	unitless
k_{mx}	6.05E-02	k_{mr}	1.65E+01	unitless
k_{my}	4.54E-02	k_{myr}	1.24E+01	unitless
k_{mz}	2.18E-01	k_{mzr}	5.98E+01	unitless
k_m	2.02E-01	k_{mr}	5.55E+01	unitless
ρ_U	2.34E+14	ρ_{Ur}	1.13E+07	g/cm^3
B	6.65E-14	B_r	1.83E-11	cm
<i>cavity</i>	4.28E-40	<i>cavity_r</i>	8.85E-33	cm^3
R_U	6.11E-16	R_{Ur}	1.26E-08	cm
V_U	9.57E-46	V_{Ur}	8.44E-24	cm^3
V_{Utotal}	1.29E+42	$V_{Utotalr}$	8.44E-24	cm^3
M_U	2.24E-31	M_{Ur}	9.56E-17	g
M_v	5.41E-21	M_{vr}	5.41E-21	g
M_{Utotal}	3.03E+56	$M_{Utotalr}$	3.03E+56	g
$time_{\pm}$	2.68E-25	$time_{r\pm}$	2.02E-20	sec
$1/time_{\pm}$	3.73E+24	$1/time_{r\pm}$	4.96E+19	$/sec$
H_U	8.49E+25	H_{Ur}	4.11E+18	$/sec$
G_U/G	3.67E+43	G_{Ur}/G	1.78E+36	unitless
<i>sherd</i>	1.35E+87	<i>sherd_r</i>	3.16E+72	unitless
Age_U	1.18E-26	Age_{Ur}	2.43E-19	sec
Age_{UG}	7.14E-05	Age_{UGr}	3.24E-01	sec
Age_{UGv}	4.59E-10	Age_{UGvr}	3.46E-05	sec
$BCST$	2.29E+02	$BCST$	2.29E+02	sec

This T_c defines superconductive phenomenon as dictated by the proton density 2.34E14 g/cm^3 and radius B of 6.65E-14 cm (8.750E-14 cm NIST reported charge radius value) which is defined at a critical temperature T_c of

$$T_c = T_{\bar{a}} = g_d m_t \hbar c^3 / (e^2 k_b) = g_d m_t c^2 / (\alpha k_b)$$

that is a consequence of a group phase reflection condition:

$$v_{dx} = \left(\frac{2}{\alpha}\right)^{\frac{1}{2}} c$$

that is justifiable in elastic resonant condition (see equations 2.1.5 and 2.1.6 and follow-on explanation) and

$$\frac{\hbar c}{e^2} = \frac{m_r}{m_t} = \frac{v_{dx}^2}{2c^2} = \text{fine structure constant} = \frac{1}{\alpha}$$

This condition 1.2 defines the quark masses in the context of an space filling elastic concept developed in section 2:

$$\begin{aligned} \text{Conservation Of Momentum} & \sum_{n=B,C,Ds,Dn} \Delta p_n \Delta x_n = 0 \\ & g_s (\pm K_B \pm K_C) \rightleftharpoons \pm K_{Ds} \pm K_{Dn} \\ & g_s (\pm K_{Br} \pm K_{Cr}) \rightleftharpoons \pm K_{Dsr} \pm K_{Dnr} \end{aligned}$$

$$\begin{aligned} \text{Conservation Of Energy} & \sum_{n=B,C,Ds,Dn} \Delta E_n \Delta t_n = 0 \\ & K_B^2 + K_C^2 = g_s (K_{Ds}^2 + K_{Dn}^2) \\ \text{Where} & K_{Br}^2 + K_{Cr}^2 = g_s (K_{Dsr}^2 + K_{Dnr}^2) \end{aligned}$$

$$2 \frac{K_A}{K_B} = \frac{B}{A} = 2 \frac{K_{Ar}}{K_{Br}} = \frac{B_r}{A_r} = 2.379329652$$

and

$$m_t = 1.003150329 E - 25 g (56.27261166 MeV/c^2)$$

$$g_s = 1.009662156$$

$$g_d = 1.001159652180760$$

(As explained in section 2.3)

The top quark is associated with energy

$$\left(\frac{4g_s}{\alpha^2}\right) \frac{\hbar^2 K_{Ar}^2}{2m_t} = \frac{\hbar^2 K_A^2}{2m_t} = 174.798 GeV (174.98 \pm .76)$$

The bottom (b) quark is associated with

$$\frac{2}{\alpha} \hbar K_{Ar} c = \hbar K_A c = 4,435 MeV (4,190 + 180 - 60)$$

verified [147]

The up (u) quark is associated with

$$\frac{2}{\alpha} \frac{1}{3} \frac{m_e}{m_t} \hbar K_{Br} c = \frac{1}{3} \frac{m_e}{m_t} \hbar K_B c = 2.82 \text{ MeV} (1.7 - 3.1)$$

The down (d) quark is associated with

$$\frac{2}{\alpha} \frac{2}{3} \frac{m_e}{m_t} \hbar K_{Br} c = \frac{2}{3} \frac{m_e}{m_t} \hbar K_B c = 5.64 \text{ MeV} (4.1 - 5.7)$$

The charm (c) quark is associated with

$$\frac{2}{\alpha} \frac{1}{3} \hbar K_{Ar} c = \frac{1}{3} \hbar K_A c = 1.48 \text{ GeV} (1.29 + .50 - .11)$$

The strange quark (s) is associated with

$$\frac{1}{3} \frac{m_e}{m_t} \frac{\hbar^2}{2m_t} (K_{Ds}^2 + K_{Dn}^2) \cdot g_s = 0.10175 \text{ MeV}$$

$$\left(\frac{4g_s}{\alpha^2}\right) \frac{1}{3} \frac{m_e}{m_t} \frac{\hbar^2}{2m_t} (K_{Dsr}^2 + K_{Dnr}^2) \cdot g_s = 0.10175 \text{ MeV}$$

$$\frac{1}{3} \frac{m_e}{m_t} \frac{\hbar^2}{2m_t} (K_B^2 + K_C^2) = 0.10175 \text{ MeV} (95 \pm 5)$$

$$\left(\frac{4g_s}{\alpha^2}\right) \frac{1}{3} \frac{m_e}{m_t} \frac{\hbar^2}{2m_t} (K_{Br}^2 + K_{Cr}^2) = 0.10175 \text{ MeV} (95 \pm 5)$$

The Delta particles $\Delta^{++}, \Delta^+, \Delta^0, \Delta^-$ are associated with

$$\frac{2}{\alpha} \frac{4}{3} \frac{g_d}{g_s} \hbar K_{Br} = \frac{4}{3} \frac{g_d}{g_s} \hbar K_B = 1232.387 \text{ MeV} (1232 \pm 2).$$

That is consistent with the neutron (n^0), electron (e^-), electron antineutrino (ν_e) and proton (p^+) state nuclear transition

$$p^+ + e^- \leftrightarrow n^0 + \nu_e$$

That is consistent with the proton (p^+) mass (m_p) state composed of standard model up quarks (2) and down quark (1)

$$m_p c^2 = \frac{g_s}{g_d^2} \frac{m_t}{m_e} \left(2 \frac{1}{3} m_{up} + 1 \frac{2}{3} m_{down} \right) c^2 \frac{\text{cavity}}{\text{chain}}$$

$$= 938.967317 \text{ MeV} (938.272046(21))$$

And also consistent with the neutron mass state

$$m_n c^2 = \frac{g_s}{g_d} \frac{m_t}{m_e} \left(1 \frac{1}{3} m_{up} + 2 \frac{2}{3} m_{down} \right) c^2$$

$$= 940.1890901 \text{ MeV} (939.565378(21))$$

Also the nuclear magneton identity exists as

$$\frac{2}{5} \frac{e\hbar}{2m_p c} = 2.785 \frac{g_s^2}{\cos(\theta)} \frac{e\hbar}{2m_t v_{dx}}$$

with the ratio 2/5 being the sphere moment of inertia factor and the constant 2.785 being equal to the experimentally observed as the nucleus of hydrogen atom, which has a magnetic moment of 2.79 nuclear magnetons.

At this nuclear length dimension ($B_{nucleus}$), the gravity energy is related to Hubble parameter (H_U) where ($\hbar = h/2\pi$)

$$hH_U = \frac{3}{2} \frac{G_U m_t^2}{B_{nucleus}}$$

and

$$B_{nucleus} = \frac{3}{16} \frac{\hbar}{m_t c} = \frac{\hbar\pi}{m_p c}$$

This proton dimensional condition conforms to Universe conditions at hundredths of second after the Big Bang and also nuclear Fermi energy of (2/3 x 56) or 38 MeV.

This point corresponds to the knee condition in the observed cosmic ray spectrum as presented in Figure 4.33.1.

The nuclear Delta particles $\Delta^{++}, \Delta^+, \Delta^0, \Delta^-$ with corresponding quark structure uuu, uud, udd, ddd, with masses of 1,232 MeV/c² are generally congruent with the trisine prediction of (4/3) $\hbar K_B c$ or 1,242 MeV/c² (compared to $\hbar K_B c$ or 932 MeV/c² for the proton 'ud' mass) where B reflects the nuclear radius $3\hbar/(16m_t c)$ or 6.65E-14 cm.

$$m_{\Delta^{++}} c^2 = \frac{g_s}{g_d} \frac{m_t}{m_e} \left(3 \frac{1}{3} m_{up} + 0 \frac{2}{3} m_{down} \right) c^2 4$$

$$= 1,231 \text{ MeV} (1,232 \text{ MeV})$$

$$m_{\Delta^+} c^2 = \frac{g_s}{g_d} \frac{m_t}{m_e} \left(2 \frac{1}{3} m_{up} + 1 \frac{2}{3} m_{down} \right) c^2 2 \\ = 1,231 \text{ MeV} (1,232 \text{ MeV})$$

$$m_{\Delta^0} c^2 = \frac{g_s}{g_d} \frac{m_t}{m_e} \left(1 \frac{1}{3} m_{up} + 2 \frac{2}{3} m_{down} \right) c^2 \frac{4}{3} \\ = 1,231 \text{ MeV} (1,232 \text{ MeV})$$

$$m_{\Delta^-} c^2 = \frac{g_s}{g_d} \frac{m_t}{m_e} \left(0 \frac{1}{3} m_{up} + 3 \frac{2}{3} m_{down} \right) c^2 \\ = 1,231 \text{ MeV} (1,232 \text{ MeV})$$

Also, the experimentally determined delta particle (6E-24 seconds) mean lifetime is consistent and understandably longer than the proton resonant *time* (2.68E-25 second from Table 2.4.1).

It is noted that the difference in neutron (m_n) and proton (m_p) masses about two electron (m_e) masses ($m_n - m_p \sim 2m_e$).

The nuclear weak force boson particles (W^-W^+) are associated with energies

$$\frac{B}{A} \frac{\hbar^2 (K_B^2 + K_C^2)}{2m_t} = 79.97 \text{ GeV}$$

$$\left(\frac{4g_s}{\alpha^2} \right) \frac{B}{A} \frac{\hbar^2 (K_{Br}^2 + K_{Cr}^2)}{2m_t} = 79.97 \text{ GeV}$$

$$\frac{B}{A} \frac{\hbar^2 (K_{Ds}^2 + K_{Dn}^2)}{2m_t} \cdot g_s = 79.97 \text{ GeV}$$

$$\left(\frac{4g_s}{\alpha^2} \right) \frac{B}{A} \frac{\hbar^2 (K_{Dsr}^2 + K_{Dnr}^2)}{2m_t} \cdot g_s = 79.97 \text{ GeV}$$

$$4\pi \frac{B}{A} \hbar (K_B + K_C) c = 79.67 \text{ GeV}$$

$$\left(\frac{2}{\alpha} \right) 4\pi \frac{B}{A} \hbar (K_{Br} + K_{Cr}) c = 79.67 \text{ GeV}$$

$$4\pi \frac{B}{A} \hbar (K_{Ds} + K_{Dn}) c \cdot g_s = 79.67 \text{ GeV}$$

$$\left(\frac{2}{\alpha} \right) 4\pi \frac{B}{A} \hbar (K_{Dsr} + K_{Dnr}) c \cdot g_s = 79.67 \text{ GeV} (80.385 \pm .01)$$

The Z boson is associated with energy

$$e \frac{\hbar^2 (K_B^2 + K_C^2)}{2m_t} = 91.37 \text{ GeV}$$

$$\left(\frac{4g_s}{\alpha^2} \right) e \frac{\hbar^2 (K_{Br}^2 + K_{Cr}^2)}{2m_t} = 91.37 \text{ GeV}$$

$$e \frac{\hbar^2 (K_{Ds}^2 + K_{Dn}^2)}{2m_t} \cdot g_s = 91.37 \text{ GeV}$$

$$\left(\frac{4g_s}{\alpha^2} \right) e \frac{\hbar^2 (K_{Dsr}^2 + K_{Dnr}^2)}{2m_t} \cdot g_s = 91.37 \text{ GeV}$$

$$4\pi \cdot e \cdot \hbar (K_B + K_C) c = 91.03 \text{ GeV}$$

$$\frac{2}{\alpha} 4\pi \cdot e \cdot \hbar (K_{Dsr} + K_{Dnr}) c \cdot g_s = 91.03 \text{ GeV}$$

$$4\pi \cdot e \cdot \hbar (K_B + K_C) c = 91.03 \text{ GeV}$$

$$\frac{2}{\alpha} 4\pi \cdot e \cdot \hbar (K_{Br} + K_{Cr}) c = 91.03 \text{ GeV} (91.1876 \pm .0021)$$

e is natural log base 2.7182818284590

The Lepton tau particle (m_τ) is associated with energy

$$\frac{2}{3} \hbar c (K_{Ds} + K_{Dn}) = \frac{2}{3} \hbar c (K_B + K_C) g_s$$

$$\frac{2}{\alpha} \frac{2}{3} \hbar c (K_{Dsr} + K_{Dnr}) = \frac{2}{\alpha} \frac{2}{3} \hbar c (K_{Br} + K_{Cr}) g_s \\ = 1.777 \text{ GeV} (1.77684(17))$$

The Lepton muon particle (m_μ) is associated with energy:

$$\frac{1}{3} \frac{m_e}{m_t} \frac{\hbar^2}{2m_t} (K_{Ds}^2 + K_{Dn}^2) g_s \\ = \frac{1}{3} \frac{m_e}{m_t} \frac{\hbar^2}{2m_t} (K_B^2 + K_C^2) \\ \left(\frac{4g_s}{\alpha^2} \right) \frac{1}{3} \frac{m_e}{m_t} \frac{\hbar^2}{2m_t} (K_{Dsr}^2 + K_{Dnr}^2) g_s \\ = \left(\frac{4g_s}{\alpha^2} \right) \frac{1}{3} \frac{m_e}{m_t} \frac{\hbar^2}{2m_t} (K_{Br}^2 + K_{Cr}^2) \\ = .1018 \text{ GeV} (.1056583668(38))$$

The Lepton electron particle (m_e) is associated with

energy:

$$\begin{aligned}
 \frac{1}{6}(g_d - 1)\hbar(K_B + K_C)c &= \frac{1}{6}(g_d - 1)\hbar(K_{Dn} + K_{Ds})\frac{1}{g_s}c \\
 \frac{2}{\alpha}\frac{1}{6}(g_d - 1)\hbar(K_{Br} + K_{Cr})c &= \frac{2}{\alpha}\frac{1}{6}(g_d - 1)\hbar(K_{Dnr} + K_{Dsr}) \\
 \frac{1}{6}\frac{\alpha}{2\pi}\hbar(K_B + K_C)c &= \frac{1}{6}\frac{\alpha}{2\pi}\hbar(K_{Dn} + K_{Ds})\frac{1}{g_s}c\frac{1}{g_s}c \\
 \frac{2}{\alpha}\frac{1}{6}\frac{\alpha}{2\pi}\hbar(K_{Br} + K_{Cr})c &= \frac{2}{\alpha}\frac{1}{6}\frac{\alpha}{2\pi}\hbar(K_{Dnr} + K_{Dsr})\frac{1}{g_s}c \\
 \frac{1}{6}\frac{e^2}{2\pi}(K_B + K_C) &= \frac{1}{6}\frac{e^2}{2\pi}(K_{Dn} + K_{Ds})\frac{1}{g_s} \\
 \frac{2}{\alpha}\frac{1}{6}\frac{e^2}{2\pi}(K_{Br} + K_{Cr}) &= \frac{2}{\alpha}\frac{1}{6}\frac{e^2}{2\pi}(K_{Dnr} + K_{Dsr})\frac{1}{g_s} \\
 &= 0.510116285 \text{ MeV} \quad (0.510998910)
 \end{aligned}$$

With the Lepton particles (m_τ, m_μ, m_e) maintaining the Koide relationship:

$$\frac{m_\tau + m_\mu + m_e}{(\sqrt{m_\tau} + \sqrt{m_\mu} + \sqrt{m_e})^2} = \frac{\text{chain}}{\text{cavity}} = \frac{2}{3}$$

The Gluon ratio is $60/25 = 2.4 \approx \pi^0/m_t \approx B/A = 2.379761271$.

$$hH_U = \frac{\text{cavity}}{\text{chain}} G_U \frac{m_t^2}{B_p}$$

The above equation provides a mechanism explaining the CERN (July 4, 2012) observed Higgs particle at 126.5 GeV as well as the astrophysical Fermi ~ 130 GeV [127]. The astrophysical ~ 130 GeV energy is sourced to a Trisine Condition 1.2 nucleosynthetic event with a fundamental G_U gravity component and generally scales with T_r .

$$g_s \frac{3}{4} \cos(\theta) G_U m_t^2 \frac{1}{\text{proton radius}} = 125.27 \text{ GeV}$$

$$g_s \frac{3}{4} \cos(\theta) G_U m_t^2 \frac{2 \sin(\theta)}{B_p} = 125.27 \text{ GeV}$$

$$g_s \frac{3}{2} \sin(\theta) \cos(\theta) G_U m_t^2 \frac{1}{B_p} = 125.27 \text{ GeV}$$

$$g_s \frac{3}{2} \frac{B}{A} \frac{1}{1 + \left(\frac{B}{A}\right)^2} G_U m_t^2 \frac{1}{B_p} = 125.27 \text{ GeV}$$

and with suitable dimensional conversions:

$$\frac{\sqrt{3}\pi^3}{16} g_s \left(\frac{B}{A}\right)^2 \frac{1}{1 + \left(\frac{B}{A}\right)^2} \frac{\hbar^4}{m_t^3 c^2 B_p^4} = 125.27 \text{ GeV}$$

falling within the measured range

$$125.36 \pm 0.37 \text{ (statistical uncertainty)}$$

$$\pm 0.18 \text{ (systematic uncertainty)}$$

$$125.36 \pm 0.41 \text{ GeV} \text{ [149]}$$

remembering that :

$$\begin{aligned}
 m_t &= \hbar^{2/3} \left(\frac{H_U}{G_U}\right)^{1/3} c^{-1/3} \cos(\theta) \\
 &= \hbar^{2/3} \left(\frac{H_{Ur}}{G_{Ur}}\right)^{1/3} c^{-1/3} \cos(\theta)
 \end{aligned}$$

$$\theta = \tan^{-1}\left(\frac{A}{B}\right) = \tan^{-1}\left(\frac{A_r}{B_r}\right)$$

Other energy levels are:

$$\hbar K_B c = 0.932 \text{ GeV}$$

$$\frac{2}{\alpha} \hbar K_{Br} c = 0.932 \text{ GeV}$$

$$\hbar K_{Dn} c = 1.020 \text{ GeV}$$

$$\frac{2}{\alpha} \hbar K_{Dnr} c = 1.020 \text{ GeV}$$

$$\hbar K_P c = 1.076 \text{ GeV}$$

$$\frac{2}{\alpha} \hbar K_{Pr} c = 1.076 \text{ GeV}$$

$$\hbar K_{Ds} c = 1.645 \text{ GeV}$$

$$\frac{2}{\alpha} \hbar K_{Dsr} c = 1.645 \text{ GeV}$$

	$\hbar K_C c = 1.707 \text{ GeV}$ $\frac{2}{\alpha} \hbar K_{Cr} c = 1.707 \text{ GeV}$ $\hbar (K_{Dn} + K_B) c = 1.953 \text{ GeV}$ $\frac{2}{\alpha} \hbar (K_{Dnr} + K_{Br}) c = 1.953 \text{ GeV}$ $\hbar (K_{Dn} + K_P) c = 2.097 \text{ GeV}$ $\frac{2}{\alpha} \hbar (K_{Dnr} + K_{Pr}) c = 2.097 \text{ GeV}$ $\hbar (K_{Ds} + K_B) c = 2.577 \text{ GeV}$ $\frac{2}{\alpha} \hbar (K_{Dsr} + K_{Br}) c = 2.577 \text{ GeV}$ $\hbar (K_B + K_C) c = 2.639 \text{ GeV}$ $\frac{2}{\alpha} \hbar (K_{Br} + K_{Cr}) c = 2.639 \text{ GeV}$ $\hbar (K_{Dn} + K_{Ds}) c = 2.665 \text{ GeV}$ $\frac{2}{\alpha} \hbar (K_{Dnr} + K_{Dsr}) c = 2.665 \text{ GeV}$ $\hbar (K_{Ds} + K_P) c = 2.721 \text{ GeV}$ $\frac{2}{\alpha} \hbar (K_{Dsr} + K_{Pr}) c = 2.721 \text{ GeV}$ $\hbar (K_{Dn} + K_C) c = 2.728 \text{ GeV}$ $\frac{2}{\alpha} \hbar (K_{Dnr} + K_{Cr}) c = 2.728 \text{ GeV}$ $\hbar (K_{Dn} + K_C) c = 2.728 \text{ GeV}$ $\frac{2}{\alpha} \hbar (K_{Dnr} + K_{Cr}) c = 2.728 \text{ GeV}$ $\hbar K_A c = 4.436 \text{ GeV}$ verified [147] $\frac{2}{\alpha} \hbar K_{Ar} c = 4.436 \text{ GeV}$ verified [147]				
1.3	z_R	8.14E+39	z_R	8.14E+39	unitless
	z_B	2.01E+13	z_B	2.01E+13	unitless
	T_a	6.53E+11	T_a	6.53E+11	$^{\circ}\text{K}$
	T_b	5.48E+13	T_{br}	5.45E+13	$^{\circ}\text{K}$
	T_c	3.28E+11	T_{cr}	3.25E+11	$^{\circ}\text{K}$
	T_d	5.98E+12	T_{dr}	5.97E+12	$^{\circ}\text{K}$
	T_i	6.54E+11	T_{ir}	6.51E+11	$^{\circ}\text{K}$
	T_j	1.03E+14	T_{jr}	1.01E+14	$^{\circ}\text{K}$
	ϵ_x	9.96E-01	ϵ_{xr}	1.00E+00	unitless
	ϵ_y	9.96E-01	ϵ_{yr}	1.00E+00	unitless

ϵ_z	1.22E-02	ϵ_{zr}	1.23E-02	unitless
ϵ	1.19E-02	ϵ_r	1.20E-02	unitless
k_{mx}	1.00E+00	k_{mr}	1.00E+00	unitless
k_{my}	7.50E-01	k_{myr}	7.50E-01	unitless
k_{mz}	3.60E+00	k_{mzr}	3.62E+00	unitless
k_m	3.34E+00	k_{mr}	3.36E+00	unitless
ρ_U	5.19E+10	ρ_{Ur}	5.11E+10	g/cm^3
B	1.10E-12	B_r	1.10E-12	cm
$cavity$	1.93E-36	$cavity_r$	1.96E-36	cm^3
R_U	2.76E-12	R_{Ur}	2.80E-12	cm
V_U	8.80E-35	V_{Ur}	9.18E-35	cm^3
V_{Utotal}	5.83E+45	$V_{Urtotal}$	9.18E-35	cm^3
M_U	4.56E-24	M_{Ur}	4.69E-24	G
M_v	6.67E-15	M_{vr}	6.67E-15	G
M_{UTotal}	3.03E+56	$M_{UTotalr}$	3.03E+56	G
$time_{\pm}$	7.32E-23	$time_{r\pm}$	7.39E-23	sec
$1/time_{\pm}$	1.37E+22	$1/time_{r\pm}$	1.35E+22	$/\text{sec}$
H_U	1.88E+22	H_{Ur}	1.86E+22	$/\text{sec}$
G_U/G	8.14E+39	G_{Ur}/G	8.03E+39	unitless
$sherd$	6.63E+79	$sherd_r$	6.45E+79	unitless
Age_U	5.31E-23	Age_{Ur}	5.39E-23	sec
Age_{UG}	4.79E-03	Age_{UGr}	4.83E-03	sec
Age_{UGv}	1.25E-07	Age_{UGvr}	1.27E-07	sec
$BCST$	3.77E+03	$BCST$	3.77E+03	sec

This temperature condition represents the undefined but potentially high energy barrier luminal state where $v_{dx} = v_{dxr} = c$ and $v_{ex} = v_{exr} > c$, $T_b = T_{br}$, $T_c = T_{cr}$, $T_d = T_{dr}$, $T_i = T_{ir} = T_a$, $T_j = T_{jr}$ and trisine length

$$B = 4\pi \text{ nuclear radius}$$

which defines a condition for the size of the proton as it ‘freezes’ out of early expanding universe nucleosynthesis state. Further, it is thought that dark matter in the form of colligative hydrogen Bose Einstein Condensate (BEC) was formed at this epoch

according to accepted criteria.

$$T \sim \frac{\hbar^2 \left(\frac{\rho}{m} \right)^{\frac{2}{3}}}{k_b m}$$

and possibly in ratios $\frac{T_1}{T_2}$ that dictate the Dark Matter to Dark Energy ratio that exists from this epoch to the present with Dark Matter loosing ~4% to gravitationally collapsed luminous matter.

$$\frac{1 - (\Omega_{\Lambda_U})}{\Omega_{\Lambda_U}} = \frac{1 - .72315}{.72315} = \frac{.27685}{.72315} = .38284$$

The ratio $\frac{T_b}{T_{cr}}$ nearly fits this Bose Einstein Condensate generation criterion.

$$\frac{T_b}{T_{cr}} = \frac{m_p \left(\frac{\Omega_{\Lambda_U}}{m_t} \right)^{\frac{2}{3}}}{m_t \left(\frac{1 - \Omega_{\Lambda_U}}{m_p} \right)^{\frac{2}{3}}} = 211$$

This compares to favorably with

$$\frac{T_b}{T_{cr}} = \frac{5.49E13}{3.28E11} = 167$$

for this epoch.

This trisine condition corresponds to the initial bent condition in the observed cosmic ray spectrum as presented in Figure 4.33.1.

Also a universe radius identity exists

$$R_U = R_{Ur} = 2.8E-12 \text{ cm}$$

Also a gravitational identity exists

$$G_U = G_{Ur} = 5.4E32 \text{ cm}^3 \text{ sec}^{-2} \text{ g}^{-1}$$

$$G_U = \frac{R_U c^2}{M_U} = \frac{R_U^3 R_U^2}{\sqrt{3} M_U} = \frac{\sqrt{3}}{4\pi} \frac{\text{cavity}_U R_U^2}{m_t}$$

$$G_{Ur} = \frac{R_{Ur} c^2}{M_{Ur}} = \frac{R_{Ur}^3 R_{Ur}^2}{\sqrt{3} M_{Ur}} = \frac{\sqrt{3}}{4\pi} \frac{\text{cavity}_r R_{Ur}^2}{m_t}$$

Also a universe density identity exists

$$\rho_U = \rho_{Ur} = 5.1E10 \text{ g cm}^{-3}$$

$$\rho_U = \frac{M_U}{V_U} = \frac{m_t}{\text{cavity}}$$

$$\rho_{Ur} = \frac{M_{Ur}}{V_{Ur}} = \frac{m_t}{\text{cavity}_r}$$

$$Age_{UG} = Age_{UGr}$$

$$Age_{UGv} = Age_{UGvr}$$

$$time_{\pm} = time_{r\pm}$$

$$B = B_r \quad A = A_r$$

$$\text{section} = \text{section}_r \quad \text{cavity} = \text{cavity}_r$$

1.3a	z_R	9.72E+34	z_R	9.72E+34	unitless
	z_B	4.60E+11	z_B	4.60E+11	unitless
	T_a	6.53E+11	T_a	6.53E+11	$^o K$
	T_b	1.25E+12	T_{br}	2.39E+15	$^o K$
	T_c	1.71E+08	T_{cr}	6.22E+14	$^o K$
	T_d	9.04E+11	T_{dr}	3.95E+13	$^o K$
	T_i	1.50E+10	T_{ir}	2.85E+13	$^o K$
	T_j	2.80E+07	T_{jr}	3.70E+20	$^o K$
	ε_x	4.36E+01	ε_{xr}	2.29E-02	unitless
	ε_y	4.36E+01	ε_{yr}	2.29E-02	unitless
	ε_z	5.34E-01	ε_{zr}	2.80E-04	unitless
	ε	5.22E-01	ε_r	2.74E-04	unitless
	k_{mx}	4.37E+01	k_{mr}	2.29E-02	unitless
	k_{my}	3.28E+01	k_{myr}	1.71E-02	unitless
	k_{mz}	1.58E+02	k_{mzr}	8.27E-02	unitless
	k_m	1.46E+02	k_{mr}	7.67E-02	unitless
	ρ_U	6.19E+05	ρ_{Ur}	4.28E+15	g/cm^3
	B	4.81E-11	B_r	2.52E-14	cm
	cavity	1.62E-31	cavity_r	2.34E-41	cm^3
	R_U	2.31E-07	R_{Ur}	3.34E-17	cm
	V_U	5.17E-20	V_{Ur}	1.56E-49	cm^3
	V_{Utotal}	4.89E+50	$V_{Urtotal}$	1.56E-49	cm^3
	M_U	3.20E-14	M_{Ur}	6.69E-34	g

M_v	1.07E-06	M_{vr}	1.07E-06	g	
$M_{U\text{Total}}$	3.03E+56	$M_{U\text{Total}r}$	3.03E+56	g	
$time_{\pm}$	1.40E-19	$time_{r\pm}$	3.86E-26	sec	
$1/time_{\pm}$	7.14E+18	$1/time_{r\pm}$	2.59E+25	$/sec$	
H_u	2.25E+17	H_{Ur}	1.55E+27	$/sec$	
G_u/G	9.72E+34	G_{Ur}/G	6.73E+44	$unitless$	
$sherd$	9.45E+69	$sherd_r$	4.52E+89	$unitless$	
Age_u	4.45E-18	Age_{Ur}	6.43E-28	sec	
Age_{UG}	1.39E+00	Age_{UGr}	1.67E-05	sec	
Age_{UGv}	2.40E-04	Age_{UGvr}	6.61E-11	sec	
$BCST$	1.65E+05	$BCST$	1.65E+05	sec	
This temperature condition defined by					
$B = \frac{m_e}{m_t} Bohr\ radius = \frac{m_e}{m_t} \frac{\hbar}{\alpha m_e c} = \frac{\hbar}{\alpha m_t c}$					
1.4	z_R	1.39E+34	z_R	1.39E+34	$unitless$
1.5	z_B	2.41E+11	z_B	2.41E+11	$unitless$
	T_a	6.53E+11	T_a	6.53E+11	$^{\circ}K$
	T_b	6.55E+11	T_{br}	4.56E+15	$^{\circ}K$
	T_c	4.69E+07	T_{cr}	2.27E+15	$^{\circ}K$
	T_d	6.54E+11	T_{dr}	5.45E+13	$^{\circ}K$
	T_i	7.83E+09	T_{ir}	5.45E+13	$^{\circ}K$
	T_j	2.10E+06	T_{jr}	4.93E+21	$^{\circ}K$
	ϵ_x	8.32E+01	ϵ_{xr}	1.20E-02	$unitless$
	ϵ_y	8.32E+01	ϵ_{yr}	1.20E-02	$unitless$
	ϵ_z	1.02E+00	ϵ_{zr}	1.47E-04	$unitless$
	ϵ	9.96E-01	ϵ_r	1.43E-04	$unitless$
	k_{mx}	8.36E+01	k_{mr}	1.20E-02	$unitless$
	k_{my}	6.27E+01	k_{myr}	8.97E-03	$unitless$
	k_{mz}	3.01E+02	k_{mzr}	4.33E-02	$unitless$
	k_m	2.80E+02	k_{mr}	4.02E-02	$unitless$
	ρ_u	8.88E+04	ρ_{Ur}	2.99E+16	g/cm^3
	B	9.19E-11	B_r	1.32E-14	cm
	$cavity$	1.13E-30	$cavity_r$	3.36E-42	cm^3

R_u	1.61E-06	R_{Ur}	4.79E-18	cm
V_u	1.75E-17	V_{Ur}	4.60E-52	cm^3
$V_{U\text{total}}$	3.41E+51	$V_{U\text{total}r}$	4.60E-52	cm^3
M_u	1.56E-12	M_{Ur}	1.38E-35	g
M_v	2.72E-05	M_{vr}	2.72E-05	g
$M_{U\text{Total}}$	3.03E+56	$M_{U\text{Total}r}$	3.03E+56	g
$time_{\pm}$	5.11E-19	$time_{r\pm}$	1.06E-26	sec
$1/time_{\pm}$	1.96E+18	$1/time_{r\pm}$	9.46E+25	$/sec$
H_u	3.22E+16	H_{Ur}	1.08E+28	$/sec$
G_u/G	1.39E+34	G_{Ur}/G	4.69E+45	$unitless$
$sherd$	1.94E+68	$sherd_r$	2.20E+91	$unitless$
Age_u	3.10E-17	Age_{Ur}	9.22E-29	sec
Age_{UG}	3.66E+00	Age_{UGr}	6.32E-06	sec
Age_{UGv}	8.77E-04	Age_{UGvr}	1.81E-11	sec
$BCST$	3.14E+05	$BCST$	3.14E+05	sec

This temperature condition represents the undefined but potentially high energy barrier luminal state where $v_e = c$, and trisine length

$$A = \frac{Bohr\ radius}{\alpha} = \frac{\hbar}{m_e c \alpha^2} = \frac{\hbar}{m_e e^2 \alpha}$$

which defines a condition for the size of the electron in its atomic orbital as it freezes out of early expanding universe radiation state. This the time frame discussed by Weinberg as the hydrogen helium formation within the first three minutes[100].

1.5	z_R	1.48E+26	z_R	1.48E+26	$unitless$
	z_B	5.29E+08	z_B	5.29E+08	$unitless$
	T_a	6.53E+11	T_a	6.53E+11	$^{\circ}K$
	T_b	1.44E+09	T_{br}	2.07E+18	$^{\circ}K$
	T_c	2.27E+02	T_{cr}	4.71E+20	$^{\circ}K$
	T_d	3.07E+10	T_{dr}	1.16E+15	$^{\circ}K$
	T_i	1.72E+07	T_{ir}	2.48E+16	$^{\circ}K$
	T_j	4.90E-05	T_{jr}	2.12E+32	$^{\circ}K$
	ϵ_x	3.79E+04	ϵ_{xr}	2.63E-05	$unitless$
	ϵ_y	3.79E+04	ϵ_{yr}	2.63E-05	$unitless$

	ε_z	4.65E+02	ε_{zr}	3.22E-07	unitless
	ε	4.54E+02	ε_r	3.15E-07	unitless
	k_{mx}	3.80E+04	k_{mr}	2.63E-05	unitless
	k_{my}	2.85E+04	k_{myr}	1.97E-05	unitless
	k_{mz}	1.37E+05	k_{mzr}	9.50E-05	unitless
	k_m	1.27E+05	k_{mr}	8.82E-05	unitless
	ρ_U	9.41E-04	ρ_{Ur}	2.82E+24	g/cm^3
	B	4.18E-08	B_r	2.90E-17	cm
	$cavity$	1.07E-22	$cavity_r$	3.56E-50	cm^3
	R_U	1.52E+02	R_{Ur}	5.08E-26	cm
	V_U	1.47E+07	V_{Ur}	5.48E-76	cm^3
	V_{Utotal}	3.21E+59	$V_{Utotalr}$	5.48E-76	cm^3
	M_U	1.39E+04	M_{Ur}	1.55E-51	g
	M_v	5.32E+08	M_{vr}	5.32E+08	g
	M_{Utotal}	3.03E+56	$M_{Utotalr}$	3.03E+56	g
	$time_{\pm}$	1.06E-13	$time_{r\pm}$	5.10E-32	sec
	$1/time_{\pm}$	9.44E+12	$1/time_{r\pm}$	1.96E+31	$/sec$
	H_U	3.42E+08	H_{Ur}	1.02E+36	$/sec$
	G_U/G	1.48E+26	G_{Ur}/G	4.42E+53	unitless
	$sherd$	2.18E+52	$sherd_r$	1.96E+107	unitless
	Age_U	2.93E-09	Age_{Ur}	9.78E-37	sec
	Age_{UG}	3.56E+04	Age_{UGr}	6.50E-10	sec
	Age_{UGv}	1.82E+02	Age_{UGvr}	8.74E-17	sec
	$BCST$	1.43E+08	$BCST$	1.43E+08	sec
The critical temperature of a generalized superconducting medium in which the Cooper Pair velocity equates to the earth orbital velocity of 7.91E05 cm/sec which would express gravitational effects to the extent that it would be apparently weightless in earth's gravitational field (See equations 2.9.1 – 2.9.4 and Table 2.9.1). Also, $k_b T_c = 1.97E-02$ eV which is close to the neutrino mass.					
1.6	z_R	3.89E+25	z_R	3.89E+25	unitless
	z_B	3.39E+08	z_B	3.39E+08	unitless
	T_a	6.53E+11	T_a	6.53E+11	oK
	T_b	9.22E+08	T_{br}	3.24E+18	oK

	T_c	9.30E+01	T_{cr}	1.15E+21	oK
	T_d	4.84E+10	T_{dr}	8.80E+12	oK
	T_i	1.10E+07	T_{ir}	3.87E+16	oK
	T_j	8.26E-06	T_{jr}	1.25E+33	oK
	ε_x	5.91E+04	ε_{xr}	1.68E-05	unitless
	ε_y	5.91E+04	ε_{yr}	1.68E-05	unitless
	ε_z	7.25E+02	ε_{zr}	2.07E-07	unitless
	ε	7.08E+02	ε_r	2.02E-07	unitless
	k_{mx}	5.94E+04	k_{mr}	1.68E-05	unitless
	k_{my}	4.45E+04	k_{myr}	1.26E-05	unitless
	k_{mz}	2.14E+05	k_{mzr}	6.09E-05	unitless
	k_m	1.99E+05	k_{mr}	5.65E-05	unitless
	ρ_U	2.48E-04	ρ_{Ur}	1.07E+25	g/cm^3
	B	6.53E-08	B_r	1.86E-17	cm
	$cavity$	4.05E-22	$cavity_r$	9.36E-51	cm^3
	R_U	5.78E+02	R_{Ur}	1.34E-26	cm
	V_U	8.08E+08	V_{Ur}	9.99E-78	cm^3
	V_{Utotal}	1.22E+60	$V_{Utotalr}$	9.99E-78	cm^3
	M_U	2.00E+05	M_{Ur}	1.07E-52	g
	M_v	4.93E+09	M_{vr}	4.93E+09	g
	M_{Utotal}	3.03E+56	$M_{Utotalr}$	3.03E+56	g
	$time_{\pm}$	2.58E-13	$time_{r\pm}$	2.09E-32	sec
	$1/time_{\pm}$	3.88E+12	$1/time_{r\pm}$	4.78E+31	$/sec$
	H_U	8.99E+07	H_{Ur}	3.89E+36	$/sec$
	G_U/G	3.89E+25	G_{Ur}/G	1.68E+54	unitless
	$sherd$	1.51E+51	$sherd_r$	2.83E+108	unitless
	Age_U	1.11E-08	Age_{Ur}	2.57E-37	sec
	Age_{UG}	6.94E+04	Age_{UGr}	3.34E-10	sec
	Age_{UGv}	4.42E+02	Age_{UGvr}	3.59E-17	sec
	$BCST$	2.23E+08	$BCST$	2.23E+08	sec
The critical temperature (T_c) of the $YBa_2Cu_3O_{7-x}$ superconductor as discovered by Paul Ching-Wu Chu, The University of Houston and which was the basis for an apparent gravitational shielding effect of .05% as observed by Podkletnov and Nieminen(see Table 2.9.1) based herein on the Cooper pair velocities at					

	this critical temperature approaching the earth orbital velocity and thereby imparting proportional apparent gravity effects on the gross superconducting $YBa_2Cu_3O_{7-x}$ material. Also, $k_b T_c = 8.01E-03$ eV which is close to the neutrino mass.						Age_U	6.28E-08	Age_{Ur}	4.56E-38	<i>sec</i>
	Age_{UG}	1.65E+05	Age_{UGr}	1.40E-10	<i>sec</i>		Age_{UGv}	1.40E+03	Age_{UGvr}	1.13E-17	<i>sec</i>
	$BCST$	3.97E+08	$BCST$	3.97E+08	<i>sec</i>		The critical temperature of an anticipated superconductor medium, in which the energy density ($m_t v_{dx} c / cavity$) or 32.4 MJ/L is equivalent to the combustion energy of gasoline. Also, $k_b T_c = 2.53E-03$ eV which is close to the neutrino mass.				
	T_c	2.93E+01	T_{cr}	3.63E+21	oK		z_R	1.25E+24	z_R	1.25E+24	<i>unitless</i>
	T_d	1.84E+10	T_{dr}	1.94E+15	oK		z_B	1.08E+08	z_B	1.08E+08	<i>unitless</i>
	T_i	6.19E+06	T_{ir}	6.89E+16	oK		T_a	6.53E+11	T_a	6.53E+11	oK
	T_j	8.22E-07	T_{jr}	1.26E+34	oK		T_b	2.93E+08	T_{br}	1.02E+19	oK
	ε_x	1.05E+05	ε_{xr}	9.46E-06	<i>unitless</i>		T_c	9.40E+00	T_{cr}	1.13E+22	oK
	ε_y	1.05E+05	ε_{yr}	9.46E-06	<i>unitless</i>		T_d	2.73E+10	T_{dr}	1.56E+13	oK
	ε_z	1.29E+03	ε_{zr}	1.16E-07	<i>unitless</i>		T_i	3.50E+06	T_{ir}	1.22E+17	oK
	ε	1.26E+03	ε_r	1.13E-07	<i>unitless</i>		T_j	8.44E-08	T_{jr}	1.23E+35	oK
	k_{mx}	1.06E+05	k_{mr}	9.46E-06	<i>unitless</i>		ε_x	1.86E+05	ε_{xr}	5.35E-06	<i>unitless</i>
	k_{my}	7.93E+04	k_{myr}	7.09E-06	<i>unitless</i>		ε_y	1.86E+05	ε_{yr}	5.35E-06	<i>unitless</i>
	k_{mz}	3.81E+05	k_{mzr}	3.42E-05	<i>unitless</i>		ε_z	2.28E+03	ε_{zr}	6.57E-08	<i>unitless</i>
	k_m	3.54E+05	k_{mr}	3.18E-05	<i>unitless</i>		ε	2.23E+03	ε_r	6.41E-08	<i>unitless</i>
	ρ_U	4.39E-05	ρ_{Ur}	6.05E+25	g/cm^3		k_{mx}	1.87E+05	k_{mr}	5.35E-06	<i>unitless</i>
	B	1.16E-07	B_r	1.04E-17	cm		k_{my}	1.40E+05	k_{myr}	4.02E-06	<i>unitless</i>
	$cavity$	2.29E-21	$cavity_r$	1.66E-51	cm^3		k_{mz}	6.72E+05	k_{mzr}	1.94E-05	<i>unitless</i>
	R_U	3.26E+03	R_{Ur}	2.37E-27	cm		k_m	6.25E+05	k_{mr}	1.80E-05	<i>unitless</i>
	V_U	1.46E+11	V_{Ur}	5.55E-80	cm^3		ρ_U	7.96E-06	ρ_{Ur}	3.33E+26	g/cm^3
	V_{Utotal}	6.90E+60	$V_{Utotalr}$	5.55E-80	cm^3		B	2.05E-07	B_r	5.91E-18	cm
	M_U	6.38E+06	M_{Ur}	3.36E-54	g		$cavity$	1.26E-20	$cavity_r$	3.01E-52	cm^3
	M_v	8.82E+10	M_{vr}	8.82E+10	g		R_U	1.80E+04	R_{Ur}	4.29E-28	cm
	M_{UTotal}	3.03E+56	$M_{UTotalr}$	3.03E+56	g		V_U	2.44E+13	V_{Ur}	3.31E-82	cm^3
	$time_{\pm}$	8.18E-13	$time_{r\pm}$	6.60E-33	<i>sec</i>		V_{Utotal}	3.80E+61	$V_{Utotalr}$	3.31E-82	cm^3
	$1/time_{\pm}$	1.22E+12	$1/time_{r\pm}$	1.51E+32	$/sec$		M_U	1.94E+08	M_{Ur}	1.10E-55	G
	H_U	1.59E+07	H_{Ur}	2.19E+37	$/sec$		M_v	1.52E+12	M_{vr}	1.52E+12	G
	G_U/G	6.88E+24	G_{Ur}/G	9.50E+54	<i>unitless</i>		M_{UTotal}	3.03E+56	$M_{UTotalr}$	3.03E+56	G
	$sherd$	4.74E+49	$sherd_r$	9.02E+109	<i>unitless</i>		$time_{\pm}$	2.55E-12	$time_{r\pm}$	2.12E-33	<i>sec</i>

	$1/time_{\pm}$	3.92E+11	$1/time_{r\pm}$	4.72E+32	/sec		M_v	2.08E+19	M_{vr}	2.08E+19	g
	H_U	2.89E+06	H_{Ur}	1.21E+38	/sec		$M_{U\text{Total}}$	3.03E+56	$M_{U\text{Total}r}$	3.03E+56	g
	G_U/G	1.25E+24	G_{Ur}/G	5.23E+55	unitless		$time_{\pm}$	1.83E-09	$time_{r\pm}$	2.96E-36	sec
	$sherd$	1.56E+48	$sherd_r$	2.74E+111	unitless		$1/time_{\pm}$	5.47E+08	$1/time_{r\pm}$	3.38E+35	/sec
	Age_U	3.46E-07	Age_{Ur}	8.27E-39	sec		H_U	1.51E+02	H_{Ur}	2.32E+42	/sec
	Age_{UG}	3.87E+05	Age_{UGr}	5.98E-11	sec		G_U/G	6.53E+19	G_{Ur}/G	1.00E+60	unitless
	Age_{UGv}	4.38E+03	Age_{UGvr}	3.63E-18	sec		$sherd$	4.26E+39	$sherd_r$	1.00E+120	unitless
	$BCST$	7.01E+08	$BCST$	7.01E+08	sec		Age_U	6.63E-03	Age_{Ur}	4.32E-43	sec
	The critical temperature of typical type I superconductor represented by niobium. This is the condition for the superconductor material in the Gravity Probe B relativity earth satellite experiment[94].						Age_{UG}	5.36E+07	Age_{UGr}	4.32E-13	sec
1.9	z_R	6.53E+19	z_R	6.53E+19	unitless		Age_{UGv}	3.13E+06	Age_{UGvr}	5.07E-21	sec
	z_B	4.03E+06	z_B	4.03E+06	unitless		$BCST$	1.88E+10	$BCST$	1.88E+10	sec
	T_a	6.53E+11	T_a	6.53E+11	$^{\circ}K$		The critical temperature of an anticipated superconductor medium, in which the energy density $(m_t c^2 / cavity)$ or 56 MeV/cavity is equivalent to the combustion energy of gasoline 37.4 MJ/L.				
	T_b	1.10E+07	T_{br}	2.72E+20	$^{\circ}K$		z_R	2.64E+12	z_R	2.64E+12	unitless
	T_c	1.31E-02	T_{cr}	8.11E+24	$^{\circ}K$		z_B	1.38E+04	z_B	1.38E+04	unitless
	T_d	2.68E+09	T_{dr}	1.33E+16	$^{\circ}K$		T_a	6.53E+11	T_a	6.53E+11	$^{\circ}K$
	T_i	1.31E+05	T_{ir}	3.25E+18	$^{\circ}K$		T_b	3.77E+04	T_{br}	7.93E+22	$^{\circ}K$
	T_j	1.65E-13	T_{jr}	6.29E+40	$^{\circ}K$		T_c	1.55E-07	T_{cr}	6.88E+29	$^{\circ}K$
	ϵ_x	4.97E+06	ϵ_{xr}	2.00E-07	unitless		T_d	1.57E+08	T_{dr}	2.28E+17	$^{\circ}K$
	ϵ_y	4.97E+06	ϵ_{yr}	2.00E-07	unitless		T_i	4.50E+02	T_{ir}	9.48E+20	$^{\circ}K$
	ϵ_z	6.10E+04	ϵ_{zr}	2.46E-09	unitless		T_j	2.29E-23	T_{jr}	4.52E+50	$^{\circ}K$
	ϵ	5.96E+04	ϵ_r	2.40E-09	unitless		ϵ_x	1.45E+09	ϵ_{xr}	6.88E-10	unitless
	k_{mx}	5.00E+06	k_{mr}	2.00E-07	unitless		ϵ_y	1.45E+09	ϵ_{yr}	6.88E-10	unitless
	k_{my}	3.75E+06	k_{myr}	1.50E-07	unitless		ϵ_z	1.78E+07	ϵ_{zr}	8.43E-12	unitless
	k_{mz}	1.80E+07	k_{mzr}	7.24E-07	unitless		ϵ	1.73E+07	ϵ_r	8.23E-12	unitless
	k_m	1.67E+07	k_{mr}	6.72E-07	unitless		k_{mx}	1.45E+09	k_{mr}	6.88E-10	unitless
	ρ_U	4.16E-10	ρ_{Ur}	6.38E+30	g/cm^3		k_{my}	1.09E+09	k_{myr}	5.16E-10	unitless
	B	5.49E-06	B_r	2.21E-19	cm		k_{mz}	5.24E+09	k_{mzr}	2.49E-09	unitless
	$cavity$	2.41E-16	$cavity_r$	1.57E-56	cm^3		k_m	4.86E+09	k_{mr}	2.31E-09	unitless
	R_U	3.44E+08	R_{Ur}	2.24E-32	cm		ρ_U	1.68E-17	ρ_{Ur}	1.57E+38	g/cm^3
	V_U	1.71E+26	V_{Ur}	4.73E-95	cm^3		B	1.60E-03	B_r	7.59E-22	cm
	$V_{U\text{total}}$	7.28E+65	$V_{U\text{total}r}$	4.73E-95	cm^3		$cavity$	5.95E-09	$cavity_r$	6.37E-64	cm^3
	M_U	7.10E+16	M_{Ur}	3.02E-64	g		R_U	8.50E+15	R_{Ur}	9.09E-40	cm

	V_U	2.57E+48	V_{Ur}	3.14E-117	cm^3
	V_{Utotal}	1.80E+73	V_{Utotal}	3.14E-117	cm^3
	M_U	4.33E+31	M_{Ur}	4.95E-79	G
	M_v	4.35E+31	M_{vr}	4.35E+31	g
	M_{UTotal}	3.03E+56	$M_{UTotalr}$	3.03E+56	g
	$time_{\pm}$	1.55E-04	$time_{r\pm}$	3.49E-41	sec
	$1/time_{\pm}$	6.46E+03	$1/time_{r\pm}$	2.87E+40	$/sec$
	H_U	6.11E-06	H_{Ur}	5.71E+49	$/sec$
	G_U/G	2.64E+12	G_{Ur}/G	2.47E+67	<i>unitless</i>
	$sherd$	6.99E+24	$sherd_r$	6.11E+134	<i>unitless</i>
	Age_U	1.64E+05	Age_{Ur}	1.75E-50	sec
	Age_{UG}	2.66E+11	Age_{UGr}	8.70E-17	sec
	Age_{UGv}	1.88E+11	Age_{UGvr}	5.98E-26	sec
	$BCST$	3.82E+13	$BCST$	3.82E+13	sec
The condition underwhich trisine energy density = black body radiation density.					
$\frac{m_t c^2}{cavity} = \frac{G_U M_U^2}{R_U V_U} = \frac{2}{8\pi} \frac{H_U^2}{G_U} = \sigma T^4 \frac{4}{c}$					
This condition defines the neutrino masses.					
The Lepton tau neutrino particle ($m_{\nu\tau}$) is associated with energy					
$\frac{2}{3} \frac{\hbar c}{3} (K_{Ds} + K_{Dn}) = \frac{2}{3} \hbar c (K_B + K_C) g_s$ $= .07389 \text{ eV}$					
The Lepton neutrino muon particle ($m_{\nu\mu}$) is associated with energy:					
$\frac{1}{3} \frac{m_e}{m_t} \frac{\hbar^2}{2m_t} (K_{Ds}^2 + K_{Dn}^2) g_s$ $= \frac{1}{3} \frac{m_e}{m_t} \frac{\hbar^2}{2m_t} (K_B^2 + K_C^2)$ $= 1.743E-13 \text{ eV}$					
The Lepton neutrino electron particle ($m_{\nu e}$) is associated with energy:					

		$\frac{1}{6} (g_d - 1) \hbar (K_B + K_C) c = \frac{1}{6} (g_d - 1) \hbar (K_{Dn} + K_{Ds}) \frac{1}{g_s} c$			
		$\frac{1}{6} \frac{\alpha}{2\pi} \hbar (K_B + K_C) c = \frac{1}{6} \frac{\alpha}{2\pi} \hbar (K_{Dn} + K_{Ds}) \frac{1}{g_s} c \frac{1}{g_s} c$			
		$\frac{1}{6} \frac{e^2}{2\pi} (K_B + K_C) = \frac{1}{6} \frac{e^2}{2\pi} (K_{Dn} + K_{Ds}) \frac{1}{g_s}$			
		$= 2.142E-5 \text{ eV}$			
		It is of special note that the hydrogen absorption 1S – 2S transition frequency at 2.465E15 Hz (121.6 nm) nearly equals the maximum black body frequency of 2.216E15 Hz			
		in this condition. This close identity is reflected in the BCST and Age_{UGv} . In essence, hydrogen-BEC dark matter closely but thermally successfully crosses this most restrictive CMBR barrier.			
1.10	z_R	1.17E+09	z_R	1.17E+09	<i>unitless</i>
	z_B	1.05E+03	z_B	1.05E+03	<i>unitless</i>
	T_a	6.53E+11	T_a	6.53E+11	$^o K$
	T_b	2.87E+03	T_{br}	1.04E+24	$^o K$
	T_c	8.99E-10	T_{cr}	1.19E+32	$^o K$
	T_d	4.33E+07	T_{dr}	8.25E+17	$^o K$
	T_i	3.43E+01	T_{ir}	1.24E+22	$^o K$
	T_j	7.72E-28	T_{jr}	1.34E+55	$^o K$
	ε_x	1.90E+10	ε_{xr}	5.24E-11	<i>unitless</i>
	ε_y	1.90E+10	ε_{yr}	5.24E-11	<i>unitless</i>
	ε_z	2.33E+08	ε_{zr}	6.42E-13	<i>unitless</i>
	ε	2.28E+08	ε_r	6.27E-13	<i>unitless</i>
	k_{mx}	1.91E+10	k_{mr}	5.24E-11	<i>unitless</i>
	k_{my}	1.43E+10	k_{myr}	3.93E-11	<i>unitless</i>
	k_{mz}	6.88E+10	k_{mzr}	1.89E-10	<i>unitless</i>
	k_m	6.39E+10	k_{mr}	1.76E-10	<i>unitless</i>
	ρ_U	7.44E-21	ρ_{Ur}	3.56E+41	g/cm^3
	B	2.10E-02	B_r	5.78E-23	cm
	$cavity$	1.35E-05	$cavity_r$	2.81E-67	cm^3
	R_U	1.92E+19	R_{Ur}	4.02E-43	cm
	V_U	2.98E+58	V_{Ur}	2.71E-127	cm^3

V_{Utotal}	4.06E+76	$V_{Urtotal}$	2.71E-127	cm^3
M_U	2.22E+38	M_{Ur}	9.67E-86	g
M_v	1.70E+37	M_{vr}	1.70E+37	g
M_{UTotal}	3.03E+56	$M_{UTotalr}$	3.03E+56	g
$time_{\pm}$	2.67E-02	$time_{r\pm}$	2.02E-43	sec
$1/time_{\pm}$	3.75E+01	$1/time_{r\pm}$	4.94E+42	$/sec$
H_U	2.70E-09	H_{Ur}	1.29E+53	$/sec$
G_u/G	1.17E+09	G_{Ur}/G	5.59E+70	$unitless$
$sherd$	1.37E+18	$sherd_r$	3.13E+141	$unitless$
Age_U	3.70E+08	Age_{Ur}	7.73E-54	sec
Age_{UG}	1.27E+13	Age_{UGr}	1.83E-18	sec
Age_{UGv}	1.22E+13	Age_{UGvr}	3.47E-28	sec
$BCST$	1.35E+30	$BCST$	1.35E+30	sec

The extant CMBR temperature at the universe scattering surface observed by the Wilkinson Microwave Anisotropy Probe (WMAP) satellite marked by coulomb energy at the *Bohr radius* $\hbar/(am_e c)$ or

$$T_b = \frac{m_e}{m_t} \frac{e^2}{k_b \text{ Bohr radius}} = \frac{m_e}{m_t} \frac{e^2 a m_e c}{k_b \hbar} = \frac{m_e^2 c^2}{m_t k_b} \alpha^2 = 2,870 \text{ K} \sim 3,000 \text{ K}$$

$$k_b T_b = m_t v_\epsilon^2 = \frac{m_e^2 c^2}{m_t} \alpha^2$$

therefore:

$$m_t^2 v_\epsilon^2 = m_e^2 c^2 \alpha^2$$

This Universe Age of 3.70E08 sec (11.7 years) as computed by:

$$Age_U = \frac{1}{H_U} = \frac{1}{\sqrt{(8\pi/2) G_u \rho_u}}$$

is considerably less than reported universe age (Age_{UGv}) (387,000 years) at last scattering. The reported value [WMAP ref:20] (376,000 years) is achieved in the trisine model by assuming a constant

Newtonian gravity G over the universe age:

$$Age_{UGv} = Age_U \sqrt{\frac{R_U c^2}{G (M_U + M_v)}}$$

$$= 1.22E13 \text{ sec (387,000 years)}$$

The trisine model indicates that gravity (G_u) even without radiation mass (M_v) changes with the Universe Age (Age_U) with results easily normalized to a universe incorrectly assumed to have a constant Newtonian gravity (G) with Universe Age (Age_U).

The ratio $T_i/T_b = 34.3/2,870 = .012$ indicates that T_i may be the source of measured millikelvin CMBR anomalies.

1.11	z_R	0.00E+00	z_R	0.00E+00	$unitless$
	z_B	0.00E+00	z_B	0.00E+00	$unitless$
	T_a	6.53E+11	T_a	6.53E+11	$^o K$
	T_b	2.72E+00	T_{br}	1.10E+27	$^o K$
	T_c	8.10E-16	T_{cr}	1.32E+38	$^o K$
	T_d	2.63E+06	T_{dr}	1.62E+17	$^o K$
	T_i	3.25E-02	T_{ir}	1.31E+25	$^o K$
	T_j	6.27E-40	T_{jr}	1.65E+67	$^o K$
	ϵ_x	2.00E+13	ϵ_{xr}	4.97E-14	$unitless$
	ϵ_y	2.00E+13	ϵ_{yr}	4.97E-14	$unitless$
	ϵ_z	2.46E+11	ϵ_{zr}	6.10E-16	$unitless$
	ϵ	2.40E+11	ϵ_r	5.95E-16	$unitless$
	k_{mx}	2.01E+13	k_{mr}	4.97E-14	$unitless$
	k_{my}	1.51E+13	k_{myr}	3.73E-14	$unitless$
	k_{mz}	7.24E+13	k_{mzr}	1.80E-13	$unitless$
	k_m	6.73E+13	k_{mr}	1.67E-13	$unitless$
	ρ_u	6.37E-30	ρ_{ur}	4.16E+50	g/cm^3
	B	2.21E+01	B_r	5.49E-26	cm
	$cavity$	1.57E+04	$cavity_r$	2.41E-76	cm^3
	R_u	2.25E+28	R_{ur}	3.44E-52	cm
	V_u	4.75E+85	V_{ur}	1.70E-154	cm^3
	V_{Utotal}	4.75E+85	$V_{Urtotal}$	1.70E-154	cm^3

M_U	3.03E+56	M_{Ur}	7.08E-104	g
M_v	2.20E+52	M_{vr}	2.20E+52	g
M_{UTotal}	3.03E+56	$M_{UTotalr}$	3.03E+56	g
$time_{\pm}$	2.96E+04	$time_{r\pm}$	1.82E-49	sec
$1/time_{\pm}$	3.38E-05	$1/time_{r\pm}$	5.48E+48	$/sec$
H_U	2.31E-18	H_{Ur}	1.51E+62	$/sec$
G_U/G	1.00E+00	G_{Ur}/G	6.54E+79	$unitless$
$sherd$	1.00E+00	$sherd_r$	4.27E+159	$unitless$
Age_U	4.33E+17	Age_{Ur}	6.62E-63	sec
Age_{UG}	4.33E+17	Age_{UGr}	5.35E-23	sec
Age_{UGv}	4.33E+17	Age_{UGvr}	3.13E-34	sec
$BCST$	3.15E+307	$BCST$	3.15E+307	sec

The background temperature of the Universe represented by the black body cosmic microwave background radiation (CMBR) of $2.728 \pm .004 \text{ } ^\circ K$ as detected in all directions of space in 60 - 630 GHz frequency range by the FIRAS instrument in the Cosmic Background Explorer (COBE) satellite and $2.730 \pm .014 \text{ } ^\circ K$ as measured at 10.7 GHz from a balloon platform [26]. The most recent NASA estimation of CMBR temperature from the Wilkinson Microwave Anisotropy Probe (WMAP) is $2.725 \pm .002 \text{ K}$. The particular temperature of $2.729 \text{ } ^\circ K$ indicated above which is essentially equal to the CMBR temperature was established by the trisine model wherein the superconducting Cooper CPT Charge conjugated pair density (see table 2.9.1) ($6.38E-30 \text{ g/cm}^3$) equals the critical density of the universe (see equation 2.11.5 and 2.11.16). Also, this temperature is congruent with an reported interstellar magnetic field of 2E-6 gauss (.2 nanotesla) [78,140] and intergalactic magnetic field)[92,93] at $1.64E-17$ gauss (see table 2.6.2).

As a general comment, a superconductor resonator should be operated (or destroyed) at about 2/3 of (T_c) for maximum effect of most properties, which are usually expressed as when extrapolated to $T = 0$ (see section 2.12). In this light, critical temperatures (T_c) in items 1.4 & 1.5 could be operated (or destroyed) up to 2/3 of the indicated temperature (793 and 1423 degree kelvin respectively). Also, the present development is for one-dimensional superconductivity. Consideration should be given to 2 and 3 dimensional superconductivity by 2 or 3 multiplier to T_c 's contained herein interpret experimental results.

2. Trisine Model Development

In this report, dimensionally (mass, length and time) mathematical relationships which link trisine geometry and superconducting theory are developed and then numerical values are presented in accordance with these relationships. Centimeter, gram and second (cgs) as well as kelvin temperature units are used unless otherwise specified with particular deference to Eugene N. Parker's electromagnetic dimensional analysis[97]. The actual model is developed in spreadsheet format with all model equations computed simultaneously, iteratively and interactively as required.

The general approach is: given a particular lattice form (in this case trisine), determine lattice momentum (p) wave vectors $K_1, K_2, K_3 \& K_4$ so that lattice cell energy(E) ($\sim K^2$) per volume is at a minimum all within a resonant $time$. The procedure is analogous to the quantum mechanical variational principle. More than four wave vectors could be evaluated at once, but four is considered sufficient.

2.1 Defining Model Relationships

The six defining model equations within the superconductor conventional tradition are presented as 2.1.1 - 2.1.4 below:

$$\oint_{Area} EdArea = \oint_{Volume} \rho_e dVolume = C \frac{e_{\pm}}{\varepsilon} \quad (2.1.1)$$

$$\frac{2m_k T_c}{\hbar^2} = \frac{(KK)}{e^{trisine} - 1} = \frac{e^{Euler}}{\pi} \frac{(KK)}{\sinh(trisine)} = K_B^2 \quad (2.1.2)$$

$$trisine = \frac{1}{D(\in_t) \cdot V} \quad (2.1.3)$$

$$f(m_t, m_p) \frac{e_{\pm} \hbar}{m_t v_e} = cavity H_c \quad (2.1.4)$$

Majorana condition

$$-i\hbar \frac{\partial}{\partial t} \Psi_+ + m_t c^2 \Psi_- = 0 \quad (2.1.5)$$

Schroedinger condition

$$-i\hbar \frac{\partial}{\partial t} \Psi_+ + \frac{1}{2} m_t v^2 \Psi_- = 0 \quad (2.1.6)$$

Reflecting(r) condition

$$v_r \sim \frac{c^2}{v} \quad K_r^2 \sim \frac{c^2}{K^2} \quad (2.1.7)$$

Dimensional Analysis for the visible and reflecting(r) condition

$$\hbar^{a1}G^{b1}c^{c1}H^{d1} = m^1l^0t^0 = \text{constant mass} \quad (2.1.8)$$

$$\hbar^{a2}G^{b2}c^{c2}H^{d2} = m^0l^1t^0 = \text{constant length} \quad (2.1.9)$$

$$\hbar^{a3}G^{b3}c^{c3}H^{d3} = m^0l^0t^1 = \text{constant time} \quad (2.1.10)$$

Equation 2.1.1 is a representation of Gauss's law with a Cooper CPT Charge conjugated pair charge contained within a bounding surface area (*Area*) defining a cell volume (*Volume*) or cell (*cavity*) with electric field (E_f) and charge density (ρ_e). Equation 2.1.2 and 2.1.3 define the superconducting model as developed by Bardeen, Cooper and Schrieffer in reference [2] and Kittel in reference [4].

Recognizing this approach and developing it further with a resonant concept, it is the further objective herein to select a particular (*wave vector*)² or (KK) based on trisine geometry (see figures 2.2.1-2.2.5) that fits the model relationship as indicated in equation 2.1.2 with K_B^2 being defined as the trisine (*wave vector*)² or (KK) associated with superconductivity of Cooper CPT Charge conjugated pairs through the lattice. This procedure establishes the trisine geometrical dimensions, then equation 2.1.4 is used to establish an effective mass function $f(m_e, m_p)$ of the particles in order for particles to flip in spin when going from trisine *cavity* to adjacent *cavity* while in thermodynamic equilibrium with critical field (H_c). The model has a geometric reflecting identity(r) implied by 2.1.7. The implementation of this method assumes the conservation of momentum (p_n) (2.1.12) and energy (E_n) (2.1.13) in visible and reflected(r) states such that:

$$\sum_{n=1,2,3,4} \Delta p_n \Delta x_n = 0 \quad (2.1.12)$$

$$\pm K_1 \pm K_2 \rightleftharpoons \pm K_3 \pm K_4$$

$$\sum_{m=1,2,3,4} \Delta p_m \Delta x_m = 0 \quad (2.1.12r)$$

$$\pm K_{r1} \pm K_{r2} \rightleftharpoons \pm K_{r3} \pm K_{r4}$$

$$\sum_{n=1,2,3,4} \Delta E_n \Delta time_n = 0$$

$$K_1 K_1 + K_2 K_2 = K_3 K_3 + K_4 K_4 + Q$$

$$\text{Where } Q = 0 \text{ (reversible process)} \quad (2.1.13)$$

$$E = \frac{\hbar^2}{2m} K^2 \sim K^2 \quad p = \hbar K \sim K$$

$$\sum_{m=1,2,3,4} \Delta E_m \Delta time_m = 0$$

$$K_{r1} K_{r1} + K_{r2} K_{r2} = K_{r3} K_{r3} + K_{r4} K_{r4} + Q_r$$

$$\text{Where } Q_r = 0 \text{ (reversible process)} \quad (2.1.13r)$$

$$E_r = \frac{\hbar^2}{2m} K_r^2 \sim K_r^2 \quad p_r = \hbar K_r \sim K_r$$

The numerical value of Q is associated with the equation 2.1.13 is associated with the non-elastic nature of a process. Q is a measure of the heat exiting the system. By stating that $Q = 0$, the elastic nature of the system is defined. An effective mass must be introduced to maintain the system elastic character. Essentially, a reversible process or reaction is defined recognizing that momentum is a vector and energy is a scalar.

These conditions of conservation of momentum (p and p_r) and energy (E , E_r or $k_b T_c$, $k_b T_{cr}$) provide the necessary condition of perfect elastic character, which must exist in the superconducting resonant state. In addition, the superconducting resonant state may be viewed as boiling of states ΔE_n , $\Delta time_n$, Δp_n , Δx_n (ΔE_m , $\Delta time_m$, Δp_m , Δx_m) on top of the zero point state in a coordinated manner.

In conjunction with the de Broglie hypothesis [77] providing momentum K and energy KK change with Lorentz transform written as

$$K \left(1 / \sqrt{1 - v^2/c^2} \right) = K\beta$$

$$KK \left(1 / \left(1 - v^2/c^2 \right) \right) = KK\beta^2 \quad (2.1.14)$$

$$\begin{aligned} K_r \left(1/\sqrt{1-v^2/c^2} \right) &= K\beta_r \\ K_r K_r \left(1/\left(1-v_r^2/c^2\right) \right) &= K_r K_r \beta_r^2 \end{aligned} \quad (2.1.14r)$$

congruent with:

$$m \left(v^2/c^2 \right) c^2 \left(1/\left(1-v^2/c^2\right) \right) = m \left(v^2/c^2 \right) c^2 \beta^2 \quad (2.1.15)$$

$$m \left(v_r^2/c^2 \right) c^2 \left(1/\left(1-v_r^2/c^2\right) \right) = m \left(v_r^2/c^2 \right) c^2 \beta_r^2 \quad (2.1.15r)$$

where the energy defined as 'KK' contains the factor v^2/c^2 , the group phase reflection (β_r) and subluminal (β) Lorentz transform conditions are allowed because in a resonant elastic condition these Lorentz transforms cancel

$$\pm K_1 \beta_1 \pm K_2 \beta_2 \rightleftharpoons \pm K_3 \beta_3 \pm K_4 \beta_4 \quad (2.1.16)$$

$$K_1 K_1 \beta_1^2 + K_2 K_2 \beta_2^2 = K_3 K_3 \beta_3^2 + K_4 K_4 \beta_4^2$$

and equivalent to:

$$\pm K_{r1} \beta_{r1} \pm K_{r2} \beta_{r2} \rightleftharpoons \pm K_{r3} \beta_{r3} \pm K_{r4} \beta_{r4} \quad (2.1.16r)$$

$$K_{r1} K_{r1} (\beta_{r1})^2 + K_{r2} K_{r2} (\beta_{r2})^2 = K_{r3} K_{r3} (\beta_{r3})^2 + K_{r4} K_{r4} (\beta_{r4})^2$$

for all values of velocity ($v_r \ll c$ or $v \ll c$) with an energy barrier at (v_r approaching c or v approaching c)

This energy barrier is shown to be at the nuclear diameter.

Conceptually, this model is defined within the context of the CPT theorem and generalized 3 dimensional parity of Cartesian coordinates (x, y, z) as follows:

$$\begin{vmatrix} x_{11} & x_{12} & x_{13} \\ y_{11} & y_{12} & y_{13} \\ z_{11} & z_{12} & z_{13} \end{vmatrix} = - \begin{vmatrix} x_{21} & x_{22} & x_{23} \\ y_{21} & y_{22} & y_{23} \\ z_{21} & z_{22} & z_{23} \end{vmatrix} \quad (2.1.17)$$

Given this parity condition defined within trisine geometrical constraints (with dimensions A and B as defined in Section 2.2) which necessarily fulfills determinate identity in equation 2.1.6b.

$$\begin{vmatrix} 0 & 0 & B_c \\ 0 & \frac{B}{\sqrt{3}} & -\frac{B}{\sqrt{3}} \\ -\frac{A}{2} & 0 & \frac{A}{2} \end{vmatrix} = - \begin{vmatrix} -B & 0 & 0 \\ 0 & \frac{B}{\sqrt{3}} & -\frac{B}{\sqrt{3}} \\ -\frac{A}{2} & 0 & \frac{A}{2} \end{vmatrix} \quad (2.1.18)$$

And further:

$$-12 \begin{vmatrix} -B & 0 & 0 \\ 0 & \frac{B}{\sqrt{3}} & -\frac{B}{\sqrt{3}} \\ -\frac{A}{2} & 0 & \frac{A}{2} \end{vmatrix} = \frac{12AB^2}{2\sqrt{3}} = 2\sqrt{3}AB^2 \quad (2.1.19)$$

$= cavity$

And further:

$$12 \begin{vmatrix} 0 & 0 & B \\ 0 & \frac{B}{\sqrt{3}} & -\frac{B}{\sqrt{3}} \\ -\frac{A}{2} & 0 & \frac{A}{2} \end{vmatrix} = \frac{12AB^2}{2\sqrt{3}} = 2\sqrt{3}AB^2 \quad (2.1.20)$$

$= cavity$

And further the reflective(r) condition:

$$12 \begin{vmatrix} 0 & 0 & B_r \\ 0 & \frac{B_r}{\sqrt{3}} & -\frac{B_r}{\sqrt{3}} \\ -\frac{A_r}{2} & 0 & \frac{A_r}{2} \end{vmatrix} = \frac{12A_r B_r^2}{2\sqrt{3}} = 2\sqrt{3}A_r B_r^2 \quad (2.1.20r)$$

$= cavity_r$

This geometry fills space lattice with hexagonal cells, each of volume ($cavity$ or $2\sqrt{3}AB^2$) ($cavity_r = 2\sqrt{3}A_r B_r^2$) and having property that lattice is equal to its reciprocal lattice. Now each cell contains a charge pair (e_+) and (e_-) in conjunction with cell dimensions (A and B) or (A_r and B_r) defining a permittivity (ϵ_x) or (ϵ_{xr}) and permeability (k_{mx}) or (k_{mrx}) such that:

$$v_{dx}^2 = \frac{c^2}{k_{mx}\epsilon_x} \quad (2.1.21)$$

and

$$v_{dxr}^2 = \frac{c^2}{k_{mxr}\epsilon_{xr}} \quad (2.1.21r)$$

Then $v_{dx\pm}$ is necessarily + or - and $(+k_{mx} + \epsilon_x) = (-k_{mx} - \epsilon_x)$

Now time (time_c) is defined as interval to traverse cell:

$$\text{time}_\pm = 2B / v_{dx\pm} \quad (2.1.22)$$

and

$$\text{time}_{dxr\pm} = 2B_r / v_{dxr\pm} \quad (2.1.22r)$$

then time_± and time_{r±} are necessarily + or -

Further: given the Heisenberg Uncertainty

$$\Delta p_x \Delta x \geq \hbar / 2 \quad \text{and} \quad \Delta E \Delta \text{time} \geq \hbar / 2 \quad (2.1.23)$$

$$\Delta p_{rx} \Delta x_r \geq \hbar / 2 \quad \text{and} \quad \Delta E_r \Delta \text{time}_r \geq \hbar / 2 \quad (2.1.23r)$$

but defined for this model satisfying a parity change geometry (A, B or A_r, B_r) and (time or time_r) reversal condition:

where: $m_t v_{dx} 2B = h$

$$m_t = \hbar^{2/3} \left(\frac{H}{G} \right)^{1/3} c^{-1/3} \cos(\theta) = 1.00E - 25g \quad (2.1.24)$$

is constant

(see Appendix I for constant mass (m_t) derivation)

$$\Delta p_x = m_t \Delta v_x$$

$$\Delta E = m_t \Delta v^2 / 2 = \frac{2 e_\pm^2}{3 \epsilon B} = \frac{h}{2 \text{time}_\pm} = k_b T_c \quad (\text{always } +)$$

$$\Delta \text{time} = \Delta x / \Delta v$$

The (B/A) ratio must have a specific ratio (2.379761271) and mass (m_t) a constant + value of 110.12275343 x electron mass (m_e) or 56.2726 MeV/c² to make this work.

(see Appendix E for background derivation based on Heisenberg Uncertainty and de Broglie condition).

The trisine symmetry (as visually seen in figures 2.2.1-2.2.5) allows movement of Cooper CPT Charge conjugated pairs with center of mass wave vector equal to zero as required by superconductor theory as presented in references [2, 4].

Wave vectors (K_c) as applied to trisine are assumed to be free particles (ones moving in the absence of any potential field) and are solutions to the one dimensional time independent Schrödinger equation 2.1.7 [3]:

$$\frac{d^2\psi}{ds^2} + \frac{2m_t}{\hbar^2} E \psi = 0 \quad (2.1.25)$$

The solution to this Schrödinger equation is in terms of a wave function (ψ):

$$\begin{aligned} \psi &= \text{Amplitude} \sin \left(\left(\frac{2m_t}{\hbar^2} E \right)^{\frac{1}{2}} s \right) \\ &= \text{Amplitude} \sin(K \cdot s) \end{aligned} \quad (2.1.26)$$

Wave vector solutions (KK) are constrained to fixed trisine cell boundaries such that energy eigen values are established by the condition s_c = S_c and ψ = 0 such that

$$\left(\frac{2m_t}{\hbar^2} E \right)^{\frac{1}{2}} S = K S = n\pi \quad (2.1.27)$$

Energy eigen values are then described in terms of what is generally called the particle in the box relationship as follows:

$$E = \frac{n^2 \hbar^2}{2m_t} \left(\frac{\pi}{S} \right)^2 \quad (2.1.28)$$

For our model development, we assume the quantum number n = 2 and this quantum number is incorporated into the wave vectors (KK) as presented as follows:

$$E = \frac{2^2 \hbar^2}{2m_t} \left(\frac{\pi}{S} \right)^2 = \frac{\hbar^2}{2m_t} \left(\frac{2\pi}{S} \right)^2 = \frac{\hbar^2}{2m_t} (KK) \quad (2.1.29)$$

This model is consistent with the Majorana equation 2.1.4 with a particular wave function satisfying the Trisine model

$$\Psi = e^{\frac{-i\pi c^2 time_{\pm}^2}{(2B)^2}} = e^{\frac{-i\pi c^2}{v_{dx}^2}} \quad (2.1.30)$$

and $m_t = \pi \hbar / (2B^2)$ or $\pi \hbar / D_c$

$$-i\hbar \frac{\partial}{\partial time} \Psi_+ + m_t c^2 \Psi_- = 0$$

$$\text{where } \Psi_+ = e^{\frac{-i\pi c^2 time_+^2}{(2B)^2}} \quad \Psi_- = e^{\frac{-i\pi c^2 time_-^2}{(2B)^2}}$$

$$\frac{(2B)^2}{time_{\pm}} = 0.06606194571 \frac{cm^2}{sec} \quad (\text{constant})$$

$$\text{and } m_t = \frac{\hbar 2\pi time_{\pm}}{(2B)^2} = 1.003008448E-25 g \quad (\text{constant})$$

Trisine geometry is described in Figures 2.2.1 – 2.2.5 is in general characterized by resonant dimensions A and B with a characteristic ratio B/A of 2.379761271 and corresponding characteristic angle (θ) where:

$$\frac{B}{A} = \frac{B_r}{A_r} = \frac{2}{\sin(1 \text{ radian})} = \frac{g_s e}{2 \text{ Euler}} = \frac{g_s 3^{1/2} e}{2} \quad (2.1.31)$$

$$\frac{B}{A} = \frac{B_r}{A_r} = \frac{1}{g_s} \zeta(3/2) \cos(\theta) = \frac{e_{\pm}^2}{\varepsilon \hbar v_{dx}} = \frac{\pi^0}{m_t} \quad (2.1.32)$$

$$\zeta(3/2) \approx 2.6124$$

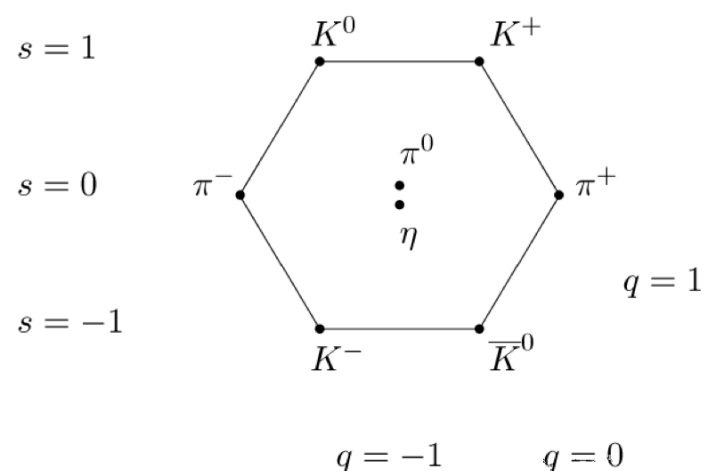
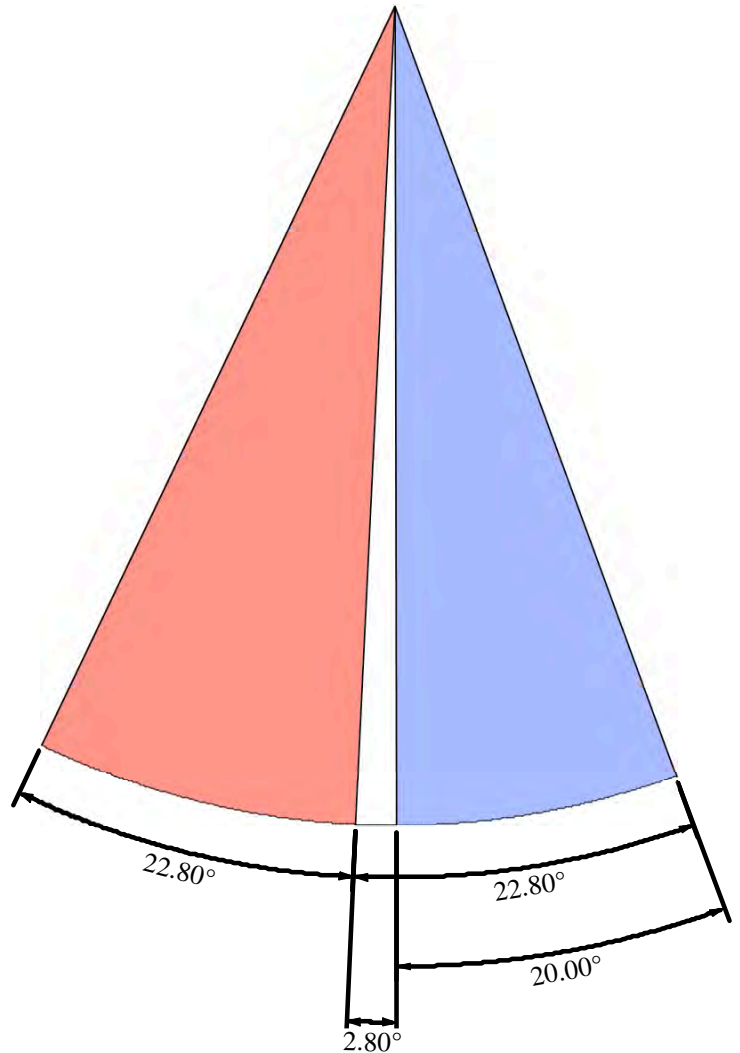
$$\theta = \tan^{-1} \left(\frac{A}{B} \right) = \tan^{-1} \left(\frac{A_r}{B_r} \right) = 22.80^\circ \quad (2.1.33)$$

$$\begin{aligned} \theta_c &= \tan^{-1} \left(\frac{A}{C} \right) = \tan^{-1} \left(\frac{A_r}{C_r} \right) \\ &= \tan^{-1} \left(\frac{\sqrt{3} A}{2 B} \right) = \tan^{-1} \left(\frac{\sqrt{3} A_r}{2 B_r} \right) = 20.00^\circ \end{aligned}$$

$$\theta - \theta_c = 2.8^\circ$$

The trisine resonant lattice model is a more general triangular formulation than the reported octal (8) ‘Noble Eightfold Path’ for establishing nature’s physical principles. The following graphic depicting standard model particles could be more comprehensively explained in terms of triangular hexagonal trisine geometry rather than Eightfold Path verbiage

Figure 2.1.1 Vilnius Divine Image Ray Angles are in conformance with θ , θ_c & $\theta - \theta_c$



The superconducting model is described with equations 2.1.34 - 2.1.40, with variable definitions described in the

remaining equations where $energy = k_b T_c$. The model again converges around a particular universal resonant transformed mass (numerically approximate to the Weinberg mass [99]):

m_t or $\hbar^{2/3} U^{1/3} c^{-1/3} \cos(\theta)$ or $\pi \hbar / (2B^2)$ or $\pi \hbar / D_c$ or $110.12275343 \times m_e$ or $56.2726 \text{ MeV}/c^2)$

and dimensional ratio (B/A) of 2.379761271

where the $(B/A) \sim$ neutral pi meson (pion) π^0/m_t .

$$energy = k_b T_c = \frac{m_t v_{dx}^2}{2} = \hbar \frac{\pi}{time_{\pm}} = \frac{\hbar^2 K_B^2}{2m_t} \quad (2.1.34)$$

$$k_b T_c = \frac{\hbar^2}{\frac{m_e m_t}{m_e + m_t} (2B)^2 + \frac{m_t m_p}{m_t + m_p} (A)^2} \quad (2.1.35)$$

$$k_b T_c = \frac{\hbar^2 (K_C^2 + K_{Ds}^2)}{2m_t} \frac{1}{e^{trisine} - 1} \quad (2.1.36)$$

$$k_b T_c = \frac{\hbar^2 (K_C^2 + K_{Ds}^2)}{2m_t} \frac{e^{Euler}}{\pi \sinh(trisine)} \quad (2.1.37)$$

$$k_b T_c = \left(\frac{1}{g_s^2} \right) \frac{cavity}{8\pi} DE \quad (2.1.38)$$

$$k_b T_c = \frac{chain}{cavity} \frac{e_{\pm}^2}{g_s \epsilon B} = \frac{e_{\pm}^2 K_B}{2\epsilon} \frac{A}{B} = \frac{e_{\pm}^2 K_B}{2\epsilon} \frac{m_t}{\pi^0} \quad (2.1.39)$$

$$k_b T_c = \frac{4\hbar v_{cz}}{time_{\pm}} \frac{1}{2\pi v_{cx}} \quad (\text{Unruh}) \quad (2.1.40)$$

Also, Bose Einstein Condensate(BEC) criteria is satisfied as:

$$cavity^{1/3} \sim \frac{h}{\sqrt{2\pi m_t k_b T_c}} \quad (2.1.24)$$

Bardeen, Cooper and Schrieffer (BCS) [2] theory is additionally adhered to by equations 2.1.34 – 2.1.40 as verified by equations 2.1.17 - 2.1.23, in conjunction with equations A.3, A.4, and A.5 as presented in Appendix A. This general approach may fall into the concept of the Majorana fermion. The Majorana fermion is its own anti-particle that has been found in the superconductivity context[121].

$$\begin{aligned} trisine &= \frac{K_B^2 + K_P^2}{K_P K_B} \\ &= \frac{1}{D(\xi) V} = -\ln\left(\frac{2}{\pi} e^{Euler} - 1\right) \\ &= 2.011 \end{aligned} \quad (2.1.41)$$

$$\begin{aligned} trisine &= \frac{K_{Br}^2 + K_{Pr}^2}{K_{Pr} K_{Br}} \\ &= \frac{1}{D(\xi_r) V_r} = -\ln\left(\frac{2}{\pi} e^{Euler} - 1\right) \\ &= 2.011 \end{aligned} \quad (2.1.41r)$$

$$\begin{aligned} \text{density of states } D(\xi_T) &= \frac{3 \text{ cavity } m_t K_C}{4\pi^3 \hbar^2} \\ &= \frac{1}{k_b T_c} \end{aligned} \quad (2.1.42)$$

$$\begin{aligned} \text{density of states } D_r(\xi_T) &= \frac{3 \text{ cavity}_r m_t K_{Cr}}{4\pi^3 \hbar^2} \\ &= \frac{1}{k_b T_{cr}} \end{aligned} \quad (2.1.42r)$$

The attractive Cooper CPT Charge conjugated pair energy (V) is expressed in equation 2.1.43:

$$V = V_r = \frac{K_P K_B}{K_B^2 + K_P^2} k_b T_c \quad (2.1.43)$$

$$V = V_r = \frac{K_P K_B}{K_{Br}^2 + K_{Pr}^2} k_b T_{cr} \quad (2.1.43r)$$

Table 2.1.1 Density of States

Condition	1.2	1.3	1.6	1.9	1.10	1.11
$T_a(^0 K)$	6.53E+11	6.53E+11	6.53E+11	6.53E+11	6.53E+11	6.53E+11
$T_b(^0 K)$	9.05E+14	5.48E+13	9.22E+08	1.10E+07	2,868	2.723
$T_{br}(^0 K)$	3.30E+12	5.45E+13	3.24E+18	2.72E+20	1.04E+24	1.10E+27
$T_c(^0 K)$	8.96E+13	3.28E+11	93.0	0.0131	8.99E-10	8.10E-16
$T_{cr}(^0 K)$	1.19E+09	3.25E+11	1.15E+21	8.11E+24	1.19E+32	1.32E+38
$z_R + 1$	3.67E+43	8.14E+39	3.89E+25	6.53E+19	1.17E+09	1.00E+00
$z_B + 1$	3.32E+14	2.01E+13	3.39E+08	4.03E+06	1.05E+03	1.00E+00
$Age_{UG} (\text{sec})$	7.14E-05	4.79E-03	6.94E+04	5.36E+07	1.27E+13	4.33E+17
$Age_{UGV} (\text{sec})$	4.59E-10	1.25E-07	4.42E+02	3.13E+06	1.22E+13	4.33E+17
$Age_U (\text{sec})$	1.18E-26	5.31E-23	1.11E-08	6.63E-03	3.70E+08	4.33E+17
V	6.12E-03	2.24E-05	6.35E-15	8.98E-19	6.14E-26	5.54E-32
V_r	8.21E-08	2.24E-05	7.91E+04	5.60E+08	8.18E+15	9.08E+21
$D(\xi)$	8.09E+01	2.21E+04	7.79E+13	5.51E+17	8.06E+24	8.94E+30
$D(\xi)_r$	6.09E+06	2.23E+04	6.32E-06	8.93E-10	6.11E-17	5.51E-23

The equation 2.1.36 array equation elements 1 and 2 along with equations 2.1.41, 2.1.42, 2.1.43, 2.1.44 and 2.1.45 are

consistent with the BCS weak link relationship:

$$k_b T_c = \frac{2e^{Euler}}{\pi} \frac{\hbar^2}{2m_t} (K_c^2 + K_{Ds}^2) e^{\frac{-1}{D(\in) V}} \quad (2.1.44)$$

$$k_b T_{cr} = \frac{2e^{Euler}}{\pi} \frac{\hbar^2}{2m_t} (K_{Cr}^2 + K_{Dsr}^2) e^{\frac{-1}{D_r(\in) V_r}} \quad (2.1.44r)$$

$$k_b T_c = \left(\frac{1}{g_s} \right) \left(\frac{chain}{cavity} \right) \frac{\hbar^2}{2m_t} \left(\frac{K_A^2}{\mathbb{C}} \right) e^{\frac{-1}{D(\in) V}} \quad (2.1.45)$$

$$k_b T_{cr} = \left(\frac{1}{g_s} \right) \left(\frac{chain_r}{cavity_r} \right) \frac{\hbar^2}{2m_t} \left(\frac{K_{Ar}^2}{\mathbb{C}} \right) e^{\frac{-1}{D_r(\in) V_r}} \quad (2.1.45r)$$

The relationship in equation 2.1.48 is based on the Bohr magneton $e\hbar/2m_e v_{ey}$ (which has dimensions of magnetic field x volume) with a material dielectric (ϵ) modified speed of light (v_{ey}) (justifiable in the context of resonant condition) and establishes the spin flip/flop as Cooper CPT Charge conjugated pairs resonate from one cavity to the next (see figure 2.3.1). The 1/2 spin factor and electron gyromagnetic factor (g_e) and superconducting gyro factor (g_s) are multipliers of the Bohr magneton where

$$g_s = \frac{3}{4} \frac{m_e}{m_t} \left(\frac{cavity}{(\Delta x \Delta y \Delta z)} - \frac{m_p}{m_e} \right) = \frac{K_{Dn}}{K_B} \cos(\theta) \\ = \frac{m_p}{m_p - m_e} \frac{m_t}{m_t - m_e} \quad (2.1.46)$$

$$g_s = \frac{3}{4} \frac{m_e}{m_t} \left(\frac{cavity_r}{(\Delta x_r \Delta y_r \Delta z_r)} - \frac{m_p}{m_e} \right) = \frac{K_{Dnr}}{K_{Br}} \cos(\theta) \\ = \frac{m_p}{m_p - m_e} \frac{m_t}{m_t - m_e} \quad (2.1.46r)$$

as related to the Dirac Number by

$$\frac{3}{4} (g_s - 1) = 2\pi (g_d - 1) \quad (2.1.47)$$

Also because particles must resonate in pairs, a symmetry is created for superconducting current to advance as bosons.

$$\frac{2}{1} \frac{\mathbb{C} e_{\pm} \hbar}{2m_e v_{ey}} = chain H_c \quad (2.1.48)$$

with reflected identity and inverted spin 1/2 vs 2/1

$$\frac{1}{2} \frac{\mathbb{C} e_{\pm} \hbar}{2m_e v_{ey}} = chain_r H_{cr}$$

The proton to electron mass ratio (m_p/m_e) is verified through the Werner Heisenberg Uncertainty Principle volume ($(\Delta x \cdot \Delta y \cdot \Delta z)$) as follows in equations 2.1.33 - 2.1.38 (2.1.33r - 2.1.38r):

$$\Delta x = \frac{\hbar}{2} \frac{1}{\Delta p_x} = \frac{\hbar}{2} \frac{1}{\Delta(\hbar K_B)} = \Delta \left(\frac{B}{2} \frac{1}{\pi} \right) \quad (2.1.49)$$

$$\Delta x_r = \frac{\hbar}{2} \frac{1}{\Delta p_{xr}} = \frac{\hbar}{2} \frac{1}{\Delta(\hbar K_{Br})} = \Delta \left(\frac{B_r}{2} \frac{1}{\pi} \right) \quad (2.1.49r)$$

$$\Delta y = \frac{\hbar}{2} \frac{1}{\Delta p_y} = \frac{\hbar}{2} \frac{1}{\Delta(\hbar K_P)} = \Delta \left(\frac{3B}{2\sqrt{3}} \frac{1}{2\pi} \right) \quad (2.1.50)$$

$$\Delta y_r = \frac{\hbar}{2} \frac{1}{\Delta p_{yr}} = \frac{\hbar}{2} \frac{1}{\Delta(\hbar K_{Pr})} = \Delta \left(\frac{3B_r}{2\sqrt{3}} \frac{1}{2\pi} \right) \quad (2.1.50r)$$

$$\Delta z = \frac{\hbar}{2} \frac{1}{\Delta p_z} = \frac{\hbar}{2} \frac{1}{\Delta(\hbar K_A)} = \Delta \left(\frac{A}{2} \frac{1}{2\pi} \right) \quad (2.1.51)$$

$$\Delta z_r = \frac{\hbar}{2} \frac{1}{\Delta p_{zr}} = \frac{\hbar}{2} \frac{1}{\Delta(\hbar K_{Ar})} = \Delta \left(\frac{A_r}{2} \frac{1}{2\pi} \right) \quad (2.1.51r)$$

$$(\Delta x \cdot \Delta y \cdot \Delta z) = \frac{1}{(2K_B)(2K_P)(2K_A)} \quad (2.1.52)$$

$$(\Delta x_r \cdot \Delta y_r \cdot \Delta z_r) = \frac{1}{(2K_{Br})(2K_{Pr})(2K_{Ar})} \quad (2.1.52r)$$

$$\frac{m_t}{m_e} = \frac{3}{4} \frac{1}{g_s} \left(\frac{cavity}{(\Delta x \Delta y \Delta z)} - \frac{m_p}{m_e} \right) \quad (2.1.53)$$

$$\frac{m_t}{m_e} = \frac{3}{4} \frac{1}{g_s} \left(\frac{cavity_r}{(\Delta x_r \Delta y_r \Delta z_r)} - \frac{m_p}{m_e} \right) \quad (2.1.53r)$$

$$g_s = \frac{3}{4} \frac{m_e}{m_t} \left(\frac{cavity}{(\Delta x \Delta y \Delta z)} - \frac{m_p}{m_e} \right) \quad (2.1.54)$$

$$g_s = \frac{3}{4} \frac{m_e}{m_t} \left(\frac{cavity_r}{(\Delta x_r \Delta y_r \Delta z_r)} - \frac{m_p}{m_e} \right) \quad (2.1.54r)$$

Equations 2.1.49 - 2.1.54 (2.1.49r - 2.1.54r) provides us with the confidence ($\Delta x \cdot \Delta y \cdot \Delta z$ is well contained within the *cavity*) ($\Delta x_r \cdot \Delta y_r \cdot \Delta z_r$ is well contained within the *cavity_r*) that we can proceed in a semi-classical manner outside the envelop of the uncertainty principle with the resonant transformed mass (m_t) and de Broglie velocities (v_d) used in this trisine superconductor model or in other words equation 2.1.55 holds.

$$\mathbb{C} \left(\frac{\hbar^2 (KK)}{2m_t} \right) = \mathbb{C} \left(\frac{1}{2} m_t v_d^2 \right) = \frac{(m_t v_d)^2}{m_t} \quad (2.1.55)$$

$$\mathbb{C} \left(\frac{\hbar^2 (K_r K_r)}{2m_t} \right) = \mathbb{C} \left(\frac{1}{2} m_t v_{dr}^2 \right) = \frac{(m_t v_{dr})^2}{m_t} \quad (2.1.55r)$$

The Meissner condition as defined by total magnetic field exclusion from trisine chain as indicated by diamagnetic susceptibility (χ) $= -1/4\pi$, as per the following equation:

$$\chi = -\frac{\mathbb{C} k_b T_c}{\text{chain } H_c^2} = -\frac{1}{4\pi} \quad (2.1.56)$$

Equation 2.1.57 provides a representation of the trisine geometry in terms of relativistic Lorentz invariant relationship that is consistent with the Majorana condition at near relativity trisine conditions 1.3 and 1.4.

$$\left(\frac{1}{2} m v^2 \right)^2 = (m \zeta c)^2 + (mc^2)^2$$

generally if $(m \text{ and } c) \neq 0$ then:

$$\zeta = \left\{ \frac{+i\sqrt{2c^2 - v^2} \sqrt{2c^2 + v^2}}{2c} \right\} \quad (2.1.57)$$

$$\left\{ \frac{-i\sqrt{2c^2 - v^2} \sqrt{2c^2 + v^2}}{2c} \right\}$$

and m compatible with

$$m_t = \pi \hbar \text{ time}_\pm / (2B^2) \text{ or } \pi \hbar / D_c$$

and v compatible with

$$v_{dx}, v_{dy}, v_{dz}, v_{ex}, v_{ey}, v_{ez}$$

to the trisine resonant condition:

$$\frac{1}{2} m_t v_{dx}^2 = \frac{1}{2} m_t v_{dx}^2$$

and m compatible with

$$m_t = \pi \hbar \text{ time}_{r\pm} / (2B_r^2) \text{ or } \pi \hbar / D_c$$

and v compatible with

$$v_{dxr}, v_{dyr}, v_{zr}, v_{ex}, v_{ey}, v_{ez}$$

to the trisine resonant condition:

$$\frac{1}{2} m_t v_{dxr}^2 = \frac{1}{2} m_t v_{dxr}^2$$

The relativity relationship is further explained in terms of the

Einstein tensor $G_{\mu\nu}$ and stress energy tensor $T_{\mu\nu}$ relationship, equation 3.22.

Table 2.1.2 with (m_t) , (m_r) . Angular frequency $(2k_b T_c / \hbar)$ (ω) & Wave Length $(2\pi c / \omega)$ or $(c \cdot \text{time})$ with plot (Conceptually this is the Schwinger limit for virtual particles).

Condition	1.2	1.3	1.6	1.9	1.10	1.11
$T_a ({}^0 K)$	6.53E+11	6.53E+11	6.53E+11	6.53E+11	6.53E+11	6.53E+11
$T_b ({}^0 K)$	9.05E+14	5.48E+13	9.22E+08	1.10E+07	2,868	2.723
$T_{br} ({}^0 K)$	3.30E+12	5.45E+13	3.24E+18	2.72E+20	1.04E+24	1.10E+27
$T_c ({}^0 K)$	8.96E+13	3.28E+11	93.0	0.0131	8.99E-10	8.10E-16
$T_{cr} ({}^0 K)$	1.19E+09	3.25E+11	1.15E+21	8.11E+24	1.19E+32	1.32E+38
$z_R + 1$	3.67E+43	8.14E+39	3.89E+25	6.53E+19	1.17E+09	1.00E+00
$z_B + 1$	3.32E+14	2.01E+13	3.39E+08	4.03E+06	1.05E+03	1.00E+00
$Age_{UG} (\text{sec})$	7.14E-05	4.79E-03	6.94E+04	5.36E+07	1.27E+13	4.33E+17
$Age_{UGV} (\text{sec})$	4.59E-10	1.25E-07	4.42E+02	3.13E+06	1.22E+13	4.33E+17
$Age_U (\text{sec})$	1.18E-26	5.31E-23	1.11E-08	6.63E-03	3.70E+08	4.33E+17
$m_t (g)$	1.00E-25	1.00E-25	1.00E-25	1.00E-25	1.00E-25	1.00E-25
$m_r (g)$	1.38E-23	5.04E-26	1.43E-35	2.02E-39	1.38E-46	1.24E-52
$m_{rr} (g)$	1.83E-28	4.99E-26	1.76E-16	1.25E-12	1.82E-05	2.02E+01
$\Delta x (\text{cm})$	1.06E-14	6.62E-09	1.75E-08	8.13E-07	3.20E-03	3.52
$\Delta y (\text{cm})$	9.17E-15	5.73E-09	1.52E-08	7.04E-07	2.77E-03	3.05
$\Delta z (\text{cm})$	2.22E-15	1.39E-09	3.68E-09	1.71E-07	6.73E-04	0.74
$\Delta x (\text{cm})$	2.90E-12	1.76E-13	2.96E-18	3.52E-20	9.20E-24	8.74E-27
$\Delta y (\text{cm})$	2.52E-12	1.52E-13	2.56E-18	3.05E-20	7.97E-24	7.57E-27
$\Delta z (\text{cm})$	6.10E-13	3.69E-14	6.22E-19	7.39E-21	1.93E-24	1.84E-27
$\omega (\text{rad/sec})$	2.35E+25	8.59E+22	2.44E+13	3.44E+09	2.35E+02	2.12E-04
Wave Length (cm)	8.03E-15	2.19E-12	7.74E-03	5.48E+01	8.00E+08	8.88E+14
$\omega (\text{rad/sec})$	3.12E+20	8.51E+22	3.00E+32	2.12E+36	3.10E+43	3.44E+49
Wave Length (cm)	6.05E-10	2.21E-12	6.28E-22	8.87E-26	6.07E-33	5.47E-39

Where (v_d) is the de Broglie velocity as in equation 2.1.41 and also related to resonant CPT time_\pm by equation 2.1.42.

$$v_{dx} = \frac{\hbar \pi}{m_t B} (1+z_R)^{1/3} \text{ or } (1+z_B)^{-1} \quad (2.1.58)$$

$$v_{dxr} = \frac{\hbar \pi}{m_t B_r} (1+z_R)^{-1/3} \text{ or } (1+z_B)^{-1} \quad (2.1.58r)$$

$$time = \frac{2 \cdot B}{v_{dx}} (1+z_R)^{-2/3} \text{ or } (1+z_B)^{-2} \quad (2.1.59)$$

$$time_r = \frac{2 \cdot B_r}{v_{dxr}} \quad (1+z_R)^{2/3} \text{ or } (1+z_B)^2 \quad (2.1.59r)$$

The relationship between (v_{dx}) and (v_{xr}) is per the group/phase velocity relationship presented in equation 2.1.60.

$$(group \text{ velocity}) \cdot (phase \text{ velocity}) = c^2$$

$$v_{dx} v_{dxr} = v_{dx} \frac{c^2}{v_{dx}} = c^2 \quad (2.1.60)$$

And the Phase velocity v_{dxr} is related to universal Hubble radius of curvature dimension R_U over cavity resonance time as well as the speed of light c over the *cavity* resonance velocity v_{dx} . At present, the phase velocity v_{dxr} is much greater than (v_{dx}) and $(v_{ex}, v_{ey} \text{ & } v_{ez})$ but in the Big Bang nucleosynthetic super luminal condition, the phase velocity v_{dxr} was less than (v_{dx}) and $(v_{ex}, v_{ey} \text{ & } v_{ez})$.

Table 2.1.3 Velocity v_{dx} phase velocity v_{dxr}

Condition	1.2	1.3	1.6	1.9	1.10	1.11
$T_a ({}^0 K)$	6.53E+11	6.53E+11	6.53E+11	6.53E+11	6.53E+11	6.53E+11
$T_b ({}^0 K)$	9.05E+14	5.48E+13	9.22E+08	1.10E+07	2,868	2.723
$T_{br} ({}^0 K)$	3.30E+12	5.45E+13	3.24E+18	2.72E+20	1.04E+24	1.10E+27
$T_c ({}^0 K)$	8.96E+13	3.28E+11	93.0	0.0131	8.99E-10	8.10E-16
$T_{cr} ({}^0 K)$	1.19E+09	3.25E+11	1.15E+21	8.11E+24	1.19E+32	1.32E+38
$z_R + 1$	3.67E+43	8.14E+39	3.89E+25	6.53E+19	1.17E+09	1.00E+00
$z_B + 1$	3.32E+14	2.01E+13	3.39E+08	4.03E+06	1.05E+03	1.00E+00
$Age_{UG} (\text{sec})$	7.14E-05	4.79E-03	6.94E+04	5.36E+07	1.27E+13	4.33E+17
$Age_{UGv} (\text{sec})$	4.59E-10	1.25E-07	4.42E+02	3.13E+06	1.22E+13	4.33E+17
$Age_U (\text{sec})$	1.18E-26	5.31E-23	1.11E-08	6.63E-03	3.70E+08	4.33E+17
$v_{dx} (\text{cm/sec})$	4.97E+11	3.00E+10	5.06E+05	6.01E+03	1.57E+00	1.49E-03
$v_{dxr} (\text{cm/sec})$	1.81E+09	2.99E+10	1.78E+15	1.49E+17	5.71E+20	6.02E+23

2.2 Trisine Geometry

The characteristic trisine resonant dimensions A and B are indicated as a function of temperature in table 2.2.1 as computed from the equation 2.2.1

$$k_b T_c = \frac{\hbar^2 K_B^2}{2m_t} = \frac{\hbar^2 K_A^2}{2m_t} \left(\frac{B}{A} \right)^2 \quad (2.2.1)$$

$$k_b T_{cr} = \frac{\hbar^2 K_{Br}^2}{2m_t} = \frac{\hbar^2 K_{Ar}^2}{2m_t} \left(\frac{B_r}{A_r} \right)^2 \quad (2.2.1r)$$

Trisine geometry is subject to Charge conjugation Parity change Time reversal (CPT) symmetry which is a fundamental symmetry of physical laws under transformations that involve the inversions of charge, parity and time simultaneously. The CPT symmetry provides the basis for creating particular resonant structures with this trisine geometrical character.

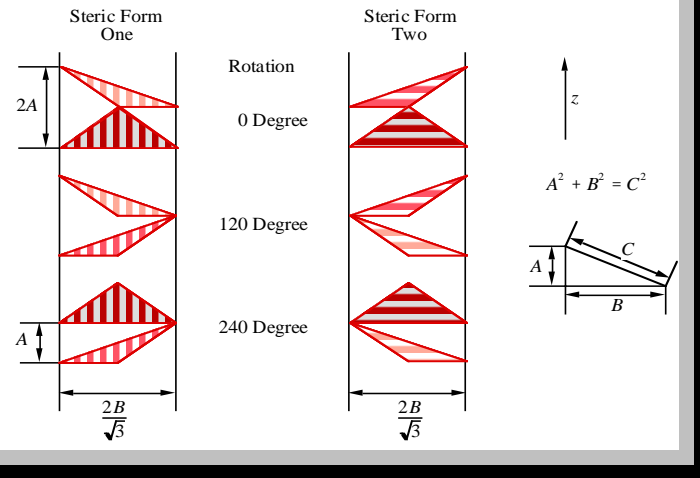
Table 2.2.1 Dimensions B and A with B vs. T_c plot

Condition	1.2	1.3	1.6	1.9	1.10	1.11
$T_a ({}^0 K)$	6.53E+11	6.53E+11	6.53E+11	6.53E+11	6.53E+11	6.53E+11
$T_b ({}^0 K)$	9.05E+14	5.48E+13	9.22E+08	1.10E+07	2,868	2.723
$T_{br} ({}^0 K)$	3.30E+12	5.45E+13	3.24E+18	2.72E+20	1.04E+24	1.10E+27
$T_c ({}^0 K)$	8.96E+13	3.28E+11	93.0	0.0131	8.99E-10	8.10E-16
$T_{cr} ({}^0 K)$	1.19E+09	3.25E+11	1.15E+21	8.11E+24	1.19E+32	1.32E+38
$z_R + 1$	3.67E+43	8.14E+39	3.89E+25	6.53E+19	1.17E+09	1.00E+00
$z_B + 1$	3.32E+14	2.01E+13	3.39E+08	4.03E+06	1.05E+03	1.00E+00
$Age_{UG} (\text{sec})$	7.14E-05	4.79E-03	6.94E+04	5.36E+07	1.27E+13	4.33E+17
$Age_{UGv} (\text{sec})$	4.59E-10	1.25E-07	4.42E+02	3.13E+06	1.22E+13	4.33E+17
$Age_U (\text{sec})$	1.18E-26	5.31E-23	1.11E-08	6.63E-03	3.70E+08	4.33E+17
$A (\text{cm})$	2.80E-14	4.62E-13	2.74E-08	2.31E-06	8.82E-03	9.29
$B (\text{cm})$	6.65E-14	1.10E-12	6.53E-08	5.49E-06	2.10E-02	2.21E+01
$A_r (\text{cm})$	7.67E-12	4.64E-13	7.82E-18	9.29E-20	2.43E-23	2.31E-26
$B_r (\text{cm})$	1.83E-11	1.10E-12	1.86E-17	2.21E-19	5.78E-23	5.49E-26

These structures have an analog in various resonant structures postulated in the field of chemistry to explain properties of delocalized π electrons in benzene, ozone and a myriad of other molecules and incorporate the Noether theorem concepts of energy – time and momentum – length symmetry.

Trisine characteristic volumes with variable names *cavity* and *chain* as well as characteristic areas with variable names *section*, *approach* and *side* are defined in equations 2.2.7 - 2.2.9. See figures 2.2.1 - 2.2.4 for a visual description of these parameters. The mirror image forms in figure 2.2.1 are in conformance with parity requirement in Charge conjugation Parity change Time reversal (CPT) theorem as established by determinant identity in equation 2.1.6b and trivially obvious in cross – product expression in equation 2.2.2 in which case an orthogonal coordinate system is right-handed, or left-handed for result $2AB$ which is later defined as trisine *cavity side* in equation 2.2.9.

Figure 2.2.1 Trisine Steric (Mirror Image) Parity Forms



Essentially, there are two mirror image *sides* to each *cavity*. At the nuclear scale (condition 1.2), such chiral geometry is consistent with the standard model (quarks, gluons etc.).

$$(2B) \times \left(\sqrt{A^2 + B^2} \right) = 2B\sqrt{A^2 + B^2} \sin(\theta) = 2AB \quad (2.2.2)$$

$$(2B_r) \times \left(\sqrt{A_r^2 + B_r^2} \right) = 2B_r\sqrt{A_r^2 + B_r^2} \sin(\theta) = 2A_r B_r \quad (2.2.2r)$$

$$cavity = 2\sqrt{3}AB^2 = \frac{4\pi A g e_U m_t}{U} \quad (2.2.3)$$

$$cavity_r = 2\sqrt{3}A_r B_r^2 = \frac{4\pi A g e_{U_r} m_t}{U} \quad (2.2.3r)$$

$$chain = \frac{2}{3} cavity \quad (2.2.4)$$

$$chain_r = \frac{2}{3} cavity_r \quad (2.2.4r)$$

A and *B* are proportional to the permeability k_m and dielectric ϵ as defined in section 2.5 with other constant factors.

$$A = \frac{A}{B} \pi x_U \frac{c}{v_{dx}} = \pi x_U \sqrt{k_{mx} \epsilon_x} \quad (2.2.5)$$

$$A_r = \frac{A_r}{B_r} \pi x_U \frac{c}{v_{dxr}} = \pi x_U \sqrt{k_{mxr} \epsilon_{xr}} \quad (2.2.5r)$$

$$B = \pi x_U \frac{c}{v_{dx}} = \pi x_U \sqrt{k_{mx} \epsilon_x} \quad (2.2.6)$$

$$B_r = \pi x_U \frac{c}{v_{dxr}} = \pi x_U \sqrt{k_{mxr} \epsilon_{xr}} \quad (2.2.6r)$$

Or in terms of the universal dimensional scale

$$B = \hbar^{\frac{1}{3}} U^{\frac{-1}{3}} c^{\frac{-2}{3}} \left(\frac{c}{v_{dx}} \right) \frac{\pi}{\cos(\theta)} \quad (2.4.4)$$

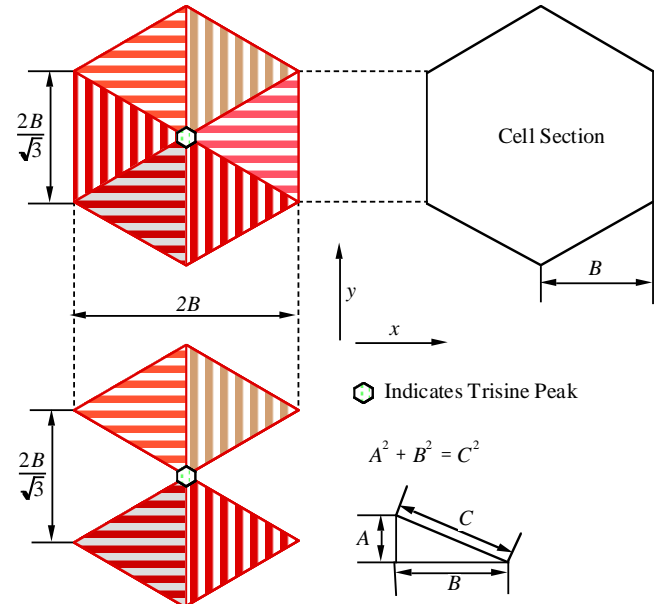
$$B_r = \hbar^{\frac{1}{3}} U^{\frac{-1}{3}} c^{\frac{-2}{3}} \left(\frac{c}{v_{dxr}} \right) \frac{\pi}{\cos(\theta)} \quad (2.4.4r)$$

Or in terms of the Kolmogorov viscosity length scale[60]

$$B = \left(\frac{1}{\sqrt{2}} \right) \left(\left(\frac{B}{A} \right)^3 \frac{m_t \nu_U time_{\pm}}{k_b T_c} \right)^{\frac{1}{4}} \quad (2.4.5)$$

$$B_r = \left(\frac{1}{\sqrt{2}} \right) \left(\left(\frac{B_r}{A_r} \right)^3 \frac{m_t \nu_U time_{r\pm}}{k_b T_{cr}} \right)^{\frac{1}{4}} \quad (2.4.5r)$$

Figure 2.2.2 Trisine Cavity and Chain Geometry from Steric (Mirror Image) Forms



The *section* is the trisine cell *cavity* projection on to the *x*, *y* plane as indicated in figure 2.2.2.

$$section = 2\sqrt{3}B^2 \quad (2.2.7)$$

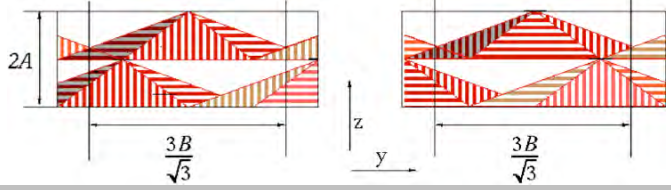
$$section_r = 2\sqrt{3}B_r^2 \quad (2.2.7r)$$

The *approach* is the trisine cell *cavity* projection on to the *y*, *z* plane as indicated in figure 2.2.3.

$$approach = \frac{1}{2} \frac{3B}{\sqrt{3}} 2A = \sqrt{3}AB \quad (2.2.8)$$

$$approach_r = \frac{1}{2} \frac{3B_r}{\sqrt{3}} 2A_r = \sqrt{3}A_r B_r \quad (2.2.8r)$$

Figure 2.2.3 Trisine *approach* from both *cavity* approaches



The *side* is the trisine cell *cavity* projection on to the x, z plane as indicated in figure 2.2.4.

$$side = \frac{1}{2} 2A 2B = 2AB \quad (2.2.9)$$

$$side_r = \frac{1}{2} 2A_r 2B_r = 2A_r B_r \quad (2.2.9r)$$

Figure 2.2.4 Trisine *side* view from both *cavity* sides

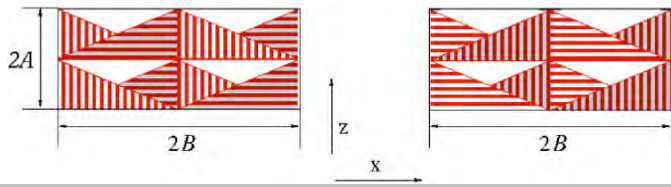
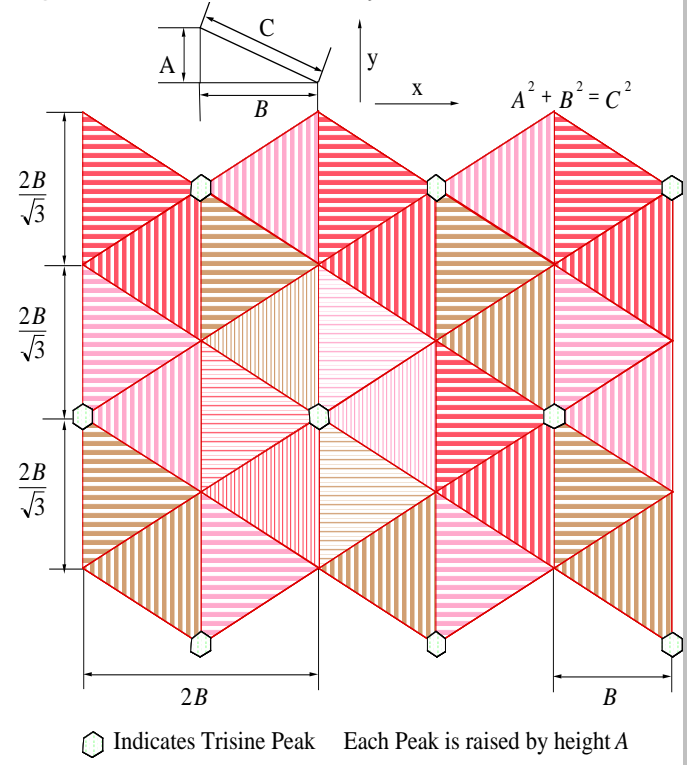


Table 2.2.2 Trisine Cavity and Section with plot

Condition	1.2	1.3	1.6	1.9	1.10	1.11
$T_a ({}^0 K)$	6.53E+11	6.53E+11	6.53E+11	6.53E+11	6.53E+11	6.53E+11
$T_b ({}^0 K)$	9.05E+14	5.48E+13	9.22E+08	1.10E+07	2,868	2.723
$T_{br} ({}^0 K)$	3.30E+12	5.45E+13	3.24E+18	2.72E+20	1.04E+24	1.10E+27
$T_c ({}^0 K)$	8.96E+13	3.28E+11	93.0	0.0131	8.99E-10	8.10E-16
$T_{cr} ({}^0 K)$	1.19E+09	3.25E+11	1.15E+21	8.11E+24	1.19E+32	1.32E+38
$z_R + 1$	3.67E+43	8.14E+39	3.89E+25	6.53E+19	1.17E+09	1.00E+00
$z_B + 1$	3.32E+14	2.01E+13	3.39E+08	4.03E+06	1.05E+03	1.00E+00
$Age_{UG} (sec)$	7.14E-05	4.79E-03	6.94E+04	5.36E+07	1.27E+13	4.33E+17
$Age_{UGv} (sec)$	4.59E-10	1.25E-07	4.42E+02	3.13E+06	1.22E+13	4.33E+17
$Age_U (sec)$	1.18E-26	5.31E-23	1.11E-08	6.63E-03	3.70E+08	4.33E+17
$cavity (cm^3)$	4.28E-40	1.93E-36	4.05E-22	2.41E-16	1.35E-05	15745
$cavity_r (cm^3)$	8.85E-33	1.96E-36	9.36E-51	1.57E-56	2.81E-67	2.41E-76

$chain (cm^3)$	2.86E-40	1.29E-36	2.70E-22	1.61E-16	8.98E-06	10497
$chain_r (cm^3)$	5.90E-33	1.31E-36	6.24E-51	1.05E-56	1.88E-67	1.61E-76
$section (cm^2)$	1.53E-26	4.19E-24	1.48E-14	1.05E-10	1.53E-03	1694
$section_r (cm^2)$	1.15E-21	4.23E-24	1.20E-33	1.69E-37	1.16E-44	1.04E-50
$approach (cm^2)$	3.22E-27	8.80E-25	3.10E-15	2.20E-11	3.21E-04	356
$approach_r (cm^2)$	2.42E-22	8.88E-25	2.52E-34	3.56E-38	2.43E-45	2.19E-51
$side (cm^2)$	3.72E-27	1.02E-24	3.58E-15	2.54E-11	3.71E-04	411
$side_r (cm^2)$	2.80E-22	1.03E-24	2.91E-34	4.11E-38	2.81E-45	2.53E-51

Figure 2.2.5 Trisine Geometry



◇ Indicates Trisine Peak Each Peak is raised by height A

2.3 Trisine Characteristic Wave Vectors

Superconducting resonant model trisine characteristic wave vectors K_{Dn} , K_{Ds} and K_C are defined in equations 2.3.1 - 2.3.3 below where K_{Dn} is the conventional Fermi surface vector.

$$K_{Dn} = \left(\frac{6\pi^2}{cavity} \right)^{\frac{1}{3}} = \left(\frac{3\pi^2 \mathbb{C}}{cavity} \right)^{\frac{1}{3}} \quad (2.3.1)$$

$$K_{Dnr} = \left(\frac{6\pi^2}{cavity_r} \right)^{\frac{1}{3}} = \left(\frac{3\pi^2 \mathbb{C}}{cavity_r} \right)^{\frac{1}{3}} \quad (2.3.1r)$$

The relationship in equation 2.3.1 represents the normal Debye wave vector (K_{Dn}) assuming the *cavity* volume

conforming to a sphere in K space and also defined in terms of K_A , K_P and K_B as defined in equations 2.3.4, 2.3.5 and 2.3.6.

See Appendix B for the derivation of equation 2.3.1.

$$K_{Ds} = \left(\frac{8\pi^3}{cavity} \right)^{\frac{1}{3}} = \left(\frac{4\pi^3 C}{cavity} \right)^{\frac{1}{3}} = (K_A K_B K_P)^{\frac{1}{3}} \quad (2.3.2)$$

$$K_{Ds} = \left(\frac{8\pi^3}{cavity} \right)^{\frac{1}{3}} = \left(\frac{4\pi^3 C}{cavity} \right)^{\frac{1}{3}} = (K_A K_B K_P)^{\frac{1}{3}} \quad (2.3.2r)$$

The relationship in equation 2.3.2 represents the normal Debye wave vector (K_{Ds}) assuming the *cavity* volume conforming to a characteristic trisine cell in K space.

See Appendix B for the derivation of equation 2.3.2.

$$K_C = \frac{4\pi}{3\sqrt{3}A} \quad (2.3.3)$$

$$K_{Cr} = \frac{4\pi}{3\sqrt{3}A_r} \quad (2.3.3r)$$

The relationship in equation 2.3.3 represents the result of equating one-dimensional and trisine density of states. See Appendix C for the derivation of equation 2.3.3.

Equations 2.3.4, 2.3.5, and 2.3.6 translate the trisine wave vectors K_C , K_{Ds} , and K_{Dn} (K_{Cr} , K_{Dsr} , and K_{Dnr}) into x, y, z Cartesian coordinates as represented by K_B , K_P and K_A (K_{Br} , K_{Pr} and K_{Ar}) respectively. The superconducting current is in the x direction.

$$K_B = \frac{2\pi}{2B} \quad (2.3.4)$$

$$K_{Br} = \frac{2\pi}{2B_r} \quad (2.3.4r)$$

$$K_P = \frac{2\pi\sqrt{3}}{3B} \quad (2.3.5)$$

$$K_{Pr} = \frac{2\pi\sqrt{3}}{3B_r} \quad (2.3.5r)$$

$$K_A = \frac{2\pi}{A} \quad (2.3.6)$$

$$K_{Ar} = \frac{2\pi}{A_r} \quad (2.3.6r)$$

Note that the sorted energy relationships of wave vectors are as follows:

$$K_A^2 > K_C^2 > K_{Ds}^2 > K_P^2 > K_{Dn}^2 > K_B^2 \quad (2.3.7)$$

$$K_{Ar}^2 > K_{Cr}^2 > K_{Dsr}^2 > K_{Pr}^2 > K_{Dnr}^2 > K_{Br}^2 \quad (2.3.7r)$$

Equation 2.3.8 relates addition of wave function amplitudes ($B/\sqrt{3}$), ($P/2$), ($B/2$) in terms of superconducting resonate energy ($k_b T_c$) congruent with Feynman[40].

$$k_b T_c = \frac{cavity}{chain \ time_{\pm}} \hbar \left(\begin{array}{l} + \frac{K_B}{2B} \left(\frac{B}{\sqrt{3}} \right)^2 \\ + \frac{K_P}{2P} \left(\frac{P}{2} \right)^2 \\ + \frac{K_A}{2A} \left(\frac{A}{2} \right)^2 \end{array} \right) \quad (2.3.8)$$

$$k_b T_{cr} = \frac{cavity_r}{chain_r \ time_{r\pm}} \hbar \left(\begin{array}{l} + \frac{K_{Br}}{2B} \left(\frac{B_r}{\sqrt{3}} \right)^2 \\ + \frac{K_{Pr}}{2P} \left(\frac{P_r}{2} \right)^2 \\ + \frac{K_{Ar}}{2A_r} \left(\frac{A_r}{2} \right)^2 \end{array} \right) \quad (2.3.8r)$$

The wave vector (K_B) and (K_{Br}), associated with the lowest energy ($\sim K_B^2$) and ($\sim K_{Br}^2$), is the carrier of the superconducting energy and in accordance with derivation in appendix A. All of the other wave vectors are contained within the cell *cavity* with many relationships with one indicated in 2.3.9 with the additional wave vector (K_C) defined in 2.3.10

$$\frac{m_e m_t}{m_e + m_t} \frac{1}{K_B^2} + \frac{m_t m_p}{m_t + m_p} \frac{1}{K_A^2} = \frac{1}{6} g_s^2 m_t \frac{1}{K_C^2} \quad (2.3.9)$$

$$K_C = \frac{1}{g_s} \frac{2\pi}{\sqrt{A^2 + B^2}} = \frac{4\pi}{3\sqrt{3}A} \quad (2.3.10)$$

The wave vector K_C is considered the hypotenuse vector because of its relationship to K_A and K_B .

The conservation of momentum and energy relationships in 2.3.11, 2.3.12 and 2.1.22 result in a convergence to a trisine lattice B/A (B/A_r) ratio of 2.379761271 and trisine mass (m_t) of 110.12275343 x electron mass (m_e). Essentially a

reversible process or reaction is defined recognizing that momentum is a vector and energy is a scalar.

Conservation Of Momentum

$$\sum_{n=B, C, Ds, Dn} \Delta p_n \Delta x_n = 0 \quad (2.3.11)$$

$$g_s (\pm K_B \pm K_C) \rightleftharpoons \pm K_{Ds} \pm K_{Dn}$$

Conservation Of Momentum

$$\sum_{n=B_r, C_r, Dsr, Dnr} \Delta p_n \Delta x_n = 0 \quad (2.3.11r)$$

$$g_s (\pm K_{Br} \pm K_{Cr}) \rightleftharpoons \pm K_{Dsr} \pm K_{Dnr}$$

Conservation Of Energy

$$\sum_{n=B, C, Ds, Dn} \Delta E_n \Delta t_n = 0 \quad (2.3.12)$$

$$K_B^2 + K_C^2 = g_s (K_{Ds}^2 + K_{Dn}^2)$$

Conservation Of Energy

$$\sum_{n=B_r, C_r, Dsr, Dnr} \Delta E_n \Delta t_n = 0 \quad (2.3.12r)$$

$$K_{Br}^2 + K_{Cr}^2 = g_s (K_{Dsr}^2 + K_{Dnr}^2)$$

The momentum and energy equations 2.3.11 and 2.3.12 solutions are exact and independent of B or A and totally dependent on the ratio B/A .

The momentum ratio is then expressed as:

$$\frac{g_s}{9} \pi \left(9 + 4\sqrt{3} \frac{B}{A} \right) = \left(\frac{B}{A} \right)^{\frac{1}{3}} \left(3 + 6^{\frac{2}{3}} \pi^{\frac{1}{3}} \right) \pi^{\frac{2}{3}} 3^{-\frac{5}{6}} \quad (2.3.13)$$

$$\frac{g_s}{9} \pi \left(9 + 4\sqrt{3} \frac{B_r}{A_r} \right) = \left(\frac{B_r}{A_r} \right)^{\frac{1}{3}} \left(3 + 6^{\frac{2}{3}} \pi^{\frac{1}{3}} \right) \pi^{\frac{2}{3}} 3^{-\frac{5}{6}} \quad (2.3.13r)$$

The energy is then expressed as:

$$\left(27 + 16 \left(\frac{B}{A} \right)^2 \right) \pi^{\frac{2}{3}} = 9 \cdot 3^{\frac{1}{3}} \left(\frac{B}{A} \right)^{\frac{2}{3}} g_s \left(3 + 2 \cdot 6^{\frac{1}{3}} \pi^{\frac{2}{3}} \right) \quad (2.3.14)$$

$$\left(27 + 16 \left(\frac{B_r}{A_r} \right)^2 \right) \pi^{\frac{2}{3}} = 9 \cdot 3^{\frac{1}{3}} \left(\frac{B_r}{A_r} \right)^{\frac{2}{3}} g_s \left(3 + 2 \cdot 6^{\frac{1}{3}} \pi^{\frac{2}{3}} \right) \quad (2.3.14r)$$

Representing an exact solution of two simultaneous equations with

Trisine size ratio $(B/A)_t$ or $(B_r/A_r)_t$,

$$= 2.379146658937169267\dots$$

Superconductorgyro-factor $g_s = 1.0098049781877999262\dots$

Another perspective of this resonant energy and momentum convergence is contained in Appendix A.

Numerical values of wave vectors are listed in Table 2.3.1.

The visible reflective luminal resonant discontinuity ($v_{dx} \sim c$) occurs at the critical temperature $T_c \sim 1.3E12$ K, $K_B \sim 5.7E12$ cm $^{-1}$ and $B \sim 5.5E-13$ cm. This discontinuity forms potential barrier providing a probable mechanism for limiting nuclear size.

Table 2.3.1 Trisine wave vectors

Condition	1.2	1.3	1.6	1.9	1.10	1.11
$T_a ({}^0 K)$	6.53E+11	6.53E+11	6.53E+11	6.53E+11	6.53E+11	6.53E+11
$T_b ({}^0 K)$	9.05E+14	5.48E+13	9.22E+08	1.10E+07	2,868	2.723
$T_{br} ({}^0 K)$	3.30E+12	5.45E+13	3.24E+18	2.72E+20	1.04E+24	1.10E+27
$T_c ({}^0 K)$	8.96E+13	3.28E+11	93.0	0.0131	8.99E-10	8.10E-16
$T_{cr} ({}^0 K)$	1.19E+09	3.25E+11	1.15E+21	8.11E+24	1.19E+32	1.32E+38
$z_R + 1$	3.67E+43	8.14E+39	3.89E+25	6.53E+19	1.17E+09	1.00E+00
$z_B + 1$	3.32E+14	2.01E+13	3.39E+08	4.03E+06	1.05E+03	1.00E+00
$Age_{UG} (sec)$	7.14E-05	4.79E-03	6.94E+04	5.36E+07	1.27E+13	4.33E+17
$Age_{UGV} (sec)$	4.59E-10	1.25E-07	4.42E+02	3.13E+06	1.22E+13	4.33E+17
$Age_U (sec)$	1.18E-26	5.31E-23	1.11E-08	6.63E-03	3.70E+08	4.33E+17
$K_B (/cm)$	4.72E+13	2.86E+12	4.81E+07	5.72E+05	1.50E+02	1.42E-01
$K_{Br} (/cm)$	1.72E+11	2.84E+12	1.69E+17	1.42E+19	5.43E+22	5.72E+25
$K_{Dn} (/cm)$	5.17E+13	3.13E+12	5.27E+07	6.26E+05	1.64E+02	1.56E-01
$K_{Dnr} (/cm)$	1.88E+11	3.11E+12	1.85E+17	1.56E+19	5.95E+22	6.26E+25
$K_{Ds} (/cm)$	8.33E+13	5.04E+12	8.49E+07	1.01E+06	2.64E+02	2.51E-01
$K_{Dsr} (/cm)$	3.04E+11	5.02E+12	2.98E+17	2.51E+19	9.59E+22	1.01E+26
$K_C (/cm)$	8.65E+13	5.23E+12	8.81E+07	1.05E+06	2.74E+02	2.60E-01
$K_{Cr} (/cm)$	3.15E+11	5.21E+12	3.09E+17	2.60E+19	9.95E+22	1.05E+26
$K_P (/cm)$	5.45E+13	3.30E+12	5.56E+07	6.60E+05	1.73E+02	1.64E-01
$K_{Pr} (/cm)$	1.99E+11	3.28E+12	1.95E+17	1.64E+19	6.27E+22	6.61E+25
$K_A (/cm)$	2.25E+14	1.36E+13	2.29E+08	2.72E+06	7.12E+02	6.76E-01
$K_{Ar} (/cm)$	8.19E+11	1.35E+13	8.04E+17	6.76E+19	2.59E+23	2.72E+26

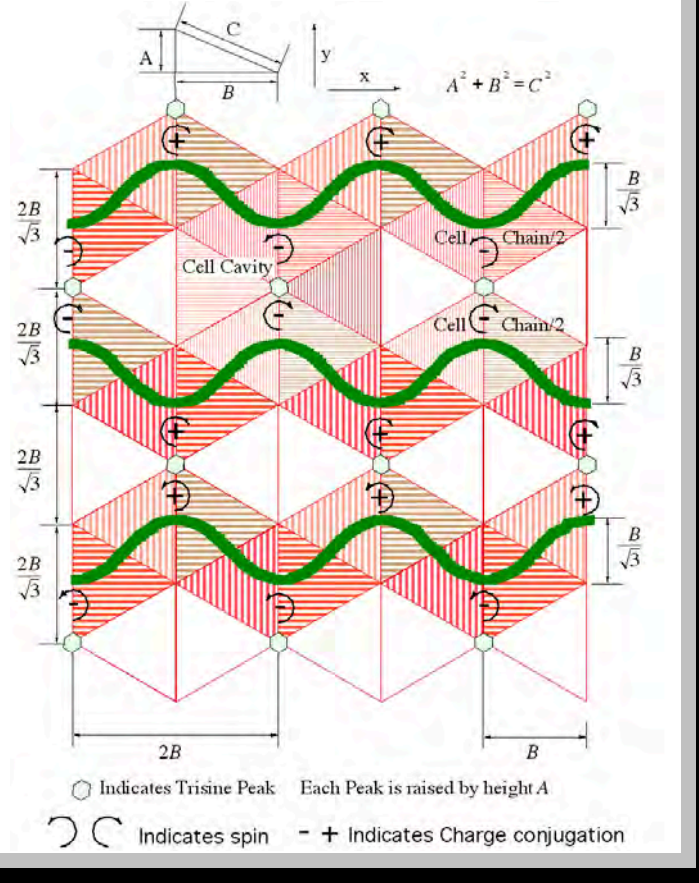
Negative and positive charge reversal as well as $time_{\pm}$ reversal takes place in mirror image parity pairs as is more visually seen in perspective presented in Figure 2.3.2.

It is important to reiterate that these triangular lattice representations are virtual and equivalent to a virtual reciprocal lattice but as geometric entities, do describe and correlate the physical data quite well.

The cavity arranged in a space filling lattice may be

considered 3D tessellated throughout the universe and congruent with the ‘dark energy’ concept scaled back to Big Bang nucleosynthesis.

Figure 2.3.1 Trisine Steric Charge Conjugate Pair Change Time Reversal CPT Geometry.



The Cartesian de Broglie velocities (v_{dx}), (v_{dy}), and (v_{dz}) are computed with the trisine Cooper CPT Charge conjugated pair residence *resonant CPT time* $_{\pm}$ and characteristic angular frequency (ω) in phase with trisine superconducting dimension ($2B$) in equations 2.4.1-2.4.5.

$$v_{dx} = \frac{\hbar K_B}{m_t} = \frac{2B}{time_{\pm}} = \frac{\omega}{2\pi} 2B \quad (2.4.1)$$

$$v_{dxx} = \frac{\hbar K_{Br}}{m_t} = \frac{2B_r}{time_{r\pm}} = \frac{\omega_r}{2\pi} 2B_r \quad (2.4.1r)$$

With $time_{\pm}$ and B as a function of the universal constant(U)

$$time_{\pm} = \hbar^{\frac{1}{3}} U^{\frac{-1}{3}} c^{\frac{-5}{3}} \left(\frac{c}{v_{dx}} \right)^2 \frac{2\pi}{\cos(\theta)} \quad (2.4.2)$$

$$time_{r\pm} = \hbar^{\frac{1}{3}} U^{\frac{-1}{3}} c^{\frac{-5}{3}} \left(\frac{c}{v_{dxx}} \right)^2 \frac{2\pi}{\cos(\theta)} \quad (2.4.2r)$$

In equation 2.4.1, note that $m_t v_{ex}/eH_c$ is the particle spin axis precession rate in the critical magnetic field (H_c). This electron spin rate is in tune with the electron moving with de Broglie velocity (v_{dx}) with a CPT residence $time_{\pm}$ in each cavity. In other words the Cooper CPT Charge conjugated pair flip spin twice per cavity and because each Cooper CPT Charge conjugated pair flips simultaneously, the quantum is an $2(1/2)$ or integer which corresponds to a boson.

$$time_{\pm} = \frac{g_s^3}{3} \frac{m_t v_{ex}}{eH_c} \quad (2.4.3)$$

$$time_{r\pm} = \frac{g_s^3}{3} \frac{m_t v_{exr}}{eH_{cr}} \quad (2.4.3r)$$

Equation 2.4.4 is a Higgs expression of superconductivity with the addition of the dielectric (ϵ or D/E) factor.

$$time_{\pm} = g_s^2 \left(\frac{2\epsilon m_t cavity}{e^2} \right)^{\frac{1}{2}} \quad (2.4.4)$$

$$time_{\pm} = g_s^2 \left(\frac{2\epsilon m_t cavity}{e^2} \right)^{\frac{1}{2}} \quad (2.4.4r)$$

Equation 2.4.5 is an expression of universal oscillation.

$$time_{\pm} = \frac{1}{\sqrt{3}} \frac{B}{A} \frac{v_{dx}}{cH_U} \quad (2.4.5)$$

$$time_{r\pm} = \frac{1}{\sqrt{3}} \frac{B_r}{A_r} \frac{v_{dxr}}{cH_{Ur}} \quad (2.4.5r)$$

Or in terms of the Kolmogorov viscosity (v_U) time scale[60]

$$time_{\pm} = \sqrt{\frac{B}{A} \frac{m_t v_U time_{\pm}}{k_b T_c}} \quad (2.4.4)$$

$$time_{r\pm} = \sqrt{\frac{B_r}{A_r} \frac{m_t v_U time_{r\pm}}{k_b T_{cr}}} \quad (2.4.4r)$$

Or in terms of universe mass and gravity dimensions

$$time_{\pm} = \frac{\hbar G_U M_U}{6 m_t A c^4} \quad (2.4.5)$$

$$time_{r\pm} = \frac{\hbar G_{Ur} M_{Ur}}{6 m_t A_r c^4} \quad (2.4.5r)$$

Then the de Broglie matter (m_t) velocities are defined:

$$v_{dy} = \frac{\hbar K_P}{m_t} = \frac{2}{\sqrt{3}} \frac{2B}{time_{\pm}} \quad (2.4.6)$$

$$v_{dyr} = \frac{\hbar K_{Pr}}{m_t} = \frac{2}{\sqrt{3}} \frac{2B_r}{time_{r\pm}} \quad (2.4.6r)$$

$$v_{dz} = \frac{\hbar K_A}{m_t} = 2 \left(\frac{B}{A} \right)^2 \frac{2A}{time_{\pm}} \quad (2.4.7)$$

$$v_{dzc} = \frac{\hbar K_{Ar}}{m_t} = 2 \left(\frac{B_r}{A_r} \right)^2 \frac{2A_r}{time_{r\pm}} \quad (2.4.7r)$$

The vector sum of the x , y and z de Broglie velocity components are used to compute a three dimensional helical or tangential de Broglie velocity (v_{dt}) as follows:

$$v_{dt} = \sqrt{v_{dx}^2 + v_{dy}^2 + v_{dz}^2} \\ = \frac{\hbar}{m_t} \sqrt{K_A^2 + K_B^2 + K_P^2} \quad (2.4.8)$$

$$v_{dTr} = \sqrt{v_{dxr}^2 + v_{dyr}^2 + v_{dzc}^2} \\ = \frac{\hbar}{m_t} \sqrt{K_{Ar}^2 + K_{Br}^2 + K_{Pr}^2} \quad (2.4.8r)$$

And in terms of reflective velocities:

$$v_{dxr} = \left(\frac{c}{v_{dx}} \right) c \quad v_{dyr} = \frac{4}{3} \left(\frac{c}{v_{dy}} \right) c \quad v_{dzc} = 4 \left(\frac{B}{A} \right)^2 \left(\frac{c}{v_{dz}} \right) c \quad (2.4.9)$$

$$\frac{1}{v_{dTr}} = \sqrt{\frac{1}{v_{dxr}^2} + \frac{1}{v_{dyr}^2} + \frac{1}{v_{dzc}^2}} \quad (2.4.10)$$

And the Majorana condition is fulfilled as follows resulting in a constant mass that can be considered a reciprocal of itself under the two time conditions $time_{+}$ and $time_{-}$ ($time_{r\pm}$ and $time_{r-}$).

Schroedinger condition

$$-i\hbar \frac{\partial}{\partial time_r} \Psi_{+} + \frac{2\pi\hbar}{2time_r} \Psi_{-} = 0 \quad (2.4.11)$$

$$\text{where } \Psi_{+} = e^{\frac{-im_t v_{dx}^2 time_{\pm}}{2\hbar}} \quad \Psi_{-} = e^{\frac{-im_t v_{dx}^2 time_{-}}{2\hbar}}$$

Majorana condition

$$-i\hbar \frac{\partial}{\partial time_r} \Psi_{+} + m_t c^2 \Psi_{-} = 0 \quad (2.4.12)$$

$$\text{where } \Psi_{+} = e^{\frac{-i\pi c^2 time_r^2}{(2B)^2}} \quad \Psi_{-} = e^{\frac{-i\pi c^2 time_{-}^2}{(2B)^2}}$$

and for both *Schroedinger* and *Majorana* conditions

$$\frac{(2B_r)^2}{time_{\pm}} = .06606194571 \frac{cm^2}{sec} \quad (2.4.13)$$

$$\text{and } m_t = \frac{\hbar 2\pi time_{\pm}}{(2B)^2} = 1.003008448E-25 g$$

Schroedinger condition

$$-i\hbar \frac{\partial}{\partial time_r} \Psi_{r+} + \frac{2\pi\hbar}{2time_r} \Psi_{r-} = 0 \quad (2.4.11r)$$

$$\text{where } \Psi_{r+} = e^{\frac{-im_t v_{dxr}^2 time_{r+}}{2\hbar}} \quad \Psi_{r-} = e^{\frac{-im_t v_{dxr}^2 time_{r-}}{2\hbar}}$$

Majorana condition

$$-i\hbar \frac{\partial}{\partial \text{time}_r} \Psi_{r+} + m_t c^2 \Psi_{r-} = 0 \quad (2.4.12r)$$

where $\Psi_{r+} = e^{\frac{-i\pi c^2 \text{time}_{r+}^2}{(2B_r)^2}}$ $\Psi_{r-} = e^{\frac{-i\pi c^2 \text{time}_{r-}^2}{(2B_r)^2}}$

and for both *Schroedinger* and *Majorana* conditions

$$\frac{(2B_r)^2}{\text{time}_{r\pm}^2} = .06606194571 \frac{\text{cm}^2}{\text{sec}} \quad (2.4.13r)$$

$$\text{and } m_t = \frac{\hbar 2\pi \text{time}_{r\pm}}{(2B_r)^2} = 1.003008448E-25 \text{ g}$$

Table 2.4.1 Listing of de Broglie velocities, trisine cell pair residence resonant *CPT time* $_{\pm}$ and characteristic frequency (ν) as a function of selected critical temperature (T_c) and black body temperature (T_b) along with a *time* $_{\pm}$ plot.

Condition	1.2	1.3	1.6	1.9	1.10	1.11
$T_a ({}^0 \text{K})$	6.53E+11	6.53E+11	6.53E+11	6.53E+11	6.53E+11	6.53E+11
$T_b ({}^0 \text{K})$	9.05E+14	5.48E+13	9.22E+08	1.10E+07	2.868	2.723
$T_{br} ({}^0 \text{K})$	3.30E+12	5.45E+13	3.24E+18	2.72E+20	1.04E+24	1.10E+27
$T_c ({}^0 \text{K})$	8.96E+13	3.28E+11	93.0	0.0131	8.99E-10	8.10E-16
$T_{cr} ({}^0 \text{K})$	1.19E+09	3.25E+11	1.15E+21	8.11E+24	1.19E+32	1.32E+38
$z_R + 1$	3.67E+43	8.14E+39	3.89E+25	6.53E+19	1.17E+09	1.00E+00
$z_B + 1$	3.32E+14	2.01E+13	3.39E+08	4.03E+06	1.05E+03	1.00E+00
$\text{Age}_{UG} (\text{sec})$	7.14E-05	4.79E-03	6.94E+04	5.36E+07	1.27E+13	4.33E+17
$\text{Age}_{UGv} (\text{sec})$	4.59E-10	1.25E-07	4.42E+02	3.13E+06	1.22E+13	4.33E+17
$\text{Age}_U (\text{sec})$	1.18E-26	5.31E-23	1.11E-08	6.63E-03	3.70E+08	4.33E+17
$v_{dx} (\text{cm/sec})$	4.97E+11	3.00E+10	5.06E+05	6.01E+03	1.57E+00	1.49E-03
$v_{dxr} (\text{cm/sec})$	1.81E+09	2.99E+10	1.78E+15	1.49E+17	5.71E+20	6.02E+23
$v_{dy} (\text{cm/sec})$	5.73E+11	3.47E+10	5.84E+05	6.94E+03	1.82E+00	1.72E-03
$v_{dyr} (\text{cm/sec})$	2.09E+09	3.45E+10	2.05E+15	1.73E+17	6.60E+20	6.95E+23
$v_{dz} (\text{cm/sec})$	2.36E+12	1.43E+11	2.41E+06	2.86E+04	7.49E+00	7.11E-03
$v_{dzc} (\text{cm/sec})$	8.61E+09	1.42E+11	8.45E+15	7.11E+17	2.72E+21	2.86E+24
$v_{dtr} (\text{cm/sec})$	2.48E+12	1.50E+11	2.53E+06	3.01E+04	7.86E+00	7.46E-03
$v_{dtr} (\text{cm/sec})$	9.04E+09	1.49E+11	8.88E+15	7.47E+17	2.85E+21	3.01E+24
$\text{time}_{\pm} (\text{sec})$	2.68E-25	7.32E-23	2.58E-13	1.83E-09	2.67E-02	2.96E+04
$\text{time}_{r\pm} (\text{sec})$	2.02E-20	7.39E-23	2.09E-32	2.96E-36	2.02E-43	1.82E-49
$\nu (\text{/sec}) \text{ Hz}$	3.73E+24	1.37E+22	3.88E+12	5.47E+08	3.75E+01	3.38E-05
$\nu_r (\text{/sec}) \text{ Hz}$	4.96E+19	1.35E+22	4.78E+31	3.38E+35	4.94E+42	5.48E+48

It is important to note that the one degree of freedom *time* $_{\pm}$ (2.96E04 sec or (164 x 3) minutes) in table 2.4.1 corresponds to a ubiquitous 160 minute resonant signal in the Universe.[68,69] and which is also consistent with the observed Active Galactic Nuclei (AGN) power spectrum. This would be an indication that the momentum and energy conserving (elastic) space lattice existing in universe space is dynamically in tune with stellar, galactic objects (Appendix H). This appears logical, based on the fact the major part of the universe mass consists of this space lattice which can be defined in other terms as dark energy and its associated matter.

Additionally, the earth's hum [87] with a harmonic of .09 Hz (f_1) as measured by seismographs is correlated to universe frequency (*1/time* $_{\pm}$) 3.38E-5 Hz (f_2) by the air/earth density unitless ratio (.0014/5.519) ($\rho_2/\rho_1 = E_2/E_1$) by a factor of approximately 2/3, which is of course *chain/cavity*. This correlation is supported by telluric atmospheric sodium oscillations on the order of 3.38E-5 Hz[88]. This phenomenon may be explained in terms of De Broglie matter wave correlations:

$$E_1/f_1 = E_2/f_2 = h \text{ and } \rho_2/\rho_1 = E_2/E_1 = f_2/f_1 .$$

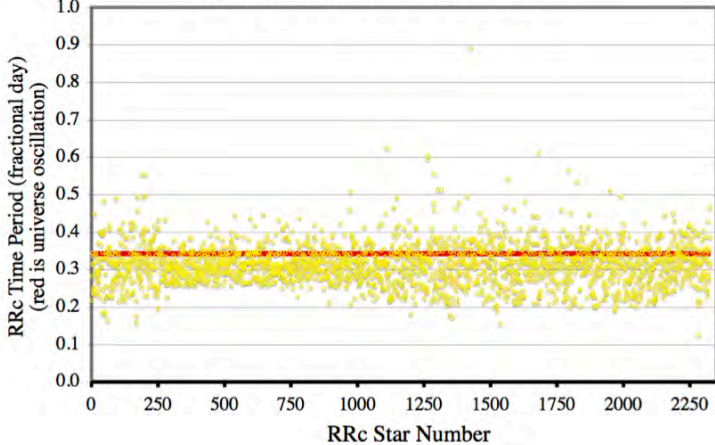
It is conceivable that these earth atmospheric resonance characteristics modulating the earth's center of mass (M) by resonant distance (r), may contribute to the flyby anomaly[86] by transferal of gravitational energy $GmM/(R+r)$ to a spacecraft of mass (m) and radius (R) from the center of mass during flyby. The increase in spacecraft energy is reported in terms of ~1 mm/sec and oscillatory universe dark energy induced earth atmospheric tidal effects result in spacecraft velocity calculated deviations of this order.

Also, an observed base oscillatory frequency of 2.91E-5 Hz has been observed in the star β Hydri that compares favorably (within 15%) to the anticipated universe frequency (*1/time* $_{\pm}$) 3.38E-5 Hz [102]. Harmonics of this base frequency are consistent with this base frequency.

This conceptual oscillatory view is supported by observed luminosity time periods for 2,327 RRc variable stars extracted from all constellations (The International Variable Star Index <http://www.aavso.org/vsx/> with 182,631 variable stars) as compiled in Figure 2.4.1. The RRc variable stars are old with low mass (with perhaps low atmospheric density), with high absolute magnitude (40 or 50 times brighter than our Sun), with sinusoidal oscillation character

and with metal-poor "Population II" star character. The RRc sinusoidal oscillation tidally (Appendix H) synchronizes with the universe trisine 'dark energy' oscillations. The average 2,327 RRc star time period is 0.316 day which differs from Table 2.4.1 prediction of 0.343 day (- 29,600 sec/(60x60x24) by 8.5% (which perhaps noncoincidentally $\sim 1/\cos(\theta)$).

Figure 2.4.1 RRc Variable Star Period



*CPT time*_± (9.23E-13 seconds) at $T_c = 26$ K is experimentally confirmed[132].

The trisine condition 1.11 (green) table 2.4.1 resonance *time* value of 29,600 seconds compares favorably with redshift adjusted Blazars[145 Figure 9] as presented in table 2.4.2.

trisine condition 1.11

(green) table 2.4.1	29,600	Seconds
	.3426	Days
	18.34	$\omega(2\pi/\text{days})$
	5.45E-02	1/ ω (days)
	-1.26	$\log_{10}(1/\omega)$ (days)

Table 2.4.2

Blazars	z_B	$1/\omega$ $(1+z_B)^{-2}$	\log_{10} $1/\omega$ $(1+z_B)^{-2}$
B2 1633+38	1.814	6.89E-03	-2.16
PKS 1424-41	1.522	8.57E-03	-2.07
B2 1520+31	1.487	8.82E-03	-2.05
PKS 0454-234	1.003	1.36E-02	-1.87
3C 454.3	0.859	1.58E-02	-1.80
3C 279	0.536	2.31E-02	-1.64
PKS 1510-089	0.360	2.95E-02	-1.53
3C 273	0.158	4.07E-02	-1.39
	0	5.45E-02	-1.26
BL Lacs			

3C 66A	0.444	2.61E-02	-1.58
PKS 0716+714	0.3	3.23E-02	-1.49
PKS 2155-304	0.116	4.38E-02	-1.36
BL Lac	0.069	4.77E-02	-1.32
Mkn 421	0.03	5.14E-02	-1.29

2.5 Dielectric Permittivity And Magnetic Permeability

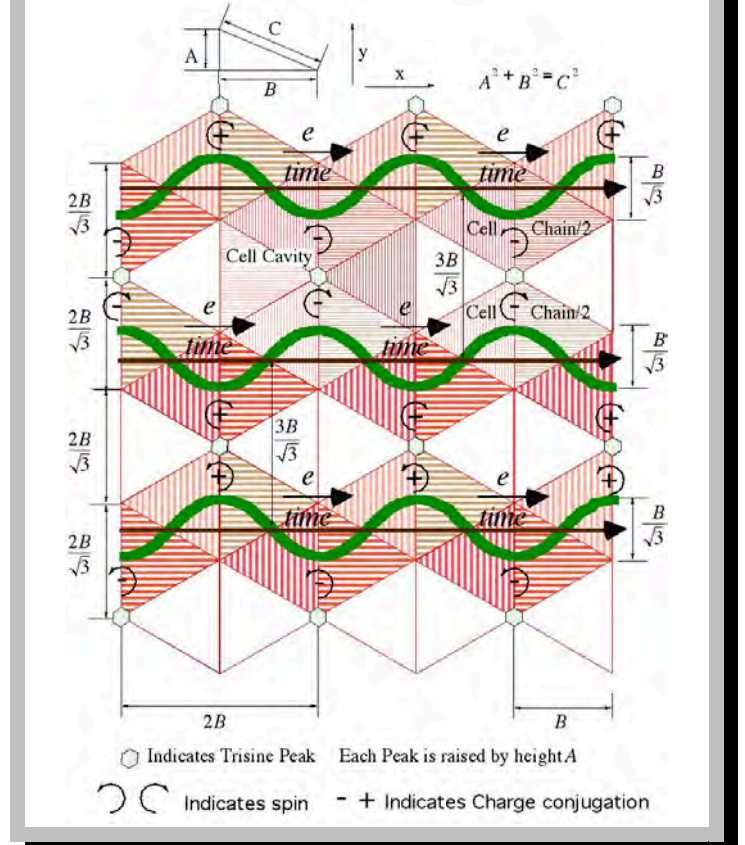
The development has origin in James Maxwell's establishment of the speed of light from previously experimentally observed constants

$$\frac{1}{\sqrt{\epsilon_0 \mu_0}} = c \left(2.998E8 \frac{m}{sec} \right)$$

$$\epsilon_0 = 8.854E-12 \frac{\text{farad}}{m} \left(\frac{\text{coulomb}^2 \text{sec}^2}{\text{kg m}^3} \right) \quad (2.5.1)$$

$$\epsilon_0 = 1.257E-6 \frac{\text{newton}}{\text{amp}^2} \left(\frac{\text{kg m}}{\text{coulomb}^2} \right)$$

Figure 2.5.1 as modified from Figure 2.3.1 Trisine Steric Charge Conjugate Pair Change Time Reversal CPT Geometry.



The material dielectric is computed by determining a displacement (D) (equation 2.5.1) and electric field (E)

(equation 2.5.2) and which establishes a dielectric (ϵ or D/E) (equation 2.5.3) and modified speed of light (v_e) (equations 2.5.4, 2.5.5). Then the superconducting fluxoid (Φ_e) (equation 2.5.6) can be calculated.

The electric field (E) is calculated by taking the translational energy $(m, v_{dx}^2/2)$ (which is equivalent to $k_b T_c$) over a distance, which is the trisine cell volume to surface ratio. This concept of the surface to volume ratio is used extensively in fluid mechanics for computing energies of fluids passing through various geometric forms and is called the hydraulic ratio.

$$\begin{aligned} E_{fx} \\ E_{fy} \\ E_{fz} \\ E_f \end{aligned} \left\{ \begin{aligned} & \frac{k_b T_c}{e2B} \\ & \frac{k_b T_c}{eP} \\ & \frac{k_b T_c}{eA} \\ & \left(E_{fx}^2 + E_{fy}^2 + E_{fz}^2 \right)^{1/2} \end{aligned} \right. \quad (2.5.2)$$

$$\begin{aligned} E_{fxr} \\ E_{fyr} \\ E_{fzr} \\ E_{fr} \end{aligned} \left\{ \begin{aligned} & \frac{k_b T_{cr}}{e2B_r} \\ & \frac{k_b T_{cr}}{eP_r} \\ & \frac{k_b T_{cr}}{eA_r} \\ & \left(E_{fxr}^2 + E_{fyr}^2 + E_{fzr}^2 \right)^{1/2} \end{aligned} \right. \quad (2.5.2r)$$

The trisine cell surface is ($section/\cos(\theta)$) and the volume is expressed as *cavity*. Note that the trisine *cavity*, although bounded by ($2section/\cos(\theta)$), still has the passageways for Cooper CPT Charge conjugated pairs ($\mathbb{C}e$) to move from cell *cavity* to cell *cavity*.

The displacement (D) as a measure of Gaussian surface containing free charges ($\mathbb{C} e_{\pm}$) is computed by taking the (4π) solid angle divided by the characteristic trisine area ($section/\cos(\theta)$) with the two(2) charges ($\mathbb{C} e_{\pm}$) contained therein and in accordance with Gauss's law as expressed in equation 2.1.1.

$$\begin{aligned} D_{fx} \\ D_{fy} \\ D_{fz} \\ D_f \end{aligned} \left\{ \begin{aligned} & \frac{\pi}{g_s} \frac{4\pi \mathbb{C}e}{approach} \\ & \frac{4\pi}{3g_s} \frac{4\pi \mathbb{C}e}{side} \\ & \frac{\sqrt{3}}{2g_s^2} \frac{4\pi \mathbb{C}e}{section} \\ & \left(D_{fx}^2 + D_{fy}^2 + D_{fz}^2 \right)^{1/2} \end{aligned} \right. \quad (2.5.3)$$

$$\begin{aligned} D_{fxr} \\ D_{fyr} \\ D_{fzr} \\ D_{fr} \end{aligned} \left\{ \begin{aligned} & \frac{\pi}{g_s} \frac{4\pi \mathbb{C}e}{approach_r} \\ & \frac{4\pi}{3g_s} \frac{4\pi \mathbb{C}e}{side_r} \\ & \frac{\sqrt{3}}{2g_s^2} \frac{4\pi \mathbb{C}e}{section_r} \\ & \left(D_{fxr}^2 + D_{fyr}^2 + D_{fzr}^2 \right)^{1/2} \end{aligned} \right. \quad (2.5.3r)$$

Now a dielectric coefficient (ϵ) can be calculated from the electric field (E) and displacement field (D) [61]. Note that $\epsilon < 1$ for group phase reflection velocities as justified by resonant condition as numerically indicated in table 2.5.1.

$$\begin{aligned} \epsilon_x \\ \epsilon_y \\ \epsilon_z \\ \epsilon \end{aligned} \left\{ \begin{aligned} & \frac{D_{fx}}{E_{fx}} \\ & \frac{D_{fy}}{E_{fy}} \\ & \frac{D_{fz}}{E_{fz}} \\ & \frac{1}{3g_s} \frac{D_f}{E_f} = \frac{3}{\frac{1}{\epsilon_x} + \frac{1}{\epsilon_y} + \frac{1}{\epsilon_z}} \end{aligned} \right. \quad (2.5.4)$$

$$\left. \begin{array}{l} \varepsilon_{xr} \\ \varepsilon_{yr} \\ \varepsilon_{zr} \\ \varepsilon_r \end{array} \right\} = \left\{ \begin{array}{l} \frac{D_{fxr}}{E_{fxr}} \\ \frac{D_{fyi}}{E_{fyi}} \\ \frac{D_{fzr}}{E_{fzr}} \\ \frac{1}{3g_s} \frac{D_{fr}}{E_{fr}} = \frac{3}{\frac{1}{\varepsilon_{xr}} + \frac{1}{\varepsilon_{yr}} + \frac{1}{\varepsilon_{zr}}} \end{array} \right. \quad (2.5.4r)$$

Velocity of light dielectric ε modified

$$\left. \begin{array}{l} v_{ex} \\ v_{ey} \\ v_{ez} \\ v_{\varepsilon} \end{array} \right\} = \left\{ \begin{array}{l} \frac{c}{\sqrt{\varepsilon_x}} \\ \frac{c}{\sqrt{\varepsilon_y}} \\ \frac{c}{\sqrt{\varepsilon_z}} \\ \frac{c}{\sqrt{\varepsilon_r}} \end{array} \right\} = \left\{ \begin{array}{l} v_{dx} \sqrt{k_{mx}} \\ v_{dy} \sqrt{k_{my}} \\ v_{dz} \sqrt{k_{mz}} \\ 2v_{dT} \sqrt{k_m} \end{array} \right. \quad (2.5.5)$$

$$\left. \begin{array}{l} v_{exr} \\ v_{eyr} \\ v_{ezr} \\ v_{\varepsilon r} \end{array} \right\} = \left\{ \begin{array}{l} \frac{c}{\sqrt{\varepsilon_{xr}}} \\ \frac{c}{\sqrt{\varepsilon_{yr}}} \\ \frac{c}{\sqrt{\varepsilon_{zr}}} \\ \frac{c}{\sqrt{\varepsilon_r}} \end{array} \right\} = \left\{ \begin{array}{l} v_{dxr} \sqrt{k_{mrx}} \\ v_{dyr} \sqrt{k_{myr}} \\ v_{dzr} \sqrt{k_{mzr}} \\ 2v_{dT} \sqrt{k_{mr}} \end{array} \right. \quad (2.5.5r)$$

Trisine incident/reflective angle (Figure 2.3.1) of 30 degrees is less than Brewster angle of $\tan^{-1}(\varepsilon/\varepsilon)^{1/2} = 45^\circ$ assuring total reflectivity as particles travel from trisine lattice cell to trisine lattice cell.

Now the fluxoid (Φ_ε) can be computed quantized according to ($\mathbb{C} e$) as experimentally observed in superconductors.

$$\Phi_\varepsilon = \frac{2\pi\hbar v_\varepsilon}{\mathbb{C} e_\pm} \quad (2.5.6)$$

What is generally called the Tao effect [65,66,67], wherein it is found that superconducting micro particles in the presence

of an electrostatic field aggregate into balls of macroscopic dimensions, is modeled by the calculated values for E in table 2.5.1. using equation 2.5.2. When the electrostatic field exceeds a critical value coincident with the critical temperature (T_b), the microscopic balls dissipate. This experimental evidence can be taken as another measure of superconductivity equivalent to the Meissner effect.

Table 2.5.1 Displacement (D) and Electric (E) Fields

Condition	1.2	1.3	1.6	1.9	1.10	1.11
$T_a ({}^0 K)$	6.53E+11	6.53E+11	6.53E+11	6.53E+11	6.53E+11	6.53E+11
$T_b ({}^0 K)$	9.05E+14	5.48E+13	9.22E+08	1.10E+07	2,868	2.723
$T_{br} ({}^0 K)$	3.30E+12	5.45E+13	3.24E+18	2.72E+20	1.04E+24	1.10E+27
$T_c ({}^0 K)$	8.96E+13	3.28E+11	93.0	0.0131	8.99E-10	8.10E-16
$T_{cr} ({}^0 K)$	1.19E+09	3.25E+11	1.15E+21	8.11E+24	1.19E+32	1.32E+38
$z_R + 1$	3.67E+43	8.14E+39	3.89E+25	6.53E+19	1.17E+09	1.00E+00
$z_B + 1$	3.32E+14	2.01E+13	3.39E+08	4.03E+06	1.05E+03	1.00E+00
$Age_{UG} (sec)$	7.14E-05	4.79E-03	6.94E+04	5.36E+07	1.27E+13	4.33E+17
$Age_{UGV} (sec)$	4.59E-10	1.25E-07	4.42E+02	3.13E+06	1.22E+13	4.33E+17
$Age_U (sec)$	1.18E-26	5.31E-23	1.11E-08	6.63E-03	3.70E+08	4.33E+17
$D_{fx} (erg/e/cm)$	1.17E+19	4.27E+16	1.21E+07	1.71E+03	1.17E-04	1.05E-10
$D_{fy} (erg/e/cm)$	1.35E+19	4.93E+16	1.40E+07	1.97E+03	1.35E-04	1.22E-10
$D_{fz} (erg/e/cm)$	6.81E+17	2.49E+15	7.07E+05	9.98E+01	6.83E-06	6.16E-12
$D_f (erg/e/cm)$	6.14E+17	2.25E+15	6.37E+05	9.00E+01	6.16E-06	5.55E-12
$D_{fxr} (erg/e/cm)$	1.55E+14	4.23E+16	1.49E+26	1.06E+30	1.54E+37	1.71E+43
$D_{fyi} (erg/e/cm)$	1.79E+14	4.88E+16	1.72E+26	1.22E+30	1.78E+37	1.98E+43
$D_{fzr} (erg/e/cm)$	9.04E+12	2.47E+15	8.71E+24	6.16E+28	9.01E+35	9.99E+41
$D_{fr} (erg/e/cm)$	8.15E+12	2.23E+15	7.85E+24	5.56E+28	8.12E+35	9.01E+41
$E_{fx} (erg/e/cm)$	1.94E+20	4.29E+16	2.05E+02	3.44E-04	6.15E-15	5.27E-24
$E_{fy} (erg/e/cm)$	2.23E+20	4.95E+16	2.36E+02	3.97E-04	7.11E-15	6.08E-24
$E_{fz} (erg/e/cm)$	9.21E+20	2.04E+17	9.74E+02	1.64E-03	2.93E-14	2.51E-23
$E_f (erg/e/cm)$	9.32E+19	2.07E+16	9.86E+01	1.66E-04	2.96E-15	2.54E-24
$E_f (volt/cm)$	2.79E+22	6.19E+18	2.96E+04	4.96E-02	8.89E-13	7.61E-22
$E_{fxr} (erg/e/cm)$	9.37E+12	4.23E+16	8.86E+30	5.28E+36	2.95E+47	3.44E+56
$E_{fyi} (erg/e/cm)$	1.08E+13	4.88E+16	1.02E+31	6.09E+36	3.40E+47	3.98E+56
$E_{fzr} (erg/e/cm)$	4.46E+13	2.01E+17	4.21E+31	2.51E+37	1.40E+48	1.64E+57
$E_{fr} (erg/e/cm)$	4.51E+12	2.04E+16	4.27E+30	2.54E+36	1.42E+47	1.66E+56
$\varepsilon_x D_{fx}/E_{fx}$	6.02E-02	9.96E-01	5.91E+04	4.97E+06	1.90E+10	2.00E+13
$\varepsilon_y D_{fy}/E_{fy}$	6.02E-02	9.96E-01	5.91E+04	4.97E+06	1.90E+10	2.00E+13
$\varepsilon_z D_{fz}/E_{fz}$	7.39E-04	1.22E-02	7.25E+02	6.10E+04	2.33E+08	2.46E+11
$\varepsilon D_f/E_f$	7.21E-04	1.19E-02	7.08E+02	5.96E+04	2.28E+08	2.40E+11
$\varepsilon_{xr} D_{fxr}/E_{fxr}$	1.65E+01	1.00E+00	1.68E-05	2.00E-07	5.24E-11	4.97E-14

ϵ_{yr}	D_{fyr}/E_{fyr}	1.65E+01	1.00E+00	1.68E-05	2.00E-07	5.24E-11	4.97E-14
ϵ_{xr}	D_{fxr}/E_{fxr}	2.03E-01	1.23E-02	2.07E-07	2.46E-09	6.42E-13	6.10E-16
ϵ_r	D_{fr}/E_{fr}	1.98E-01	1.20E-02	2.02E-07	2.40E-09	6.27E-13	5.95E-16
v_{ex} (cm/sec)		1.22E+11	3.00E+10	1.23E+08	1.34E+07	2.17E+05	6.70E+03
v_{ey} (cm/sec)		1.22E+11	3.00E+10	1.23E+08	1.34E+07	2.17E+05	6.70E+03
v_{ez} (cm/sec)		1.10E+12	2.71E+11	1.11E+09	1.21E+08	1.96E+06	6.05E+04
v_e (cm/sec)		1.12E+12	2.75E+11	1.13E+09	1.23E+08	1.99E+06	6.12E+04
v_{exr} (cm/sec)		7.36E+09	2.99E+10	7.29E+12	6.69E+13	4.13E+15	1.34E+17
v_{eyr} (cm/sec)		7.36E+09	2.99E+10	7.29E+12	6.69E+13	4.13E+15	1.34E+17
v_{ezr} (cm/sec)		6.66E+10	2.71E+11	6.60E+13	6.05E+14	3.74E+16	1.21E+18

A conversion between superconducting temperature and black body temperature is calculated in equation 2.5.9. Two primary energy related factors are involved, the first being the superconducting velocity (v_{dx}^2) to light velocity (v_e^2) and the second is normal Debye wave vector (K_{Dn}^2) to superconducting Debye wave vector (K_{Ds}^2) all of this followed by a minor rotational factor for each factor involving (m_e) and (m_p). For reference, a value of 2.729 K is used for the universe black body temperature (T_b) as indicated by experimentally observed microwave radiation by the Cosmic Background Explorer (COBE) and later satellites. Although the observed minor fluctuations (1 part in 100,000) in this universe background radiation indicative of clumps of matter forming shortly after the big bang, for the purposes of this report we will assume that the experimentally observed uniform radiation is indicative of present universe that is isotropic and homogeneous.

Now assume that the superconductor material magnetic permeability (k_m) is defined as per equation 2.5.12.

$$\begin{aligned} k_{mx} &= \begin{pmatrix} \frac{D_{fx}v_{ex}^2}{E_{fx}} & \frac{E_{fx}}{D_{fx}v_{dx}^2} \\ \frac{D_{fy}v_{ey}^2}{E_{fy}} & \frac{E_{fy}}{D_{fy}v_{dy}^2} \\ \frac{D_{fz}v_{ez}^2}{E_{fz}} & \frac{E_{fz}}{D_{fz}v_{dz}^2} \\ \frac{D_fv_e^2}{E_f} & \frac{E_f}{D_fv_{dT}^2} \end{pmatrix} = \begin{pmatrix} \frac{v_{ex}^2}{v_{dx}^2} \\ \frac{v_{ey}^2}{v_{dy}^2} \\ \frac{v_{ez}^2}{v_{dz}^2} \\ \frac{v_e^2}{v_{dT}^2} \end{pmatrix} \end{aligned} \quad (2.5.12)$$

$$\begin{aligned} k_{mxr} &= \begin{pmatrix} \frac{D_{fxr}v_{exr}^2}{E_{fxr}} & \frac{E_{fxr}}{D_{fxr}v_{dxr}^2} \\ \frac{D_{fyv_{eyr}}^2}{E_{fyv_{eyr}}} & \frac{E_{fyv_{eyr}}}{D_{fyv_{dyr}}^2} \\ \frac{D_{fzv_{ezr}}^2}{E_{fzv_{ezr}}} & \frac{E_{fzv_{ezr}}}{D_{fzv_{dzr}}^2} \\ \frac{D_{fv_{er}}^2}{E_{fv_{er}}} & \frac{E_{fv_{er}}}{D_{fv_{dT}}^2} \end{pmatrix} = \begin{pmatrix} \frac{v_{exr}^2}{v_{dxr}^2} \\ \frac{v_{eyr}^2}{v_{dyr}^2} \\ \frac{v_{ezr}^2}{v_{dzr}^2} \\ \frac{v_{er}^2}{v_{dT}^2} \end{pmatrix} \end{aligned} \quad (2.5.12r)$$

Then the de Broglie velocities (v_{dx} , v_{dy} and v_{dz}) as per equations 2.4.1, 2.4.2, 2.4.3 can be considered a sub- and super- luminal speeds of light internal to the superconductor resonant medium as per equation 2.5.13. These sub- and super- luminal resonant de Broglie velocities as presented in equation 2.5.13 logically relate to wave vectors K_A , K_B and K_P .

$$\begin{aligned} v_{dx} &= \begin{pmatrix} \frac{c}{\sqrt{k_{mx}\epsilon_x}} \\ \frac{c}{\sqrt{k_{my}\epsilon_y}} \\ \frac{c}{\sqrt{k_{mz}\epsilon_z}} \end{pmatrix} = \begin{pmatrix} \frac{v_{ex}}{\sqrt{k_{mx}}} \\ \frac{v_{ey}}{\sqrt{k_{my}}} \\ \frac{v_{ez}}{\sqrt{k_{mz}}} \end{pmatrix} \end{aligned} \quad (2.5.13)$$

$$\begin{aligned} v_{dxr} &= \begin{pmatrix} \frac{c}{\sqrt{k_{mxr}\epsilon_{xr}}} \\ \frac{c}{\sqrt{k_{myr}\epsilon_{yr}}} \\ \frac{c}{\sqrt{k_{mzr}\epsilon_{zr}}} \end{pmatrix} = \begin{pmatrix} \frac{v_{exr}}{\sqrt{k_{mxr}}} \\ \frac{v_{eyr}}{\sqrt{k_{myr}}} \\ \frac{v_{ezr}}{\sqrt{k_{mzr}}} \end{pmatrix} \end{aligned} \quad (2.5.13r)$$

Combining equations 2.5.12 and 2.5.13, the Cartesian dielectric sub- and super- luminal velocities (v_{ex} , v_{ey} & v_{ez}) can be computed and are presented in Table 2.5.3.

Table 2.5.3 Permittivities (ϵ), Permeabilities (k_m), Dielectric Velocities (v_ϵ)

Condition	1.2	1.3	1.6	1.9	1.10	1.11
$T_a ({}^0 K)$	6.53E+11	6.53E+11	6.53E+11	6.53E+11	6.53E+11	6.53E+11
$T_b ({}^0 K)$	9.05E+14	5.48E+13	9.22E+08	1.10E+07	2,868	2.723
$T_{br} ({}^0 K)$	3.30E+12	5.45E+13	3.24E+18	2.72E+20	1.04E+24	1.10E+27
$T_c ({}^0 K)$	8.96E+13	3.28E+11	93.0	0.0131	8.99E-10	8.10E-16
$T_{cr} ({}^0 K)$	1.19E+09	3.25E+11	1.15E+21	8.11E+24	1.19E+32	1.32E+38
$z_R + 1$	3.67E+43	8.14E+39	3.89E+25	6.53E+19	1.17E+09	1.00E+00
$z_B + 1$	3.32E+14	2.01E+13	3.39E+08	4.03E+06	1.05E+03	1.00E+00
Age_{UG} (sec)	7.14E-05	4.79E-03	6.94E+04	5.36E+07	1.27E+13	4.33E+17
Age_{UGv} (sec)	4.59E-10	1.25E-07	4.42E+02	3.13E+06	1.22E+13	4.33E+17
Age_U (sec)	1.18E-26	5.31E-23	1.11E-08	6.63E-03	3.70E+08	4.33E+17
$\epsilon_x D_{fx}/E_{fx}$	6.02E-02	9.96E-01	5.91E+04	4.97E+06	1.90E+10	2.00E+13
$\epsilon_y D_{fy}/E_{fy}$	6.02E-02	9.96E-01	5.91E+04	4.97E+06	1.90E+10	2.00E+13
$\epsilon_z D_{fz}/E_{fz}$	7.39E-04	1.22E-02	7.25E+02	6.10E+04	2.33E+08	2.46E+11
$\epsilon D_f/E_f$	7.21E-04	1.19E-02	7.08E+02	5.96E+04	2.28E+08	2.40E+11
$\epsilon_{xr} D_{fxr}/E_{fxr}$	1.65E+01	1.00E+00	1.68E-05	2.00E-07	5.24E-11	4.97E-14
$\epsilon_{yr} D_{fyf}/E_{fyf}$	1.65E+01	1.00E+00	1.68E-05	2.00E-07	5.24E-11	4.97E-14
$\epsilon_{xr} D_{frf}/E_{frf}$	2.03E-01	1.23E-02	2.07E-07	2.46E-09	6.42E-13	6.10E-16
$\epsilon_r D_{fr}/E_{fr}$	1.98E-01	1.20E-02	2.02E-07	2.40E-09	6.27E-13	5.95E-16
k_{mx}	6.05E-02	1.00E+00	5.94E+04	4.64E+06	1.83E+10	2.01E+13
k_{my}	4.54E-02	7.50E-01	4.45E+04	3.48E+06	1.37E+10	1.51E+13
k_{mz}	2.18E-01	3.60E+00	2.14E+05	1.67E+07	6.59E+10	7.24E+13
k_m	2.02E-01	3.34E+00	1.99E+05	1.55E+07	6.12E+10	6.73E+13
k_{mxr}	1.65E+01	1.00E+00	1.68E-05	2.15E-07	5.47E-11	4.97E-14
k_{myr}	1.24E+01	7.50E-01	1.26E-05	1.61E-07	4.10E-11	3.73E-14
k_{mzr}	5.98E+01	3.62E+00	6.09E-05	7.79E-07	1.98E-10	1.80E-13
k_{mr}	5.55E+01	3.36E+00	5.65E-05	7.23E-07	1.84E-10	1.67E-13
v_{ex} (cm/sec)	1.22E+11	3.00E+10	1.23E+08	1.34E+07	2.17E+05	6.70E+03
v_{ey} (cm/sec)	1.22E+11	3.00E+10	1.23E+08	1.34E+07	2.17E+05	6.70E+03
v_{ez} (cm/sec)	1.10E+12	2.71E+11	1.11E+09	1.21E+08	1.96E+06	6.05E+04
v_ϵ (cm/sec)	1.12E+12	2.75E+11	1.13E+09	1.23E+08	1.99E+06	6.12E+04
v_{exr} (cm/sec)	7.36E+09	2.99E+10	7.29E+12	6.69E+13	4.13E+15	1.34E+17
v_{eyr} (cm/sec)	7.36E+09	2.99E+10	7.29E+12	6.69E+13	4.13E+15	1.34E+17
v_{ezr} (cm/sec)	6.66E+10	2.71E+11	6.60E+13	6.05E+14	3.74E+16	1.21E+18
v_{er} (cm/sec)	6.74E+10	2.74E+11	6.68E+13	6.12E+14	3.79E+16	1.23E+18

Verification of equation 2.5.14 is indicated by the calculation that superconducting density ($m_t/cavity$) (table 2.9.1) and present universe density (equation 2.11.5) are equal at this Debye black body temperature (T_b) of $2.729 {}^0 K$

$$T_b = \mathbb{C} \left(\frac{k_{mx} \epsilon_x}{\epsilon} \right)^2 T_c = \mathbb{C} \left(\frac{v_\epsilon}{v_{dx}} \right)^2 T_c = m_t v_\epsilon^2 \frac{1}{k_b} \quad (2.5.14)$$

$$T_{br} = \mathbb{C} \left(\frac{k_{mxr} \epsilon_{xr}}{\epsilon_r} \right)^2 T_{cr} = \mathbb{C} \left(\frac{v_{er}}{v_{dxr}} \right)^2 T_{cr} = m_t v_{er}^2 \frac{1}{k_b} \quad (2.5.14r)$$

Based on the Cartesian dielectric velocities (v_{ex} , v_{ey} & v_{ez}), corresponding Cartesian fluxoids can be computed as per equation 2.5.16.

$$\left. \begin{array}{l} \Phi_{ex} \\ \Phi_{ey} \\ \Phi_{ez} \\ \Phi_\epsilon \end{array} \right\} = \left\{ \begin{array}{l} \frac{2\pi\hbar v_{ex}}{\mathbb{C} e_\pm} \\ \frac{2\pi\hbar v_{ey}}{\mathbb{C} e_\pm} \\ \frac{2\pi\hbar v_{ez}}{\mathbb{C} e_\pm} \\ \frac{2\pi\hbar v_\epsilon}{\mathbb{C} e_\pm} \end{array} \right\} \quad (2.5.15)$$

$$\left. \begin{array}{l} \Phi_{exr} \\ \Phi_{eyr} \\ \Phi_{ezr} \\ \Phi_{er} \end{array} \right\} = \left\{ \begin{array}{l} \frac{2\pi\hbar v_{exr}}{\mathbb{C} e_\pm} \\ \frac{2\pi\hbar v_{eyr}}{\mathbb{C} e_\pm} \\ \frac{2\pi\hbar v_{ezr}}{\mathbb{C} e_\pm} \\ \frac{2\pi\hbar v_{er}}{\mathbb{C} e_\pm} \end{array} \right\} \quad (2.5.15r)$$

The trisine residence *resonant CPT time* \pm is confirmed in terms of conventional capacitance (C) and inductance (L) resonant circuit relationships in x , y and z as well as *trisine* dimensions.

$$time_{\pm} = \left\{ \begin{array}{l} \sqrt{L_x} \sqrt{C_x} \\ \sqrt{L_y} \sqrt{C_y} \\ \sqrt{L_z} \sqrt{C_z} \\ \sqrt{L} \sqrt{C} \end{array} \right\} = \left\{ \begin{array}{l} \sqrt{\frac{\Phi_{ex} time_{\pm}}{4\pi C e v_{ex}}} \sqrt{\frac{approach \ \epsilon_x}{2\pi \ 2B}} \\ \sqrt{\frac{\Phi_{ey} time_{\pm}}{4\pi C e v_{ey}}} \sqrt{g_s \frac{\sqrt{3}}{2} \frac{side}{2\pi} \frac{\sqrt{3}\epsilon_y}{3B}} \\ \sqrt{\frac{\Phi_{ez} time_{\pm}}{4\pi C e v_{ez}}} \sqrt{\frac{2\sqrt{3}\pi}{3} \frac{section}{2\pi} \frac{\epsilon_z}{A}} \\ \sqrt{\frac{\Phi_e time_{\pm}}{4\pi C e v_e}} \sqrt{\frac{2\sqrt{3}\pi}{\cos(\theta)} \frac{section}{2\pi} \frac{\epsilon}{A}} \end{array} \right\} \quad (2.15.17)$$

$$time_{r\pm} = \left\{ \begin{array}{l} \sqrt{L_{xr}} \sqrt{C_{xr}} \\ \sqrt{L_{yr}} \sqrt{C_{yr}} \\ \sqrt{L_{zr}} \sqrt{C_{zr}} \\ \sqrt{L_r} \sqrt{C_r} \end{array} \right\} = \left\{ \begin{array}{l} \sqrt{\frac{\Phi_{exr} time_{r\pm}}{4\pi C e v_{exr}}} \sqrt{\frac{approach_r \ \epsilon_{xr}}{2\pi \ 2B_r}} \\ \sqrt{\frac{\Phi_{eyr} time_{r\pm}}{4\pi C e v_{eyr}}} \sqrt{g_s \frac{\sqrt{3}}{2} \frac{side_r}{2\pi} \frac{\sqrt{3}\epsilon_{yr}}{3B_r}} \\ \sqrt{\frac{\Phi_{ezr} time_{r\pm}}{4\pi C e v_{ezr}}} \sqrt{\frac{2\sqrt{3}\pi}{3} \frac{section_r}{2\pi} \frac{\epsilon_{zr}}{A_r}} \\ \sqrt{\frac{\Phi_e time_{r\pm}}{4\pi C e v_{er}}} \sqrt{\frac{2\sqrt{3}\pi}{\cos(\theta)} \frac{section_r}{2\pi} \frac{\epsilon}{A_r}} \end{array} \right\} \quad (2.5.17r)$$

Where relationships between Cartesian and trisine capacitance and inductance is as follows:

$$C = C_x = C_y = C_z \quad (2.5.18)$$

$$C_r = C_{xr} = C_{yr} = C_{zr} \quad (2.5.18r)$$

$$L = L_x = L_y = L_z \quad (2.5.19)$$

$$L_r = L_{xr} = L_{yr} = L_{zr} \quad (2.5.19r)$$

Table 2.5.4 Capacitance and Inductive Density

Condition	1.2	1.3	1.6	1.9	1.10	1.11
$T_a(^0K)$	6.53E+11	6.53E+11	6.53E+11	6.53E+11	6.53E+11	6.53E+11
$T_b(^0K)$	9.05E+14	5.48E+13	9.22E+08	1.10E+07	2,868	2.723
$T_{br}(^0K)$	3.30E+12	5.45E+13	3.24E+18	2.72E+20	1.04E+24	1.10E+27
$T_c(^0K)$	8.96E+13	3.28E+11	93.0	0.0131	8.99E-10	8.10E-16
$T_{cr}(^0K)$	1.19E+09	3.25E+11	1.15E+21	8.11E+24	1.19E+32	1.32E+38
$z_R + 1$	3.67E+43	8.14E+39	3.89E+25	6.53E+19	1.17E+09	1.00E+00
$z_B + 1$	3.32E+14	2.01E+13	3.39E+08	4.03E+06	1.05E+03	1.00E+00
$Age_{UG} (sec)$	7.14E-05	4.79E-03	6.94E+04	5.36E+07	1.27E+13	4.33E+17
$Age_{UGv} (sec)$	4.59E-10	1.25E-07	4.42E+02	3.13E+06	1.22E+13	4.33E+17
$Age_U (sec)$	1.18E-26	5.31E-23	1.11E-08	6.63E-03	3.70E+08	4.33E+17
C	2.36E-16	6.46E-14	2.28E-04	1.61E+00	2.36E+07	2.61E+13

C	1.78E-11	6.52E-14	1.85E-23	2.61E-27	1.79E-34	1.61E-40
$C/v (/\text{cm}^3)$	5.52E+23	3.34E+22	5.62E+17	6.68E+15	1.75E+12	1.66E+09
$C/v (/\text{cm}^3)$	2.01E+21	3.32E+22	1.97E+27	1.66E+29	6.35E+32	6.69E+35
$C/v (fd/\text{cm}^3)$	6.14E+11	3.72E+10	6.26E+05	7.44E+03	1.95E+00	1.85E-03
$C/v (fd/\text{cm}^3)$	2.24E+09	3.70E+10	2.20E+15	1.85E+17	7.06E+20	7.44E+23
L	3.06E-34	8.36E-32	2.95E-22	2.09E-18	3.05E-11	3.38E-05
L	2.30E-29	8.44E-32	2.39E-41	3.38E-45	2.31E-52	2.09E-58
$L/v (/\text{cm}^3)$	7.14E+05	4.32E+04	7.28E-01	8.65E-03	2.26E-06	2.15E-09
$L/v (/\text{cm}^3)$	2.60E+03	4.30E+04	2.56E+09	2.15E+11	8.22E+14	8.66E+17
$L/v (h/\text{cm}^3)$	6.42E+17	3.89E+16	6.54E+11	7.78E+09	2.03E+06	1.93E+03
$L/v (h/\text{cm}^3)$	2.34E+15	3.87E+16	2.30E+21	1.93E+23	7.39E+26	7.78E+29

In terms of an extended Thompson cross-section (σ_T), it is noted that the $(1/R^2)$ factor [62] is analogous to a dielectric (ϵ) equation 2.5.4. Dimensionally the dielectric (ϵ) is proportional to trisine cell length dimension.

The extended Thompson scattering cross section (σ_T) [43 equation 78.5, 62 equation 33] then becomes as in equation 2.5.20.

$$\sigma_T = \left(\frac{K_B}{K_{Ds}} \right)^2 \left(\frac{8\pi}{3} \right) \left(\frac{e_{\pm}^2}{\epsilon m_t v_{dy}^2} \right)^2 \approx side \quad (2.5.20)$$

Force(F) relationships are maintained

$$\left. \begin{array}{l} F_x \\ F_y \\ F_z \\ F \end{array} \right\} = \left\{ \begin{array}{l} \frac{\hbar K_B}{time_{\pm}} \\ \frac{\hbar K_P}{time_{\pm}} \\ \frac{\hbar K_A}{time_{\pm}} \\ \frac{\hbar \sqrt{K_B^2 + K_P^2 + K_A^2}}{time_{\pm}} \end{array} \right\} \quad (2.5.21)$$

$$\left. \begin{array}{l} F_{xr} \\ F_{yr} \\ F_{zr} \\ F_r \end{array} \right\} = \left\{ \begin{array}{l} \frac{\hbar K_{Br}}{time_{r\pm}} \\ \frac{\hbar K_{Pr}}{time_{r\pm}} \\ \frac{\hbar K_{Ar}}{time_{r\pm}} \\ \frac{\hbar \sqrt{K_{Br}^2 + K_{Pr}^2 + K_{Ar}^2}}{time_{r\pm}} \end{array} \right\} \quad (2.5.21r)$$

$$\begin{aligned} F_x \\ F_y \\ F_z \\ F \end{aligned} \left\{ = \begin{array}{l} \frac{m_t v_{dx}}{time_{\pm}} \\ \frac{m_t v_{dx}}{time_{\pm}} \\ \frac{m_t v_{dx}}{time_{\pm}} \\ \frac{m_t \sqrt{v_{dx}^2 + v_{dy}^2 + v_{dz}^2}}{time_{\pm}} \end{array} \right\} \quad (2.5.22)$$

$$\begin{aligned} F_{xr} \\ F_{yr} \\ F_{zr} \\ F_r \end{aligned} \left\{ = \begin{array}{l} \frac{m_t v_{dxr}}{time_{r\pm}} \\ \frac{m_t v_{dxr}}{time_{r\pm}} \\ \frac{m_t v_{dxr}}{time_{r\pm}} \\ \frac{m_t \sqrt{v_{dxr}^2 + v_{dyr}^2 + v_{dzr}^2}}{time_{r\pm}} \end{array} \right\} \quad (2.5.22r)$$

$$\begin{aligned} F_x \\ F_y \\ F_z \\ F \end{aligned} \left\{ = \begin{array}{l} \mathbb{C}eE_{fx} \\ \mathbb{C}eE_{fy} \\ \mathbb{C}eE_{fz} \\ \mathbb{C}e\sqrt{E_{fx}^2 + E_{fy}^2 + E_{fz}^2} \end{array} \right\} \quad (2.5.23)$$

$$\begin{aligned} F_{xr} \\ F_{yr} \\ F_{zr} \\ F_r \end{aligned} \left\{ = \begin{array}{l} \mathbb{C}eE_{fxr} \\ \mathbb{C}eE_{fyr} \\ \mathbb{C}eE_{fzr} \\ \mathbb{C}e\sqrt{E_{fxr}^2 + E_{fyr}^2 + E_{fzr}^2} \end{array} \right\} \quad (2.5.23r)$$

2.6 Fluxoid And Critical Fields

Based on the material fluxoid (Φ_{ϵ}) (equation 2.5.6), the critical fields (H_{c1}) (equation 2.6.1), (H_{c2}) (equation 2.6.2) & (H_c) (equation 2.6.3) as well as penetration depth (λ) (equation 2.6.5) and Ginzburg-Landau coherence length (ℓ)

(equation 2.6.6) are computed. Also the critical field (H_c) is alternately computed from a variation on the Biot-Savart law.

$$H_{c1} = \frac{\Phi_{\epsilon}}{\pi\lambda^2} \quad (2.6.1)$$

$$H_{c1r} = \frac{\Phi_{\epsilon}}{\pi\lambda^2} \quad (2.6.1r)$$

$$H_{c2} = \frac{4\pi \mathbb{C}}{section} \Phi_{\epsilon} \quad (2.6.2)$$

$$H_{c2r} = \frac{4\pi \mathbb{C}}{section_r} \Phi_{\epsilon r} \quad (2.6.2r)$$

$$H_c = \sqrt{H_{c1} H_{c2}} = g_s^2 \frac{B}{A} \sqrt{\pi D_f E_f} = \frac{g_s^3 m_t v_{ex}}{3e_{\pm} time_{\pm}} \quad (2.6.3)$$

$$H_{cr} = \sqrt{H_{c1r} H_{c2r}} = g_s^2 \frac{B_r}{A_r} \sqrt{\pi D_f E_f} = \frac{g_s^3 m_t v_{exr}}{3e_{\pm} time_{r\pm}} \quad (2.6.3r)$$

$$n_c = \frac{\mathbb{C}}{cavity} \quad (2.6.4)$$

$$n_c = \frac{\mathbb{C}}{cavity} \quad (2.6.4r)$$

where n_c = Ginzburg-Landau order parameter as indicated in equation D.1 in Appendix D. (2.6.4r)

And the fluxoid linked the resonant time as follows:

$$time_{\pm} = \frac{2eA}{\alpha^2 v_{ex} \Phi_{\epsilon}} \quad (2.6.5)$$

$$time_{r\pm} = \frac{2eA_r}{\alpha^2 v_{exr} \Phi_{\epsilon r}} \quad (2.6.5r)$$

Huxley [70] observed that an increasing magnetic field: quenched the URhGe superconductor at 2 tesla (20,000 gauss) initiated the URhGe superconductor at 8 tesla (80,000 gauss) quenched the URhGe superconductor at 13 tesla (130,000 gauss)

The trisine model (H_{c2}) correlates well with the reported [70] 2 tesla (20,000 gauss) with a calculated modeled superconductor magnetic critical field value (H_{c2}) of 1.8 tesla (18,000 gauss) for critical temperature (T_c) of .28 K.

At critical temperature (T_c) of .4 kelvin, the trisine model predicts superconductor magnetic critical field (H_{c2}) of 2.9 tesla (29,000 gauss), which is substantially lower than the observed 13 tesla (130,000 gauss). This could be explained in terms of the ferromagnetic properties of URhGe, which essentially mask the superconductor critical magnetic field. But it is remarkable how well the model correlates to the

observed superconducting magnetic critical field (H_{c2}) in this case.

In as much as the trisine lattice can be considered a plasma $\mathbb{C}\rho_U = \mathbb{C}m_i/cavity = \mathbb{C}M_U/V_U$, then trisine de Broglie velocities can be computed as plasma Alfvén speeds as per equation 2.6.6. Corresponding plasma Alfvén times would be congruent with $time_{\pm} = B/v_{dx}$.

$$\begin{Bmatrix} v_{dx} \\ v_{dy} \\ v_{dz} \end{Bmatrix} = \begin{Bmatrix} \frac{4}{3\sqrt{3}} \frac{A}{B} \frac{H_c}{\sqrt{\mathbb{C}\rho_U}} \\ \frac{2}{3\sqrt{3}} \frac{1}{\sqrt{\mathbb{C}\rho_U}} \frac{H_c}{B} \\ \frac{2}{3} \frac{B}{A} \frac{H_c}{\sqrt{\mathbb{C}\rho_U}} \end{Bmatrix} \quad (2.6.6)$$

$$\begin{Bmatrix} v_{dxr} \\ v_{dyr} \\ v_{dzr} \end{Bmatrix} = \begin{Bmatrix} \frac{4}{3\sqrt{3}} \frac{A_r}{B_r} \frac{H_{cr}}{\sqrt{\mathbb{C}\rho_{Ur}}} \\ \frac{2}{3\sqrt{3}} \frac{1}{\sqrt{\mathbb{C}\rho_{Ur}}} \frac{H_{cr}}{B_r} \\ \frac{2}{3} \frac{B_r}{A_r} \frac{H_{cr}}{\sqrt{\mathbb{C}\rho_{Ur}}} \end{Bmatrix} \quad (2.6.6r)$$

Also it is interesting to note that the following relationship holds

$$2\pi \frac{e_{\pm}^2 e_{\pm}^2}{A B} = m_e v_{dx}^2 m_e c^2 \quad (2.6.7)$$

$$2\pi \frac{e_{\pm}^2 e_{\pm}^2}{A_r B_r} = m_e v_{dxr}^2 m_e c^2 \quad (2.6.7r)$$

$$\lambda^2 = m_e v_{\epsilon}^2 \frac{1}{n_c} \frac{1}{e^2} \quad (2.6.8)$$

$$\lambda_r^2 = m_e v_{\epsilon r}^2 \frac{1}{n_{cr}} \frac{1}{e^2} \quad (2.6.8r)$$

From equation 2.6.8, the trisine penetration depth λ is calculated. This is plotted in the above figure along with Harshman[17] and Homes[51, 59] penetration data. The Homes data is multiplied by a factor of $(n_e chain/\mathbb{C})^{1/2}$ to get n_c in equation 2.6.8. This is consistent with $\lambda^2 = 1/(\epsilon n_c)$ in equation 2.6.8 and consistent with Uemura Plot $\lambda^2 = 1/n_c$ over short increments of penetration depth λ . It appears to be a good fit and better than the fit with data compiled by Harshman[17].

Figure 2.6.1 Experimental Harshman Data and Trisine Model Cooper CPT Charge conjugated Pair Three Dimensional Concentration as per equation 2.6.4

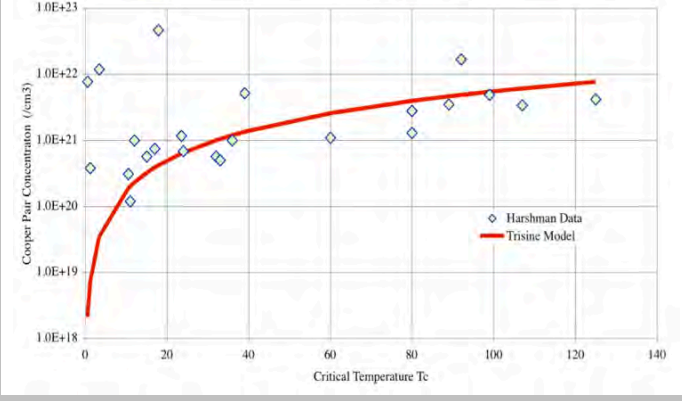
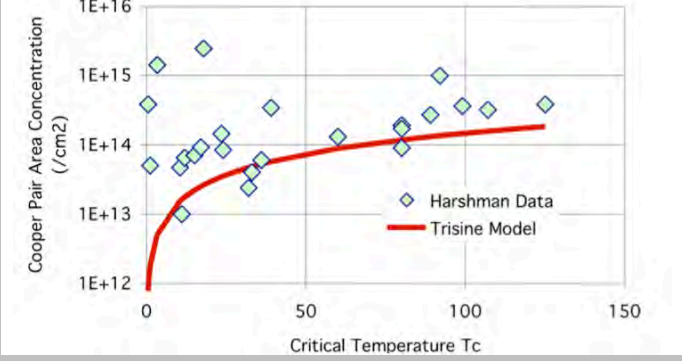


Figure 2.6.2 Experimental (Harshman Data) and Trisine Model Cooper CPT Charge conjugated Pair Two Dimensional Area Concentration or $\mathbb{C}/\text{section}$



Penetration depth and gap data for magnesium diboride MgB_2 [55], which has a critical temperature T_c of 39 K indicates a fit to the trisine model when a critical temperature of 39/3 or 13 K is assumed (see Table 2.6.1). This is interpreted as an indication that MgB_2 is a three dimensional superconductor.

Table 2.6.1 Experimental (MgB_2 Data [55]) and the related Trisine Model Prediction

	Trisine Data at T_c 39/3 K or 13 K	Observed Data [55]
Penetration Depth (nm)	276	260 ± 20
Gap (meV)	1.12	$3.3/3$ or $1.1 \pm .3$

As indicated in equation 2.5.5, the material medium dielectric sub- and super- luminal speed of light (v_{ϵ}) is a function of medium dielectric (ϵ) constant, which is calculated in general, and specifically for trisine by $\epsilon = D/E$ (equation 2.5.4). The fact that chain rather than cavity (related by 2/3 factor) must be used in obtaining a trisine model fit to Homes' data indicates that the stripe concept may be valid in as much as chains in the trisine lattice

visually form a striped pattern as in Figure 2.3.1.

See derivation of Ginzburg-Landau coherence length ℓ in equation 2.6.9 in Appendix D. It is interesting to note that $B/\xi = 2.73 \approx e$ for all T_c , which makes the trisine superconductor mode fit the conventional description of operating in the “dirty” limit. [54]

$$\xi = \sqrt{\frac{m_l}{m_e} \frac{1}{K_B^2} \frac{\text{chain}}{\text{cavity}}} \quad (2.6.9)$$

The geometry presented in Figure 2.6.4 is produced by three intersecting coherent polarized standing waves, which can be called the trisine wave function Ψ . This can be compared to figure 2.6.5, which presents the dimensional trisine geometry. Equation 2.6.10 represents the trisine wave function Ψ that is analogous to Bloch sphere vector addition of three sin functions that are 120 degrees from each other in the x y plane and form an angle 22.8 degrees with this same x y plane. Also note that 22.8 degrees is related to the (B/A) ratio by $\tan(90^\circ - 22.8^\circ) = B/A$.

Figure 2.6.3 Experimental and Trisine Model

Penetration Depth

slope -1.52

intercept -5.61

Correlation -0.950

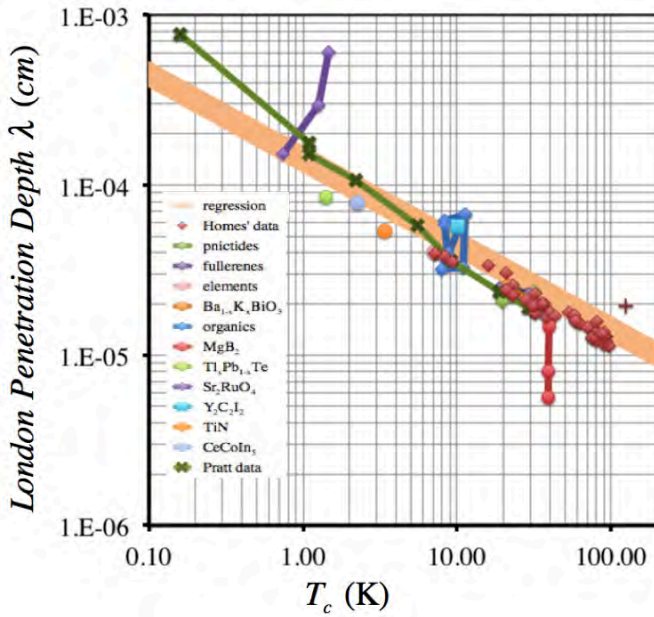
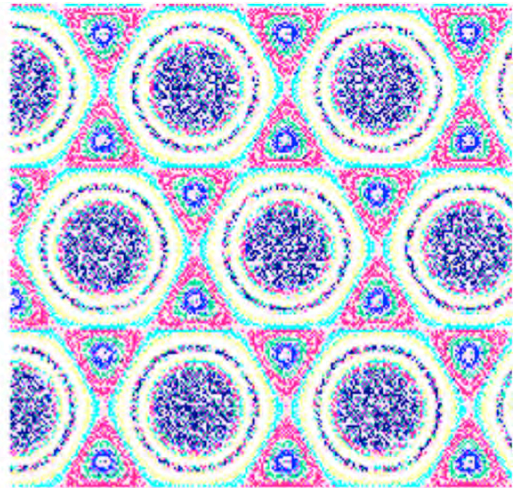


Figure 2.6.4 Trisine Geometry in the Fluxoid Mode (Interference Pattern Ψ^2)



$$\begin{aligned} \Psi = & \exp\left(\sin\left(2(a_{x1}x_0 + b_{x1}y_0 + c_{x1}z_0)\right)\right) \\ & + \exp\left(\sin\left(2(a_{x2}x_0 + b_{x2}y_0 + c_{x2}z_0)\right)\right) \\ & + \exp\left(\sin\left(2(a_{x3}x_0 + b_{x3}y_0 + c_{x3}z_0)\right)\right) \end{aligned} \quad (2.6.10)$$

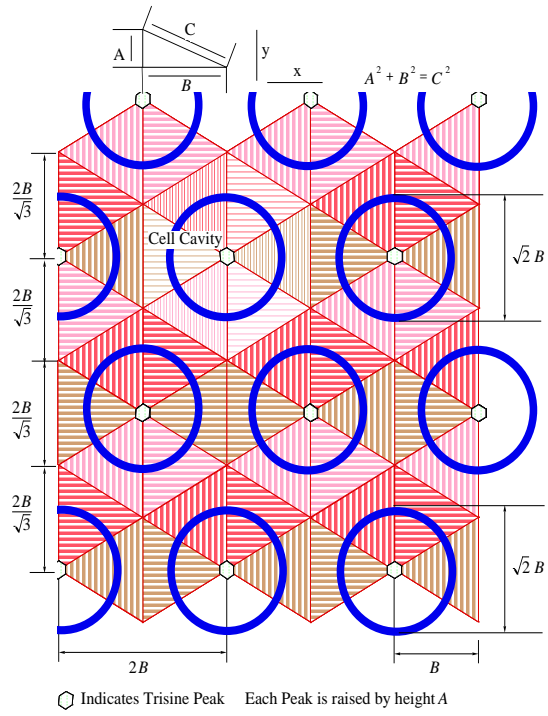
Where:

$$\begin{aligned} a_{x1} &= \cos(030^\circ) \cos(22.8^\circ) & b_{x1} &= \sin(030^\circ) \cos(22.8^\circ) \\ c_{x1} &= -\sin(030^\circ) & \\ a_{x2} &= \cos(150^\circ) \cos(22.8^\circ) & b_{x2} &= \sin(150^\circ) \cos(22.8^\circ) \\ c_{x2} &= -\sin(150^\circ) & \\ a_{x3} &= \cos(270^\circ) \cos(22.8^\circ) & b_{x3} &= \sin(270^\circ) \cos(22.8^\circ) \\ c_{x3} &= -\sin(270^\circ) & \end{aligned}$$

Functionally, the interference of these planar intersecting waves would generate Laguerre-Gaussian optical vortices (fluxoid mode and its related superconducting mode). Equation 2.6.11 is an expression of reference [96] equation A36 in terms of trisine dimensionality.

$$\frac{E_z}{P} - 3 \frac{E_y}{A} + \frac{H_{c2}}{v_e \text{time}_\pm} \sim 0 \quad (2.6.11)$$

Figure 2.6.5 Trisine Geometry in the Fluxoid Mode



n_c (/cm 3)	4.66E39	1.91E22	1.03E21	1.03E16	1.69E05	1.27E-04
n_{cr} (/cm 3)	2.26E+32	1.02E+36	2.14E+50	1.27E+56	7.11E+66	8.30E+75
λ (cm)	1.08E-11	1.78E-10	1.06E-05	8.90E-04	3.40E+00	3.58E+03
λ_r (cm)	1.79E-11	1.08E-12	1.82E-17	2.17E-19	5.67E-23	5.38E-26
ξ (cm)	1.81E-13	3.00E-12	1.78E-07	1.50E-05	5.73E-02	60.31
ξ_r (cm)	4.98E-11	3.01E-12	5.07E-17	6.03E-19	1.58E-22	1.50E-25

In table 2.6.2, note that the ratio of London penetration length (λ) to Ginzburg-Landau correlation length (ℓ) is the constant (κ) of 58. The trisine values compares favorably with London penetration length (λ) and constant (κ) of 1155(3) Å and 68 respectively as reported in reference [11, 17] based on experimental data.

Measured intergalactic magnetic field (IGMF)[92,93] $\sim 1E-15$ Gauss is consistent with critical field (H_c) value 1.64E-17 Gauss in Table 2.6.2 further verifying the trisine model at the universe 'dark energy' scale. Also, in this context, the quantity $H_c (c/v_{dx})(m_e/m_t)(2/3)$ is considered a magnetic B field that approximates Interstellar Magnetic Field (ISMF) at about 2E-6 Gauss[78,140].

Table 2.6.2 Critical Fields and Lengths

Condition	1.2	1.3	1.6	1.9	1.10	1.11
T_a (°K)	6.53E+11	6.53E+11	6.53E+11	6.53E+11	6.53E+11	6.53E+11
T_b (°K)	9.05E+14	5.48E+13	9.22E+08	1.10E+07	2,868	2.723
T_{br} (°K)	3.30E+12	5.45E+13	3.24E+18	2.72E+20	1.04E+24	1.10E+27
T_c (°K)	8.96E+13	3.28E+11	93.0	0.0131	8.99E-10	8.10E-16
T_{cr} (°K)	1.19E+09	3.25E+11	1.15E+21	8.11E+24	1.19E+32	1.32E+38
$z_R + 1$	3.67E+43	8.14E+39	3.89E+25	6.53E+19	1.17E+09	1.00E+00
$z_B + 1$	3.32E+14	2.01E+13	3.39E+08	4.03E+06	1.05E+03	1.00E+00
Age_{UG} (sec)	7.14E-05	4.79E-03	6.94E+04	5.36E+07	1.27E+13	4.33E+17
Age_{UGv} (sec)	4.59E-10	1.25E-07	4.42E+02	3.13E+06	1.22E+13	4.33E+17
Age_U (sec)	1.18E-26	5.31E-23	1.11E-08	6.63E-03	3.70E+08	4.33E+17
H_c (gauss)	3.27E+19	2.94E+16	3.42E+04	5.27E-01	5.83E-10	1.62E-17
H_{cr} (gauss)	2.62E+13	2.91E+16	2.50E+28	1.62E+33	1.47E+42	5.28E+49
H_{c1} (gauss)	4.22E+16	3.80E+13	4.43E+01	6.82E-04	7.55E-13	2.10E-20
H_{c1r} (gauss)	3.39E+10	3.76E+13	3.23E+25	2.10E+30	1.90E+39	6.83E+46
$H_c \frac{c}{v_{dx}} \frac{m_e}{m_t} \frac{2}{3}$	2.04E+20	1.83E+17	2.13E+05	3.29E+00	3.64E-09	1.01E-16
$H_{cr} \frac{c}{v_{dx}} \frac{m_e}{m_t} \frac{2}{3}$	2.63E+12	1.76E+14	2.55E+21	1.97E+24	4.66E+29	1.59E+34
H_{c2} (gauss)	2.53E+22	2.27E+19	2.65E+07	4.08E+02	4.51E-07	1.25E-14
H_{c2r} (gauss)	6.13E+13	6.81E+16	5.85E+28	3.80E+33	3.43E+42	1.24E+50

Figure 2.6.6 Critical Magnetic Field Data (gauss) compared to Trisine Model as a function of T_c

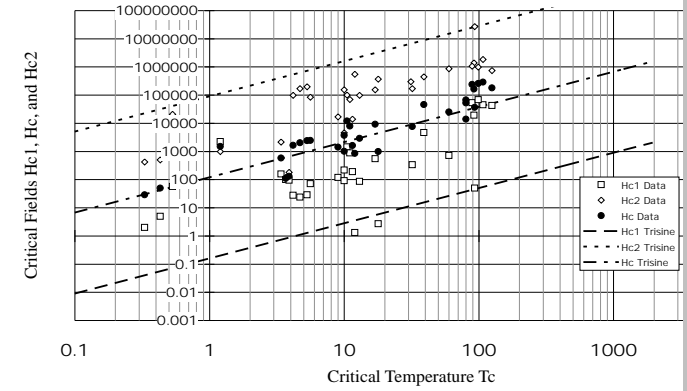


Figure 2.6.6 is graph of generally available critical field data as compile in Weast [16].

2.7 Superconductor Internal Pressure, Casimir Force And Deep Space Thrust Force (Pioneer 10 & 11)

The following pressure (p_U) values in Table 2.7.1 as based on equations 2.7.1 indicate rather high values as superconducting (T_c) increases. This is an indication of the forces that must be contained in these anticipated materials or lattices within potential barrier(c) restrictions expressed in 1.1 – 1.11. These forces are rather large for conventional materials especially at nuclear dimensions, but range to very small to the virtual lattice existing in outer space and are

considered repulsive Casimir forces (eqn 2.7.1) on evaluation of eqn 7.44, Milonni[45] with $(\pm\epsilon_1 = \pm\epsilon_3 = \pm\epsilon_2)$ and $(\pm K_1 = \mp K_3 = \pm K_2)$ with the polarities (\pm, \mp) changing in the context of CPT.

$$\text{Casimir Force(repulsive)} = \frac{\hbar K_{B\mp}}{\text{time}_\pm} \quad (2.7.1)$$

$$p_U = \left\{ \begin{array}{l} \frac{\hbar K_B}{\text{time}_\pm \text{ approach}} \\ \frac{\hbar K_P}{\text{time}_\pm \text{ side}} \\ \frac{\hbar K_A}{\text{time}_\pm \text{ section}} \end{array} \right\} = \left\{ \begin{array}{l} \frac{F_x}{\text{approach}} \\ \frac{F_y}{\text{side}} \\ \frac{F_z}{\text{section}} \end{array} \right\} = \frac{\mathbb{C} k T_c}{\text{cavity}} \quad (2.7.1a)$$

$$p_U = \frac{\sqrt{A^2 + B^2}}{B} \frac{\text{cavity}}{\text{chain}} \frac{\pi^2 \hbar v_{dx}}{240 A^4} \quad \left(\begin{array}{l} \text{Casimir} \\ \text{pressure} \end{array} \right) \quad (2.7.1b)$$

$$p_U = \left\{ \begin{array}{l} \frac{m_t v_{dx}}{\text{time}_\pm \text{ approach}} \\ \frac{m_t v_{dy}}{\text{time}_\pm \text{ side}} \\ \frac{m_t v_{dz}}{\text{time}_\pm \text{ section}} \end{array} \right\} = \frac{\mathbb{C} k_b T_c}{\text{cavity}} \quad (2.7.1c)$$

These trisine cellular pressure and force relationship are universally correlated to the gravitational force as follows assuming that the Newtonian gravitational parameter is a variable such that $G_U = R_U c^2 / M_U$.

$$F_x = 3 \frac{A}{B} \frac{G_U M_U m_t}{R_U^2} = 3 \frac{A}{B} \frac{R_U c^2}{M_U} \frac{M_U m_t}{R_U^2} = 3 \frac{A}{B} \frac{m_t c^2}{R_U} \quad (2.7.1d)$$

Cellular pressure (p_U), as expressed in eqn 2.7.1c, is congruent with the universal pressure (p_U) expressed as energy ($m_t c^2$) spread over the volumes ($\text{approach} \cdot R_U$), ($\text{side} \cdot R_U$) and ($\text{section} \cdot R_U$).

To put the calculated pressures in perspective, the C-C bond has a reported energy of 88 kcal/mole and a bond length of 1.54 Å [24]. Given these parameters, the internal chemical bond pressure (CBP) for this bond is estimated to be:

$$\begin{aligned} 88 \frac{\text{kcal}}{\text{mole}} & 4.18 \times 10^{10} \frac{\text{erg}}{\text{kcal}} \frac{1}{6.02 \times 10^{23}} \frac{\text{mole}}{\text{bond}} \frac{1}{(1.54 \times 10^{-8})^3} \frac{\text{bond}}{\text{cm}^3} \\ & = 1.67 \times 10^{12} \frac{\text{erg}}{\text{cm}^3} \end{aligned}$$

Within the context of the superconductor internal pressure numbers in table 2.7.1, the internal pressure requirement for the superconductor is less than the C-C chemical bond pressure at the order of design T_c of a few thousand degrees kelvin indicating that there is the possibility of using materials with the bond strength of carbon to chemically engineer high performance resonant superconducting materials.

In the context of interstellar space vacuum, the total pressure $m_t c^2 / \text{cavity}$ may be available (potential energy) and will be of such a magnitude as to provide for universe expansion as astronomically observed. (see equation 2.11.21). Indeed, there is evidence in the Cosmic Gamma Ray Background Radiation for energies on the order of $m_t c^2$ or 56 MeV or ($\log_{10}(\text{Hz}) = 22.13$) or (2.20E-12 cm) [73]. In the available spectrum [73], there is a hint of a black body peak at 56 MeV or ($\log_{10}(\text{Hz}) = 22.13$) or (2.20E-12 cm). This radiation has not had an identifiable source until now.

Table 2.7.1 CPT Lattice Pressure With Plot

Condition	1.2	1.3	1.6	1.9	1.10	1.11
$T_a ({}^0 K)$	6.53E+11	6.53E+11	6.53E+11	6.53E+11	6.53E+11	6.53E+11
$T_b ({}^0 K)$	9.05E+14	5.48E+13	9.22E+08	1.10E+07	2,868	2.723
$T_{br} ({}^0 K)$	3.30E+12	5.45E+13	3.24E+18	2.72E+20	1.04E+24	1.10E+27
$T_c ({}^0 K)$	8.96E+13	3.28E+11	93.0	0.0131	8.99E-10	8.10E-16
$T_{cr} ({}^0 K)$	1.19E+09	3.25E+11	1.15E+21	8.11E+24	1.19E+32	1.32E+38
$z_R + 1$	3.67E+43	8.14E+39	3.89E+25	6.53E+19	1.17E+09	1.00E+00
$z_B + 1$	3.32E+14	2.01E+13	3.39E+08	4.03E+06	1.05E+03	1.00E+00
$Age_{UG} (\text{sec})$	7.14E-05	4.79E-03	6.94E+04	5.36E+07	1.27E+13	4.33E+17
$Age_{UGv} (\text{sec})$	4.59E-10	1.25E-07	4.42E+02	3.13E+06	1.22E+13	4.33E+17
$Age_U (\text{sec})$	1.18E-26	5.31E-23	1.11E-08	6.63E-03	3.70E+08	4.33E+17
$k_b T_c / \text{cavity}$ erg/cm^3	2.89E+37	2.34E+31	3.17E+07	7.52E-03	9.21E-21	7.11E-36
$k_b T_{cr} / \text{cavity}$ erg/cm^3	1.86E+25	2.29E+31	1.69E+55	7.13E+64	5.81E+82	7.54E+97
$m_t c^2 / \text{cavity}$ erg/cm^3	2.10E+35	4.66E+31	2.23E+17	3.74E+11	6.69E+00	5.73E-09

$$p_U = \left\{ \begin{array}{l} \frac{F_x}{\text{approach}} \\ \frac{F_y}{\text{side}} \\ \frac{F_z}{\text{section}} \end{array} \right\} = \left\{ \begin{array}{l} 3 \frac{A}{B} \frac{m_t c^2}{\text{approach} \cdot R_U} \\ \frac{6}{\sqrt{3}} \frac{A}{B} \frac{m_t c^2}{\text{side} \cdot R_U} \\ 6 \frac{m_t c^2}{\text{section} \cdot R_U} \end{array} \right\} = \frac{\mathbb{C} k_b T_c}{\text{cavity}} \quad (2.7.1e)$$

$m_e c^2 / cavity_r$ erg/cm^3	1.02E+28	4.60E+31	9.63E+45	5.73E+51	3.20E+62	3.74E+71
------------------------------------	----------	----------	----------	----------	----------	----------

In comparison to CPT Lattice Pressure, Table 2.7.1a indicates Black Body Emission and Energy Density (Pressure). The rest mass CPT lattice (T_c) energy density or pressure is greater than the corresponding Black Body (T_b) energy density or pressure.

Table 2.7.1a Black Body (T_b) Emission and Energy Density

	1.2	1.3	1.6	1.9	1.10	1.11
Condition						
$T_a ({}^0 K)$	6.53E+11	6.53E+11	6.53E+11	6.53E+11	6.53E+11	6.53E+11
$T_b ({}^0 K)$	9.05E+14	5.48E+13	9.22E+08	1.10E+07	2,868	2.723
$T_{br} ({}^0 K)$	3.30E+12	5.45E+13	3.24E+18	2.72E+20	1.04E+24	1.10E+27
$T_c ({}^0 K)$	8.96E+13	3.28E+11		93.0	0.0131	8.99E-10
$T_{cr} ({}^0 K)$	1.19E+09	3.25E+11	1.15E+21	8.11E+24	1.19E+32	1.32E+38
$z_R + 1$	3.67E+43	8.14E+39	3.89E+25	6.53E+19	1.17E+09	1.00E+00
$z_B + 1$	3.32E+14	2.01E+13	3.39E+08	4.03E+06	1.05E+03	1.00E+00
$Age_{UG} (sec)$	7.14E-05	4.79E-03	6.94E+04	5.36E+07	1.27E+13	4.33E+17
$Age_{UGv} (sec)$	4.59E-10	1.25E-07	4.42E+02	3.13E+06	1.22E+13	4.33E+17
$Age_U (sec)$	1.18E-26	5.31E-23	1.11E-08	6.63E-03	3.70E+08	4.33E+17
$\sigma_s T_b^4$ $erg/cm^2/sec$	3.81E+55	5.11E+50	4.10E+31	8.19E+23	3.84E+09	3.12E-03
$\sigma_s T_{br}^4$ $erg/cm^2/sec$	6.72E+45	5.01E+50	6.23E+69	3.12E+77	6.67E+91	8.21E+103
$\sigma_s T_b^4 c/4$ erg/cm^3	5.08E+45	6.81E+40	5.48E+21	1.09E+14	5.12E-01	4.16E-13
$\sigma_s T_{br}^4 c/4$ erg/cm^3	8.96E+35	6.69E+40	8.32E+59	4.17E+67	8.90E+81	1.10E+94
$photon/cm^3$	1.51E+46	3.33E+42	1.59E+28	2.67E+22	4.79E+11	4.10E+02
$photon/cm^3$	7.29E+38	3.29E+42	6.89E+56	4.10E+62	2.29E+73	2.68E+82
wavelength cm	3.20E-16	5.29E-15	3.14E-10	2.64E-08	1.01E-04	1.06E-01
wavelength cm	8.78E-14	5.31E-15	8.95E-20	1.06E-21	2.78E-25	2.64E-28
Frequency /sec	5.32E+25	3.22E+24	5.42E+19	6.44E+17	1.69E+14	1.60E+11
Frequency /sec	1.94E+23	3.21E+24	1.90E+29	1.60E+31	6.12E+34	6.45E+37

The following figure indicates the Planck Black Body curve for CMBR at 2.729 K

The hydrogen BEC 1S-2S transition

absorbed energy	1.301E-12	erg/cm ³
absorbed freq	1.234E+15	/sec
absorbed wavelength	2.430E-05	cm
band pass	~1E-6	Hz
Ref: [90]		

is of such high frequency that CMBR intensity at 1.234E+15

/sec is negligible and band pass ~1E-6 Hz and will not degrade any intervening hydrogen dense (1 g/cc) BEC. The moles of photons(einsteins) at the tail of this curve (too far off the curve to be shown) are not enough to degrade a hydrogen dense (1 g/cc) BEC. This is further substantiate by Peebles[95] page 157 indicating electrons captured directly to the ground state emitted with not net neutral hydrogen change.

This is also the case for CMBR = 3000 K at recombination as indicated in the following figures. The moles of photons(einsteins) at the tail of this curve are not enough to degrade a hydrogen dense (1 g/cc) BEC. This is particularly true for the present universe condition where CMBR = 2.729 K.

Figure 2.7.1

Planck's Curve (Intensity vs Frequency) $T_b = 3000$ K

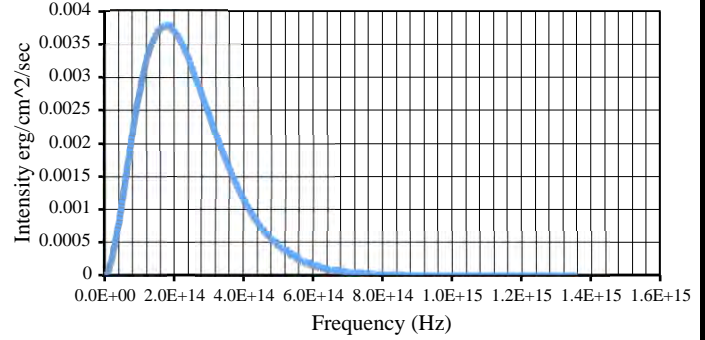
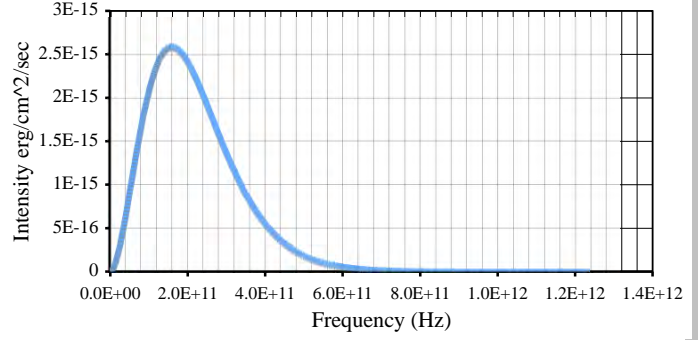


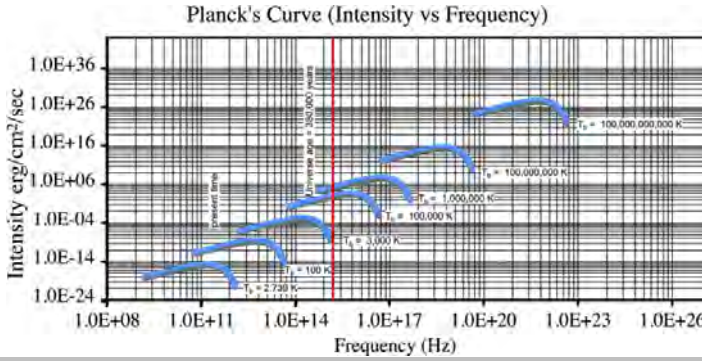
Figure 2.7.2

Planck's Curve (Intensity vs Frequency) $T_b = 2.729$ K



The red line indicates the hydrogen BEC absorption frequency of 1.234E+15 /sec in the context of universe expansion from the Big Bang nucleosynthetic event.

Figure 2.7.3



Assuming the superconducting current moves as a longitudinal wave with an adiabatic character, then equation 2.7.2 for current or de Broglie velocity (v_{dx}) holds where the ratio of heat capacity at constant pressure to the heat capacity at constant volume (δ) equals 1.

$$v_{dx} = \sqrt{\delta \text{ pressure} \frac{\text{cavity}}{m_t}} \quad (2.7.2)$$

The adiabatic nature of an expanding universe is indicated by the expansion relationships for (T_c , T_b , T_a and T_p).

$$\begin{aligned} (T = T_c, \delta = 5/3 \text{ & } p = p_U = \mathbb{C}k_b T_c / \text{cavity}) \text{ or} \\ (T = T_b, \delta = 4/3 \text{ & } p = \mathbb{C}k_b T_b / \text{cavity}) \text{ or} \\ (T = T_a, \delta = 1 \text{ & } p = \mathbb{C}k_b T_a / \text{cavity}) \text{ or} \\ (T = T_p, \delta = 1/3 \text{ & } p = \mathbb{C}k_b T_p / \text{cavity}) \end{aligned} \quad (2.7.2a)$$

$$p_1 \text{cavity}_1^\delta = p_2 \text{cavity}_2^\delta \quad (2.7.3a)$$

$$T_1 \text{cavity}_1^{\delta-1} = T_2 \text{cavity}_2^{\delta-1} \quad (2.7.3b)$$

$$T_1 p_1^{\frac{1-\delta}{\delta}} = T_2 p_2^{\frac{1-\delta}{\delta}} \quad (2.7.3c)$$

$$T_c \text{ degrees of freedom} = 2/(5/3 - 1) = 3$$

$$T_b \text{ degrees of freedom} = 2/(4/3 - 1) = 6$$

$$T_a \text{ degrees of freedom} = 2/(1 - 1) = \text{undefined}$$

$$T_p \text{ degrees of freedom} = 2/(1/3 - 1) = -3$$

Equation 2.7.2a is particularly confirmed with the equation 2.7.3d where ($\Omega_b = .037$) representing the universe luminescent fraction and

$$T_{solar} = 5780K$$

$$\sigma_s T_{solar} = 1,367,000 \text{ erg}/(\text{cm}^2 \text{ sec} \text{ AU}^2 \text{ solar mass unit})$$

and Astronomical Unit AU (distance between sun and earth)

$$AU = 1.50E13 \text{ cm} \text{ and solar mass} = 2.0E33 \text{ g}$$

$$\sigma_s T_b^4 = \left(\frac{\text{cavity}}{\text{cavity}_{\text{present}}} \right)^{\frac{4}{3}} \Omega_b \frac{M_U}{\text{solar mass}} \sigma_s T_{solar}^4 \left(\frac{AU}{R_U} \right)^2 \quad (2.7.3d)$$

It is particularly important to note this scaling relationship over universe time ($1/H_U$). Equation 2.7.3d indicates an equi-partition of energy between CMBR and universe luminescent matter (Ω_b) (commonly called baryonic matter) going back to the Big Bang. (see Appendix J)

As an extension of this work, in a report[53] by Jet Propulsion Laboratory, an unmodeled deceleration was observed in regards to Pioneer 10 and 11 spacecraft as they exited the solar system. This deceleration can be related empirically to the following dimensional correct force expression (2.7.4) where (m_t/cavity) is the mass equivalent energy density (pressure)

$$\left(m_t c^2 / \text{cavity} \right) \text{ value at } T_c = 8.11E-16 \text{ }^0K$$

representing conditions in space, which is 100 percent, transferred to an object passing through it.

$$\text{Force} = -\text{AREA} \frac{m_t}{\text{cavity}} c^2 = -\text{AREA} (\rho_U) c^2 \quad (2.7.4)$$

Note that equation 2.7.4 is similar to the conventional drag equation as used in design of aircraft with v^2 replaced with c^2 . The use of c^2 vs. v^2 means that the entire resonant energy content ($m_t c^2 / \text{cavity}$) is swept out of volume as the spacecraft passes through it. Of course $\text{Force} = Ma$, so the Pioneer spacecraft M / AREA , is an important factor in establishing deceleration, which was observed to be on the order of $8.74E-8 \text{ cm/sec}^2$.

The force equation is repeated below as the conventional drag equation in terms of Pioneer spacecraft and the assumption that space density (ρ_U) (2.11.16) is essentially what has been determined to be a potential candidate for dark energy:

$$F = Ma = C_d A_c \rho_U \frac{v^2}{2} \quad (2.7.4a)$$

where: $C_d = \frac{24}{R_e} + \frac{6}{1 + \sqrt{R_e}} + .4$ [60] empirical

and where:

$$F = \text{force} \quad M = \text{Pioneer 10 \& 11 mass}$$

$$a = \text{acceleration} \quad A_c = \text{Pioneer 10 \& 11 cross section}$$

ρ_U	= space fluid critical density (6.38E-30 g/cm ³)
v	= Pioneer 10 & 11 velocity
d	= Pioneer 10 & 11 diameter
μ_{Uc}	= absolute vacuum viscosity (1.21E-16 g/(cm sec))
ν_{Uc}	= kinematic viscosity μ_{Uc} / ρ_U (1.90E13 cm ² /sec)
R_e	= Reynolds' number = inertial force/viscous force = $\rho_U v d / \mu_U$

When the Reynolds' number (R_e) is low (laminar flow condition), then $C_d = (24/R_e)$ and the drag equation reduces to the Stokes' equation $F = 3\pi\mu_U v d$. [60]. When the Pioneer spacecraft data is fitted to this drag equation, the computed drag force is 6 orders of magnitude lower than observed values.

In other parts of this report, a model is developed as to what this dark energy actually is. The model dark energy is keyed to a 6.38E-30 g/cc value (ρ_U) (2.11.16) in trisine model (NASA observed value of 6E-30 g/cc). The proposed dark energy consists of mass units of m_t (110.12275343 x electron mass) per volume (Table 2.2.2 *cavity*- 15733 cm³). These mass units are virtual particles that exist in a coordinated lattice at base energy $\hbar\omega/2$ under the condition that momentum and energy are conserved - in other words complete elastic character. This dark energy lattice would have internal pressure (table 2.7.1) to withstand collapse into gravitational clumps.

Under these circumstances, the traditional drag equation form is valid but velocity (v) should be replaced by speed of light (c). Conceptually, the equation 2.7.4a becomes a thrust equation rather than a drag equation. Correspondingly, the space viscosity (μ_{Uc}) is computed as momentum/area or $(m_t c / (2\Delta x^2))$ where Δx is uncertainty dimension in table 2.5.1 at $T_c = 8.1\text{E-16 K}$ and as per equation 2.1.20. This is in general agreement with gaseous kinetic theory [19].

The general derivation is in one linear dimensional path (s) and in accordance with Newton's Second Law, Resonant Mass and Work-Energy Principles in conjunction with the concept of Momentum Space, which defines the trisine elastic space lattice. These considerations are developed and presented in Appendix F with path ' ds/C_t ' used here.

$$\begin{aligned}
 F \frac{s}{C_t} \Big|_B^0 &= -m_t c^2 \sqrt{1 - \frac{v^2}{c^2}} \Big|_{v_{dx}+v_0}^c = -m_t c^2 \sqrt{1 - \frac{1}{\alpha}} \Big|_{k_m \epsilon + \frac{v_0^2}{c^2}}^1 \\
 &\approx -m_t c^2 = -\frac{(m_t c)^2}{m_t} \text{ at } v_{dx} \ll c \\
 &\text{and } \left(k_m \epsilon + \frac{v_0^2}{c^2} \right) \gg 1 \\
 &= 0 \text{ at } v = c \text{ (photon has zero mass)}
 \end{aligned} \tag{2.7.5a}$$

Clearly, an adiabatic process is described wherein the change in internal energy of the system (universe) is equal in absolute magnitude to the work (related to objects moving through the universe) or Work = Energy. Momentum is transferred from the trisine elastic space lattice to the object moving through it.

The hypothesis can be stated as:

An object moving through momentum space will accelerate.

It is understood that the above development assumes that $dv/dt \neq 0$, an approach which is not covered in standard texts[61], but is assumed to be valid here because of it describes in part the actual physical phenomenon taking place when an object impacts or collides with an trisine elastic space lattice cell. The elastic space lattice cell essentially collapses ($B \rightarrow 0$) and the entire cell momentum ($m_t c$) is transferred to the object with cell permittivity (ϵ) and permeability (k_m) proceeding to a values of one(1).

In terms of an object passing through the trisine elastic space CPT lattice at some velocity (v_o), the factor (Fs/m_t) is no longer dependent of object velocity (v_o) as defined in ($v_{dx} < v_o \ll c$) but is a constant relative to c^2 which reflects the fact that the speed of light is a constant in the universe. Inspection would indicate that as (v_o) is in range ($v_{dx} < v_o \ll c$) then the observed object deceleration "a" is a constant (not tied to any particular reference frame either translational or rotational):

$$a = \frac{F}{M}$$

and specifically for object and trisine elastic space lattice relative velocities (v_o) as follows:

The sun referenced Pioneer velocity of about 12 km/s or earth (around sun) orbital velocity of 29.8 km/sec or sun (circa milky way center) rotation velocity of 400 km/sec

or the CMBR dipole of 620 km/s

or any other velocity 'v' magnitude ($0 < v < c$)

then

$$\int_B^0 F \frac{ds}{C_t} = m_t \int_{v_{dx}+v_0}^c \frac{v}{\sqrt{1 - \frac{v^2}{c^2}}} dv = m_t \int_{k_m \epsilon + \frac{v_0^2}{c^2}}^1 \frac{-1}{\alpha^2} \frac{c^2}{\sqrt{1 - \frac{1}{\alpha}}} d\alpha \tag{2.7.5}$$

do not contribute to the observed Pioneer deceleration (as observed) and (noting that $c \sim 300,000$ km/sec). and in consideration of the following established relationship:

$$F \approx -C_t \frac{m_t c^2}{s} = C_t A_c \rho_U c^2 \quad (2.7.6)$$

$$\text{where: } C_t = \frac{24}{R_{eo}} + \frac{6}{1 + \sqrt{R_{eo}}} + .4 \text{ and } R_{eo} = \frac{\rho_U c d}{\mu_{Uc}}$$

Where constant C_t is in the form of the standard fluid mechanical drag coefficient analogous to 2.7.4a, but is defined as a thrust coefficient.

This trisine model was used to analyze the Pioneer unmodeled deceleration data $8.74E-08$ cm/sec² and there appeared to be a good fit with the observed space density (ρ_U) $6E-30$ g/cm³ (trisine model (ρ_U) $6.38E-30$ g/cm³). A thrust coefficient (C_t) of 59.67 indicates a laminar flow condition. An absolute space viscosity seen ($\mu_{Uc} = m_t c / (2\Delta x^2)$) of $1.21E-16$ g/(cm sec) is established within trisine model and determines a space kinematic viscosity seen (μ_{Uc} / ρ_U) of $(1.21E-16 / 6.38E-30)$ or $1.90E13$ cm²/sec as indicated in 2.7.4a.

Table 2.7.2 Pioneer (P) Translational Calculations

P mass (M)	241,000 gram
P diameter (d)	274 cm (effective)
P cross section (A_c)	58,965 cm ² (effective)
P area/mass (A_c/M)	0.24 cm ² /g
P velocity	1,117,600 cm/sec
Pioneer Reynold's number (R_{eo})	4.31E-01 unitless
thrust coefficient (C_t)	59.67 unitless
P deceleration (a)	8.37E-08 cm/sec ²
one year thrust distance	258.51 mile
laminar thrust force	9.40E-03 dyne
time of object to stop	1.34E13 sec

These parameters are in the context of radiation pressure

$$\text{radiation pressure} = \Upsilon \sigma_s T^4 \left(\frac{4}{3c} \right)$$

with a multiplier factor F as a measure of material emissivity or absorptivity.

Pioneer recoil deceleration(a) may be then calculated as:

$$a = \text{radiation pressure } A_c / M$$

This deceleration(a) is then proportional to a net system temperature(T)⁴. This system temperature(T) scales with the RTG radioactive source half-life 87 years.

The Pioneer deceleration(a) half-life then varies with RTG half-life as $(1/2)^4 = 1/16$.

The Pioneer deceleration(aP) half_life should then be on the order of $87/16$ or 5.4 years (not ~ 25 to ~ 40 years as indicated in ref 116a). This relatively short aP half_life (~ 5 years) is correctly modeled for both Pioneers with a combination exponential decay and constant deceleration with the constant $aP(infinity)$ on the order of $8 E-8$ cm/sec².

The half_lives associated with power consumption (heat, T) ref 116 Table I are shorter than 87 years making the above argument more compelling.

Pioneer internal temperature related radiation pressure decelerations ($\Upsilon=1$) are as follows:

Temperature T (Kelvin)	Pioneer deceleration cm/sec ² due to radiation pressure
25	2.41E-10
50	3.86E-09
25	1.95E-08
100	6.17E-08
125	1.61E-07

It is difficult to escape the conclusion that the independently developed Pioneer thermal recoil model (based solely on the decay hypothesis $dx/dt = -kx$) is deficient in modeling the Pioneer anomaly.

The Jet Propulsion Laboratory (JPL), NASA raised a question concerning the universal application of the observed deceleration on Pioneer 10 & 11. In other words, why do not the planets and their satellites experience such a deceleration? The answer is in the A_c/M ratio in the modified thrust relationship.

$$a \approx -C_t \frac{m_t c^2}{M s} = -C_t \frac{A_c}{M} \rho_U c^2 = -C_t \frac{A_c}{M} \frac{m_t}{M \text{ cavity}} c^2 \quad (2.7.6a)$$

Using the earth as an example, the earth differential movement per year due to modeled deceleration of $4.94E-19$ cm/sec² would be 0.000246 centimeters (calculated as $at^2/2$, an unobservable distance amount). Also assuming the trisine superconductor resonant symmetric model, the reported 6 nanotesla (nT) ($6E-5$ gauss) interplanetary magnetic field (IMF) in the vicinity of earth, (as compared to .2 nanotesla (nT) ($2E-6$ gauss [78,140]) interstellar magnetic field congruent with CMBR) will not allow the formation of a superconductor CPT lattice due to the well known properties of a superconductor in that magnetic fields above critical fields will destroy it. In this case, the space

superconductor at $T_c = 8.1\text{E-16}$ K will be destroyed by a magnetic field above

$$H_c (c/v_{dx})(m_e/m_t)(\text{chain/cavity}) = 2.\text{E-}6 \text{ gauss (2 nT)}$$

as in table 2.6.2. It is conceivable that the IMF decreases by some power law with distance from the sun. Perhaps at some distance from the sun, the IMF diminishes to an extent and defining an associated energy condition, wherein the space superconductor resonant CPT lattice is allowed to form. This IMF condition may explain the observed ‘ramp’, ‘step’ or “kick in” of the Pioneer spacecraft deceleration phenomenon at 10 Astronomical Units (AU) (Asteroid belt distance from the sun).

Table 2.7.3 Earth Translational Calculations

Earth (M)	5.98E27	Gram
Earth (d)	1.27E09	cm
Earth cross section (A_c)	1.28E18	cm ²
Earth area/mass (A_c/M)	2.13E-10	cm ² /g
Earth velocity	2,980,010	cm/sec
Earth Reynolds number (R_{eo})	2.01E06	unitless
thrust coefficient (C_t)	0.40	unitless
thrust force (F)	2.954E09	dyne
Earth deceleration (a)	4.94E-19	cm/sec ²
one year thrust distance	0.000246	cm
laminar thrust force	4.61E-01	dyne
time for Earth to stop rotating	6.03E24	sec

Now to test the universal applicability of the unmodeled Pioneer 10 & 11 decelerations for other man made satellites, one can use the dimensions and mass of the Hubble space telescope. One arrives at a smaller deceleration of 6.79E-09 cm/sec² because of its smaller area/mass ratio. This low deceleration is swamped by other decelerations in the vicinity of earth, which would be multiples of those well detailed in reference 1, Table II Pioneer Deceleration Budget. Also the trisine elastic space CPT lattice probably does not exist in the immediate vicinity of the earth because of the earth’s milligauss magnetic field, which would destroy the coherence of the trisine elastic space CPT lattice.

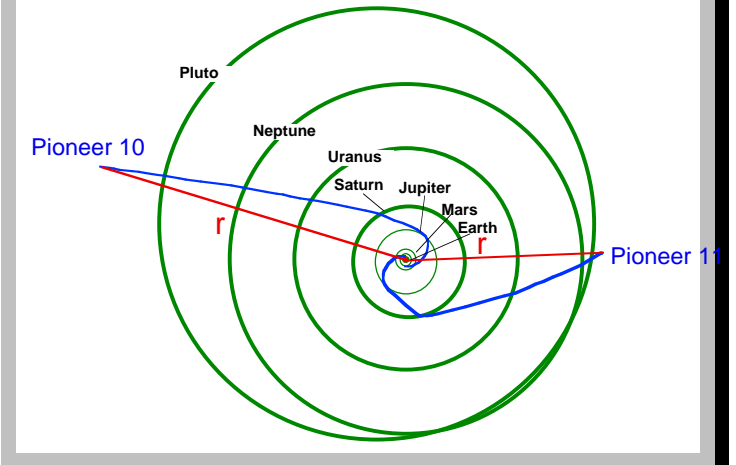
Table 2.7.4 Hubble Satellite Translational Calculations

Hubble mass (M)	1.11E07	gram
Hubble diameter (d)	7.45E02	centimeter
Hubble cross section (A_c)	5.54E05	cm ²
Hubble area/mass (A_c/M)	0.0499	cm ² /g
Hubble velocity	790,183	cm/sec
Hubble Reynolds' number (R_{eo})	1.17E00	unitless
thrust coefficient (C_t)	23.76	
thrust force (F)	7.549E-02	dyne
Hubble deceleration (a)	6.79E-09	cm/sec ²
One year thrust distance	3,378,634	cm
laminar thrust force	7.15E-08	dyne

Time for Hubble to stop rotating 1.16E14 sec
The fact that the unmodeled Pioneer 10 & 11 deceleration data are statistically equal to each other and the two space craft exited the solar system essentially 190 degrees from each other implies that the supporting fluid space density through which they are traveling is co-moving with the solar system. But this may not be the case. Assuming that the supporting fluid density is actually related to the cosmic background microwave radiation (CMBR), it is known that the solar system is moving at 500 km/sec relative to CMBR. Equivalent decelerations in irrespective to spacecraft heading relative to the CMBR would further support the hypothesis that deceleration is independent of spacecraft velocity.

Reference 150 indicates dark matter cross-section and resultant drag characteristics for 72 studied galactic collisions .47 cm²/g. The Pioneer 10 and 11 cross-sections are .24 cm²/g. The proximity of these two values is an indication of a common drag mechanism?

Figure 2.7.4 Pioneer Trajectories (NASA JPL [53]) with delineated solar satellite radial component r .



Executing a web based [58] computerized radial rate dr/dt (where r is distance of spacecraft to sun) of Pioneer 10 & 11 Figure 2.7.1), it is apparent that the solar systems exiting velocities are not equal. Based on this graphical method, the spacecraft’s velocities were in a range of about 9% (28,600 – 27,500 mph for Pioneer 10 “3Jan87 - 22July88” and 26,145 – 26,339 mph for Pioneer 11 ”5Jan87 - 01Oct90”). This reaffirms the basic thrust equation used for computation in that, velocity magnitude of the spacecraft is not a factor, only its direction with the thrust force opposite to that direction. The observed equal deceleration at different velocities would appear to rule out deceleration due to Kuiper belt dust as a source of the deceleration for a variation at 1.09² or 1.19 would be expected.

Also it is observed that the Pioneer spacecraft spin is

slowing down during periods not affected by gaseous flows or other articulated spacecraft movements. JPL[57] suggests an unmodeled deceleration rate of .0067 rpm/year or 3.54E-12 rotations/sec² during these undisturbed periods.

Now using the standard torque formula:

$$\Gamma = I\dot{\omega} \quad (2.7.7)$$

The deceleration value of 3.54E-12 rotation/sec² can be replicated assuming a Pioneer Moment of Inertia about spin axis(I) of 5.88E09 g cm² and a 'paddle' cross section area of 3,874 cm² which is 6.5% spacecraft 'frontal' cross section which seems reasonable.

Also it is important to note that the angular deceleration rate for each spacecraft (Pioneer 10, 11) is the same even though they are spinning at the two angular rates 4 and 7 rpm respectfully. This would further confirm that velocity is not a factor in measuring the space mass or energy density. The calculations below are based on NASA JPL problem set values[57]. Also, the sun is moving through the CMBR at 600 km/sec. According to this theory, this velocity would not be a factor in the spacecraft deceleration.

Table 2.7.5 Pioneer (P) Rotational Calculations

P mass (<i>M</i>)	241,000 g
P moment of inertia (<i>I</i>)	5.88E09 g cm ²
P diameter (<i>d</i>)	274 cm
P translational cross section	58,965 cm ²
P radius of gyration <i>k</i>	99 cm
P radius <i>r</i>	137 cm
P paddle cross section	3,874 cm ²
P paddle area/mass	0.02 cm ² /g
P rotation speed at <i>k</i>	4,517 cm/sec
P rotation rate change	0.0067 rpm/year
P rotation rate change	3.54E-12 rotation/sec ²
P rotation deceleration at <i>k</i>	2.20E-09 cm/sec ²
P force slowing it down (<i>F</i>)	1.32E-03 dyne
P Reynolds' number (<i>R_{eo}</i>)	4.31E-01 unitless
thrust coefficient (<i>C_v</i>)	59.67
thrust force (<i>F</i>)	1.32E-03 dyne
one year rotational distance	1,093,344 cm
P rotational laminar force	7.32E-23 dyne
time for P to stop rotating	2.05E12 sec

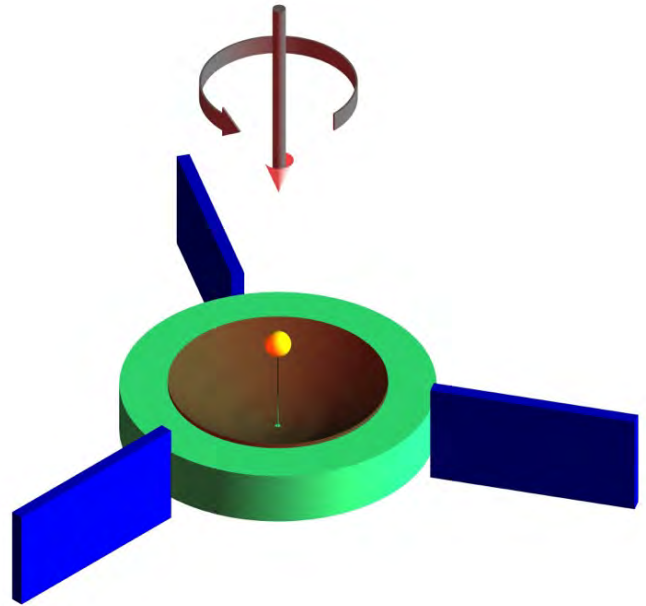
These calculations suggest a future spacecraft with general design below to test this hypothesis. This design incorporates general features to measure translational and rotational thrust. A wide spectrum of variations on this theme is envisioned. General Space Craft dimensions should be on the order of Trisine geometry *B* at $T_b = 2.711 K$ $T_c = 8.12E-16 K$ or 22 cm (Table 2.2.1) or larger. The Space Craft Reynold's number would be nearly

1 at this dimension and the resulting thrust the greatest. The coefficient of thrust would decrease towards one with larger Space Craft dimensions. It is difficult to foresee what will happen with Space Craft dimensions below present dark energy dimension *B_{present}* of 22 cm.

The spacecraft (Figure 2.7.5) would rotate on green bar axis while traveling in the direction of the green bar. The red paddles would interact with the space matter as mc^2 slowing the rotation with time in conjunction with the overall spacecraft slowing decelerating.

A basic experiment cries out here to be executed and that is to launch a series of spacecraft of varying A_c/M ratios and exiting the solar system at various angles while measuring their rotational and translational decelerations. This would give a more precise measure of the spatial orientation of dark energy in the immediate vicinity of our solar system. An equal calculation of space energy density by translational and rotational observation would add credibility to accumulated data.

Figure 2.7.5 Space craft general design to quantify translational and rotary thrust effect. Brown is parabolic antenna, green is translational capture element and blue is rotational capture element.



The assumption that the Pioneer spacecraft will continue on forever and eventually reach the next star constellation may be wrong. Calculations indicate the Pioneers will come to a stop relative to space fluid in about 400,000 years. We may be more isolated in our celestial position than previously thought.

When this thrust model is applied to a generalized design for a Solar Sail [63], a deceleration of 3.49E-05 cm/sec² is calculated which is 3 orders higher than experienced by

Pioneer spacecraft. Consideration should be given to spin paddles for these solar sails in order to accumulate spin deceleration data also. In general, a solar sail with its characteristic high A_c/M ratio such as this example should be very sensitive to the trisine elastic space CPT lattice. The integrity of the sail should be maintained beyond its projected solar wind usefulness as the space craft travels into space beyond Jupiter.

Table 2.7.6 Sail Deceleration Calculations

Sail mass (M)	300,000	gram
Sail diameter (d)	40,000	centimeter
Sail cross section (A_c)	1,256,637,000	cm^2
Sail area/mass (A_c/M)	4,189	cm^2/g
Sail velocity	1,117,600	cm/sec
Sail Reynold's number	6.30E01	unitless
thrust coefficient (C_t)	1.45	
thrust force (F)	10	dyne
Sail acceleration (a)	3.49E-05	cm/sec^2
one year thrust distance	1.73E10	Cm
laminar thrust force (F)	1.37E00	dyne
time of Sail to stop	1015	year

The following calculation establishes a distance from the sun at which the elastic space CPT lattice kicks in. There is a energy density competition between the solar wind and the elastic space CPT lattice. Assuming the charged particle density at earth is $5 / \text{cm}^3$ [57] and varying as $1/R^2$ and comparing with elastic space density of $kT/cavity$, then an equivalent energy density is achieved at 3.64 AU. This of course is a dynamic situation with solar wind changing with time, which would result in the boundary of the elastic space CPT lattice changing with time. This is monitored by a spacecraft (Advanced Composition Explorer (ACE)) at the L1 position (1% distance to sun) and can be viewed at the website <http://space.rice.edu/ISTP/dials.html>. A more descriptive term would be making the elastic space CPT lattice decoherent or coherent. It is interesting to note that the calculated boundary is close to that occupied by the Asteroids and is considered the Astroid Belt.

Table 2.7.7 Space CPT lattice intersecting with solar wind

Mercury	0.39
Venus	0.72
Earth	1.00
Mars	1.53
Jupiter	5.22
Saturn	9.57
Uranus	19.26
Neptune	30.17
Pluto	39.60
Kuiper Belt	50
	60
Oort Cloud?	80
	100
	200
	400
n at AU	3.64
	0.38 cm^{-3}

r	$1/n^{1/3}$	1.38	cm
coordination #		6	unitless
volume		0.44	cm^3
$\frac{e^2}{r}$	$\frac{1}{volume} \frac{T_c}{T_b}$	$\frac{energy}{volume}$	1.13E-34 erg / cm^3
Trisine	$\frac{k_b T_c}{cavity}$	$\frac{energy}{volume}$	1.13E-34 erg / cm^3

Now assuming the basic conservation of total kinetic and potential energy for an object in circular orbit of the sun with velocity (v_0) and at distance (R_0) equation 2.7.8 provides an indication of the time required to perturb the object out of the circular orbit in the direction of the sun.

$$v_0^2 + \frac{GM_{\odot}}{R_0} = v^2 + (v_0 - at)^2 \quad (2.7.8a)$$

$$v_0^2 + \frac{GM_{\odot}}{R_0} = v^2 + \left(v_0 - C_t \frac{\text{Area}}{M} \rho c^2 t \right)^2 \quad (2.7.8b)$$

where $v = \delta v_0$

Assuming the sun orbital velocity perturbing factor δ to be .9 and the time (t) at the estimated age of the solar system (5,000,000,000 years), then the smallest size Dark Energy Influenced objects that could remain in sun orbit are listed below as a function of distance (AU) from the sun.

Table 2.7.8a Solar Space Dark Energy Influenced object upper size vs AU

	AU	diameter (meter)
Mercury	0.39	9.04
Venus	0.72	10.67
Earth	1.00	11.63
Mars	1.53	13.04
Jupiter	5.22	18.20
Saturn	9.57	21.50
Uranus	19.26	26.10
Neptune	30.17	29.60
Pluto	39.60	31.96
Kuiper Belt	50	35.95
	60	37.57
Oort Cloud?	80	40.36
	100	41.60
	200	50.82
	400	62.24

This calculation would indicate that there is not small particle dust remaining in the solar system, which would include the Kuiper Belt and hypothesized Oort Cloud. Also, the calculated small object size would seem to be consistent with Asteroid Belt objects, which exist at the coherence/decoherence boundary for the elastic space CPT lattice.

This momentum transfer between dark energy elastic space CPT lattice and impinging objects as represented by this equations 2.7.8a and 2.7.8b analysis has implications for

large-scale galactic structures as well. Indeed, there is evidence in the Cosmic Gamma Ray Background Radiation for energies associated with this momentum transfer on the order of $m_c c^2$ or 56 MeV or ($\log_{10}(\text{Hz}) = 22.13$) or (2.20E-12 cm) [73]. In the available spectrum [73], there is a hint of a black body peak at 56 MeV or ($\log_{10}(\text{Hz}) = 22.13$) or (2.20E-12 cm). This radiation has not had an identifiable source until now.

Application of equations 2.7.8a and 2.7.8b at the Galactic scale replicate the observed constant rotation rate (220 km/sec) associated with the Milky Way Galaxy and others as well as indicated in Table 2.7.8b.

Table 2.7.8b Idealized flat rotation Milky Way Galactic Space object dark energy influenced upper size (after 13 billion years) vs galactic radius based on Milky Way mass of 2.15E11 solar masses contained within a galactic radius of 60,000 light years, galactic density (ρ_g) of 6.43E-23 g/cm³, object density (ρ_o) of 1 g/cm³ and galactic disc thickness of 12,000 light years

Galactic Radius (ly)	Object Diameter (cm)	Object A/m	Object m/A	Object Velocity (km/sec)	Object M F P (ly)	Object Optical Depth ($\rho_o d_o / \rho_g$)
5,000	10.80	0.0463	21.6	220	3.55E+05	2.82E-02
7,500	11.96	0.0418	23.9	220	3.93E+05	3.82E-02
10,000	12.85	0.0389	25.7	220	4.23E+05	4.73E-02
12,500	13.59	0.0368	27.2	220	4.47E+05	5.60E-02
15,000	14.23	0.0351	28.5	220	4.68E+05	6.41E-02
17,500	14.79	0.0338	29.6	220	4.86E+05	7.20E-02
20,000	15.29	0.0327	30.6	220	5.03E+05	7.96E-02
22,500	15.75	0.0318	31.5	220	5.18E+05	8.69E-02
25,000	16.17	0.0309	32.3	220	5.32E+05	9.41E-02
27,500	16.56	0.0302	33.1	220	5.44E+05	1.01E-01
30,000	16.92	0.0295	33.8	220	5.56E+05	1.08E-01
32,500	17.27	0.0290	34.5	220	5.68E+05	1.14E-01
35,000	17.59	0.0284	35.2	220	5.78E+05	1.21E-01
37,500	17.90	0.0279	35.8	220	5.88E+05	1.27E-01
40,000	18.19	0.0275	36.4	220	5.98E+05	1.34E-01
42,500	18.47	0.0271	36.9	220	6.07E+05	1.40E-01
45,000	18.74	0.0267	37.5	220	6.16E+05	1.46E-01
47,500	18.99	0.0263	38.0	220	6.24E+05	1.52E-01
50,000	19.24	0.0260	38.5	220	6.32E+05	1.58E-01
52,500	19.47	0.0257	38.9	220	6.40E+05	1.64E-01
55,000	19.70	0.0254	39.4	220	6.48E+05	1.70E-01
57,500	19.92	0.0251	39.8	220	6.55E+05	1.76E-01
60,000	20.14	0.0248	40.3	220	6.62E+05	1.81E-01

The upper size objects vs distance from sun as calculated above and presented in Table 2.7.8a may provide a clue for constant velocity with distance observed in galactic rotation curves (in this case 220 km/sec). The calculated mean free path of such ‘dark matter’ objects indicates that they would

be optically invisible as observed from outside the galaxy.

Dark energy and Dark matter may be very closely linked by momentum transfer forming Dark matter clumping. Reference [76] indicates non luminous but gravitational existence of dark matter clumping in the dynamics of galactic collisions and a thrust effect of the dark energy on galactic material. Reference [79] indicates the independence of dark and visible matter distribution but perhaps this independence is illusionary. According to the correlation herein, the observed dark matter distributions are composed of small dense (1 g/cc) hydrogen BEC objects (<1 meter) contributing to a space density of ~ 1.47E-23 g/cc with resulting optical path(=<1) dictating invisibility other than through the observed gravitational weak lensing effect.

Table 2.7.8c Idealized Dark Matter object dark energy influenced upper size (after 13 billion years) vs galactic radius based on Milky Way mass of 3.40E14 solar masses contained within a cluster radius of 240,000 light years, cluster density (ρ_g) of 1.47E-23 g/cm³, object density (ρ_o) of 1 g/cm³ and galactic disc thickness of 400,000 light years

Galactic Radius (ly)	Object Diameter (cm)	Object A/m	Object m/A	Object Velocity (km/sec)	Object M F P (ly)	Object Optical Depth ($\rho_o d_o / \rho_g$)
20,000	4.60	0.1088	9.2	1211	3.31E+05	1.21E-01
30,000	5.09	0.0983	10.2	1211	3.67E+05	1.64E-01
40,000	5.47	0.0915	10.9	1211	3.94E+05	2.03E-01
50,000	5.78	0.0865	11.6	1211	4.17E+05	2.40E-01
60,000	6.05	0.0827	12.1	1211	4.36E+05	2.75E-01
70,000	6.29	0.0795	12.6	1211	4.53E+05	3.09E-01
80,000	6.50	0.0769	13.0	1211	4.69E+05	3.41E-01
90,000	6.70	0.0747	13.4	1211	4.83E+05	3.73E-01
100,000	6.87	0.0727	13.7	1211	4.96E+05	4.04E-01
110,000	7.04	0.0710	14.1	1211	5.07E+05	4.34E-01
120,000	7.20	0.0695	14.4	1211	5.19E+05	4.63E-01
130,000	7.34	0.0681	14.7	1211	5.29E+05	4.91E-01
140,000	7.48	0.0669	15.0	1211	5.39E+05	5.19E-01
150,000	7.61	0.0657	15.2	1211	5.48E+05	5.47E-01
160,000	7.73	0.0647	15.5	1211	5.57E+05	5.74E-01
170,000	7.85	0.0637	15.7	1211	5.66E+05	6.01E-01
180,000	7.96	0.0628	15.9	1211	5.74E+05	6.27E-01
190,000	8.07	0.0619	16.1	1211	5.82E+05	6.53E-01
200,000	8.18	0.0611	16.4	1211	5.89E+05	6.79E-01
210,000	8.28	0.0604	16.6	1211	5.97E+05	7.04E-01
220,000	8.37	0.0597	16.7	1211	6.04E+05	7.29E-01
230,000	8.47	0.0590	16.9	1211	6.10E+05	7.54E-01
240,000	8.56	0.0584	17.1	1211	6.17E+05	7.78E-01

Reference [64] presents an experimental protocol in which a comoving optical and sodium atom lattice is studied at nanokelvin a temperature. When the moving lattice is stopped (generating laser beams extinguished), the sodium

atoms stop rather than proceeding inertially. This unexplained anomaly may be explained in a similar manner as Pioneer deceleration. The following calculation indicates a sodium atom deceleration large enough to indicate essentially an instantaneous stop.

Table 2.7.9 Sodium Atom Deceleration

sodium temperature	1.00E-06	kelvin
sodium mass	3.82E-23	gram
sodium van der Waals diameter	4.54E-08	centimeter
sodium cross-section	1.62E-15	cm ²
sodium area/mass	4.24E07	cm ² /g
optical lattice velocity	3.0	cm/sec
sodium Reynold's number	7.15E-11	unitless
thrust coefficient	3.36E11	unitless
thrust force (with C _v)	3.116E-12	dyne
sodium deceleration	8.16E10	cm/sec ²
time to stop sodium atom	3.68E-11	sec
distance to stop sodium atom	5.51E-11	cm

An experiment is envisioned whereby larger atomic clusters are decelerated in a more observable manner because of their increased mass. It assumed that such an anomalous deceleration will occur only at nanokelvin temperatures where the $k_b T$ energies are essentially zero.

It is understood that the New Horizons spacecraft launched on January 19, 2006 presents an opportunity to replicate the Pioneer 10 & 11 deceleration. The tables below provide a predictive estimate of this deceleration. Because of the New Horizons smaller area to mass ratio than Pioneer, it is anticipated that the New Horizons anomalous deceleration will be smaller than the Pioneer anomalous deceleration by a factor of about .4. Also, because the New Horizons Moment of Inertia about the spin axis is smaller than Pioneer, it is predicted that the rate of spin deceleration will be greater for the New Horizons than observed for the Pioneer space crafts.

Table 2.7.9 New Horizons (NH) Translation Predictions

New Horizons mass	470,000	gram
New Horizons diameter	210	cm (effective)
		cm ²
New Horizons cross section	34,636	(effective)
New Horizons area/mass	0.07	cm ² /g
trisine area/mass	5.58E30	cm ² /g
New Horizons velocity	1,622,755	cm/sec
New Horizons Reynold's number	3.31E-01	unitless
drag coefficient	76.82	
drag force (with drag coefficient)	1.525E-02	dyne
New Horizons deceleration	3.24E-08	cm/sec ²
one year drag distance	16,132,184	cm
laminar drag force	7.21E-03	dyne

time of New Horizons to stop	5.00E13 sec
Table 2.7.10 New Horizons (NH) Rotational Predictions	
NH mass	470,000 g
NH moment of inertia NASA JPL	4.01E09 g cm ²
NH diameter	315 cm
NH translational cross-section	77,931 cm ²
NH radius of gyration k	131 cm
NH radius r	158 cm
paddle cross-section	60,210 cm ²
paddle area/mass	1.28E-01 cm ² /g
NH rotation speed at k	5,971 cm/sec
NH rotation rate change	0.2000 rpm/year
NH rotation rate change	1.06E-10 rotation/sec ²
NH rotation deceleration at k	8.68E-08 cm/sec ²
NH force slowing it down	2.04E-02 dyne
NH Reynold's number	4.36E-01 unitless
thrust coefficient	59.09
thrust (with C _v)	2.04E-02 dyne
one year rotational thrust distance	43,139,338 cm
NH rotational laminar thrust force	1.90E-02 dyne
time for NH to stop rotating	6.88E10 sec

This New Horizons deceleration characteristics will be monitored in the vicinity of Jupiter passage on February 28, 2007 and thereafter.

In addition to the Linear and Exponential Decay Pioneer deceleration aP models presented in refs 116 & 116a, a combination Exponential Deceleration Decay To Constant Linear Deceleration approached at infinity is evaluated.

$$a_P(t) = a_P(t_0) e^{-\beta(t-t_0)\ln 2} + a_P(\text{infinity})$$

For this evaluation, stochastic data is digitized from graphical presentation in refs: 116 and 116a. Initial conditions are at January 1, 1980.

For Pioneer 10 Model, given initial $a_P(t_0) = 9.82 \times 10^{-10} \text{ m/s}^2$ at time 8.79 years from Table 2.7.11, then multivariable regression minimizing stochastic – model Root Mean Square(RMS) data from Table 2.7.13 yields the following modeled constants:

$$\beta = 1/5.00 \text{ years}$$

$$a_P(\text{infinity}) = 7.00 \times 10^{-10} \text{ m/s}^2$$

$$RMS = .224 \times 10^{-10} \text{ m/s}^2$$

This is compared to analysis with $a_P(\text{infinity}) = 0$

$$\beta = 1/61.0 \text{ years}$$

$$a_P(t_0) = 9.82 \times 10^{-10} \text{ m/s}^2$$

$$RMS = .478 \times 10^{-10} \text{ m/s}^2$$

For Pioneer 11 Model, given $a_p(t_0) = 9.274 \times 10^{-10} \text{ m/s}^2$ at 10.632 years from Table 2.7.12, then multivariable regression minimizing stochastic – model Root Mean Square(RMS) data from Table 2.7.14 yields the following modeled constants:

$$\begin{aligned}\beta &= 1/3.30 \text{ years} \\ a_p(\text{infinity}) &= 8.20 \times 10^{-10} \text{ m/s}^2 \\ RMS &= .160 \times 10^{-10} \text{ m/s}^2\end{aligned}$$

This is compared to analysis with $a_p(\text{infinity}) = 0$

$$\begin{aligned}\beta &= 1/160 \text{ years} \\ a_p(t_0) &= 9.274 \times 10^{-10} \text{ m/s}^2 \\ RMS &= .273 \times 10^{-10} \text{ m/s}^2\end{aligned}$$

Table 2.7.11 Pioneer 10
Modeled Stochastic Deceleration Data

Time(t) (years)	Stochastic a_p		Modeled a_p	
	x 10^{-10} m/s^2			
8.79	9.82	9.91		
10.78	9.33	9.20		
12.79	8.78	8.65		
14.82	8.21	8.24		
16.81	8.21	7.94		
18.80	7.39	7.71		
20.81	7.34	7.53		
22.82	7.23	7.40		
24.85	7.72	7.30		

Table 2.7.12 Pioneer 11
Modeled Stochastic Deceleration Data

Time(t) (years)	Modeled		
	Stochastic a_p	a_p	x 10^{-10}
	x 10^{-10} m/s^2	m/s ²	
10.632	9.274	9.187	
12.623	8.840	8.832	
14.631	8.358	8.604	
16.602	8.635	8.460	

Table 2.7.13 Pioneer 10
Minimized Stochastic – Model (RMS x 10^{-10} m/s^2)

$1/\beta$ years	$a_p \text{inf}$					
	x 10^{-10} m/s^2	6.80	6.90	7.00	7.10	7.20
4.80		.372	.299	.246	.228	.251
4.90		.336	.270	.230	.231	.271
5.00		.303	.247	.224	.244	.298
5.10		.274	.232	.229	.266	.330
5.40		.252	.226	.242	.294	.336

Table 2.7.14 Pioneer 11
Minimized Stochastic – Model (RMS x 10^{-10} m/s^2)

$1/\beta$ years	$a_p \text{inf}$					
	x 10^{-10} m/s^2	8.00	8.10	8.20	8.30	8.40
3.10		.325	.244	.183	.167	.205
3.20		.284	.210	.165	.175	.232
3.30		.246	.182	.160	.196	.267
3.40		.221	.164	.170	.227	.306
3.50		.183	.160	.194	.264	.349

Figure 2.7.6 Pioneer 10 deceleration profile
Stochastic data is represented by black steps with blue midpoint circles ref 116
Blue line is Pioneer deceleration decay midpoint regression

$$(10.1 \pm 1.0) 2^{-(t-t_0)/(28.8 \pm 2.0)} \text{ ref 116a} \quad (2.7.9)$$

Red line is thermal deceleration decay midpoint regression

$$(7.4 \pm 2.5) 2^{-(t-t_0)/(36.9 \pm 6.7)} \text{ ref 116a} \quad (2.7.10)$$

Green Line is Exponential Deceleration Decay To Constant Linear Deceleration

$$9.82 e^{-\frac{1}{5.00}(t-t_0) \ln 2} + 7.00 \text{ ref 116a} \quad (2.7.11)$$

with extrapolation beyond data points

Figure 2.7.6 Pioneer 10 Anomalous Deceleration $a_p \times 10^{-8} \text{ cm/sec}^2$

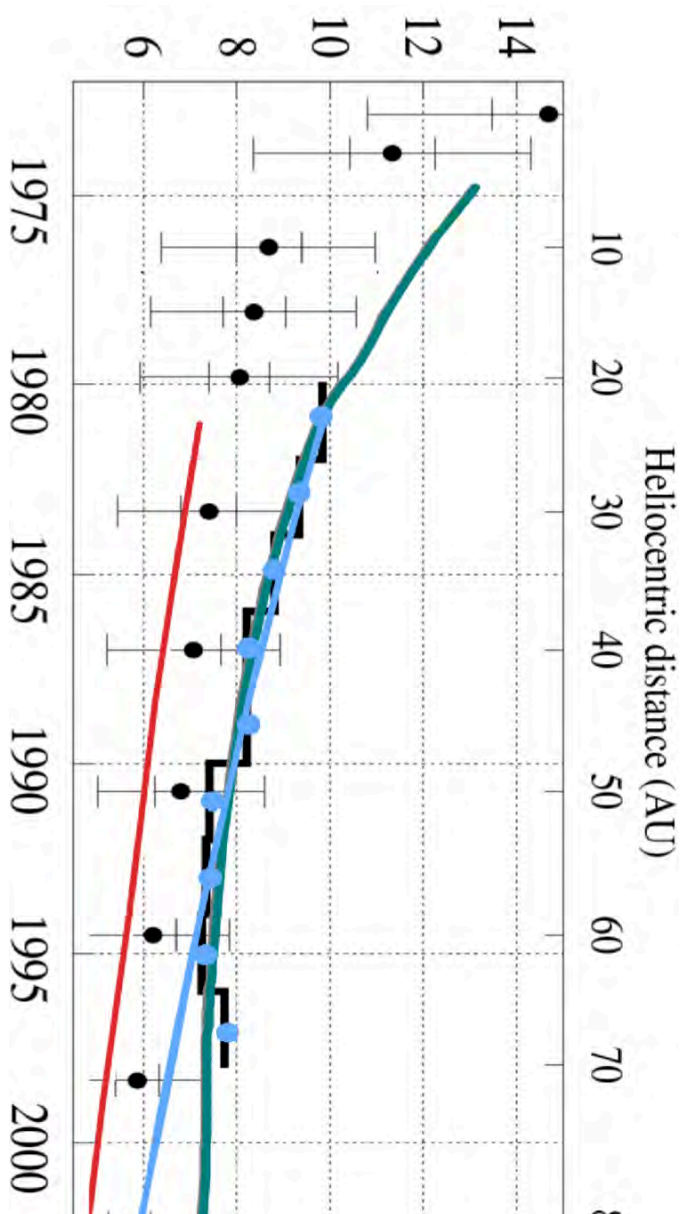


Figure 2.7.7 Pioneer 11 Anomalous Deceleration $a_p \times 10^{-8} \text{ cm/sec}^2$

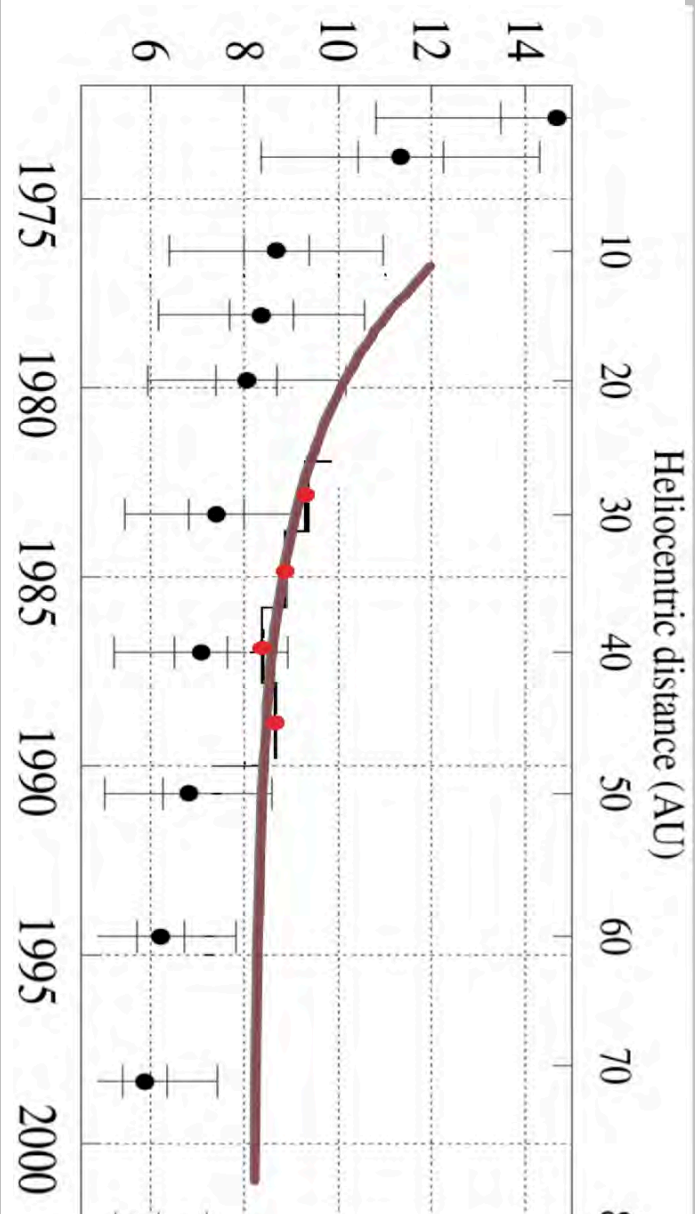


Figure 2.7.7 Pioneer 11 deceleration profile with thermal profile from Pioneer 10

Stochastic data is represented by black steps with red midpoint circles ref 116 with extrapolation beyond data points

Brown Line is Exponential Deceleration Decay To Constant Linear Deceleration

$$9.274e^{-\frac{1}{3.30}(t-t_0)\ln 2} + 8.20 \quad (2.7.12)$$

with extrapolation beyond data points.

Figures 2.7.6 and 2.7.7 indicate Pioneer thermal force has less contribution to Pioneer 10 deceleration with time approaching a constant Pioneer deceleration and not negating

$$a_p = (8.74 \pm 1.33) \times 10^{-10} \text{ m/s}^2$$

as originally suggested by John Anderson et al.[53].

Further analysis based on established theory indicates the Pioneer recoil deceleration may be calculated as:

$$\text{pressure} \times \text{pioneer area} / \text{pioneer mass} = a_p \quad (2.7.13)$$

This deceleration a_p is then proportional to a net system temperature(T)⁴.

$$\text{radiation pressure} = F\sigma_s T^4 \left(\frac{4}{3c} \right) \quad (2.7.14)$$

with a multiplier factor F as a measure of material emissivity or absorptivity.

Pioneer recoil deceleration(a_p) may be calculated as:

$$\text{radiation pressure} = F\sigma_s T^4 \left(\frac{4}{3c} \right) \quad (2.7.15)$$

Then the pioneer deceleration a_p may be represented as:

$$a_p = \frac{(\text{radiation pressure}) (\text{pioneer area})}{\text{pioneer mass}} \quad (2.7.16)$$

or

$$a_p = F\sigma_s T^4 \left(\frac{4}{3c} \right) \frac{\text{pioneer area}}{\text{pioneer mass}} \quad (2.7.17)$$

A theoretically consistent model was used[116,116a]:

$$a_p = \frac{nQ}{\text{pioneer mass } c} \quad (2.7.18)$$

where Q is directed radiation power and n represents empirically determined F and pioneer asymmetric areas.

Deceleration (a_p) as well as radiation power half_life vary as 1/4 of RTG half_life.

Deceleration (a_p) as well as radiation power half_life should then be on the order of 87.7/4 or 21.9 years

These half_lives should be considered very accurate and this accuracy is far greater than earth monitors can observe through thermal telemetry and on-board radiation pressures should follow the well established decay law $dx/dt = -kx$.

model one

$$\frac{da_p}{dt} = -ka_p = -\frac{\ln(2)}{87.2/4} a_p \quad (2.7.19)$$

The stochastic data half life more accurately follows a modified version (not addressed in refs 116,116a).

model two

$$\frac{da_p}{dt} = -k(a_p - a_{p\infty}) \quad (2.7.20)$$

indicating a_p approaches a constant value ($a_{p\infty}$) with time(t).

In summary, the references[116,116a] model the Pioneer deceleration $a_{p\infty}$ as the theoretically correct

$$a_p = \frac{\eta Q}{\text{pioneer mass } c} \quad (2.7.21)$$

with two components

$$a_p = \eta_{rtg} \frac{Q_{rtg}}{\text{pioneer mass } c} + \eta_{elec} \frac{Q_{elec}}{\text{pioneer mass } c} \quad (2.7.22)$$

Figure 2.7.8 Pioneer 10 deceleration with time after launch assuming Model two

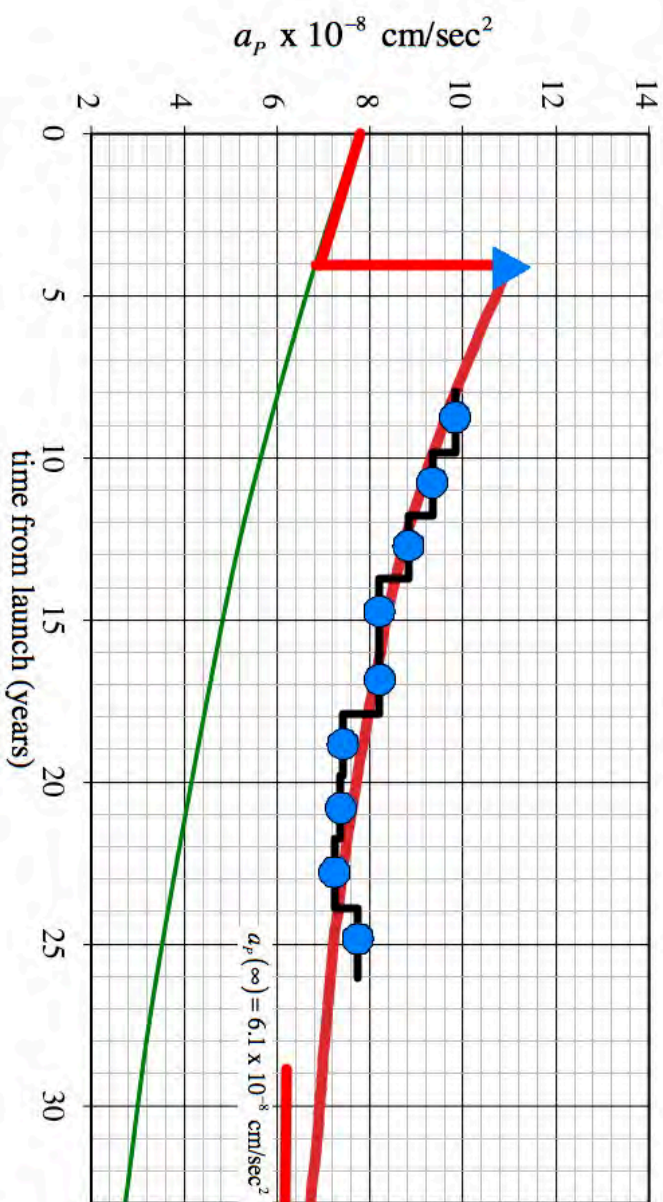
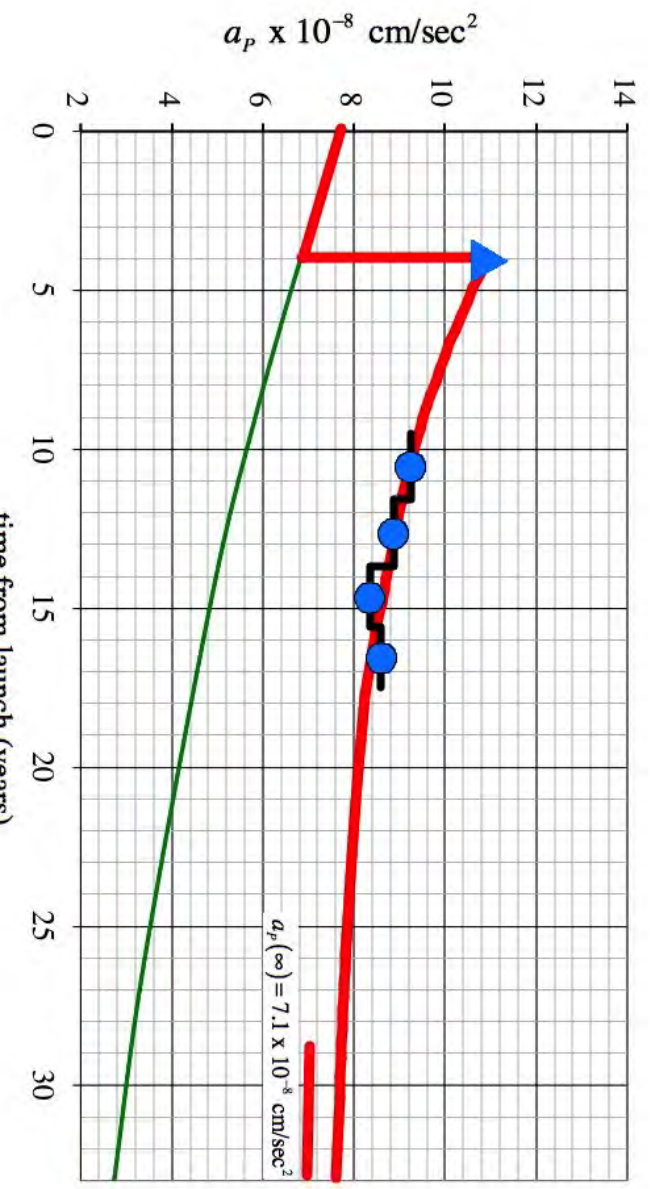


Figure 2.7.9 Pioneer 11 deceleration with time after launch assuming Model two



The data for component:

$$a_p = \eta_{elec} \frac{Q_{elec}}{\text{pioneer mass } c} \quad (2.7.23)$$

follows the relationship linked to 1/4 of RTG half life (87.7 years)

$$\frac{da_p}{dt} = -\frac{\ln(2)}{87.2/4} a_p \quad (2.7.24)$$

It is suggested that RTG deceleration component:

$$a_p = \eta_{rg} \frac{Q_{rg}}{\text{pioneer mass } c} \quad (2.7.25)$$

is directly linked to RTG 87.7 year half life[116a].

$$\frac{da_p}{dt} = -\frac{\ln(2)}{87.2} a_p \quad (2.7.26)$$

But this is theoretically not possible because of equations 2.7.16 and 2.7.17 where deceleration is related to T^4

Further, the RTG geometric design symmetry does not in principle allow for asymmetric radiation pressure contributing to a_p .

Further, the theoretical a_p identities (eqns 2.7.16 and 2.7.17)

indicates η represents empirically determined F and pioneer asymmetric areas. Any anticipated extremely small RTG manufacturing area asymmetries would contribute in a congruent extremely small manner.

Further, the RTG component decay is only about 20 percent over 25 years.

It is suggested the RTG component is incorrectly identified in refs[116,116a] as contributing to a_p . The actual contribution to model stochastic data is represented in eqn 2.7.23 plus an anomalous constant factor (aPinfinity) as represented in eqn 2.7.20 and $a_{p\infty}$ is testing the space vacuum[130] as per equation 2.11.9a.

Application of model two for stepped Pioneer 10 and 11 doppler data is represented in Figures 2.7.8 and 2.7.9.

The averaged per interval (black steps) Pioneer data are represented by blue circles.

The green line represents the electric component 2.7.23 decaying in accordance with equation 2.7.24.

The blue triangle represents the beginning of a constant Pioneer deceleration estimation in the neighborhood of the asteroid belt.

The red line follow the Pioneer deceleration from a purely electrical (thermal) (eqn 2.7.19) contribution transitioning to the electrical plus constant following model two (equation 2.7.20). Model two fits Pioneer 10 Doppler data with RMS = $.272 \times 10^{-8}$ cm/sec² and Pioneer 11 Doppler data with RMS = $.180 \times 10^{-8}$ cm/sec². The Pioneer 10 $a_{p\infty}$ is 6.1×10^{-8} cm/sec² and Pioneer 11 $a_{p\infty}$ is 7.1×10^{-8} cm/sec².

Pioneers could be probing the space vacuum viscosity in the same manner as the Voyagers test interstellar cosmic rays as they exist beyond the heliosphere (all initiated at JPL). Other object decelerations could then be dimensionally scaled to the Pioneer spacecraft. (planetary sized object deceleration would be negligible) The recently commissioned Dark Energy Survey <http://www.darkenergysurvey.org/> detailing universe expansion may be correlated to this phenomenon if galactic components are primarily of Pioneer size or smaller.

Aa. time (years after launch)(after AU to time conversion)

Bb. electric contribution to $a_{Pelec} \times 10^{-8}$ cm/sec²

n = .406 half life 24.5 years regressing [116a]

$$a_{Pelec} = 7.75 \times 10^{-8} e^{\frac{-\ln(2) \text{time after launch}}{24.5}}$$

Cc. RTG contribution to $a_{Prtg} \times 10^{-10}$ cm/sec²
n = 0.0104 half life 87.72 years (Plutonium)

$$a_{Prtg} = 3.71 \times 10^{-8} e^{\frac{-\ln(2) \text{time after launch}}{87.72}}$$

Dd. or Bb + Cc Total contribution to $a_{Px} \times 10^{-8}$ m/sec²

Ee. Doppler measured $a_{Px} \times 10^{-8}$ cm/sec²

Scenario one

Aa	Bb	Cc	Dd	Ee
8.79	6.05	3.46	9.51	9.82
10.78	5.71	3.41	9.12	9.33
12.79	5.40	3.35	8.75	8.78
14.82	5.10	3.30	8.40	8.21
16.81	4.82	3.25	8.07	8.21
18.80	4.56	3.20	7.75	7.39
20.81	4.30	3.15	7.45	7.34
22.82	4.07	3.10	7.17	7.23
24.85	3.84	3.05	6.89	7.72

Dd-Ee has RMS = .34

Statistical analysis of fin root temperatures[53a Figure 20] indicate temperature(T) half life of 130 years. This translates into power half life \sim emissivity $\times T^4$ or $130/4$ or 32.5 years. This is not reflected in reported RTG power performance. Radiation flux during Pioneer 10 Jupiter flyby (10,000 times that of Earth) did not cause differential RTG emissivity. Report [53 section C] does not provide any further mechanistic origin of Cc and none presented in [116a]. Assuming RTG contribution(Cc) is replaced by a constant(Ff) the electric(Bb) + constant(Ff) or Gg yields RMS = .33 (equal to scenario one .34) when compared to doppler(Ee)

Scenario two

Aa	Bb	Ff	Gg	Ee
8.79	6.05	3.33	9.38	9.82
10.78	5.71	3.33	9.04	9.33
12.79	5.40	3.33	8.73	8.78
14.82	5.10	3.33	8.43	8.21
16.81	4.82	3.33	8.15	8.21
18.80	4.56	3.33	7.89	7.39
20.81	4.30	3.33	7.63	7.34
22.82	4.07	3.33	7.40	7.23
24.85	3.84	3.33	7.17	7.72

Gg-Ee has RMS = .33

A more detailed model Hh minimizing RMS at .27 (the best available fit) assumes aP approaching a constant 5.9

$$a_p = (12.587 - 5.9) e^{(-.068*time)} + 5.9$$

Scenario three

Aa	Hh	Ee
8.79	9.60	9.82
10.78	9.14	9.33
12.79	8.74	8.78
14.82	8.39	8.21
16.81	8.09	8.21
18.80	7.83	7.39
20.81	7.60	7.34
22.82	7.40	7.23
24.85	7.23	7.72

Hh-Ee has RMS = .27

A Scenario three analysis of more limited Pioneer 11 data:

$$a_p = (12.587 - 7.4) e^{(-.098*time)} + 7.4$$

RMS = .18

There is statistical logic within the context of [116a] and historical Pioneer reports for a constant a_p contribution. The astrophysical importance of this constant a_p contribution demands attention. [116a] conclusions should be executed:

First,

Pioneer 11 data should be analyzed

Second,

the anomalous spin-down of both spacecraft should be addressed considering the asymmetrically electrical (door) a_p would have very little influence on the Pioneer moment of inertia (MR^2) primarily represented by the 30 foot magnetometer boom. The spin deceleration may be another

indication of constant a_p linking Pioneer rotational angular momentum to translational momentum.

Third,

Analysis early trajectory data for indication of a_p onset comparable to a constant 5.9E-8 cm/sec²

Fourth,

Address the possibility of outgassing from surface materials, with potential observable contribution to the anomalous acceleration.

Fifth,

Our understanding of systematics in the Doppler tracking data can be improved by a detailed auto correlation analysis.

Sixth,

Measure RTG paint emissivity by a thermal vacuum chamber test of a hot RTG analogue. (Resolve scenarios one and two)

Seventh,

Analyze other redundant data in the form of Deep Space Network signal strength measurements, which could be used to improve our understanding of the spacecraft's precise orientation.

2.8 Superconducting Resonant Current, Voltage And Conductance (and Homes' Law)

The superconducting electrical current (I_e) is expressed as in terms of a volume *chain* containing a Cooper CPT Charge conjugated pair moving through the trisine CPT lattice at a de Broglie velocity (v_{dx}) and the same as Maxwell's Ampere Law.

$$J_x = \frac{I_e}{area} = \frac{D_{fx}}{time_{\pm}} \quad (2.8.1)$$

$$J_{xr} = \frac{I_e}{area_r} = \frac{D_{fxr}}{time_{r\pm}} \quad (2.8.1r)$$

The superconducting mass current (I_m) is expressed as in terms of a trisine resonant transformed mass (m_t) per *cavity* containing a Cooper CPT Charge conjugated pair and the *cavity* Cooper CPT Charge conjugated pair velocity (v_{dx}).

$$J_{mx} = \frac{I_m}{area} = \left(\frac{m_t}{cavity} \right) v_{dx} \quad (2.8.2)$$

$$J_{mrx} = \frac{I_m}{area_r} = \left(\frac{m_t}{cavity_r} \right) v_{dxr} \quad (2.8.2r)$$

It is recognized that under strict CPT symmetry, there would

be zero current flow. It must be assumed that pinning of one side of CPT will result in observed current flow. Pinning (beyond that which naturally occurs) of course has been observed in real superconductors to enhance actual supercurrents. This is usually performed by inserting unlike atoms into the superconducting molecular lattice or mechanically distorting the lattice at localized points [72]. Also, there are reports that superconductor surface roughness enhances super currents by 30% [72]. This could be due to the inherent “roughness” of the CPT symmetry better expressing itself at a rough or corrugated surface rather than a smooth one.

Secondarily, this reasoning would provide reasoning why a net charge or current is not observed in a vacuum such as trisine model extended to critical space density in section 2.11.

A standard Ohm's law can be expressed as follows with the resistance expressed as the Hall quantum resistance with a value of 25,815.62 ohms (von Klitzing constant $2\pi\hbar/e_\pm^2$) in eqn 2.8.3.

$$voltage = (current) (resistance)$$

$$\frac{k_b T_c}{\mathbb{C} e_\pm} = \left(\frac{e_\pm}{\sqrt{3\alpha} \text{ approach time}} \right) \left(\frac{2\pi\hbar}{(\mathbb{C} e_\pm)^2} \right) \quad (2.8.3)$$

$$\frac{k_b T_c}{\mathbb{C} e_\pm} = \left(\frac{D_{fx}}{\text{time}} \right) \left(\frac{2\pi\hbar}{(\mathbb{C} e_\pm)^2} \right)$$

$$voltage = (current) (resistance)$$

$$\frac{k_b T_{cr}}{\mathbb{C} e_\pm} = \left(\frac{e_\pm}{\sqrt{3\alpha} \text{ approach}_r \text{ time}_r} \right) \left(\frac{2\pi\hbar}{(\mathbb{C} e_\pm)^2} \right) \quad (2.8.3r)$$

$$\frac{k_b T_{cr}}{\mathbb{C} e_\pm} = \left(\frac{D_{fxr}}{\text{time}_r} \right) \left(\frac{2\pi\hbar}{(\mathbb{C} e_\pm)^2} \right)$$

Table 2.8.1 with super current (J_s) (amp/cm^2) plot.

Condition	1.2	1.3	1.6	1.9	1.10	1.11
$T_a ({}^0 K)$	6.53E+11	6.53E+11	6.53E+11	6.53E+11	6.53E+11	6.53E+11
$T_b ({}^0 K)$	9.05E+14	5.48E+13	9.22E+08	1.10E+07	2,868	2.723
$T_{br} ({}^0 K)$	3.30E+12	5.45E+13	3.24E+18	2.72E+20	1.04E+24	1.10E+27
$T_c ({}^0 K)$	8.96E+13	3.28E+11	93.0	0.0131	8.99E-10	8.10E-16
$T_{cr} ({}^0 K)$	1.19E+09	3.25E+11	1.15E+21	8.11E+24	1.19E+32	1.32E+38
$z_R + 1$	3.67E+43	8.14E+39	3.89E+25	6.53E+19	1.17E+09	1.00E+00

$z_B + 1$	3.32E+14	2.01E+13	3.39E+08	4.03E+06	1.05E+03	1.00E+00
$Age_{UG} (\text{sec})$	7.14E-05	4.79E-03	6.94E+04	5.36E+07	1.27E+13	4.33E+17
$Age_{UGV} (\text{sec})$	4.59E-10	1.25E-07	4.42E+02	3.13E+06	1.22E+13	4.33E+17
$Age_U (\text{sec})$	1.18E-26	5.31E-23	1.11E-08	6.63E-03	3.70E+08	4.33E+17
$I_e (\text{amp/cm}^2)$	7.05E+24	9.45E+19	7.60E+00	1.52E-07	7.10E-22	5.77E-34
$I (\text{amp/cm}^2)$	1.24E+15	9.28E+19	1.15E+39	5.78E+46	1.23E+61	1.52E+73
$I_m (\text{g/cm}^2/\text{sec})$	1.16E+26	1.56E+21	1.25E+02	2.50E-06	1.17E-20	9.52E-33
$I (\text{g/cm}^2/\text{sec})$	2.05E+16	1.53E+21	1.90E+40	9.54E+47	2.04E+62	2.51E+74

Equation 2.8.4 represents the Poynting vector relationship or in other words the power per area per resonant CPT time $_\pm$ being transmitted from and absorbed in each superconducting cavity:

$$k_b T_c = \frac{m_e}{m_t} \frac{1}{2} E_x H_c (2 \text{ side}) \text{ time}_\pm v_\varepsilon \quad (2.8.4)$$

Equation 2.8.4 can be rearranged in terms of a relationship between the de Broglie velocity (v_{dx}) and modified speed of light velocity (v_{ex}) as expressed in equation 2.8.5.

$$v_{ex}^2 = \frac{\sqrt{3}}{48\pi^2} \left(\frac{m_t}{m_e} \right)^2 \frac{(\mathbb{C} e_\pm)^2}{\hbar A} B v_{dx} = \frac{1}{4} \frac{B}{A} \cdot c \cdot v_{dx} = \pi \cdot c \cdot v_{dx} \quad (2.8.5)$$

This leads to the group/phase velocity relationship (as previously stated in 2.1.30) in equation 2.8.6, which holds for the sub- and super- luminal nuclear conditions with the length dimensional transition point at the nuclear radius as established by dimensional analysis in Appendix I.

$$(v_{dx} < c, v_{ex} < c \text{ \& } v_{dxr} > c) \text{ \& } (v_{dx} > c, v_{ex} > c \text{ \& } v_{dxr} < c)$$

$$\begin{aligned}
 & (\text{group velocity}) \cdot (\text{phase velocity}(v_p)) = c^2 \\
 & (v_{dx}) \left(\frac{1}{\pi} \frac{v_{ex}^2}{v_{dx}^2} \cdot c \right) \cong \left(\frac{1}{2} v_{dx} \right) \left(\frac{\text{chain } v_{ex}^2}{\text{cavity } v_{dx}^2} \cdot c \right) \\
 & \cong (v_{dx}) \left(\frac{c}{v_{dx}} \cdot c \right) \\
 & \cong c^2
 \end{aligned} \quad (2.8.6)$$

In the Nature reference [51] and in [59], Homes reports

experimental data conforming to the empirical relationship Homes' Law relating superconducting number density ρ_s at just above T_c , superconductor conductivity σ_{dc} and T_c .

$$\rho_s \propto \sigma_{dc} T_c \quad \text{Homes' Law ref: 51} \quad (2.8.7)$$

The trisine model is developed for T_c , but using the Tanner's law observation that $n_s = n_N/4$ (ref 52), we can assume that $E_{fn} = E_{fs}/4$. This is verified by equation 2.5.1. Now substituting $I_e/(E_{fn} \text{area})$ for superconductor conductivity σ_{dc} , and using C/cavity for super current number density (ρ_s), the following dimensional relationship is obtained and is given the name Homes' constant (\mathcal{U}) while recognizing mass density (ρ_U) = $m_t \rho_s$.

(Note:

$$\sigma_{dc} (\text{cgs}) = 8.99 \times 10^11 \sigma_{dc} (\text{Siemen/cm})$$

which is dimensionally equivalent to:

$$\sigma_{dc} (e^2/(\text{erg sec cm})) = 8.99 \times 10^11 \sigma_{dc} (\text{coulomb}^2/(\text{joule sec cm}))$$

Then:

$$\sigma_{dc} = \frac{I_e}{E_{fn} \text{area}} = \frac{\frac{Cev_{dx}}{\text{chain}}}{\frac{1}{2} m_t v_{dx}^2 \frac{1}{CeA}} \quad (2.8.8)$$

All of the dimensional resources are now available to define a numerical constant that we will call the Homes' constant (\mathcal{U})

$$\begin{aligned} \mathcal{U} &= \frac{\sigma_{dc} k_b T_c}{m_t \rho_s} = \frac{\frac{Cev_{dx}}{\text{chain}}}{\frac{1}{2} m_t v_{dx}^2 \frac{1}{CeA}} \frac{1}{2} m_t v_{dx}^2 \frac{\text{cavity}}{m_t} \\ &= \frac{3\pi}{2} \frac{C^2 e_{\pm}^2 \hbar}{m_t^2} \frac{A}{B} = 191,537 \frac{\text{cm}^5}{\text{sec}^3} \end{aligned} \quad (2.8.9)$$

or

$$\rho_U = \rho_s m_t = \frac{\sigma_{dc} k_b T_c}{\mathcal{U}} \quad (\text{cgs units})$$

Equation 2.8.8 is consistent with equation 2.8.3.

The experimentally measured number density (ρ_{sm}) is calculated from plasma frequency relationship as follows:

$$\rho_{sm} = \frac{\omega_{\rho_{sm}}^2 c^2 m_t}{4\pi e^2} = \frac{\omega_m^2 m_t}{4\pi e^2} \quad (2.8.10)$$

Where the measured plasma frequency (ω_m) is related to the penetration depth (λ_m)

$$\omega_m = \frac{1}{2\pi\lambda_m} \quad (2.8.11)$$

The experimentally measured mass density ($\rho_{sm} m_e$)

compared to the trisine model $\rho_U = (m_t/\text{cavity})$ is an indicator of sample purity or fractional material superconductor phase.

It is interesting to note that this mass density ratio is mostly less than one but on occasion is greater than one indicating superconductor lattice phase overlay as allowed by Bose-Einstein statistics.

$$\text{superconductor mass density ratio} = \frac{\rho_{sm} m_t}{\rho_U} \quad (2.8.12)$$

This optical resistivity is further confirmed to be a representation of the BCS theory[138].

A modification of 2.8.9 and 2.8.12 by factor m_e/m_t is consistent with equation 2.5.15c.

$$\frac{m_t}{m_e} = \frac{1}{\sqrt{3}} \frac{\varepsilon_x + \varepsilon_y + \varepsilon_z}{\varepsilon} \quad (2.5.15c)$$

In **Table 2.8.2**, the trisine parameter (time_{\pm}) is consistent with equation 2.1.27.

The measured dielectric (ε_{dem}) is represented by:

$$\varepsilon_{dem} = \text{avg}(a, b)^{-1/2} \frac{\sigma_{dc} (\text{cgs})}{\omega_m}$$

The trisine dielectric (ε) parameter is consistent with equations 2.5.4 and 2.6.5.

the number density (ρ_{sm}) is represented by:

$$\rho_{sm} = \frac{\omega_m m_t}{4\pi e^2}$$

The trisine mass density (ρ_U) parameter is consistent with equations 2.9.1, 2.11.5, 2.11.16, 2.11.41, 2.11.42, 2.11.43, 2.11.44, 2.11.45 and 2.11.46.

The measured fractional superconductor components in the larger material matrix are represented by

$$a = \frac{\sigma_{dem} k_b T_c}{\mathcal{U} \rho_{sm} m_t} \frac{m_e}{m_t} \quad \text{and} \quad b = \frac{\rho_{sm} m_t}{\rho_U} \frac{m_e}{m_t}$$

Table 2.8.2 Superconductor optical resistivity scaling

Superconducting ref Molecule	Siemen/cm	$\sigma_{dcm} (cgS)$	$\omega_{\rho_{sm}} (cm^{-1})$	ω_m or $c\omega_{\rho_{sm}} (sec^{-1})$	$1/time_{\pm} (sec^{-1})$	ϵ_{dcm}	ϵ	$\rho_{sm} (\#/cm^3)$	$\rho_U (g/cm^3)$	$T_c (^oK)$	$(\sigma_{dcm} k_b T / (5\rho_{sm} m_t)) (m_e/m_t)$	a	$(\rho_{sm} m_t / \rho_U) (m_e/m_t)$	b	average(a,b)
[51] $YBa_2Cu_3O_{6.60}$	6,500	5.42E+15	6,400	1.92E+14 2.46E+12	261	228	1.27E+21	1.25E-04	59.00	9.27E-03	1.80E-02	1.37E-02			
[51] $YBa_2Cu_3O_{6.95}$	10,500	2.94E+15	9,950	2.98E+14 3.88E+12	241	181	3.08E+21	2.49E-04	93.20	1.13E-02	2.32E-02	1.72E-02			
[51] $Pr - YBa_2Cu_3O_{7-\delta}$	2,500	3.70E+15	3,700	1.11E+14 1.67E+12	243	277	4.26E+20	6.99E-05	40.00	5.55E-03	8.42E-03	6.99E-03			
[51] $Pr - YBa_2Cu_3O_{7-\delta}$	4,900	2.42E+15	7,350	2.20E+14 3.13E+12	197	202	1.68E+21	1.79E-04	75.00	8.53E-03	1.21E-02	1.03E-02			
[51] $YBa_2Cu_3O_{7-\delta}$	8,700	3.32E+15	9,200	2.76E+14 3.83E+12	235	183	2.63E+21	2.44E-04	92.00	9.83E-03	1.93E-02	1.46E-02			
[51] $YBa_2Cu_4O_8$	6,000	3.68E+15	8,000	2.40E+14 3.33E+12	208	196	1.99E+21	1.98E-04	80.00	9.17E-03	1.43E-02	1.17E-02			
[51] $Bi_2Ca_2SrCu_2O_{8+\delta}$	8,000	3.43E+15	8,800	2.64E+14 3.54E+12	228	190	2.41E+21	2.17E-04	85.00	1.01E-02	1.85E-02	1.43E-02			
[51] $Bi_2Ca_2SrCu_2O_{8+\delta}$	9,800	3.53E+15	9,600	2.88E+14 3.79E+12	239	184	2.87E+21	2.40E-04	91.00	1.09E-02	2.19E-02	1.64E-02			
[51] $Y / Pb - Bi_2Ca_2SrCu_2O_{8+\delta}$	2,500	3.66E+15	3,200	9.59E+13 1.46E+12	279	296	3.18E+20	5.72E-05	35.00	5.07E-03	9.01E-03	7.04E-03			
[51] $Y - Bi_2Ca_2SrCu_2O_{8+\delta}$	2,600	2.27E+15	3,800	1.14E+14 1.67E+12	240	277	4.49E+20	6.99E-05	40.00	5.85E-03	8.76E-03	7.31E-03			
[51] $Tl_2Ba_2SrCuO_{6+\delta}$	5,000	2.42E+15	6,630	1.99E+14 3.67E+12	247	187	1.37E+21	2.28E-04	88.00	5.46E-03	1.14E-02	8.41E-03			
[51] $Nd_{1.85}Ce_{0.15}CuO_4$	28,000	3.59E+15	10,300	3.09E+14 9.58E+11	244	365	3.30E+21	3.05E-05	23.00	9.86E-02	1.24E-01	1.12E-01			
[51] $La_{1.87}Sr_{0.13}CuO_4$	7,000	1.84E+15	5,600	1.68E+14 1.38E+12	256	305	9.75E+20	5.24E-05	33.00	1.70E-02	2.60E-02	2.15E-02			
[51] $La_{1.86}Sr_{0.14}CuO_4$	9,000	2.20E+15	6,000	1.80E+14 1.54E+12	291	288	1.12E+21	6.22E-05	37.00	1.64E-02	3.15E-02	2.40E-02			
[51] Nb	250,000	2.33E+15	17,600	5.28E+14 3.46E+11	338	608	9.63E+21	6.61E-06	8.30	1.33E+00	1.85E+00	1.59E+00			
[51] Nb	850,000	1.10E+15	35,800	1.07E+15 3.88E+11	310	575	3.99E+22	7.84E-06	9.30	4.63E+00	5.94E+00	5.29E+00			
[51] Pb	1,400,000	1.17E+15	41,000	1.23E+15 3.00E+11	324	653	5.23E+22	5.34E-06	7.20	8.92E+00	1.11E+01	1.00E+01			
[51] $YBa_2Cu_3O_{6.50}$	9	1.03E+15	204	6.12E+12 2.21E+12	306	241	1.29E+18	1.07E-04	53.00	1.11E-05	2.63E-05	1.87E-05			
[51] $YBa_2Cu_3O_{6.60}$	12	2.79E+15	244	7.31E+12 2.42E+12	303	230	1.85E+18	1.22E-04	58.00	1.38E-05	3.36E-05	2.37E-05			
[51] $YBa_2Cu_3O_{6.70}$	14	2.92E+15	308	9.23E+12 2.63E+12	255	221	2.95E+18	1.38E-04	63.00	1.95E-05	3.76E-05	2.85E-05			
[51] $YBa_2Cu_3O_{6.80}$	27	3.04E+15	465	1.39E+13 3.25E+12	250	198	6.72E+18	1.90E-04	78.00	3.22E-05	6.52E-05	4.87E-05			
[51] $YBa_2Cu_3O_{6.85}$	47	3.38E+15	790	2.37E+13 3.71E+12	187	186	1.94E+19	2.32E-04	89.00	7.62E-05	1.06E-04	9.12E-05			
[51] $YBa_2Cu_3O_{6.90}$	88	3.62E+15	1,003	3.01E+13 3.81E+12	210	183	3.13E+19	2.42E-04	91.50	1.18E-04	1.96E-04	1.57E-04			

[51]	$YBa_2Cu_3O_{6.95}$	220	3.67E+15	1,580	4.74E+13	3.88E+12	213	181	7.76E+19	2.49E-04	93.20	2.84E-04	4.86E-04	3.85E-04
[51]	$YBa_2Cu_3O_{6.99}$	450	3.70E+15	2,070	6.21E+13	3.75E+12	236	185	1.33E+20	2.36E-04	90.00	5.15E-04	1.01E-03	7.63E-04
[51]	$YBa_2Cu_4O_8$	320	3.64E+15	1,670	5.01E+13	3.33E+12	238	196	8.67E+19	1.98E-04	80.00	4.00E-04	7.62E-04	5.81E-04
[51]	$Tl_2Ba_2CuO_{6+\delta}$	3	3.43E+15	130	3.90E+12	3.38E+12	318	195	5.26E+17	2.01E-04	81.00	2.38E-06	7.10E-06	4.74E-06
[51]	$Hg_2Ba_2CuO_{4+\delta}$	6	3.45E+15	290	8.69E+12	4.04E+12	187	178	2.62E+18	2.64E-04	97.00	9.03E-06	1.30E-05	1.10E-05
[51]	$Nd_{1.85}Ce_{0.15}CuO_4$	2	3.77E+15	60	1.80E+12	9.58E+11	335	365	1.12E+17	3.05E-05	23.00	3.35E-06	6.67E-06	5.01E-06
[51]	$La_{1.92}Sr_{0.08}CuO_4$	1	1.84E+15	63	1.89E+12	1.17E+12	259	331	1.23E+17	4.09E-05	28.00	2.75E-06	4.03E-06	3.39E-06
[51]	$La_{1.90}Sr_{0.10}CuO_4$	2	2.03E+15	108	3.24E+12	1.33E+12	193	310	3.63E+17	5.00E-05	32.00	6.61E-06	6.78E-06	6.69E-06
[51]	$La_{1.88}Sr_{0.12}CuO_4$	4	2.17E+15	160	4.80E+12	1.33E+12	188	310	7.96E+17	5.00E-05	32.00	1.45E-05	1.43E-05	1.44E-05
[51]	$La_{1.875}Sr_{0.125}CuO_4$	5	2.17E+15	153	4.59E+12	1.33E+12	245	310	7.28E+17	5.00E-05	32.00	1.33E-05	1.88E-05	1.60E-05
[51]	$La_{1.875}Sr_{0.125}CuO_4$	7	2.17E+15	159	4.77E+12	1.33E+12	278	310	7.86E+17	5.00E-05	32.00	1.43E-05	2.45E-05	1.94E-05
[51]	$La_{1.875}Sr_{0.15}CuO_4$	16	2.17E+15	344	1.03E+13	1.58E+12	191	284	3.68E+18	6.47E-05	38.00	5.18E-05	5.53E-05	5.36E-05
[51]	$La_{1.83}Sr_{0.17}CuO_4$	32	2.36E+15	360	1.08E+13	1.50E+12	285	292	4.03E+18	5.97E-05	36.00	6.15E-05	1.14E-04	8.76E-05
[51]	$La_{1.80}Sr_{0.20}CuO_4$	95	2.30E+15	515	1.54E+13	1.33E+12	347	310	8.25E+18	5.00E-05	32.00	1.50E-04	3.58E-04	2.54E-04
[54]	$YBa_2Cu_3O_{6.95}$	4,400	2.17E+15	5,750	1.72E+14	2.92E+12	249	209	1.03E+21	1.62E-04	70.00	5.79E-03	1.12E-02	8.50E-03
[54]	$YBa_2Cu_3O_{6.95}$	6,500	3.21E+15	8,840	2.65E+14	3.33E+12	191	196	2.43E+21	1.98E-04	80.00	1.12E-02	1.55E-02	1.33E-02
[54]	$YBa_2Cu_3O_{6.95}$	9,200	3.43E+15	9,220	2.76E+14	3.54E+12	235	190	2.64E+21	2.17E-04	85.00	1.11E-02	2.13E-02	1.62E-02
[54]	$YBa_2Cu_3O_{6.95}$	10,500	3.53E+15	11,050	3.31E+14	3.90E+12	210	181	3.80E+21	2.50E-04	93.50	1.38E-02	2.31E-02	1.85E-02
[54]	$YBa_2Cu_3O_{6.60}$	6,500	3.71E+15	6,400	1.92E+14	2.46E+12	261	228	1.27E+21	1.25E-04	59.00	9.27E-03	1.80E-02	1.37E-02
[54]	$YBa_2Cu_3O_{6.95}$	10,500	2.94E+15	9,950	2.98E+14	3.88E+12	241	181	3.08E+21	2.49E-04	93.20	1.13E-02	2.32E-02	1.72E-02
[54]	$YBa_2Cu_3O_{6.95}$	8,700	3.70E+15	9,200	2.76E+14	3.83E+12	235	183	2.63E+21	2.44E-04	92.00	9.83E-03	1.93E-02	1.46E-02
[54]	$YBa_2Cu_3O_{7-\delta}$	2,500	3.68E+15	3,700	1.11E+14	1.67E+12	243	277	4.26E+20	6.99E-05	40.00	5.55E-03	8.42E-03	6.99E-03
[54]	$Pr - YBa_2Cu_3O_{7-\delta}$	4,900	2.42E+15	7,350	2.20E+14	3.13E+12	197	202	1.68E+21	1.79E-04	75.00	8.53E-03	1.21E-02	1.03E-02
[54]	$Pr - YBa_2Cu_3O_{7-\delta}$	6,000	3.32E+15	8,000	2.40E+14	3.33E+12	208	196	1.99E+21	1.98E-04	80.00	9.17E-03	1.43E-02	1.17E-02
[54]	$YBa_2Cu_3O_8$	11,500	3.43E+15	9,565	2.87E+14	3.75E+12	266	185	2.85E+21	2.36E-04	90.00	1.10E-02	2.58E-02	1.84E-02
[54]	$Bi_2Ca_2SrCu_2O_{8+\delta}$	9,800	3.64E+15	9,600	2.88E+14	3.79E+12	239	184	2.87E+21	2.40E-04	91.00	1.09E-02	2.19E-02	1.64E-02
[54]	$Bi_2Ca_2SrCu_2O_{8+\delta}$	8,500	3.66E+15	8,710	2.61E+14	3.54E+12	241	190	2.36E+21	2.17E-04	85.00	9.93E-03	1.96E-02	1.48E-02
[54]	$Bi_2Ca_2SrCu_2O_{8+\delta}$	2,500	3.53E+15	3,200	9.59E+13	1.46E+12	279	296	3.18E+20	5.72E-05	35.00	5.07E-03	9.01E-03	7.04E-03
[54]	$Y / Pb - Bi_2Ca_2SrCu_2O_{8+\delta}$	2,600	2.27E+15	3,800	1.14E+14	1.67E+12	240	277	4.49E+20	6.99E-05	40.00	5.85E-03	8.76E-03	7.31E-03
[54]	$Y - Bi_2Ca_2SrCu_2O_{8+\delta}$	4,200	2.42E+15	5,140	1.54E+14	1.79E+12	227	267	8.22E+20	7.79E-05	43.00	9.61E-03	1.37E-02	1.16E-02
[54]	$Tl_2Ba_2CuO_{6+\delta}$	5,000	2.51E+15	6,630	1.99E+14	3.67E+12	247	187	1.37E+21	2.28E-04	88.00	5.46E-03	1.14E-02	8.41E-03
[54]	$Nd_{1.85}Ce_{0.15}CuO_4$	28,000	3.59E+15	10,300	3.09E+14	9.58E+11	244	365	3.30E+21	3.05E-05	23.00	9.86E-02	1.24E-01	1.12E-01
[54]	$Pr_{1.85}Ce_{0.15}CuO_4$	30,000	1.84E+15	10,300	3.09E+14	9.58E+11	257	365	3.30E+21	3.05E-05	23.00	9.86E-02	1.33E-01	1.16E-01
[54]	$Pr_{1.85}Ce_{0.15}CuO_4$	15,000	1.84E+15	4,820	1.44E+14	8.75E+11	429	382	7.22E+20	2.66E-05	21.00	2.48E-02	6.98E-02	4.73E-02
[54]	$Pr_{1.87}Ce_{0.15}CuO_4$	50,000	1.76E+15	7,960	2.39E+14	6.67E+11	439	438	1.97E+21	1.77E-05	16.00	1.02E-01	2.66E-01	1.84E-01

[54]	$La_{1.87}Sr_{0.13}CuO_4$	7,000	1.53E+15	5,600	1.68E+14	1.33E+12	252	310	9.75E+20	5.00E-05	32.00	1.78E-02	2.64E-02	2.21E-02
[54]	$La_{1.86}Sr_{0.14}CuO_4$	9,000	2.17E+15	6,000	1.80E+14	1.50E+12	287	292	1.12E+21	5.97E-05	36.00	1.71E-02	3.20E-02	2.45E-02
[54]	$Ba_{0.62}K_{0.38}BiO_3$	3,800	2.30E+15	4,240	1.27E+14	1.29E+12	239	315	5.59E+20	4.77E-05	31.00	1.07E-02	1.45E-02	1.26E-02
[54]	$Ba_{0.60}K_{0.40}BiO_3$	4,400	2.13E+15	4,240	1.27E+14	1.17E+12	254	331	5.59E+20	4.09E-05	28.00	1.24E-02	1.77E-02	1.51E-02
[54]	$Ba_{0.54}K_{0.46}BiO_3$	6,000	2.03E+15	4,240	1.27E+14	8.75E+11	277	382	5.59E+20	2.66E-05	21.00	1.92E-02	2.79E-02	2.35E-02
[54]	Nb	250,000	1.76E+15	17,600	5.28E+14	3.46E+11	338	608	9.63E+21	6.61E-06	8.30	1.33E+00	1.85E+00	1.59E+00
[54]	Nb	850,000	1.10E+15	35,800	1.07E+15	3.88E+11	310	575	3.99E+22	7.84E-06	9.30	4.63E+00	5.94E+00	5.29E+00
[54]	Nb	1,400,000	1.17E+15	41,000	1.23E+15	3.00E+11	324	653	5.23E+22	5.34E-06	7.20	8.92E+00	1.11E+01	1.00E+01
[137]	organic	3,800	1.03E+15	1,966	5.89E+13	3.58E+11	389	597	1.20E+20	6.97E-06	8.60	1.57E-02	2.76E-02	2.17E-02
[137]	organic	3,700	1.12E+15	1,098	3.29E+13	3.46E+11	765	608	3.75E+19	6.61E-06	8.30	5.17E-03	2.74E-02	1.63E-02
[137]	organic	4,000	1.10E+15	1,019	3.05E+13	4.71E+11	953	521	3.23E+19	1.05E-05	11.30	2.80E-03	2.54E-02	1.41E-02
[137]	organic	13,150	1.29E+15	4,749	1.42E+14	4.58E+11	294	528	7.01E+20	1.01E-05	11.00	6.34E-02	8.45E-02	7.39E-02
[137]	organic	25	1.27E+15	259	7.76E+12	3.33E+11	180	619	2.08E+18	6.25E-06	8.00	3.04E-04	1.88E-04	2.46E-04
[137]	organic	6	1.08E+15	40	1.21E+12	4.71E+11	967	521	5.07E+16	1.05E-05	11.30	4.40E-06	4.06E-05	2.25E-05
[137]	organic	4	1.29E+15	38	1.14E+12	3.48E+11	714	606	4.53E+16	6.67E-06	8.35	6.18E-06	2.95E-05	1.78E-05
[137]	pnictides	18	1.11E+15	215	6.43E+12	1.32E+12	339	311	1.43E+18	4.92E-05	31.66	2.65E-05	6.67E-05	4.66E-05
[137]	pnictides	5,744	2.16E+15	4,406	1.32E+14	1.06E+12	275	347	6.04E+20	3.56E-05	25.53	1.54E-02	2.42E-02	1.98E-02
[137]	pnictides	7,871	1.94E+15	5,024	1.51E+14	1.06E+12	277	347	7.85E+20	3.57E-05	25.56	2.00E-02	3.32E-02	2.66E-02
[137]	pnictides	4,443	1.94E+15	5,120	1.53E+14	8.20E+11	154	395	8.15E+20	2.41E-05	19.69	3.08E-02	2.13E-02	2.61E-02
[137]	K_3C_{60}	1,200	1.70E+15	1,893	5.68E+13	7.92E+11	252	402	1.11E+20	2.29E-05	19.00	4.44E-03	5.87E-03	5.15E-03
[137]	Rb_3C_{60}	1,300	1.67E+15	1,966	5.89E+13	1.21E+12	316	325	1.20E+20	4.31E-05	29.00	2.54E-03	5.14E-03	3.84E-03
[137]	$CeCoIn_5$	251,064	2.06E+15	8,185	2.45E+14	9.39E+10	542	1167	2.08E+21	9.34E-07	2.25	2.03E+00	3.56E+00	2.80E+00
[137]	elements	244,565	5.75E+14	17,021	5.10E+14	3.51E+11	335	604	9.01E+21	6.76E-06	8.42	1.21E+00	1.80E+00	1.51E+00
[137]	elements	838,544	1.11E+15	34,734	1.04E+15	3.95E+11	306	569	3.75E+22	8.06E-06	9.48	4.24E+00	5.81E+00	5.02E+00
[137]	elements	1,403,835	1.18E+15	39,612	1.19E+15	2.97E+11	318	657	4.88E+22	5.25E-06	7.12	8.46E+00	1.12E+01	9.84E+00
[137]	MgB_2	40,000	1.02E+15	7,178	2.15E+14	1.65E+12	579	278	1.60E+21	6.88E-05	39.60	2.12E-02	1.35E-01	7.83E-02
[137]	MgB_2	137,000	2.41E+15	13,087	3.92E+14	1.63E+12	408	281	5.33E+21	6.73E-05	39.00	7.21E-02	4.68E-01	2.70E-01
[137]	MgB_2	49,000	2.39E+15	18,696	5.60E+14	1.63E+12	275	281	1.09E+22	6.73E-05	39.00	1.47E-01	1.67E-01	1.57E-01
[137]	$Tl_xPb_{1-x}Te$	1,111	2.39E+15	569	1.71E+13	5.88E+10	401	1475	1.01E+19	4.63E-07	1.41	1.98E-02	1.99E-02	1.99E-02
[137]	$Ba_{1-x}K_xBiO_3$	2,891	4.55E+14	4,165	1.25E+14	1.34E+12	201	310	5.39E+20	5.01E-05	32.04	9.80E-03	1.09E-02	1.03E-02
[137]	$Ba_{1-x}K_xBiO_3$	4,439	2.17E+15	4,165	1.25E+14	1.16E+12	256	332	5.39E+20	4.05E-05	27.81	1.21E-02	1.79E-02	1.50E-02
[137]	$Ba_{1-x}K_xBiO_3$	6,818	2.02E+15	4,165	1.25E+14	8.96E+11	308	378	5.39E+20	2.76E-05	21.51	1.78E-02	3.13E-02	2.46E-02
[137]	Sr_2RuO_4	4,760,000	1.78E+15	3,721	1.12E+14	6.13E+10	2209	1445	4.31E+20	4.92E-07	1.47	7.97E-01	8.37E+01	4.22E+01
[137]	Sr_2RuO_4	2,060,000	4.65E+14	5,120	1.53E+14	5.24E+10	2551	1562	8.15E+20	3.90E-07	1.26	1.90E+00	3.91E+01	2.05E+01
[137]	Sr_2RuO_4	1,380,000	4.30E+14	9,512	2.85E+14	3.08E+10	2160	2037	2.81E+21	1.76E-07	0.74	1.46E+01	3.42E+01	2.44E+01

[137]	$Y_2C_2I_2$	400	3.30E+14	391	1.17E+13	4.22E+11	758	551	4.76E+18	8.89E-06	10.12	4.88E-04	2.68E-03	1.58E-03
[137]	TiN	6,350	1.22E+15	2,159	6.47E+13	1.42E+11	319	950	1.45E+20	1.73E-06	3.40	7.62E-02	7.34E-02	7.48E-02
[74]	κ -BET ₂ GaCl ₄	250,000	7.07E+14	684	2.05E+13	6.67E+09	4087	4380	1.45E+19	1.77E-08	0.16	7.49E-01	1.33E+01	7.03E+00
[74]	(TMTSF) ₂ ClO ₄	39,000	1.53E+14	1,238	3.71E+13	4.58E+10	1370	1671	4.77E+19	3.19E-07	1.10	1.36E-01	7.92E-01	4.64E-01
[74]	a-ET ₂ NH ₄ Hg(SCN) ₄	36,000	4.02E+14	1,429	4.29E+13	4.58E+10	1105	1671	6.35E+19	3.19E-07	1.10	1.82E-01	7.32E-01	4.57E-01
[74]	β -ET ₂ IBr ₂	26,000	4.02E+14	1,747	5.24E+13	9.17E+10	910	1181	9.49E+19	9.02E-07	2.20	9.59E-02	3.74E-01	2.35E-01
[74]	λ -BET ₂ GaCl ₄	11,000	5.68E+14	2,184	6.55E+13	2.29E+11	569	747	1.48E+20	3.56E-06	5.50	3.79E-02	1.00E-01	6.89E-02
[74]	κ -ET ₂ Cu(NCS) ₂	6,000	8.99E+14	2,912	8.73E+13	3.83E+11	319	578	2.64E+20	7.71E-06	9.20	3.12E-02	4.22E-02	3.67E-02
[74]	K_3C_{60}	2,900	1.16E+15	3,276	9.82E+13	7.88E+11	223	403	3.34E+20	2.27E-05	18.90	1.34E-02	1.42E-02	1.38E-02
[74]	Rb_3C_{60}	2,500	1.67E+15	3,744	1.12E+14	1.22E+12	204	324	4.36E+20	4.38E-05	29.30	9.06E-03	9.84E-03	9.45E-03

The results for both c axis and a-b plane (ref 51) are graphically presented in the following figure 2.8.1. On average the Homes' constant calculated from data exceeds the Homes' constant derived from Trisine geometry by 1.72. There may be some degrees of freedom considerations $1 \cdot k_b T_c / 2$, $2 \cdot k_b T_c / 2$, $3 \cdot k_b T_c / 2$ that warrant looking into that may account for this divergence although conformity is noteworthy. Also 1.72 is close to $\sqrt{3}$, a value that is inherent to Trisine geometry. I will have to give this a closer look. In general, the conventional and high temperature superconductor data falls in the same pattern. I would conclude that Homes' Law can be extrapolated to any critical temperature T_c as a universal phenomenon.

Figure 2.8.1

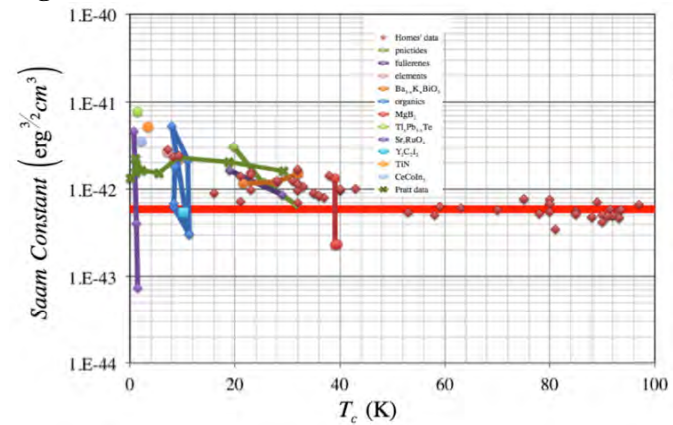


Figure 2.8.2

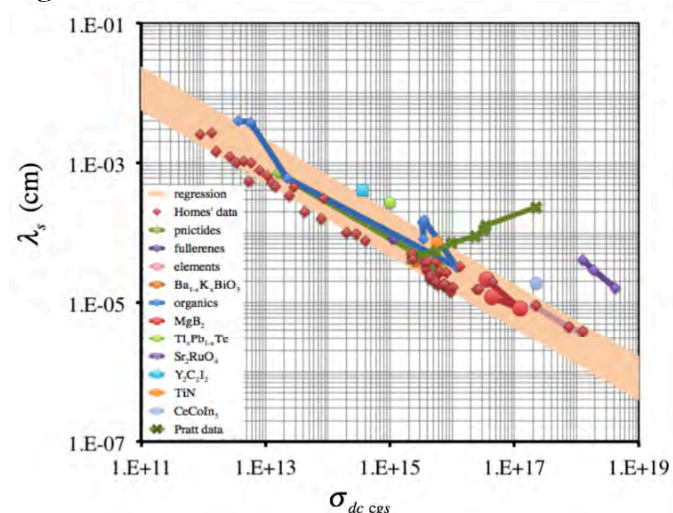


Figure 2.8.3

slope 0.965
intercept 0.136
Correlation 0.927

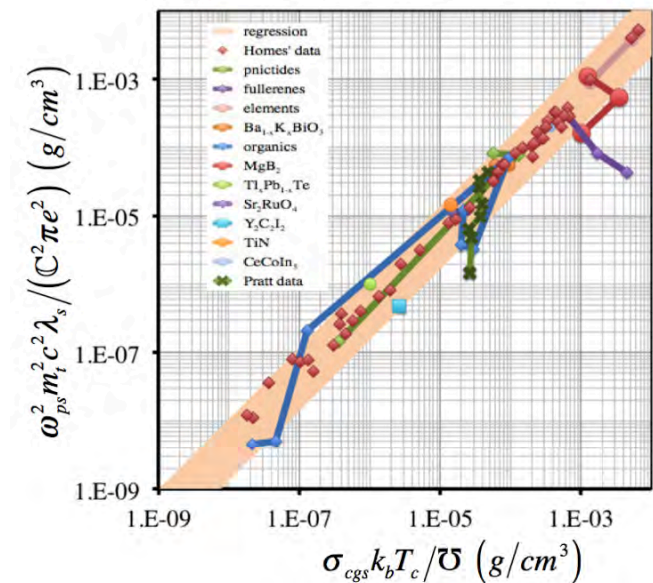


Figure 2.8.4

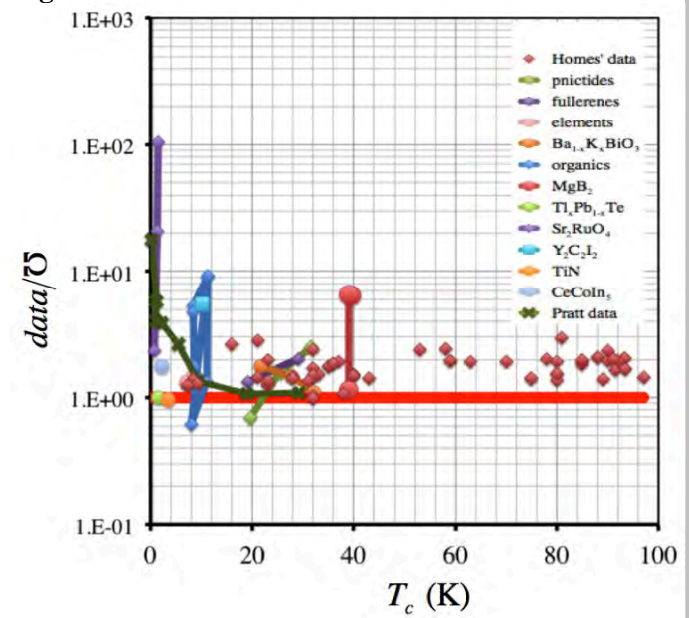
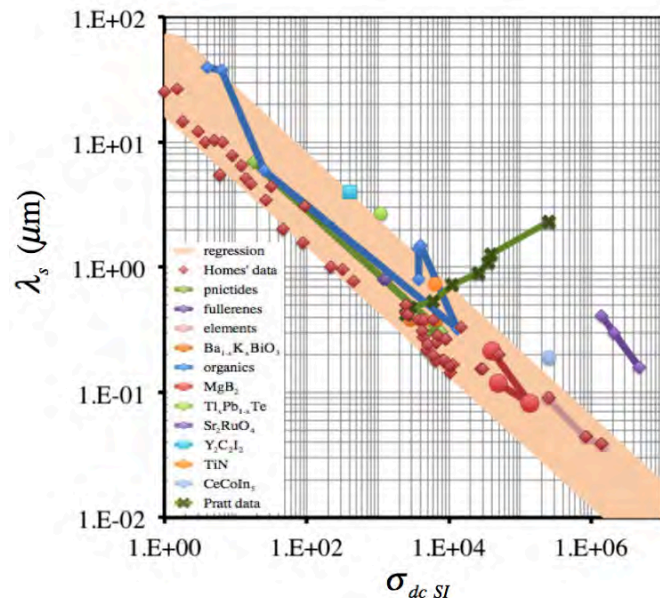
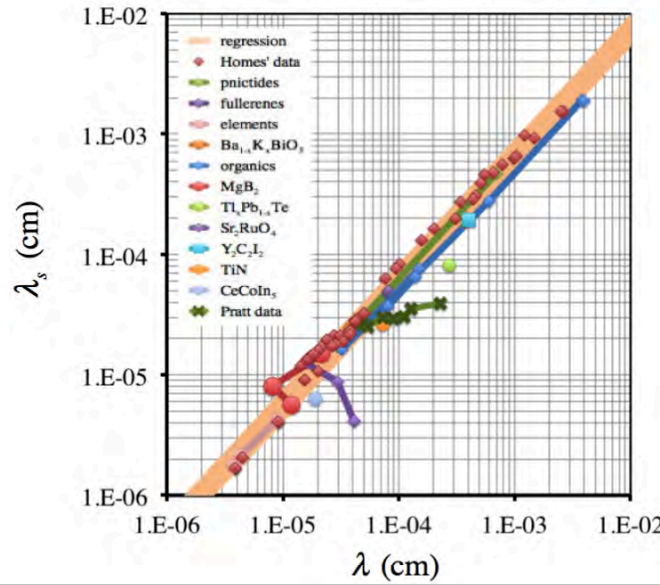


Figure 2.8.5

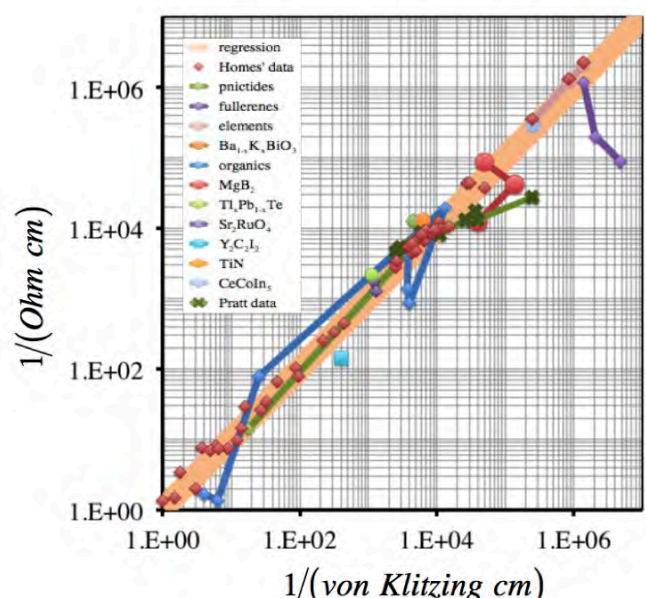
slope -1.92
 intercept 3.02
 correlation -0.886

**Figure 2.8.6**

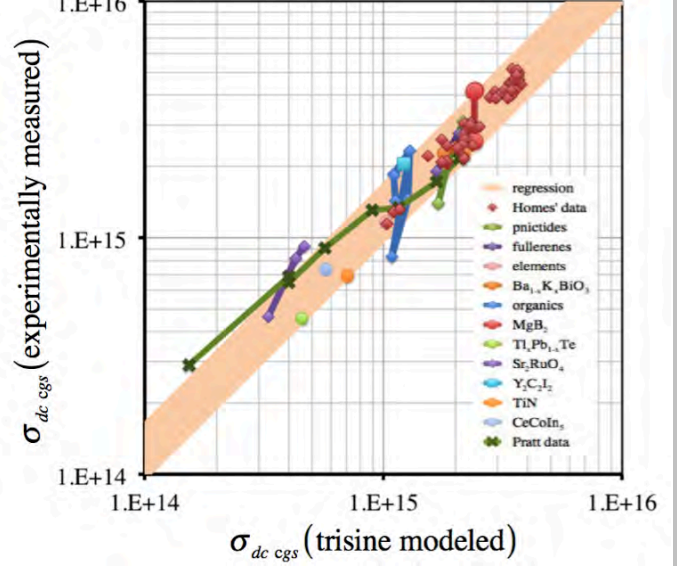
slope 0.964
 intercept 0.065
 correlation 0.978

**Figure 2.8.7**

slope 0.999
 intercept 0.00757
 correlation 0.980

**Figure 2.8.8**

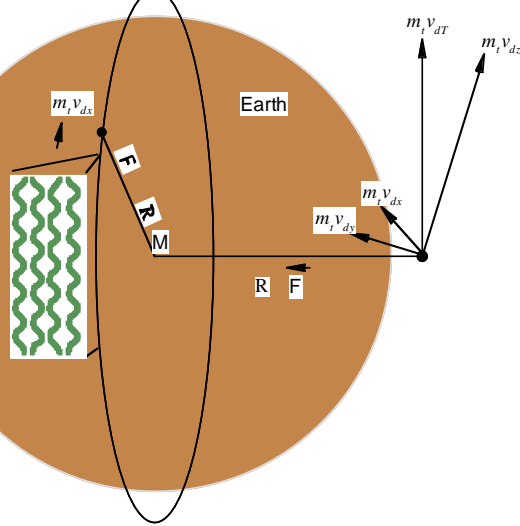
slope 0.993
 intercept 0.00743
 correlation 0.967



2.9 Superconductor Apparent Weight Reduction In A Gravitational Field

Based on the superconducting helical or tangential velocity (v_{dt}), the superconducting gravitational shielding effect (Θ) is computed based on Newton's gravitational law and the geometry as presented in Figure 2.9.1.

Figure 2.9.1 Superconductor Gravitational Model Based on Super current mass flow with Mass Velocities (v_{dx}) and (v_{dt}).



With a material density (ρ) of 6.39 g/cc [17] and the $YBa_2Cu_3O_{7-x}$ critical temperature of 93K, the gravitational apparent shielding effect (Θ_{dt}) (ρ_c/ρ) is .05% as observed by Podkletnov and Nieminen (as per following equations or extrapolating on Table 2.9.1).

$$\rho_U = \frac{m_t}{cavity} = \frac{n m_t}{2} \quad (2.9.1)$$

$$F_\uparrow = m_t \frac{v_{dx}^2}{R} = \frac{2kT_c}{R} \quad F_\downarrow = \frac{Gm_t M}{R^2} \quad (2.9.2)$$

$$\Theta_{dx} = \frac{\text{Superconducting Force } (F_{\uparrow dx})}{\text{Earth's Gravitational Force } (F_\downarrow)} \quad (2.9.3)$$

$$= \frac{\text{Earth Radius } v_{dx}^2}{\text{Earth Mass } G}$$

$$\Theta_{dt} = \frac{\text{Superconducting Force } (F_{\uparrow dt})}{\text{Earth's Gravitational Force } (F_\downarrow)} \quad (2.9.4)$$

$$= \frac{\text{Earth Radius } v_{dt}^2}{\text{Earth Mass } G}$$

Table 2.9.1 Cooper Pair Concentration and Shielding (Θ) with Plot of Cooper (C) Pair density

Condition	1.2	1.3	1.6	1.9	1.10	1.11
$T_a ({}^0 K)$	6.53E+11	6.53E+11	6.53E+11	6.53E+11	6.53E+11	6.53E+11
$T_b ({}^0 K)$	9.05E+14	5.48E+13	9.22E+08	1.10E+07	2,868	2.723
$T_{br} ({}^0 K)$	3.30E+12	5.45E+13	3.24E+18	2.72E+20	1.04E+24	1.10E+27
$T_c ({}^0 K)$	8.96E+13	3.28E+11	93.0	0.0131	8.99E-10	8.10E-16
$T_{cr} ({}^0 K)$	1.19E+09	3.25E+11	1.15E+21	8.11E+24	1.19E+32	1.32E+38
$z_R + 1$	3.67E+43	8.14E+39	3.89E+25	6.53E+19	1.17E+09	1.00E+00
$z_B + 1$	3.32E+14	2.01E+13	3.39E+08	4.03E+06	1.05E+03	1.00E+00
$Age_{UG} (\text{sec})$	7.14E-05	4.79E-03	6.94E+04	5.36E+07	1.27E+13	4.33E+17
$Age_{UGV} (\text{sec})$	4.59E-10	1.25E-07	4.42E+02	3.13E+06	1.22E+13	4.33E+17
$Age_U (\text{sec})$	1.18E-26	5.31E-23	1.11E-08	6.63E-03	3.70E+08	4.33E+17
$\rho_U (\text{g/cm}^3)$	2.34E+14	5.19E+10	2.48E-04	4.16E-10	7.44E-21	6.37E-30
Θ_{dx}	3.94E+11	1.44E+09	4.09E-01	5.77E-05	3.95E-12	3.56E-18
Θ_{dt}	9.83E+12	3.60E+10	1.02E+01	1.44E-03	9.87E-11	8.90E-17

Experiments have been conducted to see if a rotating body's weight is changed from that of a non-rotating body [21, 22, 23]. The results of these experiments were negative as they clearly should be because the center of rotation equaled the center mass. A variety of gyroscopes turned at various angular velocities were tested. Typically a gyroscope with effective radius 1.5 cm was turned at a maximum rotational frequency of 22,000 rpm. This equates to a tangential velocity of 3,502 cm/sec. At the surface of the earth, the tangential velocity is calculated to be:

$$\sqrt{gR_E} \text{ or } 791,310 \text{ cm/sec.}$$

The expected weight reduction if center of mass was different than center of rotation (r) according to equations 2.9.2 and 2.9.3 would be:

$$(3,502/791,310)^2 \text{ or } 1.964E-5$$

of the gyroscope weight. The experiments were done with gyroscopes with weights of about 142 grams. This would indicate a required balance sensitivity of $1.964E-5 \times 142$ g or 2.8 mg, which approaches the sensitivity of laboratory balances. Both positive[21] and negative results [22, 23] are experimentally observed in this area although it has been generally accepted that the positive results were spurious.

Under the geometric scenario for superconducting materials presented herein, the Cooper CPT Charge conjugated pair centers of mass and centers of rotation (r) are different making the numerical results in table 2.9.1 valid. Under this

scenario, it is the superconducting material that loses weight due to transverse Cooper pair movement relative to a center of gravity. The experimentally observed superconducting shielding effect cannot be explained in these terms.

2.10 BCS Verifying Constants and Maxwell's Equations

Equations 2.9.1 - 2.9.8 represent constants as derived from BCS theory [2] and considered by Little [5] to be primary constraints on any model depicting the superconducting phenomenon. It can be seen that the trisine model constants compare very favorably with BCS constants in brackets { }.

$$C_D = 10.2D(\epsilon_T)k_b^2 T_c \frac{\mathbb{C}}{cavity} = 10.2k_b \frac{\mathbb{C}}{cavity} \quad (2.10.1)$$

$$\gamma = \frac{2}{3}\pi^2 D(\epsilon_T)k_b^2 \frac{\mathbb{C}}{cavity} = \frac{2}{3}\pi^2 k_b \frac{\mathbb{C}}{T_c cavity} \quad (2.10.2)$$

$$\frac{1}{\mathbb{C}} \frac{\gamma T_c^2}{H_c^2} = .178 \left\{ \frac{\pi}{18} \text{ or } .170 \right\} \quad (2.10.3)$$

$$\frac{C_D}{\gamma T_c} = \frac{3 \cdot \text{jump}}{2\pi^2} \{1.52\} = 1.55 \{1.52\} \quad (2.10.4)$$

$$\frac{\hbar^2 \left(\frac{K_A^2}{\mathbb{C}} - K_{Dn}^2 \right)}{2m_t k_b T_c} = \text{jump} \{10.2\} = 10.12 \{10.2\} \quad (2.10.5)$$

$$(k_b T_c)^{3/2} cavity = \frac{3\pi^3 \hbar^3}{6^{1/2} m_t^{3/2} \left(\frac{B}{A} \right)_t} = 5.890351329 \text{E-43} \quad (2.10.6)$$

$$\approx \frac{3\cos(30^\circ)}{2.6124} \left(\frac{2\pi}{m_t} \right)^{\frac{3}{2}} \hbar^3 = \frac{3\cos(30^\circ)}{\zeta(3/2)} \left(\frac{2\pi}{m_t} \right)^{\frac{3}{2}} \hbar^3$$

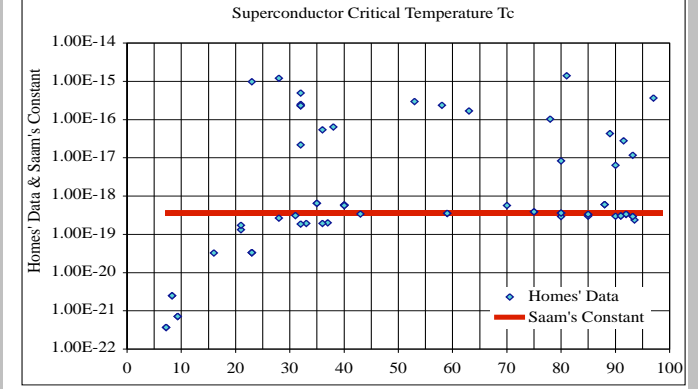
$$\frac{2e^{Euler} (K_C^2 + K_{Ds}^2)}{\pi K_B^2 \sinh(\text{trisine})} = \frac{(K_C^2 + K_{Ds}^2)}{K_B^2} \frac{2}{e^{\text{trisine}} - 1} = \mathbb{C} \quad (2.10.6a)$$

Equation 2.10.6 basically assumes the ideal gas law in the adiabatic thermodynamic condition for superconducting charge carriers and Bose Einstein Condensate.

When the $1/\rho_s$ data from reference [51, 59] is used as a measure of cavity volume in the equation 2.10.6, the following plot (figure 2.10.1) is achieved. It is a good fit for some of the data and not for others. One can only conclude that the number of charge carriers in the cavity volume varies considerably from one superconductor to another with perhaps only the Cooper CPT Charge conjugated pair being a small fraction of the total. Also, degrees of freedom may be a factor as in the kinetic theory of gas or other words – is

a particular superconductor one-, two- or three- dimensional $1 \cdot kT_c/2, 2 \cdot kT_c/2, 3 \cdot kT_c/2$ as Table 2.6.1 data for MgB_2 would imply? Also it is important to remember that Homes' data is from just above T_c and not at or below T_c .

Figure 2.10.1 Homes' Data Compared to Eqn. 2.10.6



$$\frac{\gamma T_c}{k_b} \frac{cavity}{\mathbb{C}} = \left\{ \frac{2\pi^2}{3} \right\} \quad (2.10.7)$$

$$\frac{2\Delta_o^{BCS}}{kT_c} = 2\pi e^{-Euler} \{3.527754\} \quad (2.10.8)$$

Within the context of the trisine model, it is important to note that the Bohr radius is related to the nuclear radius ($B_{nucleus}$) by this BCS gap as defined in 2.10.8

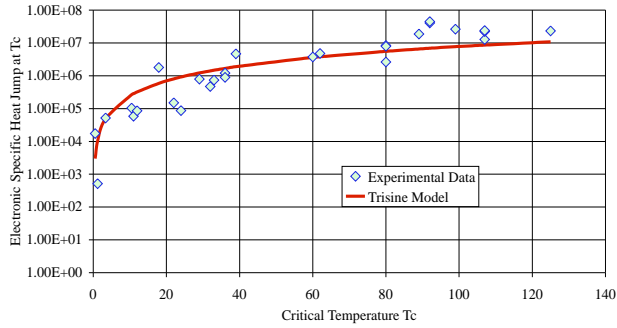
$$\frac{cavity}{\Delta x \Delta y \Delta z} \frac{m_t}{m_e} \frac{e^{Euler}}{2\pi} = \frac{\text{Bohr radius}}{B_{nucleus}} \quad (2.10.9)$$

Also the significant Euler constant is related to other universal constants

$$Euler \sim \frac{F_p}{M_u H_u c} = \frac{c^3}{M_u G_u H_u} = \frac{1}{3^{1/2}} \quad (2.10.9a)$$

Table 2.10.1 Electronic Heat Jump $k_b\mathbb{C}/cavity$ at T_c

Condition	1.2	1.3	1.6	1.9	1.10	1.11
$T_a(^0K)$	6.53E+11	6.53E+11	6.53E+11	6.53E+11	6.53E+11	6.53E+11
$T_b(^0K)$	9.05E+14	5.48E+13	9.22E+08	1.10E+07	2,868	2.723
$T_{br}(^0K)$	3.30E+12	5.45E+13	3.24E+18	2.72E+20	1.04E+24	1.10E+27
$T_c(^0K)$	8.96E+13	3.28E+11	93.0	0.0131	8.99E-10	8.10E-16
$T_{cr}(^0K)$	1.19E+09	3.25E+11	1.15E+21	8.11E+24	1.19E+32	1.32E+38
$z_R + 1$	3.67E+43	8.14E+39	3.89E+25	6.53E+19	1.17E+09	1.00E+00
$z_B + 1$	3.32E+14	2.01E+13	3.39E+08	4.03E+06	1.05E+03	1.00E+00
$Age_{UG}(sec)$	7.14E-05	4.79E-03	6.94E+04	5.36E+07	1.27E+13	4.33E+17
$Age_{UGv}(sec)$	4.59E-10	1.25E-07	4.42E+02	3.13E+06	1.22E+13	4.33E+17
$Age_U(sec)$	1.18E-26	5.31E-23	1.11E-08	6.63E-03	3.70E+08	4.33E+17
$\frac{10.2k_b\mathbb{C}}{cavity erg/cm^3}$						
	6.52E+24	1.45E+21	6.90E+06	1.16E+01	2.07E-10	1.78E-19

Figure 2.10.2 Electronic Specific Heat Jump (C_d) at T_c comparing Harshman compiled experimental data and predicted trisine values based on equation 2.10.1

Harshman [17] has compiled and reported an extended listing of electronic specific heat jump at T_c data for a number of superconducting materials. This data is reported in units of mJ/mole K^2 . With the volume per formula weight data for the superconductors also reported by Harshman and after multiplying by T_c^2 , the specific heat jump at T_c is expressed in terms of erg/cm^3 and graphed in figure 2.10.2.

In addition it is important to note a universal resonant superconductor diffusion coefficient D_c based on Einstein's 1905 publication [75] which adds to the universality of the trisine model.

$$D_c = \frac{chain}{cavity} \frac{\sqrt{3}k_b T_c}{\mu_u B} = \frac{(2B)^2}{time_x} = 2v_{dx} B \\ = 2\pi c^{\frac{1}{3}} \hbar^{\frac{1}{3}} U^{-\frac{1}{3}} \frac{1}{\cos(\theta)} = 6.60526079 \times 10^{-2} \quad (2.10.10)$$

And also in terms of the Lamb shift frequency ($\nu_{Lamb\ Shift}$) indicative of the anomalous energy difference between ($^2S_{1/2}$ and $^2P_{1/2}$) orbitals that differ in their spatial orientation. Energetics associated with spatial orientation is consistent with the trisine geometric space concept.

$$h\nu_{Lamb\ Shift} = \frac{3}{5} \frac{(\mathbb{C}e)^2}{k_{mx} \varepsilon_x B_{Bohr\ Radius}} \ln\left(\frac{B}{A}\right) \quad (2.10.11)$$

$$\text{at } T_c = 14150.44 \text{ K} \quad \nu_{Lamb\ Shift} = 1.06E+09 \text{ Hz}$$

The trisine vacuum *cavity* ratio $2B/A$ represents the *cavity* minimum/maximum frequencies generally used in Lamb Shift derivations[137].

Maxwell's equations may be expressed in trisine geometrical dimensions:

Gauss's Law (e)

$$\frac{1}{2\pi} D_{fitrisine} \frac{section}{\cos(\theta)} = \mathbb{C}e \quad (2.10.12)$$

$$\frac{1}{2g_d} (-D_{fx} approach + D_{fy} side - D_{fz} side) \cos(\theta)$$

Gauss's Law (H)

$$H section - H section = 0 \quad (2.10.13)$$

Faraday's Law

$$voltage = EMF = \frac{\hbar}{time} \frac{\pi}{\mathbb{C}e} \quad (2.10.14)$$

Ampere's Law

$$\frac{chain}{cavity} H_c \frac{v_{ex}}{K_B} = \mathbb{C}e \frac{2}{time} + D \frac{2section}{\cos(\theta)} \frac{2}{time} \quad (2.10.15)$$

2.11 Cosmological Parameters

The following relations of *Hubble radius* (R_u), *mass* (M_u), *density* (ρ_u) and *time* (T_u) in terms of the *cosmological constant* (Λ or $6C_u^2/\cos(\theta)$) are in general agreement with known data. This could be significant. The cosmological constant (Λ or $6C_u^2/\cos(\theta)$) as presented in equation 2.11.1 is based on energy/area or *trisine surface tension* (σ_T), as

well as energy/volume or *universe pressure* (p_U). The *trisine surface tension* (σ_T) is a function of (T_c) while the *universe pressure* (p_U) is the value at current CMBR temperature of $2.729^{\circ}K$ as presented in table 2.7.1 and observed by COBE [26] and WMAP. The *cosmological constant* (Λ or $6C_U^2/\cos(\theta)$) also reduces to an expression relating trisine resonant velocity transformed mass (m_t), G_U and \hbar . Also a reasonable value of 71.2 km/sec-million parsec for the Hubble constant (H_U) from equation 2.11.14 is achieved based on a *universe absolute viscosity* (μ_U) and *energy dissipation rate* (P_U).

$$C_U = \frac{16\pi G_U}{v_{dx}^4} \sigma_T = \frac{H_U}{\sqrt{3}c} = \frac{4}{\sqrt{3}\pi} \frac{m_t^3 G_U}{\hbar^2} \quad (2.11.1)$$

$$\Lambda_U = \frac{2H_U^2}{c^2 \cos(\theta)} \quad \frac{H_U}{G_U} = U = 3.46E-11 \text{ g/cm}^3$$

$$C_{Ur} = \frac{16\pi G_{Ur}}{v_{dxr}^4} \sigma_{Tr} = \frac{H_{Ur}}{\sqrt{3}c} = \frac{4}{\sqrt{3}\pi} \frac{m_t^3 G_{Ur}}{\hbar^2} \quad (2.11.1r)$$

$$\Lambda_{Ur} = \frac{2H_{Ur}^2}{c^2 \cos(\theta)} \quad \frac{H_{Ur}}{G_{Ur}} = U = 3.46E-11 \text{ g/cm}^3$$

$$\Lambda_U = 1.29E-56 \text{ cm}^{-2} \quad (\text{present})$$

$$\sigma_T = \frac{k_b T_c}{\text{section}} \quad (2.11.2)$$

$$\sigma_{Tr} = \frac{k_b T_{cr}}{\text{section}_r} \quad (2.11.2r)$$

$$\sigma_T = 5.32E-08 \text{ dyne/cm}^2 \quad (\text{present})$$

$$R_U = \frac{1}{C_U} = \frac{\sqrt{3}c}{\sqrt{4\pi G_U \rho_U}} \left(\sqrt{3} \cdot \text{Einstein radius} \right) \quad (2.11.3)$$

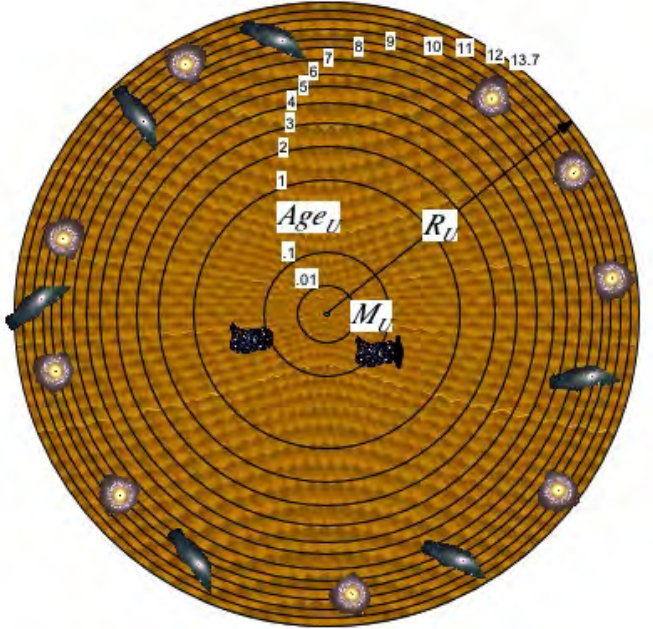
$$R_{Ur} = \frac{1}{C_{Ur}} = \frac{\sqrt{3}c}{\sqrt{4\pi G_{Ur} \rho_{Ur}}} \left(\sqrt{3} \cdot \text{Einstein radius} \right) \quad (2.11.3r)$$

The Einstein radius is sometimes called the Jeans' length [101]. The factor $\sqrt{3}$ represent an internal deviation with the trisine structure that adds an inflation factor to the static state represented by the Einstein Radius.

$$R_U = \frac{\sqrt{3}}{g_s^3} \frac{\text{cavity}}{\text{chain}} k_{mx} \varepsilon_x B \quad (2.11.4)$$

$$R_{Ur} = \frac{\sqrt{3}}{g_s^3} \frac{\text{cavity}_r}{\text{chain}_r} k_{mxr} \varepsilon_{xr} B_r \quad (2.11.4r)$$

Figure 2.11.1 Observed Universe with Mass M_U and Hubble radius of curvature R_U and smooth trisine lattice expansion (three dimensional tessellation of space) all as a function of universe age(Age_U)



Under conditions expressed in equation 2.11.42, R_U is equal to the Schwarz gravitational viscous scale.

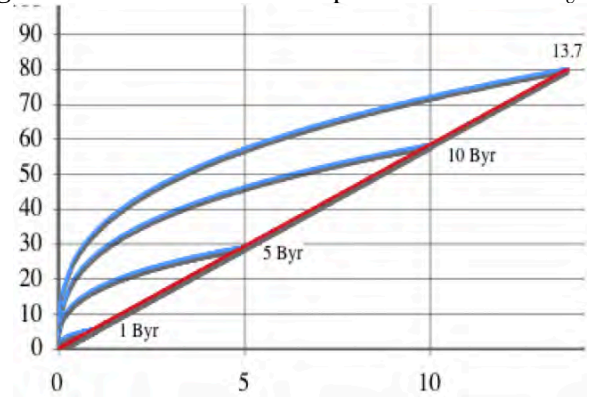
$$R_U = \frac{g_s}{3} \frac{m_t c}{\hbar 2\pi} \sqrt{\frac{3}{2}} \frac{\nu_U}{G_U \rho_U} \quad (2.11.5)$$

$$R_{Ur} = \frac{g_s}{3} \frac{m_t c}{\hbar 2\pi} \sqrt{\frac{3}{2}} \frac{\nu_{Ur}}{G_{Ur} \rho_{Ur}} \quad (2.11.5r)$$

$$\text{where } \nu_U = \nu_{Ur}$$

$$R_U = 2.25E28 \text{ cm} (\sqrt{3} c \cdot 13.71 \text{ Gyr})$$

Figure 2.11.2 The universe expands with B and R_U .



The universe R_U and Trisine Lattice as measured by cellular dimension B are equal at any proper time in Figure 2.11.2.

The mass of the universe (M_U) is established by assuming a spherical isotropic universe (center of mass in the universe center) of Hubble radius of curvature (R_U) such that a particle with the speed of light cannot escape from it as expressed in equation 2.11.6 and graphically described in figure 2.11.1.

$$M_U = R_U \cdot \frac{c^2}{G_U} = \frac{\sqrt{3}\pi}{4} \frac{\hbar^2 c^2}{m_t^3 G_U^2} = \frac{F_p}{Euler \ a_U} \quad (2.11.6)$$

$$M_{Ur} = R_{Ur} \cdot \frac{c^2}{G_{Ur}} = \frac{\sqrt{3}\pi}{4} \frac{\hbar^2 c^2}{m_t^3 G_{Ur}^2} = \frac{F_{Pr}}{Euler \ a_{Ur}} \quad (2.11.6r)$$

$$M_U = 3.02E56 \text{ g} = 3.01E61 \text{ m}_t = 3.32E83 \text{ m}_e$$

$$\rho_U = \frac{M_U}{V_U} = M_U \cdot \frac{3}{4\pi} \frac{1}{R_U^3} = \frac{4}{\pi^3} \frac{m_t^6 c^2 G_U}{\hbar^4} = \frac{m_t}{cavity} \quad (2.11.7)$$

$$\rho_{Ur} = \frac{M_{Ur}}{V_{Ur}} = M_{Ur} \cdot \frac{3}{4\pi} \frac{1}{R_{Ur}^3} = \frac{4}{\pi^3} \frac{m_t^6 c^2 G_{Ur}}{\hbar^4} = \frac{m_t}{cavity_r} \quad (2.11.7r)$$

$$\rho_U = 6.38E-30 \text{ g/cm}^3$$

This value for Universe density is much greater than the density of the universe calculated from observed celestial objects. As reported in reference [27], standard cosmology model allows accurate determination of the universe baryon density of between $1.7E-31$ to $4.1E-31 \text{ g/cm}^3$. These values are 2.7 - 6.4% of the universe density reported herein based the background universe as superconductor.

$$\begin{aligned} \text{Universe Age}(Age_U) &= \frac{R_U}{\sqrt{3}c} = \frac{\pi}{4} \frac{\hbar^2}{m_t^3 c G_U} \\ &= 4.32E17 \text{ sec (13.71 Gyr)} \end{aligned} \quad (2.11.6)$$

Equation 2.11.7 may be rearranged in terms of a universal surface constant.

$$\frac{M_U}{R_U^2} = \frac{M_{Ur}}{R_{Ur}^2} = 0.599704 \quad (2.11.6a)$$

Which compares favorability to 13.75 ± 0.13 Gyr [20]. This is an indication that the universe is expanding at the speed of light (c) but not accelerating.

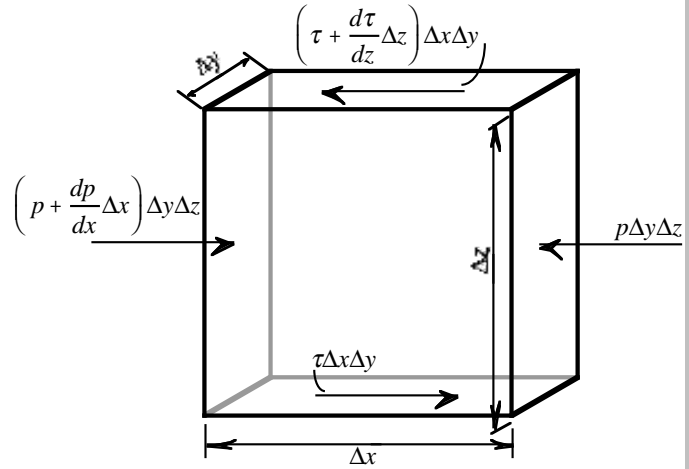
As illustrated in Figure 2.11.3 equation 2.11.14 for the Hubble constant (H_U) is derived by equating the forces acting on a cube of fluid in shear in one direction to those in

the opposite direction, or

$$\begin{aligned} p_U \Delta y \Delta z + \left[\tau + \frac{d\tau}{dz} \Delta z \right] \Delta x \Delta y \\ = \tau \Delta x \Delta y + \left[p_U + \frac{dp_U}{dx} \Delta x \right] \Delta y \Delta z \end{aligned} \quad (2.11.7)$$

$$\begin{aligned} p_{Ur} \Delta y_r \Delta z_r + \left[\tau_r + \frac{d\tau_r}{dz_r} \Delta z_r \right] \Delta x_r \Delta y_r \\ = \tau_r \Delta x_r \Delta y_r + \left[p_{Ur} + \frac{dp_{Ur}}{dx_r} \Delta x_r \right] \Delta y_r \Delta z_r \end{aligned} \quad (2.11.7r)$$

Figure 2.11.3 Shear forces along parallel planes of an elemental volume of fluid



Here p_U is the universe pressure intensity ($\mathbb{C}k_B T_c / cavity$), τ the shear intensity, and Δx , Δy , and Δz are the dimensions of the cube. It follows that:

$$\frac{d\tau}{dz} = \frac{dp_U}{dx} \quad (2.11.8)$$

$$\frac{d\tau_r}{dz_r} = \frac{dp_{Ur}}{dx_r} \quad (2.11.8r)$$

The power expended, or the rate at which the couple does work ($\tau \Delta x \Delta y$), equals the torque ($\tau \Delta x \Delta y$) Δz times the angular velocity dv/dz . Hence the universe power (P_U) consumption per universe volume (V_U) of fluid is

$$P_U/V_U = [(\tau \Delta x \Delta y) \Delta z \ dv/dz]/(\Delta x \Delta y \Delta z) = \tau (dv/dz)$$

Defining $\tau = \mu_U \ dv/dz$ and $H_U = dv/dz$

$$P_U/V_U = \mu_U (dv/dz)^2 = \mu_U H_U^2$$

or $H_U^2 = P_U/(\mu_U V_U)$

where $P_{U_1} cavity_{U_1}^{5/3} = P_{U_2} cavity_{U_2}^{5/3}$

with the exponent factor '5/3' being representative of a monatomic ideal gas adiabatic expansion and with inflation

number $\#_U$ representing the number of cavities in the universe

$$\text{and } V_U = (M_U/m_t) \text{cavity} = \#_U \text{cavity}$$

The *universe absolute viscosity* (μ_U) is based on momentum transferred per surface area as an outcome of classical kinetic theory of gas viscosity [19]. In terms of our development, the momentum changes over the *section* in each *cavity* such that:

$$\mu_U = \frac{m_t v_{dx}}{\text{section}} = \frac{1}{2} \frac{A}{B} \frac{h}{\text{cavity}} \quad (2.11.9)$$

$$\mu_{Ur} = \frac{m_t v_{dxr}}{\text{section}_r} = \frac{1}{2} \frac{A_r}{B_r} \frac{h}{\text{cavity}_r} \quad (2.11.9r)$$

Equation 2.11.10 is equivalent to entropy density derivation[130].

$$\frac{\eta}{s} = \mu_U \text{cavity} \frac{B}{A} \frac{1}{4\pi^2} = \frac{\hbar}{4\pi} \quad (2.11.10)$$

$$\frac{\eta}{s} = \mu_U \text{cavity} \frac{B}{A} \frac{1}{4\pi^2} = \frac{\hbar}{4\pi} \quad (2.11.10r)$$

Derivation of the kinematic viscosity (v_U) in terms of absolute viscosity as typically presented in fluid mechanics [18], a constant universe kinematic viscosity (v_U) is achieved in terms of Planck's constant (\hbar) and Cooper CPT Charge conjugated pair resonant transformed mass (m_t).

$$\begin{aligned} v_U &= \frac{\text{cavity}}{m_t} \mu_U = \frac{\mu_U}{\rho_U} \\ &= \pi \frac{\hbar}{m_t} \frac{A}{B} = 1.39E-02 \frac{\text{cm}^2}{\text{sec}} \end{aligned} \quad (2.11.11)$$

$$\begin{aligned} v_{Ur} &= \frac{\text{cavity}_r}{m_t} \mu_{Ur} = \frac{\mu_{Ur}}{\rho_{Ur}} \\ &= \pi \frac{\hbar}{m_t} \frac{A_r}{B_r} = 1.39E-02 \frac{\text{cm}^2}{\text{sec}} \end{aligned} \quad (2.11.11r)$$

Derivation of the Universe Energy Dissipation Rate (P_U) assumes that all of the universe mass (M_U) in a universe volume (V_U) is in the superconducting state. In other words, our visible universe contributes an insignificant amount of mass to the universe mass (M_U). This assumption appears to be valid due to the subsequent calculation of the Hubble

constant (H_U) of 71.23 km/sec-million parsec (equation 2.11.13) which falls within the experimentally observed WMAP value[20] of 71.0 ± 2.5 km/sec-million parsec.

$$P_U = \frac{A}{B} \frac{4 \cos(\theta)}{\text{Euler}} \frac{m_t c^2}{t_U} = \frac{M_U}{2} \frac{v_{dx}^2}{R_U} = \mu_U H_U^2 V_U \quad (2.11.12)$$

$$P_{Ur} = \frac{A_r}{B_r} \frac{4 \cos(\theta)}{\text{Euler}} \frac{m_t c^2}{t_U} = \frac{M_{Ur}}{2} \frac{v_{dxr}^2}{R_{Ur}} = \mu_{Ur} H_{Ur}^2 V_{Ur} \quad (2.11.12r)$$

$$P_U = P_{Ur} = 2.24E+19 \text{ erg/sec}$$

$$V_U = \frac{4}{3} \pi R_U^3 = \frac{\sqrt{3} \pi^4 \hbar^6}{16 m_t^9 G_U^3} \quad (2.11.13)$$

$$V_{Ur} = \frac{4}{3} \pi R_{Ur}^3 = \frac{\sqrt{3} \pi^4 \hbar^6}{16 m_t^9 G_{Ur}^3} \quad (2.11.13r)$$

$$= 4.74E85 \text{ cm}^3 = 3.01E81 \text{ cavitys}$$

$$\begin{aligned} H_U &= \sqrt{\frac{P_U}{\mu_U V_U}} = \frac{4 m_t^3 G_U c}{\pi \hbar^2} = \frac{F_p}{\text{Euler} M_U c} \\ &= \sqrt{3} \frac{c}{R_U} = \frac{1}{\sqrt{3}} \frac{B}{A} \frac{v_{dx}}{c} \frac{1}{\text{time}_\pm} \end{aligned} \quad (2.11.14)$$

$$\begin{aligned} H_{Ur} &= \sqrt{\frac{P_U}{\mu_{Ur} V_{Ur}}} = \frac{4 m_t^3 G_{Ur} c}{\pi \hbar^2} = \frac{F_{pr}}{\text{Euler} M_{Ur} c} \\ &= \sqrt{3} \frac{c}{R_{Ur}} = \frac{1}{\sqrt{3}} \frac{B_r}{A_r} \frac{v_{dxr}}{c} \frac{1}{\text{time}_{r\pm}} \end{aligned} \quad (2.11.14r)$$

With the universal constant mass (m_t) (analogous to the Weinberg mass[99]) established as:

$$\begin{aligned} m_t^3 &= \frac{m_t \rho_U k_b T_c \text{section}}{\sqrt{3} H_U c} \\ &= \frac{\pi^2 \rho_U \hbar^2}{H_U c} = \frac{U \hbar^2 \cos^3(\theta)}{c} \end{aligned} \quad (2.11.15)$$

$$\begin{aligned} m_t^3 &= \frac{m_t \rho_{Ur} k_b T_{cr} \text{section}_r}{\sqrt{3} H_{Ur} c} \\ &= \frac{\pi^2 \rho_{Ur} \hbar^2}{H_{Ur} c} = \frac{U \hbar^2 \cos^3(\theta)}{c} \end{aligned} \quad (2.11.15r)$$

With proximity to Heisenberg Uncertainty condition $\hbar/2$:

$$\begin{aligned} 2 \frac{\hbar}{2} &= m_t c \frac{4 m_t^2}{\pi U \hbar} = m_t c \frac{4 G_U m_t^2}{\pi H_U \hbar} \\ &= m_t c x_U = m_t c^2 t_U \end{aligned} \quad (2.11.16)$$

$$\begin{aligned} 2 \frac{\hbar}{2} &= m_t c \frac{4 m_t^2}{\pi U \hbar} = m_t c \frac{4 G_{Ur} m_t^2}{\pi H_{Ur} \hbar} \\ &= m_t c x_U = m_t c^2 t_U \end{aligned} \quad (2.11.16r)$$

$$H_U = 2.31E-18 \text{ / sec} \quad \left(71.23 \frac{\text{km}}{\text{sec}} \frac{1}{\text{million parsec}} \right)$$

$$x_U = 1.75E-13 \text{ cm} \quad (\text{nuclear dimension})$$

Now from equation 2.11.1 and 2.11.14 the *cosmological constant* (Λ_U or $6C_U^2/\cos(\theta)$) is defined in terms of the Hubble constant (H_U) in equation 2.11.17. The *cosmological constant* Λ_U is considered a scalable multiple and not addend factor

$$C_U = \left(\frac{\Lambda_U \cos(\theta)}{6} \right)^{\frac{1}{2}} = \frac{H_U}{\sqrt{3}c} = \frac{1}{R_U} = \frac{c^2}{M_U G_U} \quad (2.11.17)$$

$$C_{Ur} = \left(\frac{\Lambda_{Ur} \cos(\theta)}{6} \right)^{\frac{1}{2}} = \frac{H_{Ur}}{\sqrt{3}c} = \frac{1}{R_{Ur}} = \frac{c^2}{M_{Ur} G_{Ur}} \quad (2.11.17r)$$

$$= 4.45E-29 \text{ cm}^{-1}$$

And the Universe Escape Velocity (v_U) equivalent to the speed of light (c).

$$v_U = c = \frac{H_U R_U}{\sqrt{3}} = \sqrt{\frac{G_U M_U}{R_U}} \quad (2.11.18)$$

$$v_U = c = \frac{H_{Ur} R_{Ur}}{\sqrt{3}} = \sqrt{\frac{G_{Ur} M_{Ur}}{R_{Ur}}} \quad (2.11.18r)$$

Equation (2.11.19) implies a constant gravitational energy for any test mass(m) at any universe time epoch.

$$mv_U^2 = mc^2 = \frac{m H_U^2 R_U^2}{3} = \frac{G_U m M_U}{R_U} \quad (2.11.19)$$

$$\text{where } G_U R_U = 1.49867E+21$$

$$\text{and } \frac{M_U}{R_U^2} = .599704$$

$$mv_U^2 = mc^2 = \frac{m H_{Ur}^2 R_{Ur}^2}{3} = \frac{G_{Ur} m M_{Ur}}{R_{Ur}} \quad (2.11.19r)$$

$$\text{where } G_{Ur} R_{Ur} = 1.49867E+21$$

$$\text{and } \frac{M_{Ur}}{R_{Ur}^2} = .599704$$

Now from equation 2.11.20 and 2.11.13 the *universe mass* (M_U) is defined in terms of the Hubble constant (H_U) in equation 2.11.14.

$$M_U = \frac{m_t}{cavity} V_U = \rho_U \frac{4\pi}{3} R_U^3 \quad (2.11.20)$$

$$= \frac{\sqrt{3}c^3}{H_U G_U} = \frac{\sqrt{3}\pi\hbar^2 c^2}{4m_t^3 G_U^2} = \frac{R_U c^2}{G_U} \quad (2.11.20r)$$

$$M_{Ur} = \frac{m_t}{cavity_r} V_{Ur} = \rho_{Ur} \frac{4\pi}{3} R_{Ur}^3 \quad (2.11.20r)$$

$$= \frac{\sqrt{3}c^3}{H_{Ur} G_{Ur}} = \frac{\sqrt{3}\pi\hbar^2 c^2}{4m_t^3 G_{Ur}^2} = \frac{R_{Ur} c^2}{G_{Ur}} \quad (2.11.20r)$$

$$M_{Upresent} = \frac{P_U}{c^2} \int_{v_{dx}=c}^{v_{dx} \text{ at present}} \left(\frac{Age_{Upresent}}{Age_U} \right)^2 dAge_U$$

$$= - \frac{P_U Age_{Upresent}^2}{c^2} \left(\frac{1}{Age_{Uatpresent}} - \frac{1}{Age_{U \text{ at } vdx=c}} \right)$$

$$= 3.02E56 \text{ g} \quad (\text{conforming to condition 1.11})$$

$$\text{Number of particles} = \frac{M_{Upresent}}{m_t} = \frac{V_U}{cavity} = 3.01E81$$

Figure 2.11.4 Trisine Steric Charge Conjugate Pair Change Time Reversal CPT Geometry as depicted in Figure 2.3.1 with Relativistic Pressure ' $-p$ ', Quantum Mechanical Pressure ' p ' and Density ' ρ_U '.

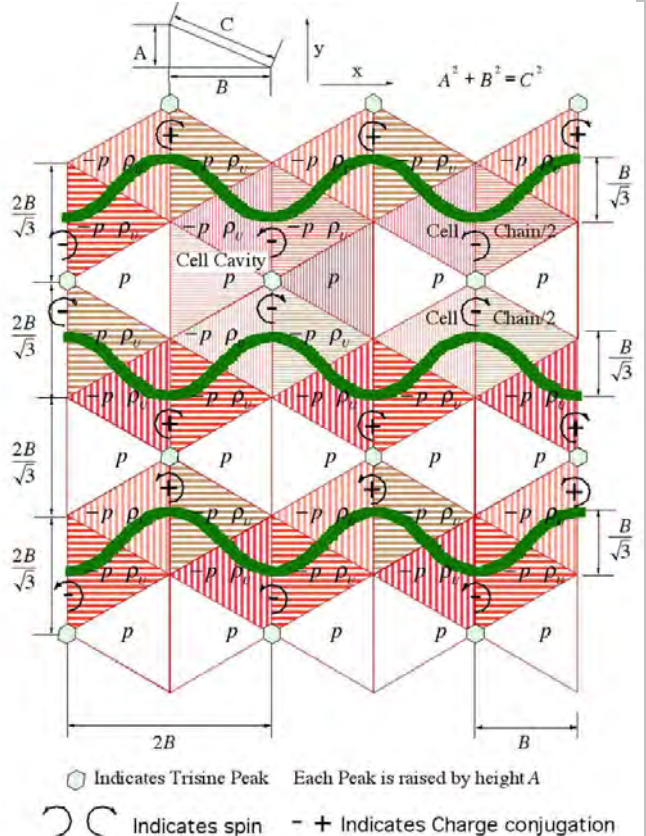
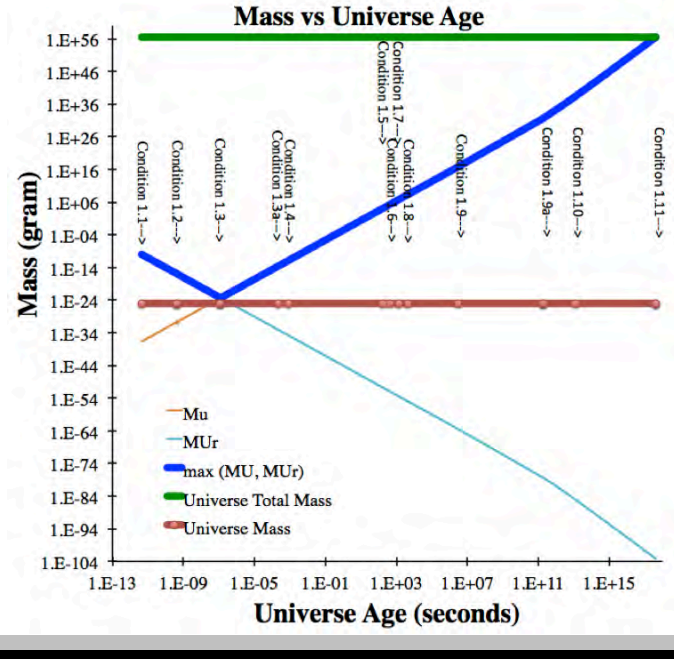
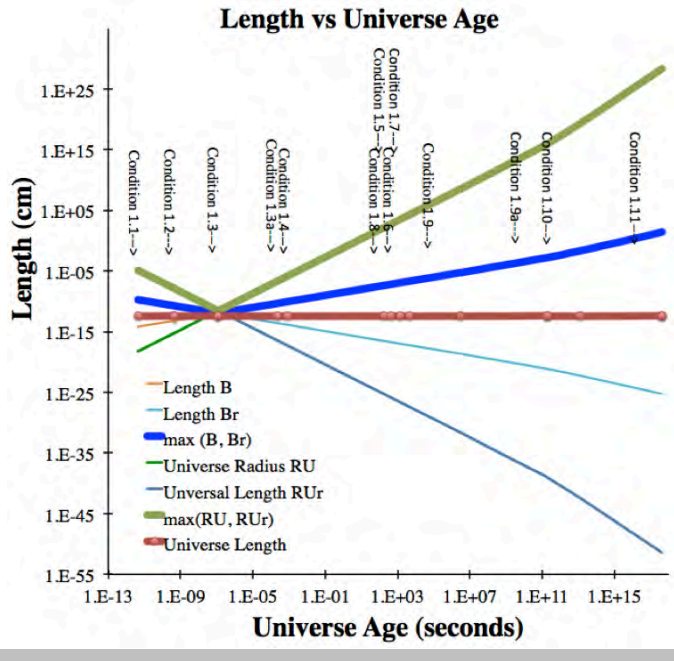


Figure 2.11.5 Graphical presentation of universe mass



The trisine model conforms to Einstein Energy Tensor equations at all lattice similarities assuming the universe mass M_U increases with time.

Figure 2.11.5a Graphical presentation of universe length



This is consistent with conventional Friedmann-Lemaitre theory for universe constant mass under assumption that universe began with extremely large number of mass points ($M_{U_{present}}/M_U \sim 1E90$) at trisine condition 1.1 each quantum mechanically in phase with each other in as much as they form a time fleeting colligative Bose Einstein Condensate

aggregation adiabatically expanding to the present. These initial $\sim 1E90$ in phase points converging in to the present one universe explains the present expanded one universe homogeneity without that group phase reflection inflation step.

Now from equation 2.11.14 and 2.11.5 the *universe density* (ρ_U) is defined in terms of the Hubble constant (H_U) in equation 2.11.21. This differs from the universe critical density equation in reference [27] by a factor of as a consequence of Robertson Walker equation 2.11.34 reduction, which indicates an expanding but not necessarily inflationary universe.

$$\begin{aligned} \rho_U &= \frac{2}{8\pi} \frac{H_U^2}{G_U} = \frac{3}{8\pi} \frac{\text{chain}}{\text{cavity}} \frac{H_U^2}{G_U} = \frac{m_t}{\text{cavity}} \\ &= \frac{1}{8\pi} \frac{c^2}{G_U} \Lambda \cos(\theta) \end{aligned} \quad (2.11.21)$$

$$\begin{aligned} \Lambda_U &= \frac{2H_U^2}{c^2 \cos(\theta)} \\ \rho_{Ur} &= \frac{2}{8\pi} \frac{H_{Ur}^2}{G_{Ur}} = \frac{3}{8\pi} \frac{\text{chain}}{\text{cavity}} \frac{H_{Ur}^2}{G_{Ur}} = \frac{m_t}{\text{cavity}_r} \\ &= \frac{1}{8\pi} \frac{c^2}{G_{Ur}} \Lambda_r \cos(\theta) \\ \Lambda_{Ur} &= \frac{2H_{Ur}^2}{c^2 \cos(\theta)} \end{aligned} \quad (2.11.21r)$$

$$\begin{aligned} \rho_U &= 6.38E-30 \frac{g}{cm^3} \\ \Omega_{\Lambda_U} &= \frac{1}{8\pi} \frac{c^2}{G_U} \Lambda_U \left(\frac{3}{8\pi} \frac{H_U^2}{G_U} \right)^{-1} \\ &= \frac{\Lambda_U c^2}{3H_U^2} = 0.72315 \\ &\approx \frac{2}{3\cos(\theta)} \end{aligned} \quad (2.11.22)$$

$$\begin{aligned} \Omega_{\Lambda_{Ur}} &= \frac{1}{8\pi} \frac{c^2}{G_{Ur}} \Lambda_{Ur} \left(\frac{3}{8\pi} \frac{H_{Ur}^2}{G_{Ur}} \right)^{-1} \\ &= \frac{\Lambda_{Ur} c^2}{3H_{Ur}^2} = 0.72315 \\ &\approx \frac{2}{3\cos(\theta)} \end{aligned} \quad (2.11.22r)$$

Now correlating equation 2.11.13 and 2.11.7, the *universe age* (Age_U) is defined in terms of the Hubble constant (H_U) in equation 2.11.23.

$$Age_U = \frac{1}{H_U} \quad (2.11.23)$$

= 4.32E+17 or 1.37E10 years

$$Universe mass creation (M_{UC}) at T_c \quad (2.11.24)$$

$$Age_{UG} = Age_U \sqrt{G_U/G} = Age_U \sqrt{R_U c^2/(GM_U)} \quad (2.11.25)$$

$$Age_{UGv} = Age_U \sqrt{R_U c^2/(G(M_U + M_v))} \quad (2.11.26)$$

$Age_{UGv} = Age_{UG} = Age_U = 13.7E+9$ years at the present time

Table 2.11.1 Vacuum Space parameters

Condition	1.2	1.3	1.6	1.9	1.10	1.11
$T_a ({}^0 K)$	6.53E+11	6.53E+11	6.53E+11	6.53E+11	6.53E+11	6.53E+11
$T_b ({}^0 K)$	9.05E+14	5.48E+13	9.22E+08	1.10E+07	2,868	2.723
$T_{br} ({}^0 K)$	3.30E+12	5.45E+13	3.24E+18	2.72E+20	1.04E+24	1.10E+27
$T_c ({}^0 K)$	8.96E+13	3.28E+11	93.0	0.0131	8.99E-10	8.10E-16
$T_{cr} ({}^0 K)$	1.19E+09	3.25E+11	1.15E+21	8.11E+24	1.19E+32	1.32E+38
$z_R + 1$	3.67E+43	8.14E+39	3.89E+25	6.53E+19	1.17E+09	1.00E+00
$z_B + 1$	3.32E+14	2.01E+13	3.39E+08	4.03E+06	1.05E+03	1.00E+00
$Age_{UG} (sec)$	7.14E-05	4.79E-03	6.94E+04	5.36E+07	1.27E+13	4.33E+17
$Age_{UGv} (sec)$	4.59E-10	1.25E-07	4.42E+02	3.13E+06	1.22E+13	4.33E+17
$Age_U (sec)$	1.18E-26	5.31E-23	1.11E-08	6.63E-03	3.70E+08	4.33E+17
$\mu_U (g/cm/sec)$	3.25E+12	7.20E+08	3.44E-06	5.77E-12	1.03E-22	8.84E-32
$\mu_{Ur} (g/cm/sec)$	1.57E+05	7.10E+08	1.49E+23	8.86E+28	4.95E+39	5.78E+48
$\sigma_U (erg/cm^2)$	8.07E+23	1.08E+19	8.70E-01	1.74E-08	8.13E-23	6.61E-35
$\sigma_{Ur} (erg/cm^2)$	1.42E+14	1.06E+19	1.32E+38	6.62E+45	1.41E+60	1.74E+72
$P_U (erg/sec)$	2.24E+19	2.24E+19	2.24E+19	2.24E+19	2.24E+19	2.24E+19
$P_{Ur} (erg/sec)$	2.24E+19	2.24E+19	2.24E+19	2.24E+19	2.24E+19	2.24E+19
$M_{UC} (g)$	3.97E+59	8.80E+55	4.20E+41	7.05E+35	1.26E+25	0.00E+00

This development would allow the galactic collision rate calculation in terms of the Hubble constant (H_U) (which is considered a shear rate in our fluid mechanical concept of the universe) in accordance with the Smolukowski relationship [12, 13, 14] where J_U represents the collision rate of galaxies of two number concentrations (n_i, n_j) and diameters (d_i, d_j):

$$J_U = \frac{1}{6} n_i n_j H_U (d_i + d_j)^3 \quad (2.11.27)$$

$$d = \frac{24}{\pi} \frac{C\sigma}{\mu_i H} \text{ After Appendix L2.12} \quad (2.11.28)$$

The superconducting Reynolds' number (R_e), which is defined as the ratio of inertial forces to viscous forces is presented in equation 2.11.20 and has the value of one(1). In terms of conventional fluid mechanics this would indicate a condition of laminar flow [18].

$$\begin{aligned} R_e &= \frac{v_{dx}}{v_U} \frac{cavity}{section} = \frac{v_{dx}}{v_U} B = \frac{v_{dx}}{v_U} 4 R_h = \frac{v_{dx}}{v_U} 4 \frac{B}{4} \\ &= \frac{m_t}{cavity} \frac{v_{dx}}{\mu} \frac{cavity}{section} = \frac{m_t v_{dx}}{\mu section} = 1 \end{aligned} \quad (2.11.29)$$

$$\begin{aligned} a_U &= \pi e^{-Euler} \left(\frac{v_{dy}^2}{2P} \right) \Bigg|_{\substack{T_c=8.11E-16 \\ T_b=2.729}} \\ &= cH_U = \frac{R_U H_U^2}{\sqrt{3}} = \sqrt{\frac{P_U c^2}{\mu_U V_U}} = 6.93 \times 10^{-8} \frac{cm}{sec^2} \end{aligned} \quad (2.11.30)$$

The numerical value of the universal acceleration (a_U) expressed in equation 2.11.30 is nearly equal to that deceleration (a) observed with Pioneer 10 & 11 [53], but this near equality is viewed as consequence of equations 2.7.6a and 2.11.31-2.11.33 for the particular dimensional characteristics (cross section (A_c), Mass (M) and thrust coefficient (C_t)) of the Pioneer space crafts (Table 2.7.2) with appropriate negative sign indicating deceleration. Free body physical analysis of such a fact (in this case the positive acceleration cH_U) would indicate the possibility of opposing component forces expressed as negative acceleration. Pioneer or any other object traveling through this universe vacuum viscosity [130] would have a negative acceleration due to their momentum transfer with the space vacuum and relative to their area/mass and may in aggregate match the positive universal cH_U .

$$a_U = cH_U = \frac{H_U^2 R_U}{\sqrt{3}} = 6.93 \times 10^{-8} \frac{cm}{sec^2} \quad (2.11.31)$$

$$a = -\frac{A_c}{M} \frac{1}{G_U} (cH_U)^2 = -7.20 \times 10^{-8} \frac{cm}{sec^2} \quad (2.11.32)$$

$$a = -C_t \frac{A_c}{M} \rho_u c^2 = -8.37 \times 10^{-8} \frac{cm}{sec^2} \quad (2.11.33)$$

Analogously, the observed type Ia supernovae acceleration interpretation may actually be due to a deceleration of our local baryonic matter (star systems, galaxies, etc.) related to momentum transfer boundary between the elastic space CPT lattice and baryonic matter (star systems, galaxies, etc.) and under the universal gravity and quantum mechanical energy relationships in equations 2.11.32 and 2.11.33.

$$\begin{aligned} m_t c^2 &= G_u \frac{m_t M_u}{R_u} \quad (2.11.34) \\ &= \frac{\sqrt{3}}{8\pi} \frac{M_u}{m_t} \frac{h^2}{2m_t} \frac{1}{R_u^2} \quad \text{where} \quad \frac{M_u}{R_u^2} = 0.599704 \text{ g/cm} \\ &= \frac{2}{3} \left(\frac{\sqrt{3}}{8\pi} \right)^2 \frac{h^2}{2m_t} \frac{1}{B_{nucleus}^2} = 3\pi k_m \varepsilon g_s \frac{h^2}{2m_t} \frac{1}{A^2} \end{aligned}$$

Eqn 2.11.34 fits well into the relativistic derivations in Appendix F and also the energy (pc) relationship:

$$\frac{1}{2} h H_u = \frac{1}{2} h \frac{\sqrt{3}c}{R_u} = \frac{3}{4} G_u \frac{m_t^2}{B_{nucleus}} = 8\pi G_u m_t^3 \frac{c}{h} \quad (2.11.35)$$

The Milky Way galactic rotational energy ($I\omega^2$) is nearly equal to relativistic energy (Mc^2) by the equipartition of energy principle where the accepted dimensions are as follows with the assumption that the Milky Way is composed of $5.8E11$ solar masses which rotated 20 times during the last 4.5 billion years (the age of the earth):

Table 2.11.2 Galactic Equipartition of Energy

Diameter	9.46E+22 <i>Cm</i>	100,000 <i>light years</i>
Radius	4.73E+22 <i>Cm</i>	50,000 <i>light years</i>
Width	2.37E+22 <i>Cm</i>	25,000 <i>light years</i>
Volume	1.66E+68 <i>cm</i> ³	1.96E+14 <i>light years</i> ³
Density	6.38E-30 <i>g/cm</i> ³	
dark energy mass	1.06E+39 <i>G</i>	<i>M</i>
dark energy	9.53E+59 <i>Erg</i>	<i>Mc</i> ²
Density	6.94E-24 <i>g/cm</i> ³	
Mass	1.15E+45 <i>G</i>	
moment of inertia (I)	1.29E+90 <i>g cm</i> ²	<i>I</i>
rotation ω	8.86E-16 <i>radian/sec</i>	1.41E-16 <i>rev/sec</i>
Energy	1.01E+60 <i>erg</i>	<i>I</i> ω^2

These ideas are consistent with an equilibrium droplet size as derived in Appendix L2.12 and shear stated in terms of H_u verses the more conventional fluid dynamic notation G .

$$\text{Universe Diameter} = \frac{24}{\pi} \frac{C\sigma}{\mu H_u} = \frac{24}{\pi} \frac{C}{H_u} c \sim R_u \quad (2.11.36)$$

$$\text{Galaxy Diameter} = \frac{24}{\pi} \frac{C\sigma}{\mu H_u} = \frac{24}{\pi} \frac{C}{H_u} v_\varepsilon \quad (2.11.36a)$$

$$\text{Solar System Diameter} = \frac{24}{\pi} \frac{C\sigma}{\mu H_u} = \frac{24}{\pi} \frac{C}{H_u} v_{dx} \quad (2.11.36b)$$

Calculations are presented in Table 2.11.3 for Dark Matter as Hydrogent Bose Einstein Condensate Concentration(C) $1 - (\Omega_{\Lambda_u}) = 1 - .72315 = .27685$.

Universe material arranges itself in accordance with

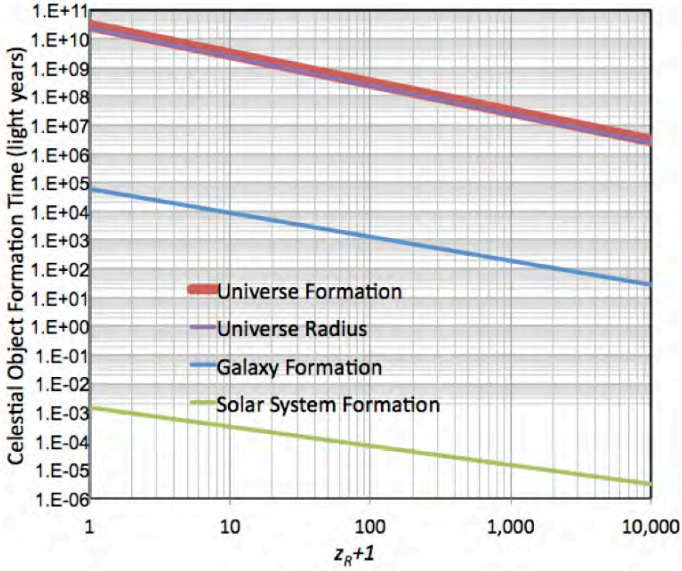
$$c, v_\varepsilon, v_{dx} \text{ or } c, \left(\frac{c}{\sqrt{\varepsilon}} \right), \left(\frac{c}{\sqrt{k_{mx}\varepsilon}} \right)$$

Table 2.11.3 Universe, Galaxy, Solar Systems Size in terms of universe expansion

Condition	1.2	1.3	1.6	1.9	1.10	1.11
$T_a ({}^0 K)$	6.53E+11	6.53E+11	6.53E+11	6.53E+11	6.53E+11	6.53E+11
$T_b ({}^0 K)$	9.05E+14	5.48E+13	9.22E+08	1.10E+07	2,868	2.723
$T_{br} ({}^0 K)$	3.30E+12	5.45E+13	3.24E+18	2.72E+20	1.04E+24	1.10E+27
$T_c ({}^0 K)$	8.96E+13	3.28E+11	93.0	0.0131	8.99E-10	8.10E-16
$T_{cr} ({}^0 K)$	1.19E+09	3.25E+11	1.15E+21	8.11E+24	1.19E+32	1.32E+38
$z_R + 1$	3.67E+43	8.14E+39	3.89E+25	6.53E+19	1.17E+09	1.00E+00
$z_B + 1$	3.32E+14	2.01E+13	3.39E+08	4.03E+06	1.05E+03	1.00E+00
$Age_{UG} (sec)$	7.14E-05	4.79E-03	6.94E+04	5.36E+07	1.27E+13	4.33E+17
$Age_{UGV} (sec)$	4.59E-10	1.25E-07	4.42E+02	3.13E+06	1.22E+13	4.33E+17
$Age_U (sec)$	1.18E-26	5.31E-23	1.11E-08	6.63E-03	3.70E+08	4.33E+17
Universe Diameter (cm)	6.18E-15	1.69E-12	5.96E-03	4.22E+01	6.16E+08	6.83E+14
Universe Diameter (lyr)	2.94E-32	3.26E-29	2.80E-17	1.82E-12	1.64E-03	5.92E+04
Galaxy Diameter (cm)	2.78E-14	3.09E-11	2.65E+01	1.72E+06	1.56E+15	5.60E+22

Galaxy Diameter (lyr)	2.94E-32	3.26E-29	2.80E-17	1.82E-12	1.64E-03	5.92E+04
Solar System Diameter (cm)	1.24E-14	3.38E-12	1.19E-02	8.43E+01	1.23E+09	1.37E+15
Solar System Diameter (lyr)	1.31E-32	3.57E-30	1.26E-20	8.91E-17	1.30E-09	1.44E-03

Figure 2.11.6 Universe, Galaxy, Solar Systems Size in terms of universe expansion



These Table 2.11.3 Galactic Formation Diameter calculations indicate present galaxies with diameters typically on the order of 2.9E-3 light years(lyr) were first formed at the first light event($T_b = 3,000\text{K}$) (possibly before) and continued to increase in size (Figure 2.11.6) to present on average 1.17E+05 light years at Age_U and Age_{UG} of 4.32E+17sec (13.7 billion years). Galactic surveys should be able to verify this relationship. Dark energy shear expressed as a changing Hubble parameter H_U was the principle mechanism. The gravitational mechanism was secondary.

In summary and referencing Stabell and Refsdal[128] and Robertson[129] the Robertson and Walker homogeneous and isotropic universe metric is:

$$ds^2 = c^2 dt^2 - R^2(t) \left[\frac{dr^2}{1 - kr^2} + r^2 (d\theta^2 + \sin^2 \theta d\phi^2) \right] \quad (2.11.37)$$

where k is equal to +1, =1 or 0, and R is a scale-factor with dimension length R not necessarily related to R_U in this paper and resulting in the following two non-trivial equations:

$$8\pi G \rho = \frac{3}{R^2} (kc^2 + \dot{R}^2) - \Lambda \quad (2.11.38)$$

$$\frac{8\pi G}{c^2} p = -\frac{2\ddot{R}}{R} - \frac{\dot{R}^2}{R^2} - \frac{kc^2}{R^2} + \Lambda \quad (2.11.39)$$

and as per Harrison[122] & D'Inverno[32], the equation 2.11.39 is integrated with constant of integration provided by equation 2.11.38.

$$\dot{R}^2 = \frac{8\pi G \rho R^2}{3} + \frac{\Lambda R^2}{3} - kc^2 \quad (2.11.40)$$

The Einstein-de Sitter universe has $k = 0$, $\Lambda = 0$ and $\Omega = 1$.

$$\dot{R}^2 = \frac{8\pi G \rho R^2}{3} \quad (2.11.41)$$

or

$$\dot{R}^2 = \left(\frac{\dot{R}}{R} \right)^2 = \frac{8\pi G \rho}{3} \quad (2.11.42)$$

That is by definition

$$H^2 = \frac{8\pi G \rho}{3} \quad (2.11.43)$$

and the universe density ρ_U

$$\rho = \frac{3}{8\pi} \frac{H^2}{G} \quad (2.11.44)$$

Given that:

$$\frac{H_{UG}}{H_U} = \left(\frac{G}{G_U} \right)^{\frac{1}{2}} \quad (2.11.45)$$

then equations 2.11.38 and 2.11.39 numerically are identified with the following equations when $k = 0$ and $\Lambda = 0$.

$$8\pi G \frac{3}{2} \rho_U = \frac{3}{B^2} (kc^2 + (H_{UG} B)^2) - \Lambda \quad (2.11.46)$$

$$\frac{8\pi G}{c^2} \frac{3}{2} \frac{m_c^2}{cavity} = -\frac{2(BH_{UG}^2)}{B} - \frac{(BH_{UG})^2}{B^2} - \frac{kc^2}{B^2} + \Lambda \quad (2.11.47)$$

And also equivalent to:

$$8\pi G_U \frac{3}{2} \rho_U = \frac{3}{B^2} (kc^2 + (H_U B)^2) - \Lambda \quad (2.11.48)$$

and

$$8\pi G_U \frac{3}{2} \rho_U = 3H_U^2 \quad (2.11.49)$$

$$\frac{8\pi G_U}{c^2} \frac{3}{2} \frac{m_t c^2}{cavity} = -\frac{2(BH_U^2)}{B} - \frac{(BH_U)^2}{B^2} - \frac{kc^2}{B^2} + \Lambda \quad (2.11.50)$$

and

$$\frac{8\pi G_U}{c^2} \frac{3}{2} \frac{m_t c^2}{cavity} = -3H_U^2 \quad (2.11.51)$$

but what is the G and H and ρ_U proper scaling? Equation 2.11.37 and 2.11.38 reduces to several expressions of this ρ_U scaling within the context of redshift 'z' with a special note to the 2/8 factor versus 3/8 factor indicating a result applicable to only 2/3 (or *chain/cavity* volume ratio) of tessellated 3D space assumed to be dark energy. The remaining 1/3 of tessellated space is assumed to be related to dark matter.

$$\rho_U (1+z)^3 = \frac{2}{8\pi} \frac{\left(H_U (1+z)^3\right)^2}{G_U (1+z)^3} \quad (2.11.52)$$

$$\rho_U (1+z)^3 = \frac{2}{8\pi} \frac{\left(H_{UG} (1+z)^{\frac{3}{2}}\right)^2}{G (1+z)^0} \quad (2.11.53)$$

$$\rho_U (1+z)^3 = \frac{m_t (1+z)^0}{cavity (1+z)^{-3}} \quad (2.11.54)$$

$$\rho_U (1+z)^3 = \frac{3}{4\pi} \frac{M_U (1+z)^{-6}}{\left(R_U (1+z)^{-3}\right)^3} = \frac{M_U (1+z)^{-6}}{V_U (1+z)^{-9}} \quad (2.11.55)$$

$$\rho_U (1+z)^3 = \frac{c}{\pi^2 \left(\hbar (1+z)^0\right)^2} H_U (1+z)^3 \left(m_t (1+z)^0\right)^3 \quad (2.11.56)$$

As the 'z+1' redshift factors indicate with their zero summation exponents, G_U approaches G at the present time from larger values at the Big Bang

and H_{UG} approaches H_U at the present time from smaller values at the Big Bang

and $1/H_{UG} = 1/H_U = 13.7$ billion years at the present time

and m_t represents a constant mass 1.003E-25 gram over all time contained in each cavity ($\sim 15,000$ cm 3 at present) tessellating volume R^3 in accordance with the CPT theory

and each *cavity* having a conservation of energy and momentum 'elastic' property and the universe mass M_U increasing from the Big Bang and the universe density ρ_U is equated to these changing conditions.

Within these scaling conditions, the university density ρ_U scaling condition 2.11.52 and 2.11.45.

$$\rho_U (1+z)^3 = \frac{2}{8\pi} \frac{\left(H_{UG} (1+z)^{\frac{3}{2}}\right)^2}{G (1+z)^0} \quad (2.11.57)$$

represents Big Bang modeling with constant Newtonian G as conventionally modeled represents the universe 'dark energy'. This is confirmed by the conventional CMBR temperature T_b universe first light representation at $z = 1100$:

$$T_b (1+z) = 3000K \text{ at } \frac{1}{H_{UG} (1+z)^{\frac{3}{2}}} = 376,000 \text{ years}$$

The universe expands R_U at the speed of light c while tessellating with *cavities* from within.

$$R_U (1+z)^{-3} = \frac{\sqrt{3}c}{H_U (1+z)^3} \quad (2.11.58)$$

$$cavity (1+z)^{-3} = \frac{4\pi}{3} \frac{m_t (1+z)^0 \left(R_U (1+z)^{-3}\right)^3}{M_U (1+z)^{-6}} \quad (2.11.59)$$

with a universal Machian mass M_U and Schwarzschild radius R_U type gravitational energy with respect to all test masses m .

$$mc^2 = G_U (1+z)^3 \frac{m M_U (1+z)^{-6}}{R_U (1+z)^{-3}} \quad (2.11.60)$$

with energy hH_U related to nuclear dimensions.

$$h (1+z)^0 H_U (1+z)^3 = G_U (1+z)^3 \frac{\left(m_t (1+z)^0\right)^2}{nuclear radius (1+z)^0} \quad (2.11.61)$$

with the constant mass m_t (considered to be the Weinberg mass[99]) related to ρ_U and H_U (density condition 2.11.44)

$$\left(m_t(1+z)^0\right)^3 = \frac{\pi^2 \left(\hbar(1+z)^0\right)^2}{c} \frac{\rho_u(1+z)^3}{H_u(1+z)^3} \quad (2.11.62)$$

and $\frac{M_u(1+z)^{-6}}{(R_u(1+z)^{-3})^2} = \text{constant}(.599704 \text{ g/cm}^3)$ (2.11.64)

indicating a continued universe synthesis. (no inflationary period required) and a decelerating expanding universe from *cavity* reference. But horizon R_u appears to be accelerating away from an observer immersed in the *cavity* tessellation.

$$\left(cavity(1+z)^{-3}\right)^{\frac{1}{3}} H_u(1+z)^3 = v(1+z)^2 \quad (2.11.65)$$

and all consistent with Einstein stress energy tensor :

$$G_{\mu\nu} = \frac{8\pi G_u}{c^4} T_{\mu\nu} \quad (2.11.66)$$

2.12 Superconducting Resonant Variance At T/Tc

Establish Gap and Critical Fields as a Function of T/T_c using Statistical Mechanics [19]

$$z_s = e^{\frac{-\hbar^2 K_B^2 \text{ chain}}{2m_t k_b T_c \text{ cavity}}} = e^{\frac{-2}{3}} \quad (2.12.1)$$

$$cavity = \frac{3\pi^3 \hbar^3}{6^{\frac{1}{2}} m_t^{\frac{3}{2}} \left(\frac{B}{A}\right)_t^{\frac{3}{2}} k_b^{\frac{3}{2}} T_c^{\frac{3}{2}}} \quad (2.12.2)$$

$$z_t = \frac{(2\pi m_t k_b T_c)^{\frac{3}{2}} cavity}{8\pi^3 \hbar^3} \approx \left(\frac{T}{T_c}\right)^{\frac{3}{2}} \quad (2.12.3)$$

$$k_t = \frac{z_t}{z_s} e^{\frac{k_b T_c}{k_b T}} = \left(\frac{T}{T_c}\right)^{\frac{3}{2}} e^{\frac{2}{3}} e^{-\frac{T_c}{T}} = \left(\frac{T}{T_c}\right)^{\frac{3}{2}} e^{\left(\frac{2}{3} - \frac{T_c}{T}\right)} \quad (2.12.4)$$

$$k_s = \frac{2}{3} - k_t = \frac{\text{chain}}{\text{cavity}} - k_t \quad (2.12.5)$$

$$\Delta_T = 1 - \frac{1}{3} \frac{T}{T_c} \frac{1}{\ln\left(\frac{1}{k_t}\right)} = 1 + \frac{1}{3} \frac{T}{T_c} \frac{1}{\ln(k_t)} \quad (2.12.6)$$

$$H_{T1}^2 = H_o^2 \left[1 - \frac{2}{3} \pi^2 \left(\frac{T}{\pi e^{-Euler} T_c} \right)^2 \right] \text{ at } \frac{T}{T_c} \sim 0 \quad (2.12.7)$$

$$H_{T2}^2 = H_o^2 k_s \quad \text{at} \quad \frac{T}{T_c} \text{ near } 1 \quad (2.12.8)$$

$$AvgH_{cT}^2 = \left[\text{if } H_{cT1}^2 > H_{cT2}^2 \text{ then } H_{cT1}^2 \text{ else } H_{cT2}^2 \right] \quad (2.12.9)$$

2.13 Superconductor Resonant Energy Content

Table 2.13.1 presents predictions of superconductivity energy content in various units that may be useful in anticipating the uses of these materials.

Table 2.13.1 Trisine Resonant Energy/Volume ($m_t c^2 / cavity$)

Condition	1.2	1.3	1.6	1.9	1.10	1.11
$T_a(^0 K)$	6.53E+11	6.53E+11	6.53E+11	6.53E+11	6.53E+11	6.53E+11
$T_b(^0 K)$	9.05E+14	5.48E+13	9.22E+08	1.10E+07	2,868	2.723
$T_{br}(^0 K)$	3.30E+12	5.45E+13	3.24E+18	2.72E+20	1.04E+24	1.10E+27
$T_c(^0 K)$	8.96E+13	3.28E+11	93.0	0.0131	8.99E-10	8.10E-16
$T_{cr}(^0 K)$	1.19E+09	3.25E+11	1.15E+21	8.11E+24	1.19E+32	1.32E+38
$z_R + 1$	3.67E+43	8.14E+39	3.89E+25	6.53E+19	1.17E+09	1.00E+00
$z_B + 1$	3.32E+14	2.01E+13	3.39E+08	4.03E+06	1.05E+03	1.00E+00
$Age_{UG}(\text{sec})$	7.14E-05	4.79E-03	6.94E+04	5.36E+07	1.27E+13	4.33E+17
$Age_{UGV}(\text{sec})$	4.59E-10	1.25E-07	4.42E+02	3.13E+06	1.22E+13	4.33E+17
$Age_v(\text{sec})$	1.18E-26	5.31E-23	1.11E-08	6.63E-03	3.70E+08	4.33E+17
erg/cm ³	2.10E+35	4.66E+31	2.23E+17	3.74E+11	6.69E+00	5.73E-09
joule/liter	2.10E+31	4.66E+27	2.23E+13	3.74E+07	6.69E-04	5.73E-13
BTU/ft ³	5.65E+29	1.25E+26	5.97E+11	1.00E+06	1.80E-05	1.54E-14
kwhr/ft ³	1.65E+26	3.67E+22	1.75E+08	2.94E+02	5.26E-09	4.50E-18
hp-hr/gallon	2.97E+25	6.57E+21	3.14E+07	5.27E+01	9.43E-10	8.07E-19
gasoline equivalent	5.66E+23	1.25E+20	5.98E+05	1.00E+00	1.80E-11	1.54E-20

Table 2.13.2 represents energy level of trisine energy states and would be key indicators material superconductor characteristics at a particular critical temperature. The BCS gap is presented as a reference energy.

Table 2.13.2 The energies (erg) and momenta (g cm/sec) associated with trisine wave vectors are presented. These energies are computed by the equation $(\hbar^2/2m_t)K^2$ and momentum $(\hbar K)$. The BCS gap (erg) is computed by the equation $(\pi/\exp(Euler))(\hbar^2/2m_t)K_B^2$.

Condition	1.2	1.3	1.6	1.9	1.10	1.11
$T_a(^0 K)$	6.53E+11	6.53E+11	6.53E+11	6.53E+11	6.53E+11	6.53E+11
$T_b(^0 K)$	9.05E+14	5.48E+13	9.22E+08	1.10E+07	2,868	2.723
$T_{br}(^0 K)$	3.30E+12	5.45E+13	3.24E+18	2.72E+20	1.04E+24	1.10E+27

$T_c ({}^0 K)$	8.96E+13	3.28E+11	93.0	0.0131	8.99E-10	8.10E-16	K_{Dnr}^2	1.97E-07	5.38E-05	1.90E+05	1.34E+09	1.96E+16	2.18E+22
$T_{cr} ({}^0 K)$	1.19E+09	3.25E+11	1.15E+21	8.11E+24	1.19E+32	1.32E+38	K_{Pr}^2	2.19E-07	5.98E-05	2.11E+05	1.49E+09	2.18E+16	2.42E+22
$z_R + 1$	3.67E+43	8.14E+39	3.89E+25	6.53E+19	1.17E+09	1.00E+00	K_{BCSr}^2	2.90E-07	7.91E-05	2.79E+05	1.98E+09	2.89E+16	3.20E+22
$z_B + 1$	3.32E+14	2.01E+13	3.39E+08	4.03E+06	1.05E+03	1.00E+00	$K_{Dsr}^2 - K_{Dnr}^2$	3.15E-07	8.59E-05	3.03E+05	2.15E+09	3.13E+16	3.48E+22
$Age_{UG} (sec)$	7.14E-05	4.79E-03	6.94E+04	5.36E+07	1.27E+13	4.33E+17	$K_{Cr}^2 - K_{Br}^2$	3.87E-07	1.06E-04	3.72E+05	2.64E+09	3.85E+16	4.27E+22
$Age_{UGv} (sec)$	4.59E-10	1.25E-07	4.42E+02	3.13E+06	1.22E+13	4.33E+17	$K_{Dnr}^2 + K_{Pr}^2$	4.16E-07	1.14E-04	4.01E+05	2.84E+09	4.14E+16	4.60E+22
$Age_U (sec)$	1.18E-26	5.31E-23	1.11E-08	6.63E-03	3.70E+08	4.33E+17	K_{Dsr}^2	5.11E-07	1.40E-04	4.93E+05	3.49E+09	5.10E+16	5.65E+22
K_B^2	1.24E-02	4.53E-05	1.28E-14	1.81E-18	1.24E-25	1.12E-31	K_{Cr}^2	5.51E-07	1.50E-04	5.31E+05	3.76E+09	5.49E+16	6.09E+22
K_{Dn}^2	1.48E-02	5.43E-05	1.54E-14	2.17E-18	1.49E-25	1.34E-31	$K_{Dsr}^2 + K_{Br}^2$	6.76E-07	1.85E-04	6.51E+05	4.61E+09	6.73E+16	7.47E+22
K_P^2	1.65E-02	6.04E-05	1.71E-14	2.42E-18	1.66E-25	1.49E-31	$K_{Dsr}^2 + K_{Dnr}^2$	7.08E-07	1.93E-04	6.82E+05	4.83E+09	7.06E+16	7.83E+22
K_{BCS}^2	2.18E-02	7.99E-05	2.26E-14	3.20E-18	2.19E-25	1.97E-31	$K_{Br}^2 + K_{Cr}^2$	7.15E-07	1.95E-04	6.89E+05	4.88E+09	7.13E+16	7.91E+22
$K_{Ds}^2 - K_{Dn}^2$	2.37E-02	8.67E-05	2.46E-14	3.47E-18	2.38E-25	2.14E-31	$K_{Dsr}^2 + K_{Pr}^2$	7.31E-07	2.00E-04	7.04E+05	4.98E+09	7.28E+16	8.07E+22
$K_C^2 - K_B^2$	2.91E-02	1.07E-04	3.02E-14	4.27E-18	2.92E-25	2.63E-31	$K_{Dnr}^2 + K_{Cr}^2$	7.48E-07	2.04E-04	7.20E+05	5.10E+09	7.45E+16	8.27E+22
$K_{Dn}^2 + K_P^2$	3.13E-02	1.15E-04	3.25E-14	4.59E-18	3.14E-25	2.83E-31	$K_{Dsr}^2 + K_{Cr}^2$	1.06E-06	2.90E-04	1.02E+06	7.25E+09	1.06E+17	1.17E+23
K_{Ds}^2	3.85E-02	1.41E-04	4.00E-14	5.65E-18	3.87E-25	3.48E-31	K_{Ar}^2	3.72E-06	1.02E-03	3.58E+06	2.54E+10	3.71E+17	4.11E+23
K_C^2	4.15E-02	1.52E-04	4.31E-14	6.08E-18	4.16E-25	3.75E-31	K_{Br}^2	1.82E-16	3.00E-15	1.78E-10	1.50E-08	5.73E-05	6.04E-02
$K_{Ds}^2 + K_B^2$	5.09E-02	1.86E-04	5.28E-14	7.46E-18	5.11E-25	4.60E-31	K_{Dnr}^2	1.99E-16	3.28E-15	1.95E-10	1.64E-08	6.27E-05	6.61E-02
$K_{Ds}^2 + K_{Dn}^2$	5.33E-02	1.95E-04	5.54E-14	7.82E-18	5.35E-25	4.82E-31	K_{Pr}^2	2.10E-16	3.46E-15	2.06E-10	1.73E-08	6.62E-05	6.97E-02
$K_B^2 + K_C^2$	5.39E-02	1.97E-04	5.59E-14	7.90E-18	5.41E-25	4.87E-31	K_{BCSr}^2	2.41E-16	3.98E-15	2.37E-10	1.99E-08	7.61E-05	8.02E-02
$K_{Ds}^2 + K_P^2$	5.50E-02	2.01E-04	5.71E-14	8.07E-18	5.52E-25	4.98E-31	$K_{Dsr}^2 - K_{Dnr}^2$	1.22E-16	2.01E-15	1.19E-10	1.00E-08	3.84E-05	4.04E-02
$K_{Dn}^2 + K_C^2$	5.63E-02	2.06E-04	5.85E-14	8.26E-18	5.65E-25	5.09E-31	$K_{Cr}^2 - K_{Br}^2$	1.51E-16	2.49E-15	1.48E-10	1.25E-08	4.76E-05	5.02E-02
$K_{Ds}^2 + K_C^2$	8.00E-02	2.93E-04	8.30E-14	1.17E-17	8.03E-25	7.24E-31	$K_{Dnr}^2 + K_{Pr}^2$	4.08E-16	6.75E-15	4.01E-10	3.37E-08	1.29E-04	1.36E-01
K_A^2	2.80E-01	1.03E-03	2.91E-13	4.11E-17	2.81E-24	2.53E-30	K_{Dsr}^2	3.20E-16	5.29E-15	3.14E-10	2.65E-08	1.01E-04	1.06E-01
K_B^2	4.98E-14	3.01E-15	5.08E-20	6.03E-22	1.58E-25	1.50E-28	K_{Cr}^2	3.32E-16	5.49E-15	3.26E-10	2.75E-08	1.05E-04	1.11E-01
K_{Dn}^2	5.45E-14	3.30E-15	5.56E-20	6.60E-22	1.73E-25	1.64E-28	$K_{Dsr}^2 + K_{Br}^2$	5.02E-16	8.29E-15	4.93E-10	4.14E-08	1.58E-04	1.67E-01
K_P^2	5.75E-14	3.48E-15	5.86E-20	6.96E-22	1.82E-25	1.73E-28	$K_{Dsr}^2 + K_{Dnr}^2$	5.19E-16	8.58E-15	5.09E-10	4.29E-08	1.64E-04	1.73E-01
K_{BCS}^2	6.62E-14	4.00E-15	6.74E-20	8.01E-22	2.10E-25	1.99E-28	$K_{Br}^2 + K_{Cr}^2$	5.14E-16	8.49E-15	5.04E-10	4.24E-08	1.62E-04	1.71E-01
$K_{Ds}^2 - K_{Dn}^2$	3.34E-14	2.02E-15	3.40E-20	4.04E-22	1.06E-25	1.00E-28	$K_{Dsr}^2 + K_{Pr}^2$	5.30E-16	8.76E-15	5.20E-10	4.38E-08	1.67E-04	1.76E-01
$K_C^2 - K_B^2$	4.14E-14	2.51E-15	4.22E-20	5.02E-22	1.31E-25	1.25E-28	$K_{Dnr}^2 + K_{Cr}^2$	5.31E-16	8.78E-15	5.21E-10	4.39E-08	1.68E-04	1.77E-01
$K_{Dn}^2 + K_P^2$	1.12E-13	6.78E-15	1.14E-19	1.36E-21	3.55E-25	3.37E-28	$K_{Dsr}^2 + K_{Cr}^2$	6.53E-16	1.08E-14	6.41E-10	5.39E-08	2.06E-04	2.17E-01
K_{Ds}^2	8.79E-14	5.32E-15	8.96E-20	1.06E-21	2.78E-25	2.64E-28	K_{Ar}^2	8.64E-16	1.43E-14	8.48E-10	7.13E-08	2.73E-04	2.87E-01
K_C	9.12E-14	5.52E-15	9.30E-20	1.10E-21	2.89E-25	2.74E-28							
$K_{Ds}^2 + K_B^2$	1.38E-13	8.33E-15	1.40E-19	1.67E-21	4.36E-25	4.14E-28							
$K_{Ds}^2 + K_{Dn}^2$	1.42E-13	8.62E-15	1.45E-19	1.72E-21	4.51E-25	4.28E-28							
$K_B^2 + K_C^2$	1.41E-13	8.53E-15	1.44E-19	1.71E-21	4.47E-25	4.24E-28							
$K_{Ds}^2 + K_P^2$	1.45E-13	8.80E-15	1.48E-19	1.76E-21	4.61E-25	4.37E-28							
$K_{Dn}^2 + K_C^2$	1.46E-13	8.82E-15	1.49E-19	1.76E-21	4.62E-25	4.38E-28							
$K_{Ds}^2 + K_C^2$	1.79E-13	1.08E-14	1.83E-19	2.17E-21	5.67E-25	5.39E-28							
K_A	2.37E-13	1.43E-14	2.41E-19	2.87E-21	7.51E-25	7.13E-28							
K_{Br}^2	1.64E-07	4.49E-05	1.58E+05	1.12E+09	1.64E+16	1.82E+22							

2.14 Superconductor Resonant Gravitational Energy

As per reference[25], a spinning nonaxisymmetric object rotating about its minor axis with angular velocity ω will radiate gravitational energy in accordance with equation 2.14.1

$$\dot{E}_g = \frac{32G}{5c^5} I_3^2 \zeta^2 \omega^6 \quad (2.14.1)$$

2.14 Superconductor Resonant Gravitational Energy

As per reference[25], a spinning nonaxisymmetric object rotating about its minor axis with angular velocity ω will radiate gravitational energy in accordance with equation 2.14.1

$$\dot{E}_g = \frac{32G}{5c^5} I_3^2 \zeta^2 \omega^6 \quad (2.14.1)$$

This expression has been derived based on weak field theory assuming that the object has three principal moments of inertia I_1, I_2, I_3 , respectively, about three principal axes $a > b > c$ and ξ is the ellipticity in the equatorial plane.

$$\xi = \frac{a-b}{\sqrt{ab}} \quad (2.14.2)$$

Equations 2.14.1 with 2.14.2 were developed from first principles (based on a quadrapole configuration) for predicting gravitational energy emitted from pulsars [25], but we use them to calculate the gravitational energy emitted from rotating Cooper CPT Charge conjugated pairs with resonant trisine mass (m_t) in the trisine resonant superconducting mode.

Assuming the three primary trisine axes $C > B > A$ corresponding to $a > b > c$ in reference [25] as presented above, then the trisine ellipticity (or measure of trisine moment of inertia) would be:

$$\xi = \frac{C-B}{\sqrt{CB}} = \frac{\text{chain } A}{\text{cavity } B} = .2795 \quad (2.14.3)$$

Assuming a mass (m_t) rotating around a nonaxisymmetric axis of resonant radius B to establish moment of inertia (I_3) then equation 2.14.1 becomes a resonant gravitational radiation emitter with no net energy emission outside of resonant *cavity*:

$$\frac{E_g}{\text{time}_\pm} = \frac{32G_U}{5} \frac{(\xi)^2 (m_t B^2)^2}{v_{dx}^5} \left(\frac{2}{\text{time}_\pm} \right)^6 \quad (2.14.4)$$

where angular velocity $\omega = 2/\text{time}_\pm$, and replacing the speed of light (c) with resonant consequential sub- and superluminal de Broglie speed of light (v_{dx}), then equation 2.14.4 in terms of dimension 'B' becomes the Newtonian gravitational energy relationship in equation 2.14.5:

$$E_g = -G_U \frac{m_t^2}{B} = -G_U \frac{m_t^2}{3\sqrt{3}B_{\text{proton}} k_m g_s} \quad (2.14.5)$$

Note the general characteristic length B related to the extended proton length. All this is consistent with the Virial Theorem.

Gravitational Potential Energy/2 = Kinetic Energy

$$\frac{1}{2} G_U m_t^2 \frac{3}{\Delta x + \Delta y + \Delta z} = \frac{1}{2} m_r v_{dx}^2 \quad (2.14.6)$$

and

$$hH_U = \frac{\text{cavity}}{\text{chain}} G_U \frac{m_t^2}{B_p} \quad (2.14.7)$$

Equation 2.14.7 provides a mechanism explaining the CERN (July 4, 2012) observed Higgs particle) at 126.5 GeV as well as the astrophysical Fermi ~ 130 GeV [127]. The astrophysical ~ 130 GeV energy is sourced to a Trisine Condition 1.2 nucleosynthetic event with a fundamental G_U gravity component.

$$g_s \frac{3}{4} \cos(\theta) G_U m_t^2 \frac{1}{\text{proton radius}} = 125.27 \text{ GeV} \quad (2.14.8)$$

$$g_s \frac{3}{4} \cos(\theta) G_U m_t^2 \frac{2 \sin(\theta)}{B_p} = 125.27 \text{ GeV} \quad (2.14.9)$$

$$g_s \frac{3}{2} \sin(\theta) \cos(\theta) G_U m_t^2 \frac{1}{B_p} = 125.27 \text{ GeV}$$

falling within the measured range

$$125.36 \pm 0.37 \text{ (statistical uncertainty)} \quad (2.14.10)$$

$$\pm 0.18 \text{ (systematic uncertainty)}$$

$$125.36 \pm 0.41 \text{ GeV} [149]$$

The Equation 2.14.7a is of the same form as 2.14.5 and in conjunction with equation 2.11.13 implies the following nuclear condition:

$$\hbar K_B \Big|_{\substack{T_c=8.95E13 \\ T_b=9.07E14}} = 8\pi \frac{\text{chain}}{\text{cavity}} m_t c \quad (2.14.11)$$

also:

$$\left\{ \frac{1}{2\epsilon_x k_m} m_t v_{dx}^2 \right. \\ \left. \frac{\text{chain}}{\text{cavity}} \frac{1}{2\epsilon_x k_m} \frac{1}{\epsilon} \frac{e^2}{B_{\text{CMBR}}} \right\}_{\substack{T_c=8.11E-16 \\ T_b=2.729}} = \frac{1}{2} m_r v_{dx}^2 \Big|_{\substack{T_c=8.11E-16 \\ T_b=2.729}}$$

$$\text{where: } 2\epsilon_x k_m = \frac{2c^2}{v_{dx}^2} \Big|_{\substack{T_c=8.11E-16 \\ T_b=2.729}} \quad (2.14.12)$$

Where m_t and m_r are related as in Equation 2.1.25 and $\Delta x, \Delta y, \Delta z$ are Heisenberg Uncertainties as expressed in equation 2.1.20.

In the case of a superconductor, the radius R is the radius of

curvature for pseudo particles described in this report as the variable B. All of the superconductor pseudo particles move in asymmetric unison, making this virial equation applicable to this particular engineered superconducting situation. This is consistent with Misner Gravitation [35] page 978 where it is indicated that gravitational power output is related to “power flowing from one side of a system to the other” carefully incorporating “only those internal power flows with a time-changing quadrupole moment”. The assumption in this report is that a super current flowing through a trisine superconducting CPT lattice has the appropriate quadrupole moment at the dimensional level of B. The key maybe a linear back and forth resonant trisine system. Circular superconducting systems such as represented by Gravity Probe B gyroscopic elements indicate the non gravitational radiation characteristic of such circular systems reinforcing the null results of mechanical gyroscopes [21, 22, 23]. The density ($m_t/cavity$) (7.96E-06 g/cm³) associated with niobium super mass currents at $T_c = 9.4$ K are subject to tidal oscillations(Appendix H) imposed by the universe dark energy at $T_c = 8.11E-16$ K with its characteristic frequency of 3.38E-5 Hz (table 2.4.1) may fundamentally and harmonically contribute to observed gyro asymptotic polhode frequency anomalies associated with Gravity Probe B (see condition 1.8) (Alex Silbergleit, John Conklin, Stanford University[94]).

Table 2.14.1 Gravity Probe B Asymptotic Gyros' Polhode Frequencies (as harmonics of present universe dark energy)

	Asymptotic Polhode Period (hours)	Asymptotic Polhode Frequency (Hz)	Asymptotic Polhode Harmonic	Asymptotic Polhode Harmonic Deviation
Gyro 1	0.867	3.20E-04	9	1.05
Gryo 3	1.529	1.82E-04	5	1.08
Gyro 2	2.581	1.08E-04	3	1.06
Gyro 4	4.137	6.71E-05	2	0.99
Universe	8.22	3.38E-05	1	1.00

2.15 Black Body Relationships[18]

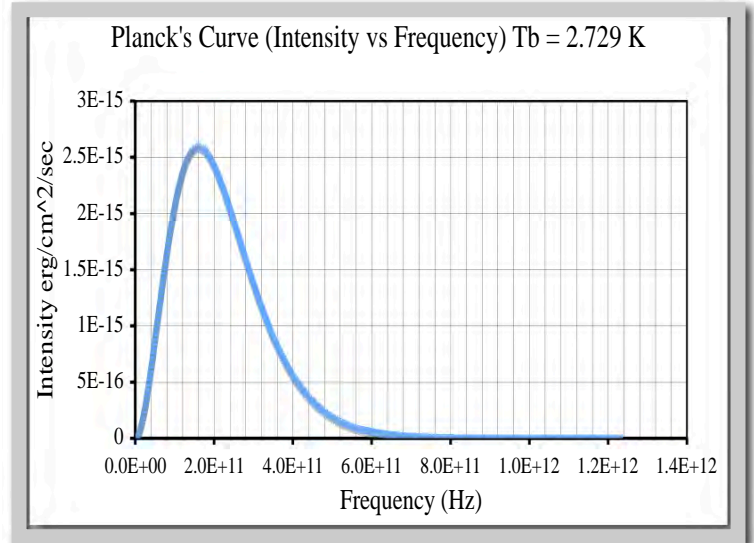
There are many unique characteristics if the Planck Black Body curve as it was introduced over 100 years ago that have been used in Universe evolutionary processes.

The number 'N' of possible frequencies in box of edge 'l' in the range ν to $\nu + d\nu$ (The '2' accounts for both oscillating electric and magnetic fields) [19 page 468]:

$$2dN = \frac{2 \cdot 4\pi l^3 \nu^2}{c^3} d\nu \quad (2.15.1)$$

Therefore:

$$2N = \frac{2 \cdot 4 \pi \nu^3}{3} l^3 \quad (2.15.2)$$



The energy ($2U$) of a system consisting of N oscillators of frequency (ν):

$$2U = \frac{2h\nu}{e^{h\nu/k_b T_b} - 1} \quad (2.15.3)$$

The energy (U) of a system consisting of N oscillators of frequency (ν):

$$\begin{aligned} 2UdN &= \frac{2h\nu 2dN}{e^{h\nu/k_b T_b} - 1} \\ &= \frac{2h\nu}{e^{h\nu/k_b T_b} - 1} \frac{2 \cdot 4\pi l^3 \nu^2}{c^3} d\nu \\ &= \frac{2h\nu^3}{e^{h\nu/k_b T_b} - 1} \frac{2 \cdot 4\pi l^3}{c^3} d\nu \end{aligned} \quad (2.15.4)$$

Or by rearranging in terms of energy density (ρ_ν)

$$2\rho_\nu d\nu = \frac{2h\nu^3}{e^{h\nu/k_b T_b} - 1} \frac{2 \cdot 4\pi}{c^3} d\nu \quad (2.15.5)$$

The energy volume density (ρ_ν) related to the surface emissivity (K_ν) which is the ratio of radiation emission (E_ν) over radiation absorption coefficient (A_ν) (The absorption coefficient (A_ν) is assumed to be 1).

$$2\rho_\nu = \frac{2 \cdot 8\pi K_\nu}{c} = \frac{2 \cdot 8\pi E_\nu}{c} \quad (2.15.6)$$

$$\frac{2 \cdot 8\pi K_v}{c} dv = \frac{2h\nu^3}{e^{h\nu/k_b T_b} - 1} \frac{2 \cdot 4\pi}{c^3} dv$$

or

$$\frac{2 \cdot 8\pi E_v}{c} dv = \frac{2h\nu^3}{e^{h\nu/k_b T_b} - 1} \frac{2 \cdot 4\pi}{c^3} dv \quad (2.15.7)$$

And by rearranging:

$$2E_v dv = \frac{2}{c^2} \frac{h\nu^3}{e^{h\nu/k_b T_b} - 1} dv \quad (2.15.8)$$

The total radiation ($2E_v$) is obtained by integrating over all frequencies (ν)

$$2 \int_0^{\infty} E_v dv = \frac{2h}{c^2} \int_0^{\infty} \frac{\nu^3}{e^{h\nu/k_b T_b} - 1} dv \quad (2.15.9)$$

The black body energy emission ($2E_v$ or energy/area/time) is:

$$2E_v = \frac{2\pi^4 k_b^4}{15c^2 h^3} T_b^4$$

$$= \sigma_s T_b^4 \quad (2.15.10)$$

$$2E_{vr} = \frac{2\pi^4 k_b^4}{15c^2 h^3} T_{br}^4$$

$$= \sigma_s T_{br}^4 \quad (2.15.10r)$$

This black body radiation emission is through a solid angle and conversion to the total energy radiated from one side of a plane then $\sigma_s = \pi \sigma_s'$.

The black body energy density ($\rho_{BBenergy}$ or energy/volume) is:

$$\rho_{BBenergy} = \sigma_s T_b^4 \frac{4}{c} \quad (2.15.11)$$

$$\rho_{BBenergy} = \sigma_s T_{br}^4 \frac{4}{c} \quad (2.15.11r)$$

The black body mass density (ρ_{BBmass} or mass/volume) is:

$$\rho_{BBmass} = \sigma_s T_b^4 \frac{4}{c^3} \quad (2.15.12)$$

$$\rho_{BBmass} = \sigma_s T_{br}^4 \frac{4}{c^3} \quad (2.15.12r)$$

The black body maximum wave length (λ_{BBmax}) is:

$$E_v dv = E_{\lambda_b} d\lambda_b$$

$$|dv| = \frac{c}{\lambda_b^2} |d\lambda_b|$$

$$2E_{\lambda_b} d\lambda_b = \frac{2hc^2}{\lambda_b^5} \frac{d\lambda_b}{e^{\frac{hc}{k_b T_b \lambda_b}} - 1}$$

$$x = \frac{ch}{\lambda_b k_b T_b} \quad \lambda_b = \frac{ch}{x k_b T_b} \quad (2.15.13)$$

Finding the differential peak:

$$\frac{dE_{\lambda_b}}{d\lambda_b} = \frac{10hc^2}{\lambda_b^6 \left(e^{\frac{hc}{k_b T_b \lambda_b}} - 1 \right)} - \frac{2h^2 c^3 e^{\frac{hc}{k_b T_b \lambda_b}}}{T_b \lambda_b^7 k_b \left(e^{\frac{hc}{k_b T_b \lambda_b}} - 1 \right)^2} = 0 \quad (2.15.14)$$

By reduction then

$$e^x (x - 5) + 5 = 0 \quad x = 4.965364560 \quad (2.15.15)$$

and

$$\lambda_{BBmax} = \frac{hc}{x k_b T_b} = \frac{hc}{4.96536456 k_b T_b} \quad (2.15.16)$$

$$\lambda_{BBmax} = \frac{hc}{x k_b T_{br}} = \frac{hc}{4.96536456 k_b T_{br}} \quad (2.15.16r)$$

BlackBody most probable energy factor based on maximum(peak) wavelength $hc/\lambda_{BBmax} = 4.965364560 k_b T_b$ and Wein displacement constant $= hc/(4.965364560 k_b) = 0.28977683 \text{ cm K}$

Differentiating 2.15.8 yields energy and frequency (ν) relationship.

$$\frac{dE_v}{d\nu} = \frac{6h\nu^2}{c^2 \left(e^{\frac{h\nu}{k_b T_b}} - 1 \right)} - \frac{2h^2 \nu^3 e^{\frac{h\nu}{k_b T_b}}}{T_b c^2 k_b \left(e^{\frac{h\nu}{k_b T_b}} - 1 \right)^2} = 0 \quad (2.15.17)$$

$$x = \frac{h\nu}{k_b T_b} \quad \nu = \frac{x k_b T_b}{h}$$

By reduction then:

$$e^x (x - 3) + 3 = 0 \quad x = 2.821439372 \quad (2.15.18)$$

Then

$$\nu_{BB\max} = \frac{2.821439372 k_b T_b}{h} \quad (2.15.19)$$

$$\nu_{BB_{br\max}} = \frac{2.821439372 k_b T_{br}}{h} \quad (2.15.19r)$$

BlackBody most probable energy factor based on maximum(peak) frequency $h\nu_{BB\max} = 2.821439372 k_b T_b$

The velocity computed by $\nu_{BB\max} \lambda_{BB\max} = 1.70E+10$ cm/sec is less than the speed of light (.568224012c). This is important consideration in performing black body energy momentum calculations.

Now for average photon number density (n)

$$nd\nu = \frac{8\pi\nu^2 d\nu}{c^3 \left(e^{\frac{h\nu}{k_b T_b}} - 1 \right)} \quad (2.15.20)$$

$$x = \frac{h\nu}{k_b T_b} \quad \nu = \frac{k_b T_b x}{h} \quad d\nu = \frac{k_b T_b dx}{h}$$

By change of variable and reduction then:

$$nd\nu = \frac{8\pi k_b^3 T_b^3 x^2 dx}{c^3 h^3 \left(e^{\frac{h\nu}{k_b T_b}} - 1 \right)} \quad (2.15.21)$$

$$\int_0^{\infty} \frac{x^2}{(e^x - 1)} = 2.404113806$$

Then

$$\int_0^{2.356763057} \frac{x^2}{(e^x - 1)} = \int_{2.356763057}^{\infty} \frac{x^2}{(e^x - 1)} \quad (2.15.22)$$

$$= \frac{2.404113806}{2} = 1.202056903$$

or

$$\rho_{BB\text{photon}} = n = 8\pi 2.404113806 \left(\frac{k_b T_b}{hc} \right)^3$$

$$\rho_{BB_{br\text{photon}}} = n = 8\pi 2.404113806 \left(\frac{k_b T_{br}}{hc} \right)^3 \quad (2.15.22r)$$

This means that half of photons (median photon density) are below $x = 2.356763057$ and half above. By similar analysis, one quarter(1/4) of photons (median photon density) are below $x = 1.40001979$ and three quarters(3/4) above and three quarters(3/4) of photons (median photon density) are below $x = 3.63027042$ and one quarter(1/4) above.

$$\nu_{BB\text{photon}} = \frac{2.356763057 k_b T_b}{h} = \frac{\zeta(3) k_b T_b}{h} \quad (2.15.23)$$

$$\nu_{BB_{br\text{photon}}} = \frac{2.356763057 k_b T_{br}}{h} = \frac{\zeta(3) k_b T_{br}}{h} \quad (2.15.23r)$$

Now for average photon energy density:

$$\rho_{\nu} d\nu = \frac{8\pi\nu^3 d\nu}{c^3 \left(e^{\frac{h\nu}{k_b T_b}} - 1 \right)} \quad (2.15.25)$$

$$x = \frac{h\nu}{k_b T_b} \quad \nu = \frac{k_b T_b x}{h} \quad d\nu = \frac{k_b T_b dx}{h}$$

By change of variable and reduction then:

$$\rho_{\nu} d\nu = \frac{8\pi k_b^4 T_b^4 x^3 dx}{c^3 h^3 (e^x - 1)} \quad (2.15.26)$$

$$\int_0^{\infty} \frac{x^3 dx}{(e^x - 1)} = 6.493939402 = \frac{\pi^4}{15}$$

Then

$$\int_0^{3.503018826} \frac{x^3 dx}{(e^x - 1)} = \int_{3.503018826}^{\infty} \frac{x^3 dx}{(e^x - 1)} \quad (2.15.27)$$

$$= \frac{6.493939402}{2} = 3.246969701$$

This means that half of photons (average photon energy density) are below $x = 3.503018826$ and half above designating a characteristic black body frequency ($\nu_{BB\text{photon}} = c/\lambda_{BB\text{photon}}$).

$$\nu_{BB\text{photon}} = \frac{c}{\lambda_{BB\text{photon}}} = \frac{3.503018826 k_b T_b}{h} \quad (2.15.28)$$

Then combining equations 2.15.21 and 2.15.24 results in a photon mean energy density.

$$\frac{\rho_v}{n} = \frac{\frac{8\pi k_b^4 T_b^4}{c^3 h^3} 6.493939402}{\frac{8\pi k_b^3 T_b^3}{c^3 h^3} 2.404113806} \quad (2.15.29)$$

$$= 2.70117803 k_b T_b = \frac{\pi^4}{30 \zeta(3)} k_b T_b$$

$$\rho_U (1+z)^3 = \rho_v (1+z)^4 = 1.62 \text{E-17 g/cm}^3$$

$$T_b = 37,200 \text{ K} \quad z_B = 13,600 \quad Age_{UG} = 8,600 \text{ years}$$

The black body photons momentum ($p_{BBmomentum}$) is:

$$p_{BBmomentum} = \frac{h}{\lambda_{BBmax}} \quad (2.15.30)$$

The black body photons in the universe ($U \# photons$) is:

$$U \# photons = \frac{\rho_{BBenergy}}{hf_{BBmax}} V_U \quad (2.15.31)$$

$$U_r \# photons = \frac{\rho_{BBenergy}}{hf_{BBmax}} V_U \quad (2.15.31r)$$

The universe viscosity due to black body photons (μ_{BB}) is:

$$\mu_{BB} = \sigma_s T_b^4 \frac{4}{c^2} \lambda_{BBmax} \quad (2.15.32)$$

$$\mu_{BBr} = \sigma_s T_{br}^4 \frac{4}{c^2} \lambda_{BBmax} \quad (2.15.32r)$$

Table 2.15.1 Universe Black Body parameters

Condition	1.2	1.3	1.6	1.9	1.10	1.11
$T_a ({}^0 K)$	6.53E+11	6.53E+11	6.53E+11	6.53E+11	6.53E+11	6.53E+11
$T_b ({}^0 K)$	9.05E+14	5.48E+13	9.22E+08	1.10E+07	2,868	2.723
$T_{br} ({}^0 K)$	3.30E+12	5.45E+13	3.24E+18	2.72E+20	1.04E+24	1.10E+27
$T_c ({}^0 K)$	8.96E+13	3.28E+11	93.0	0.0131	8.99E-10	8.10E-16
$T_{cr} ({}^0 K)$	1.19E+09	3.25E+11	1.15E+21	8.11E+24	1.19E+32	1.32E+38
$z_R + 1$	3.67E+43	8.14E+39	3.89E+25	6.53E+19	1.17E+09	1.00E+00
$z_B + 1$	3.32E+14	2.01E+13	3.39E+08	4.03E+06	1.05E+03	1.00E+00
$Age_{UG} (\text{sec})$	7.14E-05	4.79E-03	6.94E+04	5.36E+07	1.27E+13	4.33E+17
$Age_{UGv} (\text{sec})$	4.59E-10	1.25E-07	4.42E+02	3.13E+06	1.22E+13	4.33E+17

$Age_U (\text{sec})$	1.18E-26	5.31E-23	1.11E-08	6.63E-03	3.70E+08	4.33E+17
$2E_v$	3.84E+55	5.15E+50	4.14E+31	8.26E+23	3.87E+09	3.14E-03
$\rho_{BBenergy}$	5.08E+45	6.81E+40	5.48E+21	1.09E+14	5.12E-01	4.16E-13
ρ_{BBmass}	5.65E+24	7.58E+19	6.09E+00	1.22E-07	5.70E-22	4.63E-34
λ_{BBmax}	3.20E-16	5.29E-15	3.14E-10	2.64E-08	1.01E-04	1.06E-01
ν_{BBmax}	5.32E+25	3.22E+24	5.42E+19	6.44E+17	1.69E+14	1.60E+11
$\rho_{BBphoton}$	1.51E+46	3.33E+42	1.59E+28	2.67E+22	4.79E+11	4.10E+02
p_{BB}	2.07E-11	1.25E-12	2.11E-17	2.51E-19	6.56E-23	6.23E-26
μ_{BB}	5.42E+19	1.20E+16	5.74E+01	9.63E-05	1.73E-15	1.48E-24
$U \# photons$	1.44E+01	2.93E+08	1.29E+37	4.57E+48	1.42E+70	1.95E+88
$2E_v$	6.72E+45	5.01E+50	6.23E+69	3.12E+77	6.67E+91	8.21E103
$\rho_{BBenergy}$	8.96E+35	6.69E+40	8.32E+59	4.17E+67	8.90E+81	1.10E+94
ρ_{BBmass}	9.97E+14	7.44E+19	9.25E+38	4.64E+46	9.90E+60	1.22E+73
λ_{BBmax}	8.78E-14	5.31E-15	8.95E-20	1.06E-21	2.78E-25	2.64E-28
ν_{BBmax}	1.94E+23	3.21E+24	1.90E+29	1.60E+31	6.12E+34	6.45E+37
$\rho_{BBphoton}$	7.29E+38	3.29E+42	6.89E+56	4.10E+62	2.29E+73	2.68E+82
p_{BB}	7.54E-14	1.25E-12	7.40E-08	6.23E-06	2.38E-02	2.51E+01
μ_{BB}	2.63E+12	1.19E+16	2.48E+30	1.48E+36	8.26E+46	9.65E+55
$U_r \# photons$	6.97E-07	2.89E+08	5.57E+65	7.01E+88	6.82E+131	1.27E168

Black body viscosity $1.49 \text{E-24 g/(cm sec)}$ is much lower than trisine viscosity $m_c/(2\Delta x^2)$ or $1.21 \text{E-16 g/(cm sec)}$ at present universe temperature of 8.11E-16 K . This indicates negligible drag of universe objects as measured in the Pioneer 10 and 11 anomaly and dark matter impacted galactic rotation curves.

2.16 Critical Optical Volume Energy (COVE) and Schwinger Pair Production.

This section considers the concept of critical volume, which would be analogous to critical mass in atomic fission and in the context of the Lawson Criterion. The critical volume would establish a parameter beyond which the output energy would exceed the input energy. It is anticipated that this energy would have a benign character and not be usable in explosive applications. The basic principle is that a coherent beam length is not related to input power creating that beam while virtual particle generation (in accordance with the CPT theorem and Schwinger limit) is a function of length. Given that volume is length cubed, then there must be a critical volume at which the energy of created virtual particles exceeds the input power to the volume. The following is a derivation of this concept.

$$\begin{aligned}
\text{Poynting Vector}(S_{\text{Input}}) &= c \left(\frac{1}{2} \right) \left(\frac{\hbar \omega}{\text{cavity}} \right) \\
&= c \left(\frac{1}{2} \right) \left(\frac{h}{\text{cavity}} \frac{1}{\text{time}_\pm} \right) \\
&= c \left(\frac{1}{2} \right) \left(\frac{h}{\text{cavity}} \frac{v_{dx}}{2B} \right)
\end{aligned} \tag{2.16.1}$$

Now consider the potential out put power per trisine cell which is consistent with Larmor radiation of accelerated virtual particles and associated Schwinger virtual pair production within that cell and its resonant time_\pm .

$$\text{Poynting Vector}(S_{\text{Output}}) = v_{dx} \left(\frac{1}{2} \right) \left(\frac{m_t v_{dx}^2}{\text{cavity}} \right) \tag{2.16.2}$$

Now calculate trisine length for output power to balance input power.

$$\text{Length} = 2B \frac{S_{\text{Input}}}{S_{\text{Output}}} = 2B \frac{c}{v_{dx}} = 2B^2 \frac{m_t c}{\hbar \pi} = c \text{ time}_\pm \tag{2.16.3}$$

The critical volume is then:

$$\text{Critical Volume} = \text{Length}^3 = c^3 \text{time}_\pm^3 \tag{2.16.4}$$

The critical area is then:

$$\text{Critical Area} = \text{Length}^2 \tag{2.16.5}$$

Then the power requirement at criticality is:

$$\begin{aligned}
\text{Power} &= S_{\text{Input}} \text{Length}^2 = S_{\text{Output}} \frac{\text{Length}}{2B} \text{Length}^2 \\
&= \frac{1}{2} h \frac{\text{time}_\pm}{\text{cavity}} c^3
\end{aligned} \tag{2.16.6}$$

The Optical Volume incident wavelength, frequency and trisine B are:

$$\begin{aligned}
\text{Incident wavelength} &= 2c \text{ time} \\
\text{Incident frequency} &= \frac{1}{2 \text{ time}} \\
B &= \left(\frac{\hbar \pi \text{ time}}{2m_t} \right)^{1/2}
\end{aligned} \tag{2.16.6a}$$

It is envisioned that this length would be a measure of trisine lattice size necessary for criticality and in particular a defined Critical Optical Volume defined at the of intersection of three lengths. To retrieve the power, one side (+ or -) of the virtual pair would have to be pinned (perhaps optically). In this case power could be retrieved by electrically coupling lattice to a pick up coil or arranging to intercept 56 MeV radiation.

This all appears consistent with Schwinger pair production [83] per volume and area (as well as length B) and frequency (1/time) as expressed as follows as derived and verified with equations 2.16.7 - 2.16.11 with particular note to correlation with Stefan's law as express in equation 2.16.9 with a special note that $\hbar(h/2\pi)$ or $m_t(2B)^2/(2\pi \text{ time}_\pm)$:

$$\frac{\text{chain } Ee^2}{\text{cavity } DB} = \frac{\text{chain}}{\text{cavity}} \frac{\sqrt{3}BeE}{\mathbb{C}\pi \cos(\theta)} = \frac{\pi g_s \hbar}{\text{time}_\pm} \tag{2.16.7}$$

$$\begin{aligned}
\Gamma_{BP} &= \frac{1 \text{ pair } (\mathbb{C})}{B \text{ time}_\pm} \\
&= \frac{4\sqrt{3}}{3} \left(\frac{eE}{g_s \mathbb{C} 2\pi^2 \hbar \cos(\theta)} \right) \gamma
\end{aligned} \tag{2.16.8}$$

$$\begin{aligned}
\Gamma_{AP} &= \frac{1 \text{ pair } (\mathbb{C})}{\text{section time}_\pm} \\
&= \frac{4\sqrt{2} 3^{3/4}}{9} \left(\frac{eE}{g_s \mathbb{C} 2\pi^2 \hbar \cos(\theta)} \right)^{3/2} \frac{\gamma}{v_{dx}^{1/2}}
\end{aligned} \tag{2.16.9a}$$

$$\begin{aligned}
\Gamma_{AP} &= \frac{1}{2} \frac{1}{(B/A)_t} \frac{1}{k_b T_c} \text{Poynting Vector} \\
&= \frac{1}{\cos(\theta)} \frac{1}{(B/A)_t} \frac{c^2}{m_t v_{dx}^4} \sigma_s T_c^4
\end{aligned} \tag{2.16.9b}$$

$$\begin{aligned}\Gamma_{VP} &= \frac{1 \text{ pair}(\mathbb{C})}{\text{cavity time}_\pm} \\ &= \frac{16\sqrt{3}}{9} \left(\frac{B}{A}\right)_i \left(\frac{eE}{g_s \mathbb{C} 2\pi^2 \hbar \cos(\theta)}\right)^2 \frac{\gamma}{v_{dx}}\end{aligned}\quad (2.16.10)$$

And where summation is cutoff at $n = 1$ for volume $(1/n^2)$, area $(1/n^{3/2})$ and linear $(1/n)$:

$$\begin{aligned}\phi &= \frac{1}{n^2} \exp\left(\frac{-n\pi m_e^2 v_{dx}^3}{eE\hbar}\right) \\ \phi &= \frac{1}{n^{3/2}} \exp\left(\frac{-n\pi m_e^2 v_{dx}^3}{eE\hbar}\right) \\ \phi &= \frac{1}{n} \exp\left(\frac{-n\pi m_e^2 v_{dx}^3}{eE\hbar}\right)\end{aligned}\quad (2.16.11)$$

$$\gamma = \sum_{n=1}^{\infty} \phi = 0.9997 \quad \gamma = \sum_{n=1}^{\infty} \phi = 2.5493$$

Table 2.16.1 Schrödinger Virtual Pair Production per Trisine unit Length (B), per Area (section) and per Volume (cavity)

Condition	1.2	1.3	1.6	1.9	1.10	1.11
$T_a ({}^0 K)$	6.53E+11	6.53E+11	6.53E+11	6.53E+11	6.53E+11	6.53E+11
$T_b ({}^0 K)$	9.05E+14	5.48E+13	9.22E+08	1.10E+07	2,868	2.723
$T_{br} ({}^0 K)$	3.30E+12	5.45E+13	3.24E+18	2.72E+20	1.04E+24	1.10E+27
$T_c ({}^0 K)$	8.96E+13	3.28E+11	93.0	0.0131	8.99E-10	8.10E-16
$T_{cr} ({}^0 K)$	1.19E+09	3.25E+11	1.15E+21	8.11E+24	1.19E+32	1.32E+38
$z_R + 1$	3.67E+43	8.14E+39	3.89E+25	6.53E+19	1.17E+09	1.00E+00
$z_B + 1$	3.32E+14	2.01E+13	3.39E+08	4.03E+06	1.05E+03	1.00E+00
$Age_{UG} (\text{sec})$	7.14E-05	4.79E-03	6.94E+04	5.36E+07	1.27E+13	4.33E+17
$Age_{UGv} (\text{sec})$	4.59E-10	1.25E-07	4.42E+02	3.13E+06	1.22E+13	4.33E+17
$Age_U (\text{sec})$	1.18E-26	5.31E-23	1.11E-08	6.63E-03	3.70E+08	4.33E+17
E Field (V/cm)	2.79E+22	6.19E+18	2.96E+04	4.96E-02	8.89E-13	7.61E-22
$\Gamma_{BP} (\text{cm}^{-1}\text{sec}^{-1})$	5.61E+37	1.24E+34	5.93E+19	9.96E+13	1.78E+03	1.53E-06
$\Gamma_{AP} (\text{cm}^{-2}\text{sec}^{-1})$	2.43E+50	3.26E+45	2.62E+26	5.23E+18	2.45E+04	1.99E-08
$\Gamma_{VP} (\text{cm}^{-3}\text{sec}^{-1})$	8.70E+63	7.06E+57	9.55E+33	2.27E+24	2.78E+06	2.14E-09
critical volume	5.18E-43	1.06E-35	4.63E-07	1.64E+05	5.12E+26	6.99E+44

It is important to note that under unperturbed resonant

conditions, the rate of Schrödinger pair (with energy $k_b T_c$) production and pair (with energy $k_b T_c$) absorption are equal.

3. Discussion

This effort began as an attempt towards formulating a numerical and dimensional frame work towards explaining the Podkletnov's and Niemenen's [7] results but in the process, relationships between electron/proton mass, charge and gravitational forces were established which appear to be unified under this correlation with links to the cosmological constant, the dark energy of the universe, and the universe black body radiation as a continuation of its big bang origins and nuclear forces. Essentially, this effort is an attempt to explain universe stability. Most (99.99%) of the universe exists in an elastic state and does not change state at the atomic level for extremely large times. So rather than explain universe dynamics (human activity, planetary tectonics, industrial mechanics, etc), I start from the base that the universe essentially runs in place and is generally in conformance with the conservation of energy and momentum (elastic).

An importantly, the universe appears to be constructed of a visible and invisible or real and reflected nature that transforms between two at the nuclear dimension as governed by the speed of light(c) that is expressed conventionally under the concept of phase and group velocity.

Solid-state physics provides an intuitive understanding of these correlations. In solid state semiconductors, the roles of charged particles and photons in field theory are replaced by electrons in the conduction band, holes in the valence band, and phonons or vibrations of the crystal lattice.

The overall correlation is an extension to what Sir Arthur Eddington proposed during the early part of the 20th century. He attempted to relate proton and electron mass to the number of particles in the universe and the universe radius. Central to his approach was the fine structure constant:

$$1/\alpha = \hbar c/e^2$$

which he knew to be approximately equal to 137. This relationship is also found as a consequence of our development in equation 2.1.48, the difference being that a material dielectric (ϵ) modified velocity of light (v_ϵ) is used. To determine this dielectric (v_ϵ), displacement (D) and electric fields (E) are determined for Cooper CPT Charge conjugated pairs moving through the trisine CPT lattice under conditions of the trisine CPT lattice diamagnetism

equal to $-1/4\pi$ (the Meissner effect). Standard principles involving Gaussian surfaces are employed and in terms of this model development the following relationship is deduced from equation 2.1.48 repeated here

$$\frac{2 \mathbb{C}e_{\pm}\hbar}{12m_e v_{ey}} = \text{chain } H_c$$

As related to cosmological parameters

$$\rho_U = \frac{m_t}{\text{cavity}} = \frac{2}{8\pi} \frac{H_U^2}{G_U} = \frac{M_U}{V_U} = \frac{3M_U}{4\pi R_U^3} \quad (3.1)$$

$$\rho_{Ur} = \frac{m_t}{\text{cavity}_r} = \frac{2}{8\pi} \frac{H_{Ur}^2}{G_{Ur}} = \frac{M_{Ur}}{V_{Ur}} = \frac{3M_{Ur}}{4\pi R_{Ur}^3} \quad (3.1r)$$

and

$$\frac{G_U M_U H_U}{c^3} = 3^{1/2} \quad (3.2)$$

$$\frac{G_{Ur} M_{Ur} H_{Ur}}{c^3} = 3^{1/2} \quad (3.2r)$$

The extension to traditional superconductivity discussion is postulated wherein the underlying principle is resonance expressed as a conservation of energy and momentum (elastic character). The mechanics of this approach are in terms of a cell (*cavity*) defined by

momentum states: K_1, K_2, K_3 and K_4

and corresponding energy states: K_1^2, K_2^2, K_3^2 and K_4^2

by a required new mass called trisine mass (m_t), which is intermediate to the electron and proton masses. The cell dimensions can be scaled from nuclear standard model particles to universe dimensions (invariant with length ' B ', $\sim 1/K$ and related cell volumes '*cavity*' and '*chain*') with the trisine mass (m_t) remaining constant as per the following relationships expressed in terms of the superconductor critical temperature (T_c).

$$k_b T_c = h(1/\text{time}_{\pm})/2 \quad (3.3)$$

$$k_b T_{cr} = h(1/\text{time}_{r\pm})/2 \quad (3.3r)$$

$$k_b T_c = \hbar\pi/\text{time}_{\pm} \quad \text{Aharonov-Bohm effect} \quad (3.4)$$

$$k_b T_c = (h^2/(2m_t))(1/(2B)^2) \quad (3.5)$$

$$k_b T_{cr} = (h^2/(2m_t))(1/(2B_r)^2) \quad (3.5r)$$

$$k_b T_c = (1/2)m_t v_{dx}^2 \quad (3.6)$$

$$k_b T_{cr} = (1/2)m_t v_{dxr}^2 \quad (3.6r)$$

$$k_b T_c = \sqrt{3}e_{\pm}^2/(g_s g_d \epsilon 2B) \quad (3.7)$$

$$k_b T_{cr} = \sqrt{3}e_{\pm}^2/(g_s g_d \epsilon_r 2B_r) \quad (3.7r)$$

$$k_b T_c = (2/3) \left(1/\sqrt{3}\right) (A/B) (1/(4\pi)) \text{cavity } D_x E_x \quad (3.8)$$

$$k_b T_{cr} = (2/3) \left(1/\sqrt{3}\right) (A_r/B_r) (1/(4\pi)) \text{cavity } D_{xr} E_{xr} \quad (3.8r)$$

$$k_b T_c = (2/3)(1/\sqrt{3})(A/B)(1/(4\pi)) \text{cavity } E_x^2 \epsilon_x \quad (3.9)$$

$$k_b T_{cr} = (2/3)(1/\sqrt{3})(A_r/B_r)(1/(4\pi)) \text{cavity } E_{xr}^2 \epsilon_{xr} \quad (3.9r)$$

$$k_b T_c = (2/3)(1/\sqrt{3})(A/B)(1/(4\pi)) \text{cavity } D_x^2 / \epsilon_x \quad (3.10)$$

$$k_b T_{cr} = (2/3)(1/\sqrt{3})(A_r/B_r)(1/(4\pi)) \text{cavity } D_{xr}^2 / \epsilon_{xr} \quad (3.10r)$$

$$k_b T_c = (\text{chain}) H_c^2 / (8\pi) \quad (3.11)$$

$$k_b T_{cr} = (\text{chain}_r) H_{cr}^2 / (8\pi) \quad (3.11r)$$

$$k_b T_c = (\text{pressure})(\text{cavity}) \quad (3.12)$$

$$k_b T_{cr} = (\text{chain}) H_{cr}^2 / (8\pi) \quad (3.12r)$$

$$k_b T_c = m_t c^2 / (2k_{mx} \epsilon_x) \quad (3.13)$$

$$k_b T_{cr} = m_t c^2 / (2k_{mxr} \epsilon_{xr}) \quad (3.13r)$$

$$k_b T_c = m_r c^2 \quad (3.14)$$

$$k_b T_{cr} = m_r c^2 \quad (3.14r)$$

$$k_b T_c = \frac{h^2}{2\pi m_t} \left(\frac{\mathbb{C}}{\zeta(3/2) \text{chain}} \right)^{\frac{2}{3}} \cos(\theta) \quad (3.15)$$

$$k_b T_{cr} = \frac{h^2}{2\pi m_t} \left(\frac{\mathbb{C}}{\zeta(3/2) \text{chain}_r} \right)^{\frac{2}{3}} \cos(\theta) \quad (3.15r)$$

$$k_b T_c = G_U m_r M_U / R_U \quad (3.16)$$

$$k_b T_{cr} = G_{Ur} m_{rr} M_{Ur} / R_{Ur} \quad (3.16r)$$

$$k_b T_c = 4\hbar v_{xr} / R_U \quad (3.17)$$

$$k_b T_c = h^2 R_U c^2 / (8B^2 G_U M_U m_t) \quad \text{Hawking Radiation} \quad (3.18)$$

$$k_b T_{cr} = h^2 R_{Ur} c^2 / (8B^2 G_{Ur} M_{Ur} m_t) \quad \text{Hawking Radiation} \quad (3.18r)$$

$$k_b T_b = g_s^3 m_t c^2 / (4\epsilon) \quad (3.19)$$

$$k_b T_{br} = g_s^3 m_t c^2 / (4\epsilon_r) \quad (3.19r)$$

$$k_b T_a = m_t c^2 \quad (3.20)$$

$$k_b T_a = (2\pi)^{2/3} h^{4/3} c^{1/3} / (8U^{1/3} B^2 \cos(\theta)) \quad (3.21)$$

$$k_b T_{cr} = (1/2)m_t v_{dxr}^2 \quad (3.22)$$

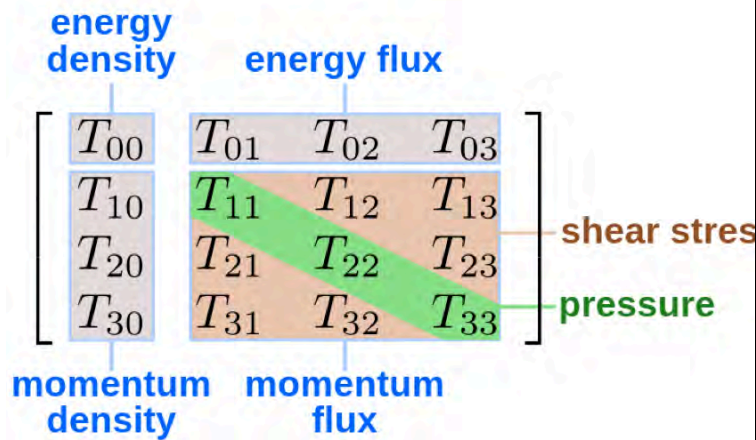
These correlations then can be placed in the form of the Einstein tensor $G_{\mu\nu}$ and stress energy tensor $T_{\mu\nu}$ relationship:

$$G_{\mu\nu} = \frac{8\pi G_U}{c^4} T_{\mu\nu} \quad (3.23)$$

And reflective tensor condition

$$G_{\mu\nu\rho} = \frac{8\pi G_{Ur}}{c^4} T_{\mu\nu\rho} \quad (3.23r)$$

where the Newton gravitational parameter (G_U) varies with universe age (Age_U) or more specifically within the context of stress energy tensor components:



and more definitively:

$$\begin{array}{l} \frac{k_b T_c}{cavity} \frac{1}{\sqrt{3}} \frac{c \sqrt{2m_t k_b T_c}}{approach \ time} \frac{2}{\sqrt{3}} \frac{Euler \ c \sqrt{2m_t k_b T_c}}{side \ time} \frac{2}{\sqrt{3}} \frac{B \ c \sqrt{2m_t k_b T_c}}{section \ time} \\ \frac{m_r c}{cavity} \frac{1}{2} \frac{\sqrt{2m_t k_b T_c}}{approach \ time} \frac{2}{\sqrt{3}} \frac{A \ m_t c}{B \ approach} \frac{2}{\sqrt{3}} \frac{A \ m_t c}{B \ side} \\ \frac{m_r c}{cavity} \frac{1}{\sqrt{3}} \frac{\sqrt{2m_t k_b T_c}}{approach \ time} \frac{Euler \ c \sqrt{2m_t k_b T_c}}{side \ time} \frac{2m_t c}{section} \\ \frac{m_r c}{cavity} \frac{2}{\sqrt{3}} \frac{Euler \ c \sqrt{2m_t k_b T_c}}{side \ time} \frac{2}{\sqrt{3}} \frac{B \ c \sqrt{2m_t k_b T_c}}{A \ section \ time} \frac{B \ c \sqrt{2m_t k_b T_c}}{A \ section \ time} \end{array}$$

$$= \frac{8\pi G_U}{c^4} \left(\frac{A}{B} \frac{c^4}{Euler} \frac{m_t^3}{h} \sqrt{\frac{1}{2m_t k_b T_c}} \right) \begin{array}{l} \frac{M_{\nu} c^2}{V_{\nu}} \frac{M_{\nu} c^2}{A_{\nu} Age_{\nu}} \frac{M_{\nu} c^2}{A_{\nu} Age_{\nu}} \frac{M_{\nu} c^2}{A_{\nu} Age_{\nu}} \\ \frac{M_{\nu} c}{V_{\nu}} \frac{M_{\nu} c^2}{V_{\nu}} \frac{M_{\nu} c}{A_{\nu}} \frac{M_{\nu} c}{A_{\nu}} \\ \frac{M_{\nu} c}{V_{\nu}} \frac{M_{\nu} c}{A_{\nu} Age_{\nu}} \frac{M_{\nu} c^2}{V_{\nu}} \frac{M_{\nu} c}{A_{\nu}} \\ \frac{M_{\nu} c}{V_{\nu}} \frac{M_{\nu} c}{A_{\nu} Age_{\nu}} \frac{M_{\nu} c}{A_{\nu} Age_{\nu}} \frac{M_{\nu} c^2}{V_{\nu}} \end{array}$$

and reflective tensor condition

$$\begin{array}{l} \frac{k_b T_{cr}}{cavity_r} \frac{1}{\sqrt{3}} \frac{c \sqrt{2m_t k_b T_{cr}}}{approach_r \ time_{rs}} \frac{2}{\sqrt{3}} \frac{Euler \ c \sqrt{2m_t k_b T_{cr}}}{side_r \ time_{rs}} \frac{2}{\sqrt{3}} \frac{B \ c \sqrt{2m_t k_b T_{cr}}}{A \ section_r \ time_{rs}} \\ \frac{m_r c}{cavity_r} \frac{1}{2} \frac{\sqrt{2m_t k_b T_{cr}}}{approach_r \ time_{rs}} \frac{2}{\sqrt{3}} \frac{A_r \ m_t c}{B_r \ approach_r} \frac{2}{\sqrt{3}} \frac{A \ m_t c}{B \ side_r} \\ \frac{m_r c}{cavity_r} \frac{1}{\sqrt{3}} \frac{\sqrt{2m_t k_b T_{cr}}}{approach_r \ time_{rs}} \frac{Euler \ c \sqrt{2m_t k_b T_{cr}}}{side_r \ time_{rs}} \frac{2m_t c}{section_r} \\ \frac{m_r c}{cavity_r} \frac{2}{\sqrt{3}} \frac{Euler \ c \sqrt{2m_t k_b T_{cr}}}{side_r \ time_{rs}} \frac{2}{\sqrt{3}} \frac{B_r \ c \sqrt{2m_t k_b T_{cr}}}{A_r \ section_r \ time_{rs}} \frac{B \ c \sqrt{2m_t k_b T_{cr}}}{A \ section_r \ time_{rs}} \end{array}$$

$$= \frac{8\pi G_{Ur}}{c^4} \left(\frac{A_r}{B_r} \frac{c^4}{Euler} \frac{m_t^3}{h} \sqrt{\frac{1}{2m_t k_b T_{cr}}} \right) \begin{array}{l} \frac{M_{\nu_r} c^2}{V_{\nu_r}} \frac{M_{\nu_r} c^2}{A_{\nu_r} Age_{\nu_r}} \frac{M_{\nu_r} c^2}{A_{\nu_r} Age_{\nu_r}} \frac{M_{\nu_r} c^2}{A_{\nu_r} Age_{\nu_r}} \\ \frac{M_{\nu_r} c}{V_{\nu_r}} \frac{M_{\nu_r} c^2}{V_{\nu_r}} \frac{M_{\nu_r} c}{A_{\nu_r}} \frac{M_{\nu_r} c}{A_{\nu_r}} \\ \frac{M_{\nu_r} c}{V_{\nu_r}} \frac{M_{\nu_r} c}{A_{\nu_r} Age_{\nu_r}} \frac{M_{\nu_r} c^2}{V_{\nu_r}} \frac{M_{\nu_r} c}{A_{\nu_r}} \\ \frac{M_{\nu_r} c}{V_{\nu_r}} \frac{M_{\nu_r} c}{A_{\nu_r} Age_{\nu_r}} \frac{M_{\nu_r} c}{A_{\nu_r} Age_{\nu_r}} \frac{M_{\nu_r} c^2}{V_{\nu_r}} \end{array}$$

Note that $8\pi G_U/c^4$ has '1/force' dimensionality as does $h\sqrt{m_t k_b T_c}/(c^4 m_t^3)$ making their ratio dimensionless but defining the quantum Einstein tensor $G_{\mu\nu}$ cellular 'curvature' as

$$G_{\mu\nu} = \frac{8\pi G_U}{c^4} T_{\mu\nu} \text{ (assuming } 1/\left(\frac{A}{B} \frac{c^4}{Euler} \frac{m_t^3}{h} \sqrt{\frac{1}{2m_t k_b T_c}}\right)$$

is multiplied into 'uv' elements of $G_{\mu\nu}$). These $G_{\mu\nu}$ curvatures are on a cosmic scale $\sim 1E28$ cm. (essentially a flat universe)

The above approach is backwards to defining Einstein tensor $G_{\mu\nu}$ in terms of the Ricci, metric tensors and scalar curvature.

$$G_{\mu\nu} = R_{\mu\nu} - (1/2) g_{\mu\nu} R$$

Note how the quantum (h) as well as charge (e) and all other parameters as reflected by correlations 3.2 – 3.17 are naturally expressed within these Einstein field equations or perhaps more correctly, solutions to the Einstein field equations with a special note that the Weinberg mass[99] is inherent to this formulation here repeated from equation 2.11.13a.

$$m_t^3 = \frac{m_t \rho_U k_b T_c \text{section}}{\sqrt{3} H_U c} = \frac{\pi^2 \rho_U \hbar^2}{H_U c} = \frac{U \hbar^2 \cos^3(\theta)}{c}$$

The triangular hexagonal cell character is generally accepted by conventional solid-state mechanics to be equivalent in momentum and real space making the energy ($\sim K^2$) and momentum ($\sim K$) cell (*cavity*) identity possible. Also, the hexagonal or triangulation energy ($\sim K^2$) and momentum ($\sim K$) have a 1/3, 2/3 character inherent to the standard model 1/3, 2/3 quark definitions.

$$\begin{array}{cccc} \frac{\sqrt{3}\text{Euler } h^4}{8\text{cavity}^2 m_t^4 c^4} & \frac{\text{Euler } h^4}{4\text{cavity}^2 m_t^4 c^3} & \frac{\text{Euler } h^4}{4\text{cavity}^2 m_t^4 c^3} & \frac{\text{Euler } h^4}{4\text{cavity}^2 m_t^4 c^3} \\ \frac{\sqrt{3}\text{Euler } h^4}{8\text{cavity}^2 m_t^4 c^5} & \frac{\sqrt{3}\text{Euler } h^4}{8\text{cavity}^2 m_t^4 c^4} & \frac{\frac{1}{3}\text{Euler}^2 h^2}{\text{cavity } m_t^2 c^3} & \frac{\frac{1}{3}\text{Euler}^2 h^2}{\text{cavity } m_t^2 c^3} \\ \frac{\sqrt{3}\text{Euler } h^4}{8\text{cavity}^2 m_t^4 c^5} & \frac{\sqrt{3}\text{Euler}^2 h^4}{4\text{cavity}^2 m_t^4 c^5} & \frac{\sqrt{3}\text{Euler } h^4}{8\text{cavity}^2 m_t^4 c^4} & \frac{\sqrt{3}\text{Euler}^2 h^3}{\text{cavity } m_t^2 c^3} \\ \frac{\sqrt{3}\text{Euler } h^4}{8\text{cavity}^2 m_t^4 c^5} & \frac{\sqrt{3}\text{Euler}^2 h^4}{4\text{cavity}^2 m_t^4 c^5} & \frac{\sqrt{3}\text{Euler } h^4}{4\text{cavity}^2 m_t^4 c^5} & \frac{\sqrt{3}\text{Euler } h^4}{8\text{cavity}^2 m_t^4 c^4} \end{array}$$

$$\begin{array}{cccc} \frac{\sqrt{3}\text{Euler } h^4}{8\text{cavity}_r^2 m_t^4 c^4} & \frac{\text{Euler } h^4}{4\text{cavity}_r^2 m_t^4 c^3} & \frac{\text{Euler } h^4}{4\text{cavity}_r^2 m_t^4 c^3} & \frac{\text{Euler } h^4}{4\text{cavity}_r^2 m_t^4 c^3} \\ \frac{\sqrt{3}\text{Euler } h^4}{8\text{cavity}_r^2 m_t^4 c^5} & \frac{\sqrt{3}\text{Euler } h^4}{8\text{cavity}_r^2 m_t^4 c^4} & \frac{\frac{1}{3}\text{Euler}^2 h^2}{\text{cavity}_r m_t^2 c^3} & \frac{\frac{1}{3}\text{Euler}^2 h^2}{\text{cavity}_r m_t^2 c^3} \\ \frac{\sqrt{3}\text{Euler } h^4}{8\text{cavity}_r^2 m_t^4 c^5} & \frac{\sqrt{3}\text{Euler}^2 h^4}{4\text{cavity}_r^2 m_t^4 c^5} & \frac{\sqrt{3}\text{Euler } h^4}{8\text{cavity}_r^2 m_t^4 c^4} & \frac{\frac{1}{3}\text{Euler}^2 h^2}{\text{cavity}_r m_t^2 c^3} \\ \frac{\sqrt{3}\text{Euler } h^4}{8\text{cavity}_r^2 m_t^4 c^5} & \frac{\sqrt{3}\text{Euler}^2 h^4}{4\text{cavity}_r^2 m_t^4 c^5} & \frac{\sqrt{3}\text{Euler}^2 h^4}{4\text{cavity}_r^2 m_t^4 c^5} & \frac{\sqrt{3}\text{Euler } h^4}{8\text{cavity}_r^2 m_t^4 c^4} \end{array}$$

$$= \frac{8\pi G_v}{c^4} \begin{array}{cccc} \frac{M_v c^2}{V_v} & \frac{M_v c^2}{A_v \text{Age}_v} & \frac{M_v c^2}{A_v \text{Age}_v} & \frac{M_v c^2}{A_v \text{Age}_v} \\ \frac{M_v c}{V_v} & \frac{M_v c^2}{V_v} & \frac{M_v c}{A_v} & \frac{M_v c}{A_v} \\ \frac{M_v c}{V_v} & \frac{M_v c}{V_v} & \frac{M_v c^2}{A_v} & \frac{M_v c}{A_v} \\ \frac{M_v c}{V_v} & \frac{M_v c}{A_v \text{Age}_v} & \frac{V_v}{A_v} & \frac{A_v}{A_v} \\ \frac{M_v c}{V_v} & \frac{M_v c}{A_v \text{Age}_v} & \frac{M_v c}{A_v \text{Age}_v} & \frac{M_v c^2}{V_v} \end{array}$$

and reflective tensor condition

$$= \frac{8\pi G_v}{c^4} \begin{array}{cccc} \frac{M_{vr} c^2}{V_{vr}} & \frac{M_{vr} c^2}{A_{vr} \text{Age}_{vr}} & \frac{M_{vr} c^2}{A_{vr} \text{Age}_{vr}} & \frac{M_{vr} c^2}{A_{vr} \text{Age}_{vr}} \\ \frac{M_{vr} c}{V_{vr}} & \frac{M_{vr} c}{V_{vr}} & \frac{M_{vr} c}{A_{vr}} & \frac{M_{vr} c}{A_{vr}} \\ \frac{M_{vr} c}{V_{vr}} & \frac{M_{vr} c}{A_{vr} \text{Age}_{vr}} & \frac{M_{vr} c^2}{V_{vr}} & \frac{M_{vr} c}{A_{vr}} \\ \frac{M_{vr} c}{V_{vr}} & \frac{M_{vr} c}{A_{vr} \text{Age}_{vr}} & \frac{M_{vr} c}{A_{vr} \text{Age}_{vr}} & \frac{M_{vr} c^2}{V_{vr}} \end{array}$$

and then assuming the Planck constant dimensional definition $\hbar(h/2\pi)$ or $m_t(2B)^2/(2\pi \text{time}_\pm)$ and $\text{cavity} = 2\sqrt{3}(A/B)B^3$ resulting in the trisine cellular curvature accelerated expansion (B/time_\pm^2) and $(B/\text{time}_\pm^2)^2$.

$$\begin{array}{cccc} \left(\frac{B}{A}\right)^2 \frac{8\text{Euler } B^2}{\sqrt{3\text{time}_\pm^4 c^4}} & \left(\frac{B}{A}\right)^2 \frac{16\text{Euler } B^2}{3\text{time}_\pm^4 c^3} & \left(\frac{B}{A}\right)^2 \frac{16\text{Euler } B^2}{3\text{time}_\pm^4 c^3} & \left(\frac{B}{A}\right)^2 \frac{16\text{Euler } B^2}{3\text{time}_\pm^4 c^3} \\ \left(\frac{B}{A}\right)^2 \frac{4\text{Euler } B^2}{\sqrt{3\text{time}_\pm^4 c^5}} & \left(\frac{B}{A}\right)^2 \frac{8\text{Euler } B^2}{\sqrt{3\text{time}_\pm^4 c^4}} & \left(\frac{B}{A}\right)^2 \frac{8\text{Euler}^2 B}{\text{time}_\pm^2 c^3} & \left(\frac{B}{A}\right)^2 \frac{8\text{Euler}^2 B}{\text{time}_\pm^2 c^3} \\ \left(\frac{B}{A}\right)^2 \frac{4\text{Euler } B^2}{\sqrt{3\text{time}_\pm^4 c^5}} & \left(\frac{B}{A}\right)^2 \frac{16\text{Euler}^2 B^2}{\sqrt{3\text{time}_\pm^4 c^4}} & \left(\frac{B}{A}\right)^2 \frac{8\text{Euler } B^2}{\sqrt{3\text{time}_\pm^4 c^4}} & \left(\frac{B}{A}\right)^2 \frac{8\text{Euler}^2 B}{\text{time}_\pm^2 c^3} \\ \left(\frac{B}{A}\right)^2 \frac{4\text{Euler } B^2}{\sqrt{3\text{time}_\pm^4 c^5}} & \left(\frac{B}{A}\right)^2 \frac{16\text{Euler}^2 B^2}{\sqrt{3\text{time}_\pm^4 c^4}} & \left(\frac{B}{A}\right)^2 \frac{16\text{Euler}^2 B^2}{\sqrt{3\text{time}_\pm^4 c^4}} & \left(\frac{B}{A}\right)^2 \frac{8\text{Euler } B^2}{\sqrt{3\text{time}_\pm^4 c^4}} \end{array}$$

$$= \frac{8\pi G_v}{c^4} \begin{array}{cccc} \frac{M_v c^2}{V_v} & \frac{M_v c^2}{A_v \text{Age}_v} & \frac{M_v c^2}{A_v \text{Age}_v} & \frac{M_v c^2}{A_v \text{Age}_v} \\ \frac{M_v c}{V_v} & \frac{M_v c^2}{V_v} & \frac{M_v c}{A_v} & \frac{M_v c}{A_v} \\ \frac{M_v c}{V_v} & \frac{M_v c}{A_v \text{Age}_v} & \frac{V_v}{A_v} & \frac{A_v}{A_v} \\ \frac{M_v c}{V_v} & \frac{M_v c}{A_v \text{Age}_v} & \frac{A_v}{A_v} & \frac{M_v c^2}{V_v} \end{array}$$

and reflective tensor condition

$$\begin{aligned}
& \left(\frac{B_r}{A_r} \right)^2 \frac{8 \text{Euler } B_r^2}{\sqrt{3 \text{time}_{rz}^4 c^4}} \quad \left(\frac{B_r}{A_r} \right)^2 \frac{16 \text{Euler } B_r^2}{3 \text{time}_{rz}^4 c^3} \quad \left(\frac{B_r}{A_r} \right)^2 \frac{16 \text{Euler } B_r^2}{3 \text{time}_{rz}^4 c^3} \quad \left(\frac{B_r}{A_r} \right)^2 \frac{16 \text{Euler } B_r^2}{3 \text{time}_{rz}^4 c^3} \\
& \left(\frac{B_r}{A_r} \right)^2 \frac{4 \text{Euler } B_r^2}{\sqrt{3 \text{time}_{rz}^4 c^5}} \quad \left(\frac{B_r}{A_r} \right)^2 \frac{8 \text{Euler } B_r^2}{\sqrt{3 \text{time}_{rz}^4 c^4}} \quad \left(\frac{B_r}{A_r} \right)^2 \frac{8 \text{Euler }^2 B_r}{\text{time}_{rz}^2 c^3} \quad \left(\frac{B_r}{A_r} \right)^2 \frac{8 \text{Euler }^2 B_r}{\text{time}_{rz}^2 c^3} \\
& \left(\frac{B_r}{A_r} \right)^2 \frac{4 \text{Euler } B_r^2}{\sqrt{3 \text{time}_{rz}^4 c^5}} \quad \left(\frac{B_r}{A_r} \right)^2 \frac{16 \text{Euler }^2 B_r^2}{\sqrt{3 \text{time}_{rz}^4 c^4}} \quad \left(\frac{B_r}{A_r} \right)^2 \frac{8 \text{Euler }^2 B_r^2}{\sqrt{3 \text{time}_{rz}^4 c^4}} \quad \left(\frac{B_r}{A_r} \right)^2 \frac{8 \text{Euler }^2 B_r}{\text{time}_{rz}^2 c^3} \\
& \left(\frac{B_r}{A_r} \right)^2 \frac{4 \text{Euler } B_r^2}{\sqrt{3 \text{time}_{rz}^4 c^5}} \quad \left(\frac{B_r}{A_r} \right)^2 \frac{16 \text{Euler }^2 B_r^2}{\sqrt{3 \text{time}_{rz}^4 c^4}} \quad \left(\frac{B_r}{A_r} \right)^2 \frac{16 \text{Euler }^2 B_r^2}{\sqrt{3 \text{time}_{rz}^4 c^4}} \quad \left(\frac{B_r}{A_r} \right)^2 \frac{8 \text{Euler } B_r^2}{\sqrt{3 \text{time}_{rz}^4 c^4}} \\
\\
& \left| \begin{array}{cccc} \frac{M_{ur} c^2}{V_{ur}} & \frac{M_{ur} c^2}{A_{ur} \text{Age}_{ur}} & \frac{M_{ur} c^2}{A_{ur} \text{Age}_{ur}} & \frac{M_{ur} c^2}{A_{ur} \text{Age}_{ur}} \\ \frac{M_{ur} c}{V_{ur}} & \frac{M_{ur} c^2}{V_{ur}} & \frac{M_{ur} c}{A_{ur}} & \frac{M_{ur} c}{A_{ur}} \\ \frac{M_{ur} c}{V_{ur}} & \frac{M_{ur} c}{A_{ur} \text{Age}_{ur}} & \frac{M_{ur} c^2}{V_{ur}} & \frac{M_{ur} c}{A_{ur}} \\ \frac{M_{ur} c}{V_{ur}} & \frac{M_{ur} c}{A_{ur} \text{Age}_{ur}} & \frac{M_{ur} c}{A_{ur} \text{Age}_{ur}} & \frac{M_{ur} c}{V_{ur}} \end{array} \right| \\
& = \frac{8\pi G_{ur}}{c^4}
\end{aligned}$$

And as a general expression of these matrices, note that
 $8\pi G_u/c^4 = 8\pi 3m_i time_{\pm} A/(M_u \hbar \pi)$

which is conceptually an expression of the impulse-momentum theorem or Newton's second law at the universal level:

$$dp/dt = c^4/(8\pi G_U) = M_U v_{dz}/(8\pi 6 time_{\pm}) = M_U \hbar \pi/(8\pi 6 m_t time_{\pm})$$

Observation of the universe from the smallest (nuclear particles) to the largest (galaxies) indicates a particularly static condition making our elastic assumption reasonable and applicable at all dimensional scales. Indeed, this is the case. This simple cellular model is congruent with proton density and radius as well as interstellar space density and energy density.

In order to scale this cellular model to these dimensions varying by 15 orders of magnitude, special relativity Lorentz transforms are justifiably suspended due to resonant cancellation in the context of the de Broglie hypothesis. This defines a sub- super- luminal resonant discontinuity ($v_{dx} \sim c$) at a critical temperature $T_c \sim 1.3\text{E}12$ K, $K_B \sim 5.7\text{E}12$ cm $^{-1}$ and $B \sim 5.5\text{E}-13$ cm. This discontinuity forms potential barrier providing a probable mechanism for limiting nuclear size.

Most importantly, the gravity force is linked to the Hubble

constant through Planck's constant. This indicates that gravity is linked to other forces at the proton scale and not the Planck scale. Indeed, when the model trisine model is scaled to the Planck scale ($B = 1.62E-33$ cm), a mass of $1.31E40$ GeV/c 2 ($2.33E16$ g) is obtained. This value would appear arbitrary. Indeed the model can be scaled to the Universe mass (M_u) of $3.02E56$ grams at a corresponding dimension (B) of $1.42E-53$ cm.

In a particular Schwinger mechanism associated with graphene structure [83] which is similar to the trisine structure projected in 2D. This is substantiated by inserting the bond length value for graphene ($B = 1.22\text{E-}8$ cm) the trisine value for potential field (E) eqn 2.5.1 and velocity (v_{dx}) eqn 2.4.1, ref 83 eqn 3 (repeated paragraph 2.16) scales nicely (within 5 parts/thousand) with the potential trisine pair production rate per area:

$$1 \text{ pair}/(\text{section time}_\pm) = 2.06\text{E}29 \text{ cm}^{-2} \text{ sec}^{-1}$$

for the graphene dimension ($f=1$ and 2.612 in denominator). And then it is noted that ref 83 eqn 1 equates (within 9 parts/thousand) trisine pair production rate per volume

$$1 \text{ pair}/(\text{cavity time}_\pm) = 3.92\text{E}37 \text{ cm}^{-3} \text{ sec}^{-1}$$

And then it is noted that by logic there exists a trisine pair production rate per length (B)

$$1 \text{ pair}/(2B \text{ time}_\pm) = 8.78 \text{E}21 \text{ cm}^{-1} \text{ sec}^{-1}$$

and this potential graphene pair creation taking place at a frequency($1/time_{\pm}$) of 1.08E14 /sec.

It is known that paper [83] assumes production of pairs out of a static classical electric field of infinite extent whereas this paper assumes a resonant condition of resonant period ' $time_{\pm}$ ' not of infinite extent but represented by condition $A_1=1$ for each cell within lattice of \sim infinite extent. The correlation can be made that a static field exists for a resonant period ' $time_{\pm}$ ' and then it flips to another 'static' condition for another resonant period ' $time_{\pm}$ '.

A correlation between trisine geometry as related to Dark Energy and DAMA is noted. The DAMA experiment is located in the Gran Sasso National Laboratory, Italy at 3500 mwe. The DAMA observed annual oscillation [84], dictates a question in terms of the following logic:

The Milky Way is moving at approximately 627 km/s (at 276 degree galactic longitude, 30 degree galactic latitude) with respect to the photons of the Cosmic Microwave Background (CMB). This has been observed by satellites such as COBE and WMAP as a dipole contribution to the CMB, as photons in equilibrium at the CMB frame get blue-shifted in the direction of the motion and red-shifted in the opposite direction.

and also: the solar system is orbiting galactic center at about

217 km/sec which is essentially additive (217 + 627) or 844 km/sec relative to CMB dipole rest frame.

and also: the earth has a velocity of 30 km/sec around the sun.

and also: refs: [84] Fig 10, harmonic DAMA/NaI experimental data and [111] Fig 10, harmonic CoGeNT experimental data indicates an annual oscillation of detected radiation flux detected on earth.

Is there a correlation of annual DAMA/ CoGeNT experimental data on earth due to earth_solar annual differential velocity projection to CMB velocity vector?

In answer to this question, the CMB 'hot spot' or 'wind origin' (+3.5 mK above the present CMBR 2.729 K) is in constellation Leo at essentially the celestial equator: <http://aether.lbl.gov/www/projects/u2/>

Given that the earth orbits the sun at 30 km/sec, the hypothesis would be that average flux would be when earth - sun line would be parallel to earth - Leo line which occurs September 1 (sun in Leo) and March 1 with maximum flux (earth against the CMB dipole wind) on December 1 and minimum (CMB dipole wind to earth's back) on June 1. This CMB dipole wind and earth solar rotation are then approximately in phase with DAMA NAI [84] Fig 10 where $t_0 = 152.5$ is ~June 1 (minimum flux). This phase relationship is congruent and also supported with the energy ratios (temperature ratio vs velocity² ratio) identity $.0035/2.732 = 30^2/(627+217)^2$ within 1 percent.

In contrast, the model presented on the DAMA web site http://people.roma2.infn.it/~dama/web/nai_dmp.html with its earth velocity 30 km/sec relative to galactic rotation indicates a maximum at this date ~June 1. Also note that the CMB 'hot spot' is essentially at the celestial equator (declination = zero). A detector optimized at pointing in this direction relative to that detectors earth latitude could conceivably have more chance of particle detection.

Also it is noted that the Pioneers 10 & 11 had annual deceleration peaks [57] that are generally in phase (maximum on December 1 and minimum on June 1) with the DAMA/CoGeNT annual flux peaks making both effects having possible correlation with dark energy

The trisine model can be adiabatically correlated to any time in the universe age. There is a correlation of X rays produced at trisine condition 1.3 with X-rays observed by DAMA/CoGeNT [148] implying a congruency between these observations and the early universe expressed in trisine condition 1.3 all within the context of the Heisenberg Uncertainty constraint. The model predicts an oscillation at ~20 particle counts per 30 days at ~1 keVee that is consistent with DAMA/CoGeNT observations and originating at

Trisine Condition 1.3 and congruent with the CMBR annual oscillations due to earth rotation around sun and its relationship to CMBR flux from above $.0035/2.732 = 30^2/(627+217)^2$.

Particle production per area and time is computed with the following equation times the CoGeNT crystal frontal area based on diameter of 2.2 cm.

$$\sigma T_{cr}^4 \xi (k_b T_r)^{-\frac{8}{8}} = \left(\frac{B}{A} \right)^{\frac{12}{8}} \frac{\pi^{\frac{8}{8}} G^{\frac{8}{8}} m_e^{\frac{47}{8}} c^{\frac{66}{8}}}{2^{\frac{67}{8}} 3^{\frac{10}{8}} 4^{\frac{8}{8}} 15^{\frac{28}{8}} \hbar^{\frac{28}{8}}} \left(\frac{B_{Present}}{R_{U_{Present}}} \right)^{\frac{6}{8}} \frac{1}{2\pi} (k_b T_r)^{-\frac{15}{8}}$$

This directional congruency apparently exists from the time of the Big Bang nucleosynthesis.

Now wind this universe age (Age_U) further back to at time in which the universe was at condition 1.2 where proton density (2.34E14 g/cc), background milieu temperature (T_c) 8.96E13 K, CMBR temperature (T_b) 9.07E14K. In the extant universe, both this CMBR (T_b) and background milieu temperature (T_c) are unobserved except for current nuclear observations (trisine condition 1.2) and cosmic rays evident in conclusion 4.33.

It is important to note that at CMBR temperature (T_b) 9.07E14K, the radiation is not longer microwave as CMBR implies, but the term is used for consistency.

At this proton density point, background milieu temperature $>$ CMBR (because of luminal - group phase reflection considerations). With adiabatic expansion, an extremely cold medium at 9.8E-10K. At this temperature, dense (~ 1 g/cm³) Bose Einstein Condensates (BEC) form from hydrogen helium created by nucleosynthesis through adiabatic expansion with milieu temperature (T_c) going to 9.8E-10K and congruent with extant CMBR (T_b) 3,000 K. or dimensionally

$$\begin{aligned} & (T_c \text{ after expansion}) / (T_c \text{ before expansion}) \\ &= (\text{density after Expansion} / \text{density before Expansion})^{2/3} \\ & (9.8E-10 / 8.96E13) = (9.01E-21 / 2.34E14)^{2/3} \end{aligned}$$

The hypothesis would be that there was a time in which the entire universe was at $T_c = 9.8E-10$ K and the extant CMBR $T_b = 3000$ K due to adiabatic expansion after the Big Bang. All the atomic entities (primarily hydrogen) would be in the form of Bose Einstein Condensates BEC's at 9.8E-10 K. This extremely low temperature would allow for dense BEC formation where the fundamental BEC formation formula:

$$k_b T_{BEC} = k_b T_c = (n / \xi (3/2))^{2/3} (h^2 / 2\pi m)$$

is modified in terms of density ($am_p/volume$ or ρ replacing n or $/volume$) and multiple proton masses (am_p):

$$k_b T_{BEC} = k_b T_c = (\rho/\xi(3/2))^{2/3} \left(h^2 / 2\pi (am_p)^{5/3} \right)$$

where $\xi(3/2) = 2.6124$

BEC's with density (1 g/cm³) could be formed at $T_{BEC} = T_c = 9.8E-10$ K with ' a ' ~ 1E6 proton masses m_p .

This condition (1.10) would not last very long as these dense (~1 g/cc) BEC's (those greater than ~1E6 cm) gravitationally collapsed resulting in heating that initiated stellar nuclear reactions distributed in galaxies with aggregate density ~1E-24 g/cc aided perhaps by the extant CMBR 3000 K at that time but leaving the residual hydrogen BECs as ~ meter objects in thermal equilibrium with all encompassing and ubiquitous T_b (T_b decreasing from 1E-9K to ~1E-16K due to further universe expansion) over the next 4.32E17 sec (13.7 billion years) gravitationally observed today as dark matter.

This extant hydrogen BEC would not be observable by the Beers Lambert Law. As generally described in elementary texts, the optical path established by this law is derived assuming that that particles may be described as having an *area* perpendicular to the path of light through a solution (or space media), such that a photon of light is absorbed if it strikes the particle, and is transmitted if it does not. Expressing the number of photons absorbed by the concentration C in direction z in the absorbing volume as dI_z , and the total number of photons incident on the absorbing volume as I_z , the fraction of photons absorbed by the absorbing volume is given by:

$dI_z/I_z = -area c dz$. There is a large difference (~6E7) in *area* for one mole of individual hydrogen atoms and that same mole in one BEC at 1 g/cc (the concentration c is the same for both cases) *area* of one mole of individual hydrogen atoms

6E23 x 1E-16 cm²/hydrogen atom ~ 6E7 cm² *area* of one mole of hydrogen BEC with density 1 g/cc ~1 cm²

There is an argument that the Intergalactic Medium (IGM) composed of 'hot' atoms would 'melt' any BECs that were there at the initial Big Bang Nucleosynthesis. In order to address this question, assume the IGM is totally ionized at the given universe critical density of ~1 proton mass per meter³. (It is very clear that this ionized IGM was not there in the beginning but ejected into space from stars etc.) Now take a 1 meter³ hydrogen BEC. It would have 100³(Avogadro's number) hydrogen atoms in it.

If there was no relative motion between the hydrogen dense (1 g/cc) BEC and the hot atoms, the hydrogen dense (1 g/cc)

BEC would not degrade. If there was relative motion between the hydrogen dense (1 g/cc) BEC and the hot atoms, the hydrogen dense (1 g/cc) BEC could travel 100³(Avogadro's number) meters or 6.023E29 meters through space before 'melting'. The length 6.023E29 meters is larger than the size of the visual universe (2.25E26 meter). There could have been multi kilometer sized hydrogen BEC's at the adiabatic expansion still remaining at nearly that size. Also, as a BEC, it would not have a vapor pressure. It would not sublime. The hydrogen dense (1 g/cc) BEC's are still with us.

The Bottom line is:

If you were Captain Kirk of the Star Ship Enterprise would you go full speed ahead into inter- intra- galactic space analogous to Captain Smith of the Titanic? I certainly would not.

4. Conclusion

A momentum and energy conserving (elastic) CPT lattice called trisine and associated superconducting theory is postulated whereby electromagnetic and gravitational forces are mediated by a particle of resonant transformed mass (110.12275343 x electron mass or 56.2726 MeV/c²) such that the established electron/proton mass is maintained, electron and proton charge is maintained and the universe radius as computed from Einstein's cosmological constant (Λ) is 1.29E-56 cm⁻², the universe mass is 3.0E56 gram, the universe density is 6.38E-30 g/cm³ and the universe age(Age_U) is 1.37E10 years.

The cosmological constant is based on a universe surface tension directly computed from a superconducting resonant energy over surface area.

The calculated universe mass and density are based on an isotropic homogeneous media filling the vacuum of space analogous to the 'aether' referred to in the 19th century (but still in conformance with Einstein's relativity theory) and could be considered a candidate for the 'cold dark matter' (or more properly 'cold dark energy') in present universe theories and as developed by Primack [80]. Universe density is 2/3 of conventionally calculated critical density. This is in conformance with currently accepted inflationary state of the universe.

The 'cold dark energy', a postulated herein, is in equilibrium with and congruent to a CMBR of 2.729 °K as has been observed by COBE, WMAP and later satellites although its temperature in terms of superconducting critical temperature is an extremely cold 8.11E-16 °K.

Also, the reported results by Podkletnov and Nieminen

wherein the weight of an object is lessened by .05% are theoretically confirmed where the object is the superconductor, although the gravitational shielding phenomenon of $YBa_2Cu_3O_{7-x}$ is yet to be explained. It is understood that the Podkletnov and Nieminen experiments have not been replicated at this time. It could be that the very high super currents that are required and theoretically possible have not been replicated from original experiment.

The trisine model provides a basis for considering the phenomenon of superconductivity in terms of an ideal gas with 1, 2 or 3 dimensions (degrees of freedom). The trisine model was developed primarily in terms of 1 dimension, but experimental data from MgB_2 would indicate a direct translation to 3 dimensions.

These trisine structures have an analog in various resonant structures postulated in the field of chemistry to explain properties of delocalized π electrons in benzene, ozone and a myriad of other molecules with conservation of energy and momentum conditions defining a superconductive (elastic) condition.

Other verifying evidence is the trisine model correlation to the ubiquitous 160-minute (~ third T_c harmonic - 29,600/(60x3) resonant oscillation [68,69] in the universe and also the model's explanation of the Tao effect [65, 66, 67].

Also dimensional guidelines are provided for design of room temperature superconductors and beyond. These dimensional scaling guidelines have been verified by Homes' Law and generally fit within the conventionally described superconductor operating in the "dirty" limit. [54]

The deceleration observed by Pioneer 10 & 11 as they exited the solar system into deep space appear to verify the existence of an space energy density consistent with the amount theoretically presented in this report. This translational deceleration is independent of the spacecraft velocity. Also, the same space density explains the Pioneer spacecraft rotational deceleration. This is remarkable in that translational and rotational velocities differ by three (3) orders of magnitude.

4.1. Universe Dark Energy is represented by a trisine elastic space CPT lattice (observed as Ω_A) which is composed of virtual particles adjacent to Heisenberg uncertainty without recourse to net matter-antimatter annihilation concepts.

4.2. Dark Energy is related to Cosmic Microwave Background Radiation (CMBR) through very large space dielectric (ϵ) (permittivity) and permeability (k) constants.

4.3. A very large trisine permittivity (dielectric) constant (6.16E10), permeability (6.26E13) and CPT equivalence makes the Dark Energy invisible to electromagnetic radiation.

4.4. A velocity independent thrust force acts on all objects passing through the trisine space CPT lattice and models the translational and rotational deceleration of Pioneer 10 & 11 spacecraft as well as dust clumping at initial stages of stellar galactic formation and deceleration of local galactic baryonic matter relative to Type 1A supernovae (an observation more conventionally reported as universe expansion acceleration).

4.5. The Asteroid Belt marks the interface between solar wind and trisine, the radial extent an indication of the dynamics of the energetic interplay of these two fields

4.6. The trisine model predicts no 'dust' in the Kuiper Belt. The Kuiper Belt is made of large Asteroid like objects.

4.7. The observed Matter Clumping in Galaxies is due to magnetic or electrical energetics in these particular areas at such a level as to destroy the coherent trisine CPT lattice.

4.8. The apparent approximately constant star rotation (~ 220 km/sec for Milky Way galaxy) with radius (R) from galactic center in galaxies is due to preponderance of galactic mass (M_d) represented by small objects (~10 - 20 cm) which rotate around the galactic center in a Keplerian manner with orbital velocity (v_d) relationship:

$$v_d^2 = \frac{GM_d}{R}$$

Stars with their apparent mass (M_s) (gravity coupled to this dark matter) appear to rotate about the galactic center at distance R with orbital velocity (v_s) relationship:

$$v_s^2 = \frac{GM_s}{R} \quad \text{where} \quad \frac{M_s}{R} \sim \text{constant}$$

This is a residual effect left over from the time when galaxies were primarily dust or small particles when the formula:

$$\text{deceleration} = C_d A \rho_U c^2$$

ρ_U = conventionally accepted space vacuum density

$$\rho_U = \frac{2}{8\pi} \frac{H_U^2}{G} \approx \frac{1}{8\pi} \frac{c^2}{G} \Lambda \cos(\theta)$$

A = dark object cross sectional area

C_t = thrust coefficient

was primarily applicable and is still applicable in as much as galaxies still consist of small particles (< a few meters) gravitationally coupled to large objects such as stars. These small particles have mean free paths ~1,000 times greater than the galactic size which indicates that they are an optically invisible form outside the galaxy and can truly be called ‘dark but real matter’. The same principle could be applied to Mira’s tail formation although these tail components are visible due to some type of emission and/or absorption mechanism.

4.9. The observed Universe (unaccelerated) Expansion is due to trisine space CPT lattice (Ω_Λ) internal pressure and is at rate defined by the speed of light (c) escape velocity. Baryonic mass within that trisine space CPT lattice ($1 - \Omega_\Lambda$) ‘B’ frame is slowing down or decelerating relative to the universe ‘ R_U ’ frame giving the appearance of expansion with distance in that R_U frame.

$$\begin{aligned} Age_U &\sim B^3 & Age_U &\sim R_U \\ dAge_U &\sim B^2 dB & dAge_U &\sim R_U^0 dR_U \\ d^2 Age_U &\sim B^1 d^2 B & d^2 Age_U &\sim R_U^{-1} d^2 R_U \\ \frac{d^2 B}{dAge_U^2} &\sim B^{-1} & \frac{d^2 R_U}{dAge_U^2} &\sim R_U^1 \end{aligned}$$

4.10. When the trisine is scaled to molecular dimensions, superconductor resonant parameters such as critical fields, penetration depths, coherence lengths, Cooper CPT Charge conjugated pair densities are modeled.

4.11. A superconductor is consider electrically neutral with balanced conjugated charge as per CPT theorem. Observed current flow is due to one CPT time frame being pinned relative to observer.

4.12. The nuclear Delta particles Δ^{++} , Δ^+ , Δ^0 , Δ^- with corresponding quark structure uuu, uud, udd, ddd, with masses of 1,232 MeV/c² are generally congruent with the trisine prediction of $(4/3)\hbar K_B c$ or 1,242 MeV/c² (compared to $\hbar K_B c$ or 932 MeV/c² for the proton ‘ud’ mass) where B reflects the nuclear radius $3\hbar/(16m_c c)$ or 6.65E-14 cm. Also, the experimentally determined delta particle (6E-24 seconds) mean lifetime is consistent and understandably

longer than the proton resonant $time_\pm$ (2.68E-25 second from Table 2.4.1).

4.13. It is noted that the difference in neutron (m_n) and proton (m_p) masses about two electron (m_e) masses ($m_n - m_p \sim 2m_e$).

4.14. The nuclear weak force boson particles (W^-W^+) are associated with energies

$$\frac{B}{A} \frac{\hbar^2 (K_B^2 + K_C^2)}{2m_t} = 79.97 \text{ GeV}$$

$$\frac{B}{A} \frac{\hbar^2 (K_{Ds}^2 + K_{Dn}^2)}{2m_t} \cdot g_s = 79.97 \text{ GeV}$$

$$4\pi \frac{B}{A} \hbar (K_B + K_C) c = 79.67 \text{ GeV}$$

$$4\pi \frac{B}{A} \hbar (K_{Ds} + K_{Dn}) c \cdot g_s = 79.67 \text{ GeV} (80.385 \pm .015)$$

The Z boson is associated with energy

$$e \frac{\hbar^2 (K_B^2 + K_C^2)}{2m_t} = 91.37 \text{ GeV}$$

$$e \frac{\hbar^2 (K_{Ds}^2 + K_{Dn}^2)}{2m_t} \cdot g_s = 91.37 \text{ GeV}$$

$$4\pi \cdot e \cdot \hbar (K_B + K_C) c = 91.03 \text{ GeV}$$

$$4\pi \cdot e \cdot \hbar (K_{Ds} + K_{Dn}) c \cdot g_s = 91.03 \text{ GeV} (91.1876 \pm .0021)$$

e is natural log base 2.7182818284590

4.15. The top quark is associated with energy

$$\frac{\hbar^2 K_A^2}{2m_t} = 174.798 \text{ GeV} (174.98 \pm .76)$$

(Fermilab Today Monday, July 21, 2014 reference:

Precision Measurement of the Top Quark Mass in

Lepton+Jets Final States

V. M. Abazov et al. (D0 Collaboration)

Phys. Rev. Lett. 113, 032002 (2014)

Published July 17, 2014)

4.16. The up (u) quark is associated with

$$\frac{1}{3} \frac{m_e}{m_t} \hbar K_B c = 2.82 \text{ MeV} (1.7 - 3.1)$$

The down (d) quark is associated with

$$\frac{2}{3} \frac{m_e}{m_t} \hbar K_B c = 5.64 \text{ MeV} (4.1 - 5.7)$$

The charm (c) quark is associated with

$$\frac{1}{3} \hbar K_A c = 1.48 \text{ GeV} (1.29 + .50 - .11)$$

4.17. The strange quark (s) is associated with

$$\frac{1}{3} \frac{m_e}{m_t} \frac{\hbar^2}{2m_t} (K_{D_s}^2 + K_B^2) = 96.13 \text{ MeV} (95 \pm 5).$$

4.18. The bottom (b) quark is associated with

$$\hbar K_A c = 4,435 \text{ MeV} (4,190 + 180 - 60)$$

verified [147]

4.19. The Gluon ratio is $60/25 = 2.4 \approx \pi^0/m_t \approx B/A = 2.379761271$.

4.20. Active Galactic Nuclei (AGN) power spectrum as typically presented in reference 89 is indicative of dark energy (related to Ω_Λ) presence as described herein and coincident with the black body nature of trisine dark energy at 8.11E-16 K at a frequency of $1/time_\pm$ or 3.38E-5 Hz.

4.20a. Anomalous Cosmic Rays (ACRs) at 56 MeV are detected by the NASA Voyager I spacecraft prior to passage, during passage and transit beyond our solar system terminal shock. The solar system terminal shock is not the source of Anomalous Cosmic Rays (ACRs). The universe matter is presently 70% composed of a cellular fluid having density 6.38E-30 g/cc as indicated by astrophysical relationship Eqns 2.11.7 and 2.11.22 and each cell cavity ($15,733 \text{ cm}^3$) composed of an ubiquitous unit mass ($m_t = 56 \text{ MeV}/c^2$) having that universe density $mt/\text{cavity} = 6.38E-30 \text{ g}/\text{cc}$.

(This universal density can be considered 'dark energy' mt is of the same order as the Weinberg mass, but it is not the same form as represented in eqn 2.11.13a.

The cellular cavity nature can best be described within the:

Charge (e_\pm) - conjugation

Parity (*trisine mirror images*) - change

Time ($time_\pm$) - reversal (CPT) theorem

In this context, when any particle or object intersects these

cavities, momentum is transferred to the particle or object resulting in an electromagnetic gamma ray release of ~ 56 MeV

(the particle slows down) (This is the mechanism for Pioneer 10 and 11 deceleration as described in chapter 2.) After their release, the 56 MeV gamma ray can interact with all particles, atoms, molecules quantum mechanically changing their energy states on the order of MeV resulting in what has come to be called:

Anomalous Cosmic Rays (ACRs)

Voyager 1 and Voyager 2 will monitor these ACR's as they proceed beyond the terminal shock as long as particles, atoms, molecules exist within interstellar and intergalactic space.

Such an hypothesis is subject to simple 'back of the envelop analysis' or more extensive computer analysis with appropriate algorithms. Essentially Voyager 1 and Voyager 2 are indirectly measuring the 'dark energy'. The presently operating FERMI satellite may directly measure the ubiquitous 56 MeV (in direct 'dark energy' measurement) in the Extra Galactic Background Gamma Ray Emission as was indicated by the previous EGRET satellite.

FERMI instrument systematics are not favorable for 56 MeV detection but such results are being processed by the FERMI team.

(FERMI 56 MeV results are eagerly awaited in conjunction with Voyager1 and Voyager2 ACR's)

4.21. The numerical and dimensional correlation between trisine lattice supercurrent and Maxwell's Ampere's Law is indicated with experimental verification by magnesium boride MgB_2 supercurrent of $1\text{E}7 \text{ amp}/\text{cm}^2$ at T_c of 39/3 K [82].

4.22. The cosmological constant (Λ) and Hubble Constant (H_U) are dimensionally related by the speed of light (c) and the trisine angle (θ) of 22.8° :

$$\Lambda_U = 2H_U^2 / (c^2 \cos(\theta))$$

and also

$$\Lambda_U = \cos(\theta)^{2/3} \left(m_e / (al_p^{1/3} m_p) \right)^6$$

4.23. The cosmological constant simple dimensionless relationship $(\Omega_{\Lambda_U} = 2/(3\cos(\theta)))$ may be a direct measure of trisine space lattice angle (θ).

$$\begin{aligned}
4.24. \text{ The present } (T_b = 2.729K) \text{ CMBR flux} &= \sigma_s T_b^4 \\
&= \\
2\cos(\theta) &\left(\frac{m_p}{m_t} \right) \left(\frac{m_t}{m_e} \right) \left(\frac{m_p}{m_e} \right) \left(\frac{2.821439372 k_B T_B}{cavity} \right) \\
&= 3.14E-03 \text{ (erg cm}^{-2} \text{ sec}^{-1})
\end{aligned}$$

Also the CMBR energy density is:

$$\sigma_s T_b^4 (4/c) = 4.20E-13 \text{ erg / cm}^3$$

Which in terms of mass density is:

$$\sigma_s T_b^4 (4/c^3) = 4.67E-34 \text{ g / cm}^3$$

or 7.32E-05 of universe critical density (ρ_U) 6.38E-30 g/cm³. Consequently, the universe critical density is a very large cold reservoir capable of maintaining hydrogen dense (1 g/cc) BEC's at the critical temperature $T_c = 8.11E-16$ K.

4.25. The Euler constant in terms of fundamental constants may be the Rosetta stone in correlating the superconducting phenomenon and in particular these two correlations.

$$\begin{aligned}
Euler \sim 1 / \sqrt{3} &= F_p / (M_U H_U c) = c^3 / (M_U G H_U) \\
Euler \sim 1 / \sqrt{3} &= -\ln \left(2\Delta_o^{BCS} / (k_b T_c) \right) / (2\pi)
\end{aligned}$$

4.26. Definition of electron mass(m_e)

$$m_e = \alpha m_p \left(\Lambda_U / \cos(\theta)^{2/3} \right)^{1/6} l_p^{1/3} = \alpha \hbar^{2/3} G_U^{-1/3} \left(\Lambda_U / \cos(\theta)^{2/3} \right)^{1/6}$$

and proton mass(m_p)

$$m_p = \hbar^2 \left(\Lambda_U \cos(\theta) / 2 \right)^{1/2} / (3G_U m_t^2)$$

provide a universal cosmological continuity with generalized superconducting equation 2.1.13b repeated here:

$$k_b T_c = \frac{\hbar^2}{\frac{m_e m_t}{m_e + m_t} (2B)^2 + \frac{m_t m_p}{m_t + m_p} (A)^2}$$

This correlation would be applicable to any superconducting equation with the proton mass(m_p) or electron mass(m_e) as a component.

4.27. The increase in spacecraft flyby energy over classical Newtonian calculation is correlated to the universe resonance with earth's atmosphere and solid earth via De Broglie matter waves and its gravitational energy transfer to the spacecraft in unsymmetrical flyby earth or other planetary passage.

4.28. The inherent Trisine B/A ratio may explain the universe alignment of galactic rotation and CMBR anomalies according to what has become called 'The Axis of Evil'

4.29. A correlation would be that there was a time in which the entire universe was at $T_b \sim 1E-9$ K and the CMBR T_c was at $\sim 3,000$ K. The correlation follows:

$$(1E-9/1E13) \sim (1E-20/2E14)^{2/3}$$

due to adiabatic expansion after the Big Bang. All the atomic entities created during the nucleosynthesis event (primarily hydrogen and helium) would be in the form of BECs at $\sim 1E-9$ K. This condition would not last very long as these clouds of BEC's gravitationally condensed resulting in heating that initiated stellar nuclear reactions distributed in galaxies with aggregate density $\sim 1E-24$ g/cc aided perhaps by the extant CMBR 3,000 K at that time but leaving the residual hydrogen BECs in thermal equilibrium with all encompassing and ubiquitous T_c decreasing from 9.80E-10K to 8.11E-16K due to further universe expansion) over the next 13.7 billion years gravitationally observed today as dark matter. This scenario would also resolve the issue of the observed hydrogen helium ratios in proto galaxies similar to nucleosynthesis values. The dark matter was simply hydrogen and helium produced by nucleosynthetic adiabatic expansion frozen out (as dense BEC's) of the rest leaving the star hydrogen and helium dynamics the same.

These hydrogen dense (1 g/cc) BEC's would be largely unnoticed by 21 cm line measurements. Assume that these primeval (through adiabatic Big Bang expansion) hydrogen dense (1 g/cc) BEC's were in rather large chunks, say 10's of kilometers in diameter. The parallel to antiparallel hydrogen (proton electron spin) configuration resulting in 21 cm line would occur randomly in the BEC chunk hydrogens at the known 2.9E-15 /sec rate. Transmittance accordance with Beer's law would indicate that the 22 cm radiation from the BEC center would be attenuated more than that from the BEC near surface resulting in a lower than reality hydrogen spatial density reading obtained by a distant observer. Also, the momentum of a hydrogen nanokelvin BEC at density of 1 g/cc would interact by momentum transfer with a photon of wavelength ~ 140 cm which is much lower than CMBR (.1 cm) or the 21 cm line.

4.30. The critical energy $k_b T_{BEC}$ (at the zero point) associated with BEC formation is related to kT_c through characteristic angle θ (22.8°) by $k_b T_c = k_b T_{BEC} \cos(\theta)$ in essence defining a BCS – BEC crossover.

4.31. A residual delta frequency (~ 3 MHz) is imposed on HI 1420.40575177 MHz (21 cm neutral hydrogen line) assuming to originate at the recombination event [98]. The residual delta frequency is imposed by continuum foreground sources.

It is suggested that the residual delta frequency is a direct indication of 'dark energy' as generally described in this paper as trisine geometry and can be quantified by the equation:

$$\frac{m_e}{m_i} \frac{c}{2B} = 6E6 \text{ Hz (6 MHz)}$$

Essentially the HI oscillatory frequency results from HI 1420.40575177 MHz electromagnetic radiation coupling with the 'dark energy' lattice with trisine geometry.

This ubiquitous trisine lattice is extremely tenuous, having a density of $6.38E-30 \text{ g/cm}^3$ ($m_i/cavity$ or M_u/V_u) and critical temperature $T_c = 8.11E-16 \text{ K}$, and this lattice making up ~ 72.3 percent of the universe back to nucleosynthetic Big Bang epoch that has come to be known as 'dark energy'.

4.32 Mantz[107] provides galaxy cluster energy as a function of redshift 'z' and analysis thereof. This cluster data is replicated in Table 4.32 without the error bars. Mantz[107] indicates a statistical relationship between $E(z)$ M2500 (10^{14} solar mass) and $k_b T$ of log log slope 1.91 ± 0.19 . Within this context, the trisine model predicts a relationship between universe density ρ_u and Age_{UG} of log log slope 2 as indicated on Figure 4.32 blue line and this relationship expressed as

$$\rho_u = (constant/Age_{UG})^2$$

where $Age_{UG} = Age_u (G_u/G)^{1/2} = (1/H_u) (G_u/G)^{1/2}$.

In the Mantz[107] analysis, $E(z) \sim (\rho(z))^{1/2}$.

This Mantz[107] relationship assumes a Newtonian universally fixed gravity (G) in

$$\rho \sim H_u^2/G \text{ and } E(z) \sim H_u$$

and is not dimensionally consistent with universe dimensional expansion. In the trisine hypothesis, the

universally constant ratio H_u/G_u eliminates the square root and establishes the relationship

$$E(z) \sim \rho_u(z) \sim H_u^2/G_u.$$

In the Mantz[107] presentation, there is no attempt to dimensionally relate $E(z)$ and $k_b T$. This may be done in the future, but the slope = 2 related to $1/Age_{UG}$ or

$$\rho_u = (\text{constant}/Age_{UG})^2$$

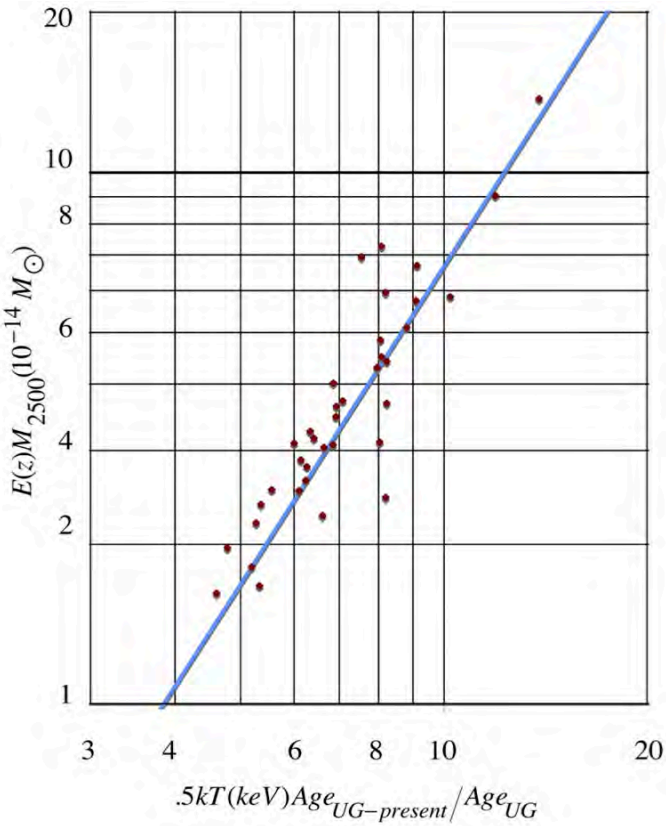
correlates the Mantz[107] analysis to the trisine model where h/Age_{UG} is energy dimensionally and related to change in galaxy cluster plasma energy $k_b T$ with z . It is concluded that Newtonian gravity changes (G_u) with z as reflected in cluster spatial and plasma dynamics.

Table 4.32 Galactic Cluster Data

Cluster	z	E(z)	M2500 (10^{14} solarmass)	$k_b T$ (keV)	E(z) M2500 (10^{14} solar mass)
3C295	0.46	1.28	1.71	5.27	2.19
Abell-1795	0.06	1.03	2.79	6.14	2.87
Abell-1835	0.25	1.14	5.87	9.11	6.66
Abell-2029	0.08	1.04	3.54	8.22	3.67
Abell-2204	0.15	1.08	4.09	8.22	4.40
Abell-2390	0.23	1.12	5.19	10.20	5.82
Abell-2537	0.30	1.16	2.67	8.03	3.11
Abell-383	0.19	1.10	2.16	5.36	2.37
Abell-478	0.09	1.04	4.11	7.96	4.28
Abell-611	0.29	1.16	2.65	6.85	3.07
Abell-963	0.21	1.11	2.74	6.64	3.03
CLJ1226.9+3332	0.89	1.65	5.46	11.90	9.03
MACSJ0011.7-1523	0.38	1.22	2.59	6.42	3.16
MACSJ0159.8-0849	0.40	1.24	4.63	9.08	5.73
MACSJ0242.6-2132	0.31	1.18	2.14	6.10	2.51
MACSJ0329.7-0212	0.45	1.27	2.56	6.34	3.25
MACSJ0429.6-0253	0.40	1.23	1.83	6.61	2.26
MACSJ0744.9+3927	0.69	1.46	3.07	8.08	4.49
MACSJ0947.2+7623	0.35	1.20	4.26	8.80	5.09
MACSJ1115.8+0129	0.36	1.20	6.02	8.08	7.24
MACSJ1311.0-0311	0.49	1.30	2.37	6.00	3.09
MACSJ1359.2-1929	0.45	1.27	2.20	6.27	2.79
MACSJ1423.8+2404	0.54	1.34	2.59	6.92	3.47
MACSJ1427.3+4408	0.49	1.30	1.88	8.19	2.44
MACSJ1427.6-2521	0.32	1.18	1.37	4.61	1.61
MACSJ1532.9+3021	0.36	1.21	3.32	6.86	4.01
MACSJ1621.6+3810	0.46	1.28	2.83	6.93	3.62
MACSJ1720.3+3536	0.39	1.23	3.02	7.08	3.71

MACSJ1931.8–2635	0.35	1.20	4.02	8.05	4.83
MACSJ2046.0–3430	0.42	1.25	1.57	4.78	1.96
MACSJ2229.8–2756	0.32	1.18	1.41	5.33	1.67
MS2137.3–2353	0.31	1.17	2.15	5.56	2.52
RXJ0439.0+0521	0.21	1.11	1.63	5.19	1.81
RXJ1347.5–1144	0.45	1.27	10.80	13.80	13.73
RXJ1504.1–0248	0.22	1.11	5.33	8.19	5.93
RXJ2129.6+0005	0.24	1.13	2.34	6.24	2.63
Zwicky=3146	0.29	1.16	5.99	7.54	6.92

Figure 4.32



4.33. A model is developed for expressing this data using the Trisine parameters developed herein within the context of Black Body theory having the basic dimensional units of energy/area/time and then scaled to universe time and volume development:

$$T_{cr} = (1/2) m_t v_{dxr}^2 / k_b = m_t c^2 / (2 k_{mxr} \epsilon_{xr} k_b)$$

$$\begin{aligned} \sigma T_{cr}^4 \xi &= \sigma T_p^4 \frac{\text{cavity}}{V_U} \frac{c}{4} \frac{\text{Age}_U}{\text{Age}_{UG}} \left(\frac{B_{Present}}{\text{R}_{U_{Present}}} \right)^{\frac{6}{8}} \frac{1}{2\pi} \\ &= \left(\frac{B}{A} \right)^{\frac{12}{8}} \frac{\pi^8 G^8 m_t^8 c^{\frac{47}{8}} \hbar^{\frac{66}{8}}}{2^{\frac{67}{8}} 3^{\frac{10}{8}} 4^{\frac{8}{8}} 15^{\frac{8}{8}} \hbar^{\frac{28}{8}}} \left(\frac{B_{Present}}{\text{R}_{U_{Present}}} \right)^{\frac{6}{8}} \frac{1}{2\pi} (k_b T_r)^{-\frac{7}{8}} \\ \sigma T_{cr}^4 \xi (k_b T_j)^{-\frac{16}{8}} &= \sigma T_{cr}^4 \frac{\text{cavity}}{V_U} \frac{c}{4} \frac{\text{Age}_U}{\text{Age}_{UG}} \left(\frac{B_{Present}}{\text{R}_{U_{Present}}} \right)^{\frac{6}{8}} \frac{1}{2\pi} (k_b T_j)^{-\frac{16}{8}} \\ &= \left(\frac{B}{A} \right)^{\frac{12}{8}} \frac{\pi^8 G^8 m_t^8 c^{\frac{47}{8}} \hbar^{\frac{66}{8}}}{2^{\frac{67}{8}} 3^{\frac{10}{8}} 4^{\frac{8}{8}} 15^{\frac{8}{8}} \hbar^{\frac{28}{8}}} \left(\frac{B_{Present}}{\text{R}_{U_{Present}}} \right)^{\frac{6}{8}} \frac{1}{2\pi} (k_b T_j)^{-\frac{7}{8}} (k_b T_j)^{-\frac{16}{8}} \\ &= \left(\frac{B}{A} \right)^{\frac{12}{8}} \frac{\pi^8 G^8 m_t^8 c^{\frac{47}{8}} \hbar^{\frac{66}{8}}}{2^{\frac{67}{8}} 3^{\frac{10}{8}} 4^{\frac{8}{8}} 15^{\frac{8}{8}} \hbar^{\frac{28}{8}}} \left(\frac{B_{Present}}{\text{R}_{U_{Present}}} \right)^{\frac{6}{8}} \frac{1}{2\pi} (k_b T_j)^{-\frac{23}{8}} \end{aligned}$$

where the resonant mass temperature (T_j) is defined as:

$$\begin{aligned} T_j &= (m_t v_{dx}^4 / 4) (1/c^2) / k_b \\ &= (m_t (v_{dx}^2 + v_{dy}^2 + v_{dz}^2)^2 / 4) (1/c^2) / k_b \\ &= \frac{1}{4} \frac{m_t c^2}{(k_m \epsilon)^2} \frac{1}{k_b} \end{aligned}$$

and resonant mass (m_r)

$$m_r = m_t v_{dx}^2 / c^2$$

and permittability (ϵ) and permittivity (ϵ) relationships

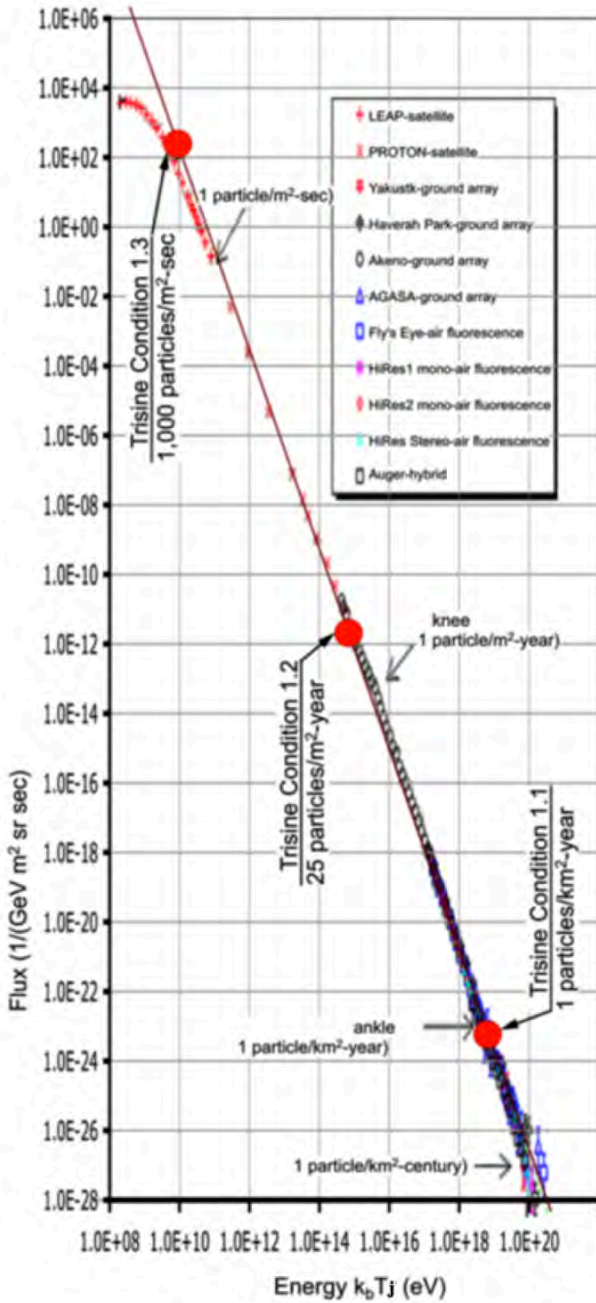
$$k_m = \frac{1}{\epsilon} \frac{1}{\frac{1}{\epsilon_x k_{mx}} + \frac{1}{\epsilon_y k_{my}} + \frac{1}{\epsilon_z k_{mz}}} \quad \epsilon = \frac{3}{\frac{1}{\epsilon_x} + \frac{1}{\epsilon_y} + \frac{1}{\epsilon_z}}$$

$$T_j = \frac{1}{4} \frac{m_t c^2}{(k_m \epsilon)^2} \frac{1}{k_b} \quad T_{jr} = \frac{1}{4} \frac{m_t c^2}{(k_{mr} \epsilon_r)^2} \frac{1}{k_b}$$

The following condition represents particle production per area and time.

$$\sigma T_{cr}^4 \xi (k_b T_j)^{-8} = \left(\frac{B}{A} \right)^{\frac{12}{8}} \frac{\pi^{\frac{8}{8}} G^{\frac{8}{8}} m_t^{\frac{47}{8}} c^{\frac{66}{8}}}{2^{\frac{67}{8}} 3^{\frac{10}{8}} 4^{\frac{8}{8}} 15^{\frac{28}{8}} \hbar^{\frac{8}{8}}} \left(\frac{B_{Present}}{R_{U_{Present}}} \right)^{\frac{6}{8}} \frac{1}{2\pi} (k_b T_j)^{-\frac{15}{8}}$$

Figure 4.33.1 Experimental Cosmic Ray data for various sources compared to the Trisine universe model



Conditions 1.1, 1.2 and 1.3 are clearly defined in Figure 4.33.1 as representing group phase reflection nucleosynthetic conditions originating the observed cosmic ray particles by various ground and satellite platforms including the recently launched Alpha Magnetic

Spectrometer-02 (AMS-02) (repeated here from the introduction) and IceTop stations [119] in the knee proximity.

1.1	z_R	3.82E+46	z_R	3.82E+46	unitless
	z_B	3.37E+15	z_B	3.37E+15	unitless
	T_a	6.53E+11	T_a	6.53E+11	°K
	T_b	9.19E+15	T_{br}	9.19E+15	°K
	T_c	9.19E+15	T_{cr}	9.19E+15	°K
	T_d	1.53E+14	T_{dr}	1.53E+14	°K
	T_i	1.10E+14	T_{ir}	1.10E+14	°K
	T_r	8.07E+22	T_{rr}	8.07E+22	°K

This energy conjunction at $T_c = T_b$ marks the beginning of the universe where time and space are not defined in a group phase reflection condition where $v_d \sim v_e \gg c$. The universe mass (M_u) is nominally at 2.08E-37 gram the radiation mass (M_v) $\sim \sqrt{3}m_t$. This nearly corresponds to the graphically displayed ankle position.

1.2	z_R	3.67E+43	z_R	3.67E+43	unitless
	z_B	3.32E+14	z_B	3.32E+14	unitless
	T_a	6.53E+11	T_a	6.53E+11	°K
	T_b	9.07E+14	T_{br}	6.05E+07	°K
	T_c	8.96E+13	T_{cr}	1.19E+09	°K
	T_d	4.80E+13	T_{dr}	8.89E+09	°K
	T_i	1.08E+13	T_{ir}	3.94E+10	°K
	T_r	7.67E+18	T_{rr}	6.98E+06	°K

This T_c defines superconductive phenomenon as dictated by the proton density 2.34E14 g/cm³ and radius B of 6.65E-14 cm (8.750E-14 cm NIST reported charge radius value) which is defined at a critical temperature T_c of

$$T_c = T_d = g_d m_t \hbar c^3 / (e^2 k_b) = g_d m_t c^2 / (\alpha k_b)$$

that is a consequence of a group phase reflection condition:

$$v_{dx} = \left(\frac{2}{\alpha} \right)^{\frac{1}{2}} c$$

that is justifiable in elastic resonant condition (see equations 2.1.5 and 2.1.6 and follow-on explanation) and

$$\frac{\hbar c}{e^2} = \frac{m_r}{m_t} = \frac{v_{dx}^2}{2c^2} = \text{fine structure constant} = \frac{1}{\alpha}$$

This nearly corresponds to the graphically displayed knee position.

1.3	z_R	8.14E+39	z_R	8.14E+39	unitless
	z_B	2.01E+13	z_B	2.01E+13	unitless
	T_a	6.53E+11	T_a	6.53E+11	°K
	T_b	5.49E+13	T_{br}	1.00E+09	°K
	T_c	3.28E+11	T_{cr}	3.25E+11	°K
	T_d	1.18E+13	T_{dr}	3.61E+10	°K
	T_i	6.54E+11	T_{ir}	6.51E+11	°K
	T_r	1.03E+14	T_{rr}	5.21E+11	°K

This temperature condition represents the undefined but potentially high energy barrier luminal state where $v_{dx} = v_{dxx} = c$ and $v_{ex} = v_{exx} > c$,
 $T_b = T_{br}$, $T_c = T_{cr}$, $T_d = T_{dr}$, $T_i = T_{ir} = T_a$, $T_j = T_{jr}$ and trisine length

$$B = 4\pi \text{ nuclear radius}$$

which defines a condition for the size of the proton as it 'freezes' out of early expanding universe nucleosynthesis

$$\sigma T_{cr}^4 \xi (k_b T_j)^{-\frac{8}{3}} = \left(\frac{B}{A}\right)^{\frac{12}{8}} \frac{\pi^8 G^8 m_t^8 c^8}{2^{\frac{67}{8}} 3^{\frac{10}{8}} 4^{\frac{8}{8}} 15^{\frac{28}{8}} \hbar^8} \left(\frac{B_{Present}}{R_{U_{Present}}}\right)^{\frac{6}{8}} \frac{1}{2\pi} (k_b T_j)^{-\frac{15}{8}}$$

Energy per nucleon Voyager 1 data is presented in Figure 4.33.2 with the intention of matching to reported cosmic ray data as presented in Figure 4.33.1.

Figure 4.33.2 Energy per nucleon Spectra for Voyager 1 for the first 295 days of 2012 Data from University of Maryland Website <http://sd-www.jhuapl.edu/VOYAGER/>

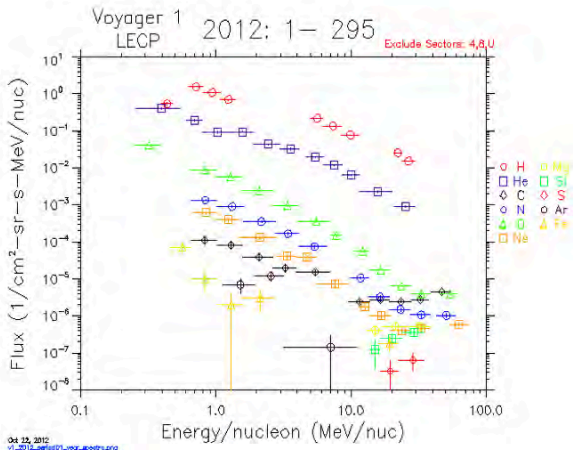
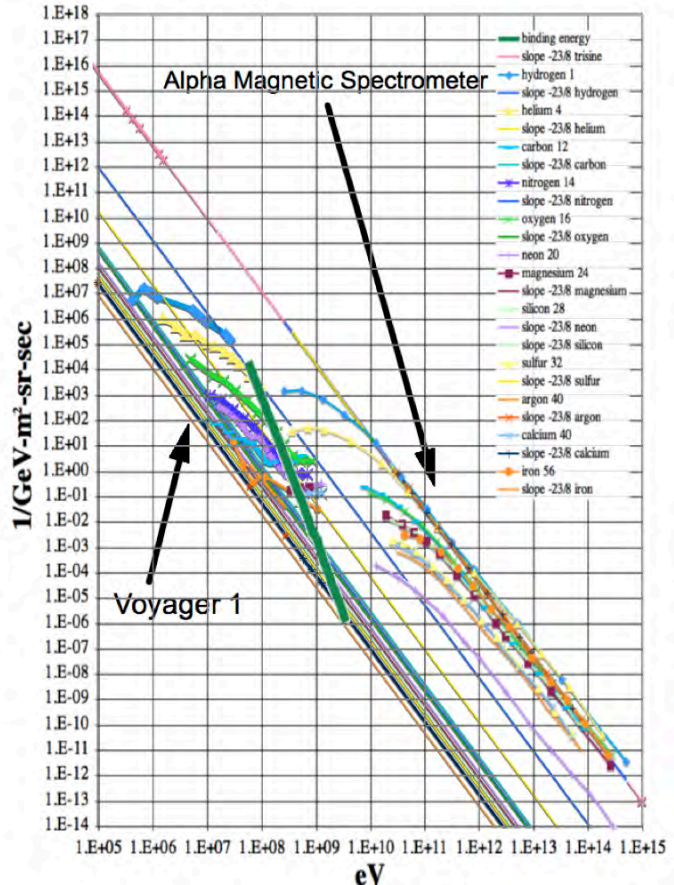


Figure 4.33.3 Dimensionally changed total energy spectra for Voyager 1 for the first 295 days of 2012 as it proceeds beyond the helio shock wave into interstellar space as an extension of Figure 4.33.1. A discontinuity is noted between Alpha Magnetic Spectrometer and Voyager 1 data and most probably defined by the isotopic binding energy.



Linear intensities have log log -23/8 slopes as per the following

$$\text{Intensity} \left(\frac{1}{\text{MeV-sec-sr-m}^2} \right) \sim \left(\text{Atomic Number} \times m_c c^2 \right)^{-\frac{23}{8}}$$

Reported isotopic binding energies including rest mass energy

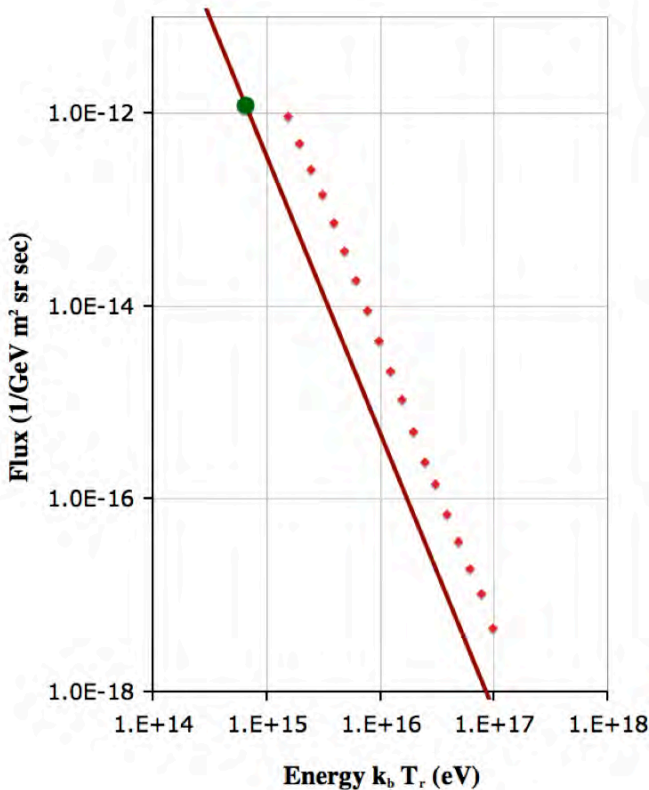
$$\left(\text{Isotopic Binding Energy} + \text{Atomic Number} \times m_c c^2 \right)^{-\frac{23}{8}}$$

(green line) are provided as a reference beyond which there may be a tendency for isotopic kinetic instability.

Selected IceCube[125 -table 3] data at the knee continues to confirm these relationships as per Figure 4.33.3.

Evidence for solar wind source and not extra helio source of tens-of-keV/n neutral ions [143] is concluded in that their log-log slope does not conform to interstellar-extragalactic log-log slope -23/8 as presented in Figure 4.33.1 of this report.

Figure 4.33.4 Experimental IceCubeCosmic Ray proton data[125, -table 3] (red squares without error bars) at the knee with Trisine Condition 1.2 (green dot) on Trisine model near universe $-23/8$ log log linear slope nucleosynthetic condition (red line).



Electron and positron flux as measured by FERMI [136 Figure 3] (with energy and nucleon conversion) is consistent with $-23/8$ log log slope as presented in Figure 4.33.1 although reported as -3 log log slope.

4.34. Also, there is an indication of a 56 MeV peak in black body curve from the Energetic Gamma Ray Experiment Telescope (EGRET) instrument aboard The Compton Gamma Ray Observatory Mission (Comptel) spacecraft, which generally observed the extra galactic diffuse background x-ray radiation. The data graphic is replicated below in Figure 4.2 by author permission [73] with the 56 MeV resonant energy superimposed. In addition the following black body equation models the log linear characteristic of the energy data with T_p conforming to the phase velocity being less then the speed of light $v_{cr} < v_{er} < c < v_e < v_c$ and approaching $v_d \sim c$.

$$\begin{aligned}\sigma T_{cr}^4 \xi &= \sigma T_{cr}^4 \frac{cavity}{V_U} \frac{c}{4} \left(\frac{1}{R_{U_{Present}}} \right)^{\frac{6}{3}} \frac{1}{2\pi} time_{\pm} H_U \\ &= \frac{2m_t^{\frac{13}{3}} c^{\frac{23}{3}}}{3^{\frac{13}{6}} 4^{\frac{6}{3}} 15^{\frac{3}{2}} \pi^{\frac{8}{3}} \hbar^{\frac{9}{2}}} \left(\frac{1}{R_{U_{Present}}} \right)^{\frac{6}{3}} \frac{1}{2\pi} \left(\frac{1}{2} \hbar H_U \right)^{\frac{1}{3}}\end{aligned}$$

or

$$= \left(\frac{B}{A} \right)^{\frac{10}{3}} - \frac{\pi^{\frac{2}{3}} m_t^{\frac{13}{3}} c^{\frac{23}{3}}}{2^{\frac{6}{3}} 3^{\frac{13}{6}} 4^{\frac{16}{3}} 15^{\frac{3}{2}} \hbar^{\frac{9}{2}}} \left(\frac{1}{R_{U_{Present}}} \right)^{\frac{6}{3}} \frac{1}{2\pi} \left(\frac{1}{2} \hbar H_U \right)^{\frac{1}{3}}$$

This equation is dimensionally correct in the CGS system with energy expressed graphically(green line) as MeV in Figures 4.34.1 to 4.34.3. Note that the abscissa is divided by an instrument 2π factor (to be checked). This graphic expression is dimensionally consistent with EGRET and FERMI featureless data and as log log linear with negative $1/3$ slope slightly different than the observed FERMI negative $1/2.41$ slope[91]. The phase velocity $v_p < c < v_e < v_d$ (and approaching $v_d \sim c$) implies that the Figures 4.34.1 to 4.34.3 data signatures reflect universe conditions ($z_B = 2.01E+13$) in the early stages of nucleosynthesis (conditions 1.1 to 1.3 as indicated in the introduction plus an interim condition 1.3a as defined below). These relic expressions as a presently observable phenomenon look back in time further than the Cosmic Microwave Background Radiation (CMBR) providing further insight into the universe evolution. Further analysis of FERMI data may provide descriptive features indicating nucleosynthetic processes

Table 4.34.1

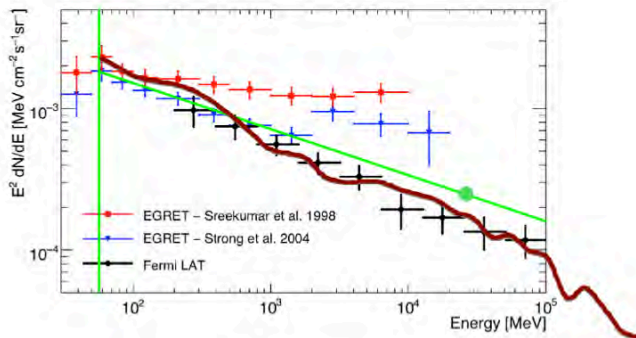
$T_c (^{\circ}K)$	1.43E+12	2.10E+12	9.73E+12	4.52E+13	2.10E+14
$T_b (^{\circ}K)$	1.15E+14	1.39E+14	2.99E+14	6.45E+14	1.39E+15
$T_{cr} (^{\circ}K)$	7.35E+10	5.01E+10	1.08E+10	2.32E+09	5.00E+08
$\sigma T_p^4 \xi$	2.03E-03	1.67E-03	7.77E-04	3.60E-04	1.67E-04
$(1/2) \hbar H_U$ (MeV)	56.27	1.00E+02	1.00E+03	1.00E+04	1.00E+05
R_U (cm)	3.04E-13	1.71E-13	1.71E-14	1.70E-15	1.70E-16
H_U (sec $^{-1}$)	1.71E+23	3.04E+23	3.04E+24	3.05E+25	3.05E+26
G_U (cm)	4.93E+33	8.77E+33	8.77E+34	8.79E+35	8.80E+36
Age_U (sec)	5.85E-24	3.29E-24	3.29E-25	3.28E-26	3.28E-27
Age_{UG} (sec)	1.59E-03	1.19E-03	3.77E-04	1.19E-04	3.77E-05

There seems to be two models tested by isotropic and galactic diffuse models that are provided by the NASA-FSSC[104].

1. Diffuse emission is from unresolved point sources that will be resolved with further analysis.
2. Diffuse emission is from unresolved sources that will never be resolved as point sources with further analysis.

Model one(1) would appear to be the easy approach. Under model two(2), one is left with the vexing question as to what is the source. Logically it could be another isotropic source analogous to the Cosmic Microwave Background Radiation (CMBR) as proposed herein.

Figure 4.34.1 Diffuse X-ray Background radiation including that from EGRET and FERMI [73, 91] with a $m_c c^2 = 56$ MeV reference cutoff energy (vertical green line) and sloping (-1/3) log log green line imposed as a remnant from Big Bang nucleosynthesis with group phase reflection Condition 1.2 as green circle. The brown line is from NASA -FSSC Pass 7 (V6) Clean (front+back) P7CLEAN_V6 iso_p7v6clean.txt converted by $x \text{ MeV}^2$ for dimensional comparison.



Inclusive in these observations would be the detected radiation from the Crab Nebula possibly correlated to its expansion shockwave. Verification is anticipated with the (FERMI) platform providing a much more detailed delineation of the extra galactic diffuse X-ray background radiation and potentially the trisine space lattice 56 MeV/c² dark energy component evidenced by interaction with known celestial bodies such as comets, planets, asteroids, stars, galaxies, intergalactic dust etcetera. Such data is presented in

The log log -1/3 slope describing Isotropic Diffuse Extragalactic Gamma radiation may be further described as having origins within group phase reflection Big Bang nucleosynthesis processes a phenomenon replicated in present standard model nuclear Asymtotic Freedom observations Figure 4.36.1

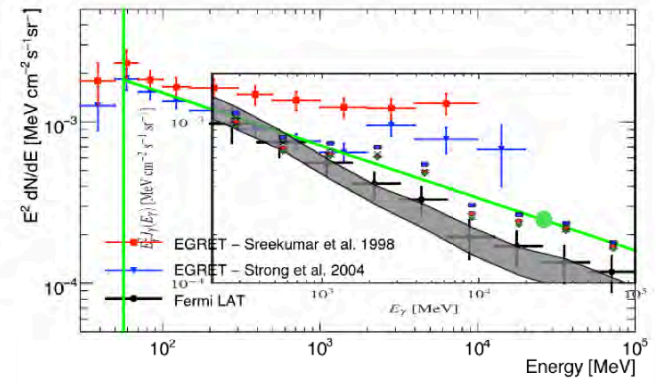
This Isotropic Diffuse Extragalactic Gamma radiation universe origin appears to be verified by the isotropic spectra[115] Fig. 29. The spectra of the isotropic component overlays with good visual agreement (log log -1/3 slope) on

Figure 4.34.1 and displayed on Figure 4.34.2 appears to support hypothesis 2 from above.

2. Diffuse emission is from unresolved sources that will never be resolved as point sources with further analysis.

The higher than isotropic FERMI energies[115] are a result of inverse Compton scattering of Big Bang isotropic energies subjected to inverse Compton scattering while transiting galactic medium such as Black Holes and energetic gases or plasmas a similar conceptual process as Sunyaev-Zeldovich effect on Cosmic Microwave Background Radiation(CMBR).

Figure 4.34.2 Diffuse X-ray Background radiation as indicated in Figure 4.34.1 and including that from FERMI [115] with a $m_c c^2 = 56$ MeV reference cutoff energy (vertical green line) and sloping (-1/3) log log green line imposed as a remnant from Big Bang nucleosynthesis with group phase reflection Condition 1.2 (green circle) and with Clean data removed and grey area correlating [115] with Fermi LAT data with uncertainty expressed in quadrature.



Fermi LAT Data from Table I [123] is replicated below and modified by Trisine Cosmic Ray photons achieving the Trisine slope of -1/3 vs the reported -1/2.438 indicating the possibility of Cosmic Ray(CR) contamination of Fermi LAT data. The following previously derived equation generates the Trisine Cosmic Ray particles:

$$\sigma T_{cr}^4 \xi(k_b T_{cr})^{\frac{8}{8}} = \left(\frac{B}{A}\right)^{\frac{12}{8}} \frac{\pi^{\frac{8}{8}} G^{\frac{8}{8}} m_t^{\frac{47}{8}} c^{\frac{66}{8}}}{2^{\frac{67}{8}} 3^{\frac{10}{8}} 4^{\frac{8}{8}} 15^{\frac{8}{8}} \hbar^{\frac{28}{8}}} \left(\frac{B_{Present}}{R_{U,Present}}\right)^{\frac{6}{8}} \frac{1}{2\pi} (k_b T_j)^{-\frac{15}{8}}$$

A 11,000 factor modifies the Fermi gamma ray n by:

$$n = n - 11,000 \times \text{Trisine CR}$$

Table 4.34.2

FERMI		Trisine(CR)																
Energy Range corrected		Particles		Energy		n flux		n flux										
		# cm ⁻² sec ⁻¹		GeV ⁻¹		MeV cm ⁻² sec ⁻¹		MeV sec ⁻¹										
GeV	GeV	n sr ⁻¹	corrected	n sr ⁻¹	MeV	n sr ⁻¹	MeV	n sr ⁻¹	MeV	67.3	70.6	181	2.31E-03	156	8.80E-11	68,950	4.18E-04	3.60E-04
4.8	5.1	7,156	3.23E-01	3,604	6.29E-08	4,950	1.54E-03	7.76E-04	81.8	70.6	148	2.11E-03	125	6.90E-11	72,400	3.62E-04	3.05E-04	
5.1	5.3	6,638	2.94E-01	3,400	5.54E-08	5,200	1.50E-03	7.67E-04	85.8	74.2	172	1.92E-03	151	7.70E-11	76,050	4.45E-04	3.91E-04	
5.3	5.6	6,295	2.70E-01	3,329	4.95E-08	5,450	1.47E-03	7.78E-04	90.1	77.9	128	1.76E-03	109	5.46E-11	79,850	3.48E-04	2.96E-04	
5.6	5.9	5,684	2.44E-01	3,002	4.21E-08	5,750	1.39E-03	7.35E-04	94.6	81.8	119	1.60E-03	101	4.85E-11	83,800	3.41E-04	2.90E-04	
5.9	6.2	5,477	2.22E-01	3,039	3.83E-08	6,050	1.40E-03	7.78E-04	99.4	85.8	129	1.47E-03	113	5.03E-11	87,950	3.89E-04	3.40E-04	
6.2	6.5	5,162	2.02E-01	2,935	3.40E-08	6,350	1.37E-03	7.80E-04	104	74.2	101	1.01E-03	90	3.32E-11	107,000	3.80E-04	3.38E-04	
6.5	6.8	4,744	1.86E-01	2,702	2.94E-08	6,650	1.30E-03	7.41E-04	110	77.9	115	9.24E-04	67	2.42E-11	112,500	3.06E-04	2.66E-04	
6.8	7.1	4,317	1.71E-01	2,437	2.52E-08	6,950	1.22E-03	6.87E-04	115	81.8	121	8.45E-04	73	2.47E-11	118,000	3.44E-04	3.05E-04	
7.1	7.5	3,944	1.56E-01	2,230	2.17E-08	7,300	1.16E-03	6.54E-04	121	85.8	127	7.70E-04	59	1.94E-11	124,000	2.98E-04	2.61E-04	
7.5	7.9	3,744	1.41E-01	2,193	1.94E-08	7,700	1.15E-03	6.74E-04	127	90.1	133	7.04E-04	62	1.94E-11	130,000	3.28E-04	2.92E-04	
7.9	8.3	3,416	1.28E-01	2,005	1.67E-08	8,100	1.10E-03	6.43E-04	133	94.6	140	6.43E-04	48	1.46E-11	136,500	2.72E-04	2.37E-04	
8.3	8.7	3,012	1.17E-01	1,723	1.40E-08	8,500	1.01E-03	5.79E-04	140	99.4	147	5.85E-04	47	1.35E-11	143,500	2.78E-04	2.44E-04	
8.7	9.1	2,763	1.07E-01	1,581	1.21E-08	8,900	9.58E-04	5.48E-04	147	104.3	154	3.35E-04	27	8.10E-12	150,500	1.83E-04	1.51E-04	
9.1	9.6	2,630	9.80E-02	1,552	1.09E-08	9,350	9.53E-04	5.62E-04	154	110	162	4.89E-04	55	1.41E-11	158,000	3.52E-04	3.20E-04	
9.6	10	2,372	8.97E-02	1,385	9.30E-09	9,800	8.93E-04	5.22E-04	162	115	170	3.45E-04	25	6.77E-12	166,000	1.87E-04	1.56E-04	
10	10.5	2,301	8.25E-02	1,394	8.50E-09	10,250	8.93E-04	5.41E-04	170	121	178	2.40E-04	22	5.64E-12	174,000	1.71E-04	1.41E-04	
10.5	11.1	2,071	7.48E-02	1,248	7.20E-09	10,800	8.40E-04	5.06E-04	178	127	187	2.37E-04	41	9.40E-12	182,500	3.13E-04	2.85E-04	
11.1	11.6	1,994	6.81E-02	1,245	6.55E-09	11,350	8.44E-04	5.27E-04	187	133	197	3.39E-04	31	7.00E-12	192,000	2.58E-04	2.31E-04	
11.6	12.2	1,936	6.23E-02	1,250	6.00E-09	11,900	8.50E-04	5.49E-04	197	140	207	3.08E-04	24	5.20E-12	202,000	2.12E-04	1.86E-04	
12.2	12.8	1,833	5.69E-02	1,208	5.36E-09	12,500	8.38E-04	5.52E-04	207	147	217	2.82E-04	27	5.55E-12	212,000	2.49E-04	2.24E-04	
12.8	13.4	1,760	5.21E-02	1,187	4.87E-09	13,100	8.36E-04	5.64E-04	217	154	228	2.57E-04	18	3.73E-12	222,500	1.85E-04	1.60E-04	
13.4	14.1	1,625	4.75E-02	1,102	4.24E-09	13,750	8.02E-04	5.44E-04	228	162	239	2.35E-04	15	3.07E-12	233,500	1.67E-04	1.43E-04	
14.1	14.8	1,519	4.33E-02	1,042	3.75E-09	14,450	7.83E-04	5.37E-04	239	170	251	2.15E-04	22	3.94E-12	245,000	2.36E-04	2.13E-04	
14.8	15.6	1,418	3.94E-02	985	3.33E-09	15,200	7.69E-04	5.34E-04	251	178	264	1.96E-04	16	2.84E-12	257,500	1.88E-04	1.66E-04	
15.6	16.3	1,396	3.60E-02	1,000	3.11E-09	15,950	7.91E-04	5.67E-04										
16.3	17.2	1,337	3.28E-02	976	2.83E-09	16,750	7.94E-04	5.79E-04										
17.2	18	1,183	2.99E-02	854	2.37E-09	17,600	7.34E-04	5.30E-04										
18	18.9	1,122	2.74E-02	821	2.13E-09	18,450	7.25E-04	5.30E-04										
18.9	19.9	1,048	2.49E-02	774	1.88E-09	19,400	7.08E-04	5.22E-04										
19.9	20.9	1,012	2.27E-02	762	1.72E-09	20,400	7.16E-04	5.39E-04										
20.9	21.9	942	2.07E-02	714	1.52E-09	21,400	6.96E-04	5.27E-04										
21.9	23	901	1.90E-02	692	1.37E-09	22,450	6.90E-04	5.31E-04										
23	24.1	825	1.73E-02	634	1.19E-09	23,550	6.60E-04	5.07E-04										
24.1	25.4	791	1.58E-02	617	1.08E-09	24,750	6.62E-04	5.16E-04										
25.4	26.6	694	1.44E-02	536	8.90E-10	26,000	6.02E-04	4.64E-04										
26.6	27.9	690	1.32E-02	545	8.40E-10	27,250	6.24E-04	4.93E-04										
27.9	29.3	653	1.20E-02	521	7.60E-10	28,600	6.22E-04	4.96E-04										
29.3	30.8	644	1.10E-02	523	7.10E-10	30,050	6.41E-04	5.21E-04										
30.8	32.4	537	9.99E-03	427	5.60E-10	31,600	5.59E-04	4.45E-04										
32.4	34	538	9.11E-03	438	5.32E-10	33,200	5.86E-04	4.77E-04										
34	35.7	490	8.31E-03	399	4.60E-10	34,850	5.59E-04	4.54E-04										
35.7	37.5	484	7.58E-03	401	4.31E-10	36,600	5.77E-04	4.78E-04										
37.5	39.3	429	6.93E-03	353	3.64E-10	38,400	5.37E-04	4.41E-04										
39.3	41.3	437	6.33E-03	367	3.54E-10	40,300	5.75E-04	4.83E-04										
41.3	43.4	386	5.77E-03	323	2.98E-10	42,350	5.34E-04	4.47E-04										
43.4	45.5	360	5.27E-03	302	2.65E-10	44,450	5.24E-04	4.39E-04										
45.5	47.8	323	4.81E-03	270	2.26E-10	46,650	4.92E-04	4.11E-04										
47.8	50.2	320	4.39E-03	272	2.14E-10	49,000	5.14E-04	4.36E-04										
50.2	52.7	289	4.00E-03	245	1.85E-10	51,450	4.90E-04	4.15E-04										
52.7	55.3	242	3.66E-03	202	1.48E-10	54,000	4.32E-04	3.60E-04										
55.3	58.1	253	3.34E-03	216	1.48E-10	56,700	4.76E-04	4.07E-04										
58.1	61	208	3.04E-03	175	1.16E-10	59,550	4.11E-04	3.45E-04										
61	64.1	208	2.78E-03	177	1.11E-10	62,550	4.34E-04	3.71E-04										
64.1	67.3	189	2.53E-03	161	9.60E-11	65,700	4.14E-04	3.53E-04										

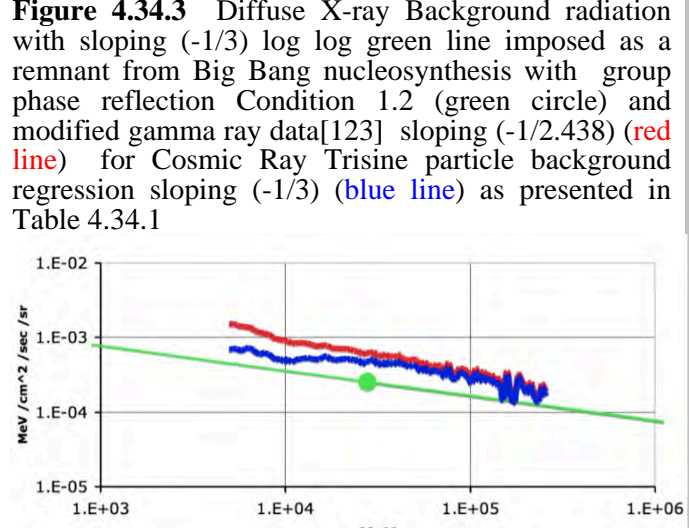
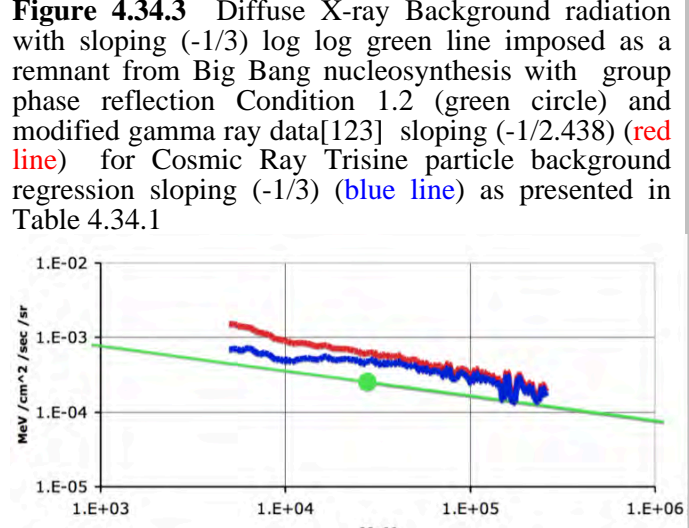
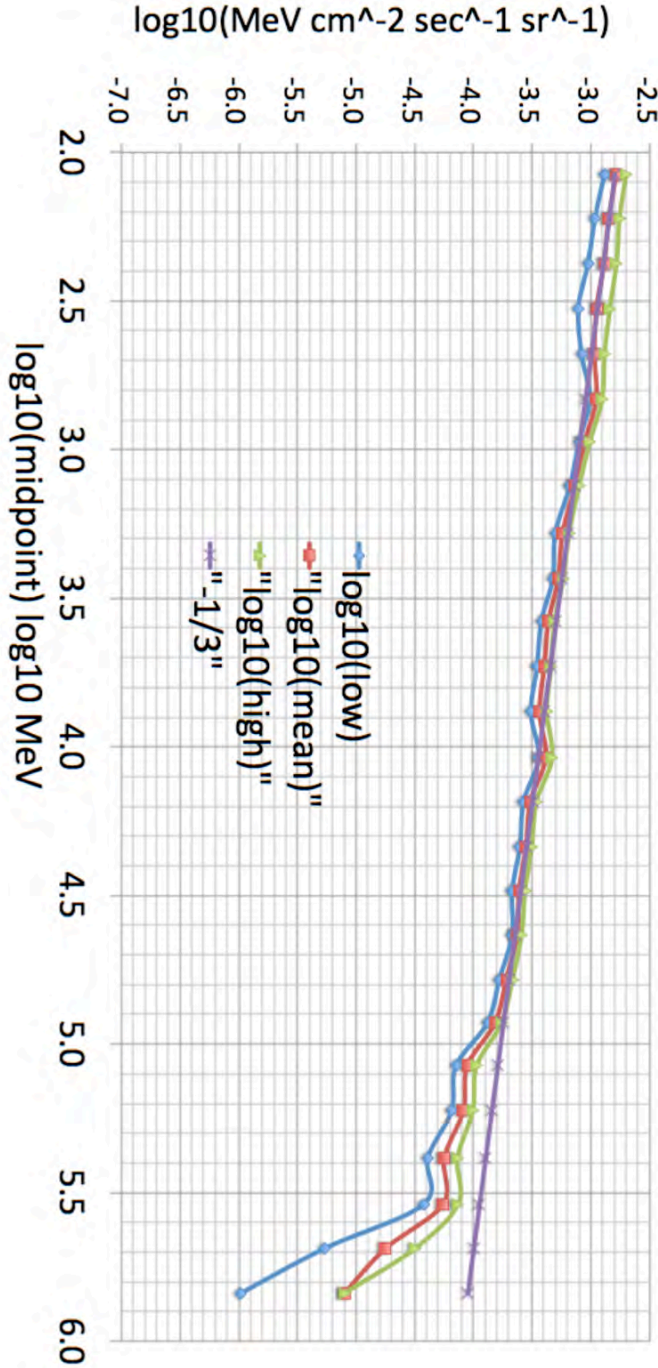


Figure 4.34.4 Diffuse X-ray Background radiation[151] with sloping (-1/3) log log green line imposed as a remnant from Big Bang nucleosynthesis with group phase reflection Condition 1.2 (green circle)



In summary, dimensional logic leads to the conclusion that empirically observed astrophysical X-Ray and Gamma Ray were created in the first second of the universe under group phase reflection Trisine Conditions 1.1 to 1.3a as presented as green circles in Figure 4.34.3. These green circles are not to any particular scale but their size is indicative becoming

larger with universe time Age_{UG} and universe size R_U while fitting the nodes of X-Ray and Gamma Ray spectra. The additional 1.3a to introductory Trisine Conditions is as follows which appears appropriate for building up atomic structures in the Big Bang event at trisine condition 1.3a:

1.3a	z_R	9.72E+34	z_R	9.72E+34	unitless
	z_B	4.60E+11	z_B	4.60E+11	unitless
	T_a	6.53E+11	T_a	6.53E+11	°K
	T_b	1.25E+12	T_{br}	2.39E+15	°K
	T_c	1.71E+08	T_{cr}	6.22E+14	°K
	T_d	9.04E+11	T_{dr}	3.95E+13	°K
	T_i	1.50E+10	T_{ir}	2.85E+13	°K
	T_j	2.80E+07	T_{jr}	3.70E+20	°K

This temperature condition defined by

$$B = \frac{m_e}{m_t} \text{Bohr radius} = \frac{m_e}{m_t} \frac{\hbar}{am_e c} = \frac{\hbar}{am_e c}$$

Equation 2.14.7a repeated here

$$hH_U = \frac{\text{cavity}}{\text{chain}} G_U \frac{m_t^2}{B_p} \quad (2.14.7a)$$

provides a mechanism explaining the CERN (July 4, 2012) observed particle at 126.5 GeV as well as the astrophysical Fermi ~130 GeV [127]. The astrophysical ~130 GeV energy is sourced to a Trisine Condition 1.2 nucleosynthetic event with a fundamental G_U gravity component.

$$\begin{aligned} & g_s^2 \frac{1}{2} hH_U \cos(\theta) \\ &= g_s^2 \frac{1}{2} \frac{\text{cavity}}{\text{chain}} G_U \frac{m_t^2}{\text{proton radius}} \cos(\theta) \\ &= 126.5 \text{ GeV} \end{aligned}$$

Also the energy MeV scaling in Figures 4.34.1, 4.34.2, 4.34.3 & 4.34.5 may be a consequence of and directly related to G_U gravity scaling.

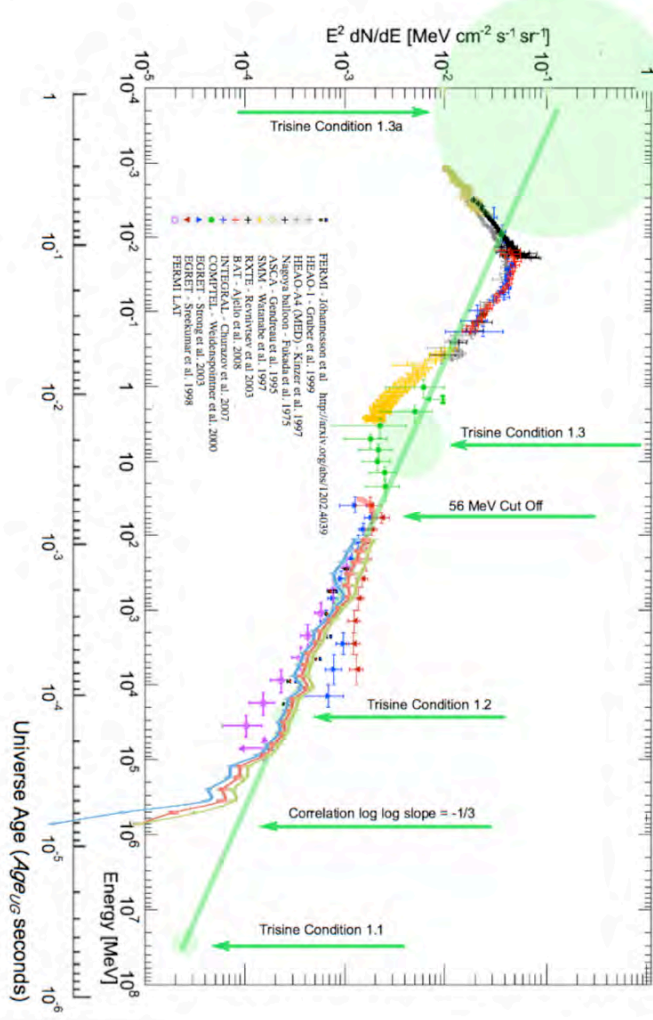
$$H_U = \frac{1}{h} \frac{\text{cavity}}{\text{chain}} G_U \frac{m_t^2}{\text{proton radius}}$$

Where $\text{proton radius} = B_p / (2 \sin(\theta))$ or $x_U / (8 \sin(\theta))$

$$= 8.59\text{E-}14 \text{ (8E-14)}$$

The value B_p represents trisine cell dimension B at Trisine Condition 1.2

Figure 4.34.5 Diffuse broader band X-ray Background radiation including that from FERMI [115, 151] with a $m_c c^2 = 56$ MeV reference cutoff energy and sloping (-1/3) log log green line imposed as a remnant from Big Bang nucleosynthesis- group phase reflection Conditions 1.1 to 1.3a expressed as green circles.



Reference [76] indicates the very existence of dark matter (observational by galactic collisions) and just such clumping thereof as well as a thrust effect of the dark energy on galactic material. Reference [79] indicates the independence of dark and visible matter distribution but perhaps this independence is illusionary. According to this correlation, the observed dark matter distributions are composed of small hydrogen dense (1 g/cc) BEC objects (<1 meter) contributing to a space density of $< 1\text{E-}23 \text{ g/cm}^3$ with resulting optical mean free path dictating invisibility other

than through the observed weak lensing effect.

4.36. The Absolute Radiometer for Cosmology, Astrophysics and Diffuse Emission(ARCADE 2) instrumented balloon was launched reporting radio measurements (3 to 90 GHz) from sky 20-30 degree radius[106]. An anomalous temperature(T) signal was measured deviant from expected the well established present universe black body temperature of 2.729 K. This anomalous signal is well fitted by the trisine model component.

$$T = T_{cr} \cdot k_m \cdot \varepsilon \cdot H_{U_{present}} / H_U$$

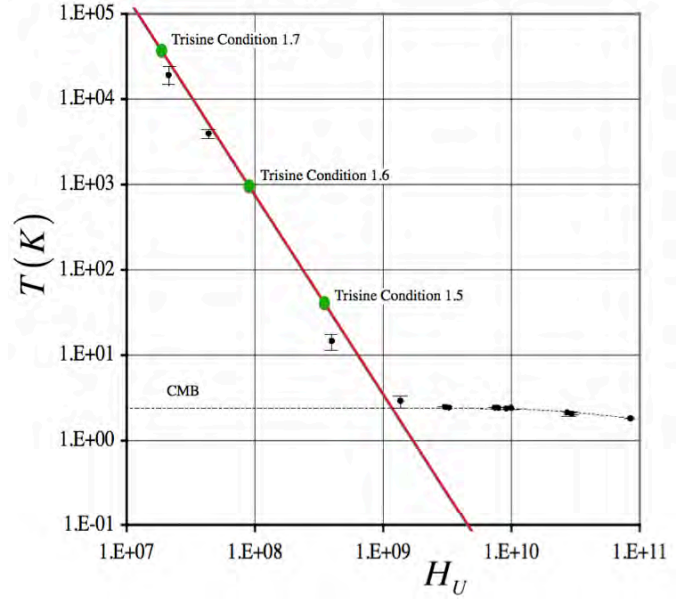
where $H_{U_{\text{present}}} = 2.31\text{E-18 }/\text{sec}$

and

$$T = T_{cr} \cdot k_m \cdot \varepsilon \cdot Age_U / Age_{U_{present}}$$

where $Age_{U_{present}} = 4.32 \times 10^{17} \text{ sec}$ (13.7 billion years)

Figure 4.36.1 ARCADE 2 Data[106] (black dots with error bars) compared with the present universe black body spectrum at 2.729K (dotted line) and trisine model red line as a function of frequency /sec as indicated by the Hubble parameter.



This data conforms to universe introductory Trisine conditions 1.5 to 1.7 or the universe at a very early stage $Age_{UIG} \sim 3.5E4$ sec or .41 days

To $Age_{UG} \sim 1.5E5$ sec or 1.7 days

where

$$Age_{UG} = Age_U \sqrt{G_U/G}$$

and k_m is the universe time variant permeability and ϵ is the universe time variant permittivity .

Also the energy H_U scaling in Figures 4.36.1 may be a consequence of and directly related to G_U gravity scaling.

$$H_U = \frac{1}{h} \frac{\text{cavity}}{\text{chain}} G_U \frac{m_t^2}{\text{proton radius}}$$

Where $\text{proton radius} = B_p / (2 \sin(\theta))$ or $x_U / (8 \sin(\theta))$
 $= 8.59 \text{E-14} (8 \text{ E-14})$

4.37. The David Gross, Frank Wilczek, and David Politzer concept of Asymtotic Freedom is naturally linked to Trisine context in the same manner as the diffuse gamma ray background as observed by EGRET and FERMI and graphically presented in Figures 4.34.1, 4.34.2 & 4.34.3 and Asymtotic data as presented by Bethke [120]. This relationship is in the context of Big Bang nucleosynthesis and Trisine Conditions 1.1 and 1.2.

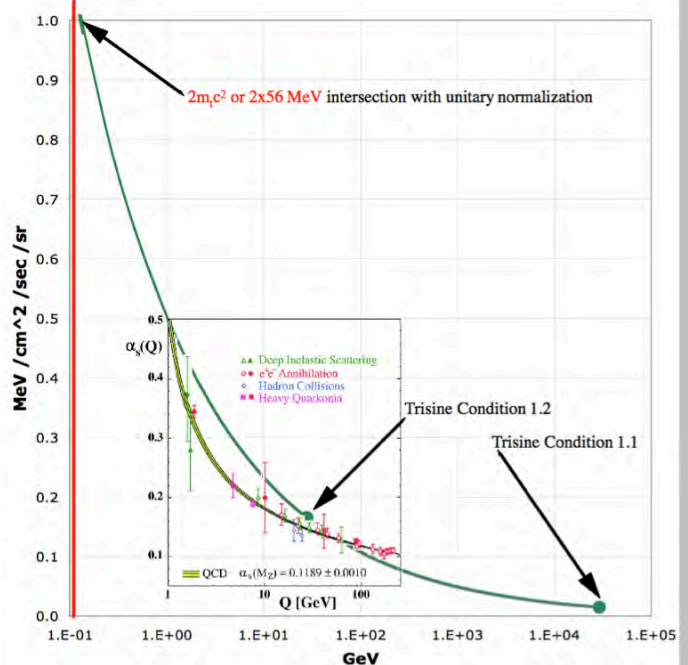
$$\begin{aligned} \sigma T_{cr}^4 \xi &= \sigma T_p^4 \frac{\text{cavity}}{V_U} \frac{c}{4} \left(\frac{1}{5.9 \text{E-19}} \right)^3 \frac{1}{2\pi} \text{time}_\pm H_U \\ &= \frac{2m_t^3 c^3}{3^6 4^3 15^3 \pi^3 \hbar^3} \left(\frac{1}{5.9 \text{E-19}} \right)^3 \frac{1}{2\pi} \left(\frac{1}{2} \hbar H_U \right)^{-\frac{1}{3}} \end{aligned}$$

or

$$= \left(\frac{B}{A} \right)^{\frac{10}{3}} \frac{\pi^{\frac{2}{3}} m_t^{\frac{13}{3}} c^{\frac{23}{3}}}{2^{\frac{6}{3}} 3^{\frac{13}{6}} 4^{\frac{3}{3}} 15^{\frac{3}{3}} \hbar^{\frac{9}{3}}} \left(\frac{1}{5.9 \text{E-19}} \right)^3 \frac{1}{2\pi} \left(\frac{1}{2} \hbar H_U \right)^{-\frac{1}{3}}$$

These two concepts are compared in Figure 4.37.1 indicating a commonality within the group phase reflection nuclear dimension. There is a normalization length dimension 5.9E-19 cm. This length dimension equals the universe Hubble radius of curvature R_U at Trisine Condition 1.1 indicative of the universe beginning. The Trisine model indicates length termination at Trisine Condition 1.1 which is far from the Planck dimensional length scale of 1.6E-33 cm.

Figure 4.37.1 Comparison between Asymtotic Freedom [Bethke-120] and Trisine Diffuse Gamma Ray Background



4.38. Within the Trisine context, the concept of entanglement or action at a distance is naturally resolved with the defined phase and group velocity definitions

$$(\text{group velocity}) \cdot (\text{phase velocity}(v_p)) = c^2$$

$$\left\{ \begin{aligned} (v_{dx}) \cdot \left(\frac{1}{\pi} \frac{v_{ex}^2}{v_{dx}^2} \cdot c \right) \\ (v_{dx}) \cdot \left(\frac{1}{\pi} \frac{v_{ey}^2}{v_{dy}^2} \cdot c \right) \\ (v_{dx}) \cdot \left(\frac{1}{\pi} \frac{v_{ez}^2}{v_{dz}^2} \cdot c \right) \end{aligned} \right\} = \left\{ \begin{aligned} (v_{dx}) \cdot \left(\frac{A}{B} \frac{1}{3^{\frac{1}{4}}} \frac{v_{ex}^2}{v_{dx}^2} \cdot c \right) \\ (v_{dx}) \cdot \left(\frac{A}{B} \frac{1}{3^{\frac{1}{4}}} \frac{v_{ey}^2}{v_{dy}^2} \cdot c \right) \\ (v_{dx}) \cdot \left(\frac{A}{B} \frac{1}{3^{\frac{1}{4}}} \frac{v_{ez}^2}{v_{dz}^2} \cdot c \right) \end{aligned} \right\} = c^2 \quad (2.1.30)$$

Table 2.1.3 indicates present universe phase velocity at $5.97 \text{E}23$ cm/sec. The average distance from the center of the Earth to the center of the Moon is $384,403$ km ($\sim 3.84 \text{E}10$ cm). Earth to moon phase velocity(v_p) travel time would be $3.84 \text{E}10 / v_p$. $3.84 \text{E}10 / 5.97 \text{E}23 = 6.43216 \text{E-24}$ sec. This extremely small number probably is unmeasurable at this time but instructive of the experimental confusion regarding entanglement or action at a distance discussions and dialogue. Indeed, entanglement and the related phase velocity(v_p) is more appropriately compared to universe dimensions $v_p = (1/3)(B/A)(R_U / \text{time}_\pm)$. It is like casting

your eyes from across the distant universe and this rate of view is comparable to the present universe phase velocity (v_p).

4.39. The OPERA experimental results[108] indicate neutrino group phase reflection velocity which was falsified by ICARUS detector at the CNGS beam and a subsequent FermiLab MINOS June 8, 2012 reported investigation. A group phase reflection result would be congruent with Trisine theory and in particular nuclear neutrino generating conditions as expressed in introductory trisine conditions 1.1 to 1.3. The nuclear generated superlumal neutrinos would transit the nuclear diameter and maintain the group phase reflection character as they pass into the surrounding media. Further nuclear neutrino generating experiments for all neutrino flavors (electron, muon, and tau and their antiparticles) are required to fully study this nuclear group phase reflection concept.

Also, observed group phase reflection motion in astrophysical radio sources may provide the basis for further confirmation of this concept in as much as the source of the these jets is nuclear in origin.

Also, there evidence of group phase reflection velocities as conducted in National Institute of Standards and Technology (NIST) experiments[118] that may feed into a more generalized view of this phenomenon.

4.40. Unidentified Infrared objects [112, 113] with observed wavelengths 3.3, 6.2, 7.7, 8.6, 11.3, 12.6 and 16.4 μm may be associated with present day trisine dark energy condition 1.11 expressing itself within galactic space resulting from dark energy and particle collisions, all within the context of the Heisenberg uncertainty constraint with Interstellar Medium proton mass (m_p) interaction with trisine mass (m_t) with trisine (not CMBR) distribution governing. This all may be consistent with bow shock micrometer emissions from bow shock the Cygnus Loop Supernova Remnant [145] resulting from momentum transfer with the ubiquitous trisine lattice.

Reported unidentified AKARI [112,113] Near- to Mid-Infrared Unidentified Emission Bands in the Interstellar Medium of the Large Magellanic Cloud as microwaves in micrometers μm .

3.3	6.2	7.7	8.6	11.3	12.6	16.4
-----	-----	-----	-----	------	------	------

And these wavelengths converted to gigaHz (GHz).

90,846	48,354	38,934	34,860	26,530	23,793	18,280
--------	--------	--------	--------	--------	--------	--------

The following are corresponding condition 1.11 trisine

harmonics corresponding to unidentified microwaves [112,113] in micrometer units μm .

$$\begin{aligned}
 & hc \left/ \left(\frac{\hbar^2}{2m_t} K_B^2 \frac{m_t}{m_e} 2 \frac{v_\epsilon^2}{v_{dx}^2} \right) \right. = \lambda_{K_B^2} \\
 & hc \left/ \left(\frac{\hbar^2}{2m_t} K_{Dn}^2 \frac{m_t}{m_e} 2 \frac{v_\epsilon^2}{v_{dx}^2} \right) \right. = \lambda_{K_{Dn}^2} \\
 & hc \left/ \left(\frac{\hbar^2}{2m_t} K_P^2 \frac{m_t}{m_e} 2 \frac{v_\epsilon^2}{v_{dx}^2} \right) \right. = \lambda_{K_P^2} \\
 & hc \left/ \left(\frac{\hbar^2}{2m_t} K_{BCS}^2 \frac{m_t}{m_e} 2 \frac{v_\epsilon^2}{v_{dx}^2} \right) \right. = \lambda_{K_{BCS}^2} \\
 & hc \left/ \left(\frac{\hbar^2}{2m_t} (K_{Ds}^2 - K_{Dn}^2) \frac{m_t}{m_e} 2 \frac{v_\epsilon^2}{v_{dx}^2} \right) \right. = \lambda_{K_{Ds}^2 - K_{Dn}^2} \\
 & hc \left/ \left(\frac{\hbar^2}{2m_t} (K_C^2 - K_B^2) \frac{m_t}{m_e} 2 \frac{v_\epsilon^2}{v_{dx}^2} \right) \right. = \lambda_{K_C^2 - K_B^2} \\
 & hc \left/ \left(\frac{\hbar^2}{2m_t} (K_{Dn}^2 + K_P^2) \frac{m_t}{m_e} 2 \frac{v_\epsilon^2}{v_{dx}^2} \right) \right. = \lambda_{K_{Dn}^2 + K_P^2} \\
 & hc \left/ \left(\frac{\hbar^2}{2m_t} K_{Ds}^2 \frac{m_t}{m_e} 2 \frac{v_\epsilon^2}{v_{dx}^2} \right) \right. = \lambda_{K_{Ds}^2} \\
 & hc \left/ \left(\frac{\hbar^2}{2m_t} K_C^2 \frac{m_t}{m_e} 2 \frac{v_\epsilon^2}{v_{dx}^2} \right) \right. = \lambda_{K_C^2} \\
 & hc \left/ \left(\frac{\hbar^2}{2m_t} (K_{Ds}^2 + K_B^2) \frac{m_t}{m_e} 2 \frac{v_\epsilon^2}{v_{dx}^2} \right) \right. = \lambda_{K_{Ds}^2 + K_B^2} \\
 & hc \left/ \left(\frac{\hbar^2}{2m_t} (K_{Ds}^2 + K_{Dn}^2) \frac{m_t}{m_e} 2 \frac{v_\epsilon^2}{v_{dx}^2} \right) \right. = \lambda_{K_{Ds}^2 + K_{Dn}^2} \\
 & hc \left/ \left(\frac{\hbar^2}{2m_t} (K_B^2 + K_C^2) \frac{m_t}{m_e} 2 \frac{v_\epsilon^2}{v_{dx}^2} \right) \right. = \lambda_{K_B^2 + K_C^2} \\
 & hc \left/ \left(\frac{\hbar^2}{2m_t} (K_{Ds}^2 + K_P^2) \frac{m_t}{m_e} 2 \frac{v_\epsilon^2}{v_{dx}^2} \right) \right. = \lambda_{K_{Ds}^2 + K_P^2} \\
 & hc \left/ \left(\frac{\hbar^2}{2m_t} (K_{Dn}^2 + K_C^2) \frac{m_t}{m_e} 2 \frac{v_\epsilon^2}{v_{dx}^2} \right) \right. = \lambda_{K_{Dn}^2 + K_C^2} \\
 & hc \left/ \left(\frac{\hbar^2}{2m_t} (K_{Ds}^2 + K_C^2) \frac{m_t}{m_e} 2 \frac{v_\epsilon^2}{v_{dx}^2} \right) \right. = \lambda_{K_{Ds}^2 + K_C^2} \\
 & hc \left/ \left(\frac{\hbar^2}{2m_t} K_A^2 \frac{m_t}{m_e} 2 \frac{v_\epsilon^2}{v_{dx}^2} \right) \right. = \lambda_{K_A^2}
 \end{aligned}$$

The AKARI spacecraft frequency spectrum is:

117,566 22,373 GHz

2.55 13.40 μm

1/Harmonic	1	2	3	4	5	6
Harmonic	1/1	1/2	1/3	1/4	1/5	1/6
$\lambda_{K_B^2}$	47.99	23.99	16.00	12.00	9.60	8.00
$\lambda_{K_{Dn}^2}$	40.05	20.02	13.35	10.01	8.01	6.67
$\lambda_{K_P^2}$	35.99	18.00	12.00	9.00	7.20	6.00
$\lambda_{K_{BCS}^2}$	27.21	13.60	9.07	6.80	5.44	4.53
$\lambda_{K_{Ds}^2 - K_{Dn}^2}$	25.05	12.53	8.35	6.26	5.01	4.18
$\lambda_{K_C^2 - K_B^2}$	20.38	10.19	6.79	5.10	4.08	3.40
$\lambda_{K_{Ds}^2 + K_P^2}$	18.96	9.48	6.32	4.74	3.79	3.16
$\lambda_{K_{Ds}^2}$	15.41	7.71	5.14	3.85	3.08	2.57
$\lambda_{K_C^2}$	14.31	7.15	4.77	3.58	2.86	2.38
$\lambda_{K_{Ds}^2 + K_B^2}$	11.67	5.83	3.89	2.92	2.33	1.94
$\lambda_{K_{Ds}^2 + K_{Dn}^2}$	11.13	5.56	3.71	2.78	2.23	1.85
$\lambda_{K_B^2 + K_C^2}$	11.02	5.51	3.67	2.76	2.20	1.84
$\lambda_{K_{Ds}^2 + K_P^2}$	10.79	5.40	3.60	2.70	2.16	1.80
$\lambda_{K_{Dn}^2 + K_C^2}$	10.54	5.27	3.51	2.64	2.11	1.76
$\lambda_{K_{Ds}^2 + K_C^2}$	7.42	3.71	2.47	1.85	1.48	1.24
$\lambda_{K_A^2}$	2.12	1.06	0.71	0.53	0.42	0.35

This trisine and stellar emission correlation represents a Compton like mechanism.

4.41. Recently quantified galactic haze may be associated with present day trisine dark energy condition 1.11 expressing itself within galactic space resulting from dark energy and particle collisions, all within the context of the Heisenberg uncertainty constraint with Interstellar Medium electron mass(m_e) interaction with trisine mass(m_t) with trisine (not CMBR) distribution governing.

The following are corresponding trisine condition 1.11 harmonics corresponding to galactic haze as frequency (GHz).

$$\left(\frac{\hbar^2}{2m_t} K_B^2 \frac{m_t}{m_p} 2 \frac{v_e^2}{v_{dx}^2} \right) / h = \nu_{K_B^2}$$

$$\left(\frac{\hbar^2}{2m_t} K_{Dn}^2 \frac{m_t}{m_p} 2 \frac{v_e^2}{v_{dx}^2} \right) / h = \nu_{K_{Dn}^2}$$

$$\left(\frac{\hbar^2}{2m_t} K_P^2 \frac{m_t}{m_p} 2 \frac{v_e^2}{v_{dx}^2} \right) / h = \nu_{K_P^2}$$

$$\left(\frac{\hbar^2}{2m_t} K_{BCS}^2 \frac{m_t}{m_p} 2 \frac{v_e^2}{v_{dx}^2} \right) / h = \nu_{K_{BCS}^2}$$

$$\left(\frac{\hbar^2}{2m_t} (K_{Ds}^2 - K_{Dn}^2) \frac{m_t}{m_p} 2 \frac{v_e^2}{v_{dx}^2} \right) / h = \nu_{K_{Ds}^2 - K_{Dn}^2}$$

$$\left(\frac{\hbar^2}{2m_t} (K_C^2 - K_B^2) \frac{m_t}{m_p} 2 \frac{v_e^2}{v_{dx}^2} \right) / h = \nu_{K_C^2 - K_B^2}$$

$$\left(\frac{\hbar^2}{2m_t} (K_{Ds}^2 + K_P^2) \frac{m_t}{m_p} 2 \frac{v_e^2}{v_{dx}^2} \right) / h = \nu_{K_{Ds}^2 + K_P^2}$$

$$\left(\frac{\hbar^2}{2m_t} K_{Ds}^2 \frac{m_t}{m_p} 2 \frac{v_e^2}{v_{dx}^2} \right) / h = \nu_{K_{Ds}^2}$$

$$\left(\frac{\hbar^2}{2m_t} K_C^2 \frac{m_t}{m_p} 2 \frac{v_e^2}{v_{dx}^2} \right) / h = \nu_{K_C^2}$$

$$\left(\frac{\hbar^2}{2m_t} (K_{Ds}^2 + K_B^2) \frac{m_t}{m_p} 2 \frac{v_e^2}{v_{dx}^2} \right) / h = \nu_{K_{Ds}^2 + K_B^2}$$

$$\left(\frac{\hbar^2}{2m_t} (K_{Dn}^2 + K_C^2) \frac{m_t}{m_p} 2 \frac{v_e^2}{v_{dx}^2} \right) / h = \nu_{K_{Dn}^2 + K_C^2}$$

$$\left(\frac{\hbar^2}{2m_t} (K_B^2 + K_C^2) \frac{m_t}{m_p} 2 \frac{v_e^2}{v_{dx}^2} \right) / h = \nu_{K_B^2 + K_C^2}$$

$$\left(\frac{\hbar^2}{2m_t} (K_{Ds}^2 + K_P^2) \frac{m_t}{m_p} 2 \frac{v_e^2}{v_{dx}^2} \right) / h = \nu_{K_{Ds}^2 + K_P^2}$$

$$\left(\frac{\hbar^2}{2m_t} (K_{Dn}^2 + K_C^2) \frac{m_t}{m_p} 2 \frac{v_e^2}{v_{dx}^2} \right) / h = \nu_{K_{Dn}^2 + K_C^2}$$

$$\left(\frac{\hbar^2}{2m_t} K_A^2 \frac{m_t}{m_p} 2 \frac{v_e^2}{v_{dx}^2} \right) / h = \nu_{K_A^2}$$

The 30 – 44 GHz Milky Way haze spectrum within Planck spacecraft frequency observational capability confirming WMAP haze detection at 23 GHz[114] with proximate trisine resonant modes shaded:

857	30	GHz
350	10,000	μm

Harmonic	1	2	3	4	5	6
1/Harmonic	1/1	1/2	1/3	1/4	1/5	1/6
Frequency GHz						
$\nu_{K_B^2}$	3.40	6.80	10.21	13.61	17.01	20.41
$\nu_{K_{Dn}^2}$	4.08	8.15	12.23	16.31	20.38	24.46
ν_{K_P}	4.54	9.07	13.61	18.15	22.68	27.22
$\nu_{K_{BCS}^2}$	6.00	12.00	18.00	24.00	30.01	36.01
$\nu_{K_{Dn}^2 - K_{Dn}^2}$	6.52	13.03	19.55	26.07	32.58	39.10
$\nu_{K_C^2 - K_B^2}$	8.01	16.02	24.03	32.04	40.05	48.06
$\nu_{K_{Dn}^2 + K_P^2}$	8.61	17.23	25.84	34.45	43.07	51.68
$\nu_{K_{Dn}^2}$	10.59	21.19	31.78	42.37	52.97	63.56
$\nu_{K_C^2}$	11.41	22.82	34.24	45.65	57.06	68.47
$\nu_{K_{Dn}^2 + K_B^2}$	14.00	27.99	41.99	55.98	69.98	83.98
$\nu_{K_{Dn}^2 + K_{Dn}^2}$	14.67	29.34	44.01	58.68	73.35	88.02
$\nu_{K_B^2 + K_C^2}$	14.81	29.63	44.44	59.26	74.07	88.89
$\nu_{K_{Dn}^2 + K_P^2}$	15.13	30.26	45.39	60.52	75.65	90.78
$\nu_{K_{Dn}^2 + K_C^2}$	15.49	30.98	46.47	61.96	77.44	92.93
$\nu_{K_{Dn}^2 + K_C^2}$	22.01	44.01	66.02	88.02	110.0	132.0
$\nu_{K_A^2}$	77.03	154.1	231.1	308.1	385.2	462.2

This trisine and galactic haze correlation represents a Compton like mechanism.

4.42. The approach in estimating Pioneer 10 and 11 deceleration (section 2) can estimate the universe dark energy anomalous acceleration but in terms of an actual deceleration of the local observer to the supernovae type 1A candle explosion events. The earth its satellite detector within the local galactic environment would be considered the observer slowing down between the supernovae type 1A event and the detection event. Equation 2.7.6 (repeated here) indicates this observer slowing or deceleration would be isotropic in as much as c^2 is constant. The parameters C_t and A_c , are characteristic of the local galactic environment and not the exploding supernovae type 1A environment.

$$F \approx -C_t \frac{m_t c^2}{s} = C_t A_c \rho_U c^2 \quad (2.7.6)$$

$$\text{where: } C_t = \frac{24}{R_{eo}} + \frac{6}{1 + \sqrt{R_{eo}}} + .4 \text{ and } R_{eo} = \frac{\rho_U cd}{\mu_{Uc}}$$

Where constant C_t is in the form of the standard fluid mechanical drag coefficient analogous to 2.7.4a, but is defined as a thrust coefficient.

This trisine model was used to analyze the Pioneer unmodeled deceleration data 8.74E-08 cm/sec² and there appeared to be a good fit with the observed space density (ρ_U) 6E-30 g/cm³ (trisine model (ρ_U) 6.38E-30 g/cm³). A thrust coefficient (C_t) of 59.67 indicates a laminar flow condition. An absolute space viscosity seen ($\mu_{Uc} = m_t c / (2\Delta x^2)$) of 1.21E-16 g/(cm sec) is established within trisine model and determines a space kinematic viscosity seen (μ_{Uc} / ρ_U) of (1.21E-16 / 6.38E-30) or 1.90E13 cm²/sec as indicated in 2.7.4a. NASA, JPL raised a question concerning the universal application of the observed deceleration on Pioneer 10 & 11. In other words, why do not the planets and their satellites experience such a deceleration? The answer is in the A_c/M ratio in the modified thrust relationship.

$$a \approx -C_t \frac{m_t c^2}{M s} = -C_t \frac{A_c}{M} \rho_U c^2 = -C_t \frac{A_c}{M} \frac{m_t}{\text{cavity}} c^2 \quad (2.7.6a)$$

Using the earth as an example, the earth differential movement

$$L_1 = \frac{1}{2} a (Age_{UGpresent}^2 - Age_{UG}^2)$$

The z factors $(1+z_R)^a$ or $(1+z_B)^b$ are presented for extrapolation of present values into the observational past consistent with tabular values in this paper. The two references $(1+z_R)^a$ or $(1+z_B)^b$ are presented representing both the universe Hubble radius of curvature R_U and trisine cellular B perspectives where $a/b = 1/3$.

L_2 scales as trisine local dimension $L_2 \sim B_{present} (1+z_R)^{-1/3}$

With relationship to universe Hubble volume V_U dimension and Hubble radius of curvature dimension R_U as follows:

$$\#_{Upresent} = \frac{m_t}{m_e} \frac{V_{Upresent}}{\text{cavity}_{present}}$$

$$\text{where } V_{Upresent} = \frac{4\pi}{3} R_{Upresent}^3$$

$$\text{and } \text{cavity}_{present} = 2\sqrt{3}AB^2 = 2\sqrt{3} \left(\frac{A}{B} \right)_t B^3$$

$$\begin{aligned}
n & \sum_1^n \left((1+z_{Rn})^w \right) \sum_1^n \left((1+z_{Rn})^w \right) \sum_1^n \left((1+z_{Rn})^w \right) \sum_1^n \left((1+z_{Rn})^w \right) \\
& \sum_1^n \left((1+z_{Rn})^w \right) \\
& \sum_1^n \left((1+z_{Rn})^w \right) \\
& \sum_1^n \left((1+z_{Rn})^w \right) \\
& \sum_1^n \left((1+z_{Rn})^w \right) \\
& \sum_1^n \left((1+z_{Rn})^w \right) \\
& \sum_1^n \left((1+z_{Rn})^w \right) \sum_1^n \left((1+z_{Rn})^w \right) \sum_1^n \left((1+z_{Rn})^w \right) \sum_1^n \left((1+z_{Rn})^w \right) \sum_1^n \left((1+z_{Rn})^w \right)
\end{aligned}$$

A

$$\begin{aligned}
n & \sum_1^n \left((1+z_{Bn})^w \right) \sum_1^n \left((1+z_{Bn})^w \right) \sum_1^n \left((1+z_{Bn})^w \right) \sum_1^n \left((1+z_{Bn})^w \right) \\
& \sum_1^n \left((1+z_{Bn})^w \right) \sum_1^n \left((1+z_{Bn})^w \right) \sum_1^n \left((1+z_{Bn})^w \right) \sum_1^n \left((1+z_{Bn})^w \right) \sum_1^n \left((1+z_{Bn})^{\frac{1}{3}} \right) \\
& \sum_1^n \left((1+z_{Bn})^w \right) \sum_1^n \left((1+z_{Bn})^w \right) \sum_1^n \left((1+z_{Bn})^w \right) \sum_1^n \left((1+z_{Bn})^{\frac{1}{3}} \right) \sum_1^n \left((1+z_{Bn})^w \right) \\
& \sum_1^n \left((1+z_{Bn})^w \right) \sum_1^n \left((1+z_{Bn})^w \right) \sum_1^n \left((1+z_{Bn})^{-\frac{1}{3}} \right) \sum_1^n \left((1+z_{Bn})^w \right) \sum_1^n \left((1+z_{Bn})^w \right) \\
& \sum_1^n \left((1+z_{Bn})^w \right) \sum_1^n \left((1+z_{Bn})^{-\frac{1}{3}} \right) \sum_1^n \left((1+z_{Bn})^w \right) \sum_1^n \left((1+z_{Bn})^w \right) \sum_1^n \left((1+z_{Bn})^w \right)
\end{aligned}$$

b

Inverse(A) x b

$ \begin{aligned} & \sum_1^n C_{t(1+z_{Rn})} \left((1+z_{Rn})^w \right)^0 \\ & \sum_1^n C_{t(1+z_{Rn})} \left((1+z_{Rn})^w \right)^1 \\ & \sum_1^n C_{t(1+z_{Rn})} \left((1+z_{Rn})^w \right)^2 \\ & \sum_1^n C_{t(1+z_{Rn})} \left((1+z_{Rn})^w \right)^3 \\ & \sum_1^n C_{t(1+z_{Rn})} \left((1+z_{Rn})^w \right)^4 \end{aligned} $	$ \begin{aligned} & a_{0R} \\ & a_{1R} \\ & a_{2R} \\ & a_{3R} \\ & a_{4R} \end{aligned} $
--	--

$$C_{t(1+z_R)} = a_{0R} \left((1+z_R)^w \right)^0 + a_{1R} \left((1+z_R)^w \right)^1 + a_{2R} \left((1+z_R)^w \right)^2 + a_{3R} \left((1+z_R)^w \right)^3 + a_{4R} \left((1+z_R)^w \right)^4$$

and combining exponents by multiplication

$$C_{t(1+z_R)} = a_{0R} + a_{1R} (1+z_R)^{1w} + a_{2R} (1+z_R)^{2w} + a_{3R} (1+z_R)^{3w} + a_{4R} (1+z_R)^{4w}$$

and similarly for B scaling:

Inverse(A) x b

$ \sum_1^n C_{t(1+z_{Bn})} \left((1+z_{Bn})^w \right)^0 $	$ a_{0B} $
$ \sum_1^n C_{t(1+z_{Bn})} \left((1+z_{Bn})^w \right)^1 $	$ a_{1B} $
$ \sum_1^n C_{t(1+z_{Bn})} \left((1+z_{Bn})^w \right)^2 $	$ a_{2B} $
$ \sum_1^n C_{t(1+z_{Bn})} \left((1+z_{Bn})^w \right)^3 $	$ a_{3B} $
$ \sum_1^n C_{t(1+z_{Bn})} \left((1+z_{Bn})^w \right)^4 $	$ a_{4B} $

$$C_{t(1+z_B)} = a_{0B} \left((1+z_B)^w \right)^0 + a_{1B} \left((1+z_B)^w \right)^1 + a_{2B} \left((1+z_B)^w \right)^2 + a_{3B} \left((1+z_B)^w \right)^3 + a_{4B} \left((1+z_B)^w \right)^4$$

and combining exponents by multiplication

$$C_{t(1+z_B)} = a_{0B} + a_{1B} (1+z_B)^{1w} + a_{2B} (1+z_B)^{2w} + a_{3B} (1+z_B)^{3w} + a_{4B} (1+z_B)^{4w}$$

$$(z_B + 1)^3 = (z_R + 1)^1$$

$$z_B = (z_R + 1)^{\frac{1}{3}} - 1 \quad z_R = (z_B + 1)^3 - 1$$

The universe expands at the speed of light c .

$$R_U = \frac{\sqrt{3}c}{H_U}$$

$$\begin{aligned}
L_{zR} &= \frac{1}{3\sqrt{3}} R_{Upresent} \int_0^{z_R} \frac{dz}{(1+z)^{1/3}} \\
&= \frac{1}{3\sqrt{3}} R_{Upresent} \left(\left(\frac{3}{2} \right) (z_R + 1)^{2/3} - \frac{3}{2} \right) \\
&= \frac{1}{3\sqrt{3}} R_{Upresent} \int_0^{(1+z_B)^{3/2}-1} \frac{dz}{(1+z)^{1/3}} \\
&= \frac{1}{3\sqrt{3}} R_{Upresent} \left(\left(\frac{3}{2} \right) (z_B^3 + 3z_B^2 + 3z_B + 1)^{2/3} - \frac{3}{2} \right)
\end{aligned}$$

And scaling as conventionally used [122 -Harrison]

$$\begin{aligned}
L_{z_B} &= \frac{1}{3^2} R_{Upresent} \int_0^{z_B} \frac{dz}{(1+z)} \\
&= \frac{1}{3^2} R_{Upresent} \ln(1+z_B) \\
&= \frac{1}{3^2} R_{Upresent} \int_0^{(z_B+1)^{1/3}-1} \frac{dz}{(1+z)} \\
&= \frac{1}{3^3} R_{Upresent} \ln(1+z_B)
\end{aligned}$$

$$\begin{aligned}
L_1 &= \int_0^{L_1} 1 dL_1 = \int_0^{z_B} \frac{1}{2} a t^2 dz_B \\
&= \int_0^{z_B} \frac{1}{2} C_{t(1+z_B)} \frac{A_c}{M} (1+z_B)^3 \rho_{present} c^2 \left((1+z_B)^{-3/2} A g e_{UGpresent} \right)^2 dz_B \\
&= \frac{A_c}{M} \rho_{present} c^2 A g e_{UGpresent}^2 \left(\frac{a_{0B} z_B}{2} \right. \\
&\quad \left. + \frac{a_{1B} (z_B (z_B + 1)^w + (z_B + 1)^w - 1)}{2w + 2} \right. \\
&\quad \left. + \frac{a_{2B} (z_B (z_B + 1)^{2w} + (z_B + 1)^{2w} - 1)}{4w + 2} \right. \\
&\quad \left. + \frac{a_{3B} (z_B (z_B + 1)^{3w} + (z_B + 1)^{3w} - 1)}{6w + 2} \right. \\
&\quad \left. + \frac{a_{4B} (z_B (z_B + 1)^{4w} + (z_B + 1)^{4w} - 1)}{8w + 2} \right) \\
&= \frac{A_c}{M} \text{factor}
\end{aligned}$$

Then normalize the object area to mass ratio A_c/M to L_{z_B} :

$$\frac{A_c}{M} = \frac{L_{z_B}}{\text{factor}}$$

Monte Carlo analysis indicates $w = -1/3.334$ with reasonable correlation only for z_B and not z_R and a clear indication of laminar fluid condition as indicated in C_t vs

R_{eo} .

Figure 4.42.1 Thrust Coefficient C_t vs $1+z_R$ Modeled (red) and Modeled Verified (blue) (a good w fit is not achievable)

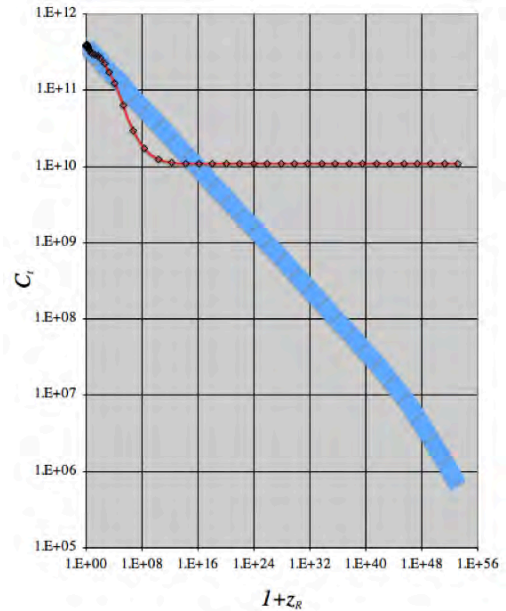
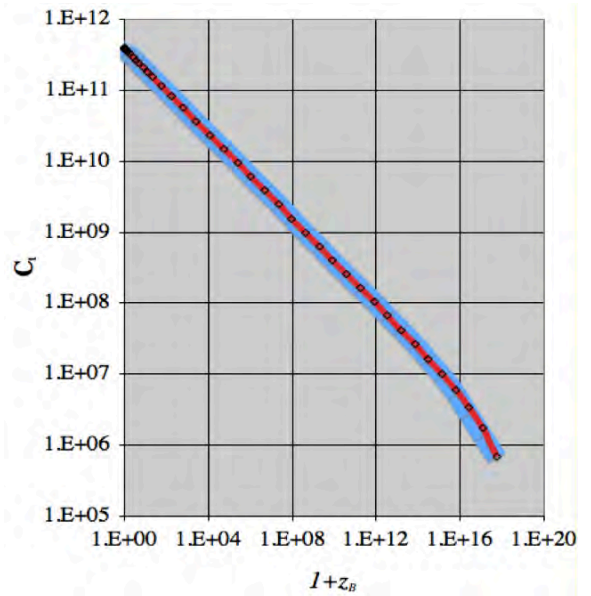


Figure 4.42.2 Thrust Coefficient C_t vs $1+z_B$ Modeled (red) and Modeled Verified (blue) (a good w fit is achievable)



For all energies represented by velocities (v) including c .

By definition the absolute magnitude(M) is the apparent magnitude(m) at a distance of 10 parsec that provides a

distance modulus $(m - M)_z$.

$$(m - M)_{z_R} = 5 \log_{10} (L_{z_R}) - 5$$

$$(m - M)_{z_B} = 5 \log_{10} (L_{z_B}) - 5$$

$$(m - M)_{z_B} = 5 \log_{10} (L_1) - 5$$

$$5 \log_{10} (L_{z_B}) - 5 = 5 \log_{10} (L_1) - 5$$

Here L_1 , L_{z_B} and L_{z_R}

have been dimensionally changed to *parsecs*

Distance modulus conversion between z_R and z_B universe scaling is as follows:

$$(m - M)_{z_R} =$$

$$5 \log_{10} \left(\sqrt{3} \ln(z_B + 1) / \left(\frac{3}{2} (z_R + 1)^{\frac{2}{3}} - \frac{3}{2} \right) 10^{\frac{((m - M)_{z_B} + 5)}{5}} \right)$$

-5

The curvature in Figure 4.42.1 is not due to accelerated expansion but dual linear expansion of universe radius R and contained lattice cellular structure with unit length B .

http://supernova.lbl.gov/Union/figures/SCPUnion2.1_mu_vs_z.txt

$Uage_{GUzR}$	z_R	$(m - M)_{z_R}$	$Uage_{GUzB}$	z_B	$(m - M)_{z_B}$
4.15E+17	0.088	34.092	4.15E+17	0.028	35.347
3.47E+17	0.158	35.383	4.02E+17	0.050	36.682
3.43E+17	0.167	35.512	4.00E+17	0.053	36.818
3.19E+17	0.225	36.105	3.91E+17	0.070	37.447
3.29E+17	0.200	36.157	3.95E+17	0.063	37.483
2.96E+17	0.286	36.851	3.81E+17	0.088	38.229
3.08E+17	0.255	36.129	3.86E+17	0.079	37.488
4.00E+17	0.053	33.424	4.21E+17	0.017	34.654
3.59E+17	0.132	35.053	4.06E+17	0.042	36.336
3.54E+17	0.142	35.351	4.05E+17	0.045	36.640
3.68E+17	0.113	34.634	4.10E+17	0.036	35.905
3.96E+17	0.060	33.350	4.20E+17	0.020	34.585
2.81E+17	0.334	37.052	3.74E+17	0.101	38.457
3.83E+17	0.084	33.834	4.15E+17	0.027	35.086
3.13E+17	0.241	36.237	3.88E+17	0.075	37.588
3.84E+17	0.082	34.231	4.16E+17	0.026	35.481
3.47E+17	0.157	35.268	4.02E+17	0.050	36.567
3.78E+17	0.095	34.292	4.13E+17	0.031	35.550
4.02E+17	0.050	32.816	4.22E+17	0.016	34.044
4.04E+17	0.047	32.715	4.23E+17	0.015	33.941
3.78E+17	0.094	34.341	4.13E+17	0.031	35.599
3.88E+17	0.075	33.813	4.17E+17	0.025	35.058
3.89E+17	0.074	33.724	4.17E+17	0.024	34.969
3.85E+17	0.080	34.118	4.16E+17	0.026	35.367
3.49E+17	0.154	35.434	4.03E+17	0.049	36.732
3.88E+17	0.075	33.864	4.17E+17	0.024	35.109
4.04E+17	0.046	32.876	4.23E+17	0.015	34.102
3.69E+17	0.111	34.691	4.10E+17	0.036	35.961

3.49E+17	0.154	35.085	4.03E+17	0.049	36.382
3.92E+17	0.067	33.613	4.19E+17	0.022	34.853
2.55E+17	0.422	37.592	3.63E+17	0.124	39.045
3.69E+17	0.112	34.551	4.10E+17	0.036	35.821
4.02E+17	0.050	32.789	4.22E+17	0.016	34.017
4.01E+17	0.051	32.997	4.22E+17	0.017	34.226
3.83E+17	0.085	34.398	4.15E+17	0.028	35.650
3.92E+17	0.067	33.734	4.19E+17	0.022	34.974
4.02E+17	0.050	32.953	4.22E+17	0.016	34.181
3.90E+17	0.071	33.843	4.18E+17	0.023	35.086
3.68E+17	0.113	34.863	4.10E+17	0.036	36.134
3.97E+17	0.059	33.718	4.20E+17	0.019	34.953
4.00E+17	0.054	33.113	4.21E+17	0.018	34.344
3.76E+17	0.098	34.468	4.13E+17	0.032	35.729
3.89E+17	0.072	33.926	4.18E+17	0.024	35.170
4.01E+17	0.051	32.774	4.22E+17	0.017	34.003
3.42E+17	0.170	35.169	4.00E+17	0.054	36.476
4.01E+17	0.052	33.149	4.22E+17	0.017	34.379
3.82E+17	0.086	33.841	4.15E+17	0.028	35.093
4.01E+17	0.052	33.031	4.22E+17	0.017	34.261
3.79E+17	0.093	34.715	4.14E+17	0.030	35.972
4.02E+17	0.051	33.115	4.22E+17	0.017	34.344
4.04E+17	0.046	32.938	4.23E+17	0.015	34.164
3.41E+17	0.172	35.646	3.99E+17	0.054	36.954
2.25E+17	0.545	37.714	3.48E+17	0.156	39.229
3.64E+17	0.123	35.057	4.08E+17	0.039	36.334
2.55E+17	0.420	37.370	3.63E+17	0.124	38.822
2.36E+17	0.498	37.344	3.53E+17	0.144	38.836
2.50E+17	0.443	37.516	3.60E+17	0.130	38.979
3.08E+17	0.254	36.323	3.86E+17	0.078	37.682
3.35E+17	0.185	35.716	3.97E+17	0.058	37.033
3.77E+17	0.096	34.670	4.13E+17	0.031	35.929
3.62E+17	0.127	35.086	4.07E+17	0.041	36.366
4.04E+17	0.046	32.791	4.23E+17	0.015	34.017
3.91E+17	0.069	33.706	4.18E+17	0.022	34.947
4.03E+17	0.049	32.947	4.22E+17	0.016	34.174
3.68E+17	0.113	34.716	4.10E+17	0.036	35.987
4.00E+17	0.053	33.020	4.21E+17	0.017	34.250
3.77E+17	0.097	34.367	4.13E+17	0.031	35.627
3.92E+17	0.068	33.671	4.18E+17	0.022	34.912
4.03E+17	0.049	32.597	4.22E+17	0.016	33.825
3.87E+17	0.077	33.557	4.17E+17	0.025	34.804
3.78E+17	0.094	34.370	4.14E+17	0.030	35.628
3.81E+17	0.087	34.267	4.15E+17	0.028	35.520
4.04E+17	0.046	33.033	4.23E+17	0.015	34.258
3.71E+17	0.107	34.711	4.11E+17	0.035	35.978
3.69E+17	0.112	34.409	4.10E+17	0.036	35.679
3.87E+17	0.076	34.010	4.17E+17	0.025	35.256
3.80E+17	0.090	34.737	4.14E+17	0.029	35.993
3.71E+17	0.107	34.225	4.22E+17	0.016	34.453
3.98E+17	0.057	33.815	4.21E+17	0.019	35.048
3.96E+17	0.060	33.522	4.20E+17	0.020	34.757
3.86E+17	0.079	34.437	4.16E+17	0.026	35.685
3.73E+17	0.105	34.579	4.11E+17	0.034	35.844
3.40E+17	0.173	35.300	3.99E+17	0.055	36.610
3.89E+17	0.074	33.932	4.17E+17	0.024	35.176
3.86E+17	0.079	34.437	4.16E+17	0.034	36.005
3.72E+17	0.104	34.740	4.12E+17	0.034	35.842
3.72E+17	0.106	34.576	4.11E+17	0.034	35.842
3.85E+17	0.080	34.111	4.16E+17	0.026	35.360
3.94E+17	0.065	33.422	4.19E+17	0.021	34.661
3.75E+17	0.099	34.634	4.12E+17	0.032	35.896
3.92E+17	0.068	33.682	4.18E+17	0.022	34.922
3.73E+17	0.104	34.615	4.12E+17	0.033	35.880
3.72E+17	0.106	34.677	4.11E+17	0.034	35.943
3.59E+17	0.132	35.117	4.06E+17	0.042	36.400

3.36E+17	0.183	35.765	3.98E+17	0.058	37.080	3.88E+17	0.074	33.807	4.17E+17	0.024	35.052
3.95E+17	0.063	33.380	4.19E+17	0.021	34.617	4.04E+17	0.046	32.725	4.23E+17	0.015	33.950
3.62E+17	0.126	35.096	4.08E+17	0.040	36.375	3.81E+17	0.088	34.294	4.15E+17	0.028	35.548
3.85E+17	0.080	34.133	4.16E+17	0.026	35.381	3.55E+17	0.141	35.261	4.05E+17	0.045	36.550
3.85E+17	0.080	34.167	4.16E+17	0.026	35.416	3.74E+17	0.102	34.704	4.12E+17	0.033	35.968
3.89E+17	0.073	33.791	4.17E+17	0.024	35.035	3.12E+17	0.244	36.228	3.88E+17	0.075	37.580
3.20E+17	0.222	36.227	3.91E+17	0.069	37.566	3.95E+17	0.062	33.420	4.20E+17	0.020	34.656
3.26E+17	0.208	35.975	3.93E+17	0.065	37.307	3.90E+17	0.071	33.892	4.18E+17	0.023	35.134
3.91E+17	0.070	33.955	4.18E+17	0.023	35.197	3.84E+17	0.083	34.010	4.16E+17	0.027	35.260
3.76E+17	0.098	34.391	4.13E+17	0.032	35.651	3.99E+17	0.055	33.118	4.21E+17	0.018	34.350
3.93E+17	0.066	33.694	4.19E+17	0.022	34.933	3.50E+17	0.152	35.390	4.03E+17	0.048	36.686
3.86E+17	0.078	34.472	4.16E+17	0.026	35.720	3.37E+17	0.180	35.650	3.98E+17	0.057	36.964
3.74E+17	0.101	34.550	4.12E+17	0.033	35.813	3.27E+17	0.204	35.987	3.94E+17	0.064	37.316
3.00E+17	0.275	36.681	3.83E+17	0.084	38.052	2.34E+17	0.506	38.063	3.52E+17	0.146	39.559
3.77E+17	0.095	34.370	4.13E+17	0.031	35.629	2.50E+17	0.440	37.456	3.60E+17	0.129	38.918
3.74E+17	0.101	34.831	4.12E+17	0.033	36.094	2.79E+17	0.341	37.079	3.73E+17	0.103	38.487
3.59E+17	0.132	35.109	4.06E+17	0.042	36.393	1.63E+17	0.918	38.449	3.12E+17	0.243	40.130
3.21E+17	0.220	36.393	3.92E+17	0.068	37.731	1.34E+17	1.189	39.278	2.92E+17	0.298	41.062
4.04E+17	0.047	33.481	4.23E+17	0.015	34.707	3.57E+17	0.137	35.100	4.06E+17	0.044	36.387
3.90E+17	0.072	33.639	4.18E+17	0.023	34.882	2.67E+17	0.379	37.122	3.68E+17	0.113	38.551
3.49E+17	0.155	35.432	4.02E+17	0.049	36.730	1.55E+17	0.984	38.903	3.07E+17	0.256	40.611
3.59E+17	0.133	34.644	4.06E+17	0.043	35.928	1.35E+17	1.175	39.358	2.93E+17	0.296	41.137
3.97E+17	0.059	33.502	4.20E+17	0.019	34.737	1.01E+17	1.630	39.727	2.67E+17	0.380	41.657
3.77E+17	0.095	34.520	4.13E+17	0.031	35.779	2.35E+17	0.504	37.562	3.53E+17	0.146	39.057
3.93E+17	0.065	33.609	4.19E+17	0.021	34.847	1.46E+17	1.065	38.988	3.01E+17	0.273	40.727
3.82E+17	0.085	34.453	4.15E+17	0.028	35.705	1.34E+17	1.184	38.989	2.93E+17	0.298	40.772
3.73E+17	0.104	34.709	4.12E+17	0.034	35.974	1.02E+17	1.622	39.654	2.67E+17	0.379	41.581
3.94E+17	0.064	33.558	4.19E+17	0.021	34.795	1.01E+17	1.630	39.342	2.67E+17	0.380	41.272
4.00E+17	0.053	33.000	4.21E+17	0.017	34.230	1.32E+17	1.206	39.703	2.91E+17	0.302	41.494
3.69E+17	0.112	34.876	4.10E+17	0.036	36.146	1.13E+17	1.451	39.434	2.76E+17	0.348	41.308
3.90E+17	0.072	33.955	4.18E+17	0.023	35.198	2.99E+17	0.280	36.624	3.82E+17	0.086	37.997
3.34E+17	0.187	35.793	3.97E+17	0.059	37.112	1.53E+17	1.003	38.808	3.06E+17	0.261	40.523
3.35E+17	0.185	35.741	3.97E+17	0.058	37.058	1.80E+17	0.796	38.666	3.23E+17	0.216	40.297
3.21E+17	0.221	36.148	3.91E+17	0.069	37.487	2.62E+17	0.396	37.141	3.66E+17	0.118	38.579
3.75E+17	0.099	34.386	4.12E+17	0.032	35.648	2.04E+17	0.652	38.027	3.36E+17	0.182	39.594
3.44E+17	0.165	35.370	4.01E+17	0.052	36.674	1.09E+17	1.502	39.439	2.73E+17	0.358	41.329
3.77E+17	0.095	34.334	4.13E+17	0.031	35.594	2.38E+17	0.489	37.787	3.54E+17	0.142	39.274
3.74E+17	0.102	34.678	4.12E+17	0.033	35.942	1.53E+17	1.003	39.093	3.06E+17	0.261	40.808
3.90E+17	0.071	33.828	4.18E+17	0.023	35.071	1.69E+17	0.874	38.541	3.16E+17	0.233	40.205
4.04E+17	0.046	33.155	4.23E+17	0.015	34.380	2.29E+17	0.528	37.649	3.50E+17	0.152	39.156
3.75E+17	0.099	34.609	4.12E+17	0.032	35.870	2.89E+17	0.309	36.782	3.78E+17	0.094	38.173
3.27E+17	0.206	35.846	3.94E+17	0.064	37.176	1.39E+17	1.130	39.275	2.96E+17	0.287	41.038
3.75E+17	0.099	34.565	4.12E+17	0.032	35.827	1.94E+17	0.704	38.372	3.31E+17	0.194	39.962
3.94E+17	0.064	33.465	4.19E+17	0.021	34.703	2.33E+17	0.509	37.806	3.52E+17	0.147	39.304
3.92E+17	0.067	33.609	4.19E+17	0.022	34.849	1.82E+17	0.779	38.937	3.24E+17	0.212	40.560
3.75E+17	0.099	34.327	4.12E+17	0.032	35.588	2.05E+17	0.644	38.076	3.37E+17	0.180	39.639
4.04E+17	0.046	33.300	4.23E+17	0.015	34.526	1.51E+17	1.017	39.047	3.04E+17	0.263	40.767
3.97E+17	0.059	33.257	4.20E+17	0.019	34.492	1.96E+17	0.694	38.454	3.32E+17	0.192	40.039
3.84E+17	0.082	34.073	4.16E+17	0.027	35.323	1.16E+17	1.400	39.448	2.79E+17	0.339	41.305
3.66E+17	0.117	34.522	4.09E+17	0.038	35.795	2.63E+17	0.395	37.308	3.66E+17	0.117	38.746
3.87E+17	0.076	33.668	4.17E+17	0.025	34.914	2.38E+17	0.491	37.628	3.54E+17	0.142	39.116
3.88E+17	0.074	33.944	4.17E+17	0.024	35.189	2.21E+17	0.564	37.794	3.46E+17	0.161	39.319
3.68E+17	0.114	34.700	4.10E+17	0.037	35.971	1.38E+17	1.139	39.077	2.96E+17	0.288	40.843
3.91E+17	0.070	33.896	4.18E+17	0.023	35.139	2.57E+17	0.416	37.351	3.63E+17	0.123	38.800
3.77E+17	0.097	34.623	4.13E+17	0.031	35.883	1.51E+17	1.018	38.827	3.04E+17	0.264	40.548
4.04E+17	0.046	32.886	4.23E+17	0.015	34.111	2.53E+17	0.429	37.254	3.62E+17	0.126	38.710
3.72E+17	0.106	34.504	4.11E+17	0.034	35.770	2.11E+17	0.613	37.955	3.41E+17	0.173	39.503
3.87E+17	0.077	33.701	4.17E+17	0.025	34.948	2.19E+17	0.576	37.864	3.44E+17	0.164	39.395
3.97E+17	0.058	33.141	4.20E+17	0.019	34.375	1.59E+17	0.951	39.086	3.10E+17	0.250	40.781
3.79E+17	0.092	34.214	4.14E+17	0.030	35.471	1.54E+17	0.990	38.942	3.07E+17	0.258	40.651
3.75E+17	0.100	34.116	4.12E+17	0.032	35.378	2.74E+17	0.356	37.220	3.71E+17	0.107	38.637
3.83E+17	0.085	34.223	4.15E+17	0.028	35.475	2.22E+17	0.560	37.828	3.46E+17	0.160	39.351
3.52E+17	0.148	35.201	4.04E+17	0.047	36.494	1.87E+17	0.750	38.414	3.27E+17	0.205	40.025
3.99E+17	0.056	33.139	4.21E+17	0.018	34.372	1.62E+17	0.927	38.517	3.12E+17	0.244	40.202
3.06E+17	0.260	36.324	3.85E+17	0.080	37.686	1.59E+17	0.946	38.580	3.10E+17	0.249	40.272

1.71E+17	0.854	38.599	3.18E+17	0.229	40.254	2.03E+17	0.658	38.142	3.36E+17	0.184	39.711
2.99E+17	0.280	36.578	3.82E+17	0.086	37.952	1.82E+17	0.783	38.463	3.24E+17	0.213	40.088
3.30E+17	0.197	35.807	3.95E+17	0.062	37.131	1.08E+17	1.516	39.263	2.73E+17	0.360	41.157
1.43E+17	1.087	39.091	2.99E+17	0.278	40.838	9.70E+16	1.709	39.827	2.63E+17	0.394	41.781
1.45E+17	1.075	39.001	3.00E+17	0.275	40.743	2.65E+17	0.385	37.236	3.67E+17	0.115	38.669
2.26E+17	0.542	37.804	3.48E+17	0.155	39.317	2.36E+17	0.496	37.695	3.54E+17	0.144	39.186
1.20E+17	1.355	39.386	2.82E+17	0.331	41.228	1.57E+17	0.965	38.818	3.09E+17	0.252	40.518
1.08E+17	1.526	39.486	2.72E+17	0.362	41.384	9.91E+16	1.670	39.950	2.65E+17	0.387	41.892
1.20E+17	1.356	39.210	2.82E+17	0.331	41.052	1.13E+17	1.453	39.426	2.76E+17	0.349	41.301
2.35E+17	0.500	37.798	3.53E+17	0.145	39.291	1.55E+17	0.979	38.780	3.07E+17	0.255	40.486
9.85E+16	1.681	39.657	2.64E+17	0.389	41.603	1.79E+17	0.801	38.728	3.22E+17	0.217	40.360
2.10E+17	0.618	37.982	3.40E+17	0.174	39.532	8.65E+16	1.924	39.303	2.53E+17	0.430	41.319
1.33E+17	1.199	39.059	2.92E+17	0.300	40.847	4.93E+16	3.252	40.904	2.10E+17	0.620	43.228
2.64E+17	0.391	37.310	3.67E+17	0.116	38.746	5.68E+16	2.870	40.244	2.20E+17	0.570	42.489
1.78E+17	0.810	38.563	3.21E+17	0.219	40.199	1.33E+17	1.197	39.175	2.92E+17	0.300	40.963
2.60E+17	0.404	37.313	3.65E+17	0.120	38.756	1.02E+17	1.628	40.134	2.67E+17	0.380	42.063
2.26E+17	0.539	37.811	3.49E+17	0.155	39.324	8.65E+16	1.924	40.383	2.53E+17	0.430	42.399
9.26E+16	1.793	39.862	2.59E+17	0.408	41.840	1.64E+17	0.907	39.066	3.13E+17	0.240	40.742
2.07E+17	0.633	38.513	3.38E+17	0.178	40.071	8.38E+16	1.986	40.017	2.50E+17	0.440	42.050
1.58E+17	0.956	39.049	3.09E+17	0.251	40.746	6.97E+16	2.375	40.231	2.35E+17	0.500	42.363
1.57E+17	0.961	38.843	3.09E+17	0.252	40.542	2.05E+16	6.645	39.992	1.56E+17	0.970	42.821
9.77E+16	1.695	39.559	2.63E+17	0.392	41.509	7.43E+16	2.235	40.254	2.40E+17	0.479	42.352
2.51E+17	0.438	37.403	3.61E+17	0.129	38.864	2.85E+16	5.128	40.907	1.75E+17	0.830	43.542
9.53E+16	1.742	39.765	2.61E+17	0.400	41.729	9.04E+16	1.839	40.432	2.57E+17	0.416	42.424
1.29E+17	1.245	39.214	2.89E+17	0.309	41.018	5.50E+16	2.952	39.801	2.18E+17	0.581	42.063
2.13E+17	0.604	37.931	3.41E+17	0.171	39.475	8.12E+16	2.049	39.783	2.48E+17	0.450	41.832
1.43E+17	1.092	39.019	2.99E+17	0.279	40.768	5.54E+16	2.937	40.927	2.18E+17	0.579	43.186
1.29E+17	1.241	39.105	2.89E+17	0.309	40.908	1.24E+17	1.300	39.421	2.85E+17	0.320	41.245
2.01E+17	0.667	38.251	3.35E+17	0.186	39.824	4.46E+16	3.550	40.594	2.03E+17	0.657	42.975
3.24E+17	0.213	36.038	3.93E+17	0.066	37.372	8.65E+16	1.924	39.751	2.53E+17	0.430	41.766
1.25E+17	1.281	39.578	2.86E+17	0.316	41.395	7.59E+16	2.190	39.883	2.42E+17	0.472	41.969
1.54E+17	0.988	38.885	3.07E+17	0.257	40.594	1.04E+17	1.594	41.266	2.68E+17	0.374	43.185
1.33E+17	1.191	39.244	2.92E+17	0.299	41.029	2.05E+17	0.643	38.627	3.37E+17	0.180	40.190
1.47E+17	1.050	38.936	3.02E+17	0.270	40.669	6.02E+16	2.724	42.130	2.24E+17	0.550	44.343
1.43E+17	1.094	38.751	2.99E+17	0.279	40.501	5.34E+16	3.035	41.872	2.15E+17	0.592	44.152
1.36E+17	1.159	39.145	2.94E+17	0.292	40.919	2.12E+17	0.610	37.756	3.41E+17	0.172	39.302
1.99E+17	0.680	38.213	3.34E+17	0.189	39.792	6.46E+16	2.554	39.781	2.29E+17	0.526	41.956
1.50E+17	1.028	38.774	3.04E+17	0.266	40.498	3.37E+16	4.480	41.933	1.85E+17	0.763	44.472
2.55E+17	0.421	37.268	3.63E+17	0.124	38.720	5.52E+16	2.944	41.044	2.18E+17	0.580	43.305
2.03E+17	0.654	38.217	3.36E+17	0.183	39.784	8.65E+16	1.924	39.786	2.53E+17	0.430	41.802
1.27E+17	1.263	39.204	2.87E+17	0.313	41.014	8.12E+16	2.049	40.222	2.48E+17	0.450	42.271
1.28E+17	1.246	39.388	2.89E+17	0.310	41.193	4.47E+16	3.541	40.765	2.03E+17	0.656	43.145
2.95E+17	0.292	36.448	3.81E+17	0.089	37.828	7.08E+16	2.341	39.995	2.37E+17	0.495	42.119
9.44E+16	1.758	39.943	2.60E+17	0.402	41.911	7.19E+16	2.308	39.671	2.38E+17	0.490	41.787
1.90E+17	0.731	38.250	3.29E+17	0.201	39.852	5.68E+16	2.870	40.426	2.20E+17	0.570	42.671
1.21E+17	1.334	39.137	2.83E+17	0.326	40.972	9.89E+16	1.674	40.264	2.64E+17	0.388	42.208
1.82E+17	0.779	38.357	3.24E+17	0.212	39.980	8.12E+16	2.049	40.353	2.48E+17	0.450	42.402
2.06E+17	0.642	38.159	3.38E+17	0.180	39.721	7.41E+16	2.242	40.060	2.40E+17	0.480	42.160
2.90E+17	0.306	36.892	3.78E+17	0.093	38.281	5.00E+16	3.212	40.226	2.11E+17	0.615	42.543
1.32E+17	1.209	39.241	2.91E+17	0.302	41.033	9.51E+16	1.744	40.349	2.61E+17	0.400	42.313
2.72E+17	0.363	37.230	3.70E+17	0.109	38.651	4.48E+16	3.533	39.937	2.03E+17	0.655	42.315
2.99E+17	0.280	36.620	3.82E+17	0.086	37.994	7.02E+16	2.362	40.855	2.36E+17	0.498	42.984
1.89E+17	0.739	38.362	3.28E+17	0.203	39.968	7.76E+16	2.144	39.751	2.44E+17	0.465	41.825
1.93E+17	0.714	38.330	3.30E+17	0.197	39.924	8.05E+16	2.068	40.767	2.47E+17	0.453	42.821
2.53E+17	0.430	37.458	3.62E+17	0.127	38.915	8.79E+16	1.894	39.195	2.54E+17	0.425	41.202
1.80E+17	0.792	38.573	3.23E+17	0.215	40.202	6.69E+16	2.470	40.631	2.32E+17	0.514	42.786
1.24E+17	1.302	39.278	2.85E+17	0.320	41.103	8.84E+16	1.881	39.562	2.55E+17	0.423	41.566
1.78E+17	0.808	38.585	3.22E+17	0.218	40.221	2.66E+16	5.424	41.416	1.71E+17	0.859	44.093
1.98E+17	0.684	38.359	3.33E+17	0.190	39.940	2.21E+16	6.256	40.524	1.61E+17	0.936	43.307
2.90E+17	0.306	36.757	3.78E+17	0.093	38.146	6.42E+16	2.568	40.276	2.29E+17	0.528	42.454
1.02E+17	1.626	39.504	2.67E+17	0.380	41.433	2.01E+16	6.739	40.660	1.55E+17	0.978	43.500
1.83E+17	0.776	38.362	3.25E+17	0.211	39.984	2.49E+16	5.698	41.471	1.67E+17	0.885	44.184
1.06E+17	1.552	39.954	2.71E+17	0.367	41.860	2.96E+16	4.979	41.460	1.77E+17	0.815	44.074
8.90E+16	1.869	40.133	2.55E+17	0.421	42.134	3.99E+16	3.896	41.326	1.95E+17	0.698	43.769
1.54E+17	0.991	38.934	3.06E+17	0.258	40.645	5.71E+16	2.855	40.467	2.20E+17	0.568	42.709

3.86E+16	4.009	41.104	1.93E+17	0.711	43.567	5.99E+16	2.735	40.087	2.24E+17	0.552	42.303
1.16E+17	1.404	39.225	2.79E+17	0.340	41.084	1.09E+17	1.503	39.544	2.73E+17	0.358	41.435
9.62E+16	1.723	39.530	2.62E+17	0.397	41.488	1.87E+16	7.121	41.130	1.52E+17	1.010	44.012
2.98E+16	4.949	41.044	1.77E+17	0.812	43.654	3.57E+16	4.277	41.210	1.88E+17	0.741	43.717
3.08E+16	4.822	40.787	1.79E+17	0.799	43.379	8.65E+16	1.924	39.795	2.53E+17	0.430	41.811
2.51E+16	5.666	40.666	1.67E+17	0.882	43.375	6.46E+16	2.554	40.225	2.29E+17	0.526	42.400
2.83E+16	5.159	41.048	1.74E+17	0.833	43.688	5.34E+16	3.035	40.297	2.15E+17	0.592	42.577
2.56E+16	5.581	40.598	1.69E+17	0.874	43.295	2.38E+16	5.913	40.898	1.64E+17	0.905	43.639
3.29E+16	4.564	40.958	1.83E+17	0.772	43.510	2.15E+16	6.403	40.644	1.59E+17	0.949	43.445
2.07E+17	0.635	37.897	3.38E+17	0.178	39.455	7.86E+16	2.117	40.004	2.45E+17	0.461	42.072
1.53E+17	1.000	39.109	3.06E+17	0.260	40.823	1.05E+17	1.576	39.755	2.69E+17	0.371	41.669
2.01E+17	0.668	38.138	3.35E+17	0.186	39.712	3.07E+16	4.832	41.121	1.79E+17	0.800	43.714
1.48E+17	1.044	39.046	3.03E+17	0.269	40.776	4.20E+16	3.733	41.043	1.99E+17	0.679	43.457
1.80E+17	0.794	38.749	3.23E+17	0.215	40.378	5.49E+16	2.957	40.408	2.17E+17	0.582	42.672
6.14E+16	2.674	40.277	2.26E+17	0.543	42.479	6.02E+16	2.724	40.062	2.24E+17	0.550	42.276
3.49E+16	4.359	40.723	1.87E+17	0.750	43.243	2.99E+16	4.930	40.763	1.78E+17	0.810	43.370
4.67E+16	3.411	40.409	2.06E+17	0.640	42.764	2.14E+16	6.415	41.175	1.59E+17	0.950	43.977
8.65E+16	1.924	40.169	2.53E+17	0.430	42.184	1.17E+17	1.392	39.440	2.80E+17	0.337	41.294
4.67E+16	3.411	40.810	2.06E+17	0.640	43.164	2.35E+16	5.968	41.558	1.64E+17	0.910	44.306
7.04E+16	2.355	40.197	2.36E+17	0.497	42.325	1.51E+17	1.015	38.915	3.05E+17	0.263	40.635
8.38E+16	1.986	39.978	2.50E+17	0.440	42.011	4.63E+16	3.435	40.652	2.05E+17	0.643	43.011
1.10E+17	1.488	39.457	2.74E+17	0.355	41.342	4.07E+16	3.835	40.656	1.97E+17	0.691	43.089
3.23E+16	4.640	41.037	1.82E+17	0.780	43.601	1.09E+17	1.499	39.536	2.74E+17	0.357	41.426
6.20E+16	2.652	40.227	2.26E+17	0.540	42.425	3.76E+16	4.097	40.698	1.92E+17	0.721	43.176
2.65E+16	5.435	41.244	1.70E+17	0.860	43.922	5.50E+16	2.952	40.479	2.18E+17	0.581	42.742
7.69E+16	2.164	40.469	2.43E+17	0.468	42.549	4.84E+16	3.305	40.424	2.08E+17	0.627	42.759
2.78E+16	5.230	41.223	1.73E+17	0.840	43.873	2.94E+16	5.009	40.774	1.76E+17	0.818	43.393
2.09E+16	6.530	40.798	1.58E+17	0.960	43.613	7.81E+16	2.129	39.972	2.44E+17	0.463	42.042
2.91E+16	5.046	41.191	1.76E+17	0.822	43.815	8.15E+16	2.042	39.975	2.48E+17	0.449	42.023
2.24E+16	6.189	40.778	1.61E+17	0.930	43.552	4.10E+16	3.810	40.626	1.97E+17	0.688	43.054
8.10E+16	2.055	39.746	2.47E+17	0.451	41.797	2.59E+16	5.539	41.539	1.69E+17	0.870	44.231
5.07E+16	3.173	40.597	2.12E+17	0.610	42.905	6.89E+16	2.404	40.199	2.34E+17	0.504	42.338
2.85E+16	5.128	41.415	1.75E+17	0.830	44.051	5.35E+16	3.027	40.930	2.15E+17	0.591	43.209
3.90E+16	3.974	40.826	1.94E+17	0.707	43.282	8.76E+16	1.900	39.753	2.54E+17	0.426	41.762
9.07E+16	1.833	39.887	2.57E+17	0.415	41.877	1.20E+17	1.347	39.501	2.82E+17	0.329	41.340
5.90E+16	2.775	40.332	2.23E+17	0.557	42.557	5.47E+16	2.967	40.135	2.17E+17	0.583	42.401
3.14E+16	4.745	40.997	1.80E+17	0.791	43.577	6.59E+16	2.505	40.908	2.31E+17	0.519	43.072
4.02E+16	3.870	40.773	1.96E+17	0.695	43.212	9.48E+16	1.750	39.729	2.61E+17	0.401	41.695
4.76E+16	3.355	40.706	2.07E+17	0.633	43.050	1.87E+17	0.750	38.293	3.27E+17	0.205	39.904
1.59E+17	0.947	38.918	3.10E+17	0.249	40.611	1.16E+17	1.406	39.354	2.79E+17	0.340	41.213
6.34E+16	2.596	40.381	2.28E+17	0.532	42.566	8.49E+16	1.961	39.854	2.51E+17	0.436	41.880
1.19E+17	1.358	39.235	2.82E+17	0.331	41.078	1.07E+17	1.532	39.652	2.72E+17	0.363	41.552
1.14E+17	1.439	39.495	2.77E+17	0.346	41.365	8.49E+16	1.961	39.900	2.51E+17	0.436	41.926
2.09E+16	6.541	41.447	1.57E+17	0.961	44.264	1.29E+17	1.243	39.370	2.89E+17	0.309	41.174
5.03E+16	3.197	40.681	2.11E+17	0.613	42.994	1.15E+17	1.417	39.522	2.78E+17	0.342	41.385
1.16E+17	1.407	39.468	2.79E+17	0.340	41.328	2.23E+17	0.557	37.895	3.47E+17	0.159	39.416
1.99E+16	6.798	41.311	1.55E+17	0.983	44.157	1.19E+17	1.363	39.410	2.81E+17	0.332	41.255
3.87E+16	4.000	40.561	1.93E+17	0.710	43.022	7.66E+16	2.170	40.273	2.43E+17	0.469	42.354
3.67E+16	4.178	40.786	1.90E+17	0.730	43.277	1.65E+17	0.902	38.584	3.14E+17	0.239	40.259
7.64E+16	2.177	40.052	2.43E+17	0.470	42.135	1.11E+17	1.471	39.543	2.75E+17	0.352	41.424
4.93E+16	3.252	40.685	2.10E+17	0.620	43.009	5.04E+16	3.189	40.502	2.11E+17	0.612	42.814
6.55E+16	2.519	40.013	2.31E+17	0.521	42.180	4.78E+16	3.339	40.036	2.08E+17	0.631	42.377
1.05E+17	1.566	39.724	2.70E+17	0.369	41.634	4.60E+16	3.451	40.454	2.05E+17	0.645	42.817
5.66E+16	2.877	40.152	2.20E+17	0.571	42.399	8.68E+16	1.918	39.876	2.53E+17	0.429	41.890
5.16E+16	3.127	40.228	2.13E+17	0.604	42.527	7.04E+16	2.355	39.948	2.36E+17	0.497	42.076
2.26E+16	6.157	41.170	1.62E+17	0.927	43.940	6.21E+16	2.645	40.031	2.26E+17	0.539	42.227
1.40E+17	1.122	39.094	2.97E+17	0.285	40.854	5.83E+16	2.804	40.641	2.22E+17	0.561	42.872
1.37E+17	1.153	39.068	2.95E+17	0.291	40.839	9.21E+16	1.803	39.366	2.58E+17	0.410	41.347
6.05E+16	2.709	40.086	2.25E+17	0.548	42.296	9.16E+16	1.815	39.439	2.58E+17	0.412	41.424
2.60E+16	5.518	40.804	1.69E+17	0.868	43.493	5.23E+16	3.088	40.452	2.14E+17	0.599	42.743
7.06E+16	2.348	40.089	2.36E+17	0.496	42.215	4.95E+16	3.244	40.734	2.10E+17	0.619	43.056
2.99E+16	4.940	40.796	1.77E+17	0.811	43.405	8.87E+16	1.875	39.726	2.55E+17	0.422	41.728
3.43E+16	4.415	41.285	1.86E+17	0.756	43.814	6.20E+16	2.652	40.314	2.26E+17	0.540	42.511
2.94E+16	4.999	41.034	1.77E+17	0.817	43.652	9.48E+16	1.750	40.589	2.61E+17	0.401	42.555
3.47E+16	4.378	40.779	1.86E+17	0.752	43.302	1.78E+17	0.807	38.440	3.22E+17	0.218	40.075

4.76E+16	3.355	39.858	2.07E+17	0.633	42.202	1.02E+16	11.167	41.769	1.24E+17	1.300	45.016
1.01E+17	1.645	39.707	2.66E+17	0.383	41.642	1.01E+16	11.247	41.487	1.24E+17	1.305	44.740
1.32E+17	1.207	39.520	2.91E+17	0.302	41.311	1.79E+17	0.798	38.925	3.22E+17	0.216	40.556
1.16E+17	1.406	39.221	2.79E+17	0.340	41.080	3.62E+16	4.223	40.594	1.89E+17	0.735	43.092
6.77E+16	2.443	39.732	2.33E+17	0.510	41.881	1.41E+16	8.800	41.146	1.38E+17	1.140	44.197
8.90E+16	1.869	40.136	2.55E+17	0.421	42.136	1.01E+16	11.278	42.155	1.23E+17	1.307	45.411
9.54E+16	1.738	39.526	2.61E+17	0.399	41.488	1.09E+16	10.620	41.739	1.27E+17	1.265	44.944
7.12E+16	2.328	40.026	2.37E+17	0.493	42.147	4.30E+16	3.657	40.742	2.00E+17	0.670	43.143
4.11E+16	3.801	40.570	1.97E+17	0.687	42.996	4.67E+16	3.411	40.569	2.06E+17	0.640	42.924
4.11E+16	3.801	40.408	1.97E+17	0.687	42.835	9.43E+15	11.813	41.773	1.21E+17	1.340	45.068
7.08E+16	2.341	40.124	2.37E+17	0.495	42.249	2.78E+16	5.230	40.864	1.73E+17	0.840	43.514
5.17E+16	3.119	40.349	2.13E+17	0.603	42.646	2.22E+16	6.245	40.759	1.61E+17	0.935	43.540
8.90E+16	1.869	40.179	2.55E+17	0.421	42.180	2.13E+16	6.449	41.468	1.58E+17	0.953	44.274
1.13E+17	1.449	39.716	2.76E+17	0.348	41.590	1.46E+16	8.582	41.537	1.40E+17	1.124	44.568
1.81E+17	0.785	38.483	3.24E+17	0.213	40.109	5.98E+16	2.738	40.294	2.24E+17	0.552	42.511
1.14E+17	1.428	39.307	2.78E+17	0.344	41.173	4.29E+16	3.666	40.580	2.00E+17	0.671	42.982
1.47E+17	1.053	38.798	3.02E+17	0.271	40.532	6.75E+16	2.450	40.223	2.33E+17	0.511	42.374
5.78E+16	2.826	40.137	2.21E+17	0.564	42.373	1.79E+16	7.365	41.331	1.50E+17	1.030	44.240
1.45E+17	1.068	38.985	3.01E+17	0.274	40.725	1.27E+16	9.532	41.343	1.33E+17	1.192	44.459
2.05E+17	0.647	38.119	3.37E+17	0.181	39.683	1.56E+16	8.156	41.019	1.43E+17	1.092	44.008
5.49E+16	2.959	40.899	2.17E+17	0.582	43.164	2.03E+16	6.692	41.000	1.56E+17	0.974	43.834
4.19E+16	3.742	40.488	1.99E+17	0.680	42.904	1.50E+16	8.394	41.613	1.41E+17	1.110	44.625
9.48E+16	1.750	39.970	2.61E+17	0.401	41.936	9.25E+15	11.978	41.521	1.20E+17	1.350	44.827
9.04E+16	1.839	39.566	2.57E+17	0.416	41.558	2.71E+16	5.332	40.830	1.72E+17	0.850	43.494
1.39E+17	1.127	39.449	2.97E+17	0.286	41.211	1.15E+16	10.254	41.406	1.29E+17	1.241	44.582
5.81E+16	2.811	40.818	2.22E+17	0.562	43.051	8.20E+15	13.067	41.423	1.15E+17	1.414	44.804
1.50E+17	1.029	38.666	3.04E+17	0.266	40.391	1.28E+16	9.475	41.497	1.34E+17	1.188	44.608
1.27E+17	1.269	39.419	2.87E+17	0.314	41.232	1.84E+16	7.206	41.402	1.51E+17	1.017	44.294
5.50E+16	2.952	41.406	2.18E+17	0.581	43.669	9.90E+15	11.407	41.707	1.23E+17	1.315	44.971
7.80E+16	2.131	39.877	2.44E+17	0.463	41.948	2.91E+16	5.039	41.018	1.76E+17	0.821	43.641
1.15E+17	1.411	39.130	2.78E+17	0.341	40.992	1.21E+16	9.867	42.103	1.31E+17	1.215	45.247
4.78E+16	3.339	40.541	2.08E+17	0.631	42.882	4.89E+16	3.275	40.186	2.09E+17	0.623	42.515
6.53E+16	2.526	40.509	2.30E+17	0.522	42.677						
1.06E+17	1.560	39.559	2.70E+17	0.368	41.468						
1.29E+17	1.243	39.057	2.89E+17	0.309	40.861						
6.42E+16	2.568	40.192	2.29E+17	0.528	42.370						
1.79E+17	0.798	38.774	3.22E+17	0.216	40.405						
1.40E+17	1.117	39.077	2.97E+17	0.284	40.835						
6.81E+16	2.429	40.049	2.34E+17	0.508	42.194						
3.22E+16	4.649	40.872	1.82E+17	0.781	43.437						
5.03E+16	3.197	40.304	2.11E+17	0.613	42.617						
1.43E+17	1.087	38.819	2.99E+17	0.278	40.566						
7.48E+16	2.222	39.960	2.41E+17	0.477	42.054						
2.14E+16	6.415	40.836	1.59E+17	0.950	43.638						
1.68E+16	7.704	41.207	1.47E+17	1.057	44.151						
2.95E+16	4.989	41.075	1.77E+17	0.816	43.691						
8.00E+16	2.080	40.266	2.46E+17	0.455	42.324						
1.83E+16	7.242	41.467	1.51E+17	1.020	44.363						
1.41E+16	8.800	41.273	1.38E+17	1.140	44.323						
2.69E+16	5.373	40.939	1.71E+17	0.854	43.608						
8.90E+15	12.312	41.720	1.19E+17	1.370	45.050						
2.02E+16	6.704	41.498	1.56E+17	0.975	44.334						
2.05E+16	6.645	41.634	1.56E+17	0.970	44.463						
3.58E+16	4.268	40.782	1.88E+17	0.740	43.288						
8.57E+15	12.652	41.523	1.17E+17	1.390	44.876						
7.88E+16	2.112	40.082	2.45E+17	0.460	42.148						
1.83E+16	7.242	41.268	1.51E+17	1.020	44.164						
1.47E+16	8.528	41.489	1.40E+17	1.120	44.514						
1.17E+16	10.090	41.858	1.30E+17	1.230	45.021						
1.27E+16	9.503	41.250	1.33E+17	1.190	44.363						
2.79E+16	5.219	40.750	1.73E+17	0.839	43.398						
1.87E+16	7.121	42.030	1.52E+17	1.010	44.912						
6.55E+16	2.519	40.212	2.31E+17	0.521	42.378						
7.52E+16	2.209	40.014	2.41E+17	0.475	42.105						
2.14E+16	6.415	41.082	1.59E+17	0.950	43.884						

where

$$m = am_p \quad \rho = \frac{m}{Vol}$$

$$n = \frac{m}{am_p Vol} = \frac{\rho}{am_p}$$

then

$$k_b T_{BEC} = \frac{h^2}{2\pi am_p} \left(\frac{\rho}{\zeta(3/2)} \right)^{\frac{2}{3}} \left(\frac{1}{am_p} \right)^{\frac{2}{3}} = \frac{h^2}{2\pi} \left(\frac{\rho}{\zeta(3/2)} \right)^{\frac{2}{3}} \left(\frac{1}{am_p} \right)^{\frac{5}{3}}$$

$$\rho = \zeta(3/2) \left(\frac{2\pi k_b T_c (am_p)^{\frac{5}{3}}}{h^2} \right)^{\frac{2}{3}}$$

$$\rho = \zeta(3/2) \left(\frac{2\pi k_b T_b (bm_p)^{\frac{5}{3}}}{h^2} \right)^{\frac{2}{3}}$$

$$\rho = \rho \text{ therefore } T_c (am_p)^{\frac{5}{3}} = T_b (bm_p)^{\frac{5}{3}}$$

and

$$a = \frac{\left(\frac{T_b (bm_p)^{\frac{5}{3}}}{T_c} \right)^{\frac{3}{5}}}{m_p}$$

$$\text{Object Spherical Perimeter } P = \pi d = A_c / d$$

$$\text{Object Hydraulic Radius } d \text{ to calculate Universe Reynolds Number Object(seen) } A_c / P = ((6/\pi) Vol)^{\frac{1}{3}} = d$$

$$\text{Object frontal area (A) to thrust } \text{cm}^2$$

$$\text{Object Spherical Diameter (d) } \text{SQRT}(4 \times A / \pi)$$

$$\text{Object number (a) of } m_p$$

$$\text{Object number (b} = 5.996\text{E+07) of } m_p$$

$$\text{Object number (a+b) of } m_p$$

$$\text{Object Mass (a+b) } m_p$$

$$\text{Object Area to Mass ratio } A_c / m = A_c / ((a+b) m_p)$$

Figure 4.42.3 Universe Particle Object Fluid Mechanical Dynamics Within the Trisine Lattice as a function of z_B

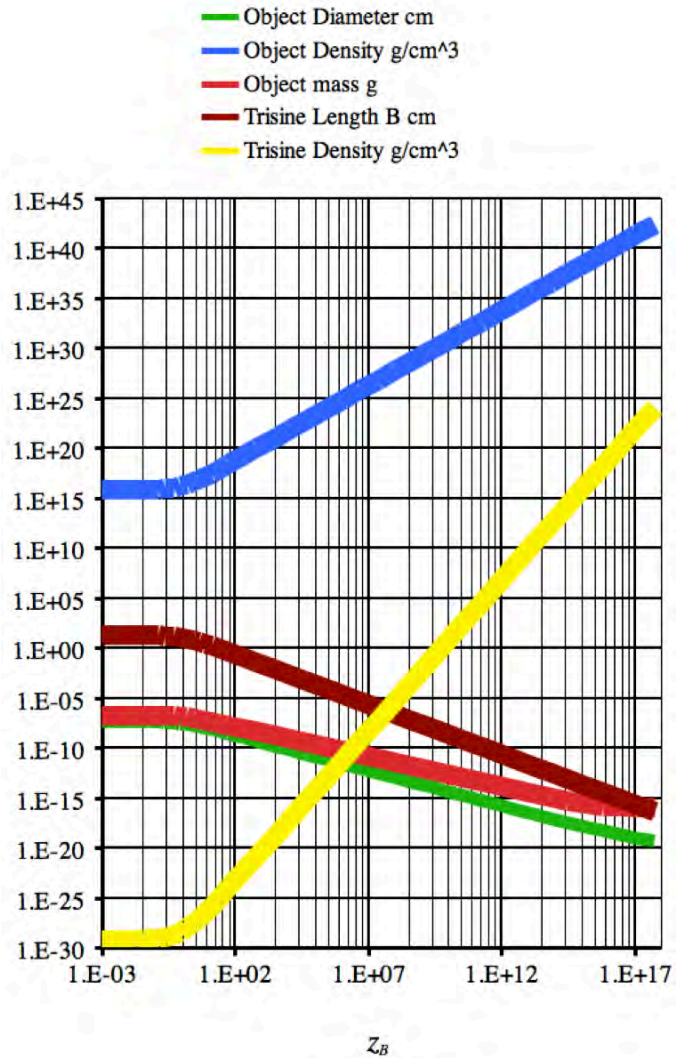
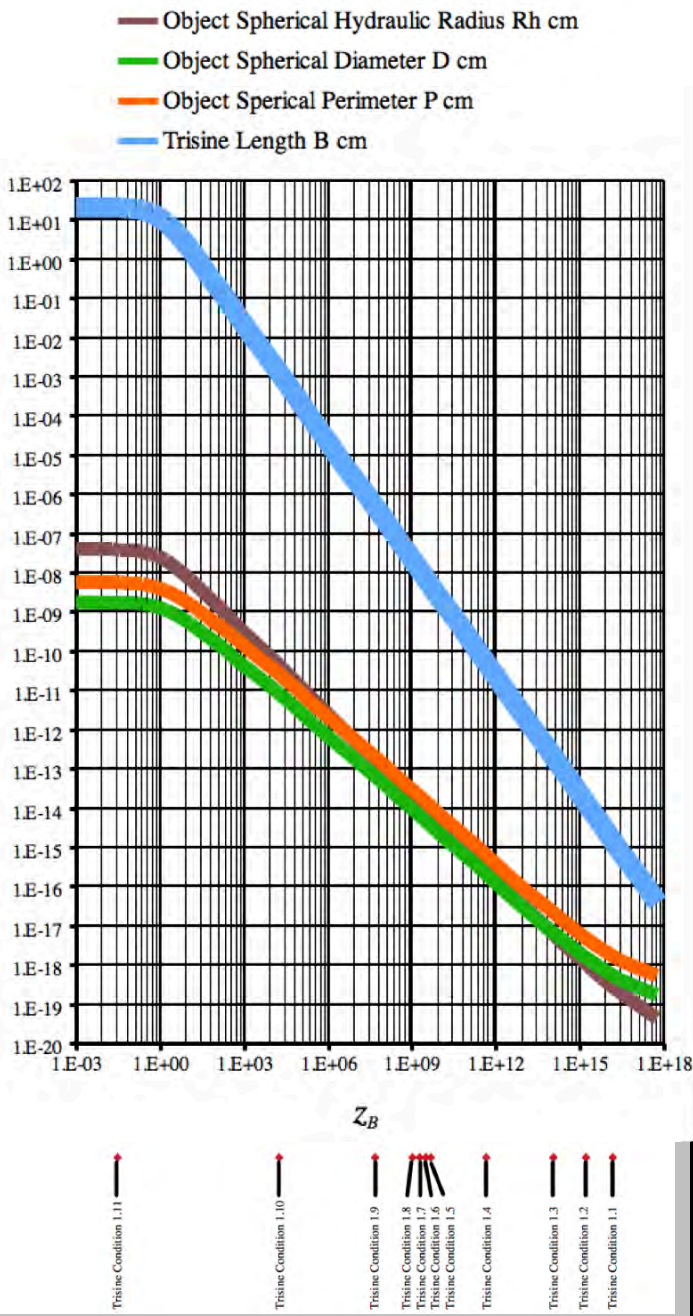
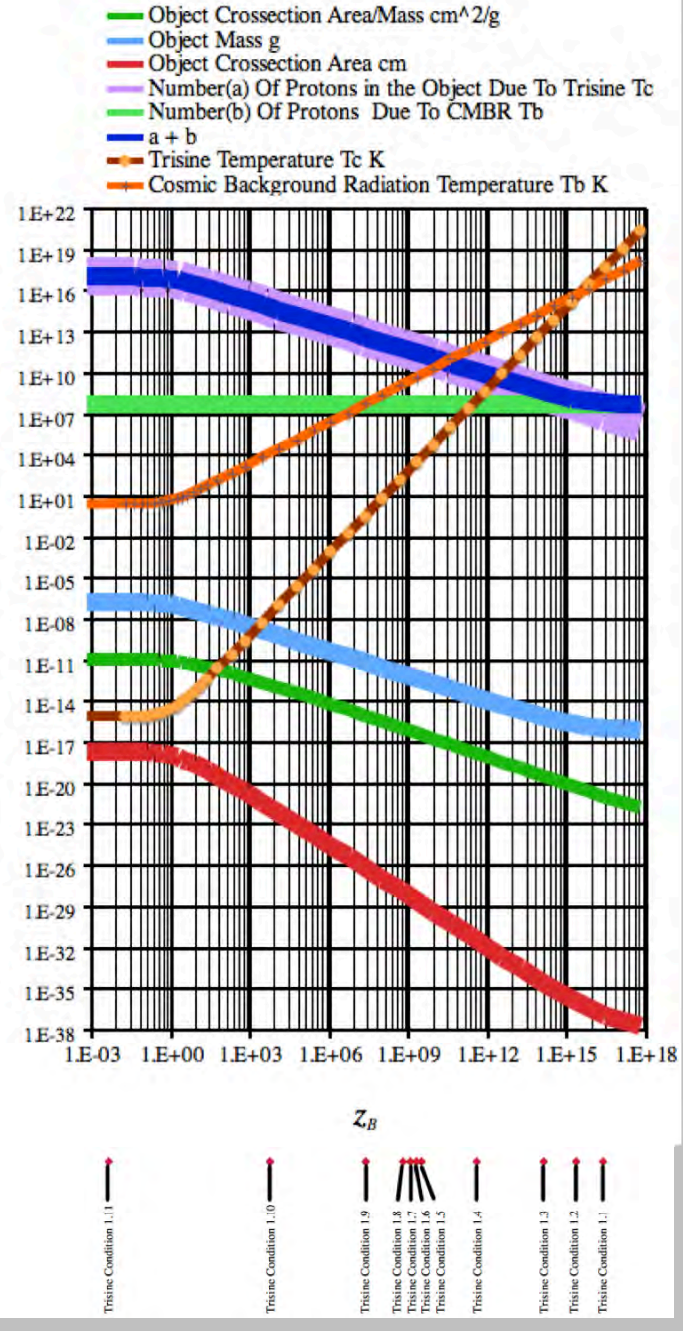


Figure 4.42.4 Extended Universe Particle Object Fluid Mechanical Dynamics Within the Trisine Background as a function of z_B



The generalized fluid model (Appendix L) is used for this universe thrust model as illustrated in Figures 4.42.3 - 4.42.9. The thrust model extends over the many orders of magnitude representing the universe at its beginning to present. The dimensional relationship between Trisine temperature T_c (dark energy) and Cosmic Microwave Background Radiation (CMBR) temperature T_b dictates a third phase (dark matter).

Figure 4.42.5 Extended Universe Particle Object Fluid Mechanical Dynamics Within the Trisine Background as a function of z_B

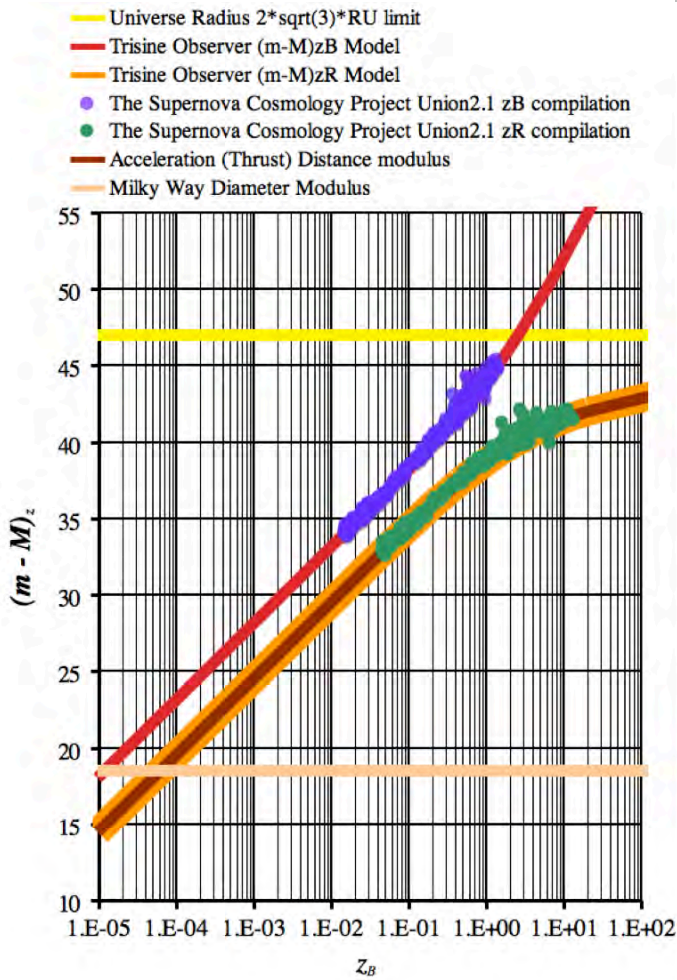


The universe is shown to be ‘thrust’ into existence much like an explosion. In this context, dark matter is essentially another baryonic phase (like ice and water) with distinct density and size characteristics that are not observed by Baryonic Acoustic Oscillations (at $z_B \sim 3,000$) which is oriented towards a continuous homogeneous gas phase.

The phase density Figures 4.42.3 (Blue line) has a slope correlation to Appendix K Figure K2. Magnitude difference can be explained in terms of particle coalescence dynamics as presented in Appendix L and in particular equation L2.14.

This thrust model assumes the unit proton mass as m_p . Other unit mass assumptions would not change the general developed relationship and may indeed provide further insights into early universe nucleosynthetic dynamics.

Figure 4.42.6 The Supernovae Cosmology Project Union 2.1 data[124] without error bars regressed with Trisine Deceleration Projection



The Type 1A supernovae when plotted in the z_B dimension (rather than z_R) further demonstrates the universe beginning expanding to the present at the speed of light c .

Figure 4.42.7 The Supernovae Cosmology Project Union 2.1 data[124] without error bars regressed with Trisine Deceleration Projection

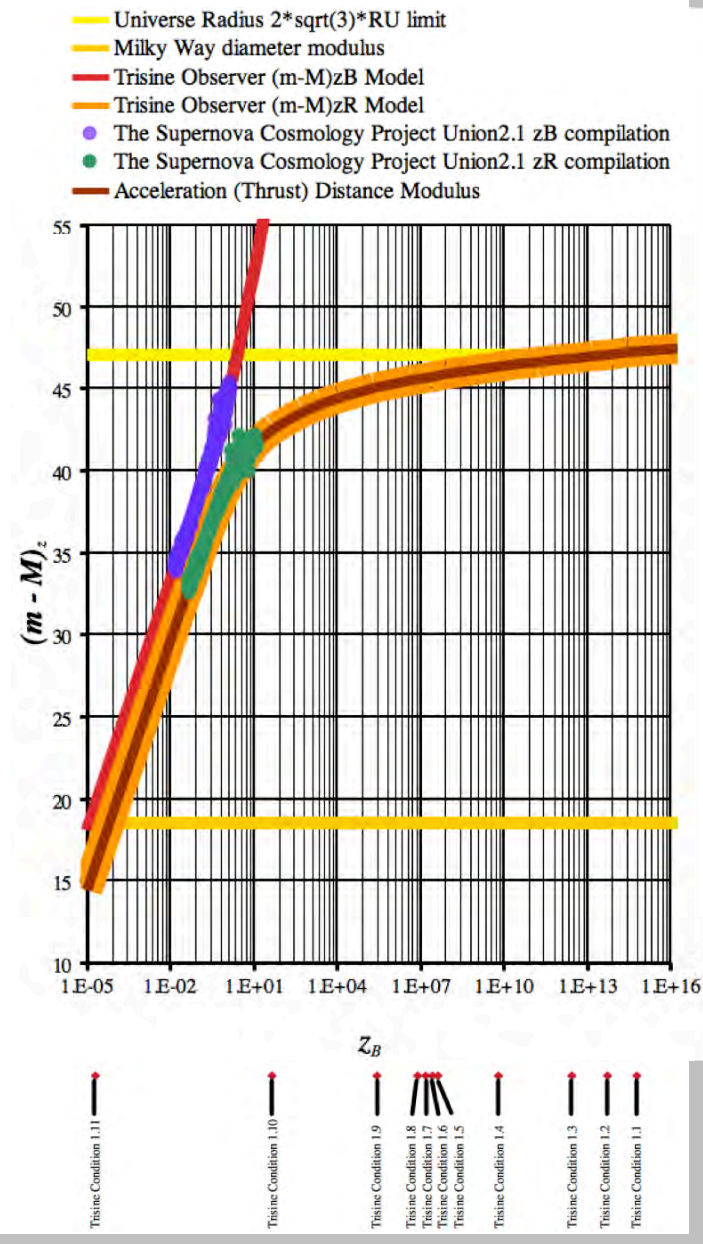
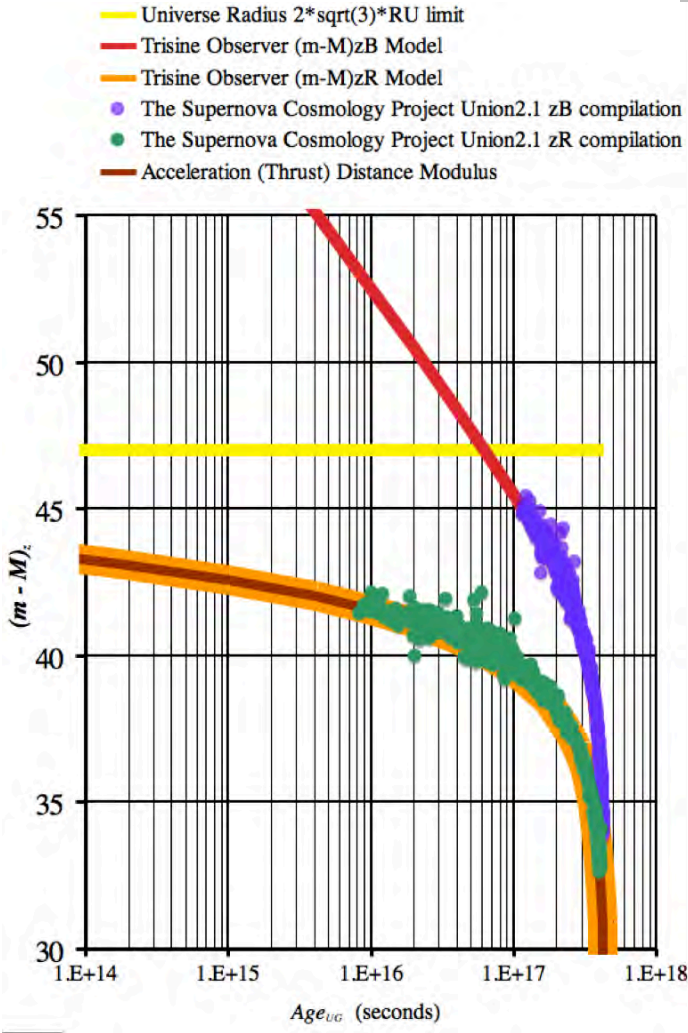
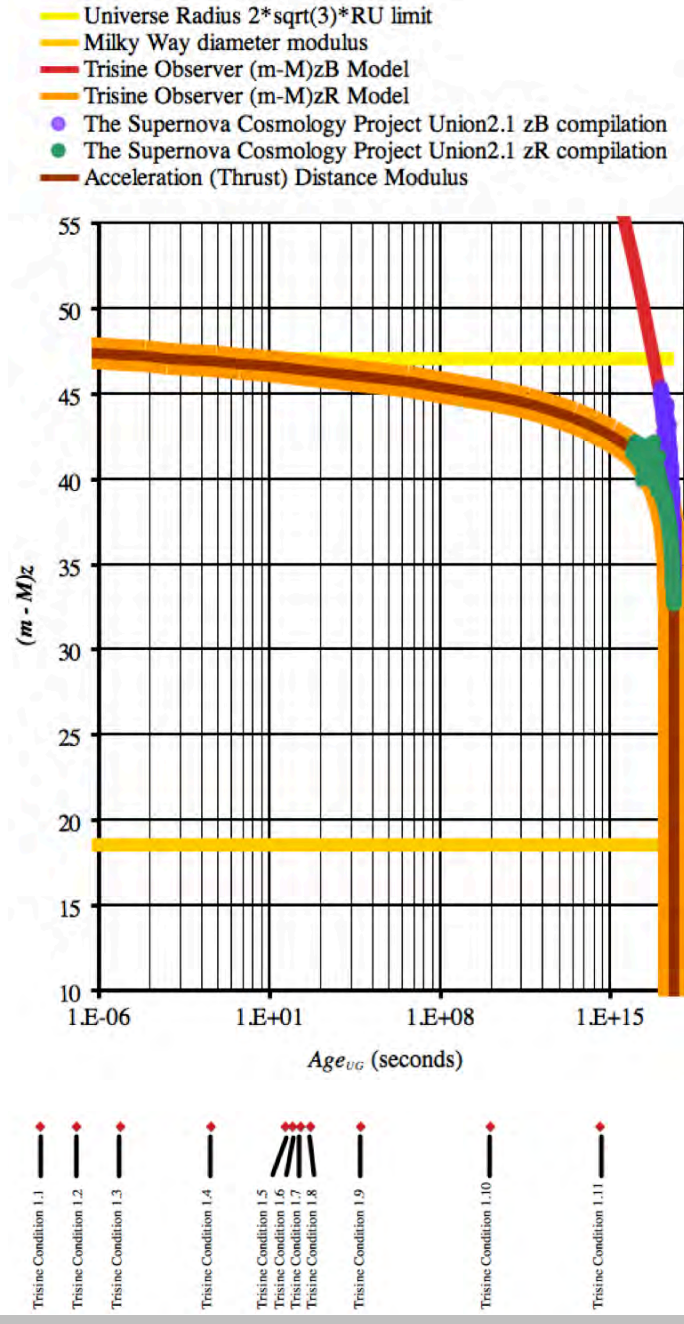


Figure 4.42.8 The Supernova Cosmology Project Union 2.1 data[124] without error bars regressed with Trisine Deceleration Projection on a Age_{UG} basis and near present time.



The Type 1A Supernovae when plotted in the Age_{UG} dimension further demonstrates the universe beginning expanding to the present at the speed of light c . This Type 1A supernovae day can be extrapolated or modeled back to the universe beginning in terms of this thrust model.

Figure 4.42.9 The Supernova Cosmology Project Union 2.1 data[124] without error bars regressed with Trisine Deceleration Projection on a Age_{UG} basis and extended universe time scale.



4.43. It is noted that time picosecond(ps) fluctuations [132] Figure 4.c are of the same order as de Broglie matter wave cellular times as a function of T_c numerically and graphically expressed in Table and Figure 2.4.

It is further noted that these De Broglie waves are an expression of the Charge conjugation, Parity change, Time reversal, CPT theorem in the space filling mode.

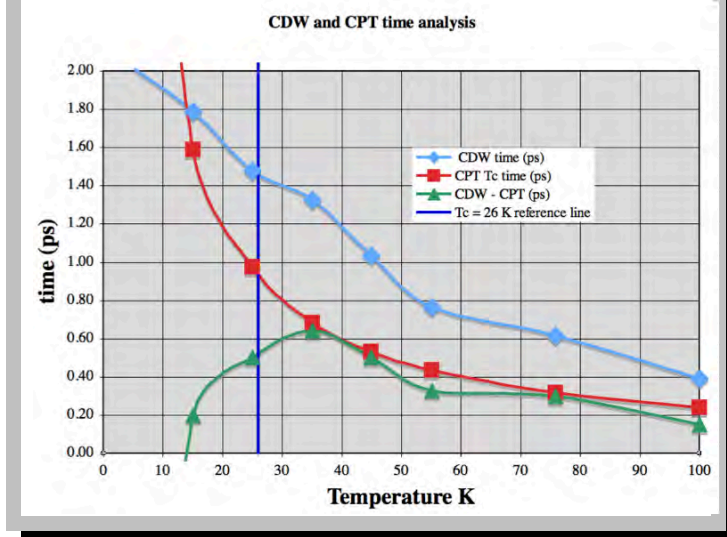
Anticipated space filling CPT times at T_c 's, your charge density wave times and their differences are as follows:

Table 4.43.1

T_c	CPT time (ps)	CDW (ps)	CDW - CPT (ps)
5.14	2.01	4.67	-2.66
15.05	1.79	1.59	0.20
24.95	1.48	0.976	0.50
35.05	1.33	0.685	0.64
44.95	1.04	0.534	0.50
55.05	0.76	0.436	0.33
75.81	0.62	0.317	0.30
100.00	0.39	0.24	0.15

Numbers are graphically presented Figure 4.43.1.

Figure 4.43.1



Space filling CPT theory, being a virtual particle concept may not always be expressed in CDW measurements, but in this case there is a peak in CDW-CPT in the upper 30K's.

(numerically similar to your intersection in Figure 4d) that may be a close indicator of your actual T_c of 26 K.

The space filling CPT is the basis of the superconductor phenomenon that may or may not be expressed as CDW.

This CPT scaling is all consistent with Homes' Law.

This concept extends into cosmological dimensions.

In additional trisine model confirmation, it is noted that the spacing between NbSe_2 stripes ([133] Figure 2 A) is $\sim 1 \text{ nm}$. This conforms to my stripe scaling Figure 2.3.1 with spacing

$$\frac{3B}{\sqrt{3}}$$

According to my scaling formula (similar to Homes law) $4 \times 1 \text{ nm}$ defined as B as in equation 2.1.13a

$$E = k_b T_c = \frac{m_t v_{dx}^2}{2} = \hbar \frac{\pi}{time_{\pm}} = \frac{\hbar^2 K_B^2}{2m_t}$$

would indicate a T_c of 7.2 K for space filling CPT.

(m_t is a universal particle with mass = $110 \times$ electron mass m_e)

Charge density waves CDW $4 \times \text{NbSe}_2$ stripes may express the difference between CDW with underlying a more fundamental CPT.

In this case[133], charge density waves CDW are expressions of electron movement directly related to universal particle m_t movement by the relationship $m_t = 110 m_e$ with charge density wave CDW spacing/superconducting wave spacing = $\sqrt{m_t/m_e}$, a relationship that is observed in this NbSe_2 superconductor but not all superconductors.

4.44. Robbert Dijkgraaf[134] provides a classical relationship based on string theory black hole dynamics.

$$F \Delta x = T_c \Delta S$$

This relationship is consistent with the following, noting that a de Broglie velocity v_{dx} replaces the speed of light c .

$$F = \frac{m_t v_{dx}}{time_{\pm}}$$

The entropy relationship is the same as Dijkgraaf[134] with a removal of π such that equation reads 2 versus 2π

$$\Delta S = \frac{2k_b v_{dx}}{\hbar} m_t \Delta x$$

The entropy has a Boltzmann constant value over all trisine dimensions recognizing the Heisenberg uncertainty relationship:

$$\frac{2v_{dx}}{\hbar} m_i \Delta x = 1$$

This is all consistent with vacuum entropy equations 2.11.9a and 2.11.10 indicating singular entropy per cavity.

4.45. Newton's second law in conjunction with Hooke's law are the basis for presenting oscillatory motion[61]

$$\text{Newtonian Force} = ma = mv \frac{dv}{dx} = -kx$$

and let

$$k = -m \frac{v}{x} \frac{dv}{dx} = -mH_U^2$$

From the third and fourth *Newtonian Force* terms we have:

$$\int mv dv + \int kx dx = 0$$

that integrates as follows with Total Energy(E) as the integration constant:

$$\frac{1}{2}mv^2 + \frac{1}{2}kx^2 = E_{kinetic} + E_{potential} = \text{Total Energy}(E)$$

The maximum potential energy $E_{potential}$ at maximum x and velocity v at 0 represents the harmonic amplitude A such that:

$$A^2 = \frac{2E}{k} = \frac{2mc^2}{k} = \frac{2mc^2}{-mH_U^2} = \frac{2c^2}{-H_U^2}$$

This equation compares nearly equivalent (2 vs 3 perhaps a *chain/cavity* relationship) eqn 2.11.14a.

$$R^2 = \frac{3c^2}{H_U^2}$$

This harmonic derivation may explain in part low angular anomalies[135] observed by the Planck spacecraft at first light as the universe bouncing against its own horizon with negative sign representing a 180 degree phase change.

4.46. A question logically develops from this line of thinking and that is "What is the source of the energy or mass density?". After the energy is imparted to the spacecraft (or other objects) passing through space, does the energy regenerate itself locally or essentially reduce the energy of universal field? And then there is the most vexing question based on the universal scaled superconductivity resonant hypothesis developed in this report and that is whether this phenomenon could be engineered at an appropriate scale for beneficial use.

One concept for realizing the capture of this essentially astrophysical concept, is to engineer an earth based congruent wave crystal reactor. Ideally, such a wave crystal reactor would be made in the technically manageable wave length (ultraviolet to microwave). Perhaps such coherent electromagnetic waves would interact at the $\hbar\omega/2$ energy level in the trisine CPT lattice pattern at the Schwinger limit with resultant virtual particle production. Conceptually a device as indicated in Figures 4.46.1, 4.46.2 and 4.46.3, may be appropriate where the green area represents reflecting, generating and polarizing surfaces of coherent electromagnetic radiation creating standing waves which interact in the intersecting zone defined by the trisine characteristic angle of (90 – 22.8) degrees and 120 degrees of each other. It is anticipated that Laguerre-Gaussian optical vortices and related superconducting modes will be spatially created in the vacuum in accordance with photon spatial positioning and total momentum (spin and angular) control, a possibility suggested by Hawton[85]. Schwinger pair production is anticipated at low electric fields because of geometrically defined permeability and permittivity associated with interfering laser beams (COVE project - Appendix N).

An alternative approach is made with the National Ignition Facility(NIF) at Livermore, CA. The question immediately arises whether the NIF could be run in a more continuous less powerful mode with selected laser standing wave beams of the trisine characteristic angle of (90 – 22.8) degrees and 120 degrees of each other with no material target and study the resultant interference pattern or lattice for virtual particles.

Above and beyond the purely scientific study of such a

lattice, it would be of primary importance to investigate the critical properties of such a lattice as the basis of providing useful energy generating mechanisms for the good of society. The major conclusion of this report is that an interdisciplinary team effort is required to continue this effort involving physicists, chemists and engineers. Each has a major role in achieving the many goals that are offered if more complete understanding of the superconducting resonant phenomenon is attained in order to bring to practical reality and bring a more complete understanding of our universe.

Figure 4.46.1 Conceptual Trisine Generator (Elastic Space CPT lattice)



Figure 4.46.2 COVE intersection of 3 standing wave fronts as generated by Vectorworks Software.

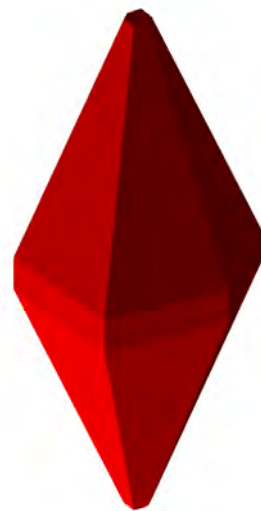
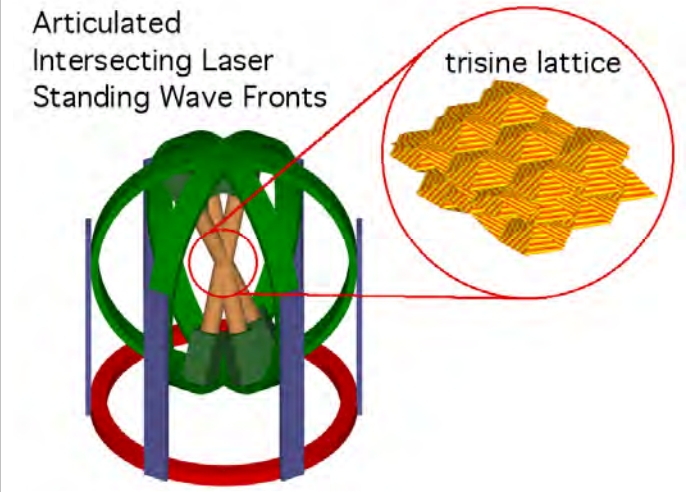


Figure 4.46.3 Conceptual Trisine Generator (Elastic Space CPT lattice) Within Articulating Motion Control Mechanism



5. Variable And Constant Definitions

Fundamental Physical Constants are from National Institute of Standards (NIST).

'Present' values represent Universe at 13.7 billion years.

The z factors $(1+z_R)^a$ or $(1+z_B)^b$ are presented for extrapolation of present values into the observational past consistent with tabular values in this paper. The two references $(1+z_R)^a$ or $(1+z_B)^b$ are presented representing both the universe Hubble radius of curvature R_U and trisine cellular B perspectives where $a/b = 1/3$.

<u>name</u>	<u>symbol</u>	<u>value</u>	<u>units</u>
Attractive Energy	V or $k_b T_c / \mathbb{C}$	5.58E-32	(present) $g \text{ cm}^2 \text{ sec}^{-2} (\text{erg})$
Attractive Energy z factors	$(1+z_R)^{2/3}$ or $(1+z_B)^2$		<i>unitless</i>
Attractive Energy	V_r or $k_b T_{cr} / \mathbb{C}$	9.08E+21	(present) $g \text{ cm}^2 \text{ sec}^{-2} (\text{erg})$
Attractive Energy z factors	$(1+z_R)^{-2/3}$ or $(1+z_B)^{-2}$		<i>unitless</i>
Black Body emission	$2E_v$ or $\sigma_s T_b^4$	3.14E-03	(present) $\text{erg cm}^{-2} \text{ sec}^{-1}$
Black Body emission z factors	$(1+z_R)^{4/3}$ or $(1+z_B)^4$		<i>unitless</i>
Black Body emission reflective	$2E_{vr}$ or $\sigma_s T_{br}^4$	9.27E+84	(present) $\text{erg cm}^{-2} \text{ sec}^{-1}$
Black Body emission reflective z factors	$(1+z_R)^{-4/3}$ or $(1+z_B)^{-4}$		<i>unitless</i>
Black Body energy/volume	$\rho_{BBenergy}$	4.20E-13	(present) erg cm^{-3}
Black Body energy/volume	$\sigma_s T_b^4 (4/c)$	4.20E-13	(present) erg cm^{-3}
Black Body energy/volume z factors	$(1+z_R)^{4/3}$ or $(1+z_B)^4$		<i>unitless</i>
Black Body energy/volume reflective	$\rho_{BBenergryr}$	1.24E+75	(present) erg cm^{-3}
Black Body energy/volume reflective	$\sigma_s T_{br}^4 (4/c)$	1.24E+75	(present) erg cm^{-3}
Black Body energy/volume reflective z factors	$(1+z_R)^{-4/3}$ or $(1+z_B)^{-4}$		<i>unitless</i>
Black Body mass/volume	ρ_{BBmass} or $\sigma_s T_b^4 (4/c^3)$	4.67E-34	(present) $g \text{ cm}^{-3}$
Black Body mass/volume z factors	$(1+z_R)^{4/3}$ or $(1+z_B)^4$		<i>unitless</i>
Black Body mass/volume reflective	$\rho_{BBmassr}$ or $\sigma_s T_{br}^4 (4/c^3)$	1.38E54	(present) $g \text{ cm}^{-3}$
Black Body mass/volume reflective z factors	$(1+z_R)^{-4/3}$ or $(1+z_B)^{-4}$		<i>unitless</i>
Black Body momentum	$\rho_{BBmomentum}$	6.24E-26	(present) $g \text{ cm sec}^{-1}$
Black Body momentum	$4.96536456 k_b T_b / c$	6.24E-26	(present) $g \text{ cm sec}^{-1}$
Black Body momentum z factors	$(1+z_R)^{-1/3}$ or $(1+z_B)^{-1}$		<i>unitless</i>
Black Body momentum reflective	$\rho_{BBmomentumr}$	4.60E-04	(present) $g \text{ cm sec}^{-1}$
Black Body momentum reflective	$4.96536456 k_b T_{br} / c$	4.60E-04	(present) $g \text{ cm sec}^{-1}$
Black Body momentum reflective z factors	$(1+z_R)^{1/3}$ or $(1+z_B)^1$		<i>unitless</i>

Black Body photons/volume	$\rho_{BB\text{photon}}$	4.12E+02	(present)	$\# \text{ cm}^{-3}$
Black Body photons/volume	$8\pi \left(k_b T_b / (hc)\right)^3 \cdot 2.404113806$	4.12E+02	(present)	$\# \text{ cm}^{-3}$
Black Body photons/volume z factors	$(1+z_R)^{3/3}$ or $(1+z_B)^3$			<i>unitless</i>
Black Body photons/volume reflective	$\rho_{BB\text{photonr}}$	1.65E+68	(present)	$\# \text{ cm}^{-3}$
Black Body photons/volume reflective	$8\pi \left(k_b T_{br} / (hc)\right)^3 \cdot 2.404113806$	1.65E+68	(present)	$\# \text{ cm}^{-3}$
Black Body photons/volume reflective z factors	$(1+z_R)^{-3/3}$ or $(1+z_B)^{-3}$			<i>unitless</i>
Black Body photons/baryon	$\rho_{BB\text{photonr}} / (\text{Avogadro} \cdot \rho_{Ur})$	1.07E+08	(present)	photon g^{-1}
Black Body photons/baryon z factors	$(1+z_R)^0$ or $(1+z_B)^0$			<i>unitless</i>
Black Body photons/baryon reflective	$\rho_{BB\text{photonr}} / (\text{Avogadro} \cdot \rho_{Ur})$	6.58E-07	(present)	$\text{photon baryon}^{-1}$
Black Body photons/baryon reflective z factors	$(1+z_R)^0$ or $(1+z_B)^0$			<i>unitless</i>
Black Body temperature (T_b)	$(1/2)(1/\mathbb{C})g_s^3 m_t v_{\epsilon}^2 (1/k_b)$	2.729	(present)	kelvin
Black Body temperature z factors	$(1+z_R)^{1/3}$ or $(1+z_B)^1$			<i>unitless</i>
Black Body temperature (T_{br}) reflective	$(1/2)(1/\mathbb{C})g_s^3 m_t v_{\epsilon r}^2 (1/k_b)$	2.01E+22	(present)	kelvin
Black Body temperature reflective z factors	$(1+z_R)^{-1/3}$ or $(1+z_B)^{-1}$			<i>unitless</i>
Black Body universe frequency	$\nu_{BB\text{max}}$	1.60E+11	(present)	sec^{-1}
Black Body universe frequency	$2.821439372 k_b T_b / h$	1.60E+11	(present)	sec^{-1}
Black Body universe frequency z factors	$(1+z_R)^{1/3}$ or $(1+z_B)^1$			<i>unitless</i>
Black Body universe frequency reflective	$\nu_{BB\text{maxr}}$	1.18E+33	(present)	sec^{-1}
Black Body universe frequency reflective	$2.821439372 k_b T_{br} / h$	1.18E+33	(present)	sec^{-1}
Black Body universe frequency reflective z factors	$(1+z_R)^{-1/3}$ or $(1+z_B)^{-1}$			<i>unitless</i>
Black Body universe mass	M_v or $V_u \sigma_s T_b^4 (4/c^3)$	2.21E+52	(present)	g
Black Body universe mass z factors	$(1+z_R)^{-5/3}$ or $(1+z_B)^{-5}$			<i>unitless</i>
Black Body universe mass reflective	M_{vr} or $V_{ur} \sigma_s T_{br}^4 (4/c^3)$	2.34E-100	(present)	g
Black Body universe mass reflective z factors	$(1+z_R)^{5/3}$ or $(1+z_B)^5$			<i>unitless</i>
Black Body universe viscosity	μ_{BB}	1.49E-24	(present)	$\text{g cm}^{-1} \text{sec}^{-1}$
Black Body universe viscosity	$\sigma_s T_b^4 (4/c^2) \lambda_{BB\text{max}}$	1.49E-24	(present)	$\text{g cm}^{-1} \text{sec}^{-1}$
Black Body universe viscosity z factors	$(1+z_R)^1$ or $(1+z_B)^3$			<i>unitless</i>
Black Body universe viscosity reflective	μ_{BBr}	5.95E+41	(present)	$\text{g cm}^{-1} \text{sec}^{-1}$
Black Body universe viscosity reflective	$\sigma_s T_{br}^4 (4/c^2) \lambda_{BB\text{maxr}}$	5.95E+41	(present)	$\text{g cm}^{-1} \text{sec}^{-1}$
Black Body universe viscosity reflective z factors	$(1+z_R)^{-1}$ or $(1+z_B)^{-3}$			<i>unitless</i>

Black Body universe wave length max	$\lambda_{BB_{max}}$	1.06E-01	(present)	cm
Black Body universe wave length max	$hc/(4.96536456 \cdot k_b T_b)$	1.06E-01	(present)	cm
Black Body universe wave length z factors	$(1+z_R)^{-1/3}$ or $(1+z_B)^{-1}$			unitless
Black Body universe wave length max reflective	$\lambda_{BB_{max,r}}$	1.44E-23	(present)	cm
Black Body universe wave length max reflective	$hc/(4.96536456 \cdot k_b T_{br})$	1.44E-23	(present)	cm
Black Body universe wave length reflective z factors	$(1+z_R)^{1/3}$ or $(1+z_B)^1$			unitless
Boltzmann constant	k_b	1.380658120E-16		$g \text{ cm}^2 \text{ sec}^{-2} \text{ Kelvin}^{-1}$
Bohr magneton	μ_B or $e\hbar/(2m_e c)$	9.27400949E-21		$erg/gauss (gauss \text{ cm}^3)$
				$g^{1/2} \text{ cm}^{5/2} \text{ sec}^{-1}$
Bohr radius	a_o or $\hbar^2/(m_e e^2)$	5.2917724924E-09		cm
	$\hbar c R_U cavity/(G m_t M_U)$			
	$\hbar c R_{Ur} cavity_r/(G m_t M_{Ur})$			
	$sherd^{1/2} \hbar c R_U cavity/(G_U m_t M_U)$			
	$sherd_r^{1/2} \hbar c R_{Ur} cavity/(G_{Ur} m_t M_{Ur})$			
Bose Einstein Condensate Survival Time	BEC_{ST} for 1 Mole (cm^3) of 1 g cm^{-3} hydrogen $BEC \text{ sec}$			
Capacitance(C_x)	approach $\epsilon_x/(4\pi B)$	2.57E+13		cm
Capacitance(C_y)	$g_s \sqrt{3}$ approach $\epsilon_y/(8\pi B)$	2.57E+13		cm
Capacitance(C_z)	$\sqrt{3}\pi$ approach $\epsilon_z/(3\pi B)$	2.57E+13		cm
Capacitance(C) z factors	$(1+z_R)^{-2/3}$ or $(1+z_B)^{-2}$			unitless
Capacitance(C_{xr})	approach $\epsilon_{xr}/(4\pi B_r)$	1.61E-40		cm
Capacitance(C_{yr})	$g_s \sqrt{3}$ approach $\epsilon_{yr}/(8\pi B_r)$	1.61E-40		cm
Capacitance(C_{zr})	$\sqrt{3}\pi$ approach $\epsilon_{zr}/(3\pi B_r)$	1.61E-40		cm
Capacitance(C_r) z factors	$(1+z_R)^{2/3}$ or $(1+z_B)^2$			unitless
Charge(e)	$(m_t c^2 x_U / \cos(\theta))^{1/2}$	4.803206799E-10		$g^{1/2} \text{ cm}^{3/2} \text{ sec}^{-1} \text{ (esu)}$
		1.60218E-19	coulomb	
Charge ² (e^2)	$m_t c^2 x_U / \cos(\theta)$	2.307077129E-19		$g \text{ cm}^3 \text{ sec}^{-2}$
Cooper CPT conjugated pair	\mathbb{C}	2	(constant)	unitless
Correlation length	ℓ	60.3	(present)	cm
Correlation length z factors	$(1+z_R)^{1/3}$ or $(1+z_B)^1$			unitless
Critical magnetic field(internal)	H_{c1} or $\Phi_\epsilon / (\pi \lambda^2)$	2.17E-20	(present)	$g^{1/2} \text{ cm}^{-1/2} \text{ sec}^{-1}$

Critical magnetic field(internal)	H_{c2} or $8\pi\Phi_\epsilon/\text{section}$	1.24E-14	(present)	$g^{1/2} \text{ cm}^{-1/2} \text{ sec}^{-1}$
Critical magnetic field(internal)	H_c or $(H_{c1}H_{c2})^{1/2}$	1.64E-17	(present)	$g^{1/2} \text{ cm}^{-1/2} \text{ sec}^{-1}$
Critical magnetic fields(internal) z factors	$(1+z_R)^{5/6}$ or $(1+z_B)^{15/6}$			unitless
Critical magnetic field(internal)	H_{cr1} or $\Phi_{er}/(\pi\lambda_r^2)$	2.30E+49	(present)	$g^{1/2} \text{ cm}^{-1/2} \text{ sec}^{-1}$
Critical magnetic field(internal)	H_{cr2} or $8\pi\Phi_{er}/\text{section}_r$	1.24E+50	(present)	$g^{1/2} \text{ cm}^{-1/2} \text{ sec}^{-1}$
Critical magnetic field(internal)	H_{cr} or $(H_{cr1}H_{cr2})^{1/2}$	5.33E+49	(present)	$g^{1/2} \text{ cm}^{-1/2} \text{ sec}^{-1}$
Critical magnetic fields(internal) z factors	$(1+z_R)^{-5/6}$ or $(1+z_B)^{-15/6}$			unitless
COVE Area	$(c \text{ time}_\pm)^2$	7.87E+29	(present)	cm^2
COVE Area z factors	$(1+z_R)^{-4/3}$ or $(1+z_B)^{-4}$			unitless
COVE Length	$(c \text{ time}_\pm)$	8.87E+14	(present)	cm
COVE Length z factors	$(1+z_R)^{-2/3}$ or $(1+z_B)^{-2}$			unitless
COVE Op frequency at in/out =1	$1/(2 \text{ time})$	1.69E-05	(present)	sec^{-1}
COVE Op frequency at in/out =1 z factors	$(1+z_R)^{2/3}$ or $(1+z_B)^2$			unitless
COVE Op wavelength at in/out =1	$2c \text{ time}$	1.77E+15	(present)	cm
COVE Op wavelength at in/out =1 z factors	$(1+z_R)^{-2/3}$ or $(1+z_B)^{-2}$			unitless
COVE Power at in/out =1	$hc^3 \text{ time}_\pm / (2 \text{ cavity})$	1.68E+05	(present)	erg sec^{-1}
COVE Power at in/out =1 z factors	$(1+z_R)^{1/3}$ or $(1+z_B)^1$			unitless
COVE Schwinger linear	$1/(B \text{ time}_\pm)$	1.53E-06	(present)	$\text{cm}^{-1} \text{ sec}^{-1}$
COVE Schwinger linear z factors	$(1+z_R)^1$ or $(1+z_B)^3$			unitless
COVE Schwinger area	$1/(\text{section time}_\pm)$	2.00E-08	(present)	$\text{cm}^{-2} \text{ sec}^{-1}$
COVE Schwinger area z factors	$(1+z_R)^{4/3}$ or $(1+z_B)^4$			unitless
COVE Schwinger volume	$1/(\text{cavity time}_\pm)$	2.15E-09	(present)	$\text{cm}^{-3} \text{ sec}^{-1}$
COVE Schwinger volume z factors	$(1+z_R)^{5/3}$ or $(1+z_B)^5$			unitless
COVE Volume	$(c \text{ time}_\pm)^3$	6.99E+44	(present)	cm^3
COVE Volume z factors	$(1+z_R)^{-6/3}$ or $(1+z_B)^{-6}$			unitless
Dirac's number - electron magnetic moment	$g_d = g_e/2$	1.009804978187790		unitless
in Bohr magnetons				
Displacement field (internal) D_{fx}	$(\pi/g_s)4\pi\mathbb{C}e/\text{approach}$	1.06E-10	(present)	$g^{1/2} \text{ cm}^{-1/2} \text{ sec}^{-1}$
Displacement field (internal) D_{fy}	$(4\pi/(3g_s))4\pi\mathbb{C}e/\text{side}$	1.22E-10	(present)	$g^{1/2} \text{ cm}^{-1/2} \text{ sec}^{-1}$
Displacement field (internal) D_{fz}	$(\sqrt{3}/(2g_s^2))4\pi\mathbb{C}e/\text{section}$	6.16E-12	(present)	$g^{1/2} \text{ cm}^{-1/2} \text{ sec}^{-1}$

Displacement field (internal) D_f	$(D_{fx}^2 + D_{fy}^2 + D_{fz}^2)^{1/2}$	1.61E-10	(present)	$g^{1/2} \text{ cm}^{-1/2} \text{ sec}^{-1}$
Displacement field (internal) $D_{ftrisine}$	$4\pi\mathbb{C}e/\text{trisine area}$	3.29E-12	(present)	$g^{1/2} \text{ cm}^{-1/2} \text{ sec}^{-1}$
	$\sqrt{2}(A/B)D_f$			
Displacement field (internal) z factors	$(1+z_R)^{2/3}$ or $(1+z_B)^2$			unitless
Displacement field (internal) D_{fxr}	$(\pi/g_s)4\pi\mathbb{C}e/\text{approach}_r$	1.71E+43	(present)	$g^{1/2} \text{ cm}^{-1/2} \text{ sec}^{-1}$
Displacement field (internal) D_{fyr}	$(4\pi/(3g_s))4\pi\mathbb{C}e/\text{side}_r$	1.98E+43	(present)	$g^{1/2} \text{ cm}^{-1/2} \text{ sec}^{-1}$
Displacement field (internal) D_{fzr}	$(\sqrt{3}/(2g_s^2))4\pi\mathbb{C}e/\text{section}_r$	9.99E+41	(present)	$g^{1/2} \text{ cm}^{-1/2} \text{ sec}^{-1}$
Displacement field (internal) D_{fr}	$(D_{fxr}^2 + D_{fyr}^2 + D_{fzr}^2)^{1/2}$	2.62E+43	(present)	$g^{1/2} \text{ cm}^{-1/2} \text{ sec}^{-1}$
Displacement field (internal) $D_{ftrisiner}$	$4\pi\mathbb{C}e/\text{trisine area}_r$	5.33E+41	(present)	$g^{1/2} \text{ cm}^{-1/2} \text{ sec}^{-1}$
	$\sqrt{2}(A_r/B_r)D_{fr}$			
Displacement field (internal) z factors	$(1+z_R)^{-2/3}$ or $(1+z_B)^{-2}$			unitless
Earth mass	M_E	5.979E27		g
Earth radius	R_E	6.371315E08		cm
Electric field (internal) E_f	$(E_{fx}^2 + E_{fy}^2 + E_{fz}^2)^{1/2}$	2.63E-23	(present)	$g^{1/2} \text{ cm}^{-1/2} \text{ sec}^{-1}$
				$(volt/cm)/299.792458$
Electric field (internal) E_{fx}	$\mathbb{C}k_b T_c / (\mathbb{C}e 2B)$	5.27E-24	(present)	$g^{1/2} \text{ cm}^{-1/2} \text{ sec}^{-1}$
Electric field (internal) E_{fy}	$\mathbb{C}k_b T_c / (\mathbb{C}e P)$	6.08E-24	(present)	$g^{1/2} \text{ cm}^{-1/2} \text{ sec}^{-1}$
Electric field (internal) E_{fz}	$\mathbb{C}k_b T_c / (\mathbb{C}e A)$	2.51E-23	(present)	$g^{1/2} \text{ cm}^{-1/2} \text{ sec}^{-1}$
Electric field (internal) $E_{ftrisine}$ $(1/g_s^2) \mathbb{C}k_b T_c \text{trisine area} / (\mathbb{C}e \text{ cavity})$	5.33E-23	(present)		$g^{1/2} \text{ cm}^{-1/2} \text{ sec}^{-1}$
Electric field (internal) z factors	$(1+z_R)^1$ or $(1+z_B)^3$			unitless
Electric field (internal) E_{fr}	$(E_{fx}^2 + E_{fy}^2 + E_{fz}^2)^{1/2}$	1.72E+57	(present)	$g^{1/2} \text{ cm}^{-1/2} \text{ sec}^{-1}$
				$(volt/cm)/299.792458$
Electric field (internal) E_{fxr}	$\mathbb{C}k_b T_{cr} / (\mathbb{C}e 2B_r)$	3.44E+56	(present)	$g^{1/2} \text{ cm}^{-1/2} \text{ sec}^{-1}$
Electric field (internal) E_{fyr}	$\mathbb{C}k_b T_{cr} / (\mathbb{C}e P_r)$	3.97E+56	(present)	$g^{1/2} \text{ cm}^{-1/2} \text{ sec}^{-1}$
Electric field (internal) E_{fzr}	$\mathbb{C}k_b T_{cr} / (\mathbb{C}e A_r)$	1.64E+57	(present)	$g^{1/2} \text{ cm}^{-1/2} \text{ sec}^{-1}$
Electric field (internal) $E_{ftrisine}$ $(1/g_s^2) \mathbb{C}k_b T_{cr} \text{trisine area}_r / (\mathbb{C}e \text{ cavity}_r)$	3.48E+57	(present)		$g^{1/2} \text{ cm}^{-1/2} \text{ sec}^{-1}$
Electric field (internal) z factors	$(1+z_R)^{-1}$ or $(1+z_B)^{-3}$			unitless
Electron gyromagnetic-factor	g_e	2.0023193043617		unitless
Electron mass (m_e)	$\alpha m_p \left(\Lambda_U^{1/6} / \cos(\theta)^{2/9} \right) l_p^{1/3}$	9.10938975E-28		g
Energy	E_{cx} or $(m_t v_{cx}^2)/2$ or $k_b T_c$	1.12E-31	(present)	$g \text{ cm}^2 \text{ sec}^{-2}$

Energy	E_{cy} or $(m_t v_{cy}^2)/2$	1.49E-31	(present)	$g \text{ cm}^2 \text{sec}^{-2}$
Energy	E_{cz} or $(m_t v_{cz}^2)/2$	2.53E-30	(present)	$g \text{ cm}^2 \text{sec}^{-2}$
Energy z factors	$(1+z_R)^{2/3}$ or $(1+z_B)^2$			<i>unitless</i>
Energy reflective	E_{xr} or $(m_t c^2)^2 2/(m_t v_{dx}^2)$	6.03E-02	(present)	$g \text{ cm}^2 \text{sec}^{-2}$
Energy reflective	E_{yr} or $(m_t c^2)^2 2/(m_t v_{dy}^2)$	5.23E-02	(present)	$g \text{ cm}^2 \text{sec}^{-2}$
Energy reflective	E_{zr} or $(m_t c^2)^2 2/(m_t v_{dz}^2)$	1.27E-02	(present)	$g \text{ cm}^2 \text{sec}^{-2}$
Energy reflective z factors	$(1+z_R)^{-2/3}$ or $(1+z_B)^{-2}$			<i>unitless</i>
Euler number -natural log base	e	2.7182818284590		<i>unitless</i>
Euler-Mascheroni constant	<i>Euler</i>	0.5772156649015		<i>unitless</i>
Fine structure constant	$\hbar c/e^2$	$1/\alpha$	137.03599936	<i>unitless</i>
	$(A/B)\sqrt{k_{mx}\epsilon_x}/\epsilon_{trisine}$	$1/\alpha$	137.03599936	<i>unitless</i>
	$\sqrt{g_s}(\epsilon/\epsilon_{trisine})^2$	$1/\alpha$	137.03599936	<i>unitless</i>
	$2\sqrt{k_{mz}\epsilon_z}/\epsilon_{trisine}$	$1/\alpha$	137.03599936	<i>unitless</i>
Fine structure constant	$\hbar c/e^2$	$1/\alpha$	137.03599936	<i>unitless</i>
	$(A_r/B_r)\sqrt{k_{mxr}\epsilon_{xr}}/\epsilon_{trisiner}$	$1/\alpha$	137.03599936	<i>unitless</i>
	$\sqrt{g_s}(\epsilon_r/\epsilon_{trisiner})^2$	$1/\alpha$	137.03599936	<i>unitless</i>
Fluxoid	Φ	2.0678539884E-7		$g^{1/2} \text{cm}^{3/2} \text{sec}^{-1}$ (<i>gauss cm</i> ²)
Fluxoid dielectric (ϵ) mod	Φ_ϵ or $h\nu_\epsilon/(\mathbb{C}e)$	8.33E-13	(present)	$g^{1/2} \text{cm}^{3/2} \text{sec}^{-1}$ (<i>gauss cm</i> ²)
Fluxoid dielectric (ϵ) mod z factors	$(1+z_R)^{1/6}$ or $(1+z_B)^{1/2}$			<i>unitless</i>
Fluxoid dielectric (ϵ) mod reflected	Φ_{er} or $h\nu_{er}/(\mathbb{C}e)$	5.13E-02	(present)	$g^{1/2} \text{cm}^{3/2} \text{sec}^{-1}$ (<i>gauss cm</i> ²)
Fluxoid dielectric (ϵ) mod reflected z factors	$(1+z_R)^{-1/6}$ or $(1+z_B)^{-1/2}$			<i>unitless</i>
Force _x	$m_t v_{dx}/\text{time}_\pm$	5.06E-33	(present)	$g \text{ cm/sec}^2$
Force _y	$m_t v_{dy}/\text{time}_\pm$	5.84E-33	(present)	$g \text{ cm/sec}^2$
Force _z	$m_t v_{dz}/\text{time}_\pm$	2.41E-32	(present)	$g \text{ cm/sec}^2$
Force	$m_t \sqrt{v_{dx}^2 + v_{dy}^2 + v_{dz}^2}/\text{time}_\pm$	2.53E-32	(present)	$g \text{ cm/sec}^2$
Force z factors	$(1+z_R)^1$ or $(1+z_B)^3$			<i>unitless</i>
Force _{xr}	$m_t v_{dxr}/\text{time}_{r\pm}$	3.31E+47	(present)	$g \text{ cm/sec}^2$
Force _{yr}	$m_t v_{dyr}/\text{time}_{r\pm}$	3.82E+47	(present)	$g \text{ cm/sec}^2$
Force _{zr}	$m_t v_{dzr}/\text{time}_{r\pm}$	1.57E+48	(present)	$g \text{ cm/sec}^2$
Force _r	$m_t \sqrt{v_{dxr}^2 + v_{dyr}^2 + v_{dzr}^2}/\text{time}_{r\pm}$	1.65E+48	(present)	$g \text{ cm/sec}^2$

Force _r <i>z</i> factors	$(1+z_R)^{-1}$ or $(1+z_B)^{-3}$		<i>unitless</i>	
Galactic diameter	$(24/\pi)(C\sigma/\mu H_U)$ or $(24/\pi)\left(Cc/\epsilon^{1/2}H_U\right)$	1.10E+23	(present)	cm
Galactic diameter <i>z</i> factors	$(1+z_R)^{-5/6}$ or $(1+z_B)^{-15/6}$			<i>unitless</i>
Hall quantum resistance	h/e^2	2.87206217786631E-08	$cm^{-1}sec$	
Hall quantum resistance (von Klitzing constant)	25812.80756			ohm
Homes' constant	\mathcal{U}	191,537	$cm^5 sec^{-3}$	
Inductance(L_x)	$\Phi_x time_{\pm}/(4\pi\mathcal{C}ev_{ex})$	3.38E-05	$cm^{-1}sec^2$	
Inductance(L_y)	$\Phi_y time_{\pm}/(4\pi\mathcal{C}ev_{ey})$	3.38E-05	$cm^{-1}sec^2$	
Inductance(L_z)	$\Phi_z time_{\pm}/(4\pi\mathcal{C}ev_{ez})$	3.38E-05	$cm^{-1}sec^2$	
Inductance(L) <i>z</i> factors	$(1+z_R)^{-2/3}$ or $(1+z_B)^{-2}$		<i>unitless</i>	
Inductance(L_{xr})	$\Phi_{xr} time_{r\pm}/(4\pi\mathcal{C}ev_{exr})$	2.09E-58	$cm^{-1}sec^2$	
Inductance(L_{yr})	$\Phi_{yr} time_{r\pm}/(4\pi\mathcal{C}ev_{eyr})$	2.09E-58	$cm^{-1}sec^2$	
Inductance(L_{zr})	$\Phi_{zr} time_{r\pm}/(4\pi\mathcal{C}ev_{ezr})$	2.09E-58	$cm^{-1}sec^2$	
Inductance(L_r) <i>z</i> factors	$(1+z_R)^{2/3}$ or $(1+z_B)^2$		<i>unitless</i>	
London penetration depth	λ or $(1/g_s)\left((m_t v_e^2/2)cavity\right)^{1/2}(\mathcal{C}e)$	3.50E+03	(present)	cm
London penetration depth <i>z</i> factors	$(1+z_R)^{-1/3}$ or $(1+z_B)^{-1}$		<i>unitless</i>	
London penetration depth	λ_r or $(1/g_s)\left((m_t v_{er}^2/2)cavity_r\right)^{1/2}(\mathcal{C}e)$	2.67E-26	(present)	cm
London penetration depth <i>z</i> factors	$(1+z_R)^{1/3}$ or $(1+z_B)^1$		<i>unitless</i>	
Lamb shift	$v_{Lamb\ shift}$	1.0578330E09	sec^{-1}	
Mole of photons	<i>einstein</i>		<i>moles of photons</i>	
Momentum vector	p_x or $m_t v_{dx}$ or $\hbar K_B$	1.50E-28	(present)	$g\ cm^{-1}sec^{-1}$
Momentum vector	p_y or $m_t v_{dy}$ or $\hbar K_P$	1.73E-28	(present)	$g\ cm^{-1}sec^{-1}$
Momentum vector	p_z or $m_t v_{dz}$ or $\hbar K_A$	7.13E-28	(present)	$g\ cm^{-1}sec^{-1}$
Momentum <i>z</i> factors	$(1+z_R)^{-1/3}$ or $(1+z_B)^{-1}$		<i>unitless</i>	
Momentum reflective vector	$(m_t c)^2/(m_t v_{dx})$	6.03E-02	(present)	$g\ cm^{-1}sec^{-1}$
Momentum reflective vector	$(m_t c)^2/(m_t v_{dy})$	5.23E-02	(present)	$g\ cm^{-1}sec^{-1}$
Momentum reflective vector	$(m_t c)^2/(m_t v_{dz})$	1.27E-02	(present)	$g\ cm^{-1}sec^{-1}$
Momentum <i>z</i> factors	$(1+z_R)^{1/3}$ or $(1+z_B)^1$		<i>unitless</i>	
Neutral pi meson (pion)	π^0	2.406176E-25	g	
Neutral pi meson (pion) in terms of trisine	$m_t (B/A)_t (g_s/g_d)$	2.407096E-25	g	

Nuclear density	$m_i/cavity_{nucleus}$	2.34E14	$g\ cm^{-3}$	
Nuclear magneton	$e\hbar/(2m_p c)$	μ_p	5.05078342E-24 $erg/gauss$ ($gauss\ cm^3$)	
			$g^{1/2}cm^{5/2}sec^{-1}$	
Permeability k_m or $(1/\epsilon)1/\left(1/(k_{mx}\epsilon_x) + 1/(k_{my}\epsilon_y) + 1/(k_{mz}\epsilon_z)\right)$		2.24E+13	(present)	<i>unitless</i>
Permeability	k_{mx}	2.01E+13	(present)	<i>unitless</i>
Permeability	k_{my}	1.51E+13	(present)	<i>unitless</i>
Permeability	k_{mz}	7.24E+13	(present)	<i>unitless</i>
Permeability z factors	$(1+z_R)^{-1/3}$ or $(1+z_B)^{-1}$			<i>unitless</i>
Permeability k_{mr} or $(1/\epsilon_r)1/\left(1/(k_{mxr}\epsilon_{xr}) + 1/(k_{myr}\epsilon_{yr}) + 1/(k_{mzr}\epsilon_{zr})\right)$		7.72E-13	(present)	<i>unitless</i>
Permeability	k_{mxr}	4.97E-14	(present)	<i>unitless</i>
Permeability	k_{myr}	6.63E-14	(present)	<i>unitless</i>
Permeability	k_{mzr}	9.22E-11	(present)	<i>unitless</i>
Permeability z factors	$(1+z_R)^{1/3}$ or $(1+z_B)^1$			<i>unitless</i>
Permittivity (dielectric)	D_{fx}/E_{fx} or ϵ_x	2.00E+13	(present)	<i>unitless</i>
Permittivity (dielectric)	D_{fy}/E_{fy} or ϵ_y	2.00E+13	(present)	<i>unitless</i>
Permittivity (dielectric)	D_{fz}/E_{fz} or ϵ_z	2.46E+11	(present)	<i>unitless</i>
Permittivity (dielectric)	$(1/(3g_s))D_f/E_f$ or ϵ	7.22E+11	(present)	<i>unitless</i>
	$3/(1/\epsilon_x + 1/\epsilon_y + 1/\epsilon_z)$	7.22E+11	(present)	<i>unitless</i>
	$\epsilon_{trisine}/(\alpha g_d^2)$	7.22E+11	(present)	<i>unitless</i>
Permittivity (dielectric)	$D_{ftrisine}/E_{ftrisine}$ or $\epsilon_{trisine}$	6.16E+10	(present)	<i>unitless</i>
Permittivity (dielectric) z factors	$(1+z_R)^{-1/3}$ or $(1+z_B)^{-1}$			<i>unitless</i>
Permittivity (dielectric ϵ)	$(1/(3g_s))D_{fr}/E_{fr}$ or ϵ_r	1.79E-15	(present)	<i>unitless</i>
Permittivity (dielectric ϵ)	$3/(1/\epsilon_{xr} + 1/\epsilon_{yr} + 1/\epsilon_{zr})$ or ϵ_r	1.79E-15	(present)	<i>unitless</i>
Permittivity (dielectric ϵ)	$\epsilon_{trisiner}/(\alpha g_d^2)$	1.79E-15	(present)	<i>unitless</i>
Permittivity (dielectric ϵ_x)	D_{fxr}/E_{fxr} or ϵ_{xr}	2.32E-12	(present)	<i>unitless</i>
Permittivity (dielectric ϵ_y)	D_{fyv}/E_{fyv} or ϵ_{yr}	4.97E-14	(present)	<i>unitless</i>
Permittivity (dielectric ϵ_z)	D_{fzr}/E_{fzr} or ϵ_{zr}	6.10E-16	(present)	<i>unitless</i>
Permittivity (dielectric $\epsilon_{trisine}$)	$D_{ftrisiner}/E_{ftrisiner}$ or $\epsilon_{trisiner}$	1.53E-16	(present)	<i>unitless</i>
Permittivity (dielectric) z factors	$(1+z_R)^{1/3}$ or $(1+z_B)^1$			<i>unitless</i>

Planck reduced constant	$\hbar(h/2\pi)$ or $m_t(2B)^2/(2\pi \text{ time}_\pm)$	1.054572675E-27	$g \text{ cm}^2 \text{ sec}^{-1}$
Planck reduced constant	$\hbar(h/2\pi)$ or $m_t(2B_r)^2/(2\pi \text{ time}_{r\pm})$	1.054572675E-27	$g \text{ cm}^2 \text{ sec}^{-1}$
Planck length (l_p)	$\hbar^{1/2} G_U^{1/2} / c^{3/2}$	1.61624E-33 (present)	cm
Planck time (t_p)	$\hbar^{1/2} G_U^{1/2} / c^{5/2}$	5.39121E-44 (present)	sec
Planck mass (m_p)	$\hbar^{1/2} c^{1/2} / G_U^{1/2}$	2.17645E-05 (present)	g
Planck energy (E_p)	$(\hbar c^5 / G_U)^{1/2}$	1.95610E+16 (present)	$g \text{ cm}^2 \text{ sec}^{-2} \text{ (erg)}$
Planck momentum (p_p)	$(\hbar c^3 / G_U)^{1/2}$	6.52483E+05 (present)	$g \text{ cm sec}^{-1}$
Planck force (F_p)	c^4 / G_U	1.21027E+49 (present)	$g \text{ cm sec}^{-2} \text{ (dyne)}$
Planck density (ρ_p)	$c^5 / (\hbar G_U^2)$	5.15500E+93 (present)	$g \text{ cm}^{-3}$
Planck acceleration (a_p)	$c^6 / (\hbar G_U)$	1.03145E+97 (present)	$cm \text{ sec}^{-2}$
Planck kinematic viscosity (ν_p)	$(c^7 / (\hbar G_U))^{1/2}$	5.56077E+53 (present)	$cm^2 \text{ sec}$
Planck absolute viscosity (μ_p)	$(c^9 / (\hbar G_U^3))^{1/2}$	2.49779E+71 (present)	$g \text{ cm}^{-1} \text{ sec}^{-1}$
Proton mass (m_p)	$(\hbar/c)(\pi/B_p)$	1.67262311E-24	g
Proton radius	$B_p / (2 \sin(\theta))$ or $x_U / (8 \sin(\theta))$	8.59E-14 (8 E-14)	cm
Resonant CPT time $time_{c\pm}$	$time_{c\pm}$	2.96E+04 (present)	sec
Resonant CPT time $time_{c\pm}$ z factors	$(1+z_R)^{-2/3}$ or $(1+z_B)^{-2}$		unitless
Resonant CPT time $time_{cr\pm}$	$time_{cr\pm}$	1.53E-49 (present)	sec
Resonant CPT time $time_{cr\pm}$ z factors	$(1+z_R)^{2/3}$ or $(1+z_B)^2$		unitless
Saam's constant (Θ)	$3\pi^3 h^3 / (6^{1/2} m_t^{3/2} (B/A))$	5.89035133E-43	$erg^{3/2} \text{ cm}^3$
Stefan's constant (σ_s)	$2\pi^5 k_b^4 / (15c^2 h^3)$	5.67040124E-05	$erg \text{ cm}^{-2} \text{ sec}^{-1}$
Superconductor gyro-factor	g_s	1.009804978188	unitless
Superconductor weak coupling constant	$2e^{Euler} / \pi$	1.133865917	unitless
Temperature Fine Structure (T_a)	$g_d m_t \hbar c^3 / (e^2 k_B)$ $g_d m_t c^2 / (\alpha k_b)$	8.96E13	kelvin
Temperature Universe (T_a)	$m_t c^2 / k_b$	6.53E+11	kelvin
	$G_U m_t M_U / (R_U k_b)$		kelvin
	$G_{Ur} m_t M_{Ur} / (R_{Ur} k_b)$		kelvin
Temperature Universe (T_a) z factors	$(1+z_R)^0$ or $(1+z_B)^0$		unitless
Temperature Critical Black Body (T_b)	$(1/2)(1/\mathbb{C}) g_s^3 m_t v_e^2 (1/k_b)$	2.729 (present)	kelvin
Temperature Critical (T_b) z factors	$(1+z_R)^{1/3}$ or $(1+z_B)^1$		unitless

Temperature Critical (T_{br})	$(1/2)m_t v_{er}^2/k_b$	2.01E+22	(present)	kelvin
Temperature Critical (T_{br}) z factors	$(1+z_R)^{-1/3}$ or $(1+z_B)^{-1}$			unitless
Temperature Critical (T_c)	$(1/2)m_t v_{dx}^2/k_b$	8.11E-16	(present)	kelvin
Temperature Critical (T_c) z factors	$(1+z_R)^{2/3}$ or $(1+z_B)^2$			unitless
Temperature Phase (T_{cr})	$(1/2)m_t v_{dxr}^2/k_b$	1.29E38	(present)	kelvin
	$m_t c^2 k_m^2 / (2k_b \pi^2)$			kelvin
Temperature Phase (T_{cr}) z factors	$(1+z_R)^{-2/3}$ or $(1+z_B)^{-2}$			unitless
Temperature Dielectric (T_d)	$m_t v_e c/k_b$	2.63E06	(present)	kelvin
Temperature Phase (T_d) z factors	$(1+z_R)^{1/6}$ or $(1+z_B)^{3/6}$			unitless
Temperature Dielectric (T_{dr})	$m_t v_{er} c/k_b$	1.62E16	(present)	kelvin
Temperature Phase (T_{dr}) z factors	$(1+z_R)^{-1/6}$ or $(1+z_B)^{-3/6}$			unitless
Temperature Momentum (T_i)	$m_t v_{dx} c/k_b$	3.25E-02	(present)	kelvin
	$\hbar K_B c/k_b$			kelvin
	$m_t c^2 / ((k_m \epsilon_x)^{1/2} k_b)$			kelvin
Temperature Momentum (T_i) z factors	$(1+z_R)^{1/3}$ or $(1+z_B)^1$			unitless
Temperature Momentum (T_{ir})	$m_t v_{dxr} c/k_b$	1.31E+25	(present)	kelvin
Temperature Momentum (T_{ir}) z factors	$(1+z_R)^{-1/3}$ or $(1+z_B)^{-1}$			unitless
Temperature Resonant (T_j)	$(m_t v_{dt}^4 / 4) (1/c^2) / k_b$	6.28E-40	(present)	kelvin
	$m_t c^2 (1/(k_m \epsilon_x) + 1/(k_m \epsilon_y) + 1/(k_m \epsilon_z))^2 / (4k_b)$			kelvin
Temperature Resonant (T_j) z factors	$(1+z_R)^{4/3}$ or $(1+z_B)^4$			unitless
Temperature Resonant (T_{jr})	$(m_t v_{dtr}^4 / 4) (1/c^2) / k_b$	8.52E+64	(present)	kelvin
	$m_t c^2 (1/(k_{mr} \epsilon_{xr}) + 1/(k_{mr} \epsilon_{yr}) + 1/(k_{mr} \epsilon_{zr}))^2 / (4k_b)$			kelvin
Temperature Resonant (T_{jr}) z factors	$(1+z_R)^{-4/3}$ or $(1+z_B)^{-4}$			unitless
Trisine angle	θ or $\tan^{-1}(A/B)$	22.7979295		angular degrees
Trisine angle	θ or $\tan^{-1}(A_r/B_r)$	22.7979295		angular degrees
Trisine angle	or $\cos^{-1}(B / (A^2 + B^2)^{1/2})$	22.7979295		angular degrees
Trisine angle	or $\cos^{-1}(B_r / (A_r^2 + B_r^2)^{1/2})$	22.7979295		angular degrees
Trisine angle	or $\cos^{-1}\left((1/(2K_B)) / \left((1/K_A)^2 + (1/(2K_B))^2\right)^{1/2}\right)$	22.7979295		angular degrees
Trisine angle	or $\cos^{-1}\left((1/(2K_{Br})) / \left((1/K_{Ar})^2 + (1/(2K_{Br}))^2\right)^{1/2}\right)$	22.7979295		angular degrees

Trisine angular relationship	$\sin(\theta)\cos(\theta) = (B/A)/\left((B/A)^2 + 1\right)$	=0.357211055	unitless	
Trisine area	<i>section</i>	$2\sqrt{3}B^2$	1,693	(present) cm^2
Trisine area	<i>approach</i>	$\sqrt{3}AB$	356	(present) cm^2
Trisine area	<i>side</i>	$2AB$	411	(present) cm^2
Trisine area	<i>trisine</i>	$4\sqrt{3}B^2/\cos(\theta)$	3,670	(present) cm^2
Trisine area z factors		$(1+z_R)^{-\frac{2}{3}}$ or $(1+z_B)^{-2}$		unitless
Trisine area reflected	<i>approach_r</i>	$\sqrt{3}A_rB_r$	2.19E-51	(present) cm^2
Trisine area reflected	<i>side_r</i>	$2A_rB_r$	2.27E-50	(present) cm^2
Trisine area reflected	<i>section_r</i>	$2\sqrt{3}B_r^2$	1.04E-50	(present) cm^2
Trisine area reflected	<i>trisine</i>	$4\sqrt{3}B_r^2/\cos(\theta)$	2.27E-50	(present) cm^2
Trisine area reflected z factors		$(1+z_R)^{\frac{2}{3}}$ or $(1+z_B)^2$		unitless
Trisine unit		<i>cell</i>		unitless
Trisine constant	<i>trisine</i>	$-\ln(2e^{Euler}/\pi - 1)$	2.010916597	unitless
Trisine density of states		$D(\xi_r)$ or $1/k_bT_c$	8.93E+30	(present) $sec^2 g^{-1} cm^{-2}$
Trisine density of states z factors		$(1+z_R)^{-\frac{2}{3}}$ or $(1+z_B)^{-2}$		unitless
Trisine density of states(reflected)		$D(\xi_r)$ or $1/k_bT_{cr}$	5.51E-23	(present) $sec^2 g^{-1} cm^{-2}$
Trisine density of states reflected z factors		$(1+z_R)^{\frac{2}{3}}$ or $(1+z_B)^2$		unitless
Trisine dimension	<i>A</i>		9.29	(present) cm
		$\pi\epsilon(m_e/m_t)$ Bohr radius		cm
Trisine dimension	<i>B</i>		22.11	(present) cm
		$\pi\epsilon(B/A)(m_e/m_t)$ Bohr radius		cm
Trisine dimension	<i>C</i>		23.98	(present) cm
Trisine dimension	<i>P</i>		38.29	(present) cm
Trisine dimensions z factors		$(1+z_R)^{-\frac{1}{3}}$ or $(1+z_B)^{-1}$		unitless
Trisine dimension	<i>A_r</i>		2.31E-26	(present) cm
		$\pi\epsilon_r(m_e/m_t)$ Bohr radius		cm
Trisine dimension	<i>B_r</i>		5.49E-26	(present) cm
		$\pi\epsilon_r(B_r/A_r)(m_e/m_t)$ Bohr radius		cm
Trisine dimension	<i>C_r</i>		5.96E-26	(present) cm
Trisine dimension	<i>P_r</i>		9.51E-26	(present) cm

Trisine dimensions z factors	$(1+z_R)^{1/3}$ or $(1+z_B)^1$		<i>unitless</i>	
Trisine magneton	$e\hbar/(2m_t c)$	μ_t	8.42151973E-23	
			<i>erg/gauss</i>	
			$gauss\ cm^3$	
			$g^{1/2}\ cm^{5/2}\ sec^{-1}$	
Trisine size ratio	$(B/A)_t$	$2/\sin(1\ radian)$	2.379146659	<i>unitless</i>
		$e^2/(\epsilon v_{dx} \hbar)$		
Trisine size ratio reflected	$(B_r/A_r)_t$	$2/\sin(1\ radian)$	2.379146659	<i>unitless</i>
		$e^2/(\epsilon_r v_{dxr} \hbar)$		
Trisine spin moment	$(2/1) (\mathbb{C} e_{\pm} \hbar / 2m_e v_{ey}) = chain\ H_e$	1.72E-13	(present)	<i>erg/gauss</i>
				$(gauss\ cm^3)$
				$g^{1/2}\ cm^{5/2}\ sec^{-1}$
Trisine spin moment z factors	$(1+z_R)^{1/6}$ or $(1+z_B)^{3/6}$			<i>unitless</i>
Trisine spin moment reflected	$(1/2) (\mathbb{C} e_{\pm} \hbar / 2m_e v_{eyr}) = chain_r\ H_{cr}$	8.56E-27	(present)	<i>erg/gauss</i>
				$(gauss\ cm^3)$
				$g^{1/2}\ cm^{5/2}\ sec^{-1}$
Trisine spin moment reflected z factors	$(1+z_R)^{-1/6}$ or $(1+z_B)^{-3/6}$			<i>unitless</i>
Trisine surface tension (σ_T)	$k_b T_c / section$	6.61E-35	(present)	$erg\ cm^{-2}$
Trisine surface tension (σ_T) z factors	$(1+z_R)^{4/3}$ or $(1+z_B)^4$			<i>unitless</i>
Trisine surface tension (σ_{Tr})	$k_b T_{cr} / section_r$	1.74E+72	(present)	$erg\ cm^{-2}$
Trisine surface tension (σ_{Tr}) z factors	$(1+z_R)^{-4/3}$ or $(1+z_B)^{-4}$			<i>unitless</i>
Trisine surface tension seen (σ_{cT})	$m_t c^2 / section$	5.32E-08	(present)	$erg\ cm^{-2}$
Trisine surface tension seen (σ_{cT}) z factors	$(1+z_R)^{2/3}$ or $(1+z_B)^2$			<i>unitless</i>
Trisine surface tension seen (σ_{cTr})	$m_t c^2 / section_r$	8.64E+45	(present)	$erg\ cm^{-2}$
Trisine surface tension seen (σ_{cTr}) z factors	$(1+z_R)^{-2/3}$ or $(1+z_B)^{-2}$			<i>unitless</i>
Trisine transformed mass	m_t or $\hbar^{2/3} U^{1/3} c^{-1/3} \cos(\theta)$	1.003150245E-25	g	
	or $\pi \hbar \ time_{\pm} / (2B^2)$ or $\pi \hbar / D_c$		(constant)	
Trisine relativistic mass	m_r or $(1/2) m_t (v_{dx}^2 / c^2)$	1.24E-52	(present)	cm^3
Trisine relativistic mass z factors	$(1+z_R)^{2/3}$ or $(1+z_B)^2$			<i>unitless</i>
Trisine relativistic mass	m_{nr} or $(1/2) m_t (v_{dxr}^2 / c^2)$	20.2	(present)	cm^3
Trisine relativistic mass z factors	$(1+z_R)^{-2/3}$ or $(1+z_B)^{-2}$			<i>unitless</i>

Trisine volume per cell	$cavity$	$2\sqrt{3}AB^2$	15,733	(present)	cm^3
Trisine volume per cell z factors		$(1+z_R)^{-1}$ or $(1+z_B)^{-3}$			<i>unitless</i>
Trisine volume per chain	<i>chain</i> or $2cavity/3$		10,497		cm^3
Trisine volume per chain z factors		$(1+z_R)^{-1}$ or $(1+z_B)^{-3}$			<i>unitless</i>
Trisine volume per cell	$cavity_r$	$2\sqrt{3}A_rB_r^2$	2.41E-76	(present)	cm^3
Trisine volume per cell z factors		$(1+z_R)^1$ or $(1+z_B)^3$			<i>unitless</i>
Trisine volume per chain	<i>chain</i> , or $2cavity_r/3$		1.61E-76		cm^3
Trisine volume per chain z factors		$(1+z_R)^1$ or $(1+z_B)^3$			<i>unitless</i>
Trisine wave vector (K_A)	$2\pi/A$		6.76E-01	(present)	cm^{-1}
Trisine wave vector (K_B)	$2\pi/(2B)$		1.41E-01	(present)	cm^{-1}
Trisine wave vector (K_C)	$4\pi/(3\sqrt{3}A)$		2.60E-01	(present)	cm^{-1}
Trisine wave vector (K_{Dn})	$(3\pi^2\mathbb{C}/cavity)^{1/3}$		1.56E-01	(present)	cm^{-1}
Trisine wave vector (K_{Ds})	$(4\pi^3\mathbb{C}/cavity)^{1/3}$		2.51E-01	(present)	cm^{-1}
Trisine wave vectors z factors		$(1+z_R)^{1/3}$ or $(1+z_B)^1$			<i>unitless</i>
Trisine wave vector (K_{Ar})	$2\pi/A_r$		2.72E+26	(present)	cm^{-1}
Trisine wave vector (K_{Br})	$2\pi/(2B_r)$		5.72E+25	(present)	cm^{-1}
Trisine wave vector (K_{Cr})	$4\pi/(3\sqrt{3}A_r)$		1.05E+26	(present)	cm^{-1}
Trisine wave vector (K_{Dnr})	$(3\pi^2\mathbb{C}/cavity_r)^{1/3}$		6.26E+25	(present)	cm^{-1}
Trisine wave vector (K_{Ds})	$(4\pi^3\mathbb{C}/cavity_r)^{1/3}$		1.01E+26	(present)	cm^{-1}
Trisine wave vectors z factors		$(1+z_R)^{-1/3}$ or $(1+z_B)^{-1}$			<i>unitless</i>
Universe absolute viscosity	μ_U or $m_t v_{dx}/section$		8.85E-32	(present)	$g\ cm^{-1}sec^{-1}$
Universe absolute viscosity z factors		$(1+z_R)^1$ or $(1+z_B)^3$			<i>unitless</i>
Universe absolute viscosity reflected	μ_U or $m_t v_{cex}/section_r$		5.78E48	(present)	$g\ cm^{-1}sec^{-1}$
Universe absolute viscosity reflected z factors	$(1+z_R)^{-1}$ or $(1+z_B)^{-3}$				<i>unitless</i>
Universe absolute (seen) viscosity	μ_{Uc} or $m_t c/(2\Delta x^2)$ or $\mathbb{C}m_t c K_B^2$		1.21E-16	(present)	$g\ cm^{-1}sec^{-1}$
Universe absolute (seen) viscosity z factors		$(1+z_R)^{2/3}$ or $(1+z_B)^{6/3}$			<i>unitless</i>
Universe absolute (seen) viscosity	μ_{Ucr} or $m_t c/(2\Delta x_r^2)$ or $\mathbb{C}m_t c K_{Br}^2$		1.97E+37	(present)	$g\ cm^{-1}sec^{-1}$
Universe absolute (seen) viscosity z factors		$(1+z_R)^{-2/3}$ or $(1+z_B)^{-6/3}$			<i>unitless</i>

Universe area	$2\pi R_U^2$	3.17E+57	(present)	cm^2
Universe area z factors	$(1+z_R)^{-2}$ or $(1+z_B)^{-6}$			<i>unitless</i>
Universe area reflected	$2\pi R_{Ur}^2$	7.42E-103	(present)	cm^2
Universe area reflected z factors	$(1+z_R)^2$ or $(1+z_B)^6$			<i>unitless</i>
Universe coordinate age	Age_U or $1/H_U$	4.32E17	(present)	<i>sec</i>
Universe coordinate age z factors	$(1+z_R)^{-1}$ or $(1+z_B)^{-3}$			<i>unitless</i>
Universe coordinate reflected age	Age_{Ur} or $1/H_{Ur}$	1.51E62	(present)	<i>sec</i>
Universe coordinate reflected age z factors	$(1+z_R)^1$ or $(1+z_B)^3$			<i>unitless</i>
Universe coordinate age at constant G	Age_{UG} or $Age_U \sqrt{G_U/G}$ $Age_U \sqrt{R_U c^2/(GM_U)}$	4.32E17	(present)	<i>sec</i>
Universe coordinate age at constant G z factors	$(1+z_R)^{-1/2}$ or $(1+z_B)^{-3/2}$			<i>unitless</i>
Universe coordinate age _v at constant G	Age_{UGv} $Age_U \sqrt{R_U c^2/(G(M_U + M_v))}$	4.32E17	(present)	<i>sec</i>
Universe coordinate age _v at constant G z factors	$(1+z_R)^{-1/2}$ or $(1+z_B)^{-3/2}$			<i>unitless</i>
Universe cosmological constant	Λ_U or $2H_U^2/c^2 \cos(\theta)$	1.29089±.23E-56	(present)	cm^{-2}
Universe cosmological constant z factors	$(1+z_R)^2$ or $(1+z_B)^6$			<i>unitless</i>
Universe cosmological constant	Ω_{Λ_U} or $c^2 \Lambda_U / (3H_U^2)$	0.72315	(constant)	<i>unitless</i>
Universe diffusion coefficient	D_c or $(2B)^2/time_{\pm} = \hbar/m_t$ or $(\hbar^{1/3} U^{-1/3} c^{1/3}) 2\pi/\cos(\theta)$	6.60526079E-2		$cm^2 \text{ sec}^{-1}$
Universe diffusion coefficient	D_c or $(2B_r)^2/time_{r\pm} = \hbar/m_t$ or $(\hbar^{1/3} U^{-1/3} c^{1/3}) 2\pi/\cos(\theta)$	6.60526079E-2		$cm^2 \text{ sec}^{-1}$
Universe energy (seen)	$m_t c^2$ or $m_U x_U^2/t_U^2$	9.01E-05	(constant)	$g \text{ cm}^2 \text{ sec}^{-2}$
Universe gravitational constancy	$G_U R_U$ or $3^{1/2} c/U$	1.4986653E+21		$cm^4 \text{ sec}^{-2} g^{-1}$
Universe gravitational constancy reflected	$G_{Ur} R_{Ur}$ or $3^{1/2} c/U$	1.4986653E+21		$cm^4 \text{ sec}^{-2} g^{-1}$
Universe gravitational energy density	$GM_U m_t / (R_U \text{cavity})$ or $sherd^{-1/2} G_U M_U m_t / (R_U \text{cavity})$ or $4\pi G \rho_U^2 c^2 / H_U^2$	5.73E-09	(constant)	$erg \text{ cm}^{-3}$
Universe gravitational energy density	$GM_{Ur} m_t / (R_{Ur} \text{cavity}_r)$ or $4\pi G \rho_{Ur}^2 c^2 / H_{Ur}^2$	5.73E-09	(constant)	$erg \text{ cm}^{-3}$
Universe gravity scaling constant	U or H_U/G_U	3.46E-11	(constant)	$g \text{ sec cm}^{-3}$

Universe gravity scaling constant	or H_{Ur}/G_{Ur}	3.46E-11	(constant)	$g \ sec \ cm^{-3}$
Universe gravity scaling constant	or $4m_t^3 c / (\pi \hbar^2)$	3.46E-11	(constant)	$g \ sec \ cm^{-3}$
Universe gravity scaling constant	or $4\pi M_U / (V_U H_U)$	3.46E-11	(constant)	$g \ sec \ cm^{-3}$
Universe gravity scaling constant	or $4\pi M_{Ur} / (V_{Ur} H_{Ur})$	3.46E-11	(constant)	$g \ sec \ cm^{-3}$
Universe gravity scaling constant	or $4\pi m_t / (cavity \ H_U)$	3.46E-11	(constant)	$g \ sec \ cm^{-3}$
Universe gravity scaling constant	or $4\pi m_t / (cavity_r \ H_{Ur})$	3.46E-11	(constant)	$g \ sec \ cm^{-3}$
Universe gravitational parameter	G_U or $R_U c^2 / M_U$ or $G (M_{Upresent} / M_U)^{1/2}$	6.67384E-8 6.67384E-8	(present) (present)	$cm^3 sec^{-2} g^{-1}$ $cm^3 sec^{-2} g^{-1}$
Universe gravitational parameter z factors	$(1+z_R)^1$ or $(1+z_B)^3$			unitless
Universe gravitational parameter	G_{Ur} or $R_{Ur} c^2 / M_{Ur}$ or $G (M_{Upresent} / M_{Ur})^{1/2}$	4.36E+72 4.36E+72	(present) (present)	$cm^3 sec^{-2} g^{-1}$ $cm^3 sec^{-2} g^{-1}$
Universe gravitational parameter z factors	$(1+z_R)^{-1}$ or $(1+z_B)^{-3}$			unitless
Universe Newtonian gravitation	G or $(sherd/sherd_{present})^{1/2} G_U$	6.67384E-8	(constant)	$cm^3 sec^{-2} g^{-1}$
Universe Newtonian gravitation	G or $(sherd_r/sherd_{present})^{1/2} G_{Ur}$	6.67384E-8	(constant)	$cm^3 sec^{-2} g^{-1}$
Universe Hubble parameter	H_U or $2^{-1/2} \cos(\theta)^{1/2} \Lambda_U^{1/2} c$	2.31E-18	(present)	sec^{-1}
Universe Hubble parameter	or $(B/A)(1/\sqrt{3})(v_{dx}/v_c)(1/time)$	2.31E-18	(present)	sec^{-1}
Universe Hubble parameter z factors	$(1+z_R)^1$ or $(1+z_B)^3$			unitless
Universe Hubble parameter	H_{Ur} or $2^{-1/2} \cos(\theta)^{1/2} \Lambda_{Ur}^{1/2} c$	1.51E+62	(present)	sec^{-1}
Universe Hubble parameter	or $(B_r/A_r)(1/\sqrt{3})(v_{dxr}/v_c)(1/time_{xr})$	1.51E+62	(present)	sec^{-1}
Universe Hubble parameter z factors	$(1+z_R)^{-1}$ or $(1+z_B)^{-3}$			unitless
Universe Hubble parameter	H_{UG} or $H_U (G/G_U)^{1/2}$	2.31E-18	(present)	sec^{-1}
Universe Hubble parameter z factors	$(1+z_R)^{1/2}$ or $(1+z_B)^{3/2}$			unitless
Universe Hubble parameter	H_{UGr} or $H_{Ur} (G/G_{Ur})^{1/2}$	1.87E+22	(present)	sec^{-1}
Universe Hubble parameter z factors	$(1+z_R)^{-1/2}$ or $(1+z_B)^{-3/2}$			unitless
Universe inflation number	$\#_U$ or $V_U m_t / (m_e cavity)$ or M_U / m_e	3.32E+83	(present)	unitless
Universe inflation number z factors	$(1+z_R)^{-2}$ or $(1+z_B)^{-6}$			unitless
Universe inflation number	$\#_{Ur}$ or $V_{Ur} m_t / (m_e cavity_r)$ or M_{Ur} / m_e	7.77E-77	(present)	unitless
Universe inflation number z factors	$(1+z_R)^2$ or $(1+z_B)^6$			unitless
Universe kinematic viscosity (seen)	ν_{Uc} or μ_{Uc} / ρ_U	1.39E13	(present)	$cm^2 sec^{-1}$
Universe kinematic viscosity (seen) z factors	$(1+z_R)^{-1/3}$ or $(1+z_B)^{-1}$			unitless

Universe kinematic viscosity (seen)	ν_{Ucr} or μ_{Ucr}/ρ_{Ur}	4.73E-14	(present)	$cm^2 sec^{-1}$
Universe kinematic viscosity (seen) z factors $(1+z_R)^{1/3}$ or $(1+z_B)^1$				<i>unitless</i>
Universe kinematic viscosity	ν_U or $(\pi A/B)x_U^2/t_U$	1.39-02	(constant)	$cm^2 sec^{-1}$
Universe kinematic viscosity	or μ_U/ρ_U	1.39-02	(constant)	$cm^2 sec^{-1}$
Universe kinematic viscosity	μ_{Ur}/ρ_{Ur}	1.39-02	(constant)	$cm^2 sec^{-1}$
Universe mass density ρ_U	$m_t/cavity$ or $2H_U^2/(8\pi G_U)$	6.38E-30	(present)	$g cm^{-3}$
Universe number density n	$\mathbb{C}/cavity$	1.27E-04	(present)	$\# cm^{-3}$
Universe mass and number density z factors $(1+z_R)^1$ or $(1+z_B)^3$				<i>unitless</i>
Universe mass density ρ_{Ur}	$m_t/cavity_r$ or $2H_{Ur}^2/(8\pi G_{Ur})$	4.16E50	(present)	$g cm^{-3}$
Universe number density n_r	$\mathbb{C}/cavity_r$	8.30E+75	(present)	$\# cm^{-3}$
Universe mass and number density z factors $(1+z_R)^{-1}$ or $(1+z_B)^{-3}$				<i>unitless</i>
Universe mass (no radiation)	M_U or $\rho_U V_U$	3.02E56	(present)	g
Universe (no radiation) mass z factors	$(1+z_R)^{-2}$ or $(1+z_B)^{-6}$			<i>unitless</i>
Universe (no radiation) mass reflective	M_{Ur} or $\rho_{Ur} V_{Ur}$	2.34E-100	(present)	g
Universe (no radiation) mass reflective z factors $(1+z_R)^2$ or $(1+z_B)^6$				<i>unitless</i>
Universe length	x_U or $(\hbar^{1/3} U^{-1/3} c^{-2/3})/\cos(\theta)$	3.51E-13	(constant)	cm
Universe time	t_U or $(\hbar^{1/3} U^{-1/3} c^{-5/3})/\cos(\theta)$	1.17E-23	(constant)	sec
Universe momentum	m_c or $m_U x_U/t_U$	3.00737E-15	(constant)	$g cm sec^{-1}$
Universe pressure	p_U or $k_b T_c/cavity$	7.11E-36	(present)	$g cm^{-1} sec^{-2}$
Universe pressure z factors	$(1+z_R)^{5/3}$ or $(1+z_B)^5$			<i>unitless</i>
Universe pressure reflective	p_{Ur} or $k_b T_{cr}/cavity_r$	7.53E+97	(present)	$g cm^{-1} sec^{-2}$
Universe pressure reflective z factors	$(1+z_R)^{-5/3}$ or $(1+z_B)^{-5}$			<i>unitless</i>
Universe Hubble radius of curvature	R_U or $\sqrt{3}c/H_U$	2.25E28	(present)	cm
Universe Hubble radius z factors	$(1+z_R)^{-1}$ or $(1+z_B)^{-3}$			<i>unitless</i>
Universe Hubble reflected radius	R_{Ur} or $\sqrt{3}c/H_{Ur}$	3.44E-52	(present)	cm
Universe Hubble reflected radius z factors	$(1+z_R)^1$ or $(1+z_B)^3$			<i>unitless</i>
Universe Hubble surface constant	M_U/R_U^2	0.599704		$g cm^{-2}$
Universe Hubble surface constant reflective	M_{Ur}/R_{Ur}^2	0.599704		$g cm^{-2}$
Universe Hubble volume	V_U or $(4\pi/3)R_U^3$	4.74E85	(present)	cm^3
Universe Hubble volume z factors	$(1+z_R)^{-3}$ or $(1+z_B)^{-9}$			<i>unitless</i>

Universe Hubble volume reflective	V_{Ur} or $(4\pi/3)R_{Ur}^3$	1.70E-154	(present)	cm^3
Universe Hubble volume reflective z factors	$(1+z_R)^3$ or $(1+z_B)^9$			<i>unitless</i>
Universe Reynolds number	R_{eU} or $\rho_U v_{dx} cavity / (\mu_U section)$	1.00	(constant)	cm
Universe Reynolds number	R_{eUr} or $\rho_{Ur} v_{dx} cavity_r / (\mu_{Ur} section_r)$	1.00	(constant)	cm
Universe sherd	$(M_{Upresent}/m_t)/(M_U/m_t)$	1	(present)	<i>unitless</i>
Universe sherd	$(V_{Upresent}/cavity_{present})/(V_U/cavity)$	1	(present)	<i>unitless</i>
Universe sherd z factors	$(1+z_R)^{-2}$ or $(1+z_B)^{-6}$			<i>unitless</i>
Universe sherd _r	$(M_{Upresent}/m_t)/(M_{Ur}/m_t)$	4.27E+159	(present)	<i>unitless</i>
Universe sherd _r	$(V_{Upresent}/cavity_{present})/(V_{Ur}/cavity_r)$	4.27E+159	(present)	<i>unitless</i>
Universe sherd _r z factors	$(1+z_R)^2$ or $(1+z_B)^6$			<i>unitless</i>
Universe z_R factor	$R_{Upresent}/R_U = 2.25E28$ cm/R_U			<i>unitless</i>
Universe z_B factor	$B_{present}/B = 22.1$ cm/B			<i>unitless</i>
Universe Total volume	V_U sherd	4.74E85	(present)	cm^3
Universe Total volume z factors	$(1+z_R)^{-1}$ or $(1+z_B)^{-3}$			<i>unitless</i>
Universe Total volume	V_{Ur} sherd _r	7.27E+05	(present)	cm^3
Universe Total volume z factors	$(1+z_R)^1$ or $(1+z_B)^3$			<i>unitless</i>
Velocity of light	c or x_U/t_U	2.997924580E10		$cm sec^{-1}$
Velocity of light	$H_U R_U / \sqrt{3}$	2.997924580E10		$cm sec^{-1}$
Velocity of light	$H_{Ur} R_{Ur} / \sqrt{3}$	2.997924580E10		$cm sec^{-1}$
Velocity of light dielectric ϵ modified	v_ϵ or $c/\sqrt{\epsilon}$ or $2v_{dx}\sqrt{k_m}$	1.21E+05	(present)	$cm sec^{-1}$
Velocity of light dielectric ϵ modified	v_{ex} or $c/\sqrt{\epsilon_x}$	1.18E+04	(present)	$cm sec^{-1}$
Velocity of light dielectric ϵ modified	v_{ey} or $c/\sqrt{\epsilon_y}$	1.36E+04	(present)	$cm sec^{-1}$
Velocity of light dielectric ϵ modified	v_{ez} or $c/\sqrt{\epsilon_z}$	5.62E+04	(present)	$cm sec^{-1}$
Velocity of light dielectric ϵ modified z factors	$(1+z_R)^{1/6}$ or $(1+z_B)^{1/2}$			<i>unitless</i>
Velocity (reflective v_{ex})	v_{exr} or $(c/v_{ex})c$ or $c/\sqrt{\epsilon_r}$	7.61E+16	(present)	$cm sec^{-1}$
Velocity (reflective v_{ey})	v_{eyr} or $(c/v_{ey})c$ or $c/\sqrt{\epsilon_{xr}}$	6.59E+16	(present)	$cm sec^{-1}$
Velocity (reflective v_{ez})	v_{ezr} or $(c/v_{ez})c$ or $c/\sqrt{\epsilon_{yr}}$	1.60E+16	(present)	$cm sec^{-1}$

Velocity (reflective v_ε)	$v_{\varepsilon r}$ or $(c/v_\varepsilon)c$ or $c/\sqrt{\varepsilon_r}$	7.44E+15	(present)	$cm\ sec^{-1}$
Velocity (reflective v_ε) z factors	$(1+z_R)^{-1/6}$ or $(1+z_B)^{-1/2}$			<i>unitless</i>
Velocity (de Broglie)	v_{dx} or $\hbar K_B/m_t$ or $c/\sqrt{\varepsilon_x k_{mx}}$	1.49E-03	(present)	$cm\ sec^{-1}$
Velocity (de Broglie)	v_{dy} or $\hbar K_P/m_t$ or $c/\sqrt{\varepsilon_y k_{my}}$	1.73E-03	(present)	$cm\ sec^{-1}$
Velocity (de Broglie)	v_{dz} or $\hbar K_A/m_t$ or $c/\sqrt{\varepsilon_z k_{mz}}$	7.11E-03	(present)	$cm\ sec^{-1}$
Velocity (de Broglie)	v_{dT} or $\sqrt{v_{dx}^2 + v_{dy}^2 + v_{dz}^2}$ or $c/\sqrt{4\varepsilon k_m}$	7.47E-03	(present)	$cm\ sec^{-1}$
Velocity (de Broglie) z factors	$(1+z_R)^{1/3}$ or $(1+z_B)^1$			<i>unitless</i>
Velocity (reflective v_{dx})	v_{dxr} or $(c/v_{dx})c$ or $c/\sqrt{\varepsilon_{xr} k_{mxr}}$	6.02E+23	(present)	$cm\ sec^{-1}$
Velocity (reflective v_{dy})	v_{dyr} or $(c/v_{dy})c$ or $c/\sqrt{\varepsilon_{yr} k_{myr}}$	5.21E+23	(present)	$cm\ sec^{-1}$
Velocity (reflective v_{dz})	v_{dzr} or $(c/v_{dz})c$ or $c/\sqrt{\varepsilon_{zr} k_{mzr}}$	1.26E+23	(present)	$cm\ sec^{-1}$
Velocity (reflective v_{dT})	$v_{dT r}$ or $\sqrt{v_{dxr}^2 + v_{dyr}^2 + v_{dzr}^2}$ or $c/\sqrt{4\varepsilon_r k_{mr}}$	8.06E+23	(present)	$cm\ sec^{-1}$
Velocity (reflective) z factors	$(1+z_R)^{-1/3}$ or $(1+z_B)^{-1}$			<i>unitless</i>
Zeta function $\zeta(n)$	$\zeta(n) = \sum_n^\infty 1/n^2$			<i>unitless</i>
Zeta function $\zeta(3/2)$		2.61237530936309		<i>unitless</i>
Zeta function $\zeta(2)$		1.64493406684823	$\pi^2/6$	<i>unitless</i>
Zeta function $\zeta(5/2)$		1.34148725725091		<i>unitless</i>
Zeta function $\zeta(3)$		1.20205690117833		<i>unitless</i>
Zeta function $\zeta(7/2)$		1.12673386618586		<i>unitless</i>
Zeta function $\zeta(4)$		1.08232323371114	$\pi^4/90$	<i>unitless</i>
Zeta function $\zeta(9/2)$		1.05470751076145		<i>unitless</i>
Zeta function $\zeta(5)$		1.03692775485763		<i>unitless</i>

Appendix A. Trisine Universal Number m_t And B/A Ratio Derivation

BCS approach [2]

$$\Delta_o^{BCS} = \frac{\hbar\omega}{\sinh\left(\frac{1}{D(\in_T)V}\right)} \quad (A.1)$$

Kittel approach [4]

$$\Delta_o = \frac{2\hbar\omega}{e^{\frac{1}{D(\in_T)V}} - 1} \quad (A.2)$$

Let the following relationship where BCS (equation A.1) and Kittel (equation A.2) approach equal each other define a particular superconducting condition.

$$k_b T_c = \begin{cases} \frac{e^{Euler}}{\pi} \frac{\hbar\omega}{\sinh\left(\frac{1}{D(\in_T)V}\right)} \\ \frac{\hbar\omega}{e^{\frac{1}{D(\in_T)V}} - 1} \end{cases} \quad (A.3)$$

$$\text{where } \frac{e^{Euler}}{\pi} = 1.133865917$$

Define:

$$\frac{1}{D(\in_T)V} = \text{trisine} \quad (A.4)$$

Then:

$$\text{trisine} = -\ln\left(\frac{2e^{Euler}}{\pi} - 1\right) = 2.01091660 \quad (A.5)$$

Given:

$$\frac{2m_t k_b T_c}{\hbar^2} = \begin{cases} \frac{(KK)_{\hbar\omega} e^{Euler}}{\pi \sinh(\text{trisine})} \\ \frac{(KK)_{\hbar\omega}}{e^{\text{trisine}} - 1} \end{cases} = K_B^2 \quad (A.6)$$

Ref: [2,4]

And within Conservation of Energy Constraint ($|n| < \infty$):

$$\left(\frac{1}{g_s}\right) (K_B^{2+n} + K_C^{2+n}) = (K_{D_s}^{2+n} + K_{D_n}^{2+n}) \quad (A.7)$$

And within Conservation of Momentum Constraint ($|n| < \infty$):

$$(g_s) (K_B^{1+n} + K_C^{1+n}) = (K_{D_s}^{1+n} + K_{D_n}^{1+n}) \quad (A.8)$$

And (KK) from table A.1:

$$(KK) = K_C^2 + K_{D_s}^2 \quad (A.9)$$

Also from table A.1:

$$\frac{2\Delta_o^{BCS}}{k_b T_c} = \frac{2\pi}{e^{Euler}} = \frac{2K_{D_s}}{K_B}^{0.065\%} \approx 3.527754 \quad (A.10)$$

Also:

$$\frac{\Delta_o}{k_b T_c} = 2 \quad (A.11)$$

Also from table A.1:

$$\text{trisine} = \frac{K_B^2 + K_P^2}{K_P K_B} \quad (A.12)$$

Table A.1 Trisine Wave Vector Multiples (KK) vs. $K_B K_B$

K	$(KK) e^{Euler}$		
	$\frac{(KK)}{K_B K_B}$	$\frac{(KK)}{K_B K_B} \frac{1}{e^{\text{trisine}} - 1}$	$\frac{K}{K_B}$
K_{D_n}	1.1981	0.1852	1.0947
K_P	1.3333	0.2061	1.1547
K_{D_s}	3.1132	0.4813	1.7646
K_C	3.3526	0.5185	1.8316
K_A	22.6300	3.4999	4.7587
$(K_C + K_{D_s})/2^{1/2}$	6.4687	1.0000	3.5962

But also using the following resonant condition in equation A.13 and by iterating equations A.7, A.8 and A.13.

$$k_b T_c = \begin{cases} \frac{\hbar^2 K_B^2}{2m_t} \\ \frac{\hbar^2}{\frac{m_e m_t}{m_e + m_t} (2B)^2 + \frac{m_t m_p}{m_t + m_p} (A)^2} \end{cases} \quad (A.13)$$

This trisine model converges at:

$$\begin{aligned} m_t/m_e &= 110.122753426 \text{ where } \alpha m_t/m_e \sim \frac{4}{5} \\ B/A &= 2.379760996 \sim 2 \csc\left(\frac{180}{\pi}\right) \sim \frac{\text{neutral pion}(\pi^0)}{m_t} \end{aligned} \quad (A.14)$$

Appendix B. Debye Model Normal And Trisine Reciprocal Lattice Wave Vectors

This appendix parallels the presentation made in ref [4 pages 121 - 122].

$$N = \begin{cases} \left(\frac{L}{2\pi}\right)^3 \frac{4\pi}{3} K_{D_n}^3 \\ \left(\frac{L}{2\pi}\right)^3 K_{D_s}^3 \end{cases} = \begin{cases} \text{Debye Spherical Condition} \\ \text{Debye Trisine Condition} \end{cases} \quad (B.1)$$

where:

$$K_{Ds} = (K_A K_B K_P)^{\frac{1}{3}} \quad (B.2)$$

$$\frac{dN}{d\omega} = \begin{bmatrix} cavity & K_{Dn}^2 \frac{dK_{Dn}}{d\omega} \\ \frac{cavity}{2\pi^2} 3K_{Ds}^2 \frac{dK_{Ds}}{d\omega} \end{bmatrix} = \begin{cases} \text{Debye Spherical Condition} \\ \text{Debye Trisine Condition} \end{cases} \quad (B.3)$$

$$K = \frac{\omega}{v} \quad (B.4)$$

$$\frac{dK}{d\omega} = \frac{1}{v} \quad (B.5)$$

$$\frac{dN}{d\omega} = \begin{cases} \frac{cavity}{2\pi^2} \frac{\omega^2}{v^3} \\ \frac{3 \cdot cavity}{8\pi^3} \frac{\omega^2}{v^3} \end{cases} = \begin{cases} \text{Debye spherical} \\ \text{Debye trisine} \end{cases} \quad (B.6)$$

$$N = \begin{cases} \frac{cavity}{6\pi^2} \frac{\omega^3}{v^3} \\ \frac{cavity}{8\pi^3} \frac{\omega^3}{v^3} \end{cases} = \begin{cases} \frac{cavity}{6\pi^2} K_{Dn}^3 \\ \frac{cavity}{8\pi^3} K_{Ds}^3 \end{cases} = \begin{cases} \text{Debye Spherical Condition} \\ \text{Debye Trisine Condition} \end{cases} \quad (B.7)$$

Given that $N = 1$ Cell

$$\begin{cases} K_{Dn} \\ K_{Ds} \end{cases} = \begin{cases} \left(\frac{6\pi^2}{cavity}\right)^{\frac{1}{3}} \\ \left(\frac{8\pi^3}{cavity}\right)^{\frac{1}{3}} \end{cases} = \begin{cases} \text{Debye Spherical Condition} \\ \text{Debye Trisine Condition} \end{cases} \quad (B.8)$$

Appendix C. One Dimension And Trisine Density Of States

This appendix parallels the presentation made in ref [4 pages 144-155].

Trisine

$$\frac{2K_C^3}{\left(\frac{2\pi}{L}\right)^3} = N \quad (C.1)$$

One Dimension

$$\xi = \frac{\hbar^2}{2m_t} N^2 \frac{\pi^2}{(2B)^2} \quad (C.2)$$

Now do a parallel development of trisine and one dimension density of states.

$$N = \begin{bmatrix} \frac{2K_C^3 \cdot cavity}{8\pi^3} \\ \left(\frac{2m_t}{\hbar^2}\right)^{\frac{1}{2}} \frac{2B}{\pi} \xi^{\frac{1}{2}} \end{bmatrix} = \begin{cases} \text{Trisine Dimensional Condition} \\ \text{One Dimensional Condition} \end{cases} \quad (C.3)$$

$$\frac{dN}{d\xi} = \begin{cases} \frac{2 \cdot cavity}{8\pi^3} \left(\frac{2m_t}{\hbar^2}\right)^{\frac{3}{2}} \frac{3}{2} \xi^{\frac{1}{2}} \\ \left(\frac{2m_t}{\hbar^2}\right)^{\frac{1}{2}} \frac{2B}{\pi} \frac{1}{2} \xi^{-\frac{1}{2}} \end{cases} = \begin{cases} \text{Trisine Dimensional Condition} \\ \text{One Dimensional Condition} \end{cases} \quad (C.4)$$

$$\frac{dN}{d\xi} = \begin{cases} \frac{2 \cdot cavity}{8\pi^3} \left(\frac{2m_t}{\hbar^2}\right)^{\frac{3}{2}} \frac{3}{2} \xi^{\frac{1}{2}} \\ \left(\frac{2m_t}{\hbar^2}\right)^{\frac{1}{2}} \frac{2B}{\pi} \frac{1}{2} \xi^{-\frac{1}{2}} \end{cases} = \begin{cases} \text{Trisine Dimensional Condition} \\ \text{One Dimensional Condition} \end{cases} \quad (C.5)$$

$$\frac{dN}{d\xi} = \begin{cases} 2 \frac{3 cavity}{8\pi^3} \left(\frac{2m_t}{\hbar^2}\right)^{\frac{3}{2}} \left(\frac{2m_t}{\hbar^2}\right)^{-\frac{1}{2}} K_C \\ \left(\frac{2m_t}{\hbar^2}\right)^{\frac{1}{2}} \frac{2B}{\pi} \frac{1}{2} \left(\frac{2m_t}{\hbar^2}\right)^{\frac{1}{2}} \frac{1}{K_B} \end{cases} = \begin{cases} \text{Trisine Dimensional Condition} \\ \text{One Dimensional Condition} \end{cases} \quad (C.6)$$

$$\frac{dN}{d\xi} = D(\xi) = \begin{cases} \frac{3 cavity}{8\pi^3} \left(\frac{2m_t}{\hbar^2}\right) K_C \\ \frac{2m_t}{\hbar^2 K_B^2} \end{cases} = \begin{cases} \text{Trisine Dimensional Condition} \\ \text{One Dimensional Condition} \end{cases} \quad (C.7)$$

Now equating trisine and one dimensional density of states results in equation C.8.

$$\begin{aligned} K_C &= \frac{8\pi^3}{3 \cdot cavity \cdot K_B^2} \\ &= \frac{4\pi}{3\sqrt{3}A} \end{aligned} \quad (C.8)$$

ξ = energy

$D(\xi)$ = density of states

Appendix D. Ginzburg-Landau Equation And Trisine Structure Relationship

This appendix parallels the presentation made in ref [4 Appendix I].

$$|\psi|^2 = \frac{\alpha}{\beta} = \frac{C}{cavity} \quad (D.1)$$

$$\frac{\alpha^2}{2\beta} = \frac{k_b T_c}{chain} = \frac{\hbar^2 K_B^2}{2m_t \cdot chain} = \frac{H_c^2}{8\pi} \quad (D.2)$$

$$\lambda = \frac{m_t v_e^2}{4\pi (\mathbb{C} \cdot e)^2 |\psi|^2} = \frac{m_t v_e^2 \beta}{4\pi q^2 \alpha} = \frac{m_t v_e^2 cavity}{4\pi (\mathbb{C} \cdot e)^2 \mathbb{C}} \quad (D.3)$$

$$\beta = \frac{\alpha^2 2m_t chain}{2\hbar^2 K_B^2} = \frac{\alpha^2 chain}{2k_b T_c} \quad (D.4)$$

$$\alpha = \beta \frac{\mathbb{C}}{cavity} = \frac{\alpha^2 2m_t chain}{2\hbar^2 K_B^2} \frac{\mathbb{C}}{cavity} = \frac{\alpha^2 chain}{2k_b T_c} \frac{\mathbb{C}}{cavity} \quad (D.5)$$

$$\alpha = k_b T_c \frac{cavity}{chain} = \frac{\hbar^2 K_B^2}{2m_t} \frac{cavity}{chain} \quad (D.6)$$

$$\ell^2 \equiv \frac{\hbar^2}{2m_e \alpha} = \frac{\hbar^2}{2m_e} \frac{2m_t \cdot chain}{\hbar^2 K_B^2 \cdot cavity} = \frac{m_t}{m_e} \frac{1}{K_B^2} \frac{chain}{cavity} \quad (D.7)$$

$$H_{c2} = \frac{\phi_e \cdot 2 \cdot 4\pi}{section} = \frac{\phi_e}{\pi \ell^2} \frac{m_t}{m_e} \frac{cavity}{chain} \quad (D.8)$$

Appendix E. Heisenberg Uncertainty within the Context of De Broglie Condition

Given Heisenberg uncertainty:

$$\Delta p_x \Delta x \geq \frac{h}{4\pi} \quad (E.1)$$

And the assumption that mass 'm' is constant then:

$$m \Delta v \Delta x \geq \frac{h}{4\pi} \quad (E.2)$$

Given de Broglie Condition:

$$p_x x = h \quad (E.3)$$

And again assuming constant mass 'm':

$$mvx = h \quad (m_t v_{dx} 2B = h) \quad (E.4)$$

Rearranging Heisenberg Uncertainty and de Broglie Condition:

$$m \geq \frac{h}{4\pi \Delta v \Delta x} \quad \text{and} \quad m = h \frac{1}{vx} \quad (E.5)$$

This implies that:

$$m \geq m \quad (E.6)$$

but a constant mass cannot be greater than itself, therefore:

$$m = m \quad (E.7)$$

therefore:

$$h \frac{1}{vx} = \frac{h}{4\pi} \frac{1}{\Delta v \Delta x} \quad (E.8)$$

And:

$$vx = 4\pi \Delta v \Delta x \quad (E.9)$$

Both the Heisenberg Uncertainty and the de Broglie condition are satisfied. Uncertainty is dimensionally within the de Broglie condition. Schrödinger in the field of quantum mechanics further quantified this idea.

Appendix F. Equivalence Principle In The Context Of Work Energy Theorem

Start with Newton's second law

$$F = \frac{dp}{dt} \quad (F.1)$$

and for constant mass

$$F = \frac{dp}{dt} = \frac{d(mv)}{dt} = m \frac{dv}{dt} \quad (F.2)$$

then given the 'work energy theorem'

$$F = \frac{dp}{dt} = \frac{d(mv)}{dt} = m \frac{dv}{dt} \frac{ds}{ds} = mv \frac{dv}{ds} \quad (F.3)$$

where $\frac{ds}{dt} = v$ and therefore: $Fds = mvdv$

where ds is test particles incremental distance along path 's'

Now given Newton's second law in relativistic terms:

$$F = \frac{dp}{dt} = \frac{d}{dt} \frac{mv}{\sqrt{1 - \frac{v^2}{c^2}}} \quad (F.4)$$

let Lorentz transform notation as 'b' :

$$b = \frac{1}{\sqrt{1 - \frac{v^2}{c^2}}} \quad (F.5)$$

therefore:

$$F = \frac{dp}{dt} = \frac{d(mb)}{dt} \quad (F.6)$$

Now transform into a work energy relationship with a K factor of dimensional units 'length/mass'

$$a \left(\frac{1}{K} \right) ds = mbv dv \quad (F.7)$$

acceleration 'a' can vary and the path 's' is arbitrary within the dimensional constraints of the equation.

Define acceleration 'a' in terms of change in Volume 'V' as:

$$\frac{d^2V}{dt^2} \frac{1}{V} = \text{constant} \quad (F.8)$$

and incremental path 'ds' as:

$$ds = 2(area)dr = 2(4\pi r^2)dr \quad (F.9)$$

'area' is the surface of the spherical volume 'V'

Now work-energy relationship becomes:

$$\frac{d^2V}{dt^2} \frac{1}{V} \frac{1}{K} 2(4\pi r^2) dr = mbvdv \quad (F.10)$$

Now integrate both sides:

$$\frac{d^2V}{dt^2} \frac{1}{V} \frac{1}{K} 2\left(\frac{4}{3}\pi r^3\right) = -\left(mc^2 - mv^2\right)b \quad (F.11)$$

for $v \ll c$ then $b \sim 1$

$$\text{and } V = \frac{4}{3} \pi r^3$$

then:

$$-\frac{d^2V}{dt^2} \frac{1}{V} \frac{2}{K} = \left(\frac{mc^2}{V} - \frac{mv^2}{V}\right) \quad (F.12)$$

and:

$$-\frac{d^2V}{dt^2} \frac{1}{V} = \frac{K}{2} \left(\frac{mc^2}{V} - \frac{mv^2}{V}\right) \quad (F.13)$$

and

$$-\frac{d^2V}{dt^2} \frac{1}{V} = \frac{K}{2} \left(\frac{mc^2}{V} - \frac{mv}{\text{time}} \left(\frac{1}{\text{area}_x} + \frac{1}{\text{area}_y} + \frac{1}{\text{area}_z}\right)\right) \quad (F.14)$$

This is the same as the Baez-Bunn narrative [144] interpretation except for the negative signs on momentum. Since momentum ' mv ' is a vector and energy ' mv^2 ' is a scalar perhaps the relationship should be expressed as:

$$-\frac{d^2V}{dt^2} \frac{1}{V} = \frac{K}{2} \begin{pmatrix} \frac{mc^2}{V} \pm \frac{mv}{\text{area}_x \text{time}} \\ \pm \frac{mv}{\text{area}_y \text{time}} \\ \pm \frac{mv}{\text{area}_z \text{time}} \end{pmatrix} \quad (F.15)$$

or perhaps in terms of spherical surface area ' area_r '

$$-\frac{d^2V}{dt^2} \frac{1}{V} = \frac{K}{2} \left(\frac{mc^2}{V} \pm \frac{mv}{\text{area}_r \text{time}}\right) \quad (F.16)$$

Lets look again at the equation F.7 and define another path ' s :

$$ds = 16\pi r dr \quad a = \frac{d^2r}{dt^2} = \text{constant} \quad (F.17)$$

then

$$a \left(\frac{2}{K}\right) 8\pi r dr = mbvdv \quad (F.18)$$

Then integrate:

$$a \left(\frac{2}{K}\right) 4\pi r^2 = -\left(mc^2 - mv^2\right)b \quad (F.19)$$

Given that:

$$K = \frac{8\pi G}{c^2} \quad (F.20)$$

and solve equation F.19 for ' a '

$$a = -\frac{Gm}{r^2} \frac{1}{b} \quad (F.21)$$

or

$$a = -\frac{Gm}{r^2} \sqrt{1 - \frac{v^2}{c^2}} \quad (F.22)$$

Does this equation correctly reflect the resonant gravitational acceleration such as a satellite orbiting the earth??

Of course this equation reduces to the standard Newtonian gravitational acceleration at ' $v \ll c$ '

$$a = -\frac{Gm}{r^2} \quad (F.23)$$

The equation F.7 would appear to be general in nature and be an embodiment of the equivalence principle. Various candidate accelerations ' a ' and geometric paths ' ds ' could be analyzed within dimensional constraints of this equation.

A simple case defined by a path ' ds/C_t ' may be appropriate for the modeling the Pioneer deceleration anomaly.

$$Ma \frac{1}{C_t} ds = F \frac{1}{C_t} ds = mbvdv \quad (F.24)$$

Where a 'thrust' constant (C_t) is associated with object of mass (M) moving on curvature ' ds '.

Appendix G. Koide Constant for Leptons - tau, muon and electron

Koide Constant for Lepton masses follows naturally from nuclear condition as defined in paragraph 1.2.

$$\begin{aligned} m_\tau &= \frac{2}{3} \hbar c (K_{Ds} + K_{Dn}) \frac{1}{c^2} \\ &= \frac{2}{3} \hbar c (K_B + K_C) \frac{g_s}{c^2} \\ &= 1.777 \text{ GeV} / c^2 \quad (1.77684(17)) \end{aligned} \quad (G1)$$

$$\begin{aligned}
m_\mu &= \frac{1}{3} \frac{m_e}{m_t} \frac{\hbar^2}{2m_t} (K_{Ds}^2 + K_{Dn}^2) \frac{g_s}{c^2} \\
&= \frac{1}{3} \frac{m_e}{m_t} \frac{\hbar^2}{2m_t} (K_B^2 + K_C^2) \frac{1}{c^2} \\
&= .1018 \text{ GeV} / c^2 \quad (.1056583668(38)) \\
m_e &= \frac{B}{A} \cos(\theta) \frac{m_e}{m_t} (g_s - 1) \hbar c (K_{Ds} + K_{Dn}) \frac{1}{c^2} \\
&= \frac{B}{A} \cos(\theta) \frac{m_e}{m_t} (g_s - 1) \hbar c (K_B + K_C) \frac{g_s}{c^2} \\
&= .0005129 \text{ GeV} / c^2 \quad (.000510998910(13)) \\
\frac{m_\tau + m_\mu + m_e}{(\sqrt{m_\tau} + \sqrt{m_\mu} + \sqrt{m_e})^2} &= \frac{\text{chain}}{\text{cavity}} = \frac{2}{3}
\end{aligned}$$

Appendix H. Active Galactic Nuclei (AGN) and Variable Star RRc Tidal Dimension (T) in Oscillating Dark Energy Matter Medium (U)

$$\frac{GM_{AGN}M_{test}}{R_{AGN}} - \frac{GM_{AGN}M_{test}}{R_{AGN} + T} = \frac{GM_U M_{test}}{R_U} - \frac{GM_U M_{test}}{R_U - B} \quad (\text{H.1})$$

$$\frac{M_{AGN}}{R_{AGN}} - \frac{M_{AGN}}{R_{AGN} + T} = \frac{M_U}{R_U} - \frac{M_U}{R_U - B} \quad (\text{H.2})$$

$$M_{AGN}T \frac{1}{R_{AGN}(R_{AGN} + T)} = M_U B \frac{1}{R_U(R_U + B)} \quad (\text{H.3})$$

$$\frac{M_{AGN}}{R_{AGN}^2} T = \frac{M_U}{R_U^2} B \approx 0.6 B \quad \text{eqn 2.11.23} \quad (\text{H.4})$$

$$\Gamma \approx 0.6 \frac{R_{AGN}^2}{M_{AGN}} B \approx 0.6 \frac{R_{AGN}^3}{M_{AGN}} \frac{B}{R_{AGN}} \approx 0.6 \frac{1}{\rho_{AGN}} \frac{B}{R_{AGN}} \quad (\text{H.5})$$

Active Galactic Nuclei (AGN) or any other interstellar gaseous medium (including planetary atmosphere) Oscillates with Dark Energy Medium (U).

Appendix I. Dimensional Analysis of \hbar, G, c, H

These calculations are presented in context of historical appreciation of the Planck Units. Mead[141] deals with the mass(m), length(l), time(t) dimensionality associated with universal constants (\hbar, G, c) known to Max Planck in 1899. The Hubble parameter(H) was conceptually unknown at that time. These relationships are independent of the particular (m, l, t) units used (in this case(cgs) gram, centimeter, second)

As a later extension of this concept, George Lemaitre

conceptually interpreted Albert Einstein's field equations in terms of universe expansion (1927)[142] which was verified by Edwin Hubble (1929).

The observed Hubble expansion value H has changed over the years and has narrowed over the last decade with WMAP and Planck spacecrafts and galactic formation changes with redshift (z) particularly with the newly commissioned dark matter survey in Chile.

In this context, there is justification to add the Hubble constant ' H ' to the physics dimensional analysis conversation.

$$\hbar, G, c, H$$

The dimensional analysis concept provides a mechanism for arrangement of these constants in order to proved investigative leads for continued experimental work.

Let H be a fundamental constant representative of an ubiquitous expanding universe (including a cosmological constant) on equal par with G, c and \hbar . In terms mass(m), length(l), and time(t), these constants are represented by their dimensional and observed numerical values:

$$\begin{aligned}
\hbar \text{ } m^1 l^2 t^{-1} &= 1.05E-27 \text{ } g^1 \text{ } cm^2 \text{ } sec^{-1} \\
G \text{ } m^{-1} l^3 t^{-2} &= 6.67E-8 \text{ } g^{-1} \text{ } cm^3 \text{ } sec^{-2} \\
c \text{ } m^0 l^1 t^{-1} &= 3.00E10 \text{ } g^0 \text{ } cm^1 \text{ } sec^{-1} \\
H \text{ } m^0 l^0 t^{-1} &= 2.31E-18 \text{ } g^0 \text{ } cm^0 \text{ } sec^{-1}
\end{aligned}$$

Below, a (m, l, t) dimensional analysis of these relationships of these constants is executed, one of these relationships being the Planck units.

Within this context, Planck units do not warrant special consideration above others.

Planck units are an expression of the limited information of Max Planck's era (circa 1900). Based on this (m, l, t) dimensional analysis (below dotted line), the following H/G (m, l, t) dimensional relationships appear to be best, because they conform to physical nuclear measurements and could be considered as a base to investigate thermodynamics and dissipative processes.

$$\begin{aligned}
H/G &= m^1 l^{-3} t^1 \quad 3.46E-11 \text{ } g \text{ } cm^{-3} \text{ } sec \\
H/G \text{ } m &= \hbar^{2/3} \left(\frac{H}{G} \right)^{1/3} c^{-1/3} \quad 1.09E-25 \text{ } G \\
H/G \text{ } l &= \hbar^{1/3} \left(\frac{H}{G} \right)^{-1/3} c^{-2/3} \quad 3.23E-13 \text{ } cm \\
H/G \text{ } t &= \hbar^{1/3} \left(\frac{H}{G} \right)^{-1/3} c^{-5/3} \quad 1.08E-23 \text{ } sec
\end{aligned}$$

Further, there is a subsequent relationship to charge (e) and the fine structure constant (α)

$$(H/G m)^{1/2} (H/G l)^{3/2} (H/G t)^{-1} e^{-1} = \alpha^{-1/2}$$

and

$$(H/G l) (H/G t)^{-1} = \text{speed of light}(c)$$

This same condition exists for Planck units.

$$(Planck m)^{1/2} (Planck l)^{3/2} (Planck t)^{-1} e^{-1} = \alpha^{-1/2}$$

and

$$(Planck l) (Planck t)^{-1} = \text{speed of light}(c)$$

The nuclear $(H/G m, H/G l, H/G t)$ dimensional result (1.09E-25 g, 3.23E-13 cm, 1.08E-23 sec) (generally consistent with trisine condition 1.2) based in part on a cosmological H appears to be incongruous, but the $(H/G m, H/G l, H/G t)$ dimensional analysis assumes a H/G constant ratio which may reflect much higher respective values of H and G at the Big Bang when nuclear particles were synthesized. G/G studies are projected to resolve this question.

The Planck unit $(Planck m, Planck l, Planck t)$ dimensional result (2.18E-5 g, 1.61E-33 cm, 5.39E-44 sec) does not share a similar physical dimensional perspective except perhaps at the very beginning of the universe (trisine condition 1.1).

Linear extrapolation of currently available G/G values indicate that G has changed less than 1 percent in universe 13.7 billion year age. But the G relationship with Universe Age may not be linear but $\sim 1/Uage$. Gravity(G) studies of early universe are required.

These universal values with appropriate 2π phase factor allow basis for trisine lattice scaling as follows:

$$2\pi m_i c H / G l = m_i v_{dx} 2B = m_i (2B)^2 / \text{time} = h$$

Dimensional analysis indicates the total set combinations worthy of investigation:

$$\begin{aligned} \hbar^{a_{11}} G^{a_{21}} l^{a_{31}} t^{a_{41}} &= m^1 l^0 t^0 & m \\ \hbar^{a_{12}} G^{a_{22}} l^{a_{32}} t^{a_{42}} &= m^0 l^1 t^0 & l \\ \hbar^{a_{13}} G^{a_{23}} l^{a_{33}} t^{a_{43}} &= m^0 l^0 t^1 & t \end{aligned}$$

with dimensionless constants

$$\begin{array}{cccc} a_{11} & a_{21} & a_{31} & a_{41} \\ a_{12} & a_{22} & a_{32} & a_{42} \\ a_{13} & a_{23} & a_{33} & a_{43} \end{array}$$

required to maintain expression mass(m), length(l), and time(t) dimensionality.

Selected four(4) groups three(3) need be selected for an exact solution in accordance with combination theory

$$4C_3 = 4.$$

$$\begin{array}{cccc} 0 & a_{21} & a_{31} & a_{41} \\ 0 & a_{22} & a_{32} & a_{42} \\ 0 & a_{23} & a_{33} & a_{43} \end{array} \quad \text{Group One(1)}$$

$$\begin{array}{cccc} a_{11} & 0 & a_{31} & a_{41} \\ a_{12} & 0 & a_{32} & a_{42} \\ a_{13} & 0 & a_{33} & a_{43} \end{array} \quad \text{Group Two(2)}$$

$$\begin{array}{cccc} a_{11} & a_{21} & 0 & a_{41} \\ a_{12} & a_{22} & 0 & a_{42} \\ a_{13} & a_{23} & 0 & a_{43} \end{array} \quad \text{Group Three(3)}$$

$$\begin{array}{cccc} a_{11} & a_{21} & a_{31} & 0 \\ a_{12} & a_{22} & a_{32} & 0 \\ a_{13} & a_{23} & a_{33} & 0 \end{array} \quad \text{Group Four(4)}$$

group one(1) corresponds to

$$\hbar^0 G^{a_{21}} c^{a_{31}} H^{a_{41}} = m^1 l^0 t^0 = M$$

$$\hbar^0 G^{a_{22}} c^{a_{32}} H^{a_{42}} = m^0 l^1 t^0 = L$$

$$\hbar^0 G^{a_{23}} c^{a_{33}} H^{a_{43}} = m^0 l^0 t^1 = T$$

where:

$$m = \hbar^0 G^{-1} c^3 H^{-1} = 1.75E+56 \text{ g}$$

$$l = \hbar^0 G^0 c^1 H^{-1} = 1.30E+28 \text{ cm}$$

$$t = \hbar^0 G^0 c^0 H^{-1} = 4.32E+17 \text{ sec}$$

$$\text{trial } l/t = 3.00E+10 \text{ cm sec}^{-1}$$

$$\text{trial } e = m^{1/2} l^{3/2} t^{-1} = 4.51E+52 \text{ g}^{1/2} \text{ cm}^{3/2} \text{ sec}^{-1}$$

group two(2) corresponds to

$$\hbar^{a_{11}} G^0 c^{a_{31}} H^{a_{41}} = m^1 l^0 t^0 = m$$

$$\hbar^{a_{12}} G^0 c^{a_{32}} H^{a_{42}} = m^0 l^1 t^0 = l$$

$$\hbar^{a_{13}} G^0 c^{a_{33}} H^{a_{43}} = m^0 l^0 t^1 = t$$

where:

$$\begin{aligned}
 m &= \hbar^1 G^0 c^{-2} H^1 &= 2.71E-66 & g \\
 l &= \hbar^{-5/2} G^0 c^{1/2} H^{1/2} &= 7.29E+63 & cm \\
 t &= \hbar^0 G^0 c^0 H^{-1} &= 4.32E+17 & sec \\
 \text{trial } l/t &= & 1.69E+46 & cm sec^{-1} \\
 \text{trial } e &= m^{1/2} l^{3/2} t^{-1} &= 2.37E+45 & g^{1/2} cm^{3/2} sec^{-1}
 \end{aligned}$$

group three(3) corresponds to

$$\begin{aligned}
 \hbar^{a_{11}} G^{a_{21}} c^0 H^{a_{41}} &= m^1 l^0 t^0 = m \\
 \hbar^{a_{12}} G^{a_{22}} c^0 H^{a_{42}} &= m^0 l^1 t^0 = l \\
 \hbar^{a_{13}} G^{a_{23}} c^0 H^{a_{43}} &= m^0 l^0 t^1 = t
 \end{aligned}$$

where:

$$\begin{aligned}
 m &= \hbar^{3/5} G^{-2/5} c^0 H^{1/5} &= 1.44E-17 & g \\
 l &= \hbar^{1/5} G^{1/5} c^0 H^{-3/5} &= 5.64E+03 & cm \\
 t &= \hbar^0 G^0 c^0 H^{-1} &= 4.32E+17 & sec \\
 \text{trial } l/t &= & 1.30E-14 & cm sec^{-1} \\
 \text{trial } e &= m^{1/2} l^{3/2} t^{-1} &= 3.71E-21 & g^{1/2} cm^{3/2} sec^{-1}
 \end{aligned}$$

group four(4) corresponds to Planck units

$$\begin{aligned}
 \hbar^{a_{11}} G^{a_{21}} c^{a_{31}} H^0 &= m^1 l^0 t^0 = m \\
 \hbar^{a_{12}} G^{a_{22}} c^{a_{32}} H^0 &= m^0 l^1 t^0 = l \\
 \hbar^{a_{13}} G^{a_{23}} c^{a_{33}} H^0 &= m^0 l^0 t^1 = t
 \end{aligned}$$

where:

$$\begin{aligned}
 m &= \hbar^{1/2} G^{-1/2} c^{1/2} H^0 &= 2.18E-5 & g \\
 l &= \hbar^{1/2} G^{1/2} c^{-3/2} H^0 &= 1.61E-33 & cm \\
 t &= \hbar^{1/2} G^{1/2} c^{-5/2} H^0 &= 5.39E-44 & sec \\
 \text{trial } l/t &= & 3.00E+10 & cm sec^{-1} \\
 \text{trial } e &= m^{1/2} l^{3/2} t^{-1} &= 5.62E-09 & g^{1/2} cm^{3/2} sec^{-1}
 \end{aligned}$$

The other exact solution alternative is to combine two constants so that all four \hbar , G , c , H can be arranged in groups of three including \hbar/H , c/H , \hbar/G , c/G , c/\hbar and H/G .

$$\begin{aligned}
 \hbar/H &= m^1 l^2 t^0 &= 4.56E-10 & g cm^2 \\
 \hbar/H m &= G^{-2/3} (\hbar/H)^{1/3} c^{4/3} &= 4.36E+15 & g \\
 \hbar/H l &= G^{1/3} (\hbar/H)^{1/3} c^{-2/3} &= 3.24E-13 & cm \\
 \hbar/H t &= G^{1/3} (\hbar/H)^{1/3} c^{-5/3} &= 1.08E-23 & sec \\
 \hbar/H l/t &= & 3.00E+10 & cm sec^{-1}
 \end{aligned}$$

$$\begin{aligned}
 \hbar/H e &= m^{1/2} l^{3/2} t^{-1} &= 1.13E+12 & g^{1/2} cm^{3/2} sec^{-1} \\
 c/H &= m^0 l^1 t^0 &= 1.30E+28 & cm \\
 c/H m &= G^{-1/3} \hbar^{2/3} (c/H)^{-1/3} &= 1.09E-25 & G \\
 c/H l &= G^0 \hbar^0 (c/H)^1 &= 1.30E+28 & cm \\
 c/H t &= G^{-1/3} \hbar^{-1/3} (c/H)^{5/3} &= 1.73E+58 & sec \\
 c/H l/t &= & 7.48E-31 & c/G \\
 c/H e &= m^{1/2} l^{3/2} t^{-1} &= 2.81E-29 & g^{1/2} cm^{3/2} sec^{-1} \\
 \hbar/G &= m^2 l^1 t^1 &= 1.58E-20 & g cm sec \\
 \hbar/G m &= H^0 (\hbar/G)^{1/2} c^{1/2} &= 2.18E-05 & g \\
 \hbar/G l &= H^{-1} (\hbar/G)^0 c^1 &= 1.30E+28 & cm \\
 \hbar/G t &= H^{-1} (\hbar/G)^0 c^0 &= 4.32E+17 & sec \\
 \hbar/G l/t &= & 3.00E+10 & cm sec^{-1} \\
 \hbar/G e &= m^{1/2} l^{3/2} t^{-1} &= 1.59E+22 & g^{1/2} cm^{3/2} sec^{-1} \\
 c/G &= m^1 l^{-2} t^1 &= 4.49E+1 & g cm^{-2} sec \\
 c/G m &= H^0 \hbar^{1/2} (c/G)^{1/2} &= 2.18E-05 & G \\
 c/G l &= H^{-1/2} \hbar^{1/4} (c/G)^{-1/4} &= 4.58E-03 & cm \\
 c/G t &= H^{-1} \hbar^0 (c/G)^0 &= 4.32E+1 & sec \\
 c/G l/t &= & 1.06E-20 & cm sec^{-1} \\
 c/G e &= m^{1/2} l^{3/2} t^{-1} &= 3.34E-24 & g^{1/2} cm^{3/2} sec^{-1} \\
 c/\hbar &= m^{-1} l^{-1} t^0 &= 2.84E+3 & g^{-1} cm^{-1} \\
 c/\hbar m &= H^{1/2} G^{-1/4} (c/\hbar)^{-3/4} &= 7.68E-36 & g \\
 c/\hbar l &= H^{-1/2} G^{1/4} (c/\hbar)^{-1/4} &= 4.58E-03 & cm \\
 c/\hbar t &= H^{-1} G^0 (c/\hbar)^0 &= 4.32E+1 & sec \\
 c/\hbar l/t &= & 1.06E-20 & cm sec^{-1} \\
 c/\hbar e &= m^{1/2} l^{3/2} t^{-1} &= 1.99E-39 & g^{1/2} cm^{3/2} sec^{-1} \\
 H/G &= m^1 l^{-3} t^1 &= 3.46E-11 & g cm^{-3} sec \\
 H/G m &= \hbar^{2/3} (H/G)^{1/3} c^{-1/3} &= 1.09E-25 & g \\
 H/G l &= \hbar^{1/3} (H/G)^{-1/3} c^{-2/3} &= 3.23E-13 & cm \\
 H/G t &= \hbar^{1/3} (H/G)^{-1/3} c^{-5/3} &= 1.08E-23 & sec \\
 H/G l/t &= & 3.00E+10 & cm sec^{-1} \\
 H/G e &= m^{1/2} l^{3/2} t^{-1} &= 5.62E-09 & g^{1/2} cm^{3/2} sec^{-1}
 \end{aligned}$$

Mead's[141] Heisenberg uncertainty logic can be applied to H/G mass(m), length(l) and time(t) which are more intuitively physical than the Planck units.
(what Planck length is physically significant at 1.61E-33 cm?)

(what Planck mass is physically significant at 2.18E-5 g?)
 (what Planck time is physically significant at 5.39-44 sec?)
 The H/G length(m) 1.09E-25 g conforms to a particle size between the electron and proton.

The H/G length(l) 3.23E-13 cm conforms to nuclear size and Compton wavelength $\hbar/(mc) = 3.51E-13$ cm.

The H/G time(t) 1.08E-23 sec conforms to typical nuclear particle decay time.

(The Standard Model predicts a top quark mean lifetime to be roughly 5E-25 sec about 20 times shorter than the timescale for strong interactions -WIKI)

Max Planck's 1899 statement is retained with the H/G units

"These necessarily retain their meaning for all times and for all civilizations, even extraterrestrial and non-human ones, and can therefore be designated as 'natural units.'"

These H/G mass(m), length(l) and time(t) may be an alternative way based on standard model physics to quantify the Hubble parameter (H) and support Mead's premise of the connection between gravity and fundamental length.

Appendix J. CMBR and Universe Luminosity Equivalence

CMBR Black Body radiation equals Milky Way luminous Black Body radiation (with reasonable dimensional assumptions)

FOR PRESENT UNIVERSE CONDITIONS

CMBR Black Body radiation equals universe luminous Black Body radiation AT ANY UNIVERSE AGE as solar type luminescent objects being 3.7 Percent of universe density ρ_U (equation 2.11.16) as presently nearly indicated (4.6 percent) by Wilkinson Microwave Anisotropy Probe (WMAP)

IF UNIVERSE DENSITY IS ADIABATICALLY EXPANDED AT THE 4/3 POWER.

(This is consistent with CMBR temperature T_b adiabatic expansion as indicated in equations 2.7.3a-c)

With the universe dimensionally described over 100's of orders of magnitude, this one percent dimensional relationship ($F = 3.7$ percent vs 4.6 percent WMAP)

OVER THE UNIVERSE AGE $1/H_U$ should be placed in the appendix of astrophysical discussion.

Calculations are as follows:

(integrated Black Body relationships are used-no /Hz)
 (full spherical relationships are used-no steradians)

0.1367	watt/(cm ² AU ² solar mass)
1,367,000	erg/(cm ² sec AU ² solar mass unit) sunBlackBody
1.50E+13	cm/AU
3.06E+32	energy total from the sun erg SunE
4.00E+11	stars in Milky Way MWstars visually observed and estimated
1.99E+33	solar mass (g) Ms
1.22E+44	energy total from the Milky Way (erg) MWstars x SunE
3.67E+22	average distance(MWR) of Milky Way stars(cm) 38,600 light years (a reasonable parameter which makes the model work)
3.85E-24	Milky Way density (g/cm ³) assumed sphere
2.04E+18	average Milky Way luminosity over spherical area defined by earth distance from sun MWstars SunE (cm/AU) ² /MWR ²
9.10E-02	Milky Way luminosity at earth (erg/sec/cm ²)
6.67E-08	Newton (G cm ³ sec ⁻² g ⁻¹)
2.31E-18	Hubble parameter (sec ⁻¹) 71.2 km/(sec million parsec)
2.25E+28	universe visible radius cm $R_U = \sqrt{3}c/H_U$ equation 2.11.6
6.38E-30	university mass density g/cm ³ $\rho_U = (2/(8\pi)) \left(H_U^2/G_U \right)$ equation 2.11.16
3.02E+56	university mass (g) $M_U = \rho_U (4\pi/3) R_U^3$ equation 2.11.15
1.52E+23	number of universe solar mass units $M_U / \text{solar mass} = M_n$
0.037	luminous fraction of the universe F
3.40E-03	universe luminosity at earth erg/cm ² /sec $F M_n \text{sunBlackBody} (cm/AU)^2/R_U^2 = UL$
4.54E-13	universe luminosity density at earth erg/cm ³ $UL/4$

3.41E-03 CMBR at $T_b = 2.7 K$ Black Body universe emission $erg/(cm^2 sec)$

$$\left(\pi^2/\left(15\hbar^3c^3\right)\right)(k_bT_b)^4$$

4.55E-13 CMBR at $T_b = 2.7 K$ energy density at earth erg/cm^3

$$(1/4)\left(\pi^2/\left(15\hbar^3c^2\right)\right)(k_bT_b)^4$$

1.00 ratio CMBR/universe luminescent BlackBody Radiation

and also:

1.00 ratio CMBR to Milky Way luminescent BlackBody Radiation

Appendix K. Hydrogen Bose Einstein Condensate as Dark Matter

A hypothesis is that the spectroscopically undetectable dark matter is actually Big Bang nucleosynthetic adiabatically produced (extremely cold nanokelvin to femtokelvin) colligative Bose Einstein Condensate(BEC) hydrogen helium at density on the order of $1 g/cm^3$ or $1 \text{ mole}/cm^3$ or $\text{Avogadro}/cm^3$. This is substantiated by the following established Bose Einstein Condensate relationship

$$k_bT_c = \left(\frac{\rho_{\text{dark matter particle density}}}{\xi \left(\frac{3}{2}\right)^{\frac{2}{3}}} \right) \frac{h^2}{2\pi m_p (am_p)^{\frac{2}{3}}}$$

that is derived from published form

$$k_bT_c = \left(\frac{n_{\text{dark matter particle density}}}{\xi \left(\frac{3}{2}\right)^{\frac{2}{3}}} \right) \frac{h^2}{2\pi m_p}$$

by a multiplier factor

$$\frac{(am_p)^{\frac{2}{3}}}{(am_p)^{\frac{2}{3}}}$$

For the universe present condition

$$T_c = 8.11\text{E-16} \text{ and } \rho_{\text{dark matter particle density}} = 1 \text{ g/cm}^3$$

then $a = 5.22\text{E}25$ superimposed states with origins in Big Bang nucleosynthesis (not presently observed under laboratory conditions)

and the hydrogen BEC volume is:

$$\frac{am_p}{\rho_{\text{dark matter particle density}}} = 87.3 \text{ cm}^3$$

or about 4.4 cm on a side.

This relationship reverts to equation 2.10.6 when $a = 1$ and mass = m_r .

The exact nature of hydrogen at these cold temperatures may also have metallic hydrogen, frozen hydrogen and/or superconducting properties.

Fact:

The observed amount of hydrogen in the universe is observed spectroscopically as neutral hydrogen through the 21 cm line assuming a Beers law.

Beers law assumption:

"Assume that particles may be described as having an area, alpha, perpendicular to the path of light through a solution (or space media), such that a photon of light is absorbed if it strikes the particle, and is transmitted if it does not."

"Expressing the number of photons absorbed by the (concentration c in) slab (in direction z) as dIz, and the total number of photons incident on the slab as Iz, the fraction of photons absorbed by the slab is given by:"

$$dIz/Iz = -\alpha c dz$$

In other words, the fraction of photons absorbed when passing through an observed slab is equal to the total opaque area of the particles in the slab.

In other words, larger particles with the same aggregate volume concentration in a supporting medium will not attenuate as many incident photons.

Issue one:

If the Big Bang nucleosynthetic hydrogen were in the form of adiabatically produced very cold chunks, their aggregate total opaque area would be much smaller than a diffuse hydrogen gas resulting in many orders of magnitude lower Beers law photon attenuation rates. Mean free paths are of multi galactic length dimensions. (These

BEC's would not be spectroscopically detected with present tools)

Issue two:

Given these primeval (through adiabatic Big Bang expansion) hydrogen dense (1 g/cc) BEC's large chunks, say 10's of kilometers in diameter, The parallel to antiparallel hydrogen (proton electron spin) configuration resulting in 21 cm line would occur randomly in the BEC chunk hydrogens at the known 2.9E-15 /sec rate. Transmittance accordance with Beer's law would indicate that the 22 cm radiation from the BEC center would be attenuated more than that from the BEC near surface resulting in a lower than reality hydrogen spatial density reading obtained by a distant observer.

Issue three:

The hydrogen dense (1 g/cc) BEC chunks should be stable relative to higher temperature of a intergalactic media (ionized gas). There is the question whether Intergalactic Medium (IGM) composed of 'hot' atoms would 'sublimate' any BECs that were adiabatically produced at the initial Big Bang. In order to address this question, assume the IGM is totally ionized at the given universe critical density of ~1 proton mass per meter³. (It is very clear that this ionized IGM was not there in the beginning but ejected into space from stars etc.) Now take a 1 meter³ hydrogen BEC. It would have 100³ x (Avogadro number) hydrogen atoms in it. If there were no relative motion between the BEC and the hot atoms, the BEC would not degrade. If there was relative motion between the BEC and the hot atoms, the BEC could travel 100³ x (Avogadro number) meters or 6.023E29 meters through space before 'melting'. The length 6.023E29 meters is larger than the size of the visual universe (2.25E26 meter). There could have been multi kilometer sized hydrogen BEC's at the adiabatic expansion still remaining at the present time and at nearly that size. Also, as a BEC, it would not have a vapor pressure. It would not sublime. The hydrogen BECs perhaps are still with us.

Issue four:

Over time, the BEC would absorb the CMBR microwave background and heat up, but how much?

Black Body Background radiation at 2.732 K emits at power density of 0.00316 erg/cm²/sec (stefan's constant x 2.7324) with wavelength at black body max at 0.106 cm (1.60531E+11 Hz)

The 1S-2S characteristic BEC hydrogen transition is at 243 nm (1.23E+15 Hz) This 1S-2S transition would have to be initiated before subsequent Rydberg transitions.

This 243 nm (1.23E+15 Hz) absorption is way out on the CMBR tale and absorbing in a band width of ~1E6 Hz with a natural line width of 1.3 Hz. [90]

Calculations indicate the einsteins absorbed at this characteristic hydrogen BEC frequency at 243 nm (band width of ~1E6 Hz with a natural line width of 1.3 Hz) from CMBR would not substantially affect hydrogen BEC chunks over universe life 13.7 billion years.

Issue five:

Even though, spectroscopically undetectable these BECs would be at the same abundance (relative concentration) as predicted by nucleosynthetic models and would be considered baryonic matter. How flexible are nucleosynthetic models as to baryonic mass generation (keeping the abundance (relative concentration to say observed helium) the same? The presently spectroscopically undetectable BECs would in principle not be spectroscopically detectable all the way back to 13.7 billion year beginning and not observable in the WMAP data.

Issue six:

These hydrogen dense (1 g/cc) BECs could be the source media for star formation (~5 percent of universe density) by gravitational collapse and as such, their residual (~25 percent of universe density) presence would be gravitationally detected by observed galactic rotation features and gravitational lensing characteristics

Issue seven:

A reference to Saha equation indicates an equilibrium among reactants in a single phase prior to recombination hydrogen + photon \leftrightarrow proton + electron

There may have been a non equilibrium condition between this phase and with another nucleosynthetic adiabatically produced solid cold BEC hydrogen phase prior to and continuing on through the recombination event and not spectroscopically observed by WMAP. (such multiphase non equilibrium reactions are important, particularly in CO_2 distribution in air phase and associated H_2CO_3 , HCO_3^- and CO_3^{2-} in water phase)

CMBR Temperature:	3,000	K
Radiated power area density:	4.593E+09	erg/cm ² /sec
Radiated power:	4.593E+09	erg/sec
radiation mass density	6.819E-22	g/cm ³
pressure=1/3 energy/volume	2.043E-01	dyne/cm ²
photon number density	5.477E+11	photon/cm ³
photon energy density	6.401E-01	erg/cm ³

Most probable energy	1.764E+14	/sec
hydrogen BEC		
absorbed energy	1.301E-12	erg/cm ³
absorbed freq	1.234E+15	/sec
absorbed wavelength	2.430E-05	cm
Ref: [90]		

Calculations indicate the einsteins absorbed by BEC at the characteristic hydrogen BEC frequency 1.234E+15 /sec (way out on the CMBR 3,000 K tail) (extremely narrow absorption band width of ~1E6 Hz with a natural line width of 1.3 Hz) would not substantially degrade extremely cold hydrogen dense (1 g/cc) BEC chunks at universe Big Bang age of 376,000 years. Indeed the BEC_{ST} at 376,000 years is 1.05E8 years. This is an estimate realizing that CMBR temperature changes with time. BEC_{ST} keeps ahead of the universe age Age_{UG} back to introductory condition 1.9 and again from introductory conditions 1.4 to 1.1.

If it assumed the BEC absorption band with approaches the nature line width of 1.3 Hz from 1E6 Hz, it is evident that the BEC_{ST} would survive through all of the universe nucleosynthetic events. It is noteworthy that under the present CMBR temperature T_b , the hydrogen BECs would survive essentially forever ($>1E300$ years – the upper limit of the current computational ability).

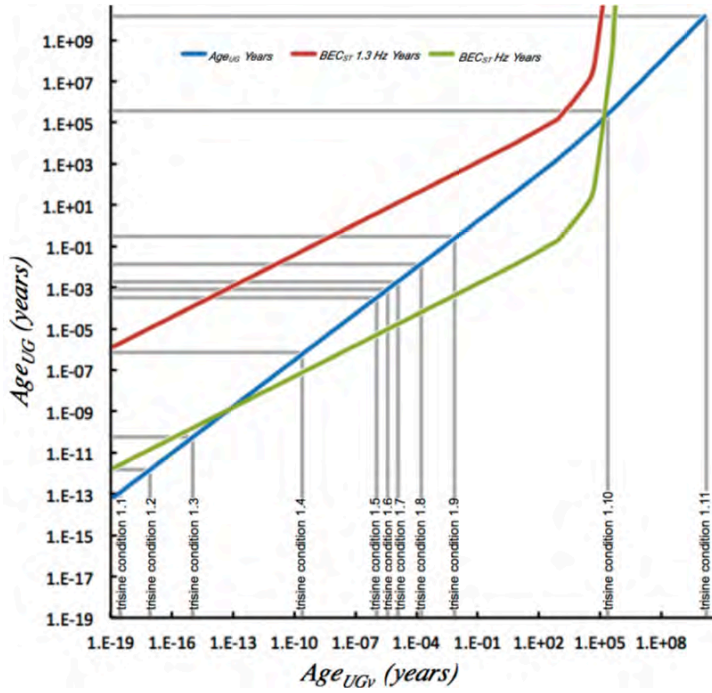
Conditions Defined In The Intro- duction	T_b kelvin	T_c kelvin	BEC	BEC_{ST} (seconds)	BEC_{ST} (seconds)	Age_{UG} (seconds)	Age_{UGv} (seconds)
				at 1E6 Hz bandwidth	at 1.3 Hz bandwidth		
1.11	2.73E+00	8.11E-16	>1.00E+300	>1.00E+300	4.32E+17	4.32E+17	
	1.00E+01	1.09E-14	>1.00E+300	>1.00E+300	6.16E+16	6.16E+16	
	2.50E+01	6.81E-14	>1.00E+300	>1.00E+300	1.56E+16	1.56E+16	
	5.00E+01	2.72E-13	>1.00E+300	>1.00E+300	5.52E+15	5.51E+15	
	1.00E+02	1.09E-12	6.12E+263	4.70E+269	1.95E+15	1.95E+15	
	2.50E+02	6.81E-12	3.47E+109	3.34E+115	4.93E+14	4.91E+14	
	5.00E+02	2.72E-11	1.50E+58	1.66E+64	1.74E+14	1.73E+14	
	1.00E+03	1.09E-10	3.69E+32	3.44E+38	6.16E+13	6.08E+13	
	2.00E+03	4.36E-10	5.64E+19	4.83E+25	2.20E+13	2.12E+13	
	2.50E+03	6.81E-10	1.63E+17	1.29E+23	1.56E+13	1.51E+13	
1.10	3.00E+03	9.80E-10	3.31E+15	2.55E+21	1.19E+13	1.14E+13	
	1.00E+04	1.09E-08	3.28E+09	2.54E+15	1.94E+12	1.73E+12	
	1.50E+04	2.45E-08	4.54E+08	3.50E+14	1.06E+12	8.96E+11	
	1.00E+05	1.09E-06	7.28E+06	5.61E+12	6.16E+10	3.21E+10	
	1.50E+05	2.45E-06	4.38E+06	3.34E+12	1.07E+03	4.75E+02	
	1.00E+06	1.09E-04	5.52E+05	4.23E+11	6.18E+01	1.17E+01	
	1.50E+06	2.45E-04	3.63E+05	2.79E+11	3.36E+01	5.24E+00	
1.9	1.9	1.18E+07	1.52E-02	4.54E+04	3.50E+10	1.52E+00	8.55E-02
	1.8	2.94E+08	9.41E+00	1.82E+03	7.51E+08	1.52E+05	1.25E+03
	1.7	5.48E+08	3.27E+01	9.76E+02	4.45E+08	6.94E+04	4.41E+02
	1.6	9.24E+08	9.30E+01	5.77E+02	4.45E+08	6.94E+04	4.41E+02
	1.5	1.45E+09	2.29E+02	3.68E+02	2.84E+08	3.53E+04	1.79E+02
	1.4	1.69E+11	3.11E+06	3.16E+00	2.44E+06	2.81E+01	1.32E-02
	1.3	5.49E+13	3.28E+11	9.72E-03	7.51E+03	4.79E-03	1.25E-07
	1.2	9.07E+14	8.96E+13	5.92E-04	4.54E+02	7.14E-05	4.57E-10
	1.1	9.19E+15	9.20E+15	5.81E-05	4.48E+01	2.21E-06	4.45E-12

1.8	2.94E+08	9.41E+00	1.82E+03	1.40E+09	3.87E+05	4.35E+03
1.7	5.48E+08	3.27E+01	9.76E+02	7.51E+08	1.52E+05	1.25E+03
1.6	9.24E+08	9.30E+01	5.77E+02	4.45E+08	6.94E+04	4.41E+02
1.5	1.45E+09	2.29E+02	3.68E+02	2.84E+08	3.53E+04	1.79E+02
1.4	1.69E+11	3.11E+06	3.16E+00	2.44E+06	2.81E+01	1.32E-02
1.3	5.49E+13	3.28E+11	9.72E-03	7.51E+03	4.79E-03	1.25E-07
1.2	9.07E+14	8.96E+13	5.92E-04	4.54E+02	7.14E-05	4.57E-10
1.1	9.19E+15	9.20E+15	5.81E-05	4.48E+01	2.21E-06	4.45E-12

For general consistency with the rest of the report, the data is also presented in seconds.

Conditions Defined In The Intro- duction	T_b kelvin	T_c kelvin	BEC	BEC_{ST} (seconds)	BEC_{ST} (seconds)	Age_{UG} (years)	Age_{UGv} (years)
				at 1E6 Hz bandwidth	at 1.3 Hz bandwidth		
1.11	2.73E+00	8.11E-16	>1.00E+300	>1.00E+300	4.32E+17	4.32E+17	
	1.00E+01	1.09E-14	>1.00E+300	>1.00E+300	6.16E+16	6.16E+16	
	2.50E+01	6.81E-14	>1.00E+300	>1.00E+300	1.56E+16	1.56E+16	
	5.00E+01	2.72E-13	>1.00E+300	>1.00E+300	5.52E+15	5.51E+15	
	1.00E+02	1.09E-12	6.12E+263	4.70E+269	1.95E+15	1.95E+15	
	2.50E+02	6.81E-12	3.47E+109	3.34E+115	4.93E+14	4.91E+14	
	5.00E+02	2.72E-11	1.50E+58	1.66E+64	1.74E+14	1.73E+14	
	1.00E+03	1.09E-10	3.69E+32	3.44E+38	6.16E+13	6.08E+13	
	2.00E+03	4.36E-10	5.64E+19	4.83E+25	2.20E+13	2.12E+13	
	2.50E+03	6.81E-10	1.63E+17	1.29E+23	1.56E+13	1.51E+13	
1.10	3.00E+03	9.80E-10	3.31E+15	2.55E+21	1.19E+13	1.14E+13	
	1.00E+04	1.09E-08	3.28E+09	2.54E+15	1.94E+12	1.73E+12	
	1.50E+04	2.45E-08	4.54E+08	3.50E+14	1.06E+12	8.96E+11	
	1.00E+05	1.09E-06	7.28E+06	5.61E+12	6.16E+10	3.21E+10	
	1.50E+05	2.45E-06	4.38E+06	3.34E+12	1.07E+03	4.75E+02	
	1.00E+06	1.09E-04	5.52E+05	4.23E+11	6.18E+01	1.17E+01	
	1.50E+06	2.45E-04	3.63E+05	2.79E+11	3.36E+01	5.24E+00	
1.9	1.9	1.18E+07	1.52E-02	4.54E+04	3.50E+10	1.52E+00	8.55E-02
	1.8	2.94E+08	9.41E+00	1.82E+03	1.40E+09	1.23E-02	1.38E-04
	1.7	5.48E+08	3.27E+01	9.76E+02	7.51E+08	4.82E-03	3.97E-05
	1.6	9.24E+08	9.30E+01	5.77E+02	4.45E+08	2.20E-03	1.40E-05
	1.5	1.45E+09	2.29E+02	3.68E+02	2.84E+08	1.12E-03	5.67E-06
	1.4	1.69E+11	3.11E+06	3.16E+00	2.44E+06	8.91E-07	4.18E-10
	1.3	5.49E+13	3.28E+11	9.72E-03	7.51E+03	1.52E-10	3.96E-15
	1.2	9.07E+14	8.96E+13	5.92E-04	4.54E+02	2.26E-12	1.45E-17
	1.1	9.19E+15	9.20E+15	5.81E-05	4.48E+01	7.01E-14	1.41E-19

These numbers are then expressed graphically following Figure K1.



The 3,000 K CMBR at 376,000 years is hot but has a very low heat capacity. It would be like touching a red to white hot space shuttle tile with your finger and not getting burned.

How would these cold hydrogen BECs coming through the recombination event be observed in Baryonic Acoustic Oscillations (BAO) (which does have a measurable BEC? dark matter component) in the context that BECs would have different masses (m) than currently modeled gaseous hydrogen?

$$BAO \text{ frequency}_{BEC} \sim \sqrt{1/m_{BEC}}$$

and

$$BAO \text{ frequency}_{\text{gaseous hydrogen}} \sim \sqrt{1/m_{\text{gaseous hydrogen}}}$$

but

$$\sqrt{1/m_{\text{gaseous hydrogen}}} \neq \sqrt{1/m_{BEC}}$$

Can 'first three minute' nucleosynthesis dynamics 'precipitate out' these cold hydrogen BECs?

The permittivity permeability model as presented in this paper allows a mechanism to do such.

Issue eight

A gravitationally unstable system loses energy (for star formation)

Assuming that the universe is a closed system that

conserves energy, then where does this gravitational energy go?

Issue nine

Superconducting particles in the universe vacuum should not clump due to magnetic field expulsion characteristic. This nonclumping is observed in dark matter observations.

Hypothesis:

The energy goes to an endothermic phase change (like solid to gas) and more specifically the change from Big Bang nucleosynthetic hydrogen Bose Einstein Condensate(H-BEC)

to hydrogen gas that with this energy transfer gaseous hydrogen is thermodynamically able to gravitationally collapse to stars.

This assumes ~30 percent of the universe is H-BEC 'dark matter' that provides a large heat sink for a small portion that endothermically absorbs energy through 'sublimation' made available for gravitationally collapsing star forming H-gas.

Hubble and Spitzer have observed early ($z = 5.7$) galaxies with a distinct red color into the infrared [109]. Could this galaxy red color be due to red shifted characteristic 1S-2S Hydrogen Bose Einstein Condensate(HBEC) at 243 nanometer red shifted

$$(1+5.7) \times 243 \text{ nanometer} = 1.63 \text{ micro meter?}$$

(in the graphically expressed beginning red detection 'within error' of [109] Figure 3 ERS-1, 2, 3, 4). Galactic formation may have this z adjusted red detection at all epochs.

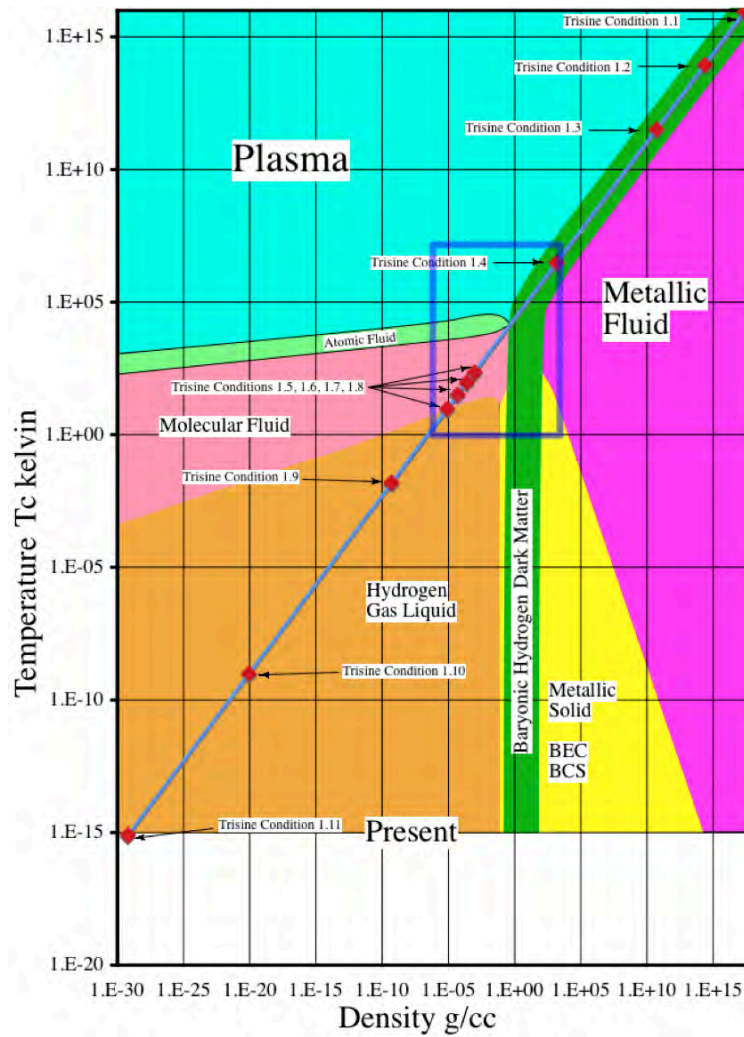
Big Bang nucleosynthetic HBEC (presently expressed as dark matter) was a robust active galactic formation source and may have contributed to the observed 13 billion year old galactic red as a portion (~4%) of HBEC was destroyed and then proceeded up the Rydberg scale before gravitational collapse in the galactic formation process all observed as a distant reddish glow.

This reddish glow should be characteristic of all early galaxies in the process formation from Big Bang nucleosynthetic HBEC.

Is this the missing link to understanding dark matter as Hydrogen Bose Einstein Condensate(HBEC)?

Figure K2 graphically presents these thoughts in terms of a expanded hydrogen phase diagram. The dark blue insert box represents available laboratory hydrogen phase data is available. Extended phase relationships are extrapolated from this available experimental data.

Figure K2 Dark Matter as Baryonic Hydrogen



A separate colder (T_c) phase than CMBR (T_b) is present from the universe beginning (initially as subatomic particles) and separates after Condition 3 as baryonic metallic (BEC and or BCS) hydrogen and retains this form (dark green) until the present time. The separate colder (T_c) phase provides the trapping (kT_c) mechanism for this baryonic metallic (BEC and or BCS) hydrogen. This baryonic metallic (BEC and or BCS) hydrogen is considered to be dark matter. It is not presently observed spectroscopically but only gravitationally.

The phase density Figures 4.42.3 (Blue line) has a slope correlation to Figure K2. The magnitude difference can be explained in terms of particle coalescence dynamics as presented in Appendix L and in particular equation L2.14.

Question?

Does transition-state theory as written in physical chemistry books and detailed in wiki Ref 1:

https://en.wikipedia.org/wiki/Transition_state_theory
enter into Big Bang Nucleosynthesis BBN

particularly with the introduction of redshift z and the colligative properties of BBN plasma as suggested by Ref 2:

Closing in on the Border Between Primordial Plasma and Ordinary Matter

http://www.bnl.gov/bnlweb/pubaf/pr/PR_display.asp?prID=1446

"the different phases exist under different conditions of temperature and density, which can be mapped out on a "phase diagram," where the regions are separated by a phase boundary akin to those that separate liquid water from ice and from steam. But in the case of nuclear matter, scientists still are not sure where to draw those boundary lines.

RHIC is providing the first clues." ?

The general reaction expression given by the transition-state theory

$$-\frac{d[A]}{dt} = \frac{k_b T}{h} [A][B]$$

$$[A] = [A_0][B_0] e^{\frac{-k_b T t}{h}}$$

Now assume T is reaction temperature that scales as

$$CMBR T_o(z+1)^1$$

and

t is universe time $1/H$ that scales as

$$t_o(z+1)^{-3}$$

then generally redshifted z transition-state theory is:

$$[A] = [A_0][B_0] e^{\frac{-k_b T_o(z+1)^1 t_o(z+1)^{-3}}{h}}$$

and by reduction

$$[A] = [A_0][B_0] e^{\frac{-k_b T_o t_o(z+1)^{-2}}{h}}$$

and specifically at two redshifts z_1 and z_2

$$[A] = [A_0][B_0] e^{\frac{-k_b T_o t_o(z_1+1)^{-2}}{h}}$$

$$[A] = [A_0][B_0] e^{\frac{-k_b T_o t_o(z_2+1)^{-2}}{h}}$$

and the ratio for two reaction temperatures T_1 and T_2 replacing temperature T_o (universe time to scaling is the same and nuclide reactant standard free energies are the same at T_1 and T_2 redshift z scaling)

$$\begin{bmatrix} A_1 \\ A_2 \end{bmatrix} = \begin{bmatrix} A_0 \\ A_0 \end{bmatrix} \begin{bmatrix} B_0 \\ B_0 \end{bmatrix} e^{-k \frac{T_{t_o}(z_1+1)^{-2}}{T_{t_o}(z_2+1)^{-2}}}$$

Taking the BBN z at 1 minute (192,000) and 3 minute (134,000)

(This is somewhat arbitrary but is in the time frame of Weinberg's book The First Three Minutes [100])

and normalizing into $k = 1$

$$\begin{bmatrix} A_1 \\ A_2 \end{bmatrix} = e^{-k \frac{T_1 1.92^{-2}}{T_2 1.34^{-2}}}$$

$$\begin{bmatrix} A_1 \\ A_2 \end{bmatrix} = e^{-k \frac{T_1 1.92^{-2}}{T_2 1.34^{-2}}}$$

$$\text{for } \frac{T_1}{T_2} = 1 \text{ then } \begin{bmatrix} A_1 \\ A_2 \end{bmatrix} = .61$$

$$\text{for } \frac{T_1}{T_2} = .8 \text{ then } \begin{bmatrix} A_1 \\ A_2 \end{bmatrix} = .68$$

and $.68/.61 = 1.11$.

(millions of other redshifted z time t and temperature T conditions could be made to make the same point)

The different reaction temperatures $T_1/T_2 = 1$ are achieved by colligative properties as suggested by Ref 2 analogous to boiling point raising without changing the nuclide reaction chemistry.

In BBN, the reaction products would be the same (standard model quarks, gluons etc) but their mass amounts would be altered.

The Ref 2 BNL RHIC experiments hint at this colligative mechanism, something that may be missed in conventional BBN calculations.

Observed H, He and Li abundances (ratios) would be the same. The universe H He masses would be different.

This is all posed as a question as to the possibility as to universe baryonic mass originating in BBN as greater than the conventionally held value at ~4%.

Appendix L. Model Development For Classical Fluid Shear and Fluid Drop Modification

This fluid work was primarily done in the 1980's as a theoretical framework for industrial separator design. As such it was done in the English (ft lb sec) system that was prevalent at that time although dimensionality dictates any

other system such as cgs or SI may be used with equal applicability with the understanding that:

$$F = M a$$

$$lb_{force} = \frac{lb_{force}}{gravity_{acceleration}} gravity_{acceleration}$$

$$\partial = \rho g$$

$$\frac{lb_{force}}{ft^3} = \frac{lb_{force}}{ft^3 gravity_{acceleration}} gravity_{acceleration}$$

Variable Definition

Fluid Viscosity (μ_1)

Fluid Specific Weight (∂_1)

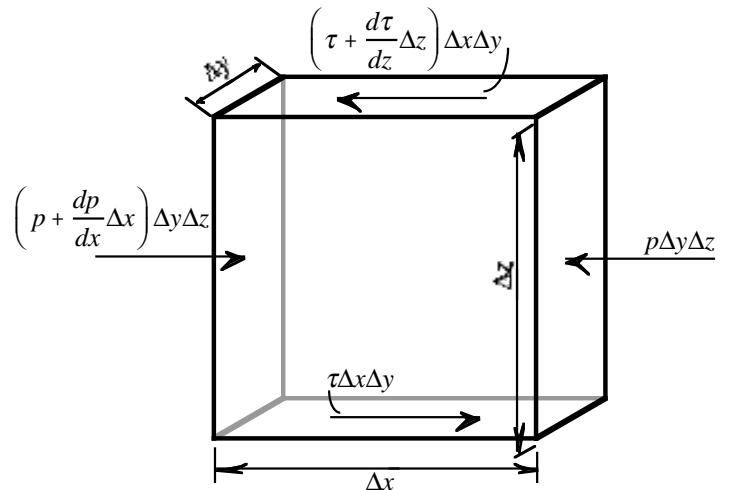
Second Phase Specific Weight (∂_2)

Gravity Acceleration (g)

L1. Introduction

The figure one display of the shear problem and following equations L1.1 and L1.2 are paraphrased from reference 1 and used as an initial starting point for this derivation or model development for the quantitative influence of shear (G) on droplet size (D) in various hydraulic functional units (HFUs) such as pipes, valves, pumps, nozzles etc.

Figure L1. Shear forces along parallel planes of an elemental volume of fluid



As illustrated in Figure L1 the fluid shear (G) is derived below by equating the forces acting on a cube of fluid in

shear in one direction to those in the opposite direction, or

$$\begin{aligned} p \Delta y \Delta z + \left[\tau + \frac{d\tau}{dz} \Delta z \right] \Delta x \Delta y \\ = \tau \Delta x \Delta y + \left[p + \frac{dp}{dx} \Delta x \right] \Delta y \Delta z \end{aligned} \quad \text{L1.1}$$

Here p is the pressure, τ the shear intensity, and Δx , Δy , and Δz are the dimensions of the cube. It follows that:

$$\frac{d\tau}{dz} = \frac{dp}{dx} \quad \text{L1.2}$$

The power expended, or the rate at which work is done by the couple $(\tau \Delta x \Delta y)$, equals the torque $(\tau \Delta x \Delta y) \Delta z$ times the angular velocity dv/dz . Therefore the power (P) consumption per volume (V) of fluid is as follows:

$$\frac{P}{V} = \frac{(\tau \Delta x \Delta y) \Delta z}{\Delta x \Delta y \Delta z} \frac{dv}{dz} = \tau \frac{dv}{dz} \quad \text{L1.3}$$

Defining $\tau = \mu dv/dz$ and $G = dv/dz$

then

$$P/V = \mu (dv/dz)^2 = \mu G^2 \text{ or as follows:}$$

$$G^2 = \frac{P}{\mu V} \quad \text{L1.4}$$

L2. Basic Model Development

Define the list of variables.

n = number of second phase fluid droplets per volume

V = volume of n second phase fluid droplets

Vol = volume of first phase supporting fluid

V/Vol = concentration(C) of second phase fluid droplets in first phase supporting fluid

D = diameter of individual second phase fluid droplets

$$\begin{aligned} S &= \text{surface area of } n \text{ second phase fluid droplets} \\ t &= \text{reactor residence time} \end{aligned}$$

From these variables the following surface, volume and droplet relationships logically follow.

$$n = \frac{6V}{\pi D^3} = \frac{S}{\pi D^2} \quad \text{L2.1}$$

$$d = \frac{6V}{S} \quad \text{and} \quad S = \frac{6V}{D} \quad \text{L2.2}$$

$$V = \frac{Sd}{6} \quad \text{L2.3}$$

As per the Smoluchowski droplet collision relationship as derived circa 1917, verified through the years and typically presented in reference 1. Droplet collision rate is directly proportional to fluid shear (G) in units of /sec.

$$\frac{1}{Vol} \frac{dn}{dt} = \frac{4}{3} \frac{n^2 d^3 G_1}{Vol^2} \frac{1}{2} \quad \text{L2.4}$$

The $1/2$ factor is introduced so that particle or drop collisions are not counted twice.

Now using the defined relationships between volume, surface area and droplet size, derive and expression for change of droplet surface area as a function of second phase fluid concentration (C), fluid shear (G) and droplet diameter (D).

$$\begin{aligned} \frac{1}{Vol} \frac{dS}{dt} &= \frac{2}{3\pi} \frac{S^2 dG_1}{Vol^2} \\ &= \frac{2}{3\pi} \frac{S^2 6VG_1}{SVol^2} = \frac{4}{\pi} \frac{SVG_1}{Vol^2} \\ &= \frac{4}{\pi} \frac{6V^2 G_1}{Vol^2 D} = \frac{24}{\pi} \frac{C^2 G_1}{D} \end{aligned} \quad \text{L2.5}$$

In terms of change in surface area per second phase fluid volume, equation L2.5 is changed by factor $C = V/Vol$. The Smoluchowski droplet collision relationship is now expressed as:

$$\frac{1}{V} \frac{dS}{dt} = \frac{24}{\pi} \frac{CG_1}{D} \quad \text{L2.6}$$

Equation L2.6 represents the increased second phase fluid surface area due to second phase fluid droplets colliding with each other, but it is well known that under conditions of shear there is a tendency for second phase fluid droplets to break up. An extreme case would be addition of second phase fluid to first phase supporting fluid in a blender and the emulsification of the second phase fluid therein.

The power (P) to create this second phase fluid surface may be expressed in terms of the Gibb's interfacial tension (energy/area) σ as in equation L2.7

$$P = \sigma \frac{dS}{dt} \quad \text{L2.7}$$

The well known (reference 1) dissipative power (P) relationship is expressed in equation L2.8 in terms of first phase supporting fluid absolute viscosity (μ) and first phase supporting fluid shear (G_1).

$$P = \mu_1 V G_1^2 \quad \text{L2.8}$$

Now equating 2.7 and 2.8

$$\mu_1 V G_1^2 = \sigma \frac{dS}{dt} \quad \text{L2.9}$$

Now again a relationship is established in equation L2.10 for change in surface area (S) per second phase fluid volume (V) per time (t) from equation L2.9.

$$\frac{1}{V} \frac{dS}{dt} = \frac{\mu_1 G_1^2}{\sigma} \quad \text{L2.10}$$

Now assume an equilibrium condition under which the coalescing of droplets equals the breakup of droplets and this is expressed by subtracting equation L2.10 from equation L2.6 and set equal to zero.

$$\frac{1}{V} \frac{dS}{dt} = \frac{24}{\pi} \frac{CG_1}{D} - \frac{\mu_1 G_1^2}{\sigma} = 0 \quad \text{L2.11}$$

Now solving equation 2.11 for D . This represents the steady state droplet diameter under a particular shear condition.

$$D = \frac{24}{\pi} \frac{C\sigma}{\mu_1 G_1} \quad \text{L2.12}$$

Equation 2.12 is the steady state condition, but it may be useful to establish the time dependent change in droplet diameter by solving the differential equation L2.11.

$$S = 6 \frac{V}{D} \quad dS = -6 \frac{V}{D^2} dD \quad \text{L2.13}$$

Therefore:

$$\frac{dD}{dt} = \frac{4CG_1 D}{\pi} - \frac{\mu G_1^2 D^2}{6\sigma} \quad \text{L2.13}$$

Solution of equation L2.13 is presented in equation L2.14.

$$D_a = \frac{\beta D_i \exp(\beta t)}{\alpha D_i (\exp(\beta t) - 1) + \beta} \quad \text{L2.14}$$

Where D_i is the initial droplet size and D_a is final droplet size,

And where:

$$\text{Constant}(\alpha) = \frac{\mu_1 G_1^2}{6\sigma} \quad \text{L2.15}$$

$$\text{and } \text{Constant}(\beta) = \frac{4C_1 G_1}{\pi}$$

And where equations L2.12 and L2.13 are equivalent to:

$$D_a = \frac{\beta}{\alpha} \quad \text{and} \quad \frac{dD}{dt} = \beta D - \alpha D^2 \quad \text{L2.16}$$

With equation L2.12 an equilibrium droplet diameter can be found and/or with equation L2.14 a time dependent droplet diameter can be found, if second phase fluid concentration (C), second phase fluid/first phase supporting fluid interfacial tension, first phase supporting

fluid absolute viscosity (μ_1) and first phase supporting fluid shear (G_1) are known. From this relationship it can be seen that second phase fluid droplet size (D) is directly proportional to second phase fluid concentration (C) (the more second phase fluid drops to collide or coalesce to form bigger drops), directly proportional to interfacial tension (σ) (the more interfacial tension (σ) the more difficult to break up drops or decrease interfacial tension (σ) by adding surfactant results in ease in drop break up), inversely proportional to first phase supporting fluid viscosity (μ_1) (the more viscous the supporting fluid, the more power is transmitted to the second phase fluid drop), and inversely proportional to first phase supporting fluid shear (G) (the more shear the smaller drop produced as in the blender analogy).

All these parameters are measurable except fluid shear (G) which can be solved by equation L2.8 by introducing conventional head loss (H), flow rate (Q) and specific gravity (δ).

$$G_1^2 = \frac{P}{\mu_1 V} = \frac{Q \delta_1 H}{\mu_1 V} = \frac{V/t \delta H}{\mu_1 V} = \frac{Vol/t \delta H}{\mu_1 Vol} = \frac{\delta_1 H}{\mu_1 t} \quad \text{L2.17}$$

Now presenting the standard Darcy Weisbach head loss (for pipe) and minor loss (for valves, elbows etc.) formulas (reference 2) and where f is the Moody friction factor (which can be explicitly calculated in turbulent and laminar regions via reference 4), g is gravity acceleration, L is pipe length, K is unitless factor for particular valve, elbow etc., R_h is hydraulic radius ($R_h = d/4$ for pipe with diameter (d)) and v is fluid velocity.

$$H = f \frac{L}{d} \frac{v^2}{2g} \quad \text{and} \quad H = K \frac{v^2}{2g} \quad \text{L2.18}$$

Now letting $v = L/t$ then

$$\frac{H}{t} = f \frac{1}{d} \frac{v^3}{2g} \quad \text{and} \quad \frac{H}{t} = \frac{K}{L} \frac{v^3}{2g} \quad \text{L2.19}$$

Now combining equations L2.17 and L2.19 then fluid

shear in the pipe or fitting can be calculated as in equation L2.20.

$$G_1^2 = \frac{\delta_1}{\mu_1} \frac{H}{t} = \frac{\delta_1}{\mu_1} f \frac{1}{d} \frac{v^3}{2g} \quad \text{L2.20}$$

and

$$G_1^2 = \frac{\delta_1}{\mu_1} \frac{H}{t} = \frac{\delta_1}{\mu_1} K \frac{v^3}{L 2g}$$

Now all of the relationships are presented in order to calculate a droplet size as a function of head loss. The Reynolds number (R_e) reference is presented in equation L2.21.

$$R_e = \frac{\delta_1 v 4 R_h}{g \mu_1} \quad \text{where } R_h \text{ is the hydraulic radius} \quad \text{L2.21}$$

The following equation L2.22 represents the classical Stokes law relationship (with two phase specific weight difference (γ_s)) to overflow rate with the principle of overflow rate (flow rate Q /(effective area (A))) as generally used to size separation devices by equating droplet settling/rising velocity (v_s) to overflow rate.

$$v_s = \frac{Q}{A} = \frac{\Delta \delta D^2}{18 \mu_1} \quad \text{L2.22}$$

L3. Model Development Including Second Phase Viscosity Contribution to Interfacial Tension

$$H_D = \frac{32 \mu_2 D v_a}{\gamma_2 D^2} \quad v_c = 2 v_a \quad \text{L3.1}$$

$$H_D = \frac{v_c - v_a}{D} = G_2 \quad \text{L3.2}$$

And therefore:

$$\frac{2 v_a - v_a}{D} = \frac{v_a}{D} = G_2 \quad \text{L3.3}$$

And:

$$H_D = \frac{32 \mu_2 G_o}{\gamma_2} \quad \text{L3.4}$$

For a sphere with diameter(D), the interfacial tension (σ_{μ_2}) is:

$$H_D = \frac{6}{\pi D^3} \frac{Energy}{\gamma_2} = \frac{6}{\gamma_2} \frac{Energy}{\pi D^2} \frac{1}{D} = \frac{6}{\gamma_2} \frac{\sigma_{\mu_2}}{D} \quad \text{L3.5}$$

For a six sided cube with each side (D), the interfacial tension (σ_{μ_2}) is:

$$H_D = \frac{1}{D^3} \frac{Energy}{\gamma_2} = \frac{6}{\gamma_2} \frac{Energy}{6D^2} \frac{1}{D} = \frac{6}{\gamma_2} \frac{\sigma_{\mu_2}}{D} \quad \text{L3.6}$$

And then combine (L3.5 or L 3.6) and L 3.4 and therefore:

$$H_D = \frac{32\mu_2 G_2}{\gamma_2} = \frac{6}{\gamma_2} \frac{\sigma_{\mu_2}}{D} \quad \text{L3.7}$$

And now solve equation L3.7 for the interfacial tension (σ_{μ_2}):

$$\sigma_{\mu_2} = \frac{16}{3} \mu_2 G_2 D \quad \text{L3.8}$$

And now from equation L1.4:

$$G_1^2 = \frac{P}{\mu_1 V} \quad \text{and} \quad G_2^2 = \frac{P}{\mu_2 V} \quad \text{L3.9}$$

Or by rearranging equation 2.9:

$$G_2 = \sqrt{\frac{\mu_1}{\mu_2}} G_1 \quad \text{L3.10}$$

Now combine equations 3.8 and 3.10:

$$\sigma_{\mu_2} = \frac{16}{3} \mu_2 \sqrt{\frac{\mu_1}{\mu_2}} G_1 D \quad \text{L3.11}$$

Now extending the basic model developed in equation

2.13 section 2 for the addition of the equivalent second phase viscosity:

$$\frac{dD}{dt} = \frac{4CG_1 D}{\pi} - \frac{\mu_1 G_1^2 D^2}{6(\sigma + \sigma_{\mu_2})} \quad \text{L3.12}$$

Now substituting equation 3.11 into equation 3.12:

$$\frac{dD}{dt} = \frac{4CG_1 D}{\pi} - \frac{\mu_1 G_1^2 D^2}{6\left(\sigma + \frac{16}{3} \mu_2 \sqrt{\frac{\mu_1}{\mu_2}} G_1 D\right)} \quad \text{L3.13}$$

L4. Charge Related Surface Tension

$$\sigma_{\pm} = \Psi_o (8RT\epsilon\epsilon_o(1000c))^{\frac{1}{2}} \sinh\left(\frac{Z\Psi_o F}{2RT}\right) \quad \text{L3.14}$$

= charge related surface tension

Where:

$$\Psi_o = \text{potential (volt) (joule/coulomb)} \quad \text{L3.15}$$

Where:

$$R = \text{Gas Constant (8.314 joule mol}^{-1} \text{ K}^{-1}\text{)} \quad \text{L3.16}$$

Where:

$$T = \text{Temperature (degree Kelvin)} \quad \text{L3.17}$$

Where:

$$\epsilon = \text{dielectric constant of first phase supporting fluid} \quad \text{L3.18}$$

Where:

$$\epsilon_o = \text{permittivity of free space (8.854 x 10}^{-12} \text{ coulomb volt}^{-1} \text{ meter}^{-1}\text{)} \quad \text{L3.13}$$

Where:

$$c = \text{molar electrolyte concentration} \quad \text{L3.19}$$

Where:

$$Z = \text{ionic charge} \quad \text{L3.20}$$

Where:

$$F = \text{Faraday constant (96485 coulomb mole}^{-1}\text{)} \quad \text{L3.21}$$

L5. References

[L5.1] Fair, Geyer and Okun, Water and Wastewater Engineering, John Wiley & Sons, Inc. New York, 1968, pages 22-9 to 22-14.

[L5.2] Vennard, Elementary Fluid Mechanics, John Wiley & Sons, Inc. New York, 1968, page 280

[L5.3] Kim, Bock and Huang, "Interfacial and Critical Phenomena in Microemulsions", a paper presented in Waves on Fluid Interfaces edited by Richard Meyer, Academic Press, New York, 1983, page 151.

[L5.4] Churchill, "Chemical Engineering", 91, Nov 7, 1977, pages 91-92

[L5.5] Provder, Particle Size Distribution II, Assessment and Characterization, ACS Symposium Series 472, ACS Washington, DC., 1991, page 140.

[L5.6] Hinze, Turbulence, McGraw-Hill Publishing Company, New York, 1975.

[L5.7] Metcalf & Eddy, Wastewater Engineering, McGraw-Hill Publishing Company, New York, 1972

[L5.8] Tishkoff, Ingebo and Kennedy, Liquid Particle Measurement Techniques, American Society for Testing and Materials, Philadelphia, PA, 1984

[L5.9] Stumm and Morgan, Aquatic Chemistry, Chemical Equilibria and Rates in Natural Waters, Third Edition, Wiley-Interscience Series of Texts and Monographs, NY, NY, 1996, page 861.

Appendix M. Classical Phase Separation

Hydraulic Functional Unit(HFU)



This work was primarily done in the 1980's as a theoretical framework for industrial separator design. As such it was done in the English (ft lb sec) system that was prevalent at that time although dimensionality dictates any other system such as cgs or SI may be used with equal applicability with the understanding that:

$$F = M a$$

$$\frac{lb_{force}}{ft^3} = \frac{lb_{force}}{ft^3} \frac{gravity}{gravity_{acceleration}}_{acceleration}$$

$$\partial = \rho g$$

$$\frac{lb_{force}}{ft^3} = \frac{lb_{force}}{ft^3} \frac{gravity}{ft^3 gravity_{acceleration}}_{acceleration}$$

Variable Definition

Fluid Viscosity (μ_1)

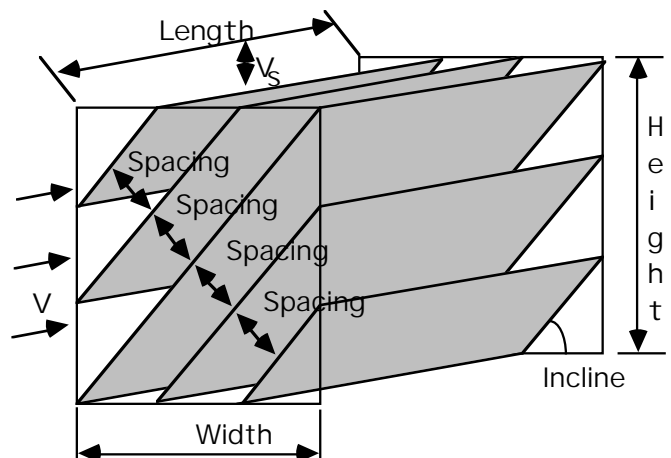
Fluid Specific Weight (∂_1)

Second Phase Specific Weight (∂_2)

Gravity Acceleration (g)

M1. PARALLEL PLATE SEPARATOR HFU

Figure M2.1



$$\text{Approach Velocity}(V) = \frac{\text{Flowrate}}{\text{Height Width}} \quad (\text{M2.1})$$

$$\text{Internal Velocity}(V_i) = \frac{V}{\text{Porosity}} \quad (\text{M2.2})$$

$$\text{Area Factor}(A_F) = \frac{\text{Spacing}}{\text{Length} \cos(\text{Incline})} \quad (\text{M2.3})$$

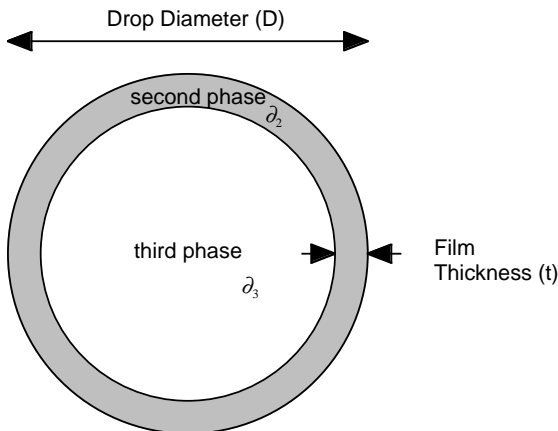
$$\text{Time}(t) = \frac{\text{Length}}{V} \quad (\text{M1.4})$$

$$\text{Head Loss Per Time} \left(\frac{H}{t} \right) = \frac{fV^3}{8gR_h} \quad (\text{M1.5})$$

$$\text{Hydraulic Radius}(R_h) = \frac{\text{Spacing}}{2} \quad (\text{M1.6})$$

M2. PARTICLE DENSITY

Figure M2.1 Third Phase Drop Coated with Second Phase



HFU Inlet Concentration (C_i)

$$C_i = C_2 + C_3 \quad (\text{M2.1})$$

Particle Film Thickness (t)

$$t = \left(1 - \frac{C_3}{C_2 + C_3} \right) \frac{D}{2} \quad (\text{M2.2})$$

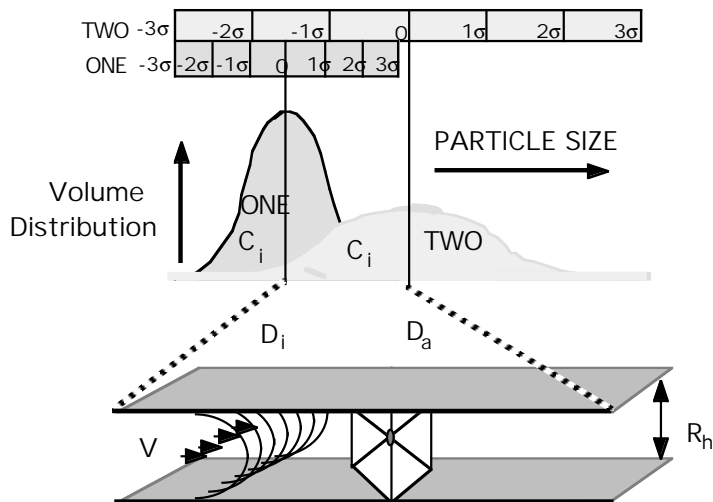
Particle Density (∂_D) on addition of a third gaseous phase

with density (∂_3)

$$\partial_D = \frac{\partial_2 (D - 2t)^3 + \partial_3 D^3}{D^3} \quad (\text{M2.3})$$

M3. PARTICLE COALESCENCE

Figure M3.1



HFU Reynolds Number (R_e)

$$R_e = \frac{\partial_1 V_i 4 R_h}{g \mu_1} \quad (\text{M3.1})$$

Churchill interim factor (E) in terms of R_e and roughness factor (r)

$$E = \left(-2.457 \ln \left(\left(\frac{7}{R_e} \right)^{.9} + .27r \right) \right)^{16} \quad (\text{M3.2})$$

Churchill Flow Friction Factor (f)

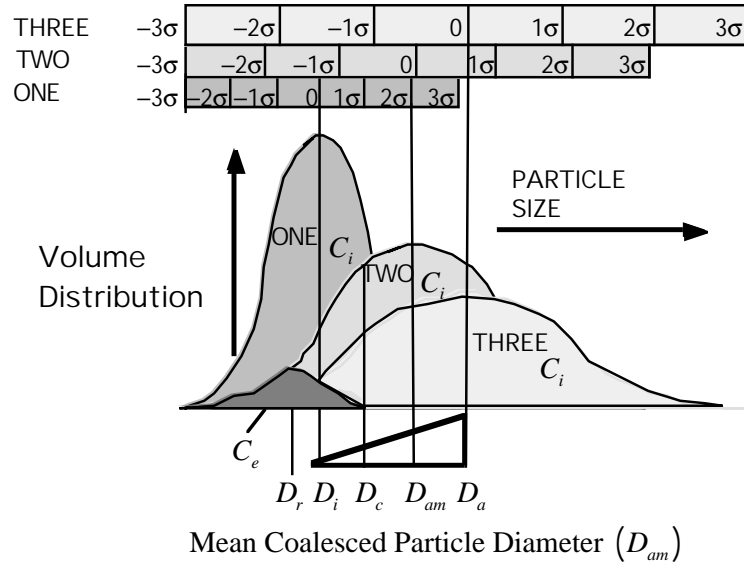
$$f = 8 \left(\left(\frac{8}{R_e} \right)^{12} + \left(\left(\frac{37530}{R_e} \right)^{16} + E \right)^{-1.5} \right)^{\frac{1}{12}} \quad (\text{M3.3})$$

Fluctuation Thermal Kinetic Shear (G_k)	Effective Surface Tension (β_e)
$G_k = \frac{8k_b T}{\mu_1 D^3}$	$\beta_e = \frac{16}{3} \mu_2 \sqrt{\frac{\mu_1}{\mu_2}} G D + \beta$ (M3.13)
Friction Factor Shear (G_f)	M4. SIMILITUDE PARTICLE
$G_f = \sqrt{\frac{\partial_1 H}{\mu_1 t}}$	Generalized HFU/Particle Similitude Assumption
Distance (R) between Particles	$HFU \ Shear(G) = Particle \ Shear \left(\frac{v_{sr}}{D_r} \right)$ (M4.1)
$R = \left(\frac{3}{2C_i} \right)^{1/3} D$	Similitude Particle Settling/Rising Velocity (v_{sr})
Coalesced Particle Diameter (D_a)	$v_{sr} = \frac{ \partial_1 - \partial_D D_r^2}{18 \mu_1}$ (M4.2)
$D_a = \frac{\delta D_i \exp(\delta t)}{\alpha D_i (\exp(\delta t) - 1) + \delta}$	Similitude Particle (D_r)
Constant(α) = $\frac{\mu_1 G^2}{6 \beta_e} - \frac{2 F_s G}{3 \pi R_h}$	$D_r = \frac{2}{3} \frac{a \mu_1 G}{ \partial_1 - \partial_D }$ (M4.3)
Constant(δ) = $\frac{4 F_p C_i G}{\pi}$	where a = Toppler Factor with typical value of 5
Surface Factor (F_s) and Sphere Factor (F_p)	M5. SETTLING/RISING PARTICLE
$F_s = \exp \left(\frac{-12 Z p}{\pi \partial_D G} \right)$	Particle Settling Velocity (v_s)
$F_p = \exp \left(\frac{-6 Z p}{\pi \partial_D G} \right)$	$v_s = A_F v_i$ (M5.1)
Gibbs Surface Tension (β).	Particle Drag Coefficient (C_d)
$\beta = \frac{Energy}{Interfacial \ Area \ between \ Phases \ 1 \ \& \ 2}$	$C_d = \frac{24}{R_{ep}} + \frac{3}{R_{ep}^{1/2}} + .34$ (M5.2)
	Particle Reynolds Number (R_{ep})
	$R_{ep} = \frac{\partial_1 v_s D_c}{g \mu_1}$ (M5.3)
	Settling/Rising Particle (D_c)

$$D_c = \frac{3C_d \partial_1 v_s^2}{4|\partial_1 - \partial_D|g} \quad (M5.4)$$

M6. PARTICLE REMOVAL

Figure M15.1



$$D_{am} = \frac{1}{3}D_i + \frac{2}{3}D_a \quad (M6.1)$$

Gaussian Influent Particle Distribution ($f(D)$)

$$f(D) = \frac{1}{\sqrt{2\pi}} \exp\left(\frac{-1}{2}\left(\frac{D_{am} - D}{\sigma}\right)^2\right) \quad (M6.2)$$

$$= \frac{1}{\sqrt{2\pi}} \exp\left(\frac{-\sigma^2}{2}\right)$$

Influent concentration (C_i)

$$C_i = \int_0^{\infty} D^n f(D) dD \quad (M6.3)$$

Camp's Particle Effluent Stokes Trial 1 (C_{e1})
and Similitude Trial 2 (C_{e2}) Effluents.

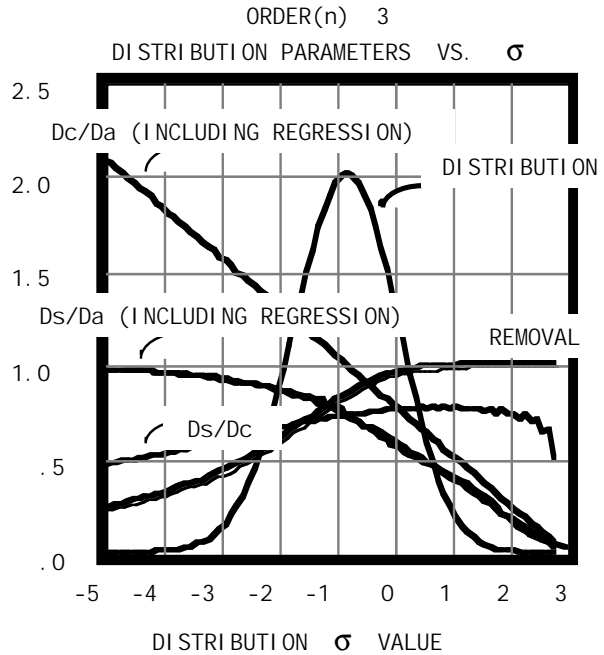
$$C_{e1} = \int_0^{D_c} \left(1 - \frac{D^2}{D_c^2}\right) D^n f(D) dD \quad (M6.4)$$

$$C_{e2} = \int_0^{aD_s} \left(1 - \frac{D^2}{(aD_s)^2}\right) D^n f(D) dD \quad (M6.5)$$

$$\text{Area Factor}(A_F) = \frac{\text{Spacing}}{\text{Length} \cos(\text{Incline})}$$

n	Distribution	n	Distribution
0	Volume	3	Number
1	Area	4	Reciprocal Diameter
2	Diameter	6	Reciprocal Volume

Figure M15.2



$$\text{HFU Effluent Time}(t) = \frac{\text{Length}}{V}$$

$$\text{Head Loss Per Time} \left(\frac{H}{t}\right) = \frac{fV^3}{8gR_h} \quad (M6.6)$$

Appendix N. Authority for Expenditure (Project Cost Estimate)

AFE number 51507
 Project Name Three Dimensional Laser Energetics
Relating Trisine Geometry to the CPT theorem
 Location Corpus Christi, Texas
 Description Apparatus and Support Facilities for 10 years
 Date May 15, 2007

				Completed Cost
PROJECT - INTANGIBLE COSTS				
Project Physicists				\$60,000,000
Project Chemists				\$60,000,000
Project Engineers				\$60,000,000
Technicians Draftsmen Electronic Electrical Specifications				\$60,000,000
Salaries management and office staff				\$20,000,000
Architectural Services				\$1,500,000
Landscaping				\$500,000
Maintenance				\$1,000,000
Office Library Supplies				\$2,000,000
Library Reference Searches				\$3,000,000
Patent Trademark Attorney Services				\$1,500,000
Legal Services				\$5,000,000
Financial Services				\$500,000
Travel				\$5,000,000
Publication Services				\$1,000,000
Marketing				\$500,000
Infrastructure maintainance				\$10,000,000
Utilities				\$1,000,000
Security				\$1,000,000
				\$0
SubTotal				\$293,500,000
Contingencies	50.00%			\$146,750,000
PROJECT - INTANGIBLE COSTS				\$440,250,000
PROJECT - TANGIBLE COSTS				
Vibration Attenuation foundation				\$5,000,000
Laser Reactor Area	5000	sq ft	\$5,000 per sq ft	\$25,000,000
Assembly Area	10000	sq ft	\$500 per sq ft	\$5,000,000
Office Laboratory Library Visualization Space	20000	sq ft	\$500 per sq ft	\$10,000,000
Office Laboratory Library Visualization Equipment Furniture				\$25,000,000
Office Laboratory Computers CAD Software Plotters Displays Printers LAN				\$10,000,000
Heating Air Conditioning				\$5,000,000
Heavy Equipment movement and placement trolleys and lifts				\$10,000,000
Test Benches and Equipment Storage				\$15,000,000
Test and Measurement Equipment				\$25,000,000
Faraday and Optical Cage				\$25,000,000
Three Dimensional Positioning System				\$5,000,000
Laser Generators				\$100,000,000
Laser Optics, Polarizers and Rectifiers				\$20,000,000
Vacuum Enclosure for Laser and Optics				\$50,000,000
Vacuum Pumping Equipment				\$5,000,000
Cryogenic Equipment				\$50,000,000
Data Sensors and Acquisition Equipment				\$50,000,000
Computers and Servers for Analysing and Storing Data				\$100,000,000
Laser Interference Reactor				\$100,000,000
PROJECT - TANGIBLE COSTS				\$640,000,000
TOTAL PROJECT COSTS				\$1,080,250,000
LEASE EQUIPMENT				
truck and sedan Vehicle				\$200,000
Out Sourcing Services				\$500,000,000
				\$0
				\$0
TOTAL LEASE EQUIPMENT				\$500,200,000
TOTAL COST				\$1,580,450,000

6. References

[1] William Melis and Richard Saam, "U. S. Patent 4,526,691", Separator Apparatus, 02 July 1985.

[2] John Bardeen, Leon Neil Cooper and John Robert Schrieffer, "Theory of Superconductivity", Physical Review, Vol 28, Number 6, December 1, 1957, pages 1175-1204.

[3] Erwin Schrödinger, "An Undulatory Theory of the Mechanics of Atoms and Molecules", Physical Review, Vol 108, Number 5, December, 1926, pages 1049-1069.

[4] Charles Kittel, Introduction to Solid State Physics, Seventh Edition, John Wiley & Sons, Inc., New York, N.Y., 1996.

[5] William A. Little, "Experimental Constraints on Theories of High Transition Temperature Superconductors", Department of Applied Physics, Stanford University, 1987. Phys. Rev. 134, A1416-A1424 (1964)

[6] Leonard Eges, "The Classical Electromagnetic Field", Dover Edition, New York, 1980.

[7] Eugene Podkletnov and R. Nieminen, "A Possibility of Gravitational Force Shielding by Bulk $YBa_2Cu_3O_{7-x}$ Superconductor", Physica C 203, (1992), 414 - 444.

[8] Sir Arthur Eddington, "The Universe and the Atom" from The Expanding Universe, Cambridge University Press.

[9] Giovanni Modanese, "Theoretical Analysis of a Reported Weak Gravitational Shielding Effect", MPI-PhT/95-44, May 1995, Max-Planck-Institut für Physik, Werner-Heisenberg-Institut, Föhringer Ring 6, D 80805 München (Germany) to appear in Europhysical Letters.

[10] Giovanni Modanese, "Role of a 'Local' Cosmological Constant in Euclidian Quantum Gravity", UTF-368/96 Jan 1996, Gruppo Collegato di Trento, Dipartimento di Fisica dell'Università I-38050 POVO (TN) - Italy

[11] J. E. Sonier et al., "Magnetic Field Dependence of the London Penetration Depth in the Vortex State of $YBa_2Cu_3O_{6.95}$ ", Triumf, Canadian Institute for Advanced Research and Department of Physics, University of British Columbia, Vancouver, British Columbia, Canada, V6T.

[12] T. R. Camp and P. C. Stein, "Velocity Gradients and Internal Work in Fluid Motion", Journal of the Boston Society Civil Engineers, 30, 219 (1943).

[13] Miron Smoluchowski, Drei Vorträge über Diffusion, Brownsche Molekularbewegung und Koagulation von Kolloidteilchen (Three Lectures on Diffusion, Brownian Motion, and Coagulation of Colloidal Particles), Phys. Z., 17, 557 (1916); Versuch einer Mathematischen Theorie der Koagulationskinetik Kolloider Lösungen (Trial of a Mathematical Theory of the Coagulation Kinetics of Colloidal Solutions), Z. Physik. Chem., 92, 129, 155 (1917).

[14] Gordon M. Fair, John C. Geyer and Daniel A. Okun, Water and Wastewater Engineering, John Wiley & Sons, Inc. New York, 1968, pages 22-9 to 22-14.

[15] Georg Joos, Theoretical Physics, translated from the first German Edition by Ira Freeman, Hafner Publishing Company, Inc., New York, 1934.

[16] Robert C. Weast and Samuel M. Selby, Handbook of Chemistry and Physics, 53 Edition, The Chemical Rubber Company, Cleveland, Ohio, 1972-73.

[17] D. R. Harshman and A. P. Mills, Jr., "Concerning the Nature of High-Tc Superconductivity: Survey of Experimental Properties and Implications for Interlayer Coupling", Physical Review B, 45, 18, 01 May 92.

[18] John K. Vennard, Fluid Mechanics, John Wiley & Sons, Inc., New York, NY, 1961.

[19] Walter J. Moore, Physical Chemistry, Prentice-Hall, Inc., Englewood Cliffs, NJ, 1962.

[20] J. L. Weiland et al., Seven-Year Wilkinson Microwave Anisotropy Probe (WMAP1) Observations: Planets and Celestial Calibration Sources, Astrophysical Journal Supplement Series, <http://arxiv.org/abs/1001.4744>

[21] Hayasaka and Takeuchi, "Anomalous Weight Reduction on a Gyroscope's Right Rotations around the Vertical Axis on the Earth", Physical Review Letters, 63, 25, December 18, 1989, p 2701-4.

[22] Faller, Hollander, and McHugh, "Gyroscope-Weighing Experiment with a Null Result", Physical Review Letters, 64, 8, February 19, 1990, p 825-6.

[23] Nitschke and Wilmarth, "Null Result for the Weight Change of a Spinning Gyroscope", Physical Review Letters, 64, 18, April 30, 1990, p 2115-16.

[24] Donald J. Cram and George S. Hammond, Organic Chemistry, McGraw-Hill Book Company, New York, NY, 1964.

[25] Kimberly, Chanmugan, Johnson, & Tohline, Millisecond Pulsars Detectable Sources of Continuous Gravitational Waves, Astrophysics J., 450:757, 1995. <http://arxiv.org/abs/astro-ph/9503092>
A theory studied, quantified and observed over several decades for the pulsar system PSR B1913+16, made by Russell A. Hulse and Joseph H. Taylor Jr. who were awarded the The Nobel Prize in Physics 1993.

[26] Staggs, Jarosik, Meyer and Wilkinson, Enrico Fermi Institute, University of Chicago, Chicago, Illinois 60637, Sept 18, 1996.

[27] Copi, Schramm and Turner, Big-bang nucleosynthesis and the baryon density of the universe, Science, 267, January 13, 1995, pp 192-8.

[28] Albert Einstein, The Meaning of Relativity, Fifth Edition, MJF Books, New York, NY, 1956.

[29] Albert Einstein, The Special and the General Theory, Three Rivers Press, New York, NY, 1961.

[30] Wolfgang Pauli, The Theory of Relativity, Dover Publications, New York, NY, 1958.

[31] Robert M. Wald, General Relativity, University of Chicago Press, Chicago, 1984.

[32] Ray D'Inverno, Introducing Einstein's Relativity, Clarendon Press, Oxford, 1995.

[33] Paul A. M. Dirac, General Theory of Relativity, Princeton University Press, Princeton, NJ, 1996.

[34] Barrett O'Neill, The Geometry of Kerr Black Holes, A K Peters, Wellesley, MA, 1995.

[35] Charles W. Misner, Kip S. Thorne & John A. Wheeler, Gravitation, W. H. Freeman and Company, New York, 1998.

[36] Rutherford Aris, Vectors, Tensors, and the Basic Equations of Fluid Mechanics, Dover Publications, New York, 1962.

[37] Heinrich W. Guggenheimer, Differential Geometry, Dover Publications, New York, 1977.

[38] Hans Schneider, George P. Barker, Matrices and Linear Algebra, Dover Publications, New York, 1962.

[39] Bernard Schutz, Geometrical Methods of Mathematical Physics, Cambridge University Press, Cambridge, 1980.

[40] Richard P. Feynman, Six Easy Pieces, Addison-Wesley Publishing Company, New York, 1995.

Richard P. Feynman, Six Not So Easy Pieces, Addison-Wesley Publishing Company, New York, 1963

Richard P. Feynman - Science Videos, The Douglas Robb Memorial Lectures, University of Auckland (New Zealand), <http://www.vega.org.uk/video/subseries/8>

[41] Jed Z. Buchwald, From Maxwell to Microphysics, University of Chicago Press, Chicago, 1973.

James Clerk Maxwell, Professor of Natural Philosophy in King's College, London, - The London, Edinburgh and Dublin Philosophical Magazine and Journal of Science [Fourth Series] March 1861 XXV. On Physical Lines of Force

Part I.—The Theory of Molecular Vortices applied to Magnetic Phenomena

Part II.—The Theory of Molecular Vortices applied to Electrical Currents.

Part III: The Theory of Molecular Vortices applied to Statical Electricity

Part IV: The Theory of Molecular Vortices applied to the Action of Magnetism on Polarized Light

[42] Leonard Eges, The Classical Electromagnetic Field, Dover Publications, New York, 1972.

[43] L. D. Landau and E. M. Lifshitz, The Classical Theory of Fields, Volume 2, Butterworth-Heinemann, Oxford, 1998.

[44] C. K. Birdsall and A. B. Langdon, Plasma Physics via Computer Simulation, Institute of Physics Publishing, Philadelphia, 1991.

[45] Peter W. Milonni, The Quantum Vacuum, An Introduction to Quantum Electrodynamics, Academic Press, New York, 1994.

[46] Claude Cohen-Tannoudju, Jacques Dupont-Roc & Gilbert Grynberg, Photons & Atoms, Introduction to Quantum Electrodynamics, John Wiley & Sons, Inc., New York, 1989.

[47] Eugen Merzbacher, Quantum Mechanics, Third Edition, John Wiley & Sons, Inc., New York, 1998.

[48] James P. Runt and John J. Fitzgerald, Dielectric Spectroscopy of Polymeric Materials, Fundamentals and Applications, American Chemical Society, Washington, DC, 1997.

[49] Michael Tinkham, Introduction to Superconductivity, McGraw-Hill Companies, New York, NY, 1996.

[50] Eugene Hecht, Optics Third Edition, Addison-Wesley, New York, NY, 1998.

[51] C. C. Homes et al., Universal Scaling Relation in High-Temperature Superconductors. *Nature*, Vol 430, 29 July 2004. <http://xxx.lanl.gov/abs/cond-mat/0404216>

[52] Jan Zaanen, Why the Temperature is High, *Nature*, Vol 430, 29 July 2004.

[53] Study of the anomalous acceleration of Pioneer 10 and 11, John D. Anderson, Philip A. Laing, Eunice L. Lau, Anthony S. Liu, Michael Martin Nieto, and Slava G. Turyshev, 11 Apr 2002 <http://arxiv.org/abs/gr-qc/0104064>

[53a] The Study of the Pioneer Anomaly: New Data and Objectives for New Investigation, Slava G. Turyshev, Viktor T. Toth, Larry R. Kellogg, Eunice L. Lau, Kyong J. Lee, 06 Mar 2006 <http://arxiv.org/abs/gr-qc/0512121>

[54] Christopher C. Homes, S. V. Dordevic, T. Valla, M. Strongin, Are high-temperature superconductors in the dirty limit <http://xxx.lanl.gov/abs/cond-mat/0410719v1>

[55] N. Klein, B.B. Jin, J. Schubert, M. Schuster, H.R. Yi, Forschungszentrum Jülich, Institute of Thin Films and Interfaces, D-52425 Jülich, Germany, A. Pimenov, A. Loidl, Universität Augsburg, Experimentalphysik V, EKM, 86135 Augsburg, Germany, S.I. Krasnosvobodtsev, P.N. Lebedev Physics Institute, Russian Academy of Sciences, 117924 Moscow, Russia, <http://xxx.lanl.gov/abs/cond-mat/0107259>, Energy gap and London penetration depth of MgB₂ films determined by microwave resonator, Submitted to Physical Review Letters, June 29, 2001. MgB₂ superconductivity originally discovered by Nagamatsu et al. 2001 Superconductivity at 39 K in MgB₂, *Nature* 410 63

[56] Directly Measured Limit on the Interplanetary Matter Density from Pioneer 10 and 11 Michael Martin Nieto, Slava G. Turyshev and John D. Anderson <http://arxiv.org/abs/astro-ph/0501626>

[57] Study of the Pioneer Anomaly: A Problem Set, Slava G. Turyshev, Michael Martin Nieto, and John D. Anderson <http://lanl.arxiv.org/abs/physics/0502123>

[58] Heliocentric Trajectories for Selected Spacecraft, Planets, and Comets, NSSDC Goddard National Spaceflight Center, <http://nssdc.gsfc.nasa.gov/space/helios/heli.html>

[59] Christopher C. Homes, S. V. Dordevic, T. Valla, M. Strongin, Scaling of the superfluid density in high-temperature superconductors, <http://xxx.lanl.gov/abs/cond-mat/0410719v2>

[60] Frank M. White, Viscous Fluid Flow, Second Edition, McGraw Hill, NY, NY, 1974

[61] Francis W. Sears and Mark W. Zemansky, University Physics, Third Edition, Addison-Wesley. Reading, MA, 1964.

[62] James L. Anderson, Thompson Scattering in an Expanding Universe, <http://xxx.lanl.gov/abs/gr-qc/9709034>

[63] Michael Martin Nieto, Slava G. Turyshev, Measuring the Interplanetary Medium with a Solar Sail, <http://xxx.lanl.gov/abs/gr-qc/0308108>

[64] Transport of atoms in a quantum conveyor belt, A. Browaeys, H. Haffner, C. McKenzie, S. L. Rolston, K. Helmerson, and W. D. Phillips, National Institute of Standards and Technology, Gaithersburg, MD 20899, USA (Dated: April 23, 2005) <http://arxiv.org/abs/cond-mat/0504606>

[65] R. Tao, X. Zhang, X. Tang and P. W. Anderson, *Phys. Rev. Lett.* 83, 5575 (1999).

[66] R. Tao, X. Xu, Y. C. Lan Y. Shiroyanagi, Electric-field induced low temperature superconducting granular balls, *Physica C* 377 (2002) 357-361

[67] R. Tao, X. Xu X and E. Amr, Magnesium diboride superconducting particles in a strong electric field, *Physica C* 398 (2003) 78-84

[68] Didkovsky L. V., Rhodes E. J., Jr., Dolgushin A.I., Haneychuk V. I., Johnson N. M., Korzennik S.G., Kotov V. A., Rose P. J., Tsap T. T. : "The first results of solar

observations made in the Crimean Astrophysical Observatory using a magneto-optical filter", 1996, Izv. Vuzov, ser. RADIOFIZIKA, Tom 39, No. 11-12, p. 1374-1380.

[69] Kotov V.A., Lyuty V. M., Haneychuk V. I. : "New evidences of the 160-minute oscillations in active galactic nuclei", 1993, Izv. Krym. Astrofiz. Obs., Tom 88, p. 47-59.

[70] Andrew Huxley, Critical Breakthrough, Science 309 1343, CEA laboratory in Grenoble and the Grenoble High Magnetic Field Laboratory (GHMFL).

[71] R. F. Klie, J. P. Buban, M. Varela, A. Franceschetti, C. Jooss, Y. Zhu, N. D. Browning, S. T. Pantelides and S. J. Pennycook, Enhanced current transport at grain boundaries in high-Tc superconductors, Nature p475, Vol 435, 26 May 2005

[72] Enhanced flux pinning in $\text{YBa}_2\text{Cu}_3\text{O}_7$ – films by nanoscaled substrate surface roughness Zu-Xin Ye, Qiang Li, Y. Hu, W. D. Si, P. D. Johnson, and Y. Zhu Appl. Phys. Lett. 87, 122502 (2005) (3 pages), BNL.

[73] Andrew W. Strong, Igor V. Moskalenko & Olaf Reimer, A New Determination Of The Diffuse Galactic and Extragalactic Gamma-Ray Emission <http://lanl.arxiv.org/abs/astro-ph/0506359>

[74] F. L. Pratt, S. J. Blundell, Universal Scaling Relations in Molecular Superconductors, Phys. Rev. Lett. 94, 097006 (2005), <http://arxiv.org/abs/cond-mat/0411754>

[75] A. Einstein, Ann. Der Physik, 17, p. 549 (1905)

[76] Marusa Bradac et al., Strong And Weak Lensing United III: Measuring The Mass Distribution Of The Merging Galaxy Cluster 1E0657-56 <http://arxiv.org/abs/astro-ph/0608408>
and A. Mahdavi et al., A Dark Core in Abell 520, <http://arxiv.org/abs/0706.3048>
and Marusa Bradac et al., Revealing the properties of dark matter in the merging cluster MACSJ0025.4-1222, <http://arxiv.org/abs/0806.2320>
and F. Gastaldello et al., Dark matter-baryons separation at the lowest mass scale: the Bullet Group, <http://arxiv.org/abs/1404.5633v2>.

[77] Louis-Victor de Broglie (1892-1987) Recherches Sur La Theorie Des Quanta (Ann. de Phys., 10 serie, t. III (Janvier-Fevrier 1925). Translation by A. F. Kracklauer

[78] Merav Opher, Edward C. Stone, Paulett C. Liewer and Tamas Gombosi, Global Asymmetry of the Heliosphere, <http://arxiv.org/abs/astro-ph/0606324>

[79] Massey R., et al. Nature, advance online publication, doi:10.1038/nature05497 (2007).

[80] Joel R. Primack. Precision Cosmology: Successes and Challenges, <http://arxiv.org/abs/astro-ph/0609541>, 19 Sep 06

[81] Schwinger, Julian, On Gauge Invariance and Vacuum Polarization, 1951, Phys. Rev., 82, 664

[82] T. Mukai, C. Hufnagel, A. Kasper, T. Meno, A. Tsukada, K. Semba, and F. Shimizu, Persistent Supercurrent Atom Chip <http://arxiv.org/abs/cond-mat/0702142>

[83] Danielle Allor, Thomas D. Cohen and David A. McGady, The Schwinger Mechanism and Graphene <http://arxiv.org/abs/0708.1471>
Thomas D. Cohen and David A. McGady, The Schwinger mechanism revisited <http://arxiv.org/abs/0807.1117>

[84] Rita Bernabei, Belli Pierluigi et al., Dark Matter Search Dip. di Fisica, Université di Roma "Tor Vergata" and INFN-Roma Tor Vergata, 00133 Roma, Italy <http://arxiv.org/abs/astro-ph/0307403>

[85] Margaret Hawton, Photon Position Eigenvectors Lead to Complete Photon Wave Mechanics, Lakehead University, Thunder Bay, Canada <http://arxiv.org/abs/0711.0112>

[86] John D. Anderson, James K. Campbell, Michael Martin Nieto, The energy transfer process in planetary flybys <http://arxiv.org/abs/astro-ph/0608087>

[87] Kiwamu Nishida, Naoki Kobayashi and Yoshio Fukao, Resonant Oscillations Between the Solid Earth and the Atmosphere Science 24 March 2000 Vol. 287. no. 5461, pp. 2244 – 2246

[88] D. Saul Davis, Paul Hickson, Glen Herriot, Chiao- Yao She Temporal variability of the telluric sodium layer Science 24 <http://arxiv.org/abs/astro-ph/0609307>

[89] K. Pounds , R. Edelson, A. Markowitz, S. Vaughan X-ray Power Density Spectrum of the Narrow Line Seyfert1 Galaxy Akn 564, <http://arxiv.org/abs/astro-ph/0101542>

[90] Thomas C. Killian, 1S-2S Spectrum of a Hydrogen Bose-Einstein Condensate, Physical Review A 61, 33611 (2000) <http://arxiv.org/abs/physics/9908002>

[91] A. A. Abdo, M. Ackermann, M. Ajello -FERMI team, The Spectrum of the Isotropic Diffuse Gamma-Ray Emission Derived From First-Year Fermi Large Area Telescope Data. <http://arxiv.org/abs/1002.3603v1>

[92] Shin'ichiro Ando, Alexander Kusenko, The Evidence for Gamma-Ray Halos Around Active Galactic Nuclei and the First Measurement of Intergalactic Magnetic Fields, <http://arxiv.org/abs/1005.1924v2>

[93] K. Dolag, M. Kachelriess, S. Ostapchenko, R. Tomas, Lower limit on the strength and filling factor of extragalactic magnetic fields, <http://arxiv.org/abs/1009.1782>

[94] Alex Silbergleit, John Conklin and the Polhode/Trapped Flux Mapping Task Team, Hansen Experimental Physics Laboratory(HEPL) Seminar, Polhode Motion, Trapped Flux, and the GP-B Science Data Analysis, July 8, 2009, Stanford University.
C. W. F. Everitt, M. Adams, W. Bencze, S. Buchman, B. Clarke, J. W. Conklin, D. B. DeBra, M. Dolphin, M. Heifetz and D. Hipkins, et al. Space Science Reviews, Volume 148, Numbers 1-4, 53-69, DOI: 10.1007/s11214-009-9524-7, Gravity Probe B Data Analysis Status and Potential for Improved Accuracy of Scientific Results From the issue entitled "Probing the Nature of Gravity: Confronting Theory and Experiments in Space / Guest Edited by C.W.F. Everitt, M.C.E. Huber, R. Kallenbach, G. Schäfer, B.F. Schutz and R.A. Treumann"
Gravity Probe B: Final Results of a Space Experiment to Test General Relativity <http://arxiv.org/abs/1105.3456>
C. W. F. Everitt, D. B. DeBra, B. W. Parkinson, J. P. Turneaure, J. W. Conklin, M. I. Heifetz, G. M. Keiser, A. S. Silbergleit, T. Holmes, J. Kolodziejczak, M. Al-Meshari, J. C. Mester, B. Muhlfelder, V. Solomonik, K. Stahl, P. Worden, W. Bencze, S. Buchman, B. Clarke, A. Al-Jadaan, H. Al-Jibreel, J. Li, J. A. Lipa, J. M. Lockhart, B. Al-Suwaidan, M. Taber, S. Wang

[95] P. J. E. Peebles, *Principles of Physical Cosmology*, Princeton University Press, Princeton, New Jersey, 1993.

[96] Oleg D. Jefimenko, A neglected topic in relativistic electrodynamics: transformation of electromagnetic integrals, <http://arxiv.org/abs/physics/0509159>

[97] Eugene N. Parker edited by David N. Spergel, *Conversations on electric and magnetic fields in the cosmos*, Princeton University Press, 2007.

[98] Abhik Ghosh1, Somnath Bharadwaj, Sk. Saiyad Ali and Jayaram N. Chengalur, GMRT observation towards detecting the Post-reionization 21-cm signal, <http://arxiv.org/abs/1010.4489>

[99] Steven Weinberg, *Gravitation and Cosmology*, John Wiley and Sons, New York, (1972)

[100] Steven Weinberg, *The First Three Minutes*, A Bantam Book, (1980)

[101] Sir James Hopwood Jeans, *Astronomy and Cosmogeny*, 2nd Ed., Cambridge University Press(1929)

[102] Timothy R. Bedding, Hans Kjeldsen, Torben Arentoft, Francois Bouchy, Jacob Brandbyge, Brendon J. Brewer, R. Paul Butler, Joergen Christensen-Dalsgaard, Thomas Dall, Soeren Frandsen, Christoffer Karoff, Laszlo L. Kiss, Mario J.P.F.G. Monteiro, Frank P. Pijpers, Teresa C. Teixeira, C. G. Tinney, Ivan K. Baldry, Fabien Carrier, Simon J. O'Toole, Solar-like oscillations in the G2 subgiant beta Hydri from dual-site observations <http://arxiv.org/abs/astro-ph/0703747>

[103] A. Das and T. Ferbel, *Introduction to Nuclear and Particles Physics*, 2nd Ed., World Scientific, London, 2003.

[104] National Aeronautics and Space Administration (NASA) Fermi Science Support Center (FSSC) <http://fermi.gsfc.nasa.gov/ssc/data/access/lat/BackgroundModels.html> isotropic_iem_v02_P6_V11_DIFFUSE.txt

[105] Mark J Hadley, The asymmetric Kerr metric as a source of CP violation <http://arxiv.org/abs/1107.1575>

[106] N. Fornengo, R. Lineros, M. Regis, M., A dark matter interpretation for the ARCADE excess? <http://arxiv.org/abs/1108.0569v1>

[107] Adam Mantz, Steven W. Allen, Implicit Priors in Galaxy Cluster Mass and Scaling Relation Determinations <http://arxiv.org/abs/1106.4052>
Adam Mantz, Steven W. Allen, David Rapetti, Harald Ebeling, The Observed Growth of Massive Galaxy Clusters I: Statistical Methods and Cosmological Constraints <http://arxiv.org/abs/0909.3098v4>

[108] The OPERA Collaboraton, Measurement of the neutrino velocity with the OPERA detector in the CNGS beam <http://arXiv:1109.4897v2>
M. Antonello et al., Measurement of the neutrino velocity with the ICARUS detector at the CNGS beam <http://arxiv.org/abs/1203.3433>

[109] J.-S. Huang, X. Z. Zheng, D. Rigopoulou, G. Magdis, G. G. Fazio, T. Wang, Four IRAC Sources with an Extremely Red H-[3.6] Color: Passive or Dusty Galaxies at $z > 4.5$? <http://arxiv.org/abs/1110.4129>

[110] C.E. Aalseth, P.S. Barbeau, N.S. Bowden, B. Cabrera, Palmer, J. Colaresi, J.I. Collar, S. Dazeley, P. de Lurgio, G. Drake, J.E. Fast, N. Fields, C.H. Greenberg, T.W. Hossbach, M.E. Keillor, J.D. Kephart, M.G. Marino, H.S. Miley, M.L. Miller, J.L. Orrell, D.C. Radford, D. Reyna, R.G.H. Robertson, R.L. Talaga, O. Tench, T.D. Van Wechel, J.F. Wilkerson, K.M. Yocom, Search for an Annual Modulation in a P-type Point Contact Germanium Dark Matter Detector <http://arxiv.org/abs/1002.4703>

[111] C.E. Aalseth, P.S. Barbeau, J. Colaresi, J.I. Collar, J. Diaz Leon, J.E. Fast, N. Fields, T.W. Hossbach, M.E. Keillor, J.D. Kephart, A. Knecht, M.G. Marino, H.S. Miley, M.L. Miller, J.L. Orrell, D.C. Radford, J.F. Wilkerson, K.M. Yocom, Results from a Search for Light-Mass Dark Matter with a P-type Point Contact Germanium Detector <http://arxiv.org/abs/1106.0650>

[112] Tamami I. Mori, Itsuki Sakon, Takashi Onaka, Hidehiro Kaneda, Hideki Umehata, Ryou Ohsawa, Observations of the Near- to Mid-Infrared Unidentified Emission Bands in the Interstellar Medium of the Large Magellanic Cloud <http://arxiv.org/abs/1109.3512>

[113] J. Kahanpaa, K. Mattila, K. Lehtinen, C. Leinert, D. Lemke, Unidentified Infrared Bands in the Interstellar Medium across the Galaxy <http://arxiv.org/abs/astro-ph/0305171>

[114] Davide Pietrobon, Krzysztof M. Gorski, James Bartlett, Anthony J. Banday, Gregory Dobler, Loris P. L. Colombo, Luca Pagano, Graca Rocha, Rajib Saha, Jeffrey B. Jewell, Sergi R. Hildebrandt, Hans Kristian Eriksen, Charles R. Lawrence, Analysis of WMAP 7-year Temperature Data: Astrophysics of the Galactic Haze <http://arxiv.org/abs/1110.5418>

[115] Gudlaugur Jóhannesson, The Fermi-LAT Collaboration, Fermi-LAT Observations of the Diffuse Gamma-Ray Emission: Implications for Cosmic Rays and the Interstellar Medium <http://arxiv.org/abs/1202.4039>

[116] Slava G. Turyshev, Viktor T. Toth, Jordan Ellis, Craig B. Markwardt, Support for temporally varying behavior of the Pioneer anomaly from the extended Pioneer 10 and 11 Doppler data sets <http://arxiv.org/abs/1107.2886>

[116a] Slava G. Turyshev, Viktor T. Toth, Gary Kinsella, Siu-Chun Lee, Shing M. Lok, Jordan Ellis, Support for the thermal origin of the Pioneer anomaly, <http://arxiv.org/abs/1204.2507>

[117] F. Francisco, O. Bertolami, P. J. S. Gil, J. Páramos, Modelling the reflective thermal contribution to the acceleration of the Pioneer spacecraft <http://arxiv.org/abs/1103.5222>

[118] Ryan T. Glasser, Ulrich Vogl, Paul D. Lett, Stimulated generation of group phase reflection light pulses via four-wave mixing <http://arxiv.org/abs/1204.0810>

[119] R. Abbasi et al., IceCube Collaboration, All-particle cosmic ray energy spectrum measured with 26 IceTop stations <http://arxiv.org/abs/1202.3039>

[120] Siegfried Bethke, Experimental Tests of Asymptotic Freedom, <http://arxiv.org/abs/hep-ex/0606035>

[121] V. Mourik, K. Zuo, S. M. Frolov, S. R. Plissard, E. P. A. M. Bakkers, L. P. Kouwenhoven, Signatures of Majorana fermions in hybrid superconductor-semiconductor nanowire devices, <http://arxiv.org/abs/1204.2792>

[122] Edward Harrison, Cosmology The Science of the Universe, Cambridge University Press, 2000

[123] M. Ackermann et al. Fermi Collaboration, Fermi LAT Search for Dark Matter in Gamma-ray Lines and the Inclusive Photon Spectrum, <http://arxiv.org/abs/1205.2739v1>

[124] N. Suzuki et al., The Hubble Space Telescope Cluster Supernova Survey: V. Improving the Dark Energy Constraints Above $z>1$ and Building an Early-Type-Hosted Supernova Sample, <http://arxiv.org/abs/1105.3470>

[125] R. Abbasi, et al., All-particle cosmic ray energy spectrum measured with 26 IceTop

[126] Richard de Grijs, An Introduction to Distance Measurement in Astronomy, John Wiley & Sons, 2011

[127] Ye Li, Qiang Yuan, Testing the 130 GeV gamma-ray line with high energy resolution detectors <http://arxiv.org/abs/1206.2241>

[128] R. Stabell and S. Refsdal, Classification of General Relativistic World Models, Monthly Notices Royal Astrophysical Society (1966), 132, 379-388

[129] Howard Percy Robertson, Relativistic Cosmology, Reviews of Modern Physics, 5, pp. 62-90, (1933)

[130] Christopher Eling, Hydrodynamics of spacetime and vacuum viscosity, <http://arxiv.org/abs/0806.3165v3>

[131] Steven Weinberg, Lectures on Quantum Mechanics, Cambridge University Press, 2013.

[132] Darius H. Torchinsky, Fahad Mahmood, Anthony T. Bollinger, Ivan Božović, Nuh Gedik, Fluctuating charge density waves in a cuprate superconductor, <http://arxiv.org/abs/1301.6128>

[133] Anjan Soumyanarayanan, Michael M. Yee Yang He, Jasper van Wezel, D.J. Rahn, K. Rossnagel, E.W. Hudson, M.R. Norman, Jennifer E. Hoffman, A quantum phase transition from triangular to stripe charge order in NbSe₂, <http://arxiv.org/abs/1212.4087>

[134] Robbert Dijkgraaf, Distinguished University Professor of Mathematical Physics at the University of Amsterdam and President of the Royal Netherlands Academy of Arts and Sciences, The End of Space and Time? Gresham College Lecture, Barnard's Inn Hall, 20 March 2012.

[135] Planck 2013 results. XXIII. Isotropy and Statistics of the CMB Planck Collaboration: <http://arxiv.org/abs/1303.5083>

[136] A. A. Abdo et al, Measurement of the Cosmic Ray e⁺ + e⁻ spectrum from 20 GeV to 1 TeV with the Fermi Large Area Telescope, The Fermi LAT Collaboration, <http://arxiv.org/abs/0905.0025>

[137] Derivation of the Lamb Shift from an Effective Hamiltonian in Non-relativistic Quantum Electrodynamics Asao Arai, Department of Mathematics, Hokkaido University Sapporo 060-0810, Japan E-mail: arai@math.sci.hokudai.ac.jp

[138] Vladimir G. Kogan, Homes scaling and BCS, <http://arxiv.org/abs/1305.3487>

[139] B. Feige, Elliptic integrals for cosmological constant cosmologies, Astronomisches Institut der Universitat Munster, April 6, 1992.

[140] L. Ben-Jaffel, M. Strumik, R. Ratkiewicz, J. Grygorczuk, The existence and nature of the interstellar bow shock, <http://arxiv.org/abs/1310.6497>

[141] C. Alden Mead, Possible Connection Between Gravitation and Fundamental Length, Physical Review Volume 135, Number 3 B 10 August, 1964.

[142] G. Lemaître (April 1927). "Un Univers homogène de masse constante et de rayon croissant rendant compte de la vitesse radiale des nébuleuses extra-galactiques". Annales de la Société Scientifique de Bruxelles (in French) 47: 49. Bibcode:1927ASSB...47...49L.

[143] S. Grzedzielski, P. Swaczyna, A. Czechowski, and M. Hilchenbach, Solar wind He pickup ions as source of tens-of-keV/n neutral He atoms observed by the HSTOF/SOHO detector, <http://arxiv.org/abs/1311.2723>

[144] John C. Baez and Emory F. Bunn, The Meaning of Einstein's Equation, <http://arxiv.org/abs/gr-qc/0103044>

[145] M. A. Sobolewska, A. Siemiginowska, B. C. Kelly, K. Nalewajko, Stochastic Modeling of the FERMI/LAT - Ray Blazar Variability, <http://arxiv.org/abs/1403.5276>

[146] R. Sankrit, J. C. Raymond, M. Bautista, T. J. Gaetz, B. J. Williams, W. P. Blair, K. J. Borkowski, K. S. Long, Spitzer IRS Observations of the XA Region in the Cygnus Loop Supernova Remnant, <http://arxiv.org/abs/1403.3676>

[147] LHCb collaboration, Observation of the resonant character of the $Z(4430)^-$ state, <http://arxiv.org/abs/1404.1903>

[148] Robert Foot, A CoGeNT confirmation of the DAMA signal, <http://arxiv.org/abs/1004.1424>

[149] Bruno Lenzi, Measurement of properties of the Higgs boson in bosonic decay channels using the ATLAS detector, <http://arxiv.org/abs/1409.4336>

[150] David Harvey, Richard Massey, Thomas Kitching, Andy Taylor, Eric Tittley, The non-gravitational interactions of dark matter in colliding galaxy clusters, <http://arxiv.org/abs/1503.07675>

[151] The Fermi LAT collaboration, The spectrum of isotropic diffuse gamma-ray emission between 100 MeV and 820 GeV, <http://arxiv.org/abs/1503.07675>